

MASARYK UNIVERSITY

FACULTY OF SCIENCE



RECETOX – Research Centre for Toxic Compounds in the Environment

GAP JUNCTIONAL INTERCELLULAR COMMUNICATION:

IN VITRO ASSESSMENT OF HAZARDOUS AND BENEFICIAL
EFFECTS OF CHEMICALS

Pavel BABICA

Habilitation thesis

BRNO 2017

BIBLIOGRAPHIC ENTRY

Habilitation thesis

Author: Pavel Babica, Ph.D.
Faculty of Science, Masaryk University
RECETOX - Research Centre for Toxic Compounds in the Environment

Habilitation field: Ecotoxicology

Title: Gap junctional intercellular communication: *in vitro* assessment of hazardous and beneficial effects of chemicals

Number of pages: 86 + Attachments

Keywords: gap junctional intercellular communication; connexin; *in vitro* cell cultures; toxicity testing; drug discovery; phenotypic screening; environmental and food toxicants; chemopreventive agents

BIBLIOGRAFICKÝ ZÁZNAM (ČESKY)

Habilitační práce

Autor: RNDr. Pavel Babica, Ph.D.
Přírodovědecká fakulta, Masarykova univerzita
RECETOX - Centrum pro výzkum toxických látek v prostředí

Obor habilitace: Ekotoxikologie

Název práce: Mezibuněčná komunikace mezerovými spoji: *in vitro* hodnocení nebezpečných a prospěšných účinků chemických látek

Počet stran: 86 + Přílohy

Klíčová slova: mezibuněčná komunikace mezerovými spoji; konexiny; *in vitro* buněčné kultury; testování toxicity; vývoj léčiv; fenotypické vyhledávání; kontaminanty životního prostředí a potravin; chemopreventivní agens

ACKNOWLEDGEMENT

I would like to thank my former mentors, who greatly influenced me throughout my scientific and teaching career, and laid the foundation for my independent research: Prof. Luděk Bláha, Prof. Blahoslav Maršálek, Prof. Brad L. Upham, Prof. James E. Trosko, and Prof. C. C. Chang.

I want to express my enormous appreciation to my current as well as former colleagues at RECETOX at Masaryk University, at the Institute of Botany of the Czech Academy of Sciences, and the Department of Pediatrics and Human Development at Michigan State University, not only for all the collaborative work we have done, but also for creating an exciting and friendly work environment, which allowed me to strive through my academic career.

My many thanks go also to all my collaborators at the other institutes, whom I was honored to collaborate with and publish together.

I would like to thank very much to my undergraduate and graduate students, for all their effort and hard work in the lab, which was fundamental for the progress and achievements of our research.

Most importantly, I would like to thank my family for their long-term support, help and understanding for my work. Special thanks go to Iva – my wife, colleague and collaborator – not only for helping me with her bright ideas and great judgment, but for being always on my side and keeping my spirit up, especially when I felt down and overwhelmed by life.

ABSTRACT

Cell- and tissue-based *in vitro* models are becoming an integral part of modern toxicological, pharmaceutical and biomedical research due to both ethical and practical reasons. Cell-based *in vitro* assays, which allow rapid, sensitive, reproducible and cost-effective evaluation of the key biological phenomena and processes, can be effectively used for hazard assessment and predictions of chemical effects on human health. Gap junctional intercellular communication (GJIC) mediated by connexin channels facilitates an exchange of small molecules between the adjacent cells and has been recognized as an essential process coordinating intra-, extra- and inter-cellular signaling pathways between the cells within a tissue. Due to increasing knowledge on the critical role of connexins and GJIC in human diseases and toxicities, compatibility of methods for GJIC assessment with advanced *in vitro* models and high-throughput setups, *in vitro* evaluation of GJIC represents an effective tool which can be utilized in the modern toxicological and pharmacological research for prediction of chemical effects on human health.

This thesis provides a commented summary of 15 original research papers, which demonstrates possible applications of *in vitro* GJIC assessment in modern toxicological and pharmacological research. GJIC can be assessed *in vitro* using a variety of methods, including techniques compatible with high-throughput screening, as well as methods which are suitable for different *in vitro* models including three-dimensional cell cultures. These *in vitro* GJIC assays were used to identify new chemical hazards represented by several organic pollutants, such as polycyclic aromatic hydrocarbons (especially methylated anthracenes and other low molecular weight PAHs), endocrine disruptors (methoxychlor, vinclozolin) or perfluorinated fatty acids. GJIC assessment was further applied to characterize molecular and cellular mechanisms of toxicity, including identification of new signal transduction pathways (phosphatidylcholine-specific phospholipase C, phospholipase A₂, mitogen-activated protein kinases, protein kinase A) and molecular targets (e.g. annexins) altered by toxicants dysregulating GJIC. *In vitro* GJIC assay was also successfully used to assess toxic potential of complex cyanobacterial water blooms or to identify synergistic interactions between natural toxins and anthropogenic contaminants. GJIC assessment was employed as a principal bioassay in an effect-directed analysis for identification of toxic compounds in complex mixtures, or in effect-based monitoring or evaluation of water treatment technologies. It was demonstrated that GJIC can be assessed in a variety of *in vitro* models representing different cell types, tissues, organs, developmental stages, health states or biological species. The effects of chemicals on GJIC, mechanisms underlying GJIC modulations, or cellular events occurring downstream of GJIC dysregulation can be then studied and interpreted within the specific biological, physiological or pathophysiological context. GJIC assessment is also a valuable tool for *in vitro* screening for cancer chemopreventive agents capable to prevent chemically-induced inhibition of GJIC, as demonstrated for example for resveratrol, quercetin or silibinin. Alternatively, restoration of GJIC in neoplastically transformed cells can be assessed *in vitro* and used in drug screening, including a bioassay-guided fractionation and identification of bioactive chemicals in complex mixtures, such as extracts of different natural products. Finally, GJIC was shown as a useful tool to evaluate potential harmful or beneficial effects and mode(s) of action of perspective biomedical applications, like applications of carbon nanotubes or treatments with pulsed electric fields.

CONTENTS

Bibliographic Entry.....	3
Bibliografický záznam (Česky).....	3
Acknowledgement.....	5
Abstract	7
Contents	9
Abbreviations.....	11
1 Introduction	15
1.1 In vitro assays for predicting chemical effects on human health.....	15
1.2 Target-based vs. phenotypic in vitro assays.....	15
1.3 new phenotypic bioassays?	16
2 Connexins and GJIC regulation.....	17
2.1 Evolutionary significance of cell-to-cell communication.....	17
2.2 Gap junction structure and GJIC regulation	18
3 Physiological and pathophysiological role of connexins and gap junctions.....	22
3.1 GJIC as a mechanism of homeostatic control in multicellular organisms	22
3.2 Connexins and gjc in human diseases	23
3.2.1 Nervous system diseases	23
3.2.2 Eye, ear and cutaneous diseases	23
3.2.3 Cardiovascular diseases	24
3.2.4 Pulmonary diseases	24
3.2.5 Diseases of digestive system.....	25
3.2.6 Renal diseases.....	25
3.2.7 Immune system and inflammatory diseases	25
3.2.8 Reproductive system diseases	25
3.2.9 Cancer	26
4 <i>In vitro</i> assessment of GJIC in toxicology and pharmacology	27
4.1 Methods for GJIC assessment	27
4.1.1 Electrophysiological measurements	27

4.1.2	endogenous metabolite transfer	27
4.1.3	Dye transfer assays	29
4.2	GJIC for identification and characterization of new chemical hazards	33
4.2.1	Inhibition of GJIC as a common but structure-dependent response to toxicants	33
4.2.2	Identification of new chemical hazards and toxicity mechanisms by GJIC assessment	34
4.3	GJIC assessment of species- and tissue-specific effects of chemicals.....	41
4.4	<i>In vivo</i> and <i>ex vivo</i> validation of <i>in vitro</i> effects on GJIC	46
4.5	GJIC assay in whole-mixture toxicity testing, effect-directed analysis and effect-based monitoring...47	
4.5.1	Whole-mixture toxicity testing of cyanobacterial extracts and exudates	48
4.5.2	Effect-based evaluation of water treatment technologies.....	51
4.6	GJIC assessment in pharmacological and biomedical research	52
4.6.1	Screening for cancer chemopreventive agents	53
4.6.2	Development of new biomedical applications	56
5	Conclusions	59
6	References.....	61
7	Author Resume	75
8	List of scholarly work published by the author	78
9	List of Attachments	83
10	Attachments.....	85

ABBREVIATIONS

2D	Two-dimensional
3D	Three-dimensional
3Rs	Replacement, Reduction and Refinement
6-TG	6-thioguanine
AhR	Aryl hydrocarbon receptor
Akt	Protein kinase B, Serine/threonine-specific protein kinase
AO	Adverse outcome
AOP	Adverse outcome pathway
AP-1	Activator protein 1
AR	Androgen receptor
ARE/Nrf2	Antioxidant responsive element/ NF-E2-related factor 2
ATP/ADP	Adenosine triphosphate/ Adenosine diphosphate
CaMKII	Calmodulin-dependent protein kinase II
Ccl2	Chemokine (C-C motif) ligand
COPD	Chronic obstructive pulmonary disease
Cox-2	Cyclooxygenase 2
Cox-2	Cyclooxygenase-2
CREB	cAMP response element-binding protein
Cx	Connexin
DDT	Dichlorodiphenyltrichloroethane
DMEM	Dulbecco's Modified Eagle Medium
EDA	Effect directed analysis
EDC	Endocrine disrupting compound
EGF	Epidermal growth factor
EGFR	Epidermal growth factor receptor
ERK1/2	Extracellular signal-regulated kinases 1/2
ER	Estrogen receptor
ERAD	Endoplasmic-reticulum-associated protein degradation

FOC	Fraction of the control
FRAP	Fluorescence recovery after photobleaching
GJIC	Gap junctional intercellular communication
GPCR/cAMP	G protein–coupled receptor/ Cyclic adenosine monophosphate
HCS/HCA	High Content Screening / High Content Analysis
HIF1A	Hypoxia-inducible factor 1-alpha
HPTE	2,2-bis-(p-hydroxyphenyl)-1,1,1-trichloroethane, the methoxychlor metabolite
HTS	High-throughput screening
IL-8	Interleukin 8
IL-DT	Incision loading-dye transfer
IP ₃	Inositol 1,4,5-triphosphate
KE	Key event
KER	key event relationship
LAMP	Local activation of fluorescent molecular probe
LC-MS	Liquid chromatography-mass spectrometry
LC-MS/MS	Liquid chromatography tandem-mass spectrometry
LPS	Lipopolysaccharide
MAPK	Mitogen-activated protein kinase
MAPK/ERK	Ras-Raf-MEK-ERK pathway
MEK	Mitogen-activated protein kinase kinase
MIE	Molecular initiating event
MMP13	Matrix metalloproteinase 13
NFκB	Nuclear Factor Kappa B
nsPEF	Nanosecond range Pulsed electric field
PAH	Polycyclic aromatic hydrocarbon
PCB	Polychlorinated biphenyls
PCDD	Polychlorinated dibenzodioxin
PC-PLC	Phosphatidylcholine-specific phospholipase C
PFOA	Perfluorooctanoic acid

PFPeA	Perfluoro-n-pentanoic acid
PKA	Protein kinase A
PKC	Protein kinase C
PKG	Protein kinase G
PLA ₂	Phospholipase A ₂
PLC	Phospholipase C
PPARs	Peroxisome proliferator-activated receptors
RT-PCR	Reverse transcription-polymerase chain reaction
RXR	Retinoid X receptor
SILAC	Stable isotope labeling with amino acids in cell culture
SL-DT	Scrape loading-dye transfer technique
SWCNT	Single-walled carbon nanotube
TNF α	Tumor necrosis factor alpha
TPA	12-O-tetradecanoylphorbol-13-acetate
VM2	Vinclozolin M2

1 INTRODUCTION

1.1 IN VITRO ASSAYS FOR PREDICTING CHEMICAL EFFECTS ON HUMAN HEALTH

Understanding **chemical effects on human health** represents one of the **essential societal needs**. Human beings are constantly being exposed to dozens of chemicals: unintentionally to those contaminating their environment or food; rather deliberately to the compounds from personal care and cosmetic products, food additives and preservatives; and finally quite on purpose via medicinal and recreational drug use and abuse. Interactions between the chemicals and organism might then result into acute or chronic **alterations of its anatomical, physiological or psychological integrity**, which are the critical determinants of the **health state** (Stokes et al., 1982).

Our interest to **understand, characterize and predict beneficial or adverse effects of chemical substances** on human beings is probably as old as the mankind itself. The effort to systematically identify compounds and exposures hazardous for human health in order to prevent, minimize, counteract or utilize their adverse health effects, has translated into the formation of modern **toxicology**, toxicity testing and risk assessment. On the other hand, modern **pharmacology** and drug discovery focuses on the identification of beneficial compounds and their effects to cure, treat, or prevent disease.

In the modern experimental toxicology and pharmacology, ***in vitro* methods** compatible with **high-throughput screening (HTS)** are becoming the major tool for **toxicity testing and drug discovery**, which is supposed to overcome not only the ethical concerns associated with the use of experimental animals, but also other constraints of animal models in terms of their low speed and throughput, high costs, limited gain of mechanistic information, poor reflection of intra-specific variability, needs for interspecies extrapolation, and overall limited predictability of the outcomes observed in humans (Shukla et al., 2010). Important milestone regarding the use *in vitro* assays in the toxicity testing was the strategic document published by the US National Academy of Science in 2007 **“Toxicity testing in the 21st Century: A vision and a strategy”**, which outlined a need for the major change in the toxicity testing in order to increase its efficiency and reduce the animal usage. This should be achieved by transitioning from current expensive and lengthy *in vivo* testing with qualitative endpoints to *in vitro* toxicity assays on human cells or cell lines using robotic HTS with mechanistic quantitative parameters (Krewski et al., 2010). This strategy placing *in vitro* toxicology and toxicity mechanisms in the foreground is also in a synergy with the long term coordinated effort aiming for reduction of animal experiments (3Rs principle) on one hand, and the increasing demands for toxicity testing and chemical hazard assessment on the other hand. Both these aspects are being strongly emphasized within the current EU legislation including promotion and support for research, development, validation and application of *in vitro* alternatives to animal testing (Daneshian et al., 2015).

1.2 TARGET-BASED VS. PHENOTYPIC IN VITRO ASSAYS

Many *in vitro* assays were designed as so-called **target-based assays** in order to evaluate interactions between chemicals and specific biochemical or molecular targets (e.g. purified recombinant receptor proteins or signaling enzymes) in high-throughput cell-free assays, or to assess perturbations of the key signaling pathways using genetically engineered cell lines with gene reporters or protein sensors allowing rapid, sensitive and high-throughput luminescence or fluorescence readouts for assessment of **nuclear receptor transactivation** (e.g. AR, ERs, PPARs, RXR, AhR), activity of other **transcription factors** (AP-1, HIF1A, NFκB, ARE/Nrf2, CREB, p53), cytokine production (IL-8, TNFα), **membrane receptor or kinase activation** (e.g. GPCR/cAMP, MAPK/ERK, Akt) (Shukla et al., 2010). Although the target-oriented approach has been quite successful in both toxicological and pharmaceutical research and screening, signaling pathways are known to be interconnected, creating complex interacting networks with many redundancies, compensatory crosstalks and feedbacks. Moreover, signaling pathways and networks are cell-type specific, thus perturbations of the same signaling pathway might result in different outcomes in different cell types, depending on species-, sex-, developmental stage-, organ- or tissue-specific cellular and physiological context. Thus, the final outcomes occurring at the higher levels of biological organization cannot be always reliably predicted from the assessment of a single or few individual target(s) or pathway(s). This

increases demands to combine multiple assays into high-throughput setups to reflect perturbations of multiple signal transduction pathways, and to rely on the application of computational and systems biology tools for modeling or predicting of biological outcomes. Despite our expanding knowledge and understanding in biology and other relevant disciplines, this approach is being inherently limited by the number of known signaling pathways which can be successfully incorporated into the high-throughput assays, as well as by the number of assays which can be actually evaluated within a given research project, and finally by our not-finite understanding of signaling pathways and networks, since new signaling pathways, mechanisms and interactions are being constantly discovered.

Phenotypic assays focusing on physiological responses and phenotypic changes, which require minimal assumptions concerning the participation of specific molecular targets and/or signaling pathways, therefore represent a very effective strategy complementary to the target-based assays. In cell-based phenotypic assays, cellular responses associated with various toxicant-induced adverse outcomes or disease-related phenotypes can be evaluated within a given cell-specific content of interacting proteins and signaling networks, and typically also in the presence of cell-cell interactions and intercellular signaling. Historically, **cell viability** represents probably most traditionally evaluated endpoint in cell-based phenotypic assays, thanks to a variety of early-on available methods allowing evaluation of cytotoxicity and proliferation in different formats, including high-throughput assays. Recent advances in cell and molecular biology, cell culture techniques, robotic platforms, detection instrumentation, microscopic and imaging systems, and computer hardware and software innovations have greatly increased the number, availability and throughput of methods and assays for evaluation of other cellular responses and phenotypic changes (Xu, 2015). *In vitro* methods and cell-based assays, which are nowadays available for routine qualitative and quantitative assessments of various cellular events linked to toxicant-induced adverse outcomes or diseased phenotypes, include alterations of **apoptosis, autophagy, cell adhesion, cell growth, cell motility, cell migration and invasion, cytoskeletal rearrangements, DNA damage and repair, membrane integrity, mitochondrial function, morphological changes** (e.g. neurite outgrowth), **nuclear translocation, oxidative stress and redox state** (Shukla et al., 2010; Zheng et al., 2013). These modern phenotypic assays can be effectively combined with biochemical or molecular-biological techniques using either **hypothesis-driven** or **exploratory approach** ('omics' technologies) in order to provide mechanistic clues and explanations by acquiring information on gene and protein expression, activity, function and regulation.

1.3 NEW PHENOTYPIC BIOASSAYS?

Considering increasing demands for toxicity testing and drug discovery, there is a continuous effort to develop and optimize **new *in vitro* cell-based assays**, which would allow to assess important toxicity- and disease-relevant cellular responses in more effective ways in terms of their efficiency, robustness, throughput, *in vivo* relevancy and ability to predict specific responses and adverse outcomes at the higher levels of biological organization. This includes development of newly designed or re-designed assays for assessment of **well-recognized phenotypic endpoints** such as cell death, migration, membrane integrity etc., but also phenotypic assays for evaluation of **other cellular and tissue processes**, whose disruption have been linked to adverse outcomes and health effects.

Gap junctional intercellular communication (GJIC) represents an evolutionary ancient cellular process founding the origin of metazoans in the phylogenetic history of life on the Earth. Although GJIC is an indispensable process for the healthy development and functioning of any animal or human being, its application in the modern toxicological and pharmacological research is relatively underrepresented in comparison to other and more traditional assays, partially due to the until-recent lack of simple and rapid methods allowing for GJIC assessment in a higher-throughput workflow or in advanced *in vitro* models.

In this habilitation thesis, GJIC will be introduced as a vital cellular process whose *in vitro* assessment provides a valuable phenotypic endpoint, which could be effectively utilized in the modern toxicological and pharmacological research. After a brief introductory information regarding the underlying principles of GJIC, its regulation and (patho-)physiological role, the candidate will summarize and comment the major findings of his postdoctoral research in order to demonstrate that:

- GJIC can be assessed *in vitro* using a variety of methods including those compatible with HTS or suitable for different *in vitro* models including three-dimensional (3D) cell cultures
- *In vitro* assessment of GJIC can be used to
 - Identify new chemical hazards, with a possibility to validate the results using *in vivo* experiments
 - Characterize molecular mechanisms of cellular and tissue toxicity
 - Assess toxic potential or bioactivity of complex mixtures and identify the bioactive components
 - Characterize species-specific, tissue- or cell-type specific effects of chemicals
 - Evaluate potentially beneficial effects of bioactive chemicals or therapeutic treatments

This thesis is built on the selection of 15 peer-reviewed publications [Attachment I-XV], which are relevant for this topic, and were co-authored by the candidate. The major claims are further supported also by several examples from the currently ongoing research.

2 CONNEXINS AND GJIC REGULATION

2.1 EVOLUTIONARY SIGNIFICANCE OF CELL-TO-CELL COMMUNICATION

Evolution of the cell-to-cell communication was the essential prerequisite for the evolutionary transition from single celled organisms into complex multicellular life forms with specialized cell types, tissues and organs. There are several extra-cellular phenotypic features underlying the evolution and morphogenesis of differentiated multicellular organisms, including most importantly (Knoll, 2011; Trosko, 2016, 2011):

- (a) mechanisms of **growth control**, where a society of grouped cells regulates their proliferation, for example by mechanisms of “contact-inhibition”;
- (b) **induction of specialized cells** (“differentiation”) through regulated expression of the selected sets of the total genomic information; and
- (c) **programmed cell death** such as apoptosis to selectively remove damaged or developmentally no-longer required cells and allow their replacement with functional cells or proper cell types.

Regulation of cell behavior in terms of their growth, differentiation or apoptosis relies on **the ability of the cells to communicate with each other** in order to coordinate their responses to different external and internal stimuli across the tissues and organs. Such coordination of cell behavior is necessary during the entire ontogenetic development, from **the early stages of embryogenesis and morphogenesis**, when an undifferentiated cell develops into a life form characterized by many specialized cell types organized in differentiated tissues and organs; till **the later developmental phases**, when proper function and regeneration of a tissue or organ depends on the constant maintenance of **tissue homeostasis** in terms of balanced proliferation, differentiation and apoptosis (Trosko 2011; 2016).

Direct cell-to-cell coupling, i.e. **direct symplastic connections between adjacent cells in the tissues**, is one of the essential mechanisms of cell communication facilitating coordination of cell behavior and responses, and thus enabling the existence of complex multicellular life. Despite their evolutionary, structural and functional differences, mechanisms of intercellular communication allowing cell-to-cell transport of various molecules can be found in one form or another in all groups of eukaryotic organisms with multicellular life forms: **gap junctions** and

so-called **tunneling nanotubes** in animals, **septal pores** in fungi, **plasmodesmata** in brown algae, green algae and plants, and possibly also **pit plugs** in red algae (Bloemendal and Kuck, 2013; Knoll, 2011; Terauchi et al., 2015).

2.2 GAP JUNCTION STRUCTURE AND GJIC REGULATION

In animals, intercellular communication is mediated primarily by **gap junctions**, which are plaque-like protein structures that form contiguous channels between the cells. Vertebrate gap junctions are built from connexins (Cxs), which are membrane proteins with tetraspan topology of four interspersed transmembrane domains connecting the cytoplasmic N-terminal region through an extracellular (E1), cytoplasmic and another extracellular (E2) loop to the C-terminal region of the connexin molecule (Figure 1). This structure is shared among the 20 rodent or 21 human connexin species encoded by the family of Gj/GJ genes. In addition to the gene names, a nomenclature of connexins based on the molecular weight predicted by DNA sequencing is commonly used. For example, Cx43 denotes connexins with a predicted molecular weight of 43 kDa, which are encoded by rodent/human genes Gja1/GJA1 (Nielsen et al., 2012). In gap junction channels, six connexin protein units are organized into a hexameric hemichannel structure termed **connexon** (Figure 1). Full gap junction channel is then formed by head-to-head docking of hemi-channels from two adjacent cells. Expression of different connexin proteins is tissue- and cell type-specific, and different connexin species can be combined within a gap junction channel: **homomeric hemi-channels** contain only one type of connexin, whereas **heteromeric connexons** are built from different connexin species (Nielsen et al., 2012). **Homotypic channels** then consist of two identical homomeric or heteromeric connexons, whereas **heterotypic channels** are created from two different homomeric or heteromeric connexons. Multiple (tens to thousands) connexin channels usually aggregate and create a **gap junction plaque** or a **gap junction** (Axelsen et al., 2013).

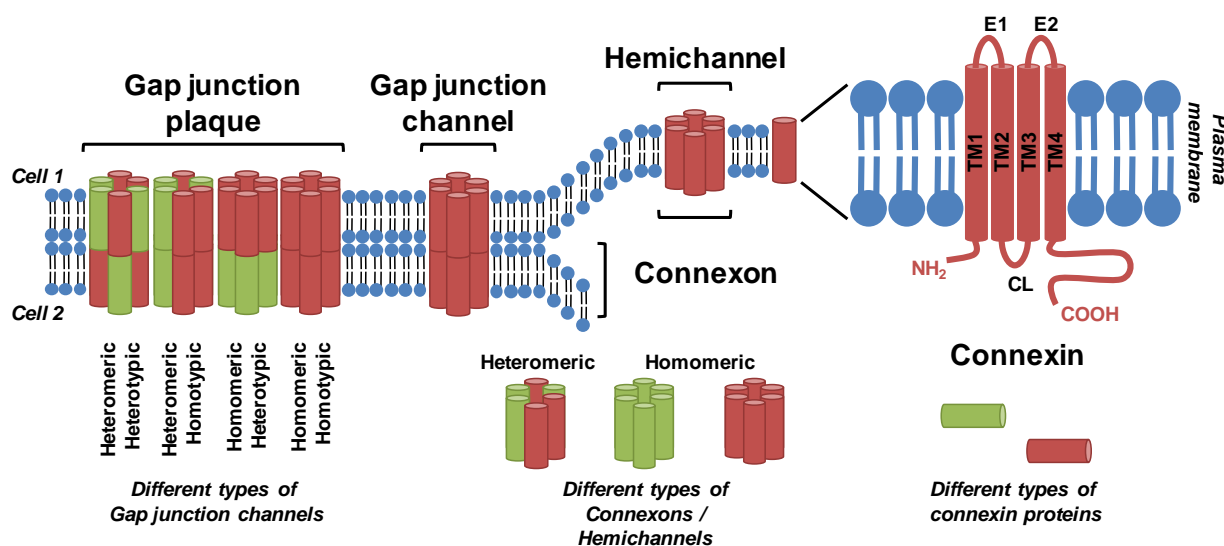


Figure 1: Connexins, connexin hemichannels and gap junction channels. Connexin monomer consists of intracellular N-terminus, C-terminus and cytoplasmic loop (CL); four transmembrane segments (TM1-4); and two extracellular loops (E1 and E2). Six connexin subunits form connexon or hemichannel, two connexons/hemichannels form a gap junction channel, multiple channels are clustered into a gap junctional plaque. Different types of connexin can be combined within one hemichannel, channel or plaque. Prepared according to (Nielsen et al., 2012; Vinken et al., 2009).

Gap junction channels allow for passing of various **ion species** carrying electrical charges, **nutrients, metabolites, signaling and regulatory molecules**, and thus provide a basis for GJIC, i.e. direct intercellular communication via exchange of soluble ions and molecules. Chemicals with a size up to **1-1.5 kDa** are known to be transported through gap junctions, including **inorganic ions (e.g. Na⁺, K⁺, Ca²⁺)**, **organic molecules, such as ATP/ADP, cAMP, inositol triphosphate (IP₃), glutamate, glutathione** (Nielsen et al., 2012) or **non-coding RNAs** (Zong et al., 2016). Different types of connexins and gap junctions might have different permeability and selectivity for the individual ions and compounds. Although cell-to-cell coupling and mediation of GJIC represents a universal and key function

of all connexins, it was also demonstrated that connexins, **connexin channels as well as hemichannels** might be involved in signaling and regulations occurring via **non-coupling mechanisms, and independently of GJIC** (Vinken et al., 2012). Correspondingly, there is also an increasing knowledge regarding the (patho-)physiological role of **pannexins**, which are proteins related to invertebrate gap junction proteins innexins with a configuration resembling connexin hemichannels, but not participating in the intercellular junctions in vertebrates (Willebrords et al., 2017).

The main focus of this thesis will be on **GJIC**, which represents a strictly controlled process regulated at several levels: (a) control of connexin gene expression, (b) connexin turnover and trafficking, (c) postranslational regulations and (d) channel gating mechanisms (**Figure 2**).

Transcription of connexin genes is regulated by a combination of ubiquitous or tissue-specific transcription factors, histone acetylation and DNA methylation. Stability and translation of connexin mRNA transcripts is modulated also by non-coding RNAs, and these epigenetic mechanisms contribute to the tissue and cell specific expression of connexin genes (Nielsen et al., 2012). GJIC permeability and selectivity will depend not only on the type(s) of connexin(s) expressed and present in the gap junctions, but also on the number of connexin channels within a gap junction plaque and the number of plaques, which are further regulated by mechanisms controlling connexin cellular fate and dynamics.

Translated connexins have a high turnover rate, with half-lives ranging from few hours up to 1.5 days, depending on the connexin type and cell type (Nielsen et al., 2012). **Folding** of connexins and disulfide bonds formation occurs

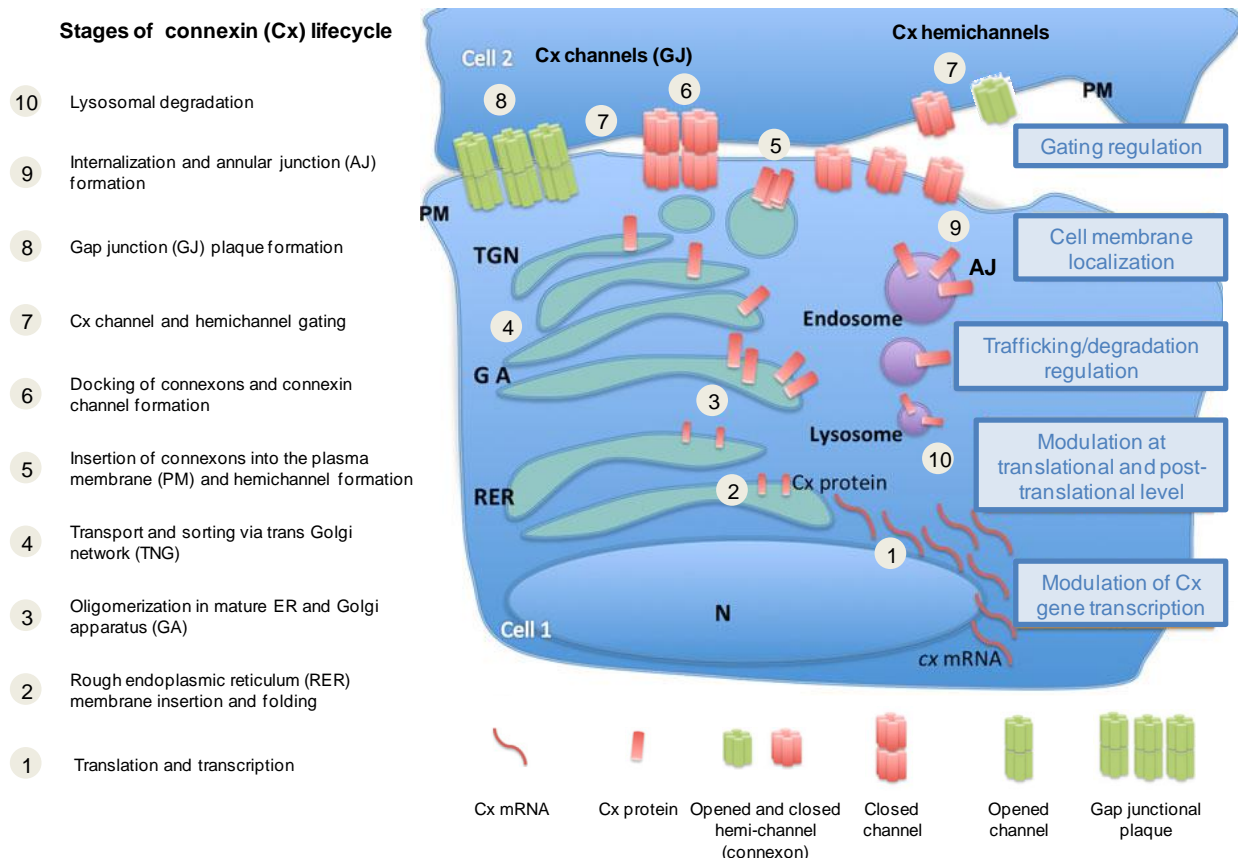


Figure 2: Formation of connexin (Cx) channels and regulation of gap junctional intercellular communication (GJIC) at different levels: (a) Transcription of connexin genes is regulated by epigenetic mechanisms; (b) Connexin maturation, trafficking and assembly, membrane localization and degradation depend on the intracellular protein and organelle machinery; (c) Connexon docking and connexon gating (opening–closing) is regulated by connexin-postranslational modifications and also by voltage-, pH-, calcium- or redox-dependent gating. Adapted from (Leone et al., 2012).

within the endoplasmic reticulum. Mature connexin molecules usually **oligomerize** in the Golgi complex, and are transported to the plasma membrane through the **Trans-Golgi network** (Leone et al., 2012). Given their short half-life, new connexons are being constantly **inserted** into the plasma membrane while removing of older ones is occurring simultaneously via **internalization**. Connexins are internalized primarily through formation of double membrane gap junction vesicles called **annular gap junctions** by clathrin-dependent endocytosis (Falk et al., 2016). Annular gap junctions are **degraded** primarily by endolysosomal or autophagosomal processes (Falk et al., 2016). Alternatively, some connexin molecules might be **recycled** back to the plasma membrane (Nielsen et al., 2012). Connexin maturation, trafficking, membrane localization, internalization or recycling is assisted and regulated by interactions with specific proteins (e.g. zonula occludens-1, caveolin, tubulin), thus dynamics of these processes is dependent on the actual context of intracellular protein and organelle machinery.

Connexin turn-over and interactions with other proteins are regulated also by **posttranslational modifications** of connexins. Major recognized posttranslational modifications of connexin molecules include SUMOylation, nitrosylation, methylation, acetylation, glutamate g-carboxylation, ubiquitination and phosphorylation (Axelsen et al., 2013). SUMOylation has been associated with an increase in both connexin expression and gap junction formation, while S-nitrosylation of connexin has been linked to the regulation of GJIC in the vasculature, as well as in the regulation of hemichannel functions. Connexin methylation and acetylation have been implicated also in the control of GJIC, whereas g-carboxylation appears to modulate Ca^{2+} -dependent gating of Cx26 (Axelsen et al., 2013).

Ubiquitination and phosphorylation represent the most studied posttranslational modifications of connexin (Axelsen et al., 2013). **Ubiquitination** is involved in connexin degradation and regulation of connexin life cycle and turnover. Newly synthesized but immature, unfolded, misfolded or damaged connexin molecules are targeted by ubiquitination for endoplasmic-reticulum-associated protein degradation (ERAD) or for proteasome degradation. Interestingly, up to 40% of newly synthesized connexins were shown to undergo ERAD, and stress-induced reduction of ERAD was demonstrated to affect number of functional gap junctions. Thus, ERAD might be also part

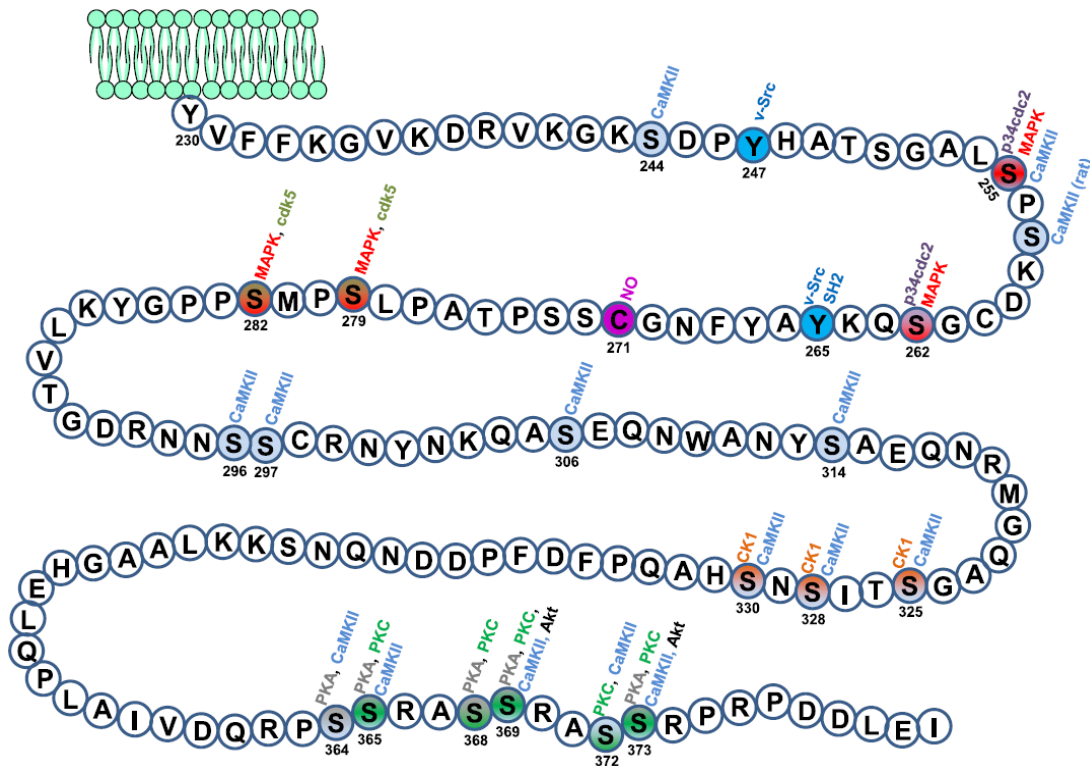


Figure 3: Post-translational modifications of connexin43 (Cx43). Schematic representation of C-terminus of Cx43 with the identified phosphosites and their specific kinases. Residue of Cystein 271 known to be modified by S-nitrosylation with nitric oxide is also highlighted. Adapted from (Pogoda et al., 2016).

of regulation of normal connexin molecules turnover (Nielsen et al., 2012). Internalization of gap junctional plaques followed by their endo-lysosomal or autophagolysosomal degradation is triggered by multiple monoubiquitination of connexins by E3 ubiquitin ligases (e.g. Nedd, Smurf2 or Trimm21) or by K63-polyubiquitination (Falk et al., 2016).

Phosphorylation is probably the most intensively investigated posttranslational modification of connexins. All connexins are phosphoproteins containing multiple phosphosites, with majority of phosphosites located in the C-terminal region (Axelsen et al., 2013; Nielsen et al., 2012; Pogoda et al., 2016). Cx43 represents the most abundant and most extensively studied mammalian connexin. In human Cx43, there have been 22 phosphosites identified within C-terminal region (**Figure 3**), which include two tyrosine residues known to be phosphorylated by Src kinases, and 20 serine residues phosphorylated in a site-specific manner by Ca^{2+} /calmodulin-dependent protein kinase II (CaMKII), mitogen activated protein kinases (MAPKs), protein kinase A (PKA), protein kinase C (PKC), casein kinase 1 (CK1), cyclin-dependent kinases (cdc5, p34cdc2) or Akt kinases (Axelsen et al., 2013; Nielsen et al., 2012; Pogoda et al., 2016). Also other kinases (protein kinase G - PKG, EGFR-tyrosine kinases) were reported to phosphorylate other types of connexin (Cx35/36, Cx32). Dephosphorylation of connexins is mediated by protein phosphatases PP1 and PP2A. Phosphorylation pattern regulates all stages of connexin life cycle, including connexin oligomerization into the connexons, trafficking and insertion into the plasma membrane, gap junction assembly and connexin degradation, thus controlling the quality and quantity of gap junctions and consequently the levels of GJIC (Axelsen et al., 2013; Nielsen et al., 2012; Pogoda et al., 2016).

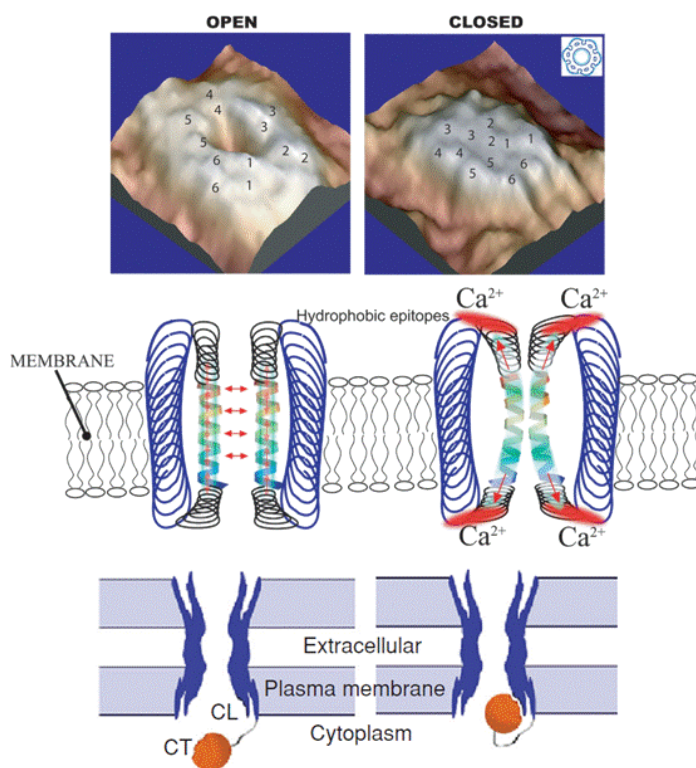


Figure 4: Examples of gating regulation of connexin (hemi)channel permeability. Atomic force microscopy topography image of the plasma membrane surface with an opened and closed Cx43 hemichannel in a calcium-free buffer (top left) and in the presence of 1.8 mM Ca^{2+} (top right). Schematic representation of hemichannel gating regulation by Ca^{2+} ions (middle) and by pH (bottom). CT - C-terminus, CL - cytoplasmic loop. Adapted from (Evans et al., 2006; Nielsen et al., 2012; Thimm et al., 2005).

Site specific phosphorylation and interplay between various phosphorylation sites appears to be also the key mechanism for direct regulation of electrical and metabolic coupling through gap junction channels via **gating mechanisms** (**Figure 4**), i.e. changes of single-channel conductance or chemical permeability achieved by conformational changes and structural rearrangements of connexin molecules or electrostatic mechanisms, but without changes in the number or composition of gap junctional plaques. In addition to phosphorylation and other posttranslational modifications, the gating of connexin channels can be directly modulated also by **transjunctional voltage** and **transmembrane potential** (Bargiello et al., 2018), **pH**, **Mg^{2+}** and **Ca^{2+} changes** (Lopez et al., 2016; Palacios-Prado et al., 2013; Wang et al., 2012), **phospholipase activity** (van Zeijl et al., 2007) or **redox signaling** (Pogoda et al., 2016; Upham and Trosko, 2009).

Taken together, functionality of GJIC represents a complex phenotypic outcome depending on the integration of different extra-, intra- and extracellular signals and signal transduction pathways either directly controlling GJIC or modulating the actual gene expression profile, including expression of connexins, expression and activity of connexin-interacting proteins or proteins involved in gap junction processing.

3 PHYSIOLOGICAL AND PATHOPHYSIOLOGICAL ROLE OF CONNEXINS AND GAP JUNCTIONS

3.1 GJIC AS A MECHANISM OF HOMEOSTATIC CONTROL IN MULTICELLULAR ORGANISMS

GJIC plays a central role in coordinating cell-to-cell communication and signal transduction pathways controlling gene expression and cell behavior in order to receive coordinated or collective responses from the cells across a tissue of multicellular organism, where virtually all differentiated cells within a solid tissue are joined by gap junctions. In the various tissues and organs of animals, four major cell types can be distinguished by their self-renewal potential and their potency, i.e. ability to differentiate into more specialized cell types: (a) **toti-potent and pluripotent stem cells**, which occur typically only during the earliest stages of ontogenetic development, and their more differentiated progeny of (b) **multipotent, oligopotent or bipolar somatic** (adult, tissue-specific or tissue-resident) stem cells, (c) the **progenitor or transiently-amplifying cells** with a finite life span, and (d) the **terminally differentiated cells**. Proper development and function of multicellular organism relies on the **maintenance of homeostatic balance** between self-renewal, differentiation, proliferation and apoptosis of these different cell types, which is achieved by delicately integrated mechanisms of extra- (hormones, cytokines, growth factors), intra- (different intracellular signaling mechanisms, such as MAPKs; NF- κ B) and also intercellular communication including GJIC (Figure 5). Without these communication mechanisms, the higher order structures and functions of multicellular organism could neither develop nor be maintained during the different stages of embryonic, fetal,

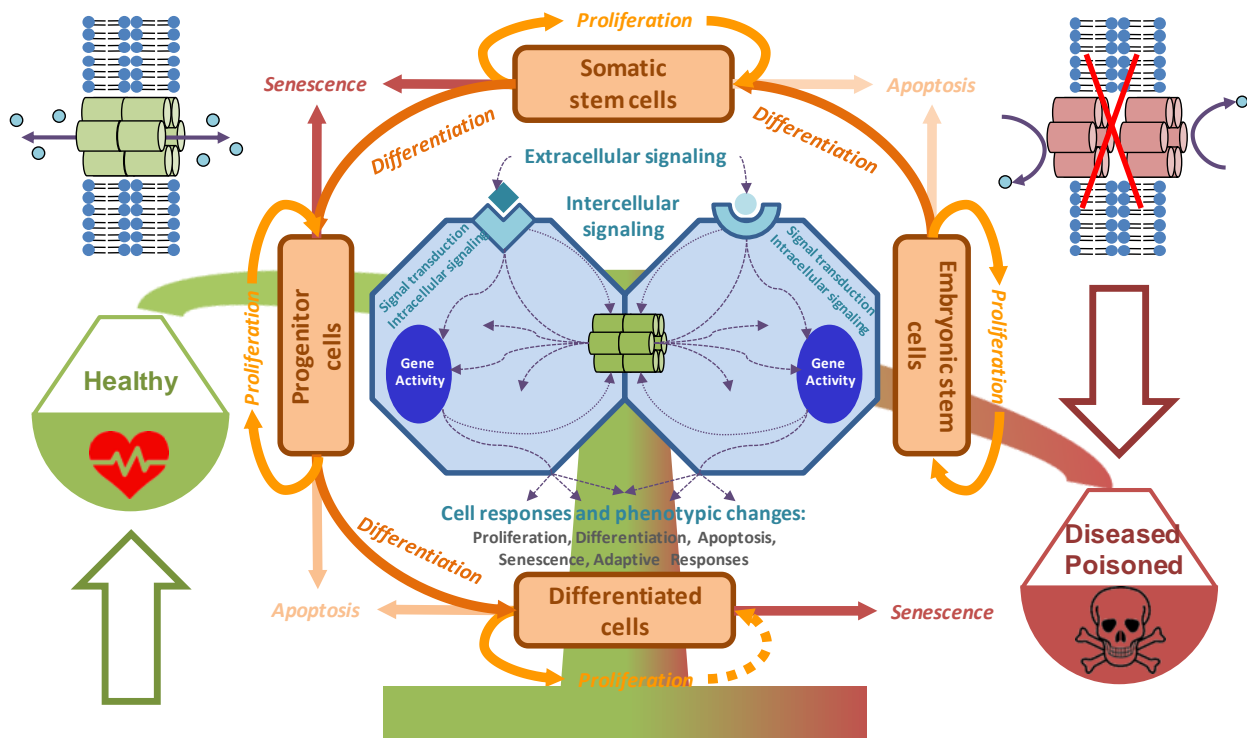


Figure 5: Gap junctions in homeostasis. Extracellular signals, such as growth factors, cytokines, hormones, toxicants, extra-cellular matrices, and cell adhesion molecules, that vary for each cell type (adult stem cell, progenitor, and terminally differentiated), interact with receptor-dependent or receptor-independent targets, which then activate intracellular signal transduction pathways that induce the transcription of genes through activated transcription factors. These specific intracellular pathways operate under cascading systems that cross-communicate with each other in controlling the expression of genes that direct the proliferation, differentiation, and apoptosis of cells within a tissue. These multiple intracellular signaling check points are further modulated by intercellular signals traversing gap junctions, thereby maintaining the homeostatic state of a tissue under physiological conditions in a healthy organism. Abnormal interruption of these integrated signaling pathways by food-related and environmental toxins/toxicants will disrupt the normal homeostatic control of cell behavior and lead to an adverse outcome or a disease. Prepared by P. Babica according to (Trosko, 2007; Upham and Trosko, 2009).

neonatal, adolescent, adult and geriatric development (Trosko, 2011).

The importance and complexity of the connexin physiological and pathophysiological role is illustrated by a variety of outcomes of different connexin knock-out models. While knock-out of some connexin genes results in embryonic or early life stage lethality due to severe developmental impairment, dysfunction of other connexins might be partially or nearly fully compensated. For example, mice knockouts for Cx32 resulted in hepatic abnormalities and susceptibility to hepatic tumors and mild peripheral neuropathies; for Cx26 resulted in embryonic lethality at day 11; for Cx31 resulted in transient placental dysmorphogenesis; for Cx43 resulted in abnormal cardiac development and subsequent embryonic death; for Cx46 resulted in cataract formation; and for Cx50 resulted in cataract formation and microphthalmia (Kelsell et al., 2001; Upham and Trosko, 2009).

3.2 CONNEXINS AND GJIC IN HUMAN DISEASES

Recent advances in life science research allowed to study connexins and gap junctions in human patients, experimental disease models and/or connexin knock-out/knock-in models, which greatly expanded our view of the role gap junctions play in physiological and pathological conditions. **Connexins and gap junctions** were clearly identified to have distinct connexin type-, cell type-, tissue-, and developmental stage-specific physiological functions, whose **direct or indirect disruption** by genetic causes, exposures to endogenous or exogenous chemicals or by physical factors, can be linked to **abnormal development or pathophysiological processes resulting in specific diseased outcomes or syndromes** (Delmar et al., 2017; Srinivas et al., 2018). In addition to the traditionally recognized cell coupling function of connexin channels, there is also an increasing amount of evidence on the (patho-)physiological importance of channel structures connecting the cells and their extracellular surroundings, including **connexin hemichannels and pannexins** (Crespo Yanguas et al., 2016; Jiang and Penuela, 2016; Maes et al., 2014).

3.2.1 NERVOUS SYSTEM DISEASES

The first human disease specifically linked to a mutation of a gap junction gene, Cx32, was the X-linked form of **Charcot-Marie-Tooth syndrome**, which is a **neuropathy** resulting from demyelination and axonal degeneration of peripheral nerves (Kleopa and Sargiannidou, 2015). In the central nervous system, connexins are expressed in neuronal, glial (astrocytes, oligodendrocytes), microglial as well as vascular cells and participate in dynamic interactions between different compartments of so-called neuro-glio-vascular unit (Leybaert et al., 2017). These interactions are required for normal brain development and function, such as synaptic transmissions and plasticity, glial signaling, vasomotor control, and blood-brain barrier permeability and integrity (Decrock et al., 2015; Gaete et al., 2014). (Dys)functions of connexin channels and hemichannels have been further implicated also in **brain ischemia-reperfusion injuries, traumatic brain and spinal cord injuries, epilepsy, brain and spinal cord tumors, migraine, inflammatory demyelinating diseases** (e.g. multiple sclerosis), **neurodegenerative diseases, Pelizaeus-Merzbacher-like disease, spastic paraplegia and maxillofacial dysplasia** (Cheung et al., 2014; Freitas-Andrade and Naus, 2016; Leybaert et al., 2017; Masaki, 2015; Moinfar et al., 2014; Moore and O'Brien, 2015; Schulz et al., 2015; Takeuchi and Suzumura, 2014; Xie et al., 2015; Yi et al., 2017).

3.2.2 EYE, EAR AND CUTANEOUS DISEASES

Connexin channels and hemichannels play a critical role in the eye development and function, where connexins are expressed in the lens epithelial cells (Cx43, Cx50) and lens fiber cells (Cx46, Cx50) to allow a flow of currents and transport of nutrients across the lens (Berthoud et al., 2014; Jiang, 2010). Mutations in Cx46 and Cx50 have been associated with **congenital cataracts and microphthalmia** (Jiang, 2010), and connexin hemichannel dysfunctions have been linked to **age- and disease-related cataracts** (Beyer and Berthoud, 2014). In the retina, Cx43 has been associated with retinal pigment epithelium losses and various retinal diseases, including **macular degeneration, glaucoma and diabetic retinopathy** (Danesh-Meyer et al., 2016; Roy et al., 2017).

Connexin mutations have been linked also to **hearing loss and hereditary deafness**. In cochlea, connexins are expressed in epithelial and connective tissue cells, but not in the sensory hair cells, and they are involved in many cochlea-specific functions. Primarily Cx26, but also Cx29, Cx30, Cx31 and Cx43 mutations are responsible nearly for half of **non-syndromic hearing losses** resulting from the impaired cochlear development or reduction of active cochlear amplification (Wingard and Zhao, 2015).

Other mutations of Cx26 or Cx30 have been linked also to **syndromic deafness**, where the hearing loss is accompanied by **cutaneous disorders**, such as **keratitis-ichthyosis-deafness syndrome**, **hystrix-like ichthyosis with deafness**, **palmoplantar keratoderma**, **Bart-Pumphrey syndrome** or **Vohwinkel syndrome** (Garcia et al., 2016; Lilly et al., 2016; Sanchez and Verselis, 2014; Xu and Nicholson, 2012). In addition, connexin gene mutations have been implicated in **oculodentodigital dysplasia**, and alterations of connexin functions can be found also in other **skin diseases**, including different types of **chronic wounds** (Cogliati et al., 2016; van Koppen and Hartmann, 2015).

3.2.3 CARDIOVASCULAR DISEASES

In the cardiovascular system, GJIC is critical for the passage of electric currents through myocardium, which is required for the propagation of the action potential across the heart and for normal cardiac rhythm (Leybaert et al., 2017). Connexin mutations have been associated with slowing impulse propagation and increased susceptibilities to **arrhythmias** (Leo-Macias et al., 2016; Michela et al., 2015; Seki et al., 2015). Electrical uncoupling of GJIC is involved in **fatal arrhythmias during myocardial infarctions** (Seki et al., 2015). Connexins and GJIC-dependent chemical coupling play a central role in the propagation of **cardiac ischemia/reperfusion injuries** (Schulz et al., 2015). Connexin remodeling has been linked to **ischemic heart diseases**, as well as to **hypertensive heart diseases**, **myocarditis**, and **myocardial fibrosis** (Cogliati et al., 2016; Michela et al., 2015; Seki et al., 2015). Changes in connexin expression, phosphorylation, distribution and altered cell-to-cell coupling have been implicated in the development of **atrial fibrillation**, which represents the most common arrhythmia (Tribulova et al., 2015).

In blood vessels, connexins are involved in the regulation of vascular tone and endothelial functions by forming gap junctional connections and/or hemichannels in the vascular smooth muscle cells, in the endothelial cells, and also so-called myoendothelial junctions between endothelial and adjacent smooth muscle cells (Ellinsworth et al., 2016; Morel, 2014). Connexins allow the passage of transverse and longitudinal signals in the vessel wall, and their alterations have been correlated with endothelial dysfunctions leading to the development of vascular diseases such as **hypertension**, **atherosclerosis**, or **restenosis** (Brisset et al., 2009; Leybaert et al., 2017; Morel, 2014; Pfenniger et al., 2013).

3.2.4 PULMONARY DISEASES

Connexins mediate communication in the different pulmonary cells, including epithelial cells (upper airway, bronchiolar and alveolar epithelium), pulmonary arterial endothelium, smooth muscle cells, alveolar macrophages, submucosal glands and lung fibroblasts. In the respiratory system, gap junctions are involved in the regulation of epithelial mucociliary clearance, including ciliary beating and mucus hydration in the upper airways, and surfactant secretion by Alveolar Type II cells (Freund-Michel et al., 2016). Connexins are also involved in regulation of mucosal defense and innate immunity responses (Bou Saab et al., 2014). Gap junctions contribute to the regulation of pulmonary blood circulation by controlling pulmonary arterial contractions and possibly also smooth muscle differentiation and hypoxic pulmonary vasoconstriction (Freund-Michel et al., 2016). Alterations of connexin expression and function in the respiratory system have been implicated in the development and persistence of different **inflammatory pulmonary diseases**, such as **asthma**, **pulmonary hypertension**, **acute lung inflammation**, **cystic fibrosis**, **idiopathic pulmonary fibrosis** (Cogliati et al., 2016; Dempsey et al., 2015; Freund-Michel et al., 2016; Willebrords et al., 2016).

3.2.5 DISEASES OF DIGESTIVE SYSTEM

In the gastrointestinal system, connexins and GJIC are required for proper gut development, maintenance of the epithelial barrier function, vascular stabilization, coordination of gastroduodenal and gut motility by coupling of smooth muscle cells and interstitial cells of Cajal, gastric acid secretion, gastric cytoprotection, intestinal nerve transmission, and also for immune responses, microbiota interactions and mucosal homeostasis (Bou Saab et al., 2014; Maes et al., 2015a, 2015b). Disruption of connexin functions have been associated with **gastroparesis, infantile hypertrophic pyloric stenosis, spontaneous neonatal gastric perforation, celiac disease, diverticular disease, Hirschsprung's disease, inflammatory bowel diseases such as Crohn's disease or ulcerative colitis, and colorectal cancer** (Diezmos et al., 2015; Maes et al., 2015a, 2015b; Sirnes et al., 2015).

Connexins are also expressed by different liver cells, including parenchymal hepatocytes as well as non-parenchymal stellate cells, Kupfer cells, cholangiocytes and sinusoidal endothelial cells. Connexins are required for proper liver development, maintenance of function and metabolic competence, and regeneration. Connexin and pannexin-dependent signaling is involved in **drug induced acute liver failure or hepatic ischemia-reperfusion injuries**, and have been implicated also in **chronic non-neoplastic liver diseases**, such as **cholestasis, liver fibrosis, cirrhosis and chronic hepatitis** (Cogliati et al., 2016; Crespo Yanguas et al., 2016; Maes et al., 2015a, 2015b; Vinken, 2012).

Connexins support distinct functions of exocrine and endocrine pancreatic secretory cells, and they are involved in the regulations of physiological secretion of pancreatic enzymes and hormones (Cigliola et al., 2015). Alterations of connexin-dependent signaling is associated with pancreatic diseases, most importantly including dysregulations of Cx36-mediated coupling in insulin-producing beta cells of the pancreatic islets, which leads to changes in insulin synthesis, secretion, beta cell survival, and **diabetes** (Bosco et al., 2011; Cigliola et al., 2013; Farnsworth and Benninger, 2014; Perez-Armendariz, 2013).

3.2.6 RENAL DISEASES

In the kidney, connexins and GJIC were implicated in the progression of **chronic kidney diseases** (Abed et al., 2015), such as diseases associated with renal **endothelial dysfunctions** (Abed et al., 2014), **diabetic nephropathy** (Hills et al., 2015), **renal endoplasmic reticulum stress, unfolded protein response and podocytopathy** (Sala et al., 2016), and dysregulations of renin-secreting cells leading to the **low renin hypertension** (Bosco et al., 2011; Kurtz, 2015; Wagner and Kurtz, 2013).

3.2.7 IMMUNE SYSTEM AND INFLAMMATORY DISEASES

Connexins and pannexins play important role also in immune cells, where they are involved in cell migration, phagocytosis, antigen presentation, terminal differentiation and maturation of T- and B-cells, T-cell reactivity and B-cell responses (Glass et al., 2015; Willebrords et al., 2016; Wong et al., 2017). Dysregulation of connexin-dependent signaling has been linked to a variety of **inflammatory diseases of cardiovascular system** (Hu et al., 2015; Leybaert et al., 2017; Morel, 2014; Pfenniger et al., 2013; Tribulova et al., 2015), **neural system** (Leybaert et al., 2017; Masaki, 2015; Sarrouilhe et al., 2017; Takeuchi and Suzumura, 2014), **lung** (Cogliati et al., 2016; Freund-Michel et al., 2016), **liver and intestine** (Cogliati et al., 2016; Diezmos et al., 2015; Maes et al., 2015a, 2015b; Willebrords et al., 2016) or **kidney** (Abed et al., 2014; Cogliati et al., 2016; Hills et al., 2015; Willebrords et al., 2016).

3.2.8 REPRODUCTIVE SYSTEM DISEASES

GJIC plays a critical role in the male reproductive system and in fertility. Connexin-dependent signaling is required for proper proliferation levels, differentiation and function of somatic testicular Sertoli and Leydig cells in the testis as well as for the epithelial cells in the epididymis (Kidder and Cyr, 2016). Alterations of connexin expression have been associated with **impaired spermatogenesis, increase of germ cell apoptosis and anarchic proliferation, loss**

of blood-testis barrier integrity, hyperplasia of androgen producing Leydig cells, and decreased sperm motility (Chevallier et al., 2013a; Cyr, 2011; Kidder and Cyr, 2016).

Gap junction proteins are present also in all organs of the female reproductive tract. Connexins are expressed in granulosa cells, cumulus cells, oocytes, uterine epithelial and stromal cells, as well as in myometrial cells. Disruption of GJIC has been implicated in **impaired folliculogenesis, oocyte deficiency, embryo implantation, placentation, vascular changes associated with pregnancy and synchronization of uterine contractions of parturition** (Christman, 2015; Winterhager and Kidder, 2015).

3.2.9 CANCER

Cancer was one of the first pathologies associated with gap junction channel impairment. GJIC-dependent integration of various extra-, intra- and inter- cellular signals across the cells within a tissue is a key component of the systems control of cellular events that allows for the coordination of cell metabolism, gene expression and cell behavior between contiguous syncytium of cells organized into a hierarchal multicellular system. This mechanism is critical for maintenance of tissue homeostasis via balanced cell proliferation, differentiation and apoptosis within a tissue (Trosko, 2011). **All cancers can be generally viewed as disorders of tissue homeostasis**, when the cancer cells are characterized by dysregulation of growth (loss of contact inhibition, self-sufficiency in growth signals, insensitivity to growth-inhibitory signals), evasion of apoptosis, and inability to terminally differentiate in combination with acquisition of phenotypic traits allowing to invade and metastase in the other parts of the body (Leone et al., 2012; Trosko, 2017). Thus, **the lack of GJIC or its disruption is a necessary prerequisite for the cell to escape normal homeostatic regulations, and to express or manifest the traits characteristic for the malignant cancer cells, or so-called ‘hallmarks of cancer’** (Trosko, 2017; Trosko et al., 2004). Inhibition of GJIC is critical especially for the rate-limiting tumor promoting phase of cancer characterized by expansion of the initiated cells, but also during cancer progression, when more traits of malignant cells are being acquired (Trosko, 2017; Trosko et al., 2004).

The role of GJIC in cancer has been extensively reviewed (Czyz et al., 2017; Jiang and Penuela, 2016; Leone et al., 2012; Trosko, 2017, 2011; Upham and Trosko, 2009; Wong et al., 2017) and its importance is supported by the following evidence: (a) exogenous and endogenous tumor promoters reversibly inhibit GJIC; (b) structure-activity relationship models showed a high concordance between inhibition of GJIC and the tumorigenicity of chemicals; (c) oncogenes inhibit GJIC; (d) tumor suppressor genes up-regulate GJIC; (e) anti-tumor promoters up-regulate GJIC; (f) restoration of GJIC in tumorigenic cells via transfection with gap junction genes results in normal growth and morphology of cells; (g) antisense gap junction genes transfected into cancer cells augment foci formation; (h) Cx32 knockout mice exhibited a 25 times higher rate of spontaneous tumors; and (i) the formation of heterotypic gap junctions between metastatic cells and cells of the target tissue leads to preferential metastasis.

Many studies demonstrated that tumor tissues and cancer cell lines have reduced levels of GJIC (Czyz et al., 2017; Jiang and Penuela, 2016; Mesnil et al., 2005), which is typically caused by aberrant expression, localization or posttranslational modifications of connexins, and by downregulations of their activity and functions via altered signaling pathways and regulatory mechanisms. Increased connexin expression and consequently GJIC levels were reported to suppress cancer growth primarily by restricting cell cycle progression and proliferation, and also increasing sensitivity of tumor cells to pro-apoptotic signals (Czyz et al., 2017; Jiang and Penuela, 2016). However, connexin expression has been positively correlated with more invasive cancers and metastasis due to modulations in cell adhesion and migration, which indicates a more complex role of connexins during different stages of cancer (Czyz et al., 2017; Naus and Laird, 2010). Connexin genes are, therefore, considered as conditional tumor suppressors (Naus and Laird, 2010).

4 IN VITRO ASSESSMENT OF GJIC IN TOXICOLOGY AND PHARMACOLOGY

As summarized in the [Chapter 2.2](#), GJIC is a process tightly controlled by changes in voltage, Ca^{2+} concentration, pH, redox balance, and also regulated by major intracellular signal transduction pathways and interactions with membrane and cytoskeleton proteins. Therefore, different types of cellular stress, modulations of different cellular events or different signal transduction pathways by **chemical exposures can result into altered GJIC**, which represents a critical biological phenomenon known to play a central role in coordinating multiple signal transduction events controlling gene expression, and whose alterations have been associated with **the onset or progress of different chronic diseases, pathologies and adverse outcomes** ([Chapter 3.2](#)). GJIC can be measured using various *in vitro*, *ex vivo* or *in vivo* techniques, which thus allow for a broad assessment of this toxicologically and pharmacologically relevant effect, as will be demonstrated in the following sections. Arguably, *in vitro* assessment of GJIC provides not only an excellent starting point to evaluate **hazardous or beneficial potential of chemicals**, but it can be also used for their further **mechanistic assessments**. Moreover, such effects on GJIC and their underlying mechanisms can be studied within a **specific biological context** of a desired cell type and tissue, normal or diseased condition, developmental stage, biological species, or level of complexity.

4.1 METHODS FOR GJIC ASSESSMENT

GJIC can be evaluated by a variety of assays, which can be principally divided into three different groups: assays based on the measurements of (a) electrical conductance (electrical coupling), (b) endogenous metabolite transfer (metabolic cooperation assays), or (c) dye transfer assay (Abbaci et al., 2008; Maes et al., 2015c; Vinken and Johnstone, 2016).

4.1.1 ELECTROPHYSIOLOGICAL MEASUREMENTS

Permeability of gap junction channels is proportional to the electrical conductance between the pair of adjacent cells. The original **dual voltage patch clamp technique** used two separate micro-electrodes introduced in each cell of a cell pair, one for current injection and another one for voltage control, to record gap junctional electrical conductance. This technique was later modified to a **double whole cell voltage clamp technique** using only one patch pipette per cell ([Figure 6A](#)), which provides a superior sensitivity, resolution capable to detect single channel conductance, and also very high time resolution. It also allows for real-time measurements of fast changes in the gap junction properties during application of a chemical or physical agent. Analysis of gap junctional electrical conductance, however, is a labor-intensive and expensive technique, which requires appropriate expertise, instrumentation and technical skills (Abbaci et al., 2008; Maes et al., 2015c).

4.1.2 ENDOGENOUS METABOLITE TRANSFER

The metabolic co-operation assays are based on the monitoring of cell-to-cell transfer of **endogenous and biologically relevant compounds**. This method was one of the first standardized bioassay for GJIC. In the original assay, wild-type Chinese hamster V79 cells (6-thioguanine-sensitive, donor) and 6-thioguanine-resistant cells (recipient) were co-cultured at high densities in which 6-thioguanine (6-TG) resistant cells do not metabolize 6-TG to a toxic metabolite, thus conferring resistance. Co-culture with the 6-TG sensitive cells results in the transfer of the toxic metabolite through gap junctions resulting in cell death, while inhibition of GJIC results in the rescue of 6-TG resistant cells by preventing the transfer of the toxic 6-TG metabolite from the 6-TG sensitive cells (Welsch and Stedman, 1983). Although an advantage of this assay is that it is minimally invasive, a major disadvantage is that it requires one week for completion, which makes extensive dose and time dependent assessments of toxicants as well as mechanistic studies impractical for assessing many chemicals (Upham et al., 2016a).

In a modified version of metabolic co-operation assay, the population of donor cells is incubated in the presence of an excess of a radiolabeled metabolic precursor (typically nucleotides or glucose), and then co-cultured with the recipient cells. The transfer of labeled metabolites after from loaded to unloaded cells during the co-culture is

evaluated by quantitative autoradiography. Discrimination between the donor and recipient cells can be assisted by the use another radioactive label or fluorescence labels, when the latter option can be also combined with fluorescence-activated cell sorting followed by analytical identification and quantification of the radioisotope-labeled metabolites in the recipient cells. This highly sensitive technique allows for a direct evaluation of the permeability of connexin channels to the endogenous molecules, however, it is relatively laborious, does not allow to evaluate rapid regulations in the channel permeability, its use might be complicated by the safety issues, and is not very quantitative or suitable for more general use (Abbaci et al., 2008).

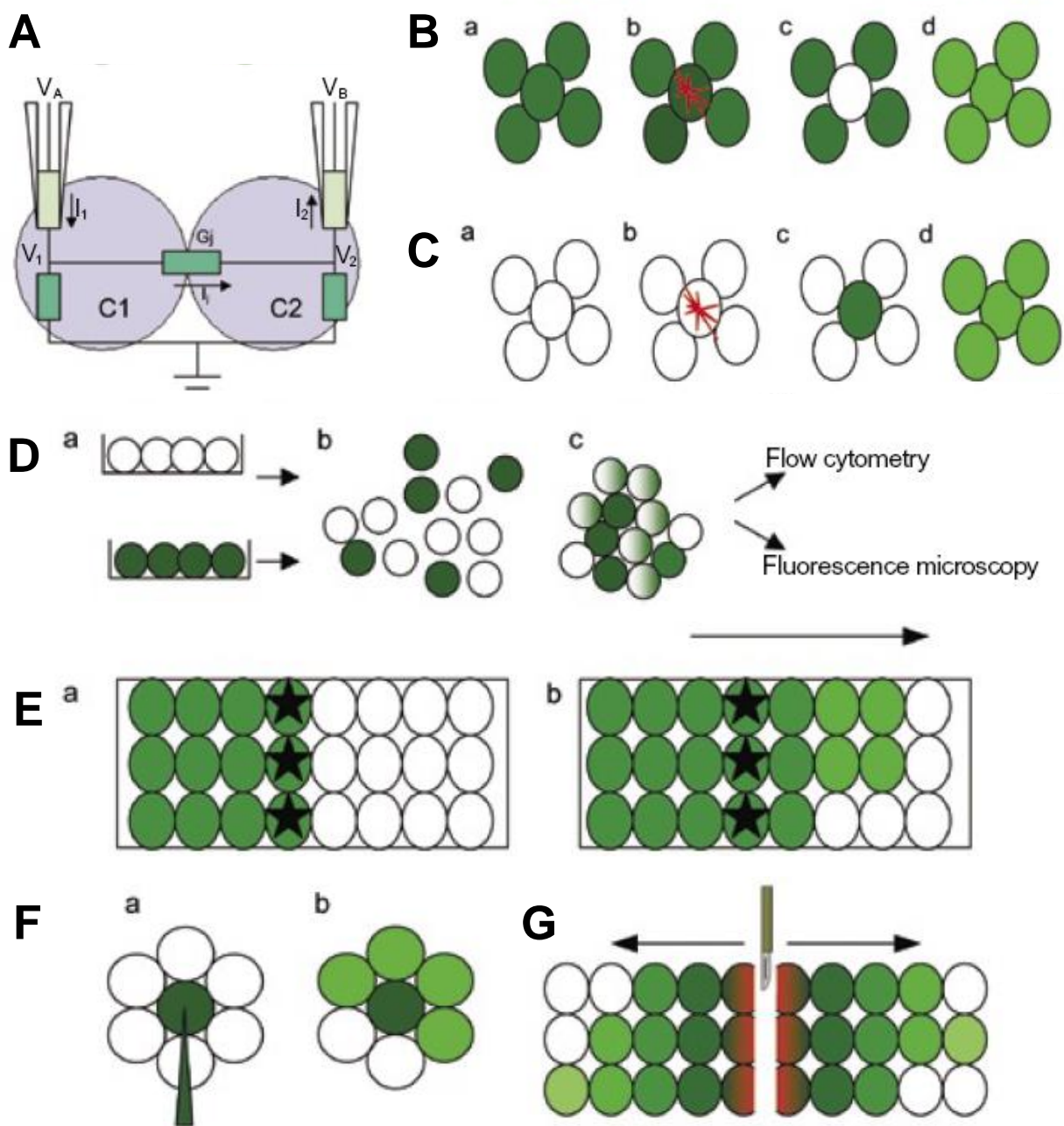


Figure 6: Methods for evaluation of GJIC. (A) Dual whole-cell patch clamp measurement; (B) Fluorescence recovery after photobleaching (FRAP); (C) Local activation of molecular fluorescent probe (LAMP); (D) Preloading assay; (E) Electroporation loading-dye transfer; (F) Microinjection assay; (G) Scrape/Scalpel loading-dye transfer. Adapted from (Abbaci et al. 2008).

Alternatively, the recipient cells can be genetically engineered cell lines expressing a luciferase gene reporter system for the detection of a selected endogenous metabolite or gap junction-permeable second messengers (e.g. IP₃). The donor cells are then stimulated to produce the endogenous metabolite, and its transfer through gap junction channels into the recipient cells can be monitored indirectly by luminescence measurements (Stains and Civitelli, 2016).

Another indirect method utilizing the transfer of endogenous metabolites is based on the tracking of **intracellular calcium waves**, whose propagation from cell-to-cell correlates with the presence of functional gap junctions. In this technique, cells are loaded with a calcium-sensitive fluorescent dye (e.g. Fura-2) and then stimulated electrically, mechanically or (photo)chemically to generate production of IP₃ triggering the actual calcium wave. The wave is tracked via monitoring of the calcium-sensor fluorescence by microscopy. The method allows for rapid kinetic measurements and can be applied also for complex *in vitro* models and perfused organs. However, it usually requires an equipment capable of fast switching between excitation filters (Abbaci et al., 2008; Maes et al., 2015c).

Intracellular calcium release can be selectively induced also in the genetically engineered donor cells, e.g. in the cells overexpressing adrenergic α 1-receptor or TrpV1 ion channel by coelenterazine. Propagation of the calcium wave into the recipient cells overexpressing calcium-sensitive bioluminescent protein aequorin can be quantified by luminescence measurements. This method was successfully optimized into a **HTS platform** (Haq et al., 2013). Another **high-throughput assay** for GJIC based on genetically engineered cell lines utilizes donor cells expressing membrane transporters for iodide ion and the acceptor cells expressing a sensor protein, whose fluorescence is quenched by iodide. When iodide is added to the co-culture of donor/acceptor cells, the iodide ions either pass from the donor cells through gap junctions into the acceptor cells and quench the fluorescence, or remain in the donor cells, if gap junction channels are absent or closed, so the fluorescence is not affected. The fluorescence is evaluated by the means of **High Content image Screening / High Content Analysis (HCS/HCA)** (Lee et al., 2015).

4.1.3 DYE TRANSFER ASSAYS

Dye transfer assays are probably most frequently used for GJIC evaluation. These assays are principally based on the introduction of a non-toxic fluorescent dye, or its precursor, into the living cells, which is followed by monitoring of gap junction-dependent cell-to-cell transfer of the fluorophore.

In **fluorescence recovery after photobleaching (FRAP) assay**, the cells are loaded with a lipophilic plasma membrane-permeable dye precursor, such as calcein acetoxymethyl ester. Upon cellular uptake, the precursor is hydrolyzed by cytoplasmic esterases into the fluorescent, membrane-impermeable but gap junction-permeable calcein. Calcein-fluorescence in a single cell is then irreversibly photobleached using a high-energy laser beam and a subsequent transfer of the fluorescent dye from neighboring cells into the photobleached cell is monitored (**Figure 6B**). FRAP can be applied to monolayer culture systems as well as to 3D *in vitro* models, such as spheroids or organotypic slices. The method is non-invasive, well-suited for time-lapse/kinetic measurements and determination of gap junction permeability coefficients. It also allows for the study of the individual cells within a population. In standardized protocols, the technique usually requires a sophisticated equipment such as confocal laser scanning microscope, and its use can be complicated by possible photodamage induced in the photobleached cells (Abbaci et al., 2008).

Alternative dye transfer technique is called **local activation of fluorescent molecular probe (LAMP)**, which uses a membrane-permeable non-fluorescent coumarin-based dye for the cell loading. Using a fluorescence microscope, the dye is photoactivated in the selected cell(s) by UV excitation light, with a subsequent monitoring of the cell-to-cell dye transfer (**Figure 6C**). The technique is non-invasive, suitable for kinetic and permeability measurements, allowing to study individual cells or cell pairs, and applicable for the 3D cultures or freshly dissected tissues (Yang and Li, 2009).

In **preloading and parachute assays**, a population of the donor cells is preloaded with a membrane-permeable dye, such as calcein acetoxymethyl ester. In the **preloading assay**, the preloaded cells are mixed with the unloaded

cells to form a monolayer together. In the **parachute assay**, the preloaded cells are seeded onto a monolayer of the unloaded cells. The transfer of the fluorescent gap junction-permeable calcein from the loaded to unloaded cells can be quantified by epifluorescence microscopy, or after cell harvesting by flow-cytometry (**Figure 6D**). The donor and recipient cells can be distinguished by using fluorophores for permanent cell labeling and tracking, such as Di-I. The method is non-invasive, suitable for studies of circulating cells, and measurements of GJIC function in large populations of cells. Both preloading as well as parachute assay have been adopted for **high-throughput setup** including the use of HCA for image acquisition and analysis (Dukic et al., 2017; Li et al., 2003; Roemer et al., 2013). Microfluidic-based techniques can be also utilized to selective pre-load calcein acetoxymethyl ester into a defined region of adherent cells and then monitor calcein transfer into the area of unloaded cells and are also **compatible with HTS** (Chen and Lee, 2010).

Electroporation loading-dye transfer assays utilize electroporation to introduce fluorescent dye into a selected population of the cells. The cells can be grown on special slides, where the half of the slide is coated with an electrically conductive and optically transparent surface (Ennaji et al., 1995). A membrane-impermeable fluorescent dye, such as Lucifer Yellow, is added to the culture medium, and an electric pulse is applied. It leads to formation of transient pores in the plasma membrane and dye penetration into the cells grown on the conductive part of the slide. Migration of the dye through gap junction channels from the permeabilized (loaded) cells to non-permeabilized (unloaded) ones is monitored by fluorescence microscopy (**Figure 6E**). Alternatively, electroporation loading can be also done by a pair of microelectrodes, which are positioned using a micromanipulator above the monolayer cell culture and can electroporate a defined area of the cell (De Vuyst et al., 2008).

Membrane-impermeable dyes, such as fluorescein or Lucifer Yellow, can be also introduced into the selected cells by **intracellular microinjection** using a micropipette and micromanipulator (**Figure 6F**). This technique allows to select and study dye transfer from the individual targeted cells, but it is relatively laborious and time-consuming in the traditional setup. However, it has been recently automated into a **high-throughput format** utilizing robotic

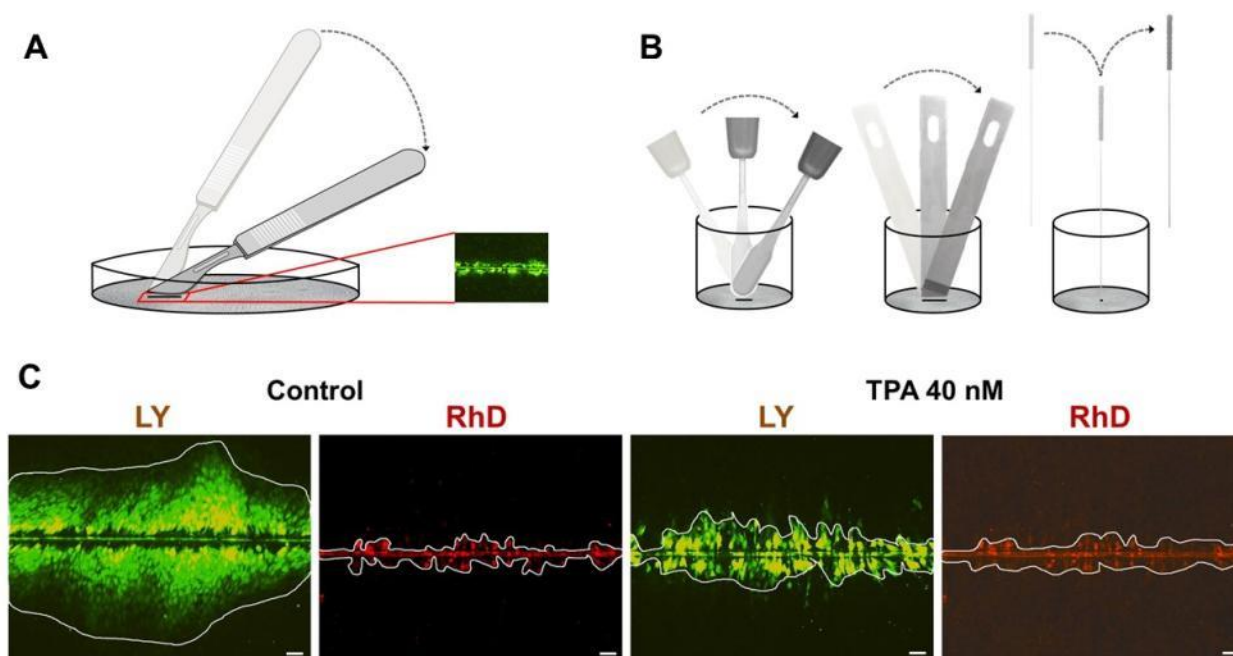


Figure 7: Scalpel loading procedure (SL-DT). (A) Scalpel loading technique done by surgical scalpel with a curved blade in 35 mm dishes, and (B) different types of blades suitable for SL-DT assay in microplate wells, including a curved blade, a flat blade, and an acupuncture needle. (C) Images obtained by SL-DT assay, applying Lucifer Yellow (LY), which transfers through functional gap junction channels, and rhodamine-dextran (RhD), which is retained in the loaded cells. The GJIC function is evaluated by analyzing net transfer of LY (the area at which LY diffuses), excluding RhD-stained regions. Representative images showing GJIC after the 1 h exposure of mouse Sertoli TM4 cells to the model tumor promoter, TPA (12-O-tetradecanoylphorbol-13-acetate), at the concentration of 40 nM was reduced to FOC (the fraction of the control) = 0.13 when compared with the solvent control (Control). Scale bar = 50 μ m. Adapted from (Babica et al., 2016b) [Attachment I].

microinjection (Liu et al., 2014). As an alternative to fluorescent dyes, endogenous molecules such as serotonin or neurobiotin can be microinjected, and their cell-to-cell transfer can be then detected by immunocytochemistry (Hou et al., 2013). These microinjection-based techniques are suitable not only for monolayer cultures, but also for 3D cultures, explantates or *in vivo* experiments.

Another commonly used technique for *in vitro* assessment of GJIC is so-called **scrape loading-dye transfer assay (SL-DT)** (Figure 6G). This technique has been used as **the principal assay for GJIC evaluation in the research papers reported in this thesis [Attachment I-XV]**, and thus will be described in more detail in the following section.

4.1.3.1 SCRAPE/SCALPEL LOADING-DYE TRANSFER ASSAY

The original **SL-DT** was reported by (El Fouly et al., 1987). This technique uses a membrane-impermeable and gap junction-permeable fluorescent dye, typically Lucifer Yellow, which is introduced into adherent cells grown in a Petri dish by scraping with a rubber policeman or wooden probe (El Fouly et al., 1987). This technique has been slightly modified during the recent years, when the relatively invasive scraping step was replaced by a clean-cutting with a sharp blade, such as surgical scalpel blade. This later version was dubbed as **“scalpel loading-dye transfer”** technique, and the modified protocol has been reported in recent publications (Babica et al., 2016b; Upham et al., 2016a) [Attachment I-II].

The SL-DT utilizes dilithium salt of Lucifer Yellow hydrazine (457 Da, negatively charged), which is dissolved in a phosphate buffered solution and added to the rinsed monolayer of the experimental cells. Lucifer Yellow is introduced to the cells by cutting the monolayer by a gentle roll with a scalpel blade or a microblade, or by a pricking of the cell monolayer by a thin needle (Figure 7A-B). This method allows to successfully load the fluorescent dye into the cells, presumably as a result of mechanical perturbation of the membrane, in a reproducible manner which minimizes the area of loaded cells and is not leading to an extensive cell damage or detachment. It becomes incorporated by the cells along the cut. As normal membrane permeability is re-established, the Lucifer Yellow becomes trapped within the cytoplasm and move from the dye-loaded cells into adjacent ones connected by functional gap junction channels. The amount of dye transferred from one cell to its neighbor that it is in contact with, is dependent on the number of coupling gap junctions and the gating properties of individual channels. To determine which cells are initially loaded after the scrape, other fluorescent dyes (e.g. rhodamine-dextran, MW 10,000, or dialkylcarbocyanine) that are too large to traverse the gap junction channel are concurrently used with the diffusional dye to serve as an additional control (Figure 7C). After a defined incubation period (usually 3-10 min), the cells are rinsed, fixated with phosphate-buffered formaldehyde, and the extent of dye transfer is documented microscopically. The extent of GJIC is typically quantified using image analysis to determine a control-normalized area of communicating (i.e. Lucifer Yellow labeled) cells (Babica et al., 2016b; Upham et al., 2016a) [Attachment I-II].

SL-DT is an invasive assay which allows to investigate GJIC levels simultaneously in large populations of the cells, but it is not conducive in studying GJIC in small cell populations, particularly between cell pairs, in cultures with low cell densities, in cases when the extent of junctional coupling is small, or when the specific cells within the culture need to be examined individually. In addition, the GJIC status of cell types of irregular shape are not easily quantified using this assay. Although this approach is not well suited for 3D systems, its modification called **incision loading-dye transfer (IL-DT)** (Upham et al., 2016a) [Attachment II] can be used for GJIC assessment in freshly dissected tissues, also in combination with *in vivo* or *ex vivo* exposures to the tested chemicals (see Chapter 4.4). The major advantages of the SL-DT assay are its simplicity and minimum requirements for the special equipment or skills, especially in contrast to the other methods such as whole cell patch clamp, microinjection, electroporation. This method is versatile and can be used virtually for any adherent primary cells or permanent cell lines capable to grow to confluent or nearly confluent cell densities, with several examples shown in the Figure 8.

As indicated above, there is a variety of tools which can be used for the dye loading in SL-DT assay, some of them compatible with a microplate format. In our laboratory, we have recently **adapted SL-DT assay for the standard 24-, 48- or 96-well cell culture microplates** (Babica et al., 2016b) [Attachment I]. This modified microplate version of SL-DT assay allowed to **increase the throughput of the assay by using fully-motorized automated microscopes**

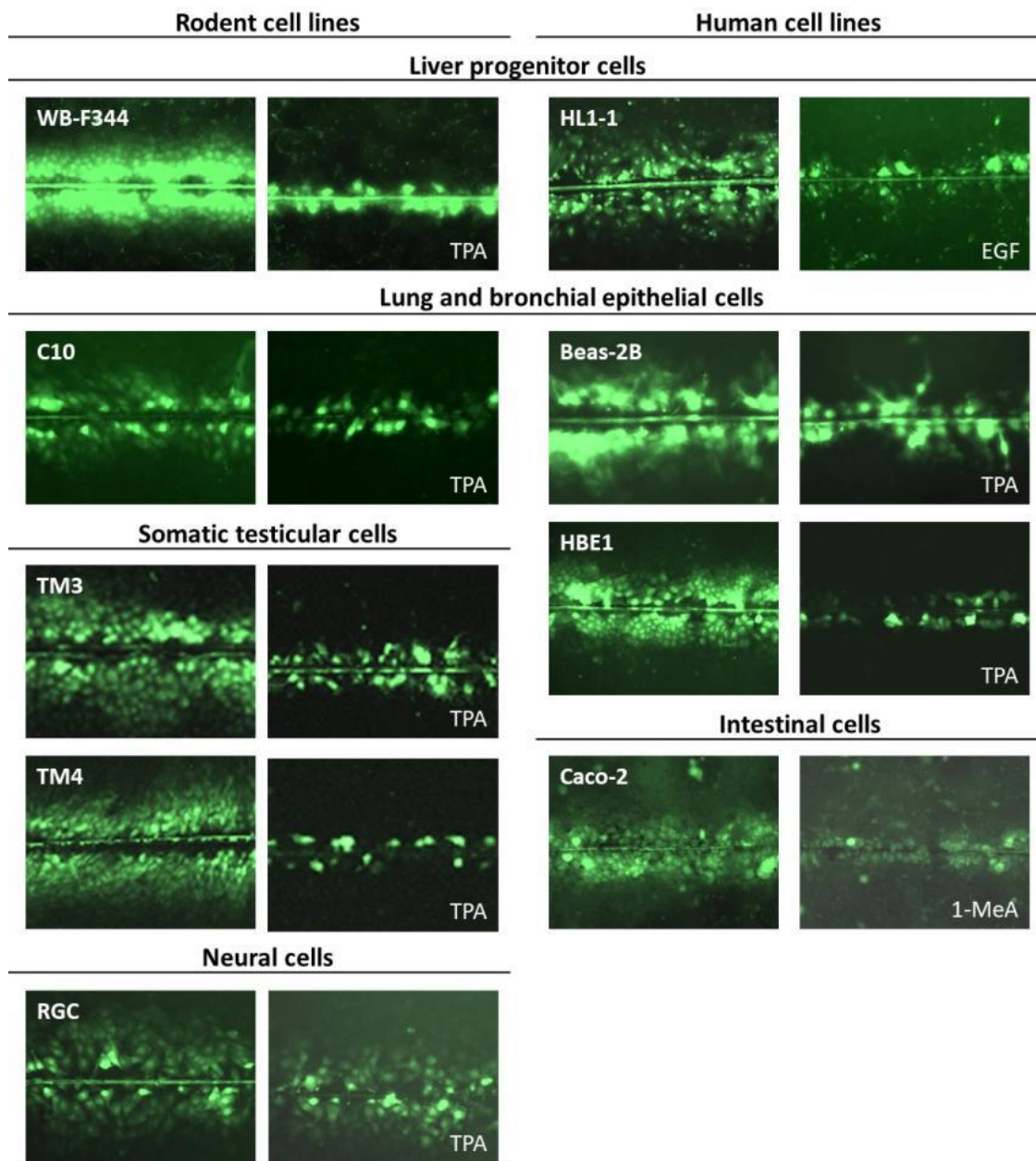


Figure 8: Evaluation of GJIC by SL-DT assay in different rodent and human permanent cell lines. WB-F344 - rat liver epithelial (oval) cells; C10 - mouse lung epithelial cells; TM3 - mouse Leydig cells; TM4 - mouse Sertoli cells; RGC - rat glial cells; HL1-1 - adult human liver stem cells; Beas-2B, HBE1 - human bronchial epithelial cells; Caco-2 - human epithelial colorectal adenocarcinoma. Microphotographs show the communication in the non-treated cells (left) or the cells treated with chemicals inhibiting GJIC (right). 1-MeA - 1-methylanthracene, EGF – epidermal growth factor, TPA - 12-O-tetradecanoylphorbol-13-acetate. Prepared by P. Babica from his experimental results.

or HCA readers for image acquisition. We are currently developing scripts for analysis of these images using an open source platform Fiji/ImageJ, which will **automate also the image analysis for quantification of GJIC**, as well as other cellular parameters possibly evaluated by this assay. We are currently incorporating fluorophores allowing for detection of dead cells (e.g. propidium iodide) into the SL-DT protocol along with simultaneous nuclear staining to easily determine also the total number of the cells within the image (Čtveráčková et al., 2017; Yawer et al., 2017). This modified SL-DT assay provides a very **simple, cost-effective and (semi-) high-throughput assay for the simultaneous evaluation and quantification of cell-to-cell communication, cell viability and cell density/proliferation within one test (Figure 9)**. Moreover, this assay is opened for further development, including

HCA evaluation of other cellular endpoints, such as discrimination between apoptosis-necrosis or cell cycle assessment, which can be derived from the dead cell staining and/or the pattern of nuclei staining (Elstein and Zucker, 1994; Ribble et al., 2005; Roukos et al., 2015).

Thus, *in vitro* assessment of GJIC using a SL-DT method and eventually its modified microplate version are adaptable for the needs of HTS, and might represent a perspective technique, which could be utilized for multiparametric *in vitro* screening and simultaneous assessment of chemical effects on intercellular communication, cell proliferation, apoptosis and cytotoxicity.

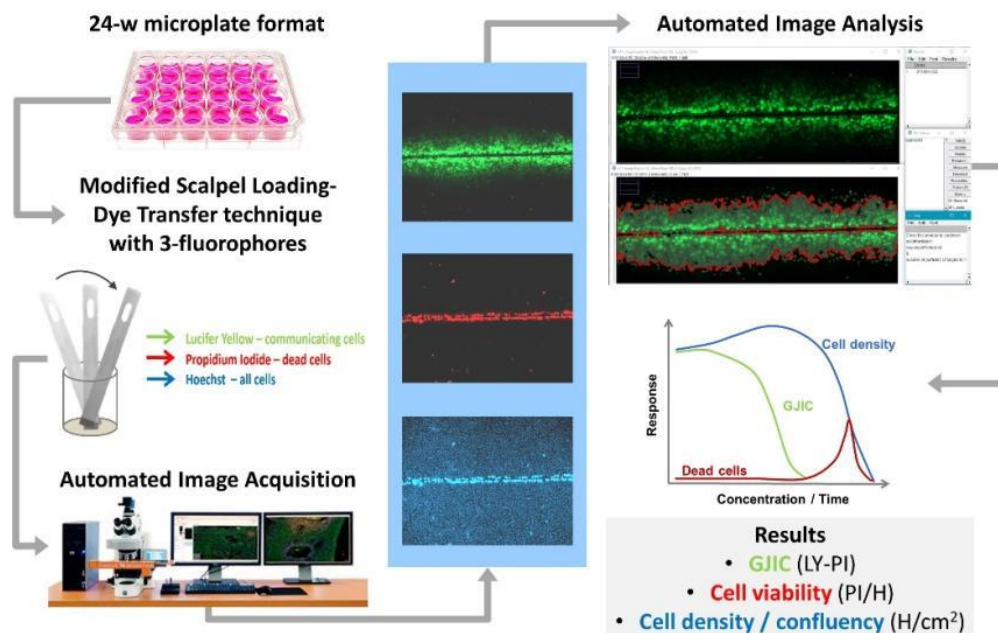


Figure 9: Schematic representation of (semi-) high-throughput *in vitro* multiparametric assay, which is currently being optimized for the simultaneous evaluation of GJIC, cytotoxicity and cell density / growth. LY – Lucifer yellow, PI – propidium iodide, H – Hoechst 33342. Adapted from conference proceedings co-authored by P. Babica (Čtveráčková et al., 2017; Yawer et al., 2017), paper in preparation.

4.2 GJIC FOR IDENTIFICATION AND CHARACTERIZATION OF NEW CHEMICAL HAZARDS

4.2.1 INHIBITION OF GJIC AS A COMMON BUT STRUCTURE-DEPENDENT RESPONSE TO TOXICANTS

Among the very first chemicals identified as modulators of GJIC were not only well-recognized tumor promoters, such as 12-O-tetradecanoylphorbol-13-acetate (TPA) (Murray and Fitzgerald, 1979; Yotti and Trosko, 1979), but also organochlorine pesticides DDT, lindane and chlordane, aldrin, dieldrin, endrin, heptachlor and methoxychlor (Kurata et al., 1982; Tsushimoto et al., 1983), or cigarette smoke (Hartman and Rosen, 1983). Since then, many prominent environmental and food toxicants, pharmaceutical agents or biotoxins were identified as potent inhibitors of GJIC: including **polycyclic aromatic hydrocarbons (PAHs)**, **polychlorinated dibenzodioxins (PCDDs)**, **polychlorinated biphenyls (PCBs)**, **organochlorine pesticides** (pentachlorophenol, hexachlorobenzene, toxaphene, alachlor), **organophosphate pesticides** (e.g. malathion, parathion), **organic solvents** (e.g. ethanol), **fluorinated fatty acids**, **phthalates**, **peroxides**, **biotoxins** (e.g. phorbol esters, lipopolysaccharides - LPS, ochratoxins, patulin, gossypol), **drugs** (clofibrate, phenobarbital, methapyrilene), or **metals** (Vinken et al., 2009).

The observed effects on GJIC were repeatedly demonstrated to be **structure-specific** (Figure 10). This phenomenon was well reported for **PAHs**, where the inhibitory effects were observed for low molecular weight

PAHs with 3-4 benzene rings possessing a “bay” or “bay-like” region (Blaha et al., 2002; Rummel et al., 1999; Upham et al., 1998b; Weis et al., 1998). Thus, low molecular weight PAHs, such as methylated anthracenes or fluoranthene, which are known to be the predominant PAHs in the cigarette smoke, are the most potent inhibitors of GJIC, while the less abundant but frequently studied genotoxic and AhR-activating higher molecular weights PAHs have only weak effects on GJIC (Blaha et al., 2002; Rummel et al., 1999; Upham et al., 1998b; Weis et al., 1998). Among **PCBs**, the strong inhibition of GJIC is elicited by non-coplanar PCBs, such as PCB153, while AhR-activating coplanar congeners like PCB126 do not inhibit GJIC (Machala et al., 2003). Diametrically different effects were reported also for **fluorinated fatty acids** with different carbon chain lengths (Hu et al., 2002; Upham et al., 1998a), **phthalates** with different types and lengths of ester side-chains (Klimova, 2015), **organic peroxides** with aliphatic or aromatic functional groups (Upham et al., 2007), different types of **bile acids** (Noda et al., 1981; Umeda et al., 1980), or various **hexachlorocyclohexane isomers** (Kurata et al., 1982). It indicates that **the effects of chemicals on GJIC depend on specific structure-dependent interactions with molecular and cellular targets, and do not seem to be a consequence of general cell or membrane perturbations, cell stress or cytotoxicity.**

4.2.2 IDENTIFICATION OF NEW CHEMICAL HAZARDS AND TOXICITY MECHANISMS BY GJIC ASSESSMENT

The examples of PAHs, PCBs, phthalates or organic peroxides also illustrate, that the effects on GJIC do not often correlate with the structure-dependent effects on the well-recognized toxicity mechanisms, such as induction of DNA damage, oxidative stress or activation of nuclear receptors such as AhR or PPARs. Thus, ***in vitro* evaluation of GJIC might help to identify completely new hazardous properties of chemical compounds**, which might not be revealed by *in vitro* assays targeting specific signaling pathways or toxicity mechanisms.

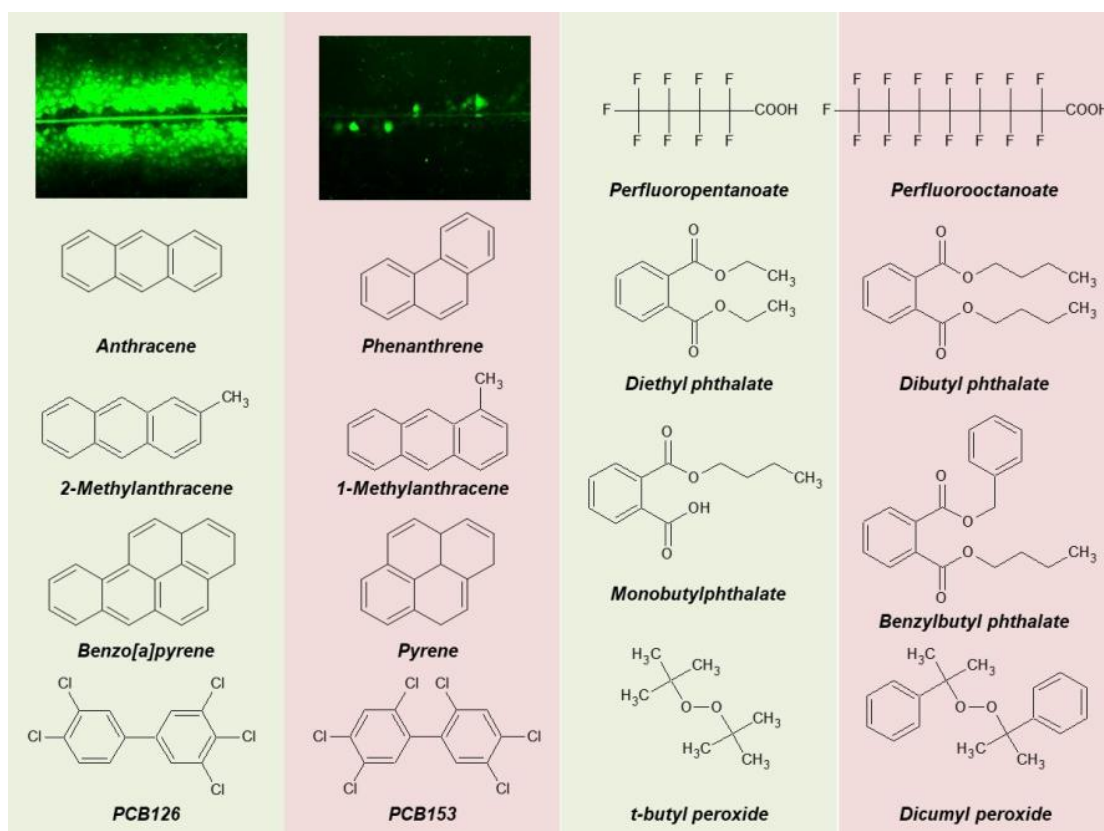


Figure 10: Structure-dependent effects on GJIC. Chemicals with the green background did not inhibit GJIC in rat liver epithelial cell line WB-F344, while the chemicals with red background were identified as potent inhibitors of GJIC. Prepared according to (Upham et al. 1998, 2007; Blaha et al. 2002; Machala et al. 2003; Klimova 2015).

In fact, *in vitro* inhibition of GJIC induced by these compounds is often elicited after relatively short exposure periods (<60 min), which suggests that altered mechanisms of GJIC control involve, at least initially, **rapid changes in the signal transduction pathways** regulating the connexin channel gating or intracellular trafficking, rather than alterations of gene expression mediated for example by transactivation of nuclear receptors such as AhR or PPARs. Several intracellular signaling pathways responsible for the regulation of gap junction channel gating have been found to be targeted by GJIC-inhibiting toxicants. Activation of MEK (MAPK kinase), either by activators of receptor tyrosine kinases-Raf-pathway like **epidermal growth factor (EGF)**, or by PKC activators like **TPA**, resulting in the **activation of MAPK ERK1/2 and phosphorylation of consensus sequences of Cx43 by PKC and ERK1/2** (see **Figure 3**), is probably one of the best understood mechanisms of GJIC dysregulation (Rivedal and Opsahl, 2001; Ruch et al., 2001; Sirnes et al., 2009; Warn-Cramer et al., 1998). Also other inhibitors of GJIC were reported to activate MAPK/ERK pathway, such as **arachidonic acid** (Rao et al., 1994), **lower molecular weight PAHs** (Blaha et al., 2002; Weis et al., 1998), **pentachlorophenol** (Corcelle et al., 2007), **lindane** (Mograbai et al., 2003), **DDT** (Han et al., 2008), **PCB153** (Machala et al., 2003), or **benzoylperoxide** and **dicumylperoxide** (Upham et al., 2007). Other known inhibitors were reported to activate PKC, such as **diacylglycerol kinase inhibitor R59022** (Matowe and Ginsberg, 1996), **18 β -glycyrrhetic acid** (Huang et al., 2003; Liang et al., 2008), or **alachlor** (Bagchi et al., 1997). However, experimental results indicated that the activation of MAPK ERK1/2 alone is not sufficient to inhibit GJIC (Hossain et al., 1999). Moreover, rapid inhibition of GJIC induced by MAPK ERK1/2 activating toxicants, such as **PCB153** (Machala et al., 2003) or **dicumylperoxide** (Upham et al., 2007) was found to be independent of MAPK ERK1/2 activation but **dependent on the activity of phosphatidylcholine-specific phospholipase C (PC-PLC)**. This indicates that *in vitro* assessment of GJIC can help to **identify new molecular and biochemical processes, which are targeted by toxic chemicals**.

Therefore, we focused on further characterization of rapid molecular and signaling responses to **1-methylanthracene**, which represents environmentally relevant PAH, known to be abundant also in the cigarette smoke (Upham et al., 2008a) [**Attachment III**]. 1-methylanthracene, but not 2-methylanthracene was found to rapidly (<10 min) dysregulates GJIC in rat liver epithelial cells WB-F344 (**Figure 11A**). WB-F344 represent a model epithelial cell line expressing Cx43, which is the major connexin protein responsible for the maintenance of GJIC and tissue homeostasis in many different cell types, tissues and organs. Moreover, these cells possess characteristics of liver bipotent progenitor or 'oval' cells, which have been implicated in liver tumor promotion and carcinogenesis (Vondracek and Machala, 2016). While having normal diploid karyotype and non-tumorigenic phenotype, WB-F344 cells can undergo neoplastic transformation as a result of mutagenization, chemical exposures or oncogene activation, which was found to be accompanied with dysregulation of GJIC, aberrant connexin phosphorylation, localization and/or expression (DeoCampo et al., 2000; Hayashi et al., 1998; Ogawa et al., 2005; Oh et al., 1993). Forced re-expression of connexin and/or restoration of GJIC in transformed cells decrease their tumorigenicity and reverse the phenotype of normal cells (Rae et al., 1998; Ruch et al., 1993). Thus, WB-F344 cells represent a relevant *in vitro* model for studies of liver tumor promotion and disruption of progenitor cell-dependent tissue homeostasis.

The **GJIC-inhibiting effects of 1-methylanthracene** induced in WB-F344 cells were accompanied also by activation of **MAPKs ERK1/2 and p38** (**Figure 11B**). However, inhibition of GJIC was not associated with altered phosphorylation of Cx43, and connexin-internalization occurred only in the later phases of exposure, which indicated that other than ERK1/2-dependent mechanism were involved in GJIC dysregulation. GJIC inhibition was found to be associated with activation of **phospholipase A₂ (PLA₂)** and also **PC-PLC** (**Figure 11C-D**). Finally, experiments with a series of pharmacological inhibitors of different signal transduction pathways revealed that 1-methylanthracene-induced **inhibition of GJIC was dependent on PC-PLC activation** and also **facilitated by PKA** (**Figure 11E-F**), while activation of MAPKs and PLA₂ occurred independently of PC-PLC (**Figure 11G-H**).

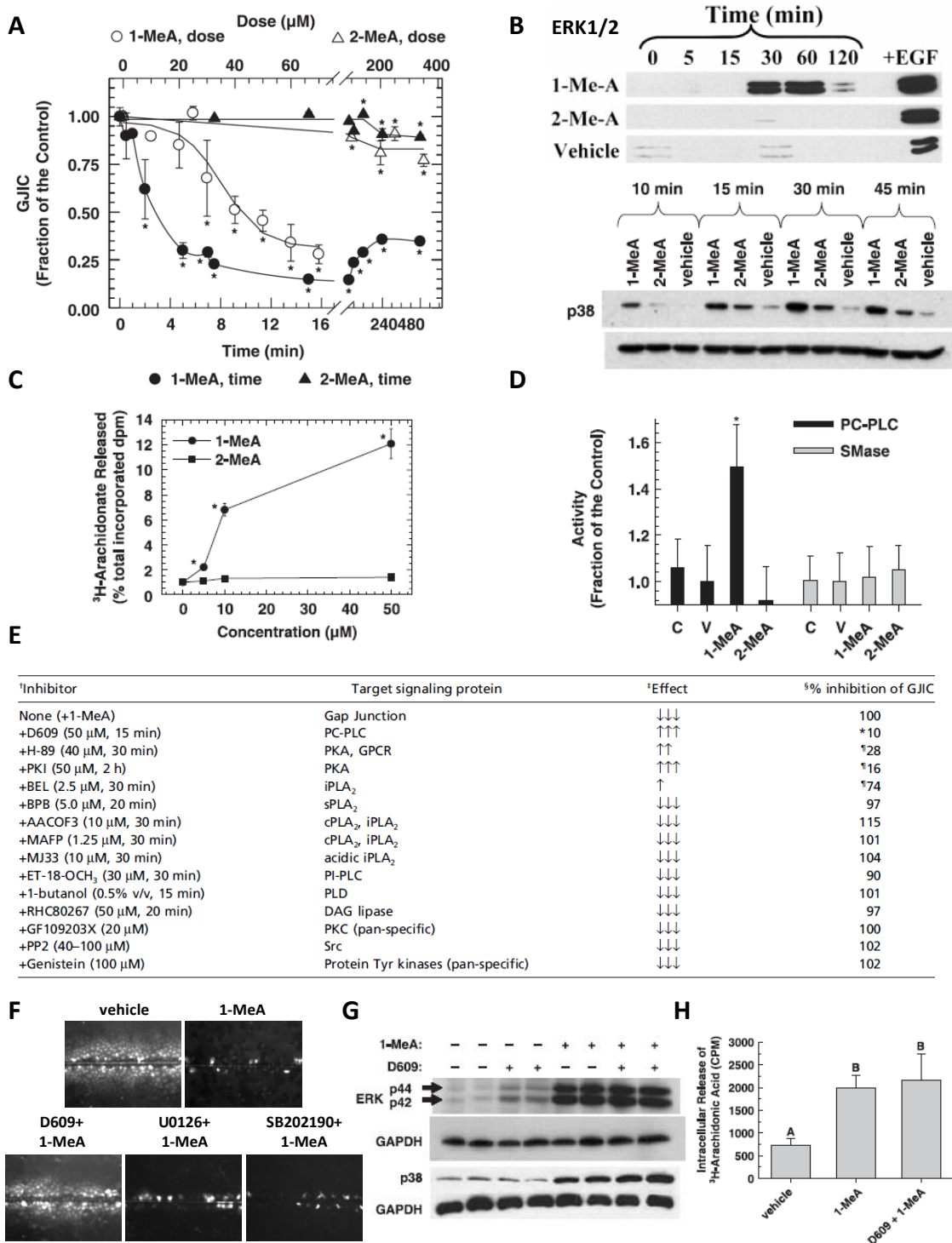


Figure 11: Effects of methylated anthracenes on intercellular and intracellular signaling in rat liver epithelial cells WB-F344. 1-methylanthracene (1-MeA), but not 2-methylanthracene (2-MeA) (A) inhibited GJIC (15 min exposure or 75 µM concentration), (B) activated MAPK ERK1/2 and p38 (75 µM), (C) phospholipase A₂ (PLA₂; measured as a release of arachidonic acid, 15 min exposure); (D) phosphatidylcholine-specific phospholipase C (PC-PLC; 100 µM for 15 min). (E) Inhibition of GJIC by 1-MeA (75 µM, 10 min) was prevented by D609, an inhibitor of PC-PLC, but (F) not by inhibitors of MEK-ERK1/2 and p38 pathways, U0126 and SB202190; (G-H) D609 did not prevent 1-MeA-dependent activation of ERK1/2, p38 (75 µM, 30 min) or PLA₂ (75 µM, 15 min). GJIC was evaluated by SL-DT assay, MAPK activity by Western blotting, release of tritiated arachidonic acid by liquid scintillation counter, PC-PLC activity by Amplex Red PC-PLC assay. Adapted from (Upham et al., 2008a) [Attachment III] and (Rummel et al., 1999).

To complement these **hypothesis-driven mechanistic experiments**, which investigated alterations of individual signal transduction pathways, we also utilized an **exploratory proteomic approach** to identify rapid signaling events occurring specifically in response to 1-methylanthracene. These experiments were designed with respect to the chemically-induced inhibition of GJIC viewed as the critical cellular event of interest, thus (a) the concentrations effectively inhibiting GJIC were used (b) in combination with exposure times associated with the onset of GJIC inhibition (5 min), and (c) 2-methylanthracene was used as the primary negative control to take into the account any effects resulting from general cell perturbations not specifically linked to structure-dependent activity of 1-methylanthracene. Relative changes in the membrane proteome were quantified using **Stable Isotope Labeling with Amino Acid in Cell Culture (SILAC)** technique, where the experimental 1-methylanthracene-treated were labeled by a heavy ^{13}C -Lys isotope (H), while unlabeled (L, ^{12}C -Lys) 2-methylanthracene-treated cells were used as a control (Upham et al., 2011, 2008b). The exposed H and L cells were pooled, membrane and cytosolic protein fractions were separated, the samples trypsin-digested and peptides analyzed and identified by tandem mass spectrometry and *de novo* peptide sequencing. For 192 out of 516 successfully identified proteins, both H

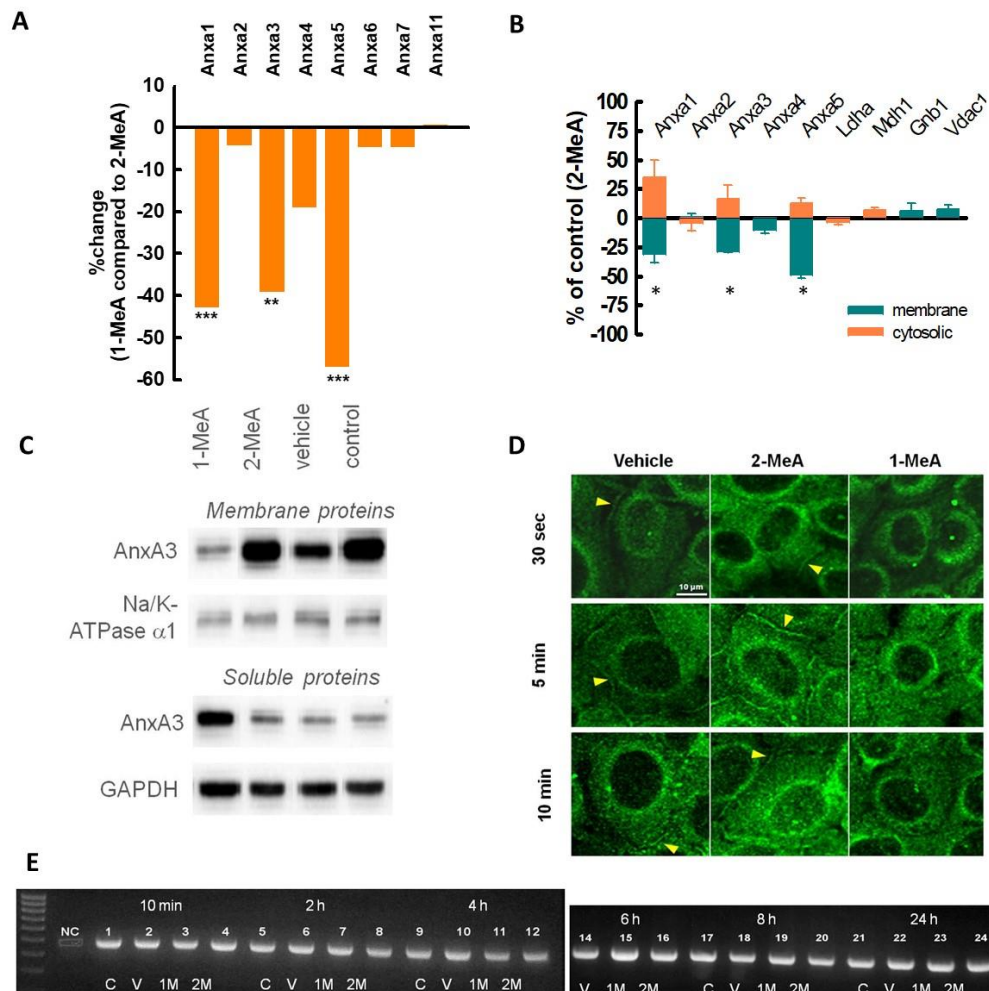


Figure 12: Rapid signaling events induced by 1-methylanthracene (1-MeA) in rat liver epithelial cells WB-F344. (A) Proteomic SILAC experiment revealed that, among 192 quantified proteins with SILAC ratios, proteins from annexin (Anxa) family were specifically depleted in the membrane proteome of 1-MeA-treated cells (70 μM , 5 min) in comparison to 2-methylanthracene (2-MeA)-treated cells. (B) Independent SILAC experiment confirmed that decrease of annexin A1, A2 and A5 in the fraction of membrane proteome was accompanied by their reciprocal increase in the fraction of soluble cytosolic proteins, while housekeeping proteins such as Ldha, Mdh1, Gnb1 or Vdac1 were not affected. Immunodetection of Annexin A3 (AnxA3) by (C) Western blotting and (D) immunocytochemistry confirmed membrane-to-cytosol translocation of the annexin in response to 1-MeA but not to 2-MeA. (E) Expression of *Annexin A3* gene was affected neither by 1-MeA (1M) nor 2-MeA (2M) exposure (70 μM) as analyzed by RT-PCR. C - control, V - vehicle (solvent) control. Adapted from conference proceedings co-authored by P. Babica (Babica et al., 2009; Upham et al., 2016b, 2011, 2008b), paper in preparation.

and L peptides were detected and SILAC H/L ratios could be determined. The proteins from annexin family were the most significantly affected, when annexin A1, A3 and A5 were found to be significantly depleted in the membrane proteome of 1-methylanthracene treated cells (Figure 12A). Subsequent proteomic experiment revealed that 1-methylanthracene-dependent decrease of annexin A1, A3 and A5 in the membrane protein fraction leads to their reciprocal increase in the fraction of soluble cytosolic proteins (Figure 12B). These results were confirmed also by Western blotting analysis of annexin A1-A5 (a representative image of annexin A3 is shown in the Figure 12C) and immunocytochemistry (Figure 12D). The changes observed at the protein level were not a result of altered gene expression, as confirmed by reverse transcription-polymerase chain reaction (RT-PCR) (a representative image of annexin A3 is shown in the Figure 12E), indicating that the observed changes in annexin proteins are probably caused by their translocation from membrane to cytosol. Moreover, translocation of annexin A3 from the plasma membrane was effectively prevented by pre-treatment of the cells with PC-PLC inhibitor, D609 (Figure 12D). Knock-down of AnxA3 by siRNA did not prevent 1-MeA induced dysregulation of GJIC, but did stimulate the 1-methylanthracene-induced release of arachidonic acid. Correspondingly, annexins have been previously identified as inhibitors of PLA₂. Therefore, it can be hypothesized that annexins closely interact with phospholipases in the plasma membrane until translocated to cytosol in response to a GJIC-inhibiting PAH, and the subsequent phospholipase-induced events then regulate the release of lipid derived second messengers and dysregulation of GJIC (Babica et al., 2009; Upham et al., 2016b, 2011, 2008b). These studies demonstrate that **inhibition of GJIC can be considered as the critical biological event to which both upstream and downstream**

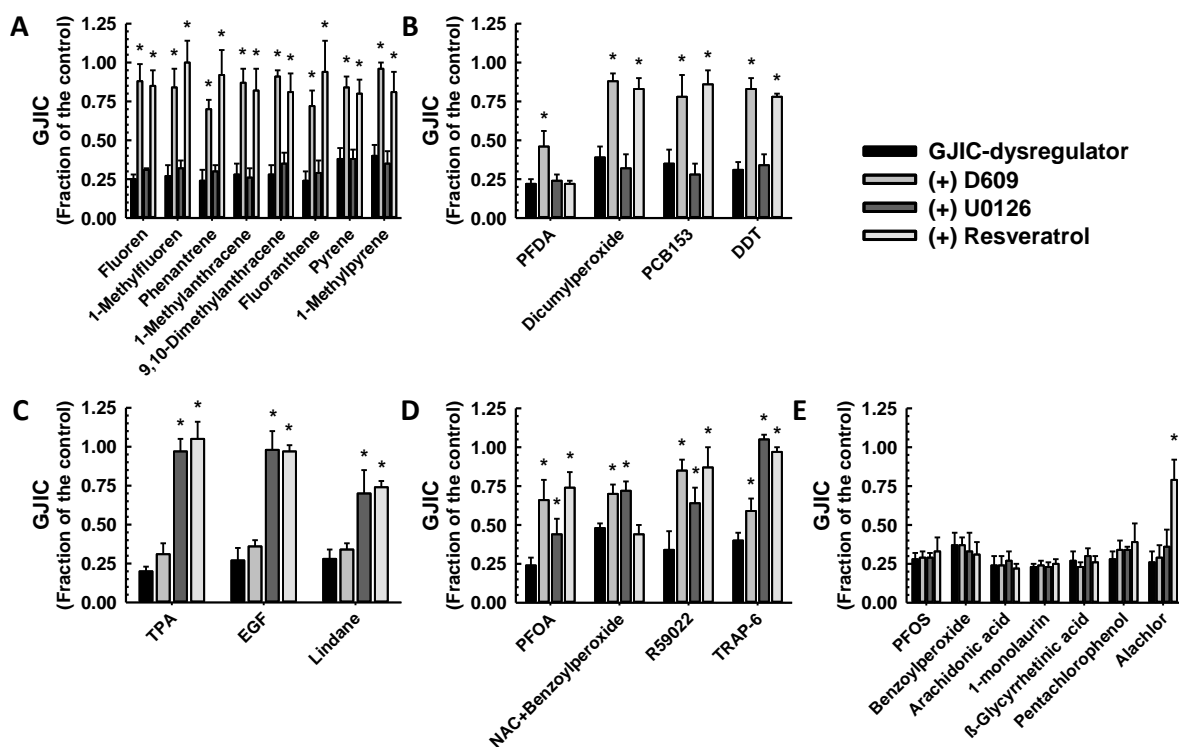


Figure 13: Different chemicals dysregulate GJIC via different mechanisms in rat liver epithelial cells WB-F344. (A-B) PC-PLC-dependent dysregulators of GJIC; (C) MAPK-ERK1/2-dependent dysregulators; (D) Both PC-PLC and MEK-ERK1/2-dependent dysregulators; (E) PC-PLC and MAPK-ERK1/2-independent dysregulators. WB-F344 cells were pre-treated with PC-PLC inhibitor D609 (50 μ M, 20 min), MEK inhibitor (i.e. upstream regulator of ERK1/2) U0126 (20 μ M, 30 min) or resveratrol (100 μ M, 15 min), then the GJIC dysregulators were added: Fluorene (100 μ M, 10 min), 1-methylfluorene (70 μ M, 10 min), phenanthrene (70 μ M, 10 min), 1-methylanthracene (70 μ M, 10 min), 9,10-dimethylanthracene (100 μ M, 10 min), fluoranthene (70 μ M, 10 min), pyrene (70 μ M, 10 min), 1-methylpyrene (70 μ M, 10 min), perfluorodecanoic acid (PFDA; 50 μ M, 20 min), dicumylperoxide (50 μ M, 15 min), PCB153 (50 μ M, 30 min), DDT (30 μ M, 20 min), 12-O-tetradecanoylphorbol-13-acetate (TPA; 10 nM, 30 min), EGF (5 ng/mL, 30 min), lindane (60 μ M, 25 min), perfluorooctanoic acid (PFOA; 80 μ M, 10 min), NAC+benzoylperoxide (the cells were treated with 1 mM N-acetylcysteine for 15 min to prevent oxidative stress-dependent cytotoxicity prior the addition of 200 μ M benzoylperoxide for 15 min), diacylglycerol kinase inhibitor R59022 (30-50 μ M, 10 min), thrombin receptor activating peptide-6 (TRAP-6; 50 μ M, 30 min), perfluorooctanesulfonic acid (PFOS; 40 μ M, 20 min), benzoylperoxide (200 μ M, 15 min), arachidonic acid (70-100 μ M, 15 min), 1-monolaurin (150 μ M, 10 min), 18 β -glycyrrhetic acid (30 μ M, 15 min), pentachlorophenol (50 μ M, 10 min) and alachlor (185 μ M, 25 min). GJIC was evaluated by SL-DT assay. Adapted from (Sovadinová et al., 2015) [Attachment IV].

signaling events can be anchored. Evaluation of GJIC can be then used as the principal *in vitro* assay for further identification of mechanisms associated with the inhibition of GJIC either in **hypothesis-driven research or to design ‘omics’ experiments**, both successfully leading to the **identification of the new molecular targets and signaling pathways**, such as PC-PLC or annexins. **Mechanistic understanding might not only provide links to the other toxicologically-relevant events and adverse outcomes, but could be also utilized to define new *in vitro* biomarkers for hazard identification and assessment.**

The experiments with 1-methylantracene further indicated that PC-PLC represents the key regulator of GJIC, which might be responsible for GJIC dysregulation occurring independently on the traditionally recognized regulatory mechanisms through MAPK MEK-ERK1/2 or PKC. Therefore, we conducted an ***in vitro* survey of 25 different chemicals to elucidate their major mechanism of GJIC inhibition: PC-PLC-dependent, MEK-ERK1/2-dependent, or other** (Sovadinová et al., 2015) [Attachment IV]. Different toxicants, growth factors and signal pathway modulators were found to dysregulate GJIC via **different mechanisms** in rat liver epithelial cells WB-F344 (Figure 13). Although many of these chemicals are known to activate MAPK ERK1/2, this signaling pathway was involved in GJIC dysregulation only by limited number of compounds. **Majority of compounds thus inhibited GJIC through MEK-ERK1/2-independent mechanisms, with PC-PLC-dependent dysregulation of GJIC being relatively prevalent and robust response by all lower molecular weight PAHs, dicumylperoxide, PCB153, DDT, and partially also by perfluorodecanoic and perfluorooctanoic acid (PFOA).** However, large group of chemicals dysregulated GJIC through signaling pathways other than MEK-ERK1/2 or PC-PLC. Interestingly, different signaling mechanisms responsible for GJIC were in some instances implicated even for chemically related compounds, such as different fluorinated fatty acids (PFOA, perfluorodecanoic or perfluorooctanesulfonic acid), different organochlorine pesticides (DDT, lindane, pentachlorophenol, alachlor), or different organic peroxides (dicumylperoxide, benzoylperoxide). Thus, not only the general ability of environmental toxicants to target GJIC depends on their structure, but also the **mechanisms responsible for GJIC dysregulation might be structure-dependent.** ***In vitro* assessment of GJIC allows to effectively pinpoint these mechanisms and the signaling events leading to dysregulated intercellular communication and other downstream effects.**

The implication of PC-PLC as the key regulator of GJIC and probably common target of environmental toxicants in rat liver progenitor cells was further supported by a study, which focused on the effects of **methoxychlor and vinclozolin** on rapid signaling events (Babica et al., 2016c) [Attachment V]. Pesticides methoxychlor and vinclozolin are potent **endocrine-disrupting compounds (EDCs)**, known to alter male and female reproductive system, neuroendocrine and immune system, reproductive and social behavior (Manikkam et al., 2014; van Ravenzwaay et al., 2013). The effects induced by these compounds were found to be transmitted into the offspring via mechanisms of epigenetic inheritance. Interactions of methoxychlor and vinclozolin and their metabolites with sex hormone receptors, such as estrogen receptor (ER) or androgenic receptor (AR) and subsequent changes in the expression of the genes transcriptionally controlled by the ligand-activated ER/AR represent well-recognized and traditionally studied mechanism of methoxychlor and vinclozolin toxicity (Cummings, 1997; Gaido et al., 2000; Wong et al., 1995). Hydroxylated metabolites of methoxychlor, such as HPTE (2,2-bis-(p-hydroxyphenyl)-1,1,1-trichloroethane), are potent agonists of ER α and weak antagonists of ER β and AR. Vinclozolin metabolites, vinclozolin M1 and M2, are strong antagonists of AR and moderate agonists to progesterone receptor and ERs. However, there is an increasing evidence that both endogenous hormones, as well as several environmental EDCs, can also act via so-called **non-genomic signaling mechanisms**, which represents primarily membrane-initiated rapid signaling events occurring independently of alterations of gene transcription induced by ligand-activated nuclear receptors (Watson et al., 2014; Wong and Walker, 2013). These mechanisms include also processes known to be involved in the regulation of GJIC, such as rapid modulations of Ca²⁺ or K⁺ channel activity, Ca²⁺ levels, or activity of major intracellular signal transduction pathways, such as PLC / PKC, PKG, PKA, adenylyl cyclase, Akt, Src, or MAPKs ERK1/2, p38 and SAPK/JNK (see Chapter 2.2). These rapid mechanisms of non-genomic signaling were also implicated in the modulation of GJIC in response to various endogenous or synthetic estrogens and androgens (Herve et al., 1996; Iwase et al., 2006; Lyng et al., 2000; Pluciennik et al., 1996), bisphenol A (Lee et al., 2014), ioxynil, ioxynil octanoate (Leithe et al., 2010), nonylphenol (Aravindakshan and Cyr, 2005), fluorinated fatty acids, DDT or lindane (Sovadinová et al., 2015) [Attachment IV]. Interestingly, **methoxychlor and vinclozolin were also found to induce a rapid (<5 min) dysregulation of GJIC accompanied by activation/phosphorylation of MAPK ERK1/2 and p38** (Figure 14). Inhibition of GJIC by vinclozolin was also associated with rapid **hyperphosphorylation**

and internalization of Cx43 (Figure 14). The effects on GJIC were prevented by an inhibitor of PC-PLC and, in the case of vinclozolin, also by p38 inhibitor. However, neither MEK inhibitor or modulators of ER and AR (estradiol, HPTE, ICI182,780, testosterone, flutamide, vinclozolin M2) were able to prevent effects of methoxychlor or

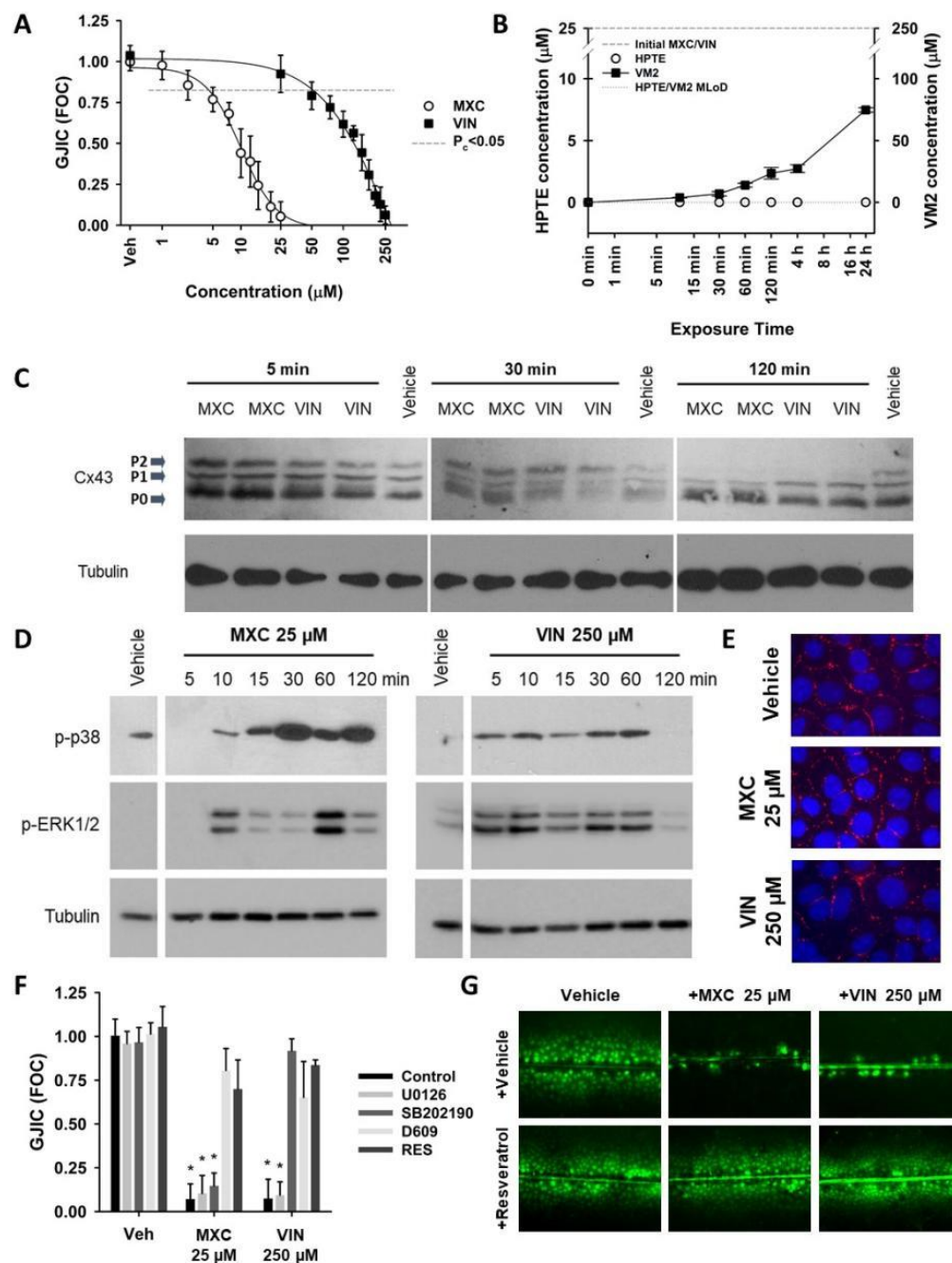


Figure 14: Effects of methoxychlor (MXC) and vinclozolin (VIN) on GJIC and MAPKs in rat liver epithelial cells WB-344. (A) MXC and VIN induced rapid inhibition of GJIC (30 min exposure is shown); (B) Concentrations of MXC and VIN metabolites HPTE and vinclozolin M2 (VM2) in cell culture medium during the experiments (MLoD - method limit of detection); (C) Effects on phosphorylation of Cx43 (MXC 25 μM, VIN 250 μM); (D) Activation of MAPKs ERK1/2 and p38; (E) Immunocytochemistry of Cx43 in the cells treated for 30 min; (F) Effects of inhibitors of MEK-ERK1/2 pathway (U0126), p38 (SB202190) and PC-PLC (D609) and resveratrol (RES) inhibition of GJIC induced by 10 min exposure to MXC or VIN; (G) Microphotographs showing preventive effects of resveratrol on GJIC dysregulation by 10 min treatment with MXC or VIN. GJIC was evaluated by SL-DT assay, MAPK and Cx43 phosphorylation by Western blotting, Cx43 localization by immunocytochemistry, HPTE and VM2 were analyzed by LC-MS/MS. FOC – Fraction of the Control. Adapted from (Babica et al., 2016c) [Attachment V].

vinclozolin on GJIC. Interestingly, some of the ER- or AR-ligands, such as estradiol, HPTe, flutamide and VM2 also inhibited GJIC, although via a slower and presumably genomic signaling-dependent mechanism (Babica et al., 2016c) [Attachment V]. Since no biotransformation of methoxychlor to HPTe was detected by instrumental analysis, and formation of vinclozolin M2 was slower than the onset of GJIC inhibition and MAPK activation (Figure 14), the rapid signaling events were probably caused by the **parental compounds**, not the metabolites. We provided most likely the very first report that prototypical EDCs, methoxychlor and vinclozolin, can **rapidly inhibit GJIC and activate ERK1/2, p38 and PC-PLC independently of ER or AR-dependent genomic signaling** (Babica et al., 2016c) [Attachment V]. **These newly recognized rapid alterations of intercellular and intracellular signaling might represent another mechanism possibly contributing to the effects of EDCs on disruption of epigenetic developmental programming, alterations of tissue development and organ function, and transgenerational inheritance** (Casati et al., 2015).

4.3 GJIC ASSESSMENT OF SPECIES- AND TISSUE-SPECIFIC EFFECTS OF CHEMICALS

Although WB-F344 cells have been repeatedly proven to be a useful model to study effects of toxicants on Cx43-dependent GJIC in liver progenitor cells (Vondracek and Machala, 2016), the effects on GJIC observed in one particular *in vitro* model should not be undoubtedly extrapolated to the other cell types, since **connexin expression, gap junction function and regulation depend on the biological and physiological context (Chapters 2 and 3)**. Consequently, **effects of toxic chemicals on GJIC**, as well as specific mechanisms underlying the eventual GJIC inhibition, might be also **cell type-, tissue- and organ-specific**. As illustrated in the Chapter 4.1 (Figure 8), GJIC can be evaluated in different cell types representing various tissues and organs, which provides an excellent opportunity to investigate effects of chemicals on GJIC in the desired biological context.

Methoxychlor is known to **impair development and function of male reproductive system** in rodent *in vivo* studies, where induced hormonal imbalances, atrophy of sexual organs, and deteriorations of sperm production (Aoyama and Chapin, 2014). Cx43-mediated GJIC, which was found to be targeted by methoxychlor in the rat liver epithelial cells (Babica et al., 2016c) [Attachment V], plays a critical role in the function of **somatic testicular Leydig or Sertoli cells** (see Chapter 3), which are known to be essential for sex hormone production, gametogenesis and reproduction (Kidder and Cyr, 2016). The results of our recent and still ongoing study

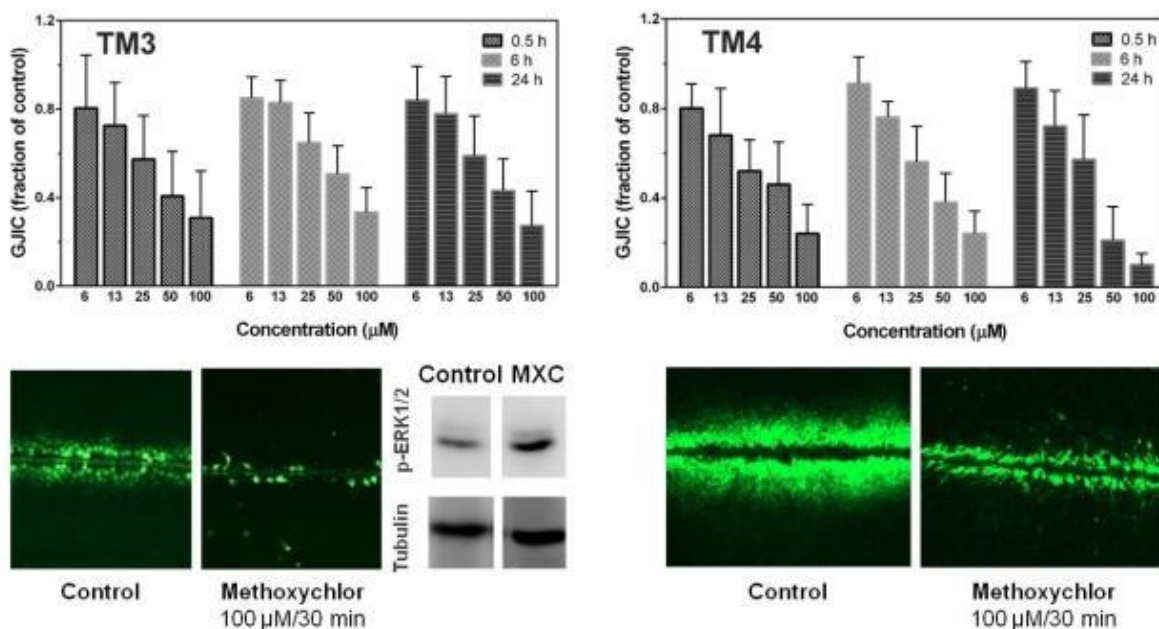


Figure 15 Effects of methoxychlor (MXC) on GJIC and MAPK ERK1/2 in mouse somatic testicular Leydig TM3 and Sertoli TM4 cells. Western blot image shows the control cells and the cells treated with 100 µM MXC for 30 min. GJIC was evaluated by SL-DT assay, MAPK-ERK1/2 activation by Western blotting. Adapted from conference proceedings co-authored by P. Babica (Sovadinová et al., 2017b; Yawer et al., 2017), paper in preparation.

(Sovadinová et al., 2017b; Yawer et al., 2017) revealed that **methoxychlor induces rapid (within 30 min) and permanent inhibition (≥ 24 h) of GJIC also in mouse Leydig TM3 cells and mouse Sertoli TM4 cells (Figure 15)**. Similar to WB-F344 cells, GJIC dysregulation was also accompanied with **activation of MAPK-ERK1/2 in Leydig TM3 cells**. Another example of cell type-specific effects of toxicants on GJIC is represented by the activity of **low molecular weight PAHs in mouse Leydig TM3 cells** in contrast to **mouse Sertoli TM4 cells**. 1-methylanthracene, fluorene, fluoranthene, but not 2-methylanthracene or benzo(a)pyrene, were found to inhibit GJIC in Leydig TM3 cells (Figure 16), which indicated a similar pattern of structure-dependent activity as in the previous experiments with rat liver cells WB-F344 (Blaha et al., 2002) (Upham et al., 2008a) [Attachment III]. However, the effects of 1-methylanthracene on GJIC were attenuated by an inhibitor of MEK-ERK1/2 pathway (Figure 16), which implies a **different mechanism responsible for 1-methylanthracene-induced inhibition of GJIC in TM3 cells in comparison with WB-F344 cells**. Nevertheless, none of the tested PAHs was found to alter GJIC in TM4 Sertoli cells, further indicating that the effects of chemicals on GJIC might be cell type-specific (Babica et al., 2013; Sovadinová et al., 2017b; Yawer et al., 2017).

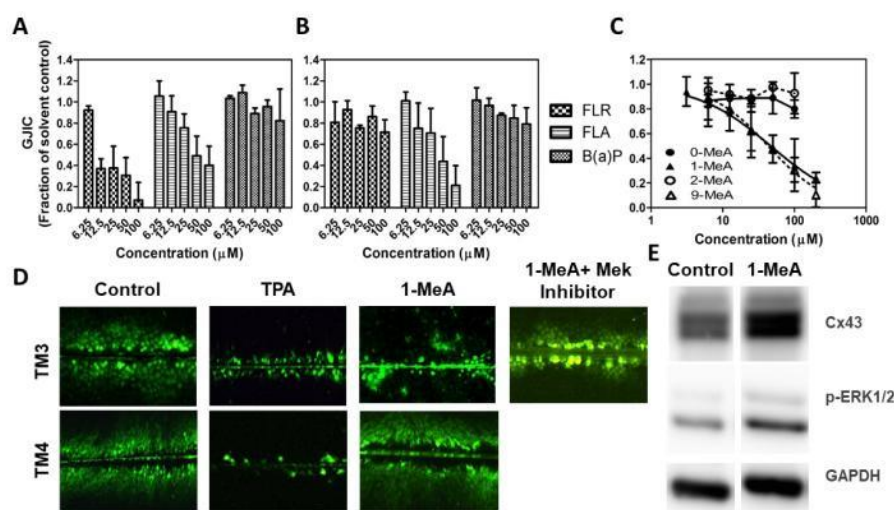


Figure 16: Effects of polycyclic aromatic hydrocarbons on GJIC and related signaling events in mouse Leydig TM3 and Sertoli TM4 cells. Fluorene (FLR) and fluoranthene (FLA) but not benzo(a)pyrene (BaP) inhibited GJIC in Leydig TM3 cells after (A) 30 min or (B) 24 h. (C) 1-methylanthracene and 9-methylanthracene (1-MeA, 9-MeA) but not anthracene (0-MeA) or 2-methylanthracene (2-MeA) inhibited GJIC in Leydig TM3 cells after 30 min exposure. (D) 12-O-tetradecanoylphorbol-13-acetate (TPA) but not 1-MeA (100 μ M) inhibited GJIC in Sertoli TM4 cells, 1-MeA-induced inhibition of GJIC was prevented by PD98059, an inhibitor of MEK-ERK1/2 pathway. (E) 1-MeA (100 μ M, 30 min) did alter phosphorylation of Cx43 and activation of ERK1/2. GJIC was evaluated by SL-DT assay, MAPK-ERK1/2 and Cx43 were evaluated by Western blotting. Adapted from conference proceedings co-authored by P. Babica (Babica et al., 2013; Sovadinová et al., 2017b; Yawer et al., 2017), paper in preparation.

mouse epithelial lung cells C10 (Osgood et al., 2013) [Attachment VI]. These cells were derived from BALB/c mouse **alveolar type II pneumocytes (type II cells)**, which express Cx43 as the major connexin (along with other connexin types). Type II cells are critical in the defense of the alveolar space from inhaled pollutants and maintenance of homeostasis. In addition, type II cells maintain gas exchange, secrete surfactant, have a metabolic capacity, and play a role in lung immunity through secretion of cytokines and chemokines. Similar to the previous results with WB-F344 cells, **1-methylanthracene but not 2-methylanthracene induced rapid inhibition of GJIC in C10 cells (Figure 17)**, followed by **internalization and degradation of Cx43**. Inhibition of GJIC was induced by **non-cytotoxic concentrations**, and GJIC was restored upon removal of 1-methylanthracene from the cell culture. Furthermore, the inhibition of GJIC by 1-methylanthracene was associated with **activation of MAPKs ERK1/2 and p38 (Figure 17)**. It has been observed that inhibition of GJIC induced by 1-methylanthracene was prevented by inhibitor of p38 but not MEK-ERK1/2 inhibitors, which indicates that **p38 pathway was responsible for dysregulation of GJIC** in this type of cells. MAPK p38 is known to be active in inflammatory lung diseases like

Apparently, low molecular weight PAHs can elicit quite different effects on GJIC in different cells or tissues. Since these compounds represent prevalent atmospheric contaminants which are also abundant in the cigarette smoke and secondhand cigarette smoke, it was particularly interesting to characterize effects of low molecular PAHs in **airway epithelial cells**, where a dysregulation of GJIC might represent a mechanism eventually contributing to the adverse outcomes induced by inhalation exposure to these compounds, such as development of chronic pulmonary diseases or lung tumor promotion. Therefore, we studied the effects of selected **methylated anthracenes** on GJIC also in

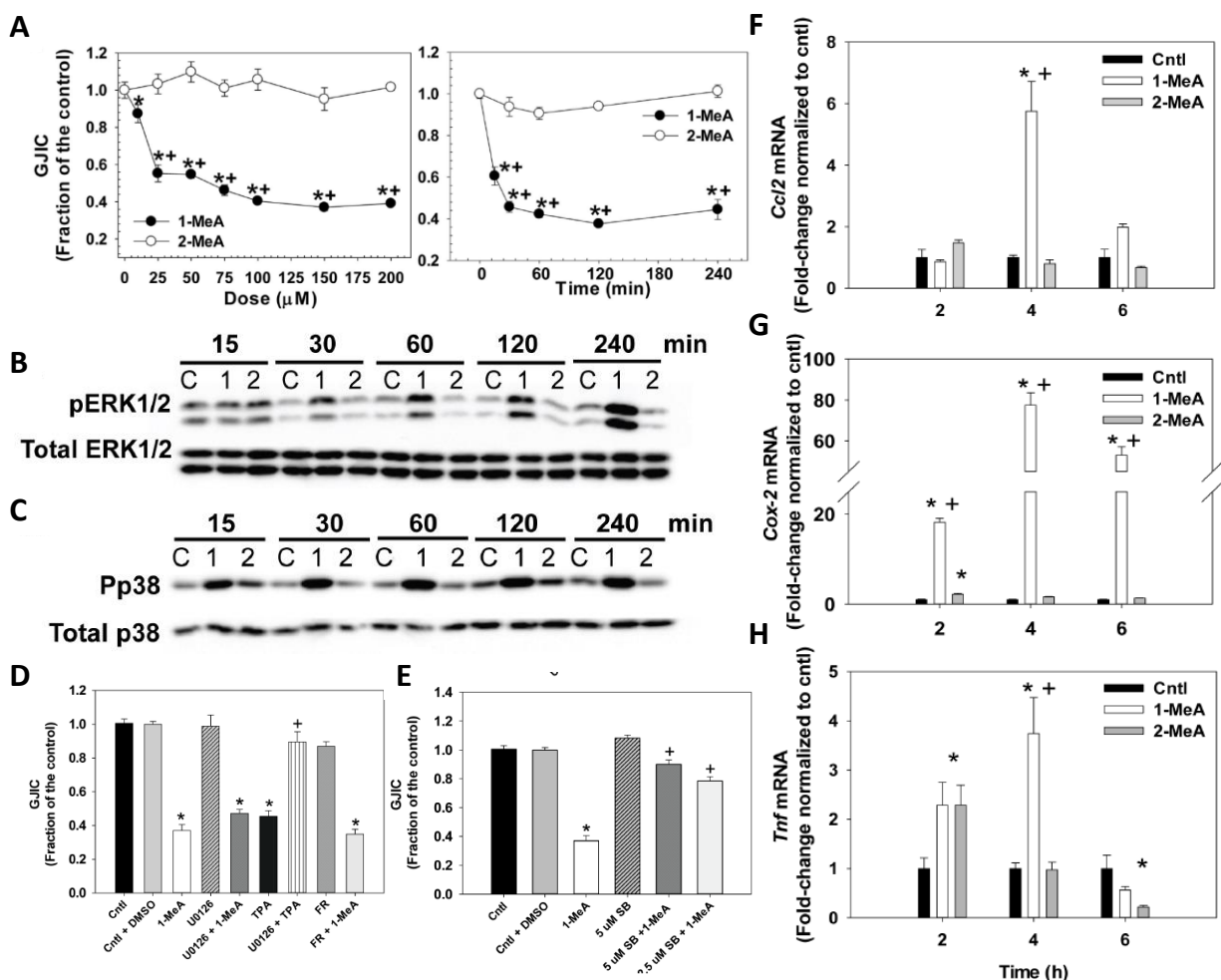


Figure 17: Effects of methylated anthracenes in mouse lung epithelial cells C10. 1-methylanthracene (1-MeA) but not 2-methylanthracene (2-MeA) (A) inhibited GJIC and (B-C) activated MAPK-ERK1/2 and p38 (at concentration 75 μM). GJIC inhibition induced by 1-MeA (75 μM, 30 min) was (D) not prevented by the inhibitors of MEK-ERK1/2 pathway, U0126 and FR180204, but they were (E) prevented by p38 inhibitor, SB202190. (F-G) The effects of 1-MeA but not 2-MeA (75 μM) were associated with increased expression of inflammatory genes, Ccl2 (chemokine CC-motif ligand), Cox-2 (cyclooxygenase 2) and Tnf (tumor necrosis factor α). GJIC was evaluated by SL-DT assay, MAPK activation by Western blotting, inflammatory genes by PCR. Cntl - control; TPA - 12-O-tetradecanoylphorbol-13-acetate. Adapted from (Osgood et al., 2013) [Attachment VI].

chronic obstructive pulmonary disease (COPD), and has been shown to be induced in the lung exposed to cigarette smoke, which suggested that GJIC dysregulation and p38 activation might be also associated also with pro-inflammatory responses and signaling. Indeed, 1-methylanthracene but not 2-methylanthracene induced gene expression of **inflammatory markers: Chemokine (C-C motif) ligand (Ccl2), Cyclooxygenase 2 (Cox-2) and Tnf** (Osgood et al., 2013) [Attachment VI]. P38-dependent modulations of chemokine and cytokine expression were confirmed also by a follow-up transcriptomic and proteomic study with C10 cells exposed to 1-methylanthracene, fluoranthene or their binary (1:1) mix (Osgood et al., 2017). The effects of the binary 1-methylanthracene-fluoranthene mix were more potent than those of the individual chemicals, and the mix was found to alter in a p38-dependent manner expression of **major inflammatory genes and pathways** (e.g. *Cox2*, *Ccl2*, *Cxcl1*, *Lif*, *IL6*, *Egfr1*, *Ccl7*, *Vcam1*, *Vegfa*). P38 was also responsible for **increased expression of Mmp-13 protein and decreased expression of Mmp inhibitor Timp-1**, which is similar to their expression pattern COPD patients, where these proteins play a critical role in tissue remodeling and disease progression. Thus, rapid dysregulation of GJIC and upregulation of p38 by low molecular weight PAHs seems to be mechanistically connected to chronic disease-relevant effects occurring at the tissue level (Osgood et al., 2017).

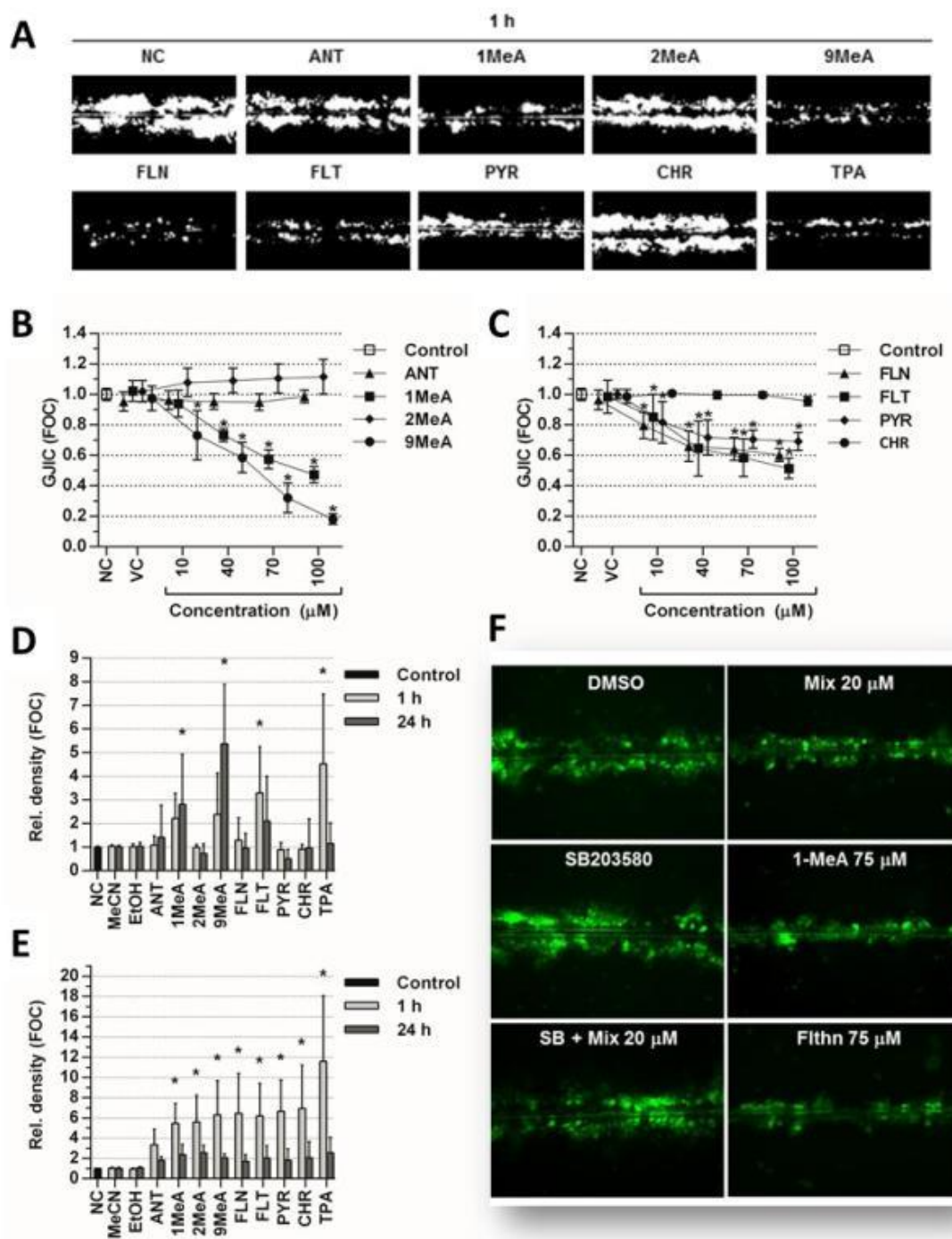


Figure 18: Effects of selected polycyclic aromatic hydrocarbons (PAHs) on GJIC and MAPK activity in human bronchial epithelial cells HBE1. 1-methylanthracene and 9-methylanthracene (1-MeA, 9-MeA), fluorene (FLN), fluoranthene (FLT) and pyrene (PYR) but not anthracene (ANT), 2-methylanthracene (2-MeA) or chrysene (CHR) inhibited GJIC in HBE1 cells after (A) 1 h exposure or (B-C) 24 h exposure. Effects of PAHs (100 μM) on (D) MAPK-ERK1/2 and (E) p38 activity. (F) GJIC inhibition induced by a binary mix of 20 μM 1-MeA and 20 μM Fluoranthene (Mix 20 μM) was blocked by an p38 inhibitor, SB203580 (SB). GJIC was evaluated by SL-DT assay, MAPK activation by Western blotting. FOC - Fraction of the Control; TPA - 12-O-tetradecanoylphorbol-13-acetate. Adapted from diploma thesis co-supervised by P. Babica (Brózman, 2015) and a conference proceeding co-authored by P. Babica (Brózman et al., 2017), paper in preparation.

Interspecies differences might also pose a significant limitation of rodent testing to predict toxic effects of chemicals in humans from animal tests (Cunningham, 2002; Krewski et al., 2010). Some of these differences might be manifested also at the molecular and cellular level, and result in the different outcomes between rodent and human cell lines (Jemnitz et al., 2008), thus **confirmation of *in vitro* data using a human cell line might provide an additional level of evidence towards predicting the effects in human beings**. Importantly, our recent experiments revealed that **low molecular weight PAHs** induce inhibition also in **human bronchial epithelial cells HBE1** with a similar structure-dependent effects on GJIC like in WB-F344 cells or C10 cells (Brózman, 2015; Brózman et al., 2017), when 1- and 9- methylanthracene, fluorene, fluoranthene and pyrene inhibited GJIC, while anthracene, 2-methylanthracene and chrysene did not have effected on GJIC (Figure 18). **MAPK ERK1/2** was activated in a similar structure-specific manner, being most potently activated by GJIC-inhibiting 1-methylanthracene, 9-methylanthracene and fluoranthene. Interestingly, GJIC inhibitors fluorene and pyrene had only little effects on MAPK-ERK1/2, which indicates that these chemicals might act differently in respect to ERK1/2 activation than in WB-F344 or C10 cells (Figure 18). **MAPK p38** was found to be transiently activated by all PAHs under the study, regardless their structure (Figure 18). However, **dysregulation of GJIC** induced by the binary mix of 1-methylanthracene and fluoranthene was **prevented by p38 inhibitor** (Figure 18), which suggests that activation of p38 pathway played an essential role in the effects on GJIC, but p38 itself was not sufficient to decrease GJIC and co-action of other signaling pathways was probably needed. **These results revealed that low molecular weight PAHs induce similar effects on GJIC in both human HBE1 cells and mouse C10 cells**, although p38 does not seem have an exclusive role in GJIC dysregulation in human cells.

PC-PLC was implicated as the key regulator of GJIC in response of WB-F344 rat liver cells to several environmental toxicants, including low molecular weight PAHs, PCB153, DDT, dicumylperoxide, PFOA (Sovadinová et al., 2015) [Attachment IV], methoxychlor or vinclozolin (Babica et al., 2016c) [Attachment V]. However, 1-methylanthracene, a known PC-PLC-activator (Upham et al., 2008a) [Attachment III], has been just found either not to inhibit GJIC in certain cell lines, such as Sertoli TM4 cells (Figure 16), or to inhibit GJIC through a MAPK pathway in some other cells, such as mouse lung epithelial cells C10 (Osgood et al., 2013) [Attachment VI] or human bronchial epithelial cell line HBE1 (Figure 18). Therefore, we decided to investigate the structure-

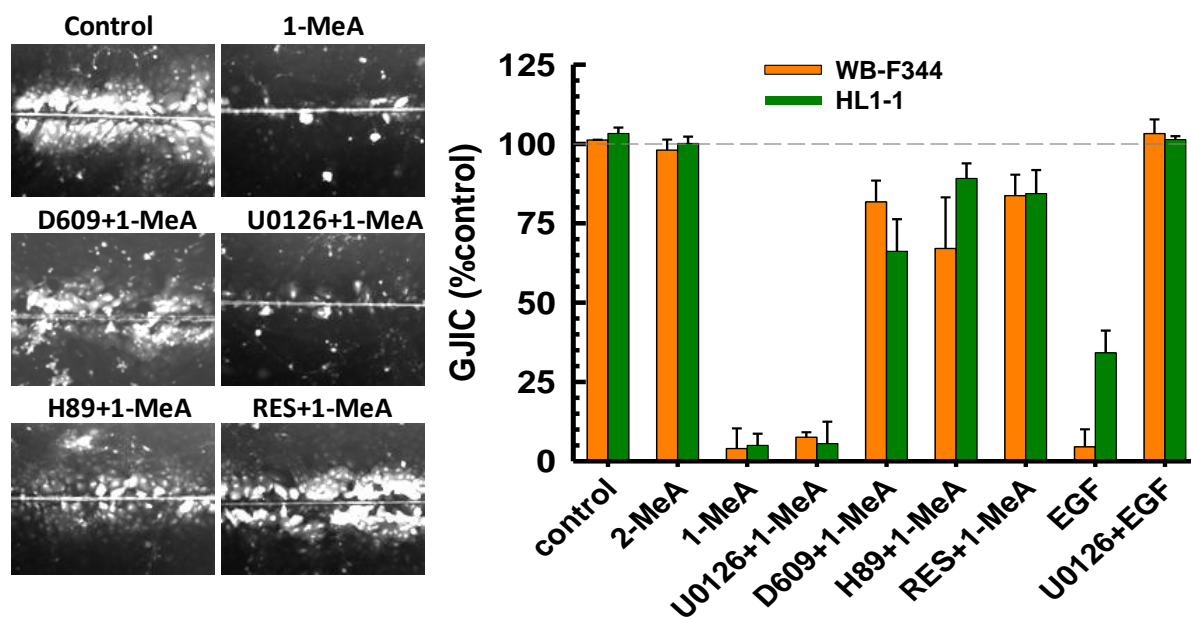


Figure 19: Effects of methylated anthracenes on GJIC in adult human liver stem cells HL1-1. 1-methylanthracene (1-MeA) but not 2-methylanthracene (2-MeA) inhibited GJIC (150 μ M, 20 min). The effects of 1-MeA were prevented by pre-treatment with D609, an inhibitor of PC-PLC, H89, an inhibitor of PKA, and resveratrol (RES, 200 μ M, 120 min). U0126, an MEK-ERK1/2 pathway inhibitor, did not have effect on 1-MeA-induced dysregulation of GJIC, while prevented the effects of epidermal growth factor (EGF). GJIC was evaluated by SL-DT assay. Graph provides a comparison between the effects on GJIC in rat liver epithelial cells WB-F344 and human liver stem cells HL1-1. Adapted from a conference proceeding co-authored by P. Babica (Park et al., 2008), paper in preparation.

dependent effects of **methylated anthracenes** as well as the basic mechanisms identified in the studies with rat liver progenitor WB-F344 cells also in a human liver cell line. For this purpose, we used recently isolated **adult human liver stem cells HL1-1**, which have characteristics of liver stem or progenitor cells, including expression of Oct-4, α -fetoprotein, vimentin, Thy-1/CD90, high proliferation capacity, and ability to undergo hepatic differentiation (Chang et al., 2004; Kim et al., 2013, 2009; Shi et al., 2014). Upon differentiating HL1-1 cells in a high calcium DMEM-based medium (Kim, 2011), these cells developed functional GJIC. 1-methylanthracene was found to inhibit GJIC, while 2-methylanthracene did not have a significant effect on cell-to-cell communication (Park et al., 2008). Similarly to WB-F344 cells, **GJIC dysregulation by 1-methylanthracene was prevented by a PC-PLC inhibitor as well as by a PKA inhibitor, but not by a MEK-ERK1/2 inhibitor (Figure 19)**. This provides additional evidence that PC-PLC-dependent inhibition of GJIC represents an important mechanism induced by 1-methylanthracene and possibly other environmental toxicants not only in rat liver epithelial cells, but also in adult human liver stem cells. Chemically-induced alterations of homeostatic control mechanisms, such as GJIC, in populations of **adult liver stem or progenitor cells** might be particularly important for the development of **chronic toxicities and diseases**, given the important role these cells play in liver tissue renewal, regeneration and repair, and increasing number of studies, which have linked alterations of liver stem cells by model toxicants to the development of hepatic carcinoma or other chronic liver diseases, such as liver fibrosis (Font-Burgada et al., 2015; Knight et al., 2007; Wang and Jacob, 2011; Zhi et al., 2016).

4.4 IN VIVO AND EX VIVO VALIDATION OF IN VITRO EFFECTS ON GJIC

The traditional cultures of adherent mammalian cells grown in monolayers provide a convenient *in vitro* model allowing for effective assessment of GJIC by a variety of methods (Chapter 4.1). However, it is being more increasingly recognized that such '2-dimensional' (2D) cultures, due to their simplistic and unphysiological microenvironment, do not often properly recapitulate many critical properties of the cells and tissues *in vivo*. Thus, responses of 2D cultured cells to the chemicals might not correspond to their *in vivo* effects. **Validation of the effects on GJIC observed in 2D monolayer cultures using more complex *in vitro* systems**, such as 3D cell and organoid cultures, ***ex vivo* experiments** with tissue slices, or ***in vivo* GJIC assessment**, might be a key step to better understand the ***in vivo* relevance of *in vitro* results**. Some techniques introduced in the Chapter 4.1 can be adapted also for *ex vivo* evaluation of GJIC in organs and tissues. These techniques include also SL-DT protocol, which can be modified into IL-DT, as previously described (Babica et al., 2016b; Upham et al., 2016a) [Attachment I-II].

It has been reported previously, that some of the rodent liver tumor promoters and well-recognized *in vitro* inhibitors of GJIC were found to inhibit GJIC also in the liver of *in vivo* exposed Fischer 344 rats. These chemicals included pentachlorophenol (Sai et al., 2000), 2-acetylaminofluorene (Krutovskikh et al., 1991), phenobarbital and polychlorinated biphenyls (Kolaja et al., 2000; Krutovskikh et al., 1995), pregnenolone-16 α -carbonitrile (Kolaja et al., 2000), cadmium (Jeong et al., 2000), clofibrate, DDT (Krutovskikh et al., 1995) and perfluorosulfonic acids (Hu et al., 2002).

In the following study, we investigated GJIC inhibiting effects of PFOA, which is an important environmental contaminant, hepatotoxicant, liver tumor promoter and endocrine disrupter. The initial studies reported that perfluorinated fatty acids inhibit GJIC in WB-F344 cells in a structure dependent manner, where inhibition of GJIC was a function of perfluorinated carbon lengths ranging from C7 to C10 (Figure 20). Our follow-up experiments (Upham et al., 2009) [Attachment VII] revealed that single dose (intraperitoneal injection, 100 mg/kg of body weight) of rodent liver tumor promoter phenobarbital, C8 PFOA but not C5 perfluoropentanoic acid (PFPeA) induced hepatomegaly in F344 rats after 24 h - 1 week exposure. The effects on the liver weight were not associated with liver injury (Upham et al., 2009) [Attachment VII]. *Ex vivo* evaluation of GJIC by IL-DT method revealed that PFOA but not PFPeA inhibited GJIC in the liver of *in vivo* exposed rats (Figure 20). In addition, PFOA, but not PFPeA were then also found to activate MAPK ERK1/2 in WB-F344 cells (Figure 20). PFOA was observed to inhibit GJIC *in vitro* via a mixed PC-PLC- and MEK-ERK1/2-dependent mechanism (Figure 13). Similarly to *in vivo* results, the effective concentrations of PFOA required to inhibit GJIC *in vitro* were also not cytotoxic, since WB-F344 cells incubated for 48 h with PFOA did not show any morphological abnormalities, and after the transfer into

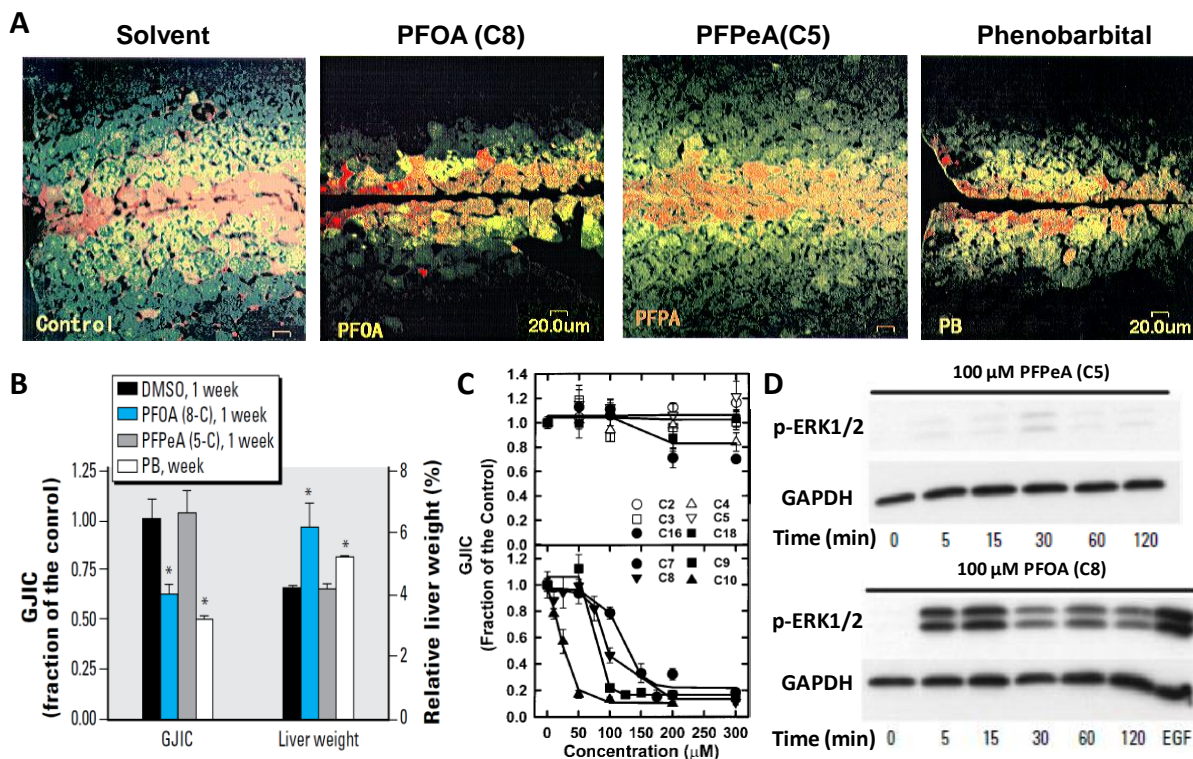


Figure 20: *In vivo* and *in vitro* effects of fluorinated fatty acids on GJIC. (A) *Ex vivo* incision loading-dye transfer (IL-DT) assay of GJIC in liver tissues from F344 rats exposed *in vivo* (intraperitoneal single dose administration, 100 mg/kg body weight) to solvent (DMSO), phenobarbital (PB) perfluorooctanoic acid (PFOA), perfluoropentanoic acid (PFPeA) - effects 24 h post-treatment; (B) relative changes in GJIC levels in liver tissue and changes in the relative liver weight in F344 rats exposed *in vivo* to DMSO, PB, PFOA and PFPeA – effects 1 week post-treatment; (C) *In vitro* inhibition of GJIC by fluorinated fatty acids with different carbon chain lengths (PFPeA = C5; PFOA = C8) evaluated by SL-DT assay in rat liver epithelial cells WB-F344 (20 min exposure); (D) *in vitro* effects of PFPeA and PFOA on MAPK ERK1/2 activation in WB-F344 cells evaluated by Western blotting. EGF – epidermal growth factor (20 ng/mL, 15 min). Adapted from (Upham et al., 1998) and (Upham et al., 2009) [Attachment VII].

a fresh medium without PFOA, the cells completely restored GJIC (Upham et al., 2009) [Attachment VII]. These results suggest that the *in vitro* rat liver epithelial cell assay system is a good predictor of the *in vivo* effects of chemicals on gap junctions in the liver tissue of rodents.

Recently, we investigated also effects of methoxychlor on GJIC inhibition *ex vivo* (Sovadinová et al., 2017b; Yawer et al., 2017). Endocrine disrupter methoxychlor was identified to be a potent inhibitor of GJIC not only in rat liver WB-F344 cells (Babica et al., 2016c) [Attachment V], but also in both mouse Leydig TM3 and Sertoli TM4 cells. Correspondingly, methoxychlor dysregulated GJIC also in rat seminiferous tubules exposed *ex vivo* (Sovadinová et al., 2017b; Yawer et al., 2017), which further indicates that GJIC results obtained from *in vitro* experiments are likely to be relevant also for *in vivo* situation.

4.5 GJIC ASSAY IN WHOLE-MIXTURE TOXICITY TESTING, EFFECT-DIRECTED ANALYSIS AND EFFECT-BASED MONITORING

The previous Chapters (Chapters 4.2-4.4) focused on the use of *in vitro* GJIC assessment to identify hazards and characterize toxicity mechanisms of the individual chemicals. Although human risk assessment and environmental risk assessment of chemicals mainly focuses on exposures to individual chemicals and mostly considering only a single source, human beings and the environment are continuously exposed to enormous number of chemicals and their combinations often coming from multiple sources. Thus, there is an increasing demand for novel tools which could support human and environmental risk assessment of mixtures. In this respect, *in vitro* assays can support mixture risk assessment by providing a better understanding of the underlying mechanisms of combined

effects. This approach includes also **whole-mixture testing**, where the environmental mixtures of unknown composition can be tested to evaluate their hazardous potential to alter a specific mechanism of molecular or cellular toxicity (Kienzler et al., 2016). Although the compounds responsible for the response remain unknown, *in vitro* assays can be then used in a combination with fractionation procedures and chemical analytical methods in **effect-directed analysis (EDA)** to identify causative agents of specific adverse effects (Brack, 2003; Hong et al., 2016). Moreover, **effect-based tools**, such as *in vitro* bioassays targeting different toxic modes of action, are currently being implemented into the monitoring guidelines for water quality assessment to complement the classical chemical analyses with additional information and to provide more integrative view of toxic potential of complex mixtures consisting of (i) high priority target contaminants, (ii) other potentially toxic but not-yet fully characterized compounds as well as (iii) toxic (by-)products of transformation or degradation formed by natural processes or during water treatment (Wernersson et al., 2015).

4.5.1 WHOLE-MIXTURE TOXICITY TESTING OF CYANOBACTERIAL EXTRACTS AND EXUDATES

Massive proliferations of toxic cyanobacteria and formation of so-called **water blooms** in aquatic ecosystems represent an emerging environmental and human health problem. Frequency, intensity and duration of cyanobacterial water blooms in fresh and coastal waters have been increasing over the past decades due to human activities, including anthropogenic eutrophication and climate change (Paerl and Otten, 2013; Visser et al., 2016). Several secondary metabolites of cyanobacterial origin have been identified as potent toxins and potential threat for human health. The major and well-recognized **cyanobacterial toxins (cyanotoxins)** include: (1) cyclic heptapeptides microcystins and pentapeptides nodularins, (2) tricyclic guanidine alkaloid cylindrospermopsin, (3) bicyclic amine alkaloid anatoxin-a, (4) cyclic N-hydroxyguanine organophosphate anatoxin-a(S), (5) carbamate alkaloids saxitoxins. These compounds have been identified, and their toxicity and ecotoxicity have been at least partially characterized and understood, which allowed for an assessment and management of health risks associated with human exposures via cyanotoxin-contaminated drinking or recreational water, or cyanotoxin-contaminated food or food supplements (Buratti et al., 2017; Miller et al., 2017).

Tumor promotion and carcinogenesis represent an adverse outcome, which might be affected by exposure to toxic cyanobacteria, since increased incidence of liver or colorectal cancers have been associated with increased occurrence of cyanobacterial water blooms and cyanotoxins, such as microcystin-LR (Svircev et al., 2017). **Microcystin-LR** has been recognized as a liver tumor promoter (Buratti et al., 2017), currently classified as a possible human carcinogen (Class 2B) by International Association for Research on Cancer (Grosse et al., 2006). Another cyanotoxin linked to carcinogenesis is cytotoxic and genotoxic **cylindrospermopsin** (Buratti et al., 2017). As discussed in the **Chapter 3**, inhibition of GJIC is strongly associated with carcinogenic process, especially its tumor promotion phase (Czyz et al., 2017; Trosko, 2017, 2011; Trosko et al., 2004).

In addition to these well-recognized cyanotoxins, cyanobacteria can produce hundreds of **other secondary metabolites** (e.g. various peptidic, lipopeptidic, heterocyclic aromatic compounds) and **other components of cyanobacterial biomass** (such as cyanobacterial LPS), which were shown to be **bioactive**, but they are usually not considered in toxicological studies or risk assessment of cyanobacteria (Buratti et al., 2017; Dittmann et al., 2015; Méjean and Ploux, 2013). However, many *in vitro* as well as *in vivo* studies repeatedly demonstrated that the toxicity of complex cyanobacterial extracts does usually not correspond to the content of the known and identified cyanotoxins (Burýšková et al., 2006; Hrouzek et al., 2016; Palíková et al., 2007; Smutna et al., 2014), which indicates that there are **other not-yet-identified compounds of cyanobacterial origin** contributing to the toxicity of cyanobacterial biomass.

We used *in vitro* assessment of GJIC to evaluate tumor-promoting potential of cyanobacterial extracts in a rat liver epithelial cells WB-F344 (Bláha et al., 2010) [**Attachment VIII**]. **GJIC was found to be rapidly inhibited (<30 min)** by methanolic **extracts from natural water blooms** dominated by common water bloom-forming cyanobacterial species: *Aphanizomenon flos-aquae* (most pronounced effects), *Planktothrix aghardii*, *Microcystis aeruginosa* and *Woronichinia naegeliana* (least effective) (**Figure 21**). Similar effects were observed also with extracts from **laboratory single strain cultures** of *Aph. flos-aquae* CCALA008 and *M. aeruginosa* PCC7806, while extracts from

cultures of heterotrophic Gram negative bacterium *Klebsiella terrigena* CCM3568 or green alga *Chlamydomonas reinhardtii* UTEX2246 had only weak or no effects on GJIC (Figure 21). Similarly, **MAPK ERK1/2 was activated** only by extracts from cyanobacteria, but neither by bacterial nor green algal extract (Figure 21). Apparently, the effects on GJIC did not correlate with the content or production of microcystins, which were detected only in *M. aeruginosa* and *P. aghardii* extracts, but not in GJIC-inhibiting and MAPK-activating extracts from *Aphanizomenon* sp. or *Woronichinia* sp. (Bláha et al., 2010) [Attachment VIII]. Moreover, pure cyanotoxins microcystin-LR and cylindrospermopsin, had no effects on GJIC or MAPKs. This study thus provided **the very first evidence on the existence of novel cyanobacterial metabolites exhibiting in vitro tumor promoting potential** (Bláha et al., 2010) [Attachment VIII].

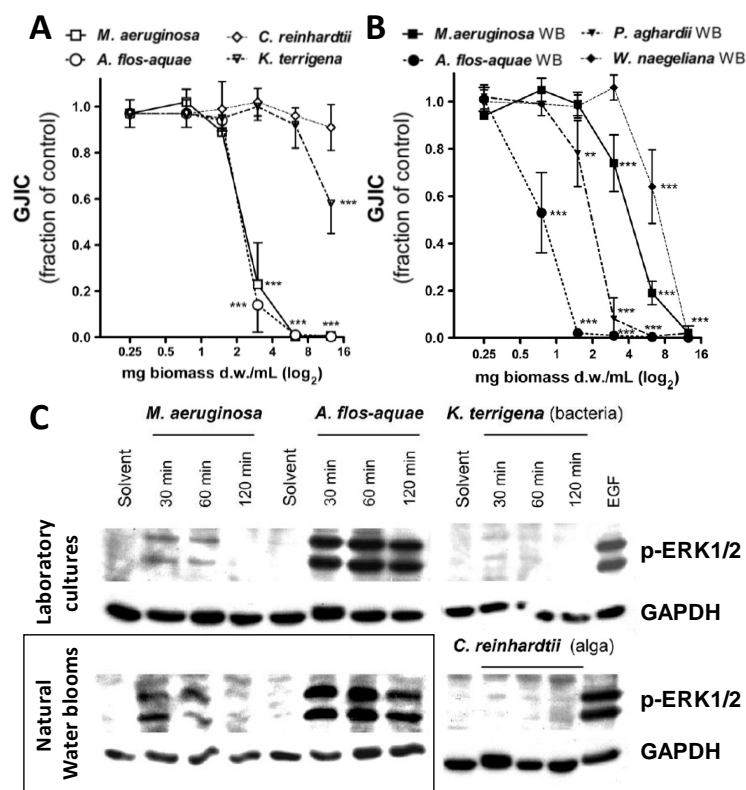


Figure 21: Effects of cyanobacterial extracts on GJIC and MAPK ERK1/2 in rat liver epithelial cells WB-F344. (A) GJIC inhibition (30 min) by extracts of laboratory cultures of cyanobacterium *Microcystis aeruginosa* PCC7806 and *Aphanizomenon flos-aquae* CCALA008, green alga *Chlamydomonas reinhardtii* UTEX2246 and bacterium *Klebsiella terrigena* CCM3568; (B) GJIC inhibition (30 min) by extracts of natural water blooms (WB) dominated by *M. aeruginosa*, *A. flos-aquae*, *Planktothrix aghardii* and *Woronichinia naegeliana*; (C) effects of extracts of cyanobacterial, green alga and bacterium laboratory culture and cyanobacterial water bloom on MAPK ERK1/2 (30 min). GJIC was evaluated by SL-DT assay, MAPK-ERK1/2 activation by Western blotting. EGF – epidermal growth factor (5 ng/ml, 30 min). Adapted from (Bláha et al., 2010) [Attachment VIII].

In the following study, GJIC-inhibitory potencies were evaluated in a broader set of ten cultured cyanobacterial strains, as well as in six samples of natural water blooms (Nováková et al., 2011) [Attachment IX]. The effects on GJIC were evaluated not only for the extracts, but in the case of cultures also for their exudates, i.e. cell-free spent culture medium, which was concentrated and purified by solid phase extraction (Oasis HLB and activated carbon). This step was supposed to reduce the complexity of the tested samples and possibly narrow down the fraction containing GJIC-inhibiting metabolites. The results showed, that extracts from natural water blooms effectively inhibited GJIC (Figure 22). The extracts from laboratory cultures of *Anabaena flos-aquae* UTEX1444, *Aph. flos-aquae* SAG 31.87, *Aphanizomenon gracile* RCX06, *M. aeruginosa* PCC 7806 (microcystin-producing), *Cylindrospermopsis raciborskii* SAG 1.97, *Planktothrix aghardii* CCALA159 (microcystin-producing) and SAG 32.79 (microcystin-producing) also rapidly inhibited GJIC, whereas much weaker effects were induced by *Aphanizomenon klebahnii* CCALA 009 and no inhibition was induced by extracts of *Aph. flos-aquae* PCC7905 (cylindrospermopsin-producing) and *Aph. gracile* SAG 31.79 (Figure 22). The exudates from laboratory cultured strains also inhibited GJIC, but their activity did not clearly correspond to the activity of the

extracts, since the most potent effects were induced by *Aph. flos-aquae* PCC 7905 and SAG 31.87, *Aph. gracile* RCX06 and SAG 31.79, *C. raciborskii* SAG 1.97 and *M. aeruginosa* PCC7806 (Figure 22). Apparently, GJIC-inhibiting chemicals can be released from cyanobacterial cells to the surrounding medium. In agreement with the previous study, no correlation with microcystin or cylindrospermopsin content in the extracts or exudates was found. These results indicate that putative tumor promoting compound(s) inhibiting GJIC can be associated with a wide range of different species of bloom-forming cyanobacteria, but the production as well as distribution of these compounds between the intracellular (extracts) and extracellular (exudates) compartments in the cultures are obviously

species- and strain- specific, which could explain the lack of clear relationship between toxicities of extracts and exudates. Also, the possibility that different agents were responsible for the effects of extracts and exudates cannot be excluded, as well as the modulation of the observed effects by other compounds present in the extract or exudate (Nováková et al., 2011) [Attachment IX]. The exudate of *C. raciborskii* SAG 1.97, which induced very pronounced effects on GJIC, was then fractionated by semi-preparative reversed phased HPLC, and the collected fractions assessed for GJIC inhibition (Nováková et al., 2013). The most activity was associated with two non-polar fractions, which were further fractionated and evaluated for their GJIC inhibiting potencies. The final LC-high resolution MS analyses of the bioactive subfractions identified a chemical compound with a molecular formula $C_{18}H_{34}O_3$, whose presence was associated with the subfractions inhibiting GJIC. The experiments with signal pathway inhibitors revealed, that the compound was inhibiting GJIC via EGFR- and MEK-ERK1/2-depedent mechanism (Nováková et al., 2013), i.e. through a different pathway than common among different environmental toxicants, such as low molecular weight PAHs or PCBs (Sovadinová et al., 2015) [Attachment IV].

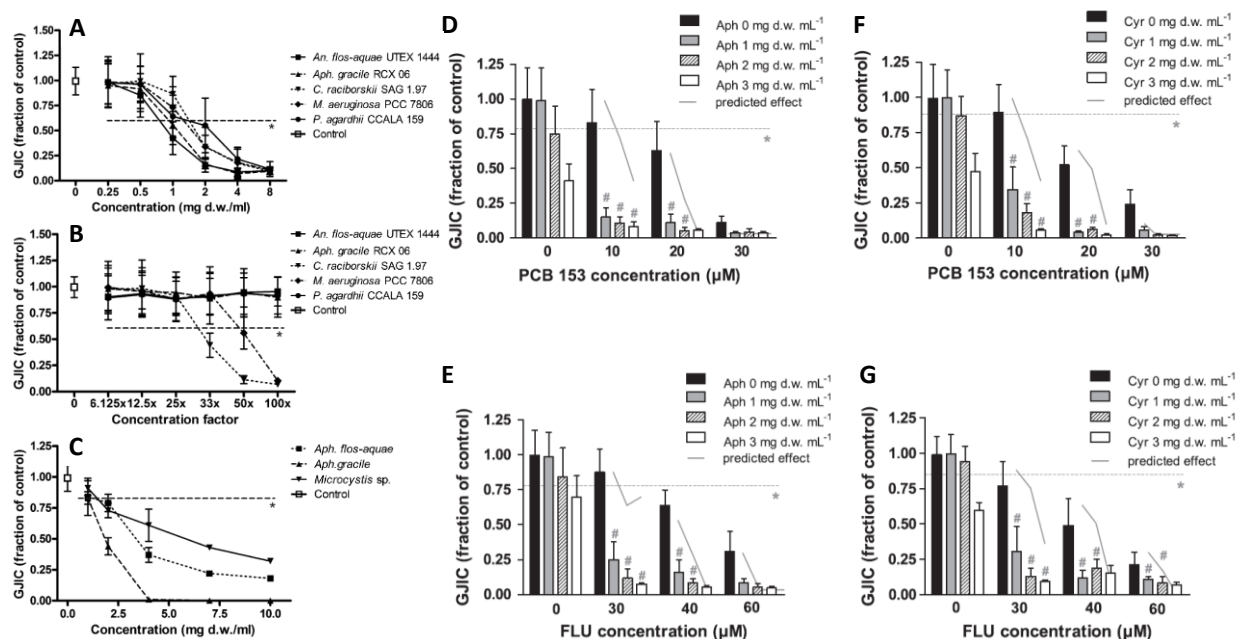


Figure 22: Effects of cyanobacterial extracts and exudates on GJIC and their potentiation by co-exposure with anthropogenic contaminants in rat liver epithelial cells WB-F344. GJIC-inhibiting effects of (A) extracts and (B) exudates of several cyanobacterial strains and (C) extracts of water blooms dominated by different cyanobacterial species; synergistic effects of cyanobacterial extracts from (D-E) *Aphanizomenon gracile* RCX06 or (F-G) *Cylindrospermopsis raciborskii* SAG 1.97 and anthropogenic contaminants (D, F) PCB153 or (E, G) fluoranthene. Exposure time was 30 min in all experiments. GJIC was evaluated by SL-DT assay. Asterisks indicate significant difference from the solvent control, crosses indicate significant difference from the values predicted by an effect-addition model. D.w. - dry weight. Adapted from (Nováková et al., 2011) [Attachment IX] and (Nováková et al., 2012) [Attachment X].

Since there is an evidence that **exposures to toxic cyanobacteria enhance effects of other non-cyanobacterial environmental toxicants and stressors**, such as heavy metals or viral infections (Pikula et al., 2010), or pesticides (Cerbin et al., 2010), we also investigated GJIC-inhibiting potencies of cyanobacterial extracts and cyanotoxins in mixtures with well-recognized environmentally relevant inhibitors of GJIC, fluoranthene and PCB153 (Nováková et al., 2012) [Attachment X]. A binary mixture of PCB 153 with fluoranthene was found to elicit a simple additive effect on GJIC, which further supports the information on the similar mechanism of GJIC dysregulation by these two chemicals, i.e. through the PC-PLC-dependent pathway (Sovadinová et al., 2015) [Attachment IV]. Similarly, the effects of binary mixture of extracts from two cyanobacterial strains, *Aph. gracile* RCX06 and *C. raciborskii* SAG 1.97, were also additive. The effects of extracts or anthropogenic contaminants on GJIC were not modulated by microcystin-LR (up to 100 μ M) and cylindrospermopsin (up to 60 μ M), which further indicated that these cyanotoxins do not target GJIC in the rat liver epithelial cells WB-F344 (Novakova2012) [Attachment X]. However, the **binary mixtures of anthropogenic contaminants (PCB 153 or fluoranthene) and cyanobacterial extracts (Aph.**

gracile or *C. raciborskii*) induced significant synergistic effects on GJIC (Figure 22). Nearly complete GJIC inhibition could be observed in the binary mixtures of such concentrations of the individual components, which separately did not cause any significant effect (Figure 22). While mixture toxicity of various environmental contaminants is being intensively studied, most studies are dealing with mixtures of chemicals sharing some general similarity or mechanism of action, whereas experiments with mixtures containing widely divergent components (e.g., organics vs. metals) or chemicals in a combination with non-chemical stressors are much less common (Nováková et al., 2012) [Attachment X].

In addition to the first information about alterations of this type of tumor promotion-relevant events by novel types of metabolites, our studies provided new evidence on toxic interactions between cyanobacterial metabolites and environmental anthropogenic contaminants, and thus highlighted the importance of combined toxic effects of chemicals in complex environmental mixtures.

4.5.2 EFFECT-BASED EVALUATION OF WATER TREATMENT TECHNOLOGIES

Occurrence of toxic cyanobacteria in aquatic ecosystems presents a challenge to drinking water treatment facilities producing drinking water from cyanobacteria-contaminated surface water. Although different risk management strategies have been suggested and elaborated to minimize human health risks caused by cyanobacteria and their toxins in drinking water (He et al., 2016; Merel et al., 2013; Sklenar et al., 2016; Westrick et al., 2010), they have primarily focused on the elimination of cyanobacterial biomass or removal of the selected well-identified cyanotoxins. However, the existing treatment techniques and strategies should be evaluated not only for their efficiency (i) to remove targeted priority pollutants (e.g. microcystins or cylindrospermopsin in the case of cyanobacterial toxins), but also (ii) to eliminate other potentially harmful and toxic components of the complex material which may not be fully chemically characterized; and (iii) to form of new harmful metabolites / toxic by-products during the application of the water treatment technology (Prasse et al., 2015). Thus, the use of complementary chemical and biological tools (i.e. instrumental analyses and effect-based bioassays) in the monitoring plans is encouraged (Maier et al., 2015; Wernersson et al., 2015). *In vitro* assessment of GJIC has been successfully used along with chemical analysis as a principal bioassay to study tumor promoting activity of water chlorination by-products (Hakulinen et al., 2004; Nishikawa et al., 2006) or to assess the efficiency of removing different anthropogenic contaminants and their toxic by-products with ozone, including PAHs (Herner et al., 2001; Luster-Teasley et al., 2005, 2002; Upham et al., 1995) and various pesticides (Masten et al., 2001; Upham et al., 1997; Wu et al., 2007).

Since toxic cyanobacteria seem to be generally capable of producing not only well-recognized tumor promoting microcystins, but also other water soluble but not-yet fully identified compounds shown to inhibit GJIC and activate MAPK ERK1/2 (Bláha et al., 2010; Nováková et al., 2012, 2011) [Attachment VIII-X], we decided to use GJIC and MAPK evaluation to compare the efficacy of two commonly used drinking water treatment technologies, chlorination and ozonation, for reducing tumor promoting potential of cyanobacterial extract of natural water bloom of *M. aeruginosa* (Sovadinová et al., 2017a) [Attachment XI]. The chemical analyses showed that ozone effectively removed microcystins in the extract and reduced its ability to inhibit GJIC and activate MAPK ERK1/2 in WB-F344 cells (Figure 23). Chlorination leading to a comparable decrease of total organic carbon in the extract was much less effective in both removing microcystins and reducing the effects on GJIC. Moreover, activation of ERK1/2 actually slightly increased in the extracts treated with a high chlorine dose, indicating a possible formation of toxic by-products. Both treatment techniques were less effective in reducing on MAPK p38 activation by the extract (Sovadinová et al., 2017a) [Attachment XI]. Our study thus points to the advances of ozonation approach and demonstrates that *in vitro* evaluation of GJIC and MAPKs represent a simple and sensitive bioassay for assessment of tumor promoting potential of complex cyanobacterial extracts, which is also suitable for effect-based studies focusing on the elimination of these hazardous properties of contaminated water.

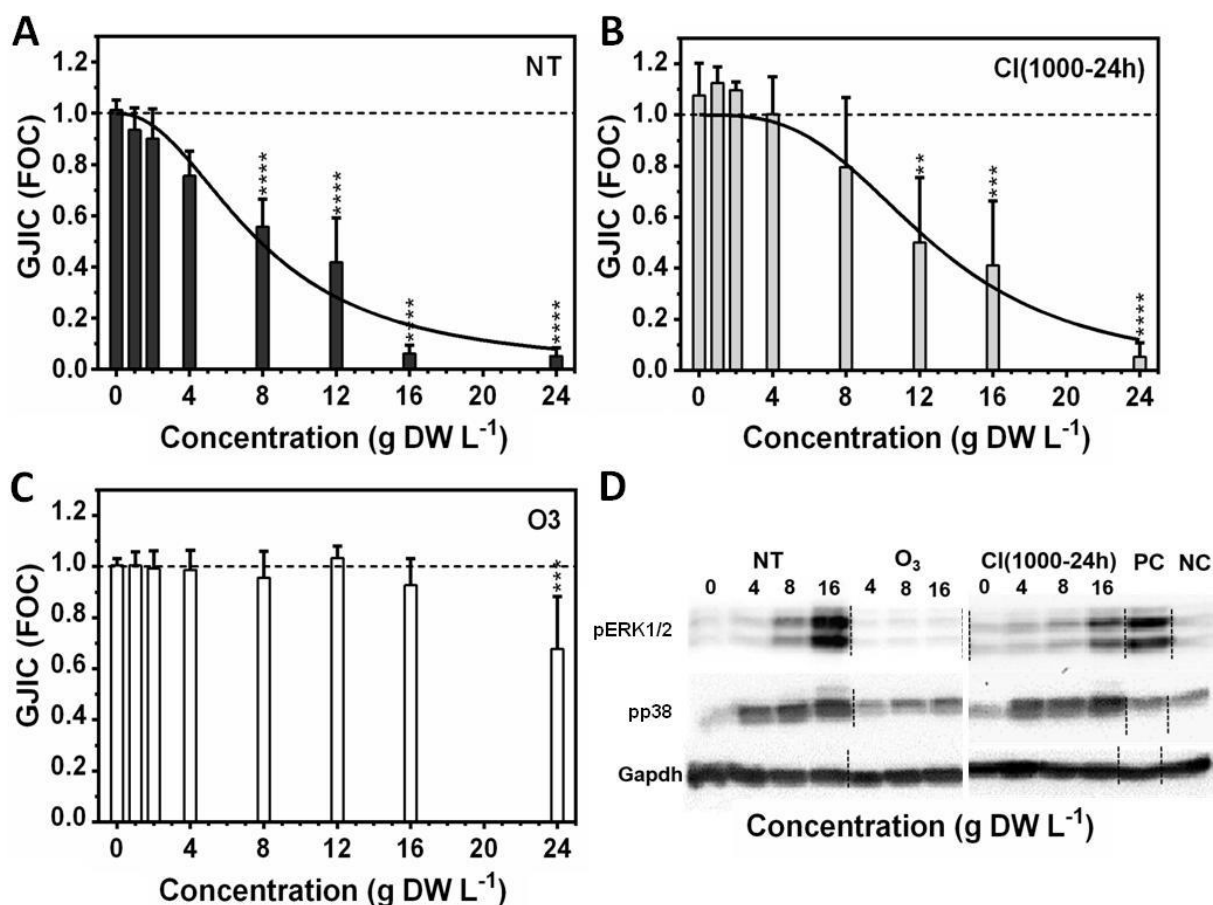


Figure 23: Effects of complex and chlorine- or ozone-treated cyanobacterial extract on GJIC and MAPKs in rat liver epithelial cells WB-F344. Inhibition of GJIC by (A) non-treated (NT) extract of *Microcystis aeruginosa* water bloom, (B) extract treated with a chlorine dose of 1000 mg/L for 24 h (Cl(1000-24h)), and (C) ozone-treated extract (5 mg/L, 1 L/min for 30 min); (D) activation of MAPK ERK1/2 and p38 by non-treated and treated cyanobacterial extracts. Effects were evaluated after 30 min exposure. GJIC was evaluated by SL-DT assay, MAPK activation by Western blotting. DW - dry weight; PC - positive control (12-O-tetradecanoyl phorbol-13-acetate, 10 nM, 30 min). Adapted from (Sovadinová et al., 2017a) [Attachment XI].

4.6 GJIC ASSESSMENT IN PHARMACOLOGICAL AND BIOMEDICAL RESEARCH

With the increasing evidence on the critical role of connexins and pannexins in the etiology of different human diseases (Chapter 3), there is an extensive research exploiting potential use of connexins and pannexins in various clinical applications. This includes eventual use of GJIC, connexins and pannexins either as diagnostic markers, or considering them as a therapeutic targets in human disease prevention, protection or treatment (Delmar et al., 2017; Willebrords et al., 2017). Several recent reviews discussed in the detail the clinical and therapeutic potential of connexins in the diagnosis and therapies of **retinal** (Danesh-Meyer et al., 2016; Jiang, 2010), **cochlear** (Lilly et al., 2016; Xu and Nicholson, 2012), **skin** (van Koppen and Hartmann, 2015), **neural** (Hu et al., 2015; Schulz et al., 2015; Seki et al., 2015; Tribulova et al., 2015), **cardiovascular** (Dempsey et al., 2015; Freund-Michel et al., 2016), **respiratory** (Hills et al., 2015; Sala et al., 2016), **liver** (Crespo Yanguas et al., 2016; Maes et al., 2015b; Vinken, 2012), **gastrointestinal** and **reproductive** (Chevallier et al., 2013a, 2013b; Christman, 2015), **oncogenic** (Czyz et al., 2017; Jiang and Penuela, 2016; Leone et al., 2012) **diabetic** (Cigliola et al., 2013; Farnsworth and Benninger, 2014; Goudis et al., 2015; Perez-Armendariz, 2013) and **wound healing** (Kleopa and Sargiannidou, 2015; Masaki, 2015;

Moinfar et al., 2014; Moore and O'Brien, 2015; Takeuchi and Suzumura, 2014; Xie et al., 2015) diseases and disorders .

In vitro assessment of connexins and GJIC could be then effectively used to screen for medically or pharmacologically interesting compounds which are able to **modulate GJIC and other connexin functions in a desired manner** (Willebrords et al., 2017), such as blocking the cell-cell communication in order to reduce propagation of injury during ischemia (Lee et al., 2015; Li et al., 2003) or to alter specific protein interactions (Dukic et al., 2017). Furthermore, *in vitro* assessment of GJIC in the **cells representing a specific diseased phenotype** can be utilized to evaluate the ability of pharmacological agents or other medical treatments to **induce or restore connexin-dependent functions** of a normal healthy cell or tissue. Since **cancer** represents a prime example of a disease which has been strongly linked to the impairment of connexin expression and function (**Chapter 3**), it was shown that *in vitro* assessment of GJIC can be effectively utilized in the screening for chemopreventive dietary or pharmaceutical agents capable to **attenuate GJIC-inhibiting effects of chemical tumor promoters in normal cells or restore GJIC in cancer cells** (Leone et al., 2012).

4.6.1 SCREENING FOR CANCER CHEMOPREVENTIVE AGENTS

Tumor promotion phase of cancer is typically associated with a dysregulation of GJIC, and chemical tumor promoters, mitogenic chemicals and stimuli were found to be potent inhibitors of GJIC (Leone et al., 2012; Trosko, 2017; Vinken et al., 2009). Since tumor promotion represents a reversible and rate-limiting step of cancer, it provides a window of opportunity for lowering the risks of cancer by dietary chemoprevention or eventually by therapeutic interventions with synthetic drugs. Various dietary chemicals or synthetic drugs with known **chemopreventive activity have been found to prevent tumor promoter-induced dysregulation of GJIC**, which might represent an important mechanism contributing to their chemopreventive effects (Leone et al., 2012). While most of the studies reporting that chemopreventive agents can attenuate chemically-induced inhibition of GJIC were done with model tumor promoters, such as TPA, butylated hydroxytoluene or hydrogen peroxide (Leone et al., 2012), there is much less information about the **interactions of chemopreventive agents with environmental tumor promoters and toxicants**. It has been reported that **oleoresins from tomato and grape seed extract** can prevent inhibition of GJIC induced by mercury chloride (Leone et al., 2010; Zefferino et al., 2008); **salidroside** blocked effects of cadmium (Zou et al., 2015); **chaetoglobosin K** can attenuate the effects of endosulfan and dieldrin (Matesic et al., 2001); **quercetin** effects of DDT (Warngard et al., 1987); a **green tea extract and its constituents** can block inhibition of GJIC induced by DDT (Sigler and Ruch, 1993); paraquat, phenobarbital (Ruch et al., 1989) or dimethylnitrosamine (Takahashi et al., 2004).

After the initial reports that **resveratrol**, a dietary phytoalexin and well-recognized chemopreventive agent, can attenuate inhibition of GJIC elicited by **TPA** (Nielsen et al., 2000), it has been also reported that resveratrol blocks also inhibition of GJIC induced by **dicumylperoxide** (Upham et al., 2007). Our further *in vitro* experiments with WB-F344 cells revealed that resveratrol can attenuate also GJIC inhibition induced by **PFOA** (Upham et al., 2009) [**Attachment VII**]. Moreover, the survey of **25 different inhibitors of GJIC** showed that resveratrol had significant preventive effects on the GJIC inhibiting activity of all chemicals dysregulating GJIC via a PC-PLC-dependent mechanism, a MEK-ERK1/2-dependent mechanism, or a combined MEK-ERK1/2 and PC-PLC-dependent mechanism (**Figure 13**), whereas compounds dysregulating GJIC through an alternative pathways were not affected by resveratrol with the exception of alachlor (Sovadinová et al., 2015) [**Attachment IV**]. These findings strongly suggest that **resveratrol might be targeting PC-PLC pathway** and thus preventing GJIC inhibition caused by PC-PLC-dependent inhibitors, as well as to interfere with most likely **redox-dependent activation of MAPK ERK1/2 pathway**, which could explain its preventive activity towards MEK-ERK1/2-dependent inhibitors of GJIC (Upham et al., 2009). In agreement with this hypothesis, the effects of **methoxychlor and vinclozolin**, which represent other PC-PLC-dependent inhibitors of GJIC (Babica et al., 2016c) [**Attachment V**], were also found to be attenuated by resveratrol (**Figure 14**). Finally, the preventive effects of resveratrol against 1-methylanthracene-induced inhibition of GJIC observed in rat liver epithelial cells WB-F344 (Sovadinová et al., 2015) [**Attachment IV**] were confirmed also in a **human relevant in vitro model of adult human liver stem cells HL1-1** (**Chapter 4.3, Figure 19**).

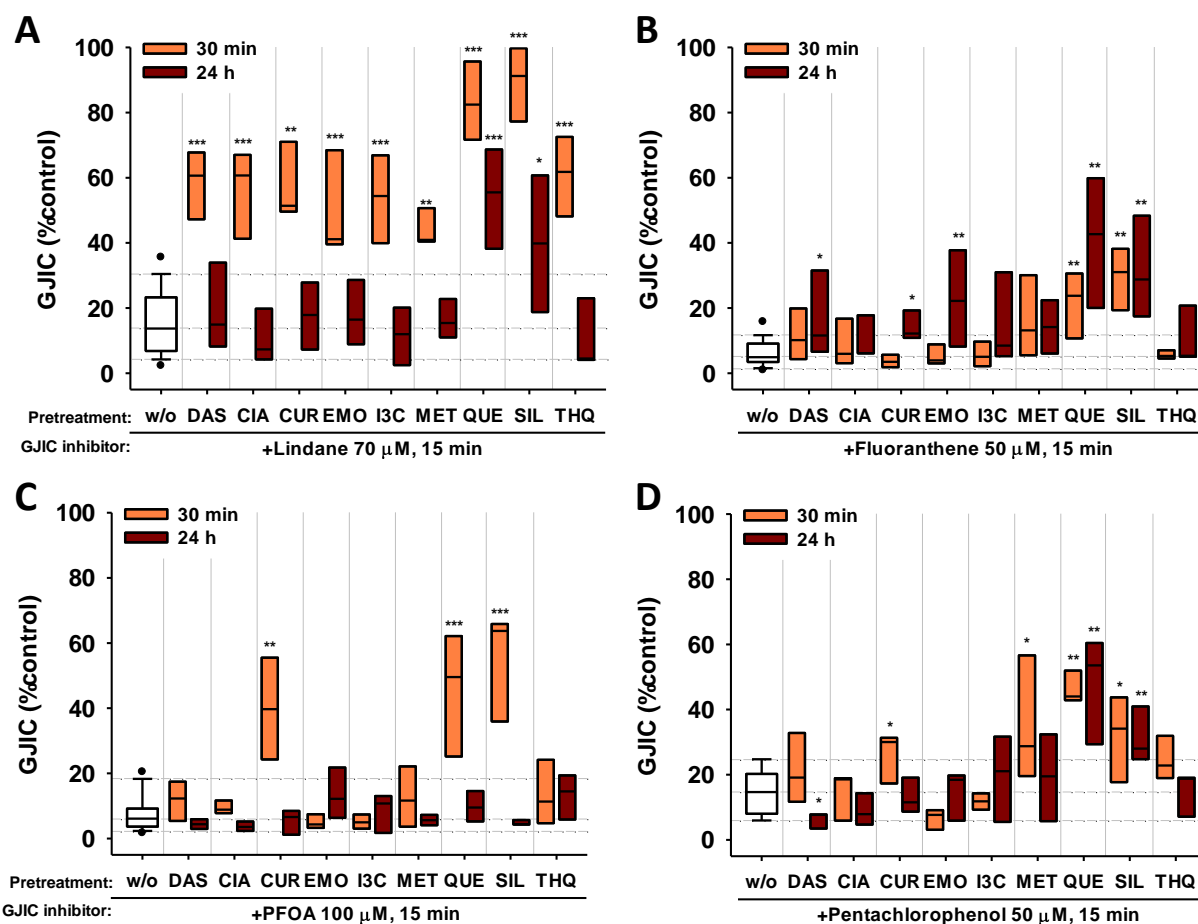


Figure 24: Chemopreventive agents attenuated inhibition of GJIC induced by environmental toxicants in rat liver epithelial cells WB-F344. (A) Lindane, MEK-ERK1/2-dependent dysregulator of GJIC; (B) Fluoranthene, PC-PLC-dependent dysregulator of GJIC; (C) PFOA, both MEK-ERK1/2-dependent dysregulator of GJIC; (D) Pentachlorophenol, MEK-ERK1/2- and PC-PLC-independent dysregulator of GJIC. Prior the addition of GJIC inhibitor, the cells were pretreated for 30 min or 24 h with allylsulfide (DAS, 500 μ M), cinnamic acid (CIA, 100 μ M), curcumin, (CUR, 1 μ M), emodin (EMO, 10 μ M), indole-3-carbinol (I3C, 10 μ M), metformin (MET, 1000 μ M), quercetin (QUE, 100 μ M for 30 min or 25 μ M for 24 h), silibinin (SIL, 100 μ M for 30 min or 50 μ M for 24 h), thymoquinone (THQ, 10 μ M). Data represent medians, 25th and 75th percentiles (boxes), 10th and 90th percentiles (whiskers) of at least three independent experiments. Dashed horizontal lines indicate median value, 25th and 75th percentile of the treatment with GJIC inhibitor only (w/o). Values significantly different from the treatment with GJIC inhibitor only are labeled by asterisks. Adapted from (Babica et al., 2016a) [Attachment XII].

Following these experimental results, we conducted another study to investigate whether also other chemopreventive agents can prevent inhibition of GJIC induced by environmental toxicants, and whether their eventual preventive effects will depend on the GJIC inhibitor or its mechanism of GJIC dysregulation (Babica et al., 2016a) [Attachment XII]. The tested chemopreventive agents included nine commercially available chemicals previously implicated in cancer chemoprevention: **polyphenols quercetin, silibinin and curcumin, simple phenol indol-3 carbinol, quinones thymoquinone and emodin, unsaturated aromatic carboxylic acid cinnamic acid, the organosulphurcompound diallyl sulfide, and an antidiabetic drug, biguanide metformin**. Rat liver epithelial cells WB-F344 were pretreated for 30 min or 24 h with a chemopreventive agent and then a GJIC inhibitor was added for additional 15 min. Six different GJIC inhibitors were used, namely **TPA, lindane** (both MEK-ERK1/2-dependent inhibitors of GJIC), **fluoranthene, DDT** (both PC-PLC-dependent inhibitors), **PFOA** (mixed MEK-ERK1/2-dependent inhibitor of GJIC) and **pentachlorophenol** (neither MEK-ERK1/2- nor PC-PLC-dependent inhibitor of GJIC). All chemopreventive chemicals were able to attenuate the effects of at least one GJIC inhibitor, namely lindane (Figure 24). Quercetin and silibinin elicited the most pronounced effects, preventing the dysregulation of GJIC by all the GJIC-inhibitors but DDT (Babica et al., 2016a) [Attachment XII]. Metformin and curcumin attenuated the

effects of three GJIC-inhibitors, whereas the other chemopreventive agents prevented the effects of two (diallyl sulfide, emodin) or one (indole-3 carbinol, thymoquinone) GJIC-inhibitor. The effects of MEK-ERK1/2-dependent inhibitors of GJIC were more effectively prevented by shorter pre-treatment with chemopreventive chemicals (e.g. lindane, **Figure 24A**), while longer incubation induced more pronounced effects on PC-PLC-dependent inhibitors, such as fluoranthene (**Figure 24B**). Preventive effects of chemopreventive agents were apparently dependent on the type of compound (its chemistry, structure and mode probably of action) as well as on the type of GJIC-inhibitor and its mechanism of GJIC dysregulation (Babica et al., 2016a) [**Attachment XII**]. This indicates that the chemopreventive effects were mediated through specific modulations of different signaling pathways involved in GJIC control, rather than being a result of a generally shared biochemical or molecular mechanism. Such prevention of inhibition of GJIC induced by environmental toxicants represents an important mechanism contributing to the chemopreventive activity of dietary chemicals and supplements during tumor promotion, when the effects of environmental and food toxicants can be counteracted by co-exposure to chemopreventive agents from diet or dietary supplements, and thus lowering the cancer risks. Significant attenuation of chemically induced inhibition of GJIC was observed in 27 (50%) out of 54 possible combinations of nine chemopreventive agents with six GJIC inhibitors (Babica et al., 2016a) [**Attachment XII**], which demonstrates that ***in vitro* evaluations of GJIC could be used as an effective tool for screening of chemicals for chemopreventive activity.**

Cancer or transformed cells where **GJIC levels were reduced due to an oncogenic event** can be also utilized in the screening for chemopreventive and anticancer compounds. WB-ras cell line represents a genetically engineered cell line, which was derived from normal WB-F344 cells by overexpressing **H-ras oncogene** (Defejter et al., 1990). **Normal WB-F344 cells** have a functional Cx43-mediated GJIC, exhibit contact inhibition of growth, have a low ability to growth on soft agar, and are non-tumorigenic *in vivo*. On the other hand, **neoplastically transformed WB-ras cells** have a typical diseased phenotype of cancer cells, including an aberrant expression, localization and phosphorylation of Cx43, low level of GJIC, lack of contact growth inhibition, ability to grow on soft agar and formation of metastazing tumors *in vivo* (Defejter et al., 1990; Hayashi et al., 1998). Chemopreventive compounds such as **lovastatin** (Ruch et al., 1993), **caffeic acid phenylester** (Lee et al., 2004; Na et al., 2000), **4-phenyl-3-butenic acid** (Burns et al., 2015; Sunman et al., 2004), **suberoylanilide hydroxamic acid** and **trichostatin A** (Ogawa et al., 2005) were found to increase GJIC in WB-ras cells. In our recent research, we have found that GJIC in

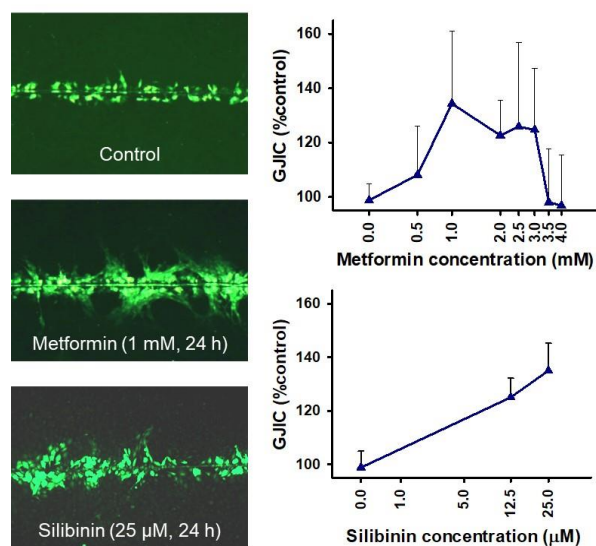


Figure 25: Chemopreventive agents restored oncogene-inhibited GJIC in WB-ras cells. WB-F344 cells transformed by H-ras oncogene were exposed to metformin or silibinin for 24 h, GJIC was evaluated by SL-DT assay. Adapted from a diploma thesis supervised by P. Babica (Lenčešová, 2012) and a conference proceeding co-authored by P. Babica (Čtveráčková et al., 2017), paper in preparation.

WB-ras cells can be also restored for example by **silibinin**, a flavonoid from milk thistle seeds, or biguanide **metformin** (**Figure 25**) (Čtveráčková et al., 2017; Lenčešová, 2012). Furthermore, *in vitro* assessment of GJIC in WB-ras cells can be effectively used also as the principal method in **bioassay-guided fractionation** for identification of the active components and chemicals in the **bioactive extracts from various natural products**. This approach was applied to identify β -sitosterol as an active compound in psyllium extract which was responsible for the restoration of GJIC in WB-ras cells (Nakamura et al., 2005, 2004). We are currently using WB-ras cell line and semi-automated / semi-high throughput multiparametric assay optimized in our lab for the simultaneous evaluation of GJIC, cell proliferation and viability (**Figure 9**) in screening for chemopreventive activities of compounds, which were recently isolated from *Paulownia tomentosa* fruits (Hanakova et al., 2015) or from zooxanthellate jellyfish *Cotylorhiza tuberculata* (Leone et al., 2015, 2013). **High-throughput *in vitro* assessment of GJIC could be thus used for evaluation of chemopreventive and anticancer potential of known chemical entities, or for identification of new bioactive compounds in the complex matrices.**

4.6.2 DEVELOPMENT OF NEW BIOMEDICAL APPLICATIONS

In addition to drug discovery and screening for new pharmacologically relevant chemicals or treatments, GJIC assessment can be also utilized in biomedical research of molecular and cellular mechanisms **which might be targeted by perspective therapeutic procedures or treatments, or for evaluation of potential unwanted side effects of new therapies and biomedical applications.**

Single-walled carbon nanotubes (SWCNTs) represent a class of material with extraordinary mechanical, electrical, optical and thermal properties, with a wide variety of possible applications including biomedical field (Liang and Chen, 2010). SWCNTs are being investigated as near-infrared optical **biosensors, bioprobes, molecular imaging contrast agents, photothermal therapy enhancers,** as well as **drug carriers** to specifically deliver various

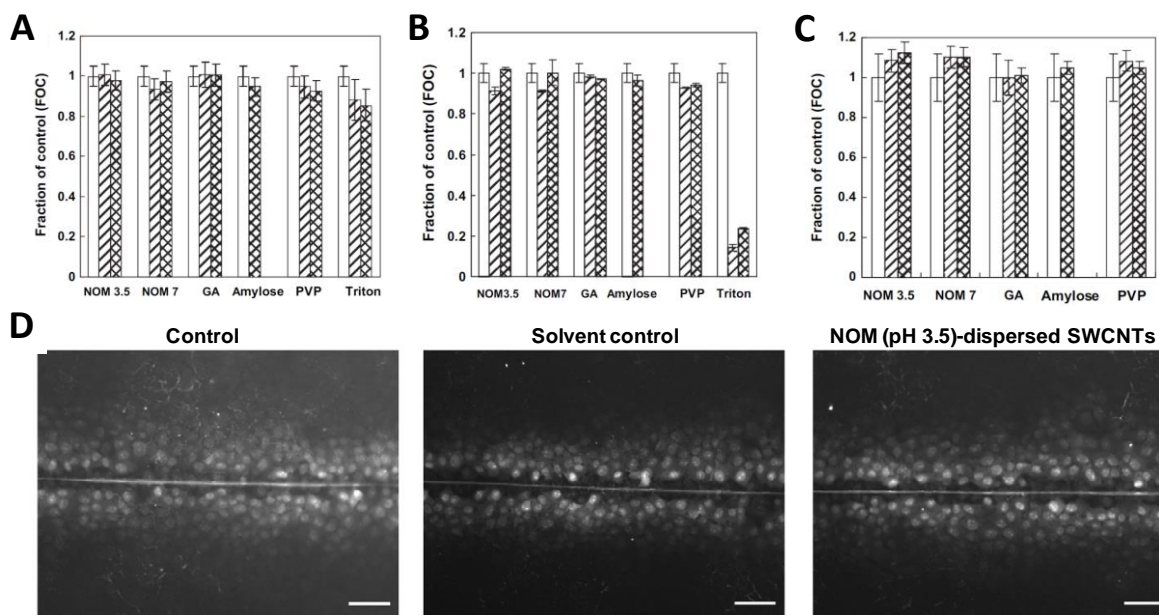


Figure 26: In vitro effects of dispersed single-walled carbon nanotubes (SWCNTs). (A) Effects on viability of *Escherichia coli* (48 h exposure in LB medium), (B) viability of rat liver epithelial cells WB-F344 (neutral red dye uptake, 24 h exposure), and (C) GJIC in WB-F344 cells (24 h exposure) and (D) representative images of GJIC assessment. Labels of x-axis indicate the dispersant type: Suwannee River Natural Organic Matter (NOM) with pH 3.5 (NOM3.5) or pH 7 (NOM7); arabic gum (GA); polyvinyl pyrrolidone (PVP); Triton X-100 (Triton). Open bars correspond to non-treated controls, hatched bars correspond to solvent controls, and cross-hatched bars correspond to dispersed SWCNTs. Adapted from (Alpatova et al., 2010) [Attachment XIII].

anticancer drugs, proteins and nucleic acids to the diseased tissues and maximize the bioavailability of the drugs by improving solubility and increasing circulation time (Gao et al., 2016; Jain et al., 2015; Liang and Chen, 2010). However, the use of SWCNTs is impeded by their **low solubility** in polar solvents and their tendency to aggregate in aqueous solutions including biological fluids and liquids. Another issue complicating biomedical applications of SWCNTs is associated with their highly reactive surface, which provides a great opportunity for a variety of surface modifications, but might result into eventual **unintentional deleterious interactions with biomolecules, cells and tissues** (Gao et al., 2016). There have been different strategies and approaches aiming to increase solubility of SWCNTs in aqueous solutions, as well as to suppress toxicity of SWCNTs. **Non-covalent functionalization of SWCNTs** is an effective strategy which aids the dispersion process of SWCNTs in aqueous medium but minimizes changes in their electrical or mechanical properties. In our study, SWCNTs were functionalized by different dispersants, including arabic gum, Triton X-100, amylose, natural organic matter from Suwannee River, and polyvinyl pyrrolidone (Alpatova et al., 2010) [Attachment XIII]. These dispersing agents allowed to prepare SWCNTs suspensions where charge and the average effective hydrodynamic diameter of suspended SWCNTs as well as the concentration of exfoliated SWCNTs in the dispersion remained relatively stable over a period of 4 weeks (Alpatova et al., 2010) [Attachment XIII]. The **functionalized and dispersed SWCNTs were not cytotoxic for**

Escherichia coli (3-48 h exposure) or rat liver epithelial cells WB-F344 (30 min-24 h exposure), with the exception of SWCNTs dispersed in Triton X-100, where the dispersing agent itself elicited toxic effects, as apparent from the solvent control treatments (Figure 26). Dispersions of SWCNTs also did not alter with GJIC in WB-F344 cells (Figure 26), a critical process for the maintenance of tissue homeostasis. **Non-covalent functionalization of SWCNTs with non-toxic dispersants was found to be a useful method for the preparation of stable aqueous suspensions of SWCNTs, which seemed to be biocompatible and thus potentially suitable for biomedical applications** (Alpatova et al., 2010) [Attachment XIII].

Pulsed electric fields (PEFs) have been recognized to induce **different biological effects depending on pulse duration and field strength**. Pulses in the range of **milli- to microseconds** primarily affect the outer membrane, while shorter pulses with duration in the **nanosecond range (nsPEFs)** have a more pronounced effect on **intercellular structures**. Treatments with nsPEFs were found to **inhibit tumor growth** and nsPEFs are being considered as a perspective tool for **cancer therapy** (Breton and Mir, 2012). There are several processes and signaling pathways, which can be triggered by nsPEFs, including the formation of pores in the plasma membrane, the release of calcium from intracellular stores, the breakdown of the cytoskeleton, and induction of apoptosis (Scarlett et al., 2009; Stacey et al., 2011; Thompson et al., 2014). These cellular events might result in modulations of GJIC, which is important for the regulation of cell growth control, differentiation and apoptosis, and plays a critical role in the carcinogenesis (Chapter 3). With respect to the lack of data regarding the effects of nsPEFs on GJIC, we studied effects of nsPEFs on intercellular communication, intracellular signaling, and structural changes in WB-F344 cells (Steuer et al., 2016) [Attachment XIV]. We found that non-cytotoxic treatments with nsPEFs (20 pulses of 100 ns duration) induced **rapid dysregulation of GJIC**, which become more pronounced with increasing field strength (10-20 kV). Maximum inhibition of GJIC occurred 15 min after the treatment, which appears to be relatively late to be a result of a direct membrane depolarization. The effects on GJIC were only **transient**, and communication recovered within 24 h post-treatment (Figure 27). Alongside GJIC inhibition, **amount of Cx43 mRNA was decreased** within 30-60 min post-treatment, but this effect was becoming gradually less pronounced and after 24-48 h recovering nearly to the control level (Figure 27). GJIC inhibition was also associated with a transient **hyperphosphorylation and internalization of Cx43** (Steuer et al., 2016) [Attachment XIV]. **MAPK ERK1/2 were activated** during 30-60 min, but after 6 h decreasing back to the control level (Figure 27). Interestingly, **p38 was not activated till 6 h post-treatment** (Figure 27). Alterations of GJIC, Cx43 and MAPKs were accompanied by transient (5-60 min) **disruption of cytoskeletal actin filaments**, while tight junctional proteins **zonula occludens-1 remained intact**. Altogether, the inhibition of GJIC was unlikely caused by a mechanical separation of the cells, membrane disruption or depolarization, but most likely resulted from nsPEF-induced modulation of intracellular processes and signaling leading to Cx43 alterations and GJIC dysregulation (Steuer et al., 2016) [Attachment XIV]. Although inhibition of GJIC and activation of MAPKs have been associated with tumor promoting and carcinogenic events, these effects induced by nsPEFs were only transient. In order to evaluate whether these transient changes might be translated into other and more permanent alterations of cell phenotype, we investigated effects of nsPEFs on the **cell elasticity, cell migration and anchorage-independent growth** (Steuer et al., 2017) [Attachment XV]. Treatment with nsPEF rapidly (within 8 min post treatment) **decreased elasticity of WB-F344 cells, but only transiently** and not to the levels of elastic modulus observed in tumorigenic WB-ras cells (Figure 27). Decrease in the elastic modulus correlated with reorganization of actin filaments, which also recovered app. 60 min after the treatment (Steuer et al., 2017) [Attachment XV]. However, these changes did not have any significant effects on the cell migration or soft agar growth (Figure 27). Treatments with nsPEF thus seem to be **suitable for the cancer therapies without posing a risk to induce further pro-carcinogenic events in surviving cells that were incidentally exposed to sub-lethal electric fields** (Steuer et al., 2017) [Attachment XV]. In fact, the ability of nsPEFs to transiently downregulate GJIC without inducing tumor promoting or carcinogenic changes might be utilized in other biomedical applications, where transient suppression of GJIC might represent desired therapeutic outcome, such as chronic wound healing (Wright et al., 2009). **Investigation of GJIC can provide deeper mechanistic insights into the alterations of signaling and cellular events by nsPEFs, which could then contribute to the further improvement and development of nsPEFs treatments and therapies.**

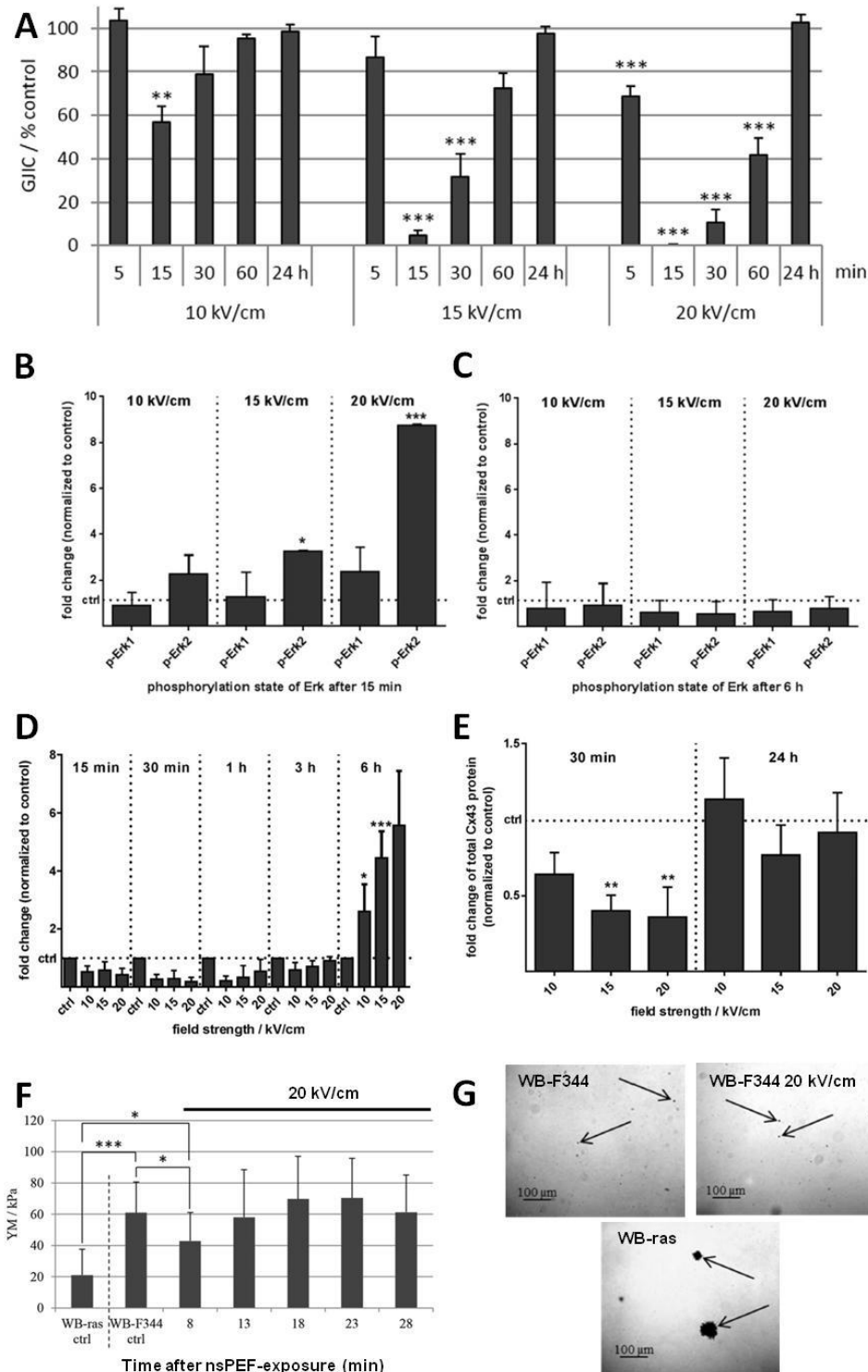


Figure 27: Effects of nanosecond pulsed electric fields (nsPEFs) on GJIC and related cellular events in rat liver epithelial cells WB-F344 at the different time points after the treatment. Effects of nsPEFs (20 pulses of 100 ns) of different field strengths (10-20 kV/cm) on (A) GJIC, (B-C) MAPK ERK1/2, (D) MAPK p38, (E) connexin 43 (Cx43) protein level, (F) elastic modulus (Young's modulus, YM), and (G) ability to growth on soft agar (Giemsa stained colonies obtained after 3 weeks of growth of control or nsPEF-treated cells). GJIC was evaluated by SL-DT assay, (B-E) were evaluated by Western blotting, YM was evaluated by atomic force microscopy. H-ras transformed WB-F344 cells (WB-ras) were used as a positive control for elastic modulus and soft agar growth. Adapted from (Steuer et al., 2017, 2016) [Attachment XIV-XV].

5 CONCLUSIONS

The demands on chemical testing and evaluation of their biological effects are ever increasing. *In vitro* assays allow acquiring large amount of data about the effects of chemicals on different biological phenomena with unprecedented speed and capacity, and can be effectively used for predictions of chemical effects on human health. **Experimental assessment of connexin-dependent functions including GJIC** can provide toxicologically and pharmacologically relevant information about the potential of chemicals to alter this physiologically important process, whose disruption appears to be the key cellular and tissue event associated with the onset and/or progress of different chronic diseases, pathologies and adverse outcomes (**Chapter 3**). Connexin functions and GJIC can be evaluated *in vitro* using a variety of methods, including techniques which are compatible with **high-throughput setups** (**Chapter 4.1**). *In vitro* evaluation of GJIC thus represents a **phenotypic assay** capable to identify and characterize **potential of chemicals either to disrupt or restore** this key mechanism responsible for the maintenance of **tissue homeostasis, proper development and functioning of multicellular organisms**. Within the work presented in this thesis, such effects were identified for several environmental toxicants (e.g. 1-methylanthracene, PFOA, methoxychlor, vinclozolin; **Chapter 4.2**) or medically promising compounds or treatments (e.g. dietary phytochemicals, pulsed electric fields, carbon nanotubes; **Chapter 4.6**). In addition to the assessment of **defined chemical entities**, GJIC can be used as the primary bioassay also for assessment of **hazard potential of complex mixtures** (e.g. cyanobacterial biomass), and utilized in effect-based monitoring or effect-directed analysis (**Chapter 4.5**). In an analogous manner, GJIC assessment can be utilized for evaluation of **beneficial effects** of complex extracts from natural products with subsequent isolation and **identification of the bioactive components using a bioassay-guided fractionation and analysis** (**Chapter 4.6**).

Since GJIC function at any given moment represents an integrated outcome of the actual signal transduction network and gene expression profile, modulations of GJIC can result from (a) alterations of gene expression due to transcriptional or epigenetic regulations, as well as from (b) rapid changes in signaling pathways controlling connexin channel gating, connexin trafficking or degradation. In essence, the effects on GJIC can reflect **alterations of signal transduction pathways and gene expression pattern via 'non-genotoxic' or 'epigenetic' mechanisms**, i.e. mechanisms not including alterations of genetic information. These mechanisms involve not only transcriptional activations or so-called genomic signaling mechanisms, which are currently in the focus of many high-throughput *in vitro* assays, but also **rapidly occurring signaling events such as phospholipase or kinase activation**, which was demonstrated for several environmental chemicals (e.g. lower molecular weight PAHs, PFOA, methoxychlor, vinclozolin; **Chapter 4.2**) or dietary phytochemicals and chemopreventive agents (e.g. silibinin, metformin; **Chapter 4.6**).

Although the mechanisms controlling GJIC are quite complex, there is a continuous progress in our understanding of GJIC regulation and several major regulatory mechanisms have been identified and characterized in detail. Thus, time- and concentration-dependent alterations of GJIC in the specific context of a particular *in vitro* model provide **immediate mechanistic clues**, which can be subsequently **tested in hypothesis-driven experiments**, or **explored using 'omics' technologies** in experiments specifically designed to decipher signaling events occurring upstream or downstream GJIC inhibition. This approach has been used to discover activation of the key signal transduction pathways and regulatory proteins, such as PC-PLC or annexins, in response to GJIC inhibitors (**Chapter 4.2**).

Specific physiological functions and regulatory mechanisms of GJIC are often dependent on the species, organ, tissue, cell type or developmental stage of an organism. Possibility to evaluate GJIC using **different *in vitro* models** would therefore provide an excellent opportunity to study the **effects on GJIC in a particular physiological or pathophysiological cellular/tissue context**. This would allow more reliable data interpretation and better predictions of possible *in vivo* outcomes. Different *in vitro* models which might be considered for GJIC evaluation include models representing **different cell types** (primary cells, immortalized cell lines, somatic stem and progenitor cells, pluripotent stem cells) obtained from different **species** (rodent, human, or other animals), different **organs** (brain, liver, lung, etc.), different **developmental stages** of organism (embryonic, fetal, adult) or different **health conditions** (e.g. normal vs. diseased cells, such as transformed or cancer cells). Use of different types of cells and models to study GJIC and differences in their responses to GJIC inhibitors were shown in **Chapter 4.1 (Figure 8)**. Specific examples of tissue-specific and GJIC-inhibiting effects and mechanisms were then provided

for methylated anthracenes or methoxychlor for human or rodent **liver, pulmonary or testicular *in vitro* models** (Chapter 4.3). In addition to the traditionally used monolayer monocultures of adherent cells, GJIC evaluation is principally possible also in advanced and physiologically more relevant *in vitro* models, such as co-cultures or 3D cell cultures (Chapter 4.1), which are becoming more increasingly used in biomedical research, toxicology and pharmacology. Validation of GJIC-inhibiting effects observed in rodent monolayer *in vitro* models was demonstrated using *ex vivo* assessment of GJIC in rat liver tissue of *in vivo* exposed animals, or using *ex vivo* exposed rat testicular tissue (Chapter 4.4).

GJIC and its *in vitro* assessment can be possibly incorporated also into the new emerging toxicological concepts, such as **Adverse Outcome Pathways (AOPs)**, which is currently gaining a momentum within the toxicological community, and has been formally recognized, endorsed and promoted by the key regulatory agencies and organizations, including Organization for Economic Cooperation and Development (OECD), Joint Research Centre of the European Commission or the US EPA (Vinken et al., 2017). AOP is a structured clear-cut mechanistic representation of the critical toxicological effects, that are propagated (1) from the initial interaction of a chemical with a molecular target (so-called **Molecular Initiating Event, MIE**); (2) through a series of toxicologically-relevant biological events (so-called **Key Events, KEs**) over the different levels of biological organization (cells, tissues, organs); (3) and leading to a defined adverse effect (**Adverse Outcome, AO**) that is observed at the individual or population level (Vinken et al., 2017). Causal relationships linking MIE, KEs and AO are then described by **Key Event Relationships (KER)**, which are established using the existing mechanistic knowledge. From the perspective of the AOP framework, well-defined alterations of connexin- or GJIC- functions might be seen as putative KE(s). Such KE(s) could be then linked via newly established KERs to already recognized KE(s) and incorporated into an existing AOP, or eventually used in a development of a new AOP. **Within the AOP framework, *in vitro* assessment of GJIC should effectively become a tool for predicting specific adverse outcomes and health hazards.**

Compatibility of GJIC assessment with high-throughput setup, advanced *in vitro* models, together with an increasing knowledge on the role and importance of connexins and GJIC in human diseases and toxicities, it would allow to use the *in vitro* evaluation of this evolutionary ancient cellular process for the prediction of chemical effects in the 21st century.

6 REFERENCES

- Abbaci, M., Barberi-Heyob, M., Blondel, W., Guillemin, F., Didelon, J., 2008. Advantages and limitations of commonly used methods to assay the molecular permeability of gap junctional intercellular communication. *Biotechniques* 45, 33–62.
- Abed, A., Dussault, J.C., Boffa, J.J., Chatziantoniou, C., Chadjichristos, C.E., 2014. Connexins in renal endothelial function and dysfunction. *Cardiovasc Hematol Disord Drug Targets* 14, 15–21.
- Abed, A.B., Kavvadas, P., Chadjichristos, C.E., 2015. Functional roles of connexins and pannexins in the kidney. *Cell Mol Life Sci* 72, 2869–2877.
- Alpatova, A.L., Shan, W., Babica, P., Upham, B.L., Rogensues, A.R., Masten, S.J., Drown, E., Mohanty, A.K., Alocilja, E.C., Tarabara, V. V., 2010. Single-walled carbon nanotubes dispersed in aqueous media via non-covalent functionalization: Effect of dispersant on the stability, cytotoxicity, and epigenetic toxicity of nanotube suspensions. *Water Res* 44, 505–520.
- Aoyama, H., Chapin, R.E., 2014. Reproductive toxicities of methoxychlor based on estrogenic properties of the compound and its estrogenic metabolite, hydroxyphenyltrichloroethane. *Vitam Horm* 94, 193–210.
- Aravindakshan, J., Cyr, D.G., 2005. Nonylphenol alters connexin 43 levels and connexin 43 phosphorylation via an inhibition of the p38-mitogen-activated protein kinase pathway. *Biol Reprod* 72, 1232–1240.
- Axelsen, L.N., Calloe, K., Holstein-Rathlou, N.H., Nielsen, M.S., 2013. Managing the complexity of communication: regulation of gap junctions by post-translational modification. *Front Pharmacol* 4, 130.
- Babica, P., Ctverackova, L., Lencesova, Z., Trosko, J.E., Upham, B.L., 2016a. Chemopreventive Agents Attenuate Rapid Inhibition of Gap Junctional Intercellular Communication Induced by Environmental Toxicants. *Nutr Cancer* 68, 827–837.
- Babica, P., Kubincová, P., Basu, A., Sovadinová, I., 2013. Polycyclic aromatic hydrocarbons and male reproductive system: the role of junctional intercellular communication, in: SETAC North America 34th Annual Meeting - Book of Abstracts. Nashville, TN, p. 286.
- Babica, P., Park, J.S., Sovadinova, I., Blaha, L., Whitten, D.A., Wilkerson, C.G., Trosko, J.E., Upham, B.L., 2009. Tumor Promotion-relevant Cell Signaling: Key Roles of Annexins and Phospholipases. *Vitr Cell Dev Biol* 45, S42–S42.
- Babica, P., Sovadinová, I., Upham, B., 2016b. Scrape loading/dye transfer assay, in: *Methods in Molecular Biology - Gap Junction Protocols*. pp. 133–144. doi:10.1007/978-1-4939-3664-9_9
- Babica, P., Zurabian, R., Kumar, E.R., Chopra, R., Mianeki, M.J., Park, J.-S., Jaša, L., Trosko, J.E., Upham, B.L., 2016c. Methoxychlor and vinclozolin induce rapid changes in intercellular and intracellular signaling in liver progenitor cells. *Toxicol Sci* 153, 174–185. doi:10.1093/toxsci/kfw114
- Bagchi, D., Bagchi, M., Tang, L., Stohs, S.J., 1997. Comparative in vitro and in vivo protein kinase C activation by selected pesticides and transition metal salts. *Toxicol Lett* 91, 31–37.
- Bargiello, T.A., Oh, S., Tang, Q., Bargiello, N.K., Dowd, T.L., Kwon, T., 2018. Gating of Connexin Channels by transjunctional-voltage: Conformations and models of open and closed states. *Biochim Biophys Acta* 1860, 22–39. doi:10.1016/j.bbammem.2017.04.028
- Berthoud, V.M., Minogue, P.J., Osmolak, P., Snabb, J.I., Beyer, E.C., 2014. Roles and regulation of lens epithelial cell connexins. *FEBS Lett* 588, 1297–1303.
- Beyer, E.C., Berthoud, V.M., 2014. Connexin hemichannels in the lens. *Front Physiol* 5, 20.
- Bláha, L., Babica, P., Hilscherová, K., Upham, B.L., Blaha, L., Babica, P., Hilscherova, K., Upham, B.L., 2010. Inhibition of gap-junctional intercellular communication and activation of mitogen-activated protein kinases by cyanobacterial extracts - Indications of novel tumor-promoting cyanotoxins? *Toxicon* 55, 126–134.
- Blaha, L., Kapplova, P., Vondracek, J., Upham, B., Machala, M., 2002. Inhibition of gap-junctional intercellular communication by environmentally occurring polycyclic aromatic hydrocarbons. *Toxicol Sci* 65, 43–51.
- Bloemendal, S., Kuck, U., 2013. Cell-to-cell communication in plants, animals, and fungi: a comparative review. *Naturwissenschaften* 100, 3–19.
- Bosco, D., Haefliger, J.A., Meda, P., 2011. Connexins: key mediators of endocrine function. *Physiol Rev* 91, 1393–1445.
- Bou Saab, J., Losa, D., Chanson, M., Ruez, R., 2014. Connexins in respiratory and gastrointestinal mucosal immunity. *FEBS Lett* 588, 1288–1296.
- Brack, W., 2003. Effect-directed analysis: a promising tool for the identification of organic toxicants in complex

- mixtures? *Anal Bioanal Chem* 377, 397–407. doi:10.1007/s00216-003-2139-z
- Breton, M., Mir, L.M., 2012. Microsecond and nanosecond electric pulses in cancer treatments. *Bioelectromagnetics* 33, 106–123. doi:10.1002/bem.20692
- Brisset, A.C., Isakson, B.E., Kwak, B.R., 2009. Connexins in vascular physiology and pathology. *Antioxid Redox Signal* 11, 267–282.
- Brózman, O., 2015. Epigenetické mechanismy toxicity v in vitro modelu dýchací soustavy. Diploma (M.Sc.) thesis, RECETOX, Masaryk University.
- Brózman, O., Novák, J., Osgood, R.S., Bauer, A.K., Babica, P., Labohá, P., 2017. In vitro model to study effects of environmental contaminants on gap junctional intercellular communication in human airway epithelial cells, in: *International Gap Junction Conference - Book of Abstracts*. Glasgow, UK.
- Buratti, F.M., Manganelli, M., Vichi, S., Stefanelli, M., Scardala, S., Testai, E., Funari, E., 2017. Cyanotoxins: producing organisms, occurrence, toxicity, mechanism of action and human health toxicological risk evaluation. *Arch Toxicol* 91, 1049–1130. doi:10.1007/s00204-016-1913-6
- Burns, T.J., Ali, A., Matesic, D.F., 2015. Comparative effects of 4-phenyl-3-butenoic acid and vorinostat on cell growth and signaling. *Anticancer Res* 35, 775–784.
- Burýšková, B., Hilscherová, K., Babica, P., Vrškova, D., Maršálek, B., Bláha, L., 2006. Toxicity of complex cyanobacterial samples and their fractions in *Xenopus laevis* embryos and the role of microcystins. *Aquat Toxicol* 80, 346–354.
- Casati, L., Sendra, R., Sibilía, V., Celotti, F., 2015. Endocrine Disrupters: the new players able to affect the epigenome. *Front Cell Dev Biol* 3, 37. doi:10.3389/fcell.2015.00037
- Cerbin, S., Kraak, M.H.S., de Voogt, P., Visser, P.M., Van Donk, E., 2010. Combined and single effects of pesticide carbaryl and toxic *Microcystis aeruginosa* on the life history of *Daphnia pulex*. *Hydrobiologia* 643, 129–138.
- Chang, C.-C., Tsai, J.L., Kuo, K.K., Wang, K.H., Chiang, C.-H., Kao, A.P., Tai, M.-H., Trosko, J.E., 2004. Expression of Oct-4, alpha fetoprotein and vimentin, and lack of gap-junctional intercellular communication (GJIC) as common phenotypes for human adult liver stem cells and hepatoma cells. *AAOHN Meet Abstr* 2004, 642–b–.
- Chen, S., Lee, L.P., 2010. Non-invasive microfluidic gap junction assay. *Integr Biol* 2, 130–138.
- Cheung, G., Chever, O., Rouach, N., 2014. Connexons and pannexons: newcomers in neurophysiology. *Front Cell Neurosci* 8, 348.
- Chevallier, D., Carette, D., Gilleron, J., Segretain, D., Pointis, G., 2013a. The emerging role of connexin 43 in testis pathogenesis. *Curr Mol Med* 13, 1331–1344.
- Chevallier, D., Carette, D., Segretain, D., Gilleron, J., Pointis, G., 2013b. Connexin 43 a check-point component of cell proliferation implicated in a wide range of human testis diseases. *Cell Mol Life Sci* 70, 1207–1220.
- Christman, G.M., 2015. Gap Junctions in Leiomyomas and the Human Female Reproductive Tract. *Semin Reprod Med* 33, 287–297.
- Cigliola, V., Allagnat, F., Berchtold, L.A., Lamprianou, S., Haefliger, J.A., Meda, P., 2015. Role of Connexins and Pannexins in the Pancreas. *Pancreas* 44, 1234–1244.
- Cigliola, V., Chellakudam, V., Arabieter, W., Meda, P., 2013. Connexins and beta-cell functions. *Diabetes Res Clin Pr* 99, 250–259.
- Cogliati, B., Menecier, G., Willebrords, J., Da Silva, T.C., Maes, M., Pereira, I. V., Crespo Yanguas, S., Hernandez-Blazquez, F.J., Dagli, M.L., Vinken, M., 2016. Connexins, Pannexins, and Their Channels in Fibroproliferative Diseases. *J Membr Biol* 249, 199–213.
- Corcelle, E., Dierbi, N., Mari, M., Nebout, M., Fiorini, C., Fenichel, P., Hofman, P., Poujeol, P., Mograbi, B., 2007. Control of the autophagy maturation step by the MAPK ERK and p38 - Lessons from environmental carcinogens. *Autophagy* 3, 57–59.
- Crespo Yanguas, S., Willebrords, J., Maes, M., da Silva, T.C., Veloso Alves Pereira, I., Cogliati, B., Zaidan Dagli, M.L., Vinken, M., 2016. Connexins and pannexins in liver damage. *Excli J* 15, 177–186.
- Čtveráčková, L., Brózman, O., Dydowiczová, A., Babica, P., 2017. In vitro assessment of gap junctional intercellular communication for identification and characterization of chemopreventive and anticancer compounds, in: *9th International Conference Analytical Cytometry - Abstracts*. Prague, Czech Republic, pp. 87–88.
- Cummings, A.M., 1997. Methoxychlor as a model for environmental estrogens. *Crit Rev Toxicol* 27, 367–379.
- Cunningham, M.L., 2002. A Mouse Is Not a Rat Is Not a Human: Species Differences Exist. *Toxicol Sci* 70, 157–158. doi:10.1093/toxsci/70.2.157

- Cyr, D.G., 2011. Connexins and pannexins: Coordinating cellular communication in the testis and epididymis. *Spermatogenesis* 1, 325–338.
- Czyz, J., Piwowarczyk, K., Paw, M., Luty, M., Wrobel, T., Catapano, J., Madeja, Z., Ryszawy, D., 2017. Connexin-dependent intercellular stress signaling in tissue homeostasis and tumor development. *Acta Biochim Pol* 64, 377–389. doi:10.18388/abp.2017_1592
- Danesh-Meyer, H. V., Zhang, J., Acosta, M.L., Rupenthal, I.D., Green, C.R., 2016. Connexin43 in retinal injury and disease. *Prog Retin Eye Res* 51, 41–68.
- Daneshian, M., Busquet, F., Hartung, T., Leist, M., 2015. Animal use for science in Europe. *ALTEX* 32, 261–274.
- De Vuyst, E., De Bock, M., Decrock, E., Van Moorhem, M., Naus, C., Mabilde, C., Leybaert, L., 2008. In Situ Bipolar Electroporation for Localized Cell Loading with Reporter Dyes and Investigating Gap Junctional Coupling. *Biophys J* 94, 469–479. doi:10.1529/biophysj.107.109470
- Decrock, E., De Bock, M., Wang, N., Bultynck, G., Giaume, C., Naus, C.C., Green, C.R., Leybaert, L., 2015. Connexin and pannexin signaling pathways, an architectural blueprint for CNS physiology and pathology? *Cell Mol Life Sci* 72, 2823–2851.
- Defejter, A.W., Ray, J.S., Weghorst, C.M., Klaunig, J.E., Goodman, J.I., Chang, C.C., Ruch, R.J., Trosko, J.E., 1990. Infection of Rat-Liver Epithelial-Cells with V-Ha-Ras - Correlation between Oncogene Expression, Gap Junctional Communication, and Tumorigenicity. *Mol Carcinog* 3, 54–67.
- Delmar, M., Laird, D.W., Naus, C.C., Nielsen, M.S., Verselis, V.K., White, T.W., 2017. Connexins and Disease. *Cold Spring Harb Perspect Biol* a029348. doi:10.1101/cshperspect.a029348
- Dempsey, Y., Martin, P., Upton, P.D., 2015. Connexin-mediated regulation of the pulmonary vasculature. *Biochem Soc Trans* 43, 524–529.
- DeoCampo, N.D., Wilson, M.R., Trosko, J.E., 2000. Cooperation of bcl-2 and myc in the neoplastic transformation of normal rat liver epithelial cells is related to the down-regulation of gap junction-mediated intercellular communication. *Carcinogenesis* 21, 1501–1506.
- Diezmos, E.F., Bertrand, P.P., Liu, L., 2015. Purinergic Signaling in Gut Inflammation: The Role of Connexins and Pannexins. *Front Neurosci* 10, 311.
- Dittmann, E., Gugger, M., Sivonen, K., Fewer, D.P., 2015. Natural Product Biosynthetic Diversity and Comparative Genomics of the Cyanobacteria. *Trends Microbiol* 23, 642–652. doi:10.1016/j.tim.2015.07.008
- Dukic, A.R., McClymont, D.W., Tasken, K., 2017. A Cell-Based High-Throughput Assay for Gap Junction Communication Suitable for Assessing Connexin 43-Ezrin Interaction Disruptors Using IncuCyte ZOOM. *SLAS Discov Adv life Sci R D* 22, 77–85. doi:10.1177/1087057116669120
- El Fouly, M.H., Trosko, J.E., Chang, C.C., 1987. Scrape-loading and dye transfer - a rapid and simple technique to study gap junctional intercellular communication. *Exp Cell Res* 168, 422–430.
- Ellinsworth, D.C., Sandow, S.L., Shukla, N., Liu, Y., Jeremy, J.Y., Gutterman, D.D., 2016. Endothelium-Derived Hyperpolarization and Coronary Vasodilation: Diverse and Integrated Roles of Epoxyeicosatrienoic Acids, Hydrogen Peroxide, and Gap Junctions. *Microcirculation* 23, 15–32.
- Elstein, K.H., Zucker, R.M., 1994. Comparison of cellular and nuclear flow cytometric techniques for discriminating apoptotic subpopulations. *Exp Cell Res* 211, 322–331. doi:10.1006/excr.1994.1094
- Ennaji, M.M., Schwartz, J.L., Mealing, G., Belbaraka, L., Parker, C., Parentaux, M., Jouishomme, H., Arella, M., Whitfield, J.F., Phipps, J., 1995. Alterations in Cell-Cell Communication in Human Papillomavirus Type-16 (Hpv16) Transformed Rat Myoblasts. *Cell Mol Biol* 41, 481–498.
- Evans, W.H., De Vuyst, E., Leybaert, L., 2006. The gap junction cellular internet: connexin hemichannels enter the signalling limelight. *Biochem J* 397, 1–14. doi:10.1042/BJ20060175
- Falk, M.M., Bell, C.L., Kells Andrews, R.M., Murray, S.A., 2016. Molecular mechanisms regulating formation, trafficking and processing of annular gap junctions. *BMC Cell Biol* 17, 22.
- Farnsworth, N.L., Benninger, R.K., 2014. New insights into the role of connexins in pancreatic islet function and diabetes. *FEBS Lett* 588, 1278–1287.
- Font-Burgada, J., Shalapour, S., Ramaswamy, S., Hsueh, B., Rossell, D., Umemura, A., Taniguchi, K., Nakagawa, H., Valasek, M.A., Ye, L., Kopp, J.L., Sander, M., Carter, H., Deisseroth, K., Verma, I.M., Karin, M., 2015. Hybrid Periportal Hepatocytes Regenerate the Injured Liver without Giving Rise to Cancer. *Cell* 162, 766–779.
- Freitas-Andrade, M., Naus, C.C., 2016. Astrocytes in neuroprotection and neurodegeneration: The role of connexin43 and pannexin1. *Neuroscience* 323, 207–221.
- Freund-Michel, V., Muller, B., Marthan, R., Savineau, J.P., Guibert, C., 2016. Expression and role of connexin-based

- gap junctions in pulmonary inflammatory diseases. *Pharmacol Ther* 164, 105–119.
- Gaete, P.S., Lillo, M.A., Figueroa, X.F., 2014. Functional role of connexins and pannexins in the interaction between vascular and nervous system. *J Cell Physiol* 229, 1336–1345.
- Gaido, K.W., Maness, S.C., McDonnell, D.P., Dehal, S.S., Kupfer, D., Safe, S., 2000. Interaction of methoxychlor and related compounds with estrogen receptor alpha and beta, and androgen receptor: structure-activity studies. *Mol Pharmacol* 58, 852–858.
- Gao, Z., Varela, J.A., Groc, L., Lounis, B., Cognet, L., 2016. Toward the suppression of cellular toxicity from single-walled carbon nanotubes. *Biomater Sci* 4, 230–244. doi:10.1039/c5bm00134j
- Garcia, I.E., Bosen, F., Mujica, P., Pupo, A., Flores-Munoz, C., Jara, O., Gonzalez, C., Willecke, K., Martinez, A.D., 2016. From Hyperactive Connexin26 Hemichannels to Impairments in Epidermal Calcium Gradient and Permeability Barrier in the Keratitis-Ichthyosis-Deafness Syndrome. *J Invest Dermatol* 136, 574–583.
- Glass, A.M., Snyder, E.G., Taffet, S.M., 2015. Connexins and pannexins in the immune system and lymphatic organs. *Cell Mol Life Sci* 72, 2899–2910.
- Goudis, C.A., Korantzopoulos, P., Ntalas, I. V, Kallergis, E.M., Liu, T., Ketikoglou, D.G., 2015. Diabetes mellitus and atrial fibrillation: Pathophysiological mechanisms and potential upstream therapies. *Int J Cardiol* 184, 617–622.
- Grosse, Y., Baan, R., Straif, K., Secretan, B., El Ghissassi, F., Cogliano, V., 2006. Carcinogenicity of nitrate, nitrite, and cyanobacterial peptide toxins. *Lancet Oncol* 7, 628–629.
- Hakulinen, P., Maki-Paakkanen, J., Naarala, J., Kronberg, L., Komulainen, H., 2004. Potent inhibition of gap junctional intercellular communication by 3-chloro-4-(dichloromethyl)-5-hydroxy-2(5H)-furanone (MX) in BALB/c 3T3 cells. *Toxicol Lett* 151, 439–449. doi:10.1016/j.toxlet.2004.03.012
- Han, E.H., Kim, J.Y., Kim, H.K., Hwang, Y.P., Jeong, H.G., 2008. o,p'-DDT induces cyclooxygenase-2 gene expression in murine macrophages: Role of AP-1 and CRE promoter elements and PI3-kinase/Akt/MAPK signaling pathways. *Toxicol Appl Pharmacol* 233, 333–342.
- Hanakova, Z., Hosek, J., Babula, P., Dall'Acqua, S., Vaclavik, J., Smejkal, K., 2015. C-Geranylated Flavanones from *Paulownia tomentosa* Fruits as Potential Anti-inflammatory Compounds Acting via Inhibition of TNF-alpha Production. *J Nat Prod* 78, 850–863.
- Haq, N., Grose, D., Ward, E., Chiu, O., Tigue, N., Dowell, S.J., Powell, A.J., Chen, M.X., 2013. A high-throughput assay for connexin 43 (Cx43, GJA1) gap junctions using codon-optimized aequorin. *Assay Drug Dev Technol* 11, 93–100. doi:10.1089/adt.2012.469
- Hartman, T.G., Rosen, J.D., 1983. Inhibition of metabolic cooperation by cigarette smoke condensate and its fractions in V-79 Chinese hamster lung fibroblasts. *Proc Natl Acad Sci U S A* 80, 5305–5309.
- Hayashi, T., Nomata, K., Chang, C.C., Ruch, R.J., Trosko, J.E., 1998. Cooperative effects of v-myc and c-Ha-ras oncogenes on gap junctional intercellular communication and tumorigenicity in rat liver epithelial cells. *Cancer Lett* 128, 145–154.
- He, X., Liu, Y.-L., Conklin, A., Westrick, J., Weavers, L.K., Dionysiou, D.D., Lenhart, J.J., Mouser, P.J., Szlag, D., Walker, H.W., 2016. Toxic cyanobacteria and drinking water: Impacts, detection, and treatment. *Harmful Algae* 54, 174–193. doi:https://doi.org/10.1016/j.hal.2016.01.001
- Herner, H.A., Trosko, J.E., Masten, S.J., 2001. The epigenetic toxicity of pyrene and related ozonation byproducts containing an aldehyde functional group. *Environ Sci Technol* 35, 3576–3583. doi:10.1021/es0106117
- Herve, J.C., Pluciennik, F., Verrecchia, F., Bastide, B., Delage, B., Joffre, M., Deleze, J., 1996. Influence of the molecular structure of steroids on their ability to interrupt gap junctional communication. *J Membr Biol* 149, 179–187.
- Hills, C.E., Price, G.W., Squires, P.E., 2015. Mind the gap: connexins and cell-cell communication in the diabetic kidney. *Diabetologia* 58, 233–241.
- Hong, S., Giesy, J.P., Lee, J.-S., Lee, J.-H., Khim, J.S., 2016. Effect-directed analysis: Current status and future challenges. *Ocean Sci J* 51, 413–433. doi:10.1007/s12601-016-0038-4
- Hossain, M.Z., Jagdale, A.B., Ao, P., Boynton, A.L., 1999. Mitogen-activated protein kinase and phosphorylation of connexin43 are not sufficient for the disruption of gap junctional communication by platelet-derived growth factor and tetradecanoylphorbol acetate. *J Cell Physiol* 179, 87–96.
- Hou, M.L., Li, Y.Q., Paul, D.L., 2013. A novel, highly sensitive method for assessing gap junctional coupling. *J Neurosci Methods* 220, 18–23.
- Hrouzek, P., Kapuscik, A., Vacek, J., Voracova, K., Paichlova, J., Kosina, P., Voloshko, L., Ventura, S., Kopecky, J.,

2016. Cytotoxicity evaluation of large cyanobacterial strain set using selected human and murine in vitro cell models. *Ecotoxicol Environ Saf* 124, 177–185. doi:10.1016/j.ecoenv.2015.10.020
- Hu, W.Y., Jones, P.D., Upham, B.L., Trosko, J.E., Lau, C., Giesy, J.P., 2002. Inhibition of gap junctional intercellular communication by perfluorinated compounds in rat liver and dolphin kidney epithelial cell lines in vitro and sprague-dawley rats in vivo. *Toxicol Sci* 68, 429–436.
- Hu, Y.F., Chen, Y.J., Lin, Y.J., Chen, S.A., 2015. Inflammation and the pathogenesis of atrial fibrillation. *Nat Rev Cardiol* 12, 230–243.
- Huang, S.H., Wu, J.C., Hwang, R.D., Yeo, H.L., Wang, S.M., 2003. Effects of 18 beta-glycyrrhetic acid and steroidogenesis acid on the junctional in rat adrenocortical cells. *J Cell Biochem* 90, 33–41.
- Iwase, Y., Fukata, H., Mori, C., 2006. Estrogenic compounds inhibit gap junctional intercellular communication in mouse Leydig TM3 cells. *Toxicol Appl Pharmacol* 212, 237–246.
- Jain, A., Homayoun, A., Bannister, C.W., Yum, K., 2015. Single-walled carbon nanotubes as near-infrared optical biosensors for life sciences and biomedicine. *Biotechnol J* 10, 447–459. doi:10.1002/biot.201400168
- Jemnitz, K., Veres, Z., Monostory, K., Kobori, L., Vereczkey, L., 2008. Interspecies differences in acetaminophen sensitivity of human, rat, and mouse primary hepatocytes. *Toxicol In Vitro* 22, 961–967. doi:10.1016/j.tiv.2008.02.001
- Jeong, S.H., Habeebu, S.S.M., Klaassen, C.D., 2000. Cadmium decreases gap junctional intercellular communication in mouse liver. *Toxicol Sci* 57, 156–166.
- Jiang, J.X., 2010. Gap junctions or hemichannel-dependent and independent roles of connexins in cataractogenesis and lens development. *Curr Mol Med* 10, 851–863.
- Jiang, J.X., Penuela, S., 2016. Connexin and pannexin channels in cancer. *BMC Cell Biol* 17 Suppl 1, 12.
- Kelsell, D.P., Dunlop, J., Hodgins, M.B., 2001. Human diseases: clues to cracking the connexin code? *Trends Cell Biol* 11, 2–6.
- Kidder, G.M., Cyr, D.G., 2016. Roles of connexins in testis development and spermatogenesis. *Semin Cell Dev Biol* 50, 22–30. doi:10.1016/j.semcdb.2015.12.019
- Kienzler, A., Bopp, S.K., van der Linden, S., Berggren, E., Worth, A., 2016. Regulatory assessment of chemical mixtures: Requirements, current approaches and future perspectives. *Regul Toxicol Pharmacol* 80, 321–334. doi:https://doi.org/10.1016/j.yrtph.2016.05.020
- Kim, S., 2011. Application of human liver stem cells for receptor-mediated toxicogenomic study. Doctoral thesis in Biochemistry and Molecular Biology - Environmental Toxicology, Michigan State University, East Lansing.
- Kim, S., Dere, E., Burgoon, L.D., Chang, C.C., Zacharewski, T.R., 2009. Comparative Analysis of AhR-Mediated TCDD-Elicited Gene Expression in Human Liver Adult Stem Cells. *Toxicol Sci* 112, 229–244.
- Kim, S., Kiyosawa, N., Burgoon, L.D., Chang, C.C., Zacharewski, T.R., 2013. PPARalpha-mediated responses in human adult liver stem cells: In vivo/in vitro and cross-species comparisons. *J Steroid Biochem Mol Biol* 138, 236–247.
- Kleopa, K.A., Sargiannidou, I., 2015. Connexins, gap junctions and peripheral neuropathy. *Neurosci Lett* 596, 27–32.
- Klimova, Z., 2015. Účinky endokrinných disruptorů na in vitro biomarkery epigenetické toxicity. Diploma (M.Sc.) thesis, Dept. of Biochemistry, Masaryk University Masaryk University.
- Knight, B., Akhurst, B., Matthews, V.B., Ruddell, R.G., Ramm, G.A., Abraham, L.J., Olynyk, J.K., Yeoh, G.C., 2007. Attenuated liver progenitor (oval) cell and fibrogenic responses to the choline deficient, ethionine supplemented diet in the BALB/c inbred strain of mice. *J Hepatol* 46, 134–141. doi:10.1016/j.jhep.2006.08.015
- Knoll, A.H., 2011. The Multiple Origins of Complex Multicellularity. *Annu Rev Earth Planet Sci* 39, 217–239. doi:10.1146/annurev.earth.031208.100209
- Kolaja, K.L., Engelken, D.T., Klaassen, C.D., 2000. Inhibition of gap-junctional-intercellular communication in intact rat liver by nongenotoxic hepatocarcinogens. *Toxicology* 146, 15–22.
- Krewski, D., Acosta, D., Andersen, M., Anderson, H., Bailar, J.C., Boekelheide, K., Brent, R., Charnley, G., Cheung, V.G., Green, S., Kelsey, K.T., Kerkvliet, N.I., Li, A.A., McCray, L., Meyer, O., Patterson, R.D., Pennie, W., Scala, R.A., Solomon, G.M., Stephens, M., Yager, J., Zeise, L., 2010. Toxicity Testing in the 21st Century: a Vision and a Strategy. *J Toxicol Environ Heal B-Critical Rev* 13, 51–138.
- Krutovskikh, V.A., Mesnil, M., Mazzoleni, G., Yamasaki, H., 1995. Inhibition of Rat-Liver Gap Junction Intercellular Communication by Tumor-Promoting Agents in-Vivo - Association with Aberrant Localization of Connexin Proteins. *Lab Investig* 72, 571–577.

- Krutovskikh, V.A., Oyamada, M., Yamasaki, H., 1991. Sequential-Changes of Gap-Junctional Intercellular Communications During Multistage Rat-Liver Carcinogenesis - Direct Measurement of Communication In Vivo. *Carcinogenesis* 12, 1701–1706.
- Kurata, M., Hirose, K., Umeda, M., 1982. Inhibition of metabolic cooperation in Chinese hamster cells by organochlorine pesticides. *GANN* 73, 217–221.
- Kurtz, A., 2015. Connexins, renin cell displacement and hypertension. *Curr Opin Pharmacol* 21, 1–6.
- Lee, H.S., Park, E.J., Oh, J.H., Moon, G., Hwang, M.S., Kim, S.Y., Shin, M.K., Koh, Y.H., Suh, J.H., Kang, H.S., Jeon, J.H., Rhee, G.S., Hong, J.H., 2014. Bisphenol A exerts estrogenic effects by modulating CDK1/2 and p38 MAP kinase activity. *Biosci Biotechnol Biochem* 78, 1371–1375.
- Lee, J.Y., Choi, E.J., Lee, J., 2015. A new high-throughput screening-compatible gap junctional intercellular communication assay. *BMC Biotechnol* 15, 90.
- Lee, K.W., Chun, K.S., Lee, J.S., Kang, K.S., Surh, Y.J., Lee, H.J., 2004. Inhibition of cyclooxygenase-2 expression and restoration of gap junction intercellular communication in H-ras-transformed rat liver epithelial cells by caffeic acid phenethyl ester, in: *Signal Transduction Pathways, Chromatin Structure, and Gene Expression Mechanisms as Therapeutic Targets*. New York Acad Sciences, New York, pp. 501–507.
- Leithe, E., Kjenseth, A., Bruun, J., Sirnes, S., Rivedal, E., 2010. Inhibition of connexin43 gap junction channels by the endocrine disruptor ioxynil. *Toxicol Appl Pharmacol* 247, 10–17.
- Lenčešová, Z., 2012. In vitro metody pro studium chemopreventivních účinků fytochemikálií. Diploma (M.Sc.) thesis, RECETOX, Masaryk University.
- Leo-Macias, A., Agullo-Pascual, E., Delmar, M., 2016. The cardiac connexome: Non-canonical functions of connexin43 and their role in cardiac arrhythmias. *Semin Cell Dev Biol* 50, 13–21.
- Leone, A., Lecci, R.M., Durante, M., Meli, F., Piraino, S., 2015. The Bright Side of Gelatinous Blooms: Nutraceutical Value and Antioxidant Properties of Three Mediterranean Jellyfish (Scyphozoa). *Mar Drugs* 13, 4654–4681.
- Leone, A., Lecci, R.M., Durante, M., Piraino, S., 2013. Extract from the zooxanthellate jellyfish *Cotylorhiza tuberculata* modulates gap junction intercellular communication in human cell cultures. *Mar Drugs* 11, 1728–1762.
- Leone, A., Longo, C., Trosko, J.E., 2012. The chemopreventive role of dietary phytochemicals through gap junctional intercellular communication. *Phytochem Rev* 11, 285–307. doi:DOI 10.1007/s11101-012-9235-7
- Leone, A., Zefferino, R., Longo, C., Leo, L., Zacheo, G., 2010. Supercritical CO₂-Extracted Tomato Oleoresins Enhance Gap Junction Intercellular Communications and Recover from Mercury Chloride Inhibition in Keratinocytes. *J Agric Food Chem* 58, 4769–4778.
- Leybaert, L., Lampe, P.D., Dhein, S., Kwak, B.R., Ferdinandy, P., Beyer, E.C., Laird, D.W., Naus, C.C., Green, C.R., Schulz, R., 2017. Connexins in Cardiovascular and Neurovascular Health and Disease: Pharmacological Implications. *Pharmacol Rev* 69, 396–478. doi:10.1124/pr.115.012062
- Li, Z., Yan, Y., Powers, E.A., Ying, X., Janjua, K., Garyantes, T., Baron, B., 2003. Identification of gap junction blockers using automated fluorescence microscopy imaging. *J Biomol Screen* 8, 489–499. doi:10.1177/1087057103257309
- Liang, F., Chen, B., 2010. A review on biomedical applications of single-walled carbon nanotubes. *Curr Med Chem* 17, 10–24.
- Liang, J.Y., Wang, S.M., Chung, T.H., Yang, S.H., Wu, J.C., 2008. Effects of 18-glycyrrhetic acid on serine 368 phosphorylation of connexin43 in rat neonatal cardiomyocytes. *Cell Biol Int* 32, 1371–1379.
- Lilly, E., Sellitto, C., Milstone, L.M., White, T.W., 2016. Connexin channels in congenital skin disorders. *Semin Cell Dev Biol* 50, 4–12.
- Liu, J., Siragam, V., Chen, J., Fridman, M.D., Hamilton, R.M., Sun, Y., 2014. High-throughput measurement of gap junctional intercellular communication. *Am J Physiol Hear Circ Physiol* 306, H1708–13.
- Lopez, W., Ramachandran, J., Alsamarah, A., Luo, Y., Harris, A.L., Contreras, J.E., 2016. Mechanism of gating by calcium in connexin hemichannels. *Proc Natl Acad Sci U S A* 113, E7986–E7995. doi:10.1073/pnas.1609378113
- Luster-Teasley, S.L., Ganey, P.E., DiOrio, M., Ward 3rd, J.S., Maleczka Jr., R.E., Trosko, J.E., Masten, S.J., 2005. Effect of byproducts from the ozonation of pyrene: biphenyl-2,2',6,6'-tetracarbaldehyde and biphenyl-2,2',6,6'-tetracarboxylic acid on gap junction intercellular communication and neutrophil function. *Env Toxicol Chem* 24, 733–740. doi:10.1897/04-679.1
- Luster-Teasley, S.L., Yao, J.J., Herner, H.H., Trosko, J.E., Masten, S.J., 2002. Ozonation of chrysene: Evaluation of

- byproduct mixtures and identification of toxic constituent. *Environ Sci Technol* 36, 869–876. doi:10.1021/es011090q
- Lyng, F.M., Jones, G.R., Rommerts, F.F.G., 2000. Rapid androgen actions on calcium signaling in rat Sertoli cells and two human prostatic cell lines: Similar biphasic responses between 1 picomolar and 100 nanomolar concentrations. *Biol Reprod* 63, 736–747.
- Machala, M., Blaha, L., Vondracek, J., Trosko, J.E., Scott, J., Upham, B.L., 2003. Inhibition of gap junctional intercellular communication by noncoplanar polychlorinated biphenyls: Inhibitory potencies and screening for potential mode(s) of action. *Toxicol Sci* 76, 102–111.
- Maes, M., Cogliati, B., Crespo Yanguas, S., Willebrords, J., Vinken, M., 2015a. Roles of connexins and pannexins in digestive homeostasis. *Cell Mol Life Sci* 72, 2809–2821.
- Maes, M., Crespo Yanguas, S., Willebrords, J., Cogliati, B., Vinken, M., 2015b. Connexin and pannexin signaling in gastrointestinal and liver disease. *Transl Res* 166, 332–343.
- Maes, M., Crespo Yanguas, S., Willebrords, J., Vinken, M., 2015c. Models and methods for in vitro testing of hepatic gap junctional communication. *Toxicol Vitro* 30, 569–577.
- Maes, M., Decrock, E., Cogliati, B., Oliveira, A.G., Marques, P.E., Dagli, M.L., Menezes, G.B., Mennecier, G., Leybaert, L., Vanhaecke, T., Rogiers, V., Vinken, M., 2014. Connexin and pannexin (hemi)channels in the liver. *Front Physiol* 4, 405.
- Maier, D., Blaha, L., Giesy, J.P., Henneberg, A., Kohler, H.-R., Kuch, B., Osterauer, R., Peschke, K., Richter, D., Scheurer, M., Triebkorn, R., 2015. Biological plausibility as a tool to associate analytical data for micropollutants and effect potentials in wastewater, surface water, and sediments with effects in fishes. *Water Res* 72, 127–144. doi:10.1016/j.watres.2014.08.050
- Manikkam, M., Haque, M.M., Guerrero-Bosagna, C., Nilsson, E.E., Skinner, M.K., 2014. Pesticide methoxychlor promotes the epigenetic transgenerational inheritance of adult-onset disease through the female germline. *PLoS One* 9, e102091.
- Masaki, K., 2015. Early disruption of glial communication via connexin gap junction in multiple sclerosis, Balo's disease and neuromyelitis optica. *Neuropathology* 35, 469–480.
- Masten, S.J., Tian, M., Upham, B.L., Trosko, J.E., Trosko, E., 2001. Effect of selected pesticides and their ozonation by-products on gap junctional intercellular communication using rat liver epithelial cell lines. *Chemosphere* 44, 457–465.
- Matesic, D.F., Blommel, M.L., Sunman, J.A., Cutler, S.J., Cutler, H.G., 2001. Prevention of organochlorine-induced inhibition of gap junctional communication by chaetoglobosin K in astrocytes. *Cell Biol Toxicol* 17, 395–408.
- Matowe, W.C., Ginsberg, J., 1996. Effects of the diacylglycerol kinase inhibitor, R59022, on TSH-stimulated iodide organification in porcine thyroid cells. *Pharmacology* 53, 376–383.
- Méjean, A., Ploux, O., 2013. Chapter Six: A Genomic View of Secondary Metabolite Production in Cyanobacteria, *Genomics* o. ed. Academic Press Ltd., Elsevier Science Ltd.
- Merel, S., Walker, D., Chicana, R., Snyder, S., Baures, E., Thomas, O., 2013. State of knowledge and concerns on cyanobacterial blooms and cyanotoxins. *Environ Int* 59, 303–327.
- Mesnil, M., Crespín, S., Avanzo, J.L., Zaidan-Dagli, M.L., 2005. Defective gap junctional intercellular communication in the carcinogenic process. *Biochim Biophys Acta* 1719, 125–145.
- Michela, P., Velia, V., Aldo, P., Ada, P., 2015. Role of connexin 43 in cardiovascular diseases. *Eur J Pharmacol* 768, 71–76.
- Miller, T.R., Beversdorf, L.J., Weirich, C.A., Bartlett, S.L., 2017. Cyanobacterial Toxins of the Laurentian Great Lakes, Their Toxicological Effects, and Numerical Limits in Drinking Water. *Mar Drugs* 15. doi:10.3390/md15060160
- Mograbí, B., Corcelle, E., Defamie, N., Samson, M., Nebout, M., Segretain, D., Fenichel, P., Pointis, G., 2003. Aberrant connexin 43 endocytosis by the carcinogen lindane involves activation of the ERK/mitogen-activated protein kinase pathway. *Carcinogenesis* 24, 1415–1423.
- Moinfar, Z., Dambach, H., Faustmann, P.M., 2014. Influence of drugs on gap junctions in glioma cell lines and primary astrocytes in vitro. *Front Physiol* 5, 186.
- Moore, K.B., O'Brien, J., 2015. Connexins in neurons and glia: targets for intervention in disease and injury. *Neural Regen Res* 10, 1013–1017.
- Morel, S., 2014. Multiple roles of connexins in atherosclerosis- and restenosis-induced vascular remodelling. *J Vasc Res* 51, 149–161.
- Murray, A.W., Fitzgerald, D.J., 1979. Tumor Promoters Inhibit Metabolic Cooperation in Cocultures of Epidermal

- and 3t3-Cells. *Biochem Biophys Res Commun* 91, 395–401.
- Na, H.K., Wilson, M.R., Kang, K.S., Chang, C.C., Grunberger, D., Trosko, J.E., 2000. Restoration of gap junctional intercellular communication by caffeic acid phenethyl ester (CAPE) in a ras-transformed rat liver epithelial cell line. *Cancer Lett* 157, 31–38.
- Nakamura, Y., Trosko, J.E., Chang, C.C., Upham, B.L., 2004. psyllium extracts decreased neoplastic phenotypes induced by the Ha-Ras oncogene transfected into a rat liver oval cell line. *Cancer Lett* 203, 13–24.
- Nakamura, Y., Yoshikawa, N., Hiroki, I., Sato, K., Ohtsuki, K., Chang, C.C., Upham, B.L., Trosko, J.E., 2005. beta-sitosterol from psyllium seed husk (*Plantago ovata* Forsk) restores gap junctional intercellular communication in Ha-ras transfected rat liver cells. *Nutr Cancer-an Int J* 51, 218–225.
- Naus, C.C., Laird, D.W., 2010. Implications and challenges of connexin connections to cancer. *Nat Rev Cancer* 10, 435–441.
- Nielsen, M., Ruch, R.J., Vang, O., 2000. Resveratrol reverses tumor-promoter-induced inhibition of gap-junctional intercellular communication. *Biochem Biophys Res Commun* 275, 804–809.
- Nielsen, M.S., Axelsen, L.N., Sorgen, P.L., Verma, V., Delmar, M., Holstein-Rathlou, N.H., 2012. Gap junctions. *Compr Physiol* 2, 1981–2035.
- Nishikawa, A., Sai, K., Okazaki, K., Son, H.Y., Kanki, K., Nakajima, M., Kinae, N., Nohmi, T., Trosko, J.E., Inoue, T., Hirose, M., 2006. MX, a by-product of water chlorination, lacks in vivo genotoxicity in gpt delta mice but inhibits gap junctional intercellular communication in rat WB cells. *Environ Mol Mutagen* 47, 48–55. doi:10.1002/em.20167
- Noda, K., Umeda, M., Ono, T., 1981. Effects of various chemicals including bile acids and chemical carcinogens on the inhibition of metabolic cooperation. *Gan* 72, 772–776.
- Nováková, K., Babica, P., Adamovský, O., Bláha, L., 2011. Modulation of gap-junctional intercellular communication by a series of cyanobacterial samples from nature and laboratory cultures. *Toxicon* 58, 76–84.
- Nováková, K., Bláha, L., Babica, P., 2012. Tumor promoting effects of cyanobacterial extracts are potentiated by anthropogenic contaminants – Evidence from in vitro study. *Chemosphere* 89, 30–37.
- Nováková, K., Kohoutek, J., Adamovský, O., Brack, W., Krauss, M., Blaha, L., 2013. Novel metabolites in cyanobacterium *Cylindrospermopsis raciborskii* with potencies to inhibit gap junctional intercellular communication. *J Hazard Mater* 262C, 571–579.
- Ogawa, T., Hayashi, T., Tokunou, M., Nakachi, K., Trosko, J.E., Chang, C.C., Yorioka, N., 2005. Suberoylanilide hydroxamic acid enhances gap junctional intercellular communication via acetylation of histone containing connexin 43 gene locus. *Cancer Res* 65, 9771–9778.
- Oh, S.Y., Dupont, E., Madhukar, B. V., Briand, J.P., Chang, C.C., Beyer, E., Trosko, J.E., 1993. Characterization of Gap Junctional Communication-Deficient Mutants of a Rat-Liver Epithelial-Cell Line. *Eur J Cell Biol* 60, 250–255.
- Osgood, R.S., Upham, B.L., Bushel, P.R., Velmurugan, K., Xiong, K.-N., Bauer, A.K., 2017. Secondhand Smoke-Prevalent Polycyclic Aromatic Hydrocarbon Binary Mixture-Induced Specific Mitogenic and Pro-inflammatory Cell Signaling Events in Lung Epithelial Cells. *Toxicol Sci* 157, 156–171. doi:10.1093/toxsci/kfx027
- Osgood, R.S., Upham, B.L., Hill, T., Helms, K.L., Velmurugan, K., Babica, P., Bauer, A.K., 2013. Polycyclic aromatic hydrocarbon-induced signaling events relevant to inflammation and tumorigenesis in lung cells are dependent on molecular structure. *PLoS One* 8, e65150.
- Paerl, H.W., Otten, T.G., 2013. Harmful Cyanobacterial Blooms: Causes, Consequences, and Controls. *Microb Ecol* 65, 995–1010.
- Palacios-Prado, N., Hoge, G., Marandykina, A., Rimkute, L., Chapuis, S., Paulauskas, N., Skeberdis, V.A., O'Brien, J., Pereda, A.E., Bennett, M.V.L., Bukauskas, F.F., 2013. Intracellular magnesium-dependent modulation of gap junction channels formed by neuronal connexin36. *J Neurosci* 33, 4741–4753. doi:10.1523/JNEUROSCI.2825-12.2013
- Palíková, M., Krejčí, R., Hilscherová, K., Babica, P., Navrátil, S., Kopp, R., Bláha, L., 2007. Effect of different cyanobacterial biomasses and their fractions with variable microcystin content on embryonal development of carp (*Cyprinus carpio* L.). *Aquat Toxicol* 81, 312–318.
- Park, J.S., Babica, P., Sovadinová, I., Trosko, J.E., Chang, C.C., Upham, B., 2008. The effects of polycyclic aromatic hydrocarbons on adult human epithelial liver stem cell line, in: *The First Midwest Conference on Stem Cell Biology and Therapy - Book of Abstracts*. Rochester, MI, p. 52.
- Perez-Armendariz, E.M., 2013. Connexin 36, a key element in pancreatic beta cell function. *Neuropharmacology* 75, 557–566.

- Pfenniger, A., Chanson, M., Kwak, B.R., 2013. Connexins in atherosclerosis. *Biochim Biophys Acta* 1828, 157–166.
- Pikula, J., Bandouchova, H., Hilscherova, K., Paskova, V., Sedlackova, J., Adamovsky, O., Knotkova, Z., Lany, P., Machat, J., Marsalek, B., Novotny, L., Pohanka, M., Vitula, F., 2010. Combined exposure to cyanobacterial biomass, lead and the Newcastle virus enhances avian toxicity. *Sci Total Environ* 408, 4984–4992.
- Pluciennik, F., Verrecchia, F., Bastide, B., Herve, J.C., Joffre, M., Deleze, J., 1996. Reversible interruption of gap junctional communication by testosterone propionate in cultured sertoli cells and cardiac myocytes. *J Membr Biol* 149, 169–177.
- Pogoda, K., Kameritsch, P., Retamal, M.A., Vega, J.L., 2016. Regulation of gap junction channels and hemichannels by phosphorylation. *BMC Cell Biol* 17. doi:10.1186/s12860-016-0099-3
- Prasse, C., Stalter, D., Schulte-Oehlmann, U., Oehlmann, J., Ternes, T.A., 2015. Spoilt for choice: A critical review on the chemical and biological assessment of current wastewater treatment technologies. *Water Res* 87, 237–270. doi:10.1016/j.watres.2015.09.023
- Rae, R.S., Mehta, P.P., Chang, C.C., Trosko, J.E., Ruch, R.J., 1998. Neoplastic phenotype of gap-junctional intercellular communication-deficient WB rat liver epithelial cells and its reversal by forced expression of connexin 32. *Mol Carcinog* 22, 120–127.
- Rao, G.N., Baas, A.S., Glasgow, W.C., Eling, T.E., Runge, M.S., Alexander, R.W., 1994. Activation of Mitogen-Activated Protein-Kinases by Arachidonic-Acid and Its Metabolites in Vascular Smooth-Muscle Cells. *J Biol Chem* 269, 32586–32591.
- Ribble, D., Goldstein, N.B., Norris, D.A., Shellman, Y.G., 2005. A simple technique for quantifying apoptosis in 96-well plates. *BMC Biotechnol* 5, 12.
- Rivedal, E., Opsahl, H., 2001. Role of PKC and MAP kinase in EGF- and TPA-induced connexin43 phosphorylation and inhibition of gap junction intercellular communication in rat liver epithelial cells. *Carcinogenesis* 22, 1543–1550.
- Roemer, E., Lammerich, H.P., Conroy, L.L., Weisensee, D., 2013. Characterization of a gap-junctional intercellular communication (GJIC) assay using cigarette smoke. *Toxicol Lett* 219, 248–253.
- Roukos, V., Pegoraro, G., Voss, T.C., Misteli, T., 2015. Cell cycle staging of individual cells by fluorescence microscopy. *Nat Protoc* 10, 334–348.
- Roy, S., Jiang, J.X., Li, A.-F., Kim, D., 2017. Connexin channel and its role in diabetic retinopathy. *Prog Retin Eye Res* 61, 35–59. doi:10.1016/j.preteyeres.2017.06.001
- Ruch, R.J., Cheng, S.J., Klaunig, J.E., 1989. Prevention of cytotoxicity and inhibition of intercellular communication by antioxidant catechins isolated from Chinese green tea. *Carcinogenesis* 10, 1003–1008.
- Ruch, R.J., Madhukar, B. V, Trosko, J.E., Klaunig, J.E., 1993. Reversal of Ras-Induced Inhibition of Gap-Junctional Intercellular Communication, Transformation, and Tumorigenesis by Lovastatin. *Mol Carcinog* 7, 50–59.
- Ruch, R.J., Trosko, J.E., Madhukar, B. V, 2001. Inhibition of connexin43 gap junctional intercellular communication by TPA requires ERK activation. *J Cell Biochem* 83, 163–169.
- Rummel, A.M., Trosko, J.E., Wilson, M.R., Upham, B.L., 1999. Polycyclic aromatic hydrocarbons with bay-like regions inhibited gap junctional intercellular communication and stimulated MAPK activity. *Toxicol Sci* 49, 232–240.
- Sai, K., Kanno, J., Hasegawa, R., Trosko, J.E., Inoue, T., 2000. Prevention of the down-regulation of gap junctional intercellular communication by green tea in the liver of mice fed pentachlorophenol. *Carcinogenesis* 21, 1671–1676.
- Sala, G., Badalamenti, S., Ponticelli, C., 2016. The Renal Connexome and Possible Roles of Connexins in Kidney Diseases. *Am J Kidney Dis* 67, 677–687.
- Sanchez, H.A., Verselis, V.K., 2014. Aberrant Cx26 hemichannels and keratitis-ichthyosis-deafness syndrome: insights into syndromic hearing loss. *Front Cell Neurosci* 8, 354.
- Sarrouilhe, D., Dejean, C., Mesnil, M., 2017. Connexin43- and Pannexin-Based Channels in Neuroinflammation and Cerebral Neuropathies. *Front Mol Neurosci* 10, 320. doi:10.3389/fnmol.2017.00320
- Scarlett, S.S., White, J.A., Blackmore, P.F., Schoenbach, K.H., Kolb, J.F., 2009. Regulation of intracellular calcium concentration by nanosecond pulsed electric fields. *Biochim Biophys Acta* 1788, 1168–1175.
- Schulz, R., Gorge, P.M., Gorbe, A., Ferdinandy, P., Lampe, P.D., Leybaert, L., 2015. Connexin 43 is an emerging therapeutic target in ischemia/reperfusion injury, cardioprotection and neuroprotection. *Pharmacol Ther* 153, 90–106.
- Seki, A., Nishii, K., Hagiwara, N., 2015. Gap junctional regulation of pressure, fluid force, and electrical fields in the

- epigenetics of cardiac morphogenesis and remodeling. *Life Sci* 129, 27–34.
- Shi, X., Chang, C.-C., Basson, M.D., Upham, B., Wei, L., Zhang, P., 2014. Alcohol Disrupts Human Liver Stem/Progenitor Cell Proliferation and Differentiation. *J Stem Cell Res Ther* 4, 205. doi:10.4172/2157-7633.1000205
- Shukla, S.J., Huang, R., Austin, C.P., Xia, M., 2010. The Future of Toxicity Testing: A Focus on In Vitro Methods Using a Quantitative High Throughput Screening Platform. *Drug Discov Today* 15, 997–1007.
- Sigler, K., Ruch, R.J., 1993. Enhancement of Gap Junctional Intercellular Communication in Tumor Promoter-Treated Cells by Components of Green Tea. *Cancer Lett* 69, 15–19.
- Sirnes, S., Kjenseth, A., Leithe, E., Rivedal, E., 2009. Interplay between PKC and the MAP kinase pathway in Connexin43 phosphorylation and inhibition of gap junction intercellular communication. *Biochem Biophys Res Commun* 382, 41–45.
- Sirnes, S., Lind, G.E., Bruun, J., Fykerud, T.A., Mesnil, M., Lothe, R.A., Rivedal, E., Kolberg, M., Leithe, E., 2015. Connexins in colorectal cancer pathogenesis. *Int J cancer* 137, 1–11. doi:10.1002/ijc.28911
- Sklenar, K., Westcrick, J., Szlag, D., 2016. Managing Cyanotoxins in Drinking Water: A Technical Guidance Manual for Drinking Water Professionals. American Water Works Association & Water Research Foundation, Denver, CO.
- Smutna, M., Babica, P., Jarque, S., Hilscherova, K., Marsalek, B., Haeba, M., Blaha, L., 2014. Acute, chronic and reproductive toxicity of complex cyanobacterial blooms in *Daphnia magna* and the role of microcystins. *Toxicol* 79, 11–18.
- Sovadinová, I., Babica, P., Adamovský, O., Alpatova, A., Tarabara, V., Upham, B., Bláha, L., 2017a. Chlorination and ozonation differentially reduced the microcystin content and tumour promoting activity of a complex cyanobacterial extract. *Adv Oceanogr Limnol* 8, 107–120. doi:10.4081/aiol.2017.6342
- Sovadinová, I., Babica, P., Boke, H., Kumar, E., Wilke, A., Park, J.-S., Trosko, J.E., Upham, B.L., 2015. Phosphatidylcholine specific PLC-induced dysregulation of gap junctions, a robust cellular response to environmental toxicants, and prevention by resveratrol. *PLoS One* 10, e0124454.
- Sovadinová, I., Yawer, A., Raška, J., Labohá, P., Kubincová, P., Babica, P., 2017b. The role of gap-junctional intercellular communication in male reproductive system: a target for reproductive toxicants, in: *International Gap Junction Conference - Book of Abstracts*. Glasgow, UK.
- Srinivas, M., Verselis, V.K., White, T.W., 2018. Human diseases associated with connexin mutations. *Biochim Biophys Acta* 1860, 192–201. doi:10.1016/j.bbame.2017.04.024
- Stacey, M., Fox, P., Buescher, S., Kolb, J., 2011. Nanosecond pulsed electric field induced cytoskeleton, nuclear membrane and telomere damage adversely impact cell survival. *Bioelectrochemistry* 82, 131–134. doi:10.1016/j.bioelechem.2011.06.002
- Stains, J.P., Civitelli, R., 2016. A functional assay to assess connexin 43-mediated cell-to-cell communication of second messengers in cultured bone cells. *Methods Mol Biol - Gap Junction Protoc* 1437, 193–201. doi:10.1007/978-1-4939-3664-9_14
- Steuer, A., Schmidt, A., Laboha, P., Babica, P., Kolb, J.F., 2016. Transient suppression of gap junctional intercellular communication after exposure to 100-nanosecond pulsed electric fields. *Bioelectrochemistry* 112, 33–46.
- Steuer, A., Wende, K., Babica, P., Kolb, J.F., 2017. Elasticity and tumorigenic characteristics of cells in a monolayer after nanosecond pulsed electric field exposure. *Eur Biophys J* 46, 567–580. doi:10.1007/s00249-017-1205-y
- Stokes, J. 3rd, Noren, J., Shindell, S., 1982. Definition of terms and concepts applicable to clinical preventive medicine. *J Community Heal* 8, 33–41.
- Sunman, J.A., Foster, M.S., Folse, S.L., May, S.W., Matesic, D.F., 2004. Reversal of the transformed phenotype and inhibition of peptidylglycine alpha-monooxygenase in Ras-transformed cells by 4-phenyl-3-butenoic acid. *Mol Carcinog* 41, 231–246.
- Svircev, Z., Drobac, D., Tokodi, N., Mijovic, B., Codd, G.A., Meriluoto, J., 2017. Toxicology of microcystins with reference to cases of human intoxications and epidemiological investigations of exposures to cyanobacteria and cyanotoxins. *Arch Toxicol* 91, 621–650. doi:10.1007/s00204-016-1921-6
- Takahashi, H., Nomata, K., Mori, K., Matsuo, M., Miyaguchi, T., Noguchi, M., Kanetake, H., 2004. The preventive effect of green tea on the gap junction intercellular communication in renal epithelial cells treated with a renal carcinogen. *Anticancer Res* 24, 3757–3762.
- Takeuchi, H., Suzumura, A., 2014. Gap junctions and hemichannels composed of connexins: potential therapeutic targets for neurodegenerative diseases. *Front Cell Neurosci* 8, 189.

- Terauchi, M., Nagasato, C., Motomura, T., 2015. Plasmodesmata of brown algae. *J Plant Res* 128, 7–15.
- Thimm, J., Mechler, A., Lin, H., Rhee, S., Lal, R., 2005. Calcium-dependent open/closed conformations and interfacial energy maps of reconstituted hemichannels. *J Biol Chem* 280, 10646–10654. doi:10.1074/jbc.M412749200
- Thompson, G.L., Roth, C., Tolstykh, G., Kuipers, M., Ibey, B.L., 2014. Disruption of the actin cortex contributes to susceptibility of mammalian cells to nanosecond pulsed electric fields. *Bioelectromagnetics* 35, 262–272. doi:10.1002/bem.21845
- Tribulova, N., Egan Benova, T., Szeiffova Bacova, B., Vicenczova, C., Barancik, M., 2015. New aspects of pathogenesis of atrial fibrillation: remodelling of intercalated discs. *J Physiol Pharmacol* 66, 625–634.
- Trosko, J.E., 2017. Reflections on the use of 10 IARC carcinogenic characteristics for an objective approach to identifying and organizing results from certain mechanistic studies. *Toxicol Res Appl* 1, 1–10. doi:10.1177/2397847317710837
- Trosko, J.E., 2016. Evolution of Microbial Quorum Sensing to Human Global Quorum Sensing: An Insight into How Gap Junctional Intercellular Communication Might Be Linked to the Global Metabolic Disease Crisis. *Biology (Basel)* 5, 29.
- Trosko, J.E., 2011. The gap junction as a “Biological Rosetta Stone”: implications of evolution, stem cells to homeostatic regulation of health and disease in the Barker hypothesis. *J Cell Commun Signal* 5, 53–66.
- Trosko, J.E., 2007. Gap junctional intercellular communication as a biological “Rosetta stone” in understanding, in a systems biological manner, stem cell behavior, mechanisms of epigenetic toxicology, chemoprevention and chemotherapy. *J Membr Biol* 218, 93–100.
- Trosko, J.E., Chang, C.C., Upham, B.L., Tai, M.H., 2004. Ignored hallmarks of carcinogenesis: Stem cells and cell-cell communication. *Ann N Y Acad Sci* 1028, 192–201.
- Tsushimoto, G., Chang, C.C., Trosko, J.E., Matsumura, F., 1983. Cyto-toxic, mutagenic, and cell-cell communication inhibitory properties of DDT, lindane, and chlordane on Chinese-Hamster cells-in vitro. *Arch Environ Contam Toxicol* 12, 721–730.
- Umeda, M., Noda, K., Ono, T., 1980. Inhibition of metabolic cooperation in Chinese hamster cells by various chemical including tumor promoters. *Gan* 71, 614–620.
- Upham, B.L., Babica, P., Park, J.-S., Whitten, D.A., Wilkerson, C.G., 2011. Determining Early Signaling Response to Environmental Toxicants Using Novel Proteomic Approaches. *Vitr Cell Dev Biol* 47, S42–S43.
- Upham, B.L., Blaha, L., Babica, P., Park, J.S., Sovadinová, I., Pudrith, C., Rummel, A.M., Weis, L.M., Sai, K., Tithof, P.K., Guzvic, M., Vondracek, J., Machala, M., Trosko, J.E., 2008a. Tumor promoting properties of a cigarette smoke prevalent polycyclic aromatic hydrocarbon as indicated by the inhibition of gap junctional intercellular communication via phosphatidylcholine-specific phospholipase C. *Cancer Sci* 99, 696–705.
- Upham, B.L., Boddy, B., Xing, X., Trosko, J.E., Masten, S.J., 1997. Non-genotoxic effects of selected pesticides and their disinfection by-products on gap junctional intercellular communication. *Ozone Sci Eng* 19, 351–369.
- Upham, B.L., Deocampo, N.D., Wurl, B., Trosko, J.E., 1998a. Inhibition of gap junctional intercellular communication by perfluorinated fatty acids is dependent on the chain length of the fluorinated tail. *Int J Cancer* 78, 491–495.
- Upham, B.L., Guzvic, M., Scott, J., Carbone, J.M., Blaha, L., Coe, C., Li, L.L., Rummel, A.M., Trosko, J.E., 2007. Inhibition of gap junctional intercellular communication and activation of mitogen-activated protein kinase by tumor-promoting organic peroxides and protection by resveratrol. *Nutr Cancer* 57, 38–47.
- Upham, B.L., Park, J.-S., Babica, P., Sovadinová, I., Rummel, A.M., Trosko, J.E., Hirose, A., Hasegawa, R., Kanno, J., Sai, K., 2009. Structure-activity-dependent regulation of cell communication by perfluorinated fatty acids using in vivo and in vitro model systems. *Environ Health Perspect* 117, 545–551.
- Upham, B.L., Sovadinová, I., Babica, P., 2016a. Gap Junctional Intercellular Communication: A Functional Biomarker to Assess Adverse Effects of Toxicants and Toxins, and Health Benefits of Natural Products. *J Vis Exp* 118, e54281. doi:10.3791/54281
- Upham, B.L., Sovadinová, I., Park, J.S., Whitten, D.A., Wilkerson, C.G., Babica, P., 2016b. Annexins: A Potential Biomarker for Identifying Tumor Promoting Activity of Environmental Contaminants. *Vitr Cell Dev Biol* 52, S44–S44.
- Upham, B.L., Trosko, J.E., 2009. Oxidative-Dependent Integration of Signal Transduction with Intercellular Gap Junctional Communication in the Control of Gene Expression. *Antioxid Redox Signal* 11, 297–307.
- Upham, B.L., Weis, L.M., Trosko, J.E., 1998b. Modulated gap junctional intercellular communication as a biomarker

- of PAH epigenetic toxicity: Structure-function relationship. *Environ Health Perspect* 106, 975–981.
- Upham, B.L., Whitten, D.A., Wilkerson, C.G., Park, J.S., Sovadinová, I., Babica, P., Trosko, J.E., Blaha, L., 2008b. Mapping signaling pathways that control gap junction function using modern proteomic approaches. *Vitr Cell Dev Biol* 44, S34–S34.
- Upham, B.L., Yao, J.J., Trosko, J.E., Masten, S.J., 1995. Determination of the Efficacy of Ozone Treatment Systems Using a Gap Junction Intercellular Communication Bioassay. *Environ Sci Technol* 29, 2923–2928.
- van Koppen, C.J., Hartmann, R.W., 2015. Advances in the treatment of chronic wounds: a patent review. *Expert Opin Ther Pat* 25, 931–937.
- van Ravenzwaay, B., Kolle, S.N., Ramirez, T., Kamp, H.G., 2013. Vinclozolin: a case study on the identification of endocrine active substances in the past and a future perspective. *Toxicol Lett* 223, 271–279.
- van Zeijl, L., Ponsioen, B., Giepmans, B.N.G., Ariaens, A., Postma, F.R., Várnai, P., Balla, T., Divecha, N., Jalink, K., Moolenaar, W.H., 2007. Regulation of connexin43 gap junctional communication by phosphatidylinositol 4,5-bisphosphate. *J Cell Biol* 177, 881–891.
- Vinken, M., 2012. Gap junctions and non-neoplastic liver disease. *J Hepatol* 57, 655–662.
- Vinken, M., Decrock, E., Leybaert, L., Bultynck, G., Himpens, B., Vanhaecke, T., Rogiers, V., 2012. Non-channel functions of connexins in cell growth and cell death. *Biochim Biophys Acta - Biomembr* 1818, 2002–2008.
- Vinken, M., Doktorova, T., Decrock, E., Leybaert, L., Vanhaecke, T., Rogiers, V., 2009. Gap junctional intercellular communication as a target for liver toxicity and carcinogenicity. *Crit Rev Biochem Mol Biol* 44, 201–222.
- Vinken, M., Johnstone, S.R., 2016. Gap Junction Protocols. *Methods Mol Biol*. doi:10.1007/978-1-4939-3664-9
- Vinken, M., Knapen, D., Vergauwen, L., Hengstler, J.G., Angrish, M., Whelan, M., 2017. Adverse outcome pathways: a concise introduction for toxicologists. *Arch Toxicol*. doi:10.1007/s00204-017-2020-z
- Visser, P.M., Verspagen, J.M.H., Sandrini, G., Stal, L.J., Matthijs, H.C.P., Davis, T.W., Paerl, H.W., Huisman, J., 2016. How rising CO₂ and global warming may stimulate harmful cyanobacterial blooms. *Harmful Algae* 54, 145–159. doi:10.1016/j.hal.2015.12.006
- Vondracek, J., Machala, M., 2016. Environmental Ligands of the Aryl Hydrocarbon Receptor and Their Effects in Models of Adult Liver Progenitor Cells. *Stem Cells Int* 2016, 4326194.
- Wagner, C., Kurtz, A., 2013. Distribution and functional relevance of connexins in renin-producing cells. *Pflugers Arch* 465, 71–77.
- Wang, B., Jacob, S.T., 2011. Role of cancer stem cells in hepatocarcinogenesis. *Genome Med* 3, 11.
- Wang, X., Xu, X., Ma, M., Zhou, W., Wang, Y., Yang, L., 2012. pH-dependent channel gating in connexin26 hemichannels involves conformational changes in N-terminus. *Biochim Biophys Acta* 1818, 1148–1157. doi:10.1016/j.bbamem.2011.12.027
- Warn-Cramer, B.J., Cottrell, G.T., Burt, J.M., Lau, A.F., 1998. Regulation of connexin-43 gap junctional intercellular communication by mitogen-activated protein kinase. *J Biol Chem* 273, 9188–9196.
- Warngard, L., Flodstrom, S., Ljungquist, S., Ahlborg, U.G., 1987. Interaction between quercetin, TPA and DDT in the V79 metabolic cooperation assay. *Carcinogenesis* 8, 1201–1205.
- Watson, C.S., Hu, G.Z., Paulucci-Holthausen, A.A., 2014. Rapid actions of xenoestrogens disrupt normal estrogenic signaling. *Steroids* 81, 36–42.
- Weis, L.M., Rummel, A.M., Masten, S.J., Trosko, J.E., Upham, B.L., 1998. Bay or baylike regions of polycyclic aromatic hydrocarbons were potent inhibitors of gap junctional intercellular communication. *Environ Health Perspect* 106, 17–22.
- Welsch, F., Stedman, D.B., 1983. Inhibition of metabolic cooperation between Chinese hamster V79 cells by structurally diverse teratogens. *Teratology* 27, A83.
- Wernersson, A.-S., Carere, M., Maggi, C., Tusil, P., Soldan, P., James, A., Sanchez, W., Dulio, V., Broeg, K., Reifferscheid, G., Buchinger, S., Maas, H., Van Der Grinten, E., O’Toole, S., Ausili, A., Manfra, L., Marziali, L., Polesello, S., Lacchetti, I., Mancini, L., Lilja, K., Linderoth, M., Lundeborg, T., Fjällborg, B., Porsbring, T., Larsson, D.G.J., Bengtsson-Palme, J., Förlin, L., Kienle, C., Kunz, P., Vermeirssen, E., Werner, I., Robinson, C.D., Lyons, B., Katsiadaki, I., Whalley, C., den Haan, K., Messiaen, M., Clayton, H., Lettieri, T., Carvalho, R.N., Gawlik, B.M., Hollert, H., Di Paolo, C., Brack, W., Kammann, U., Kase, R., 2015. The European technical report on aquatic effect-based monitoring tools under the water framework directive. *Environ Sci Eur* 27, 1–11. doi:10.1186/s12302-015-0039-4
- Westrick, J.A., Szlag, D.C., Southwell, B.J., Sinclair, J., 2010. A review of cyanobacteria and cyanotoxins removal/inactivation in drinking water treatment. *Anal Bioanal Chem* 397, 1705–1714.

- Willebrords, J., Crespo Yanguas, S., Maes, M., Decrock, E., Wang, N., Leybaert, L., Kwak, B.R., Green, C.R., Cogliati, B., Vinken, M., 2016. Connexins and their channels in inflammation. *Crit Rev Biochem Mol Biol* 1–27.
- Willebrords, J., Maes, M., Crespo Yanguas, S., Vinken, M., 2017. Inhibitors of connexin and pannexin channels as potential therapeutics. *Pharmacol Ther* 180, 144–160. doi:10.1016/j.pharmthera.2017.07.001
- Wingard, J.C., Zhao, H.B., 2015. Cellular and Deafness Mechanisms Underlying Connexin Mutation-Induced Hearing Loss - A Common Hereditary Deafness. *Front Cell Neurosci* 9, 202.
- Winterhager, E., Kidder, G.M., 2015. Gap junction connexins in female reproductive organs: implications for women's reproductive health. *Hum Reprod Updat* 21, 340–352. doi:10.1093/humupd/dmv007
- Wong, C., Kelce, W.R., Sar, M., Wilson, E.M., 1995. Androgen receptor antagonist versus agonist activities of the fungicide vinclozolin relative to hydroxyflutamide. *J Biol Chem* 270, 19998–20003.
- Wong, P., Laxton, V., Srivastava, S., Chan, Y.W.F., Tse, G., 2017. The role of gap junctions in inflammatory and neoplastic disorders (Review). *Int J Mol Med* 39, 498–506. doi:10.3892/ijmm.2017.2859
- Wong, R.L.Y., Walker, C.L., 2013. Molecular pathways: Environmental estrogens activate nongenomic signaling to developmentally reprogram the epigenome. *Clin Cancer Res* 19, 3732–3737.
- Wright, C.S., van Steensel, M.A.M., Hodgins, M.B., Martin, P.E.M., 2009. Connexin mimetic peptides improve cell migration rates of human epidermal keratinocytes and dermal fibroblasts in vitro. *Wound Repair Regen* 17, 240–249. doi:10.1111/j.1524-475X.2009.00471.x
- Wu, J., Lin, L., Luan, T., Chan Gilbert, Y.S., Lan, C., 2007. Effects of organophosphorus pesticides and their ozonation byproducts on gap junctional intercellular communication in rat liver cell line. *Food Chem Toxicol* 45, 2057–2063. doi:10.1016/j.fct.2007.05.006
- Xie, H.Y., Cui, Y., Deng, F., Feng, J.C., 2015. Connexin: a potential novel target for protecting the central nervous system? *Neural Regen Res* 10, 659–666.
- Xu, J., Nicholson, B.J., 2012. The role of connexins in ear and skin physiology - functional insights from disease-associated mutations. *Biochim Biophys Acta* 1828, 167–178.
- Xu, J.J., 2015. Cellular imaging: a key phenotypic screening strategy for predictive toxicology. *Front Pharmacol* 6, 191. doi:10.3389/fphar.2015.00191
- Yang, S., Li, W.-H., 2009. Assaying dynamic cell-cell junctional communication using noninvasive and quantitative fluorescence imaging techniques: LAMP and infrared-LAMP. *Nat Protoc* 4, 94–101. doi:10.1038/nprot.2008.219
- Yawer, A., Laboha, P., Dydowiczova, A., Brozman, O., Sychrova, E., Kubincova, P., Babica, P., Sovadinova, I., 2017. Gap junction intercellular communication in testicular cells: implications for male reproductive health., in: 9th International Conference Analytical Cytometry - Abstracts. Prague, Czech Republic, p. 105.
- Yi, C., Koulakoff, A., Giaume, C., 2017. Astroglial connexins as a therapeutic target for Alzheimer's disease. *Curr Pharm Des [Epub ahead of print]*. doi:10.2174/1381612823666171004151215
- Yotti, L.P., Trosko, J.E., 1979. Inhibition of Metabolic Cooperation in Mammalian Tissue-Culture Cells by Phorbol-Myristate Acetate. *Vitr Tissue Cult Assoc* 15, 208–209.
- Zefferino, R., Leone, A., Piccaluga, S., Cincione, R., Ambrosi, L., 2008. Mercury modulates interplay between IL-1beta, TNF-alpha, and gap junctional intercellular communication in keratinocytes: mitigation by lycopene. *J Immunotoxicol* 5, 353–360.
- Zheng, W., Thorne, N., McKew, J.C., 2013. Phenotypic screens as a renewed approach for drug discovery. *Drug Discov Today* 18, 1067–1073.
- Zhi, X.-S.S., Xiong, J., Zi, X.-Y.Y., Hu, Y.-P.P., 2016. The potential role of liver stem cells in initiation of primary liver cancer. *Hepatol Int* 10, 893–901. doi:10.1007/s12072-016-9730-9
- Zong, L., Zhu, Y., Liang, R., Zhao, H.B., 2016. Gap junction mediated miRNA intercellular transfer and gene regulation: A novel mechanism for intercellular genetic communication. *Sci Rep* 6, 19884.
- Zou, H., Liu, X., Han, T., Hu, D., Wang, Y., Yuan, Y., Gu, J., Bian, J., Zhu, J., Liu, Z.P., 2015. Salidroside Protects against Cadmium-Induced Hepatotoxicity in Rats via GJIC and MAPK Pathways. *PLoS One* 10, e0129788.

7 AUTHOR RESUME

RNDr. Pavel Babica, Ph.D.

✉ babica@recetox.muni.cz

Born:

- 1978, Kroměříž, Czech Republic

Education:

- 2006 Ph.D. in Environmental Chemistry (Masaryk University, Brno, Czech Republic)
- 2005 RNDr. degree in Ecotoxicology (Masaryk University, Brno, Czech Republic)
- 2002 M.Sc. in Ecotoxicology, *summa cum laude* (Masaryk University, Brno, Czech Republic)



Work experience:

- 2012-present Research Scientist, Masaryk University, RECETOX – Research Centre for Toxic Compounds in the Environment, Brno, Czech Republic
- 2003-present Research Scientist (part time), Institute of Botany of the Czech Academy of Sciences Department of Experimental Phycology and Ecotoxicology, Brno, Czech Republic
- 2006-2010 Visiting Research Associate, Michigan State University, Department Pediatrics and Human Development & Food Safety and Toxicology Center, East Lansing, MI, USA)

Research topics – key words:

- *In vitro* toxicology, *In vitro* mammalian cell cultures; Stem cell-based *in vitro* models; Disruption of tissue homeostasis; Tumor promotion; Gap junctional intercellular communication (GJIC); Toxic cyanobacteria; Cyanotoxins

Awards:

- 2007 The First Place Award for The Best Poster Presentation in Postdoctoral fellow/Research Associate Category in the fall meeting of The Michigan Society of Toxicology
- 2007 The Rector's Award for the best students in doctoral programs (Masaryk University, Brno, CZ)
- 2006 The Dean's Award for the best students in doctoral programs (Faculty of Sciences, Masaryk University, Brno, CZ)
- 2003 The Best Platform Presentation in the Environmental section of the Student's Scientific Conference (organized by the Slovak Academy of Sciences)
- 2002 1st -2nd place in the competition of the Diploma Theses organized by Tocoen Ltd.

Attended courses:

- Applied *In Vitro* Toxicology Course (ESTIV/ApTox, Cascais, Portugal, 2015)
- Advanced microscopical techniques (CEITEC and Faculty of Science, Masaryk University, Brno, CZ, 2013)
- Analyses of structures and interactions of biomolecules (Institute of Biophysics, CAS, Brno, CZ, 2011)
- Mutagenization of Toxic Cyanobacterium Planktothrix (Institute for Limnology, Austrian Academy of Sciences, Technology Center, Mondsee, Austria, 2011)
- Summer School of Environmental Chemistry and Ecotoxicology (RECETOX, Masaryk University, Brno, CZ, 2005)
- Summer School of Environmental Modeling (AUC Nové Hradky, The Faculty of Biological Sciences, University of South Bohemia, CZ, 2003)

Research Projects:

- 2017-2020 “NaToxAq” - Natural Toxins and Drinking Water Quality - From Source to Tap (MSCA-ITN No. 722493, co-hosted by RECETOX, Masaryk University, *co-supervisor of an early stage researcher / Ph.D. candidate*)
- 2016-2018 “Importance of Toll-like receptors in intestinal epithelium response to cyanobacterial water bloom” (GACR 16-24949S, hosted by Institute of Biophysics, CAS, co-hosted by RECETOX, Masaryk University, *co-principal investigator*)
- 2015-2017 “Role of the stem and differentiated cells in hepatotoxicity and hepatocarcinogenicity induced by cyanotoxins” (GACR 15-12408S, RECETOX, Masaryk University, *research team member*)
- 2012-2014 “Novel in vitro approach for identification of chemopreventive effects and mechanisms of phytochemicals” (MSMT KONTAKT II LH12034, Institute of Botany, CAS, *principal investigator*)
- 2012 “New methods for monitoring of hazardous drinking water contaminants - cyanobacterial toxins” (Thomas Bata Foundation, Institute of Botany, CAS, *principal investigator*)
- 2011-2013 “A novel approach for monitoring, toxicity evaluation and risk assessment of cyanobacterial toxins – a use of passive samplers” (SoMoPro 2SGA2858, Institute of Botany, CAS, *principal investigator*)
- 2008-2010 “Tumor promotional mechanisms of cyanobacterial metabolites” (GAČR 524/08/0496, Masaryk University/Institute of Botany, CAS, *research team member*)
- 2006-2010 “Epigenetic toxicity of polyaromatic hydrocarbons” (NIEHS R01 ES013268-01A2, Michigan State University, *postdoctoral researcher*)
- 2004-2006 “Toxic cyanobacteria in the Czech Republic” (GAAV KJB6005411, Institute of Botany, CAS, *research team member*)
- 2003-2005 “Strategies for Microcystis sp. overwintering - signal function of microcystin? ” (GACR 206/03/1215, Institute of Botany, CAS, *research team member*)
- 2004 “Allelopathic effects of microcystins in aquatic environment” (FRVS TO G4 545/2004, RECETOX, Masaryk University, *principal investigator*).

Teaching:

RECETOX, Faculty of Science, Masaryk University, Brno: Introduction to the study of Special Biology (2016-present), Modern methods in Ecotoxicology (2014-present), Advanced seminar in ecotoxicology (2014-present), Seminar for Ecotoxicology (2014), Summer School of Environmental Chemistry and Ecotoxicology (2005-2006)

Mentoring/supervising:

B.Sc. theses: **8 successfully defended, and 1 co-supervised in progress** at Faculty of Science, Masaryk University, Brno, CZ

M.Sc. theses: **8 supervised and 2 co-supervised and successfully defended, 2 supervised, and 1 co-supervised in progress** at Faculty of Science, Masaryk University, Brno, CZ (11); at Department of Physiology and Biochemistry of Animals, University of Greifswald, Germany (1); and at Faculty of Pharmacy, University of Veterinary and Pharmaceutical Sciences, Brno, CZ (1)

Ph.D. theses: **7 supervised and 3 co-supervised in progress** at Faculty of Science, Masaryk University, Brno, CZ (9), and at Faculty of Science, University of South Bohemia, Ceske Budejovice, CZ (1)

Presentations and conferences:

- Author or co-author of more than 150 conference contributions, active personal participation at >30 major **international conferences and workshops including 8 lectures** (4 invited lectures), **3 extramural invited lectures** at universities or research institutions, >20 lectures at national conferences and workshops

Lectures at international conferences or workshops

- Babica, P., Sovadinová, I., Upham, B. (2016): Gap junctional intercellular communication: A biomarker for assessing environmental stressors and chemopreventive compounds. In: **Central and Eastern European Conference on Health and the Environment – CEECHE 2016**, Prague, CZ, Apr 10-14, 2016 (*lecture*)
- Babica, P. (2015): 2D and 3D in vitro models to study disruption of liver tissue homeostasis. In: **Alternatives for pharmacological and toxicity testing - with special focus on 2D and 3D liver in vitro models**, workshop organized by RECETOX, Masaryk University, Brno, CZ, Sep 24, 2015 (*invited lecture*)

- Babica, P., Upham, B. (2015): Gap junction Function: A Biomarker for Elucidating Toxicant-Induced Mechanisms of Tissue Dysfunction. In: **54th annual meeting of Society of Toxicology**, San Diego, CA, USA, Mar 22-26, 2015 (*invited lecture*)
- Babica, P., Novaková, K., Adamovský, O., Bláha, L. (2014): Cyanobacterial toxins and human health –tumor promoting and carcinogenic effects. In: **Trends in Natural Products Research 2014**, 23-25 June, 2014 (*invited lecture*)
- Babica, P., Jaša, L., Sadílek, J., Kohoutek, J., Straková, L., Maršálek, B. (2013): Application of passive sampling for assessment of microcystin contamination and removal efficiency in drinking water treatment plants. In: **SETAC North America 34th Annual Meeting**, Nashville, TN, USA, Nov 17-21, 2013 (*lecture*)
- Babica, P., Novák, J., Sovadinová, I. (2013): Study of Paracrine Signaling between Leydig and Sertoli Cells Using Impedance Analysis. In: **2nd Conference on Impedance-Based Cellular Assays**, Budapest, Hungary, Aug 21-23, 2013 (*lecture*)
- Babica, P., Sovadinová, I., Lenčešová, Z., Trosko, J., Upham, B. (2012): In vitro assessment of gap junctional intercellular communication (GJIC) as a tool for identification and characterization of chemopreventive activity of phytochemicals. In: **Natural Anticancer Drugs 2012**, Olomouc, CZ, Jun 30-Jul 4, 2012 (*lecture*)
- Babica, P., Bláha, L., Kopp, R., Hilscherová, K., Pašková, V., Adamovský, O., Maršálek, B., Palíková, M., Krejčí, R., Navrátil, S. (2006): Microcystin bioaccumulation and biomarker responses in fish exposed to cyanobacterial blooms. In: **RESLIM 2006 Satellite Workshop - Cyanobacterial water blooms: effects, consequences and management**, Brno, CZ, Sep 1-2, 2006 (*invited lecture*)

Invited extramural lectures at universities and research institutes

- Babica, P. (2017): Gap junctional intercellular communication: a powerful biomarker of toxicant-induced tissue dysfunction. Invited Lecture at the Department of Physiology and Biochemistry of Animals, **University of Greifswald**, Greifswald, Germany, Apr 5, 2017
- Babica, P. (2014): Gap junctional intercellular communication – in vitro biomarker for evaluation of epigenetic effects of chemicals. In: Seminar at **Leibniz Institut für Plasma Forschung und Technologie**, Greifswald, Germany, March 25, 2014
- Babica, P. (2004): “Cyanotoxiny”. In: Sinice vodních květů – proč se jich tak bojíme? Seminar at the Department of Botany, Faculty of Science, **Charles University**, Prague, CZ, Nov 23, 2004

Publications:

- **41 papers in Web of Science (WoS) database**
 - h-index (WoS): 15; 838 citations in total; 20.49 citations per item [Nov 21, 2017]
 - JCR ranking of journals publishing author's work: Q1: 49%; Q2: 22%; Q3: 22%; Q4: 7%
- **4 additional papers in Scopus database**
- **4 papers in other peer-reviewed international journals**
- **3 book chapters**
- **5 papers in peer-reviewed national journals**
- **1 edited special issue of peer-reviewed international journal**
- **3 popularization papers**
- **1 utility patent**

Database links:

- Researcher ID: <http://www.researcherid.com/rid/B-2587-2013>
- ORCID: <http://orcid.org/0000-0001-6399-3554>
- ResearchGate: https://www.researchgate.net/profile/Pavel_Babica2
- Scopus: <https://www.scopus.com/authid/detail.uri?authorId=22933632100>

8 LIST OF SCHOLARLY WORK PUBLISHED BY THE AUTHOR

Articles published in scholarly journals listed in the Web of Science / JCR database		IF¹	Q²	Cit.³
[1]	Sharma, A., Bányiová, K., Babica, P. , El Yamani, N., Collins, A. R., Čupr, P.* (2017): Different DNA damage response of cis and trans isomers of commonly used UV filter after the exposure on adult human liver stem cells and human lymphoblastoid cells. <i>Science of the Total Environment</i> 593-594: 18-26.	4.900	Q1	0
[2]	Steuer, A., Wende, K., Babica, P. , Kolb J.F.* (2017): Elasticity and Tumorigenic Characteristics of cells in a monolayer after nanosecond pulsed electric field exposure. <i>European Biophysics Journal</i> 46(6): 567-580.	1.472	Q4	0
[3]	Babica, P.* , Čtveráčková, L., Lenčesová Z., Trosko, J., Upham B. (2016): Chemopreventive agents attenuate rapid inhibition of gap junctional intercellular communication induced by environmental toxicants. <i>Nutrition and Cancer</i> 68(5): 827-837.	2.447	Q3	2
[4]	Babica, P.* , Zurabian, R., Kumar, E.R., Chopra, R., Mianeki, M., Park, J.-S., Jasa, L., Trosko, J., Upham, B. (2016): Methoxychlor and vinclozolin induce rapid changes in intracellular and intercellular signaling in liver progenitor cells. <i>Toxicological Sciences</i> 153(1): 174-185.	4.081	Q1	2
[5]	Kollár, P., Šmejkal, K., Salmonová, H., Vlková, E., Lepšová-Skácelová, O., Balounová, Z., Rajchard, J., Cvačka, J., Jasa, L., Babica, P. , Pazourek, J.* (2016): Assessment of chemical impact of invasive bryozoan <i>Pectinatella magnifica</i> on the environment: Cytotoxicity and antimicrobial activity of <i>P. magnifica</i> extracts. <i>Molecules</i> 21(11): 1476-1489.	2.861	Q2	1
[6]	Machalová-Šišková, K., Jančula, D., Drahoš, B., Machala, L., Babica, P. , Godoy-Alonso, P., Trávníček, Z., Maršálek, B., Sharma, V. K., Zbořil, R.* (2016): High-valent iron (FeVI, FeV, and FeIV) species in water: Characterization and oxidative transformation of estrogenic hormones. <i>Physical Chemistry Chemical Physics</i> 18(28): 18802-18810.	4.123	Q1	3
[7]	Steuer, A., Schmidt, A., Labohá, P., Babica, P. , Kolb, J.F.* (2016): Transient suppression of gap junctional intercellular communication after exposure to 100-nanosecond pulsed electric fields. <i>Bioelectrochemistry</i> 112: 33-46.	3.346	Q1	1
[8]	Upham, B.*, Sovadinová, I., Babica, P. (2016): Gap junctional intercellular communication: a functional biomarker to assess adverse effects of toxicants and toxins, and health benefits of natural products. <i>Journal of Visualised Experiments</i> 118: e54281.	1.232	Q2	0
[9]	Adamovský, O.*, Moosová, Z., Pekarová, M., Basu, A., Babica, P. , Šviháková-Šindlerová, L., Kubala, L., Bláha, L. (2015): Immunomodulatory potency of microcystin, an important water polluting cyanobacterial toxin. <i>Environmental Science and Technology</i> 49(20): 12457-12464.	6.198	Q1	11
[10]	Sovadinová, I., Babica, P. , Boke, H., Kumar, E.R., Wilke, A., Park, J.S., Trosko, J.E., Upham, B.* (2015): Phosphatidylcholine specific phospholipase C dysregulation of gap junctional intercellular communication, a robust cellular response to environmental toxicants, and prevention by resveratrol. <i>PLOS One</i> 10(5): e0124454.	2.806	Q1	6

[11]	Jančula, D., Straková, L., Sadílek, J., Maršálek, B., Babica, P.* (2014): Survey of cyanobacterial toxins in the Czech water reservoirs – the first observation of neurotoxic saxitoxins. <i>Environmental Science and Pollution Research</i> 21(13): 8006-8015.	2.741	Q2	13
[12]	Smutná, M., Babica, P. , Jarque, S., Hilscherová, K., Haeba, M., Bláha, L.* (2014): Acute, chronic and reproduction toxicity of complex cyanobacterial blooms to <i>Daphnia magna</i> and the role of microcystins. <i>Toxicon</i> 79: 11-18.	1.927	Q3	11
[13]	Jančula, D.*, Maršálek, B., Babica, P. (2013): Photodynamic effects of 31 different phthalocyanines on human keratinocyte cell line HaCaT. <i>Chemosphere</i> 93(6): 870-874.	4.208	Q1	1
[14]	Osgood, R.O., Upham, B. L., Hill, T., Helms, K. L., Velmurugan, K., Babica, P. , Bauer, A.K.* (2013): Polycyclic aromatic hydrocarbon-induced signaling events relevant to inflammation and tumorigenesis in lung cells are dependent on molecular structure. <i>PLoS ONE</i> 8(6): e65150.	2.806	Q1	9
[15]	Nováková, K., Bláha, L., Babica, P.* (2012): Tumor promoting effects of cyanobacterial extracts are potentiated by anthropogenic contaminants – Evidence from in vitro study. <i>Chemosphere</i> 89 (1): 30-37.	4.208	Q1	5
[16]	Bártová, K.*, Hilscherová, K., Babica, P. , Maršálek, B. (2011): Extract of <i>Microcystis</i> water bloom affects cellular differentiation in filamentous cyanobacterium <i>Trichormus variabilis</i> (Nostocales, Cyanobacteria). <i>Journal of Applied Phycology</i> 23(6): 967-973.	2.616	Q1	8
[17]	Bártová, K., Hilscherová, K., Babica, P. , Maršálek, B., Bláha, L.* (2011): Effects of microcystin and complex cyanobacterial samples on growth and oxidative stress parameters in green alga <i>Pseudokirchneriella subcapitata</i> and comparison with the effects of model oxidative stressor, herbicide paraquat. <i>Environmental Toxicology</i> 26(6): 641–648.	2.937	Q1	13
[18]	Nováková, K., Babica, P.* , Adamovský, O., Bláha, L. (2011): Modulation of gap-junctional intercellular communication by a series of cyanobacterial samples from nature and laboratory cultures. <i>Toxicon</i> 58(1): 76-84.	1.927	Q3	14
[19]	Alpatova, A.L., Shan, W., Babica, P. , Rogensues, A. R., Masten, S. J., Drown, E., Mohanty, A. K., Upham, B. L., Alocilja, E. C., Tarabara, V. V.* (2010): Single-walled carbon nanotubes dispersed in aqueous media via non-covalent functionalization: Effect of dispersant on the stability, cytotoxicity, and epigenetic toxicity of nanotube suspensions. <i>Water Research</i> 44(2): 505-520.	6.942	Q1	106
[20]	Bláha, L.*, Bláhová, L., Kohoutek, J., Adamovský, O., Babica, P. , Maršálek, B. (2010): Temporal and spatial variability of cyanobacterial toxins microcystins in three interconnected freshwater reservoirs. <i>Journal of the Serbian Chemical Society</i> 75(9): 1303-1312.	0.822	Q4	10
[21]	Bláha, L., Babica, P.* , Hilscherová, K., Upham, B. (2010): Inhibition of gap-junctional intercellular communication and activation of mitogen-activated protein kinases by cyanobacterial extracts - indications of novel tumor promoting cyanotoxins? <i>Toxicon</i> 55(1): 126-134.	1.927	Q3	12
[22]	Upham, B.*, Park, J.S., Babica, P. , Sovadinová, I., Rummel, A., Trosko, J., Hirose, A., Hasegawa, R., Kanno, J. and Sai, K. (2009): Structure-activity-dependent regulation of cell communication by perfluorinated acids using in vivo and in vitro model systems. <i>Environmental Health Perspectives</i> 117(4): 545-551.	9.776	Q1	22
[23]	Bernardová, K., Babica, P. , Maršálek, B., Bláha, L.* (2008): Isolation and endotoxin activities of lipopolysaccharides from cyanobacterial cultures and complex water blooms and comparison with the effects of heterotrophic bacteria and green alga. <i>Journal of Applied Toxicology</i> 28(1): 72-77.	3.159	Q2	20

[24]	Bláhová, L., Babica, P. , Adamovský, O., Kohoutek, J., Maršálek B., Bláha, L.* (2008): Analyses of cyanobacterial toxins microcystins and cylindrospermopsin in water bloom samples and drinking waters from the Czech Republic and evaluation of health risks. <i>Environmental Chemistry Letters</i> 6(4): 223-227.	3.594	Q1	27
[25]	Kohoutek, J., Babica, P. , Bláha, L., Maršálek, B.* (2008): A novel approach for monitoring of cyanobacterial toxins - development and evaluation of the passive sampler for microcystins. <i>Analytical and Bioanalytical Chemistry</i> 390(4): 1167-1172.	3.431	Q1	15
[26]	Pašková, V., Adamovský, O., Pikula, J., Skocovská, B., Bandouchová, H., Horáková, J., Babica, P. , Maršálek, B., Hilscherová, K.* (2008): Detoxification and oxidative stress responses along with microcystins accumulation in Japanese quail exposed to cyanobacterial biomass. <i>Science of the Total Environment</i> 398(1-3): 34-47.	4.900	Q1	29
[27]	Upham, B.*, Bláha, L., Babica, P. , Park, J.S., Sovadinová, I., Pudrith, C., Rummel, A., Weis, L., Sai, K., Tithof, P., Guzvic, M., Vondracek, J., Machala, M., Trosko, J. (2008): Tumor promoting properties of a cigarette smoke prevalent polycyclic aromatic hydrocarbon as indicated by the inhibition of gap junctional intercellular communication via phosphatidylcholine-specific phospholipase C. <i>Cancer Science</i> 99(4): 696-705.	3.974	Q2	22
[28]	Adamovský, O., Kopp, R., Hilscherová, K., Babica, P. , Palíková, M., Pašková, V., Navrátil, S., Maršálek, B., Bláha, L.* (2007): Microcystin kinetics (bioaccumulation, elimination) and biochemical responses in common carp and silver carp exposed to toxic cyanobacterial blooms. <i>Environmental Toxicology and Chemistry</i> 26(12): 2687-2693.	2.951	Q2	48
[29]	Babica, P.* , Hilscherová, K., Bártová K., Maršálek, B., Bláha, L. (2007): Effects of dissolved microcystins on growth of planktonic photoautotrophs. <i>Phycologia</i> 46(2): 137-142.	1.826	Q2	31
[30]	Bláhová, L., Babica, P. , Maršálková, E., Maršálek, B., Bláha, L.* (2007): Concentrations and seasonal trends of extracellular microcystins in freshwaters of the Czech Republic – Results of the National Monitoring Program. <i>Clean</i> 35(4): 348-354.	1.473	Q3	18
[31]	Palíková, M.*, Krejčí, R., Hilscherová, K., Babica, P. , Navrátil, S., Kopp, R., Bláha, L. (2007): Effect of different cyanobacterial biomasses and their fractions with variable microcystin content on embryonal development of carp (<i>Cyprinus carpio</i> L.). <i>Aquatic Toxicology</i> 81(3): 312-318.	4.129	Q1	50
[32]	Palíková, M.*, Krejčí, R., Hilscherová, K., Burýšková, B., Babica, P. , Navrátil, S., Kopp, R., Bláha, L. (2007): Effects of different oxygen saturation to activity of complex biomass and aqueous crude extract of cyanobacteria during embryonal development in carp (<i>Cyprinus carpio</i> L.). <i>Acta Veterinaria Brno</i> 76 (2): 291-299.	0.415	Q4	4
[33]	Skočovská, B., Hilscherová, K., Babica, P. , Adamovský, O., Bandouchová, H., Horáková, J., Knotková, Z., Maršálek, B., Pašková, V., Pikula, J.* (2007): Effects of cyanobacterial biomass on the Japanese quail. <i>Toxicon</i> 49(7): 793-803.	1.927	Q3	18
[34]	Addico, G.*, Hardege, J., Komarek, J., Babica, P. , de Graft-Johnson, K.A.A. (2006): Cyanobacteria species identified in the Weiya and Kpong reservoirs, Ghana, and their implications for drinking water quality with respect to microcystin. <i>African Journal of Marine Science</i> 28(2): 451-456.	1.229	Q3	4
[35]	Babica, P.* , Bláha, L., Maršálek, B. (2006): Exploring the natural role of microcystins - a review of effects on photoautotrophic organisms. <i>Journal of Phycology</i> 42(1): 9-20.	2.608	Q1	134

[36]	Babica, P.* , Kohoutek, J., Bláha, L., Adamovský, O., Maršálek, B. (2006): Evaluation of extraction approaches linked with ELISA and HPLC for analyses of microcystin-LR, -RR and -YR in freshwater sediments with different organic material content. <i>Analytical and Bioanalytical Chemistry</i> 385(8): 1545-1551.	3.431	Q1	56
[37]	Burýšková, B., Hilscherová, K., Babica, P. , Vršková, D., Maršálek, B., Bláha, L.* (2006): Toxicity of complex cyanobacterial samples and their fractions in <i>Xenopus laevis</i> embryos and the role of microcystins. <i>Aquatic Toxicology</i> 80(4): 346-354.	4.129	Q1	44
[38]	Pavlova, V.* Babica, P. , Todorova, D., Bratanova, Z., Maršálek, B. (2006): Contamination of some reservoirs and lakes in Republic of Bulgaria by microcystins. <i>Acta Hydrochimica et Hydrobiologica</i> 34(5): 437-441.	0.907	Q3	14
[39]	Zeisbergerová, M.* Babica, P. , Košťál, V., Šrámková, M., Bláha, L., Glatz, Z., Kahle, V. (2006): Separation of microcystins on monolithic electrochromatography columns. <i>Journal of Chromatography B</i> 841(1-2): 140-144.	2.603	Q2	15
[40]	Babica, P.* , Bláha, L., Maršálek, B. (2005): Removal of microcystins by phototrophic biofilms – a microcosm study. <i>Environmental Science and Pollution Research</i> 12(6): 369-374.	2.741	Q2	25
[41]	Bláha, L.* Babica, P. , Vilalta, E. and Maršálek, B. (2004): Geosmin occurrence in riverine cyanobacterial mats: is it causing a significant health hazard? <i>Water Science and Technology</i> 49(9): 307-312.	1.197	Q3	6

Articles published in scholarly journals or proceedings listed in the Scopus database		IF ¹	Q ²	Cit. ³
[42]	Steuer, A., Schmidt, A., Babica, P. , Kolb, J.F.* (2015): Effects of nanosecond pulsed electric fields on cell-cell communication in a monolayer. In: <i>Proceedings of 1st World Congress on Electroporation and Pulsed Electric Fields</i> (Eds.: Jarm, T., Kramar, P.), p. 192-195, IFMBE Proceedings Vol. 53. Springer.	---	---	0
[43]	Addico, G. N. D.* Babica, P. , Kohoutek, J., de Graft-Johnson, K.A.A. (2012): Microcystin-RR Like Toxin Identified in the Cyanobacterium <i>Anabaena flos-aquae</i> Strain CCAP 1403/13B Culture. <i>West African Journal of Applied Ecology</i> 19(1): 9-16.	---	Q4	0
[44]	Addico, G. N. D.* Babica, P. , Kohoutek, J., de Graft-Johnson, K. A. A. (2010): Levels of Demethylated Microcystin - RR ([D - Asp3] MCYST-RR) and Five Other Putative Microcystins Identified in a Culture of <i>Planktothrix</i> sp. Strain CCAP 1460/13. <i>West African Journal of Applied Ecology</i> 17: 37-53.	---	Q4	0
[45]	Bláha, L.* Babica, P. , Maršálek, B. (2009): Toxins produced in cyanobacterial water blooms - toxicity and risks. <i>Interdisciplinary Toxicology</i> 2: 36-41.	---	Q3	60

Articles published in another international peer-reviewed journals (not listed in the above categories)		IF ¹	Q ²	Cit. ³
[46]	Addico, G. N. D.* Babica, P. , Kohoutek, J., deGraft-Johnson, K.A.A., Babica, P. (2017): Cyanobacteria and cyanotoxin contamination in untreated and treated drinking water in Ghana. <i>Advances in Oceanography and Limnology</i> 8(1): 92-106.			
[47]	Sovadinová, I.* Babica, P. , Adamovský O., Alpatova, A., Tarabara, V., Upham, B., Bláha, L. (2017): Chlorination and ozonation differentially reduced the microcystin content and tumour promoting activity of a complex cyanobacterial extract. <i>Advances in Oceanography and Limnology</i> 8(1): 107-120.	---	---	0

[48]	Stoyneva-Gaertner, M. P.*, Descy, J.-P., Latli, A., Uzunov, B., Pavlova, V., Bratanova, Z., Babica, P., Maršálek, B., Meriluoto, J., Spoof, L. (2017): Assessment of cyanoprokaryote blooms and of cyanotoxins in Bulgaria in a 15-years period (2000-2015). <i>Advances in Oceanography and Limnology</i> 8(1): 131-152.	---	---	0
[49]	Kopp R.*, Mareš J., Kubiček Z., Babica P. (2005): The influence of toxic cyanobacterial water blooms on the hematological indicators of silver carp (<i>Hypophthalmichthys molitrix</i> Val.). <i>Oceanological and Hydrobiological Studies</i> 34 (supplement 3): 85-92.	0.544	Q4	0
[50]	Maršálek, B.*, Bláha, L., Babica, P. (2003): Analyses of microcystins in the biomass of <i>Pseudanabaena limnetica</i> collected in Znojmo reservoir. <i>Czech Phycology</i> 3: 195-197.	---	---	0

Article published in a Czech peer-reviewed journal included in the List of non-impact peer-reviewed journals published in the Czech Republic		IF ¹	Q ²	Cit. ³
[51]	Jančula, D.*, Babica, P. , Straková, L., Sadílek, J., Maršálek, B. (2013): Saxitoxin - neurotoxin produkovaný sinicemi v povrchových vodách České republiky. <i>Vodní hospodářství</i> 63(12): 406-409.	---	---	0
[52]	Holba, M.*, Matysíková, J., Došek, M., Jančula, D., Mikula, P., Maršálek, B. Maršálková, E., Babica, P. , Novák, Šišková, K., Zbořil, R., Kejvalová, K. (2013): Dočištění a hygienizace komunálního odtoku z ČOV pomocí směsi železanů/železičanů a nanočástic nulamocného železa. <i>Vodní hospodářství</i> 63(5): 144-149.	---	---	0
[53]	Sovadinová, I.*, Babica, P. , Adamovský O., Alpatova, A., Upham, B. (2011): Epigenetická toxicita komplexních vzorků cyanobaktérií - vliv ozonizace a chlorace. <i>Bulletin VÚRH</i> 47(2011/4): 27-35.	---	---	0
[54]	Bártová, K.*, Babica, P. , Hilscherová, K., Bláha, L. (2007): Vliv toxinu sinic - microcystinu - na rust a biomarkery u fytoplanktonních organismu. <i>Bulletin VÚRH</i> 43(4): 11-16.	---	---	0
[55]	Kohoutek, J.*, Adamovský, O., Babica, P. , Maršálek, B., Maršálková, E., Ocelka, T., Jančula, D. (2007): Využití pasivních vzorkovačů pro detekci cyanotoxinů v povrchových vodách. <i>Bulletin VÚRH</i> 43(3): 43-48.	---	---	0

Chapter(s) in a scholarly book publication		IF ¹	Q ²	Cit. ³
[56]	Babica P.* , Sovadinová, I., Upham, B. (2016): Scrape loading / dye transfer. In: <i>Methods in Molecular Biology Vol. 1437 - Gap Junction Protocols</i> (Eds.: Vinken, M. , Johnstone, S.), pp. 133-144, Springer, ISBN 978-1-4939-3662-5.	---	---	1
[57]	Maršálek, B.*, Babica, P. (2014): Optical sensors for detection of cyanobacteria. In: <i>Encyclopedia of Aquatic Ecotoxicology</i> (Eds.: Férard, J.F. and Blaise, C.), p. 805-814. Springer, ISBN-10: 9400750404 ISBN-13: 978-9400750401, 1221 pp.	---	---	0
[58]	Maršálek, B.*, Bláha, L., Bláhová, L., Babica, P. (2005): Czech Republic: Management and Regulation of Cyanobacteria and Cyanotoxins. In: <i>Current approaches to cyanotoxin risk assessment, risk management and regulations in different countries</i> (Eds.: Chorus, I.), pp. 37-39. <i>WaBoLu – Heft 02-05</i> , Federal Environmental Agency (Umweltbundesamt), Dessau, Germany, ISSN:0175-4211.	---	---	0

¹JCR impact factor 2016; ²JCR Rank 2016 for the journals listed in the WoS database, and SJR Rank 2016 for the journals listed in the Scopus database; ³ Number of unique citations w/o self-citations combined from WoS and Scopus (up to Nov 21, 2017); * indicates the corresponding author

9 LIST OF ATTACHMENTS

This thesis is based on following original research papers and publications co-authored by the candidate, which have been cited throughout the thesis and their full-texts are provided in the Attachments. Asterisks indicate the corresponding author.

- I. **Babica, P.***, Sovadinová, I., Upham, B.L., 2016. Scrape loading/dye transfer assay, in: *Methods in Molecular Biology - Gap junction Protocols*. pp. 133–144.
- II. Upham, B.L.*, Sovadinová, I., **Babica, P.**, 2016. Gap junctional Intercellular Communication: A Functional Biomarker to Assess Adverse Effects of Toxicants and Toxins, and Health Benefits of Natural Products. *Journal of Visualized Experiments* 118, e54281.
- III. Upham, B.L.*, Blaha, L., **Babica, P.**, Park, J.S., Sovadinova, I., Pudrith, C., Rummel, A.M., Weis, L.M., Sai, K., Tithof, P.K., Guzvic, M., Vondracek, J., Machala, M., Trosko, J.E., 2008. Tumor promoting properties of a cigarette smoke prevalent polycyclic aromatic hydrocarbon as indicated by the inhibition of gap junctional intercellular communication via phosphatidylcholine-specific phospholipase C. *Cancer Science* 99, 696–705.
- IV. Sovadinová, I., **Babica, P.**, Boke, H., Kumar, E., Wilke, A., Park, J.-S., Trosko, J.E., Upham, B.L.* , 2015. Phosphatidylcholine specific PLC-induced dysregulation of gap junctions, a robust cellular response to environmental toxicants, and prevention by resveratrol. *PLoS One* 10, e0124454.
- V. **Babica, P.***, Zurabian, R., Kumar, E.R., Chopra, R., Mianecky, M.J., Park, J.-S., Jaša, L., Trosko, J.E., Upham, B.L., 2016. Methoxychlor and vinclozolin induce rapid changes in intercellular and intracellular signaling in liver progenitor cells. *Toxicological Sciences* 153, 174–185.
- VI. Osgood, R.S., Upham, B.L., Hill, T., Helms, K.L., Velmurugan, K., **Babica, P.**, Bauer, A.K.* , 2013. Polycyclic aromatic hydrocarbon-induced signaling events relevant to inflammation and tumorigenesis in lung cells are dependent on molecular structure. *PLoS One* 8, e65150.
- VII. Upham, B.L.* , Park, J.-S., **Babica, P.**, Sovadinová, I., Rummel, A.M., Trosko, J.E., Hirose, A., Hasegawa, R., Kanno, J., Sai, K., 2009. Structure-activity-dependent regulation of cell communication by perfluorinated fatty acids using in vivo and in vitro model systems. *Environmental Health Perspectives* 117, 545–551.
- VIII. Bláha, L., **Babica, P.***, Hilscherová, K., Upham, B.L., 2010. Inhibition of gap-junctional intercellular communication and activation of mitogen-activated protein kinases by cyanobacterial extracts - Indications of novel tumor-promoting cyanotoxins? *Toxicon* 55, 126–134.
- IX. Nováková, K., **Babica, P.***, Adamovský, O., Bláha, L., 2011. Modulation of gap-junctional intercellular communication by a series of cyanobacterial samples from nature and laboratory cultures. *Toxicon* 58, 76–84.
- X. Nováková, K., Bláha, L., **Babica, P.***, 2012. Tumor promoting effects of cyanobacterial extracts are potentiated by anthropogenic contaminants – Evidence from in vitro study. *Chemosphere* 89, 30–37.
- XI. Sovadinová, I.* , **Babica, P.**, Adamovský, O., Alpatova, A., Tarabara, V., Upham, B., Bláha, L., 2017. Chlorination and ozonation differentially reduced the microcystin content and tumour promoting activity of a complex cyanobacterial extract. *Advances in Oceanography and Limnology* 8, 107–120.

- XII. **Babica, P.***, Čtveráčková, L., Lenčešová, Z., Trosko, J.E., Upham, B.L., 2016. Chemopreventive Agents Attenuate Rapid Inhibition of Gap junctional Intercellular Communication Induced by Environmental Toxicants. *Nutrition and Cancer* 68, 827–837.
- XIII. Alpatova, A.L., Shan, W., **Babica, P.**, Upham, B.L., Rogensues, A.R., Masten, S.J., Drown, E., Mohanty, A.K., Alocilja, E.C., Tarabara, V. V.*, 2010. Single-walled carbon nanotubes dispersed in aqueous media via non-covalent functionalization: Effect of dispersant on the stability, cytotoxicity, and epigenetic toxicity of nanotube suspensions. *Water Research* 44, 505–520.
- XIV. Steuer, A., Schmidt, A., Labohá, P., **Babica, P.**, Kolb, J.F.*, 2016. Transient suppression of gap junctional intercellular communication after exposure to 100-nanosecond pulsed electric fields. *Bioelectrochemistry* 112, 33–46.
- XV. Steuer, A., Wende, K., **Babica, P.**, Kolb, J.F.*, 2017. Elasticity and tumorigenic characteristics of cells in a monolayer after nanosecond pulsed electric field exposure. *European Biophysics Journal* 46, 567–580.

10 ATTACHMENTS

- I. **Babica, P.***, Sovadinová, I., Upham, B.L., 2016. Scrape loading/dye transfer assay, in: *Methods in Molecular Biology - Gap Junction Protocols*. pp. 133–144.

Scrape Loading/Dye Transfer Assay

Pavel Babica, Iva Sovadinová, and Brad L. Upham

Abstract

The scrape loading/dye transfer (SL/DT) technique is a simple functional assay for the simultaneous assessment of gap junctional intercellular communication (GJIC) in a large population of cells. The equipment needs are minimal and are typically met in standard cell biology labs, and SL/DT is the simplest and quickest of all the assays that measure GJIC. This assay has also been adapted for *in vivo* studies. The SL/DT assay is also conducive to a high-throughput setup with automated fluorescence microscopy imaging and analysis to elucidate more samples in shorter time, and hence can serve a broad range of *in vitro* pharmacological and toxicological needs.

Key words Dye coupling, Dye transfer, Ex vivo assessment, Gap junctional intercellular communication assessment, High throughput, In vitro assay, Incision loading, Lucifer Yellow, Scalpel loading, Scrape loading, Tracers

1 Introduction

Dye coupling methods are by far the most frequently used assay for the assessment of GJIC, mainly because of their ease of use. Of all the techniques used to measure GJIC, the scrape loading/dye transfer (SL/DT) assay is the fastest and simplest. Most protocols are modification of the one first reported by El-Fouly et al. [1]. This technique has since been widely used to elucidate the GJIC status of many cell types in various biological circumstances in different scientific areas such as carcinogenesis, embryogenesis, growth control, or endocrine disruption (for review, *see* [2–6]). This visual method allows to assess GJIC in a large population of cells. It is therefore particularly useful when a large screen of multiple conditions is required or when different regions of a cell monolayer have to be compared within the same culture dish [2]. The SL/DT assay can be effectively used as a tool to determine the qualitative and quantitative presence or absence of GJIC as well as demonstrate the concentration-dependent inhibition of GJIC [3, 7–9].

The SL/DT assay relies on the introduction of small (MW <900), nonpermeable dyes (for review, *see* [2, 10]) into living cells that are traced in their intercellular movement through gap junctions. As the reference dye, dilithium salt of Lucifer Yellow hydrazine (LY, MW 457, negatively charged) is the most popular dye currently in use. This tracer has a high fluorescence efficiency, which ensures its detection in minute levels [10]. LY is introduced by scraping a monolayer of cells and becomes incorporated by cells along the scrape, presumably as a result of some mechanical perturbation of the membrane (Fig. 1). As normal permeability is reestablished, the LY becomes trapped within the cytoplasm and move from the dye-loaded cells into adjacent ones connected by functional gap junctional channels [2]. This dye transfer is monitored and quantified by fluorescent microscopy in multiple cells almost simultaneously. The amount of dye transferred from one cell to its neighbor that it is in contact with is dependent on the number of gap

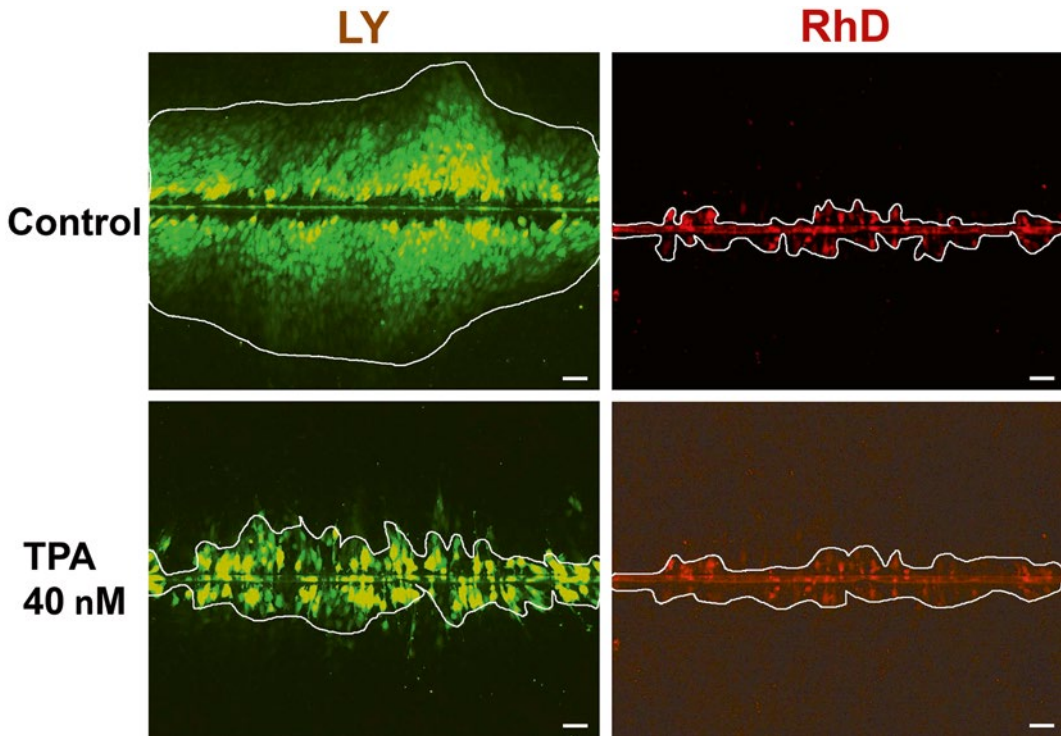


Fig. 1 Scrape load dye transfer analysis in mouse Sertoli cells. Images obtained by SL/DT assay, applying Lucifer Yellow CH dilithium salt (LY, MW 457), which transfers through functional gap junction channels, and rhodamine-dextran (RhD, MW 10,000), which is retained in the scraped cells. The GJIC function is evaluated by analyzing net transfer of LY (the area at which LY diffuses), excluding RhD-stained regions. GJIC after the 1-h exposure of mouse Sertoli TM4 cells to the model tumor promoter, TPA (12-O-tetradecanoylphorbol-13-acetate), at the concentration of 40 nM was reduced to FOC (the fraction of the control) = 0.13 when compared with the solvent control. Scale bar = 50 μ m

junctions that are coupled and the gating properties of individual channels. The distance or area at which the dye diffuses during a certain period away from the scrape line is a quantitative measurement of GJIC capacity. To determine which cells are initially loaded after the scrape, other fluorescent dyes (e.g., rhodamine-dextran, MW 10,000, or dialkylcarbocyanine) that are too large to traverse the gap junction channel are concurrently used with the diffusional dye to serve as an additional control (Fig. 1). These large fluorescent macromolecules that cannot diffuse across gap junctions are useful in ensuring that the intercellular transfer of the gap junction diffusible-reference dye is actually dependent on gap junctions and is not accounted for by alternative pathways, such as cytoplasmic membrane fusions, cytoplasmic bridge formation at the end of mitosis or due to membrane damage, which can occur after scraping [1, 11].

The SL/DT assay is an invasive technique but has been successfully demonstrated to assess compounds that disrupt GJIC. However, this assay is not conducive in studying GJIC in small cell populations, particularly between cell pairs, and also in cultures with low cell densities, or when the extent of junctional coupling is small, or when specific cells need to be observed [2]. In addition, the GJIC status of cell types of irregular shape is not easily quantified using this assay. For example, GJIC of neuronal cells or long spindly fibroblast cannot be easily quantified because the distance or area at which the dye diffuses cannot be easily “trackable” and quantified [11]. This approach is also not well suited to three-dimensional (3D) systems. The local activation of molecular fluorescent probe (LAMP) method has been recently improved (the so-called infrared-LAMP assay) and allows to examine cell-cell coupling in three dimensions [12, 13]. However, for the time being, two-dimensional cell culture systems still serve as a valuable tool in cell biology and toxicology research [5].

The major advantages of the SL/DT are as follows: (1) simplicity, (2) not a necessity of the special equipment or skills that are needed for other methods such as microinjection, (3) a rapid and simultaneous assessment of GJIC in a large number of cells, (4) conducive to a high-throughput setup with automated fluorescence microscopy imaging and analysis, and (5) its adaptation for *in vivo* studies followed by *ex vivo* assessment of GJIC in tissue slices from experimental animals [5]. An *ex vivo* GJIC assay, the incision loading/dye transfer method (IL/DT), is very similar to the *in vitro* protocol [14–16]. The IL/DT may be useful for rapidly screening tumorigenic compounds for setting doses for studies of carcinogenesis [14].

The basic technique described in this chapter has been adapted after the method of El-Fouly [1]. Rather than more invasive scrape with rubber policeman or wooden probe, the dye loading step in this protocol involves a clean cut with a sharp

blade, such as surgical scalpel. This modified technique can be thus called scalpel loading/dye transfer assay and is amendable to many cell types with minimal or no modifications. This assay has been extensively applied to determine changes in GJIC in a wide variety of mammalian (including human) cell types after treatment with many kind of toxicants such as tumor promoters, endocrine disruptors, pesticides, or developmental toxicants. Additionally, this assay has been successful in screening for compounds that can either prevent toxicant-induced disruption of GJIC or reverse the effects of these toxicants or endogenous oncogenes.

2 Materials

1. Cells of interest and appropriate media.
2. Cell culture plates, e.g., 35 mm dishes, or multiwell plates, e.g., 6/12/24/48/96 wells.
3. Phosphate buffered saline (PBS) buffer with calcium and magnesium (CaMg-PBS; *see Note 1*): 137 mM NaCl (8 g/L), 2.68 mM KCl (0.2 g/L), 8.10 mM Na₂HPO₄ (1.15 g/L), 1.47 mM KH₂PO₄ (0.2 g/L), 0.68 mM CaCl₂ (0.075 g/L), 0.49 mM MgCl₂ (0.047 g/L). The pH is adjusted to 7.2. The CaMg-PBS is filter sterilized and can be stored at room temperature.
4. LY-dye solution: 1 mg/mL Lucifer Yellow CH dilithium salt (LY, MW 457) (*see Note 2*) and 1 mg/mL rhodamine-dextran (RhD, MW 10,000, optional, *see Note 3*) in CaMg-PBS. The solution is filter sterilized and can be stored for weeks in the dark at 4 °C (*see Note 4*).
5. Surgical scalpel blade or micro-knife with a curved, flat, or needle blade as appropriate (Fig. 2) to fit into the cell culture plasticware used (*see Note 5*).
6. 10% Formalin solution (i.e., approximately 4% formaldehyde) in CaMg-PBS (*see Note 6*).
7. 25 mL pipettes with a pipette aid or manual bulb, automatic pipette 100–1000 µL or Pasteur pipette with a bulb, waste container, parafilm, aluminum foil.
8. Inverted epifluorescent microscope or confocal microscope with appropriate filters (LY: excitation at 428 nm, emission at 536 nm; RhD: excitation at 555 nm, emission at 580 nm).
9. Camera, CCD or CMOS camera coupled to the microscope, computer, image acquisition and analysis software.

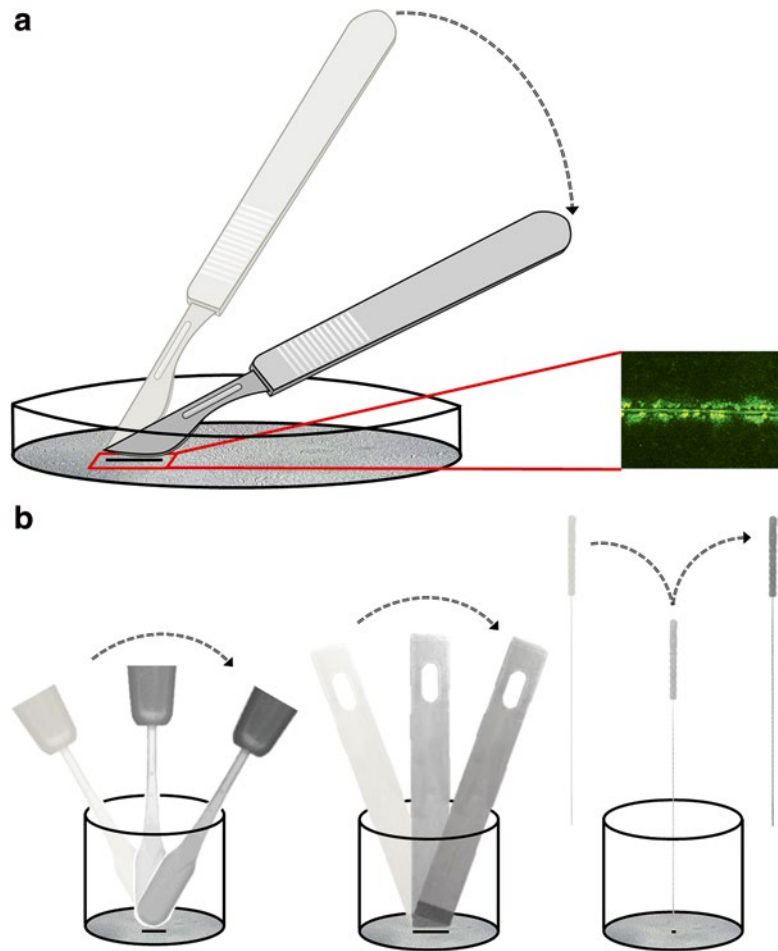


Fig. 2 *The scrape loading procedure. (a)* Scrape loading technique done by surgical scalpel with a curved blade in 35 mm dishes. *(b)* Different types of blades suitable for SL/DT assay in microplate wells, including a curved blade (*left*), a flat blade (*middle*), and an acupuncture needle (*right*)

3 Methods

3.1 General Procedure

1. Grow cells to confluency in suitable cultivation medium under appropriate conditions for the desired cell type (*see Note 7*).
2. Visually check the health of the cells for expected morphologies and sterile conditions prior to the start of the experiments.
3. Remove cells from the incubator and discard medium by gently pouring off the medium or by siphoning with a pipette into a waste container (*see Notes 8 and 9*).

4. Rinse cells gently three times with CaMg-PBS using a pipette (*see Note 10*) and discard the CaMg-PBS by gently pipetting off into a waste container.
5. Add sufficient LY-dye solution (warmed up to 37 °C) to cover the cell monolayer (*see Note 11*).
6. Load the dye into the cells by gently placing the tip of a surgical steel blade with a curved edge in contact with the cell monolayer and then rolling the blade in one direction over its curved edge as indicated in Fig. 2a (*see Note 12*). If using multiwell plates, use a micro-knife with a curved or flat blade, or an acupuncture needle (*see Note 5*) to gently prick the cells (Fig. 2b).
7. Typically, three cuts are done for each dish or multiwell plate well. The areas for cell loading are randomly selected in the central part of the plate/well (*see Note 13*).
8. Incubate the dish or multiwell plate, undisturbed and under minimum illumination for 3–6 min at room temperature to allow the LY dye to travel through several adjacent cell layers (3 and more) via functional gap junctions (*see Note 14*).
9. Cover the plate, to limit the exposure of the LY-dye solution to light during the incubation to avoid fluorescence photobleaching of the dye.
10. Aspirate the LY-dye solution from plate/wells (*see Note 15*) and then rinse cells three times with CaMg-PBS to remove all extracellular dye (*see Notes 10 and 16*).
11. Fix the cells by adding sufficient 10% formalin solution to cover the cells (*see Notes 11 and 17*).
12. The cells can be viewed immediately using an inverted epifluorescence microscope or confocal microscope with appropriate filters.
13. Acquire three representative LY/RhD images per plate/well (*see Note 18*).
14. A bright field or phase contrast image should be acquired for each field of view (*see Note 19*).
15. Fixed cells can be air-dried overnight, stored in the dark for extended periods (months with no detectable decrease in dye intensity), and rehydrated with formalin solution for viewing.
16. Store the plates sealed in parafilm and covered in aluminum foil.

3.2 Quantification of GJIC Using Morphometric Software

1. The degree of GJIC can be measured using a variety of methods (*see Note 20*) [17].
2. The fluorescent distance or the area of the dye spread can be quantified using a morphometric software package. We use ImageJ, a free public domain imaging software package from

the National Institute of Health (<http://imagej.nih.gov/ij/>), with a subroutine for determining fluorescence area of a fluorescent image.

3. To obtain a corrected fluorescence area value for LY and RhD, the fluorescent areas of digitized images (e.g., Fig. 1) are subtracted from background fluorescence obtained at an area of the monolayer well away from any scrape lines within the same test plate (*see Note 21*).
4. To calculate the net transfer of LY, the areas of LY and RhD fluorescence are subtracted from each other for each field of view (i.e., $\text{Area}^{\text{LY}} - \text{Area}^{\text{RhD}}$) (*see Note 22*).
5. The net LY areas of individual images can then be normalized to the averaged net area from negative or solvent control dishes to obtain the fraction of the control (GJIC-FOC)

$$\text{GJIC FOC}_{\text{Treatment}} = \frac{\left(\text{Area}_{\text{Treatment}}^{\text{LY}} - \text{Area}_{\text{Treatment}}^{\text{RhD}} \right)}{\left(\text{Area}_{\text{Control(Averaged)}}^{\text{LY}} - \text{Area}_{\text{Control(Averaged)}}^{\text{RhD}} \right)}$$

6. GJIC-FOC values of individual images can be then grouped by the individual dishes or treatment conditions for further data evaluation and statistical analyses to allow relative comparisons between the control and the treatments, for concentration and time response analyses, or for comparisons between independent experiments.

4 Notes

1. Calcium chloride must be added before the magnesium chloride to avoid irreversible precipitation of the salts. This buffered solution should not be sterilized by autoclave because of salt precipitation but should be rather filter sterilized through a sterile 0.22 μm filter. Calcium and magnesium cations are added to the PBS buffer to maintain cell adhesion and prevent a monolayer of cells from lifting, i.e., detaching from the bottom of culture dishes or plates. However, some cell types may be sensitive to this level of Ca^{2+} . This problem may be alleviated by preparing the LY-dye solution in CaMg-free PBS.
2. Some junction channels exclude anionic molecules like LY, for example, connexin 45 [2, 18, 19]. For these channels, smaller cationic dyes such as biotin conjugate (e.g., Neurobiotin [16, 20] or Biotin [21]) are recommended. To be detected, biotin conjugates should be visualized with either streptavidin coupled to a fluorochrome (cyanine dyes, fluorescein, or rhodamine) or to horseradish peroxidase. If the connexin channels of a particular cell type are unknown, then SL/DT using LY as the transfer dye is not enough to elucidate GJIC status in these cells.

3. Use LY-dye solution with RhD if there is a need to identify which cells are initially loaded with the dye. RhD is a large dye that does not pass through gap junctions, while LY does pass through gap junctions.
4. The LY-dye solution must be warmed to 37 °C before use on the cells.
5. Surgical scalpel with a curved blade is suitable for 35 mm dishes (Fig. 2a). Micro-knives and blade holders with curved blades, flat blades, or ultrafine needle blades (e.g., acupuncture needles) with dimensions fitting multiwell plate wells are suitable for SL/DT in setups allowing for higher throughput (Fig. 2b).
6. The formalin solution should be prepared in a chemical fume hood and safety goggles and gloves should be worn. Shelf-life of this solution is approximately 3 months.
7. The growth phase at which a SL/DT experiment is done is critical. Typically, cells which have reached confluency and are no longer actively dividing (“contact inhibition”) are the most suitable for the SL/DT assay. For new cells that have not been previously assessed for GJIC, the growth conditions, i.e., cell seeding density as well as culture time, must be optimized. In addition, the passage number must be noted during GJIC experiments because the passage number can play a significant role in functioning GJIC in a given cell type. Many cells have abundant PDGF (platelet-derived growth factor) receptors. PDGF inhibits GJIC in several cell lines [22], thus conducting GJIC experiments with cells grown in medium supplemented with fetal bovine serum (FBS) poses problem due to the high levels PDGF in FBS. Transferring the cells to FBS free for 2–4 h can overcome this problem. Due to the unnatural two-dimensional environments of the traditional in vitro assays, some cell types may not establish GJIC in the traditional medium or plastic. Some cell types need specific culture conditions to express functional GJIC such as extracellular matrix-coated plates (e.g., mammary CID-9 cell line [23]) or low or high calcium medium (e.g., mouse epidermal cell line [24]). Some cell types such as mouse testicular cell lines TM3 and TM4 can detach from the bottom of tissue culture plates during the washing steps. Growing cells on gelatin-coated plates can overcome this problem.
8. Culture medium containing hazardous waste must be properly disposed.
9. This and the subsequent steps are usually done on the lab bench at room temperature.
10. We typically use a 25 mL pipette, which is sufficient volume to rinse several 35 mm cell culture dishes or a 6- to 96-well multiwell plate.

11. We typically use about 1 mL of solution per 35 mm cell culture dish or per well of 6- or 12-well plate, 0.5 mL per well of 24-well plate, 0.25 mL per well of 48-well plate, 0.1 mL per well of 96-well plate.
12. The key principle of proper loading technique is to put the tip or apex of the blade to the bottom of the dish or multiwell plate well and then roll the blade over its cutting edge against the cell monolayer or to gently prick the monolayer with the tip of a thin acupuncture needle. This action is minimally invasive and provides a very clean line or spot of loading. Do not slice or scratch the monolayer, but only apply gentle pressure to minimize physical effects of this step. A sharp blade or point is important to prevent a large separation or empty hole between the cells that were loaded resulting in high variability.
13. This scrape loading step is done at the lab bench without use of a microscope. If you want to assess GJIC in any specific area of special interests that you found during microscopic examination, then use a marker to indicate where the scrape line needs to be placed, or use the microscope. The three cuts per dish or well should be aligned in parallel, and in the case of multiwell plates also geometrically parallel with the base of the well.
14. The optimal incubation time varies between different cell types, depending on the level of communication and attachment properties of the cells [8]. Incubation up to 10 min might be required for some cell cultures. For a set experiment duration, different rates of dye diffusion through homotypic channels is correlated to the number of gap junction channels [25]. If processing several dishes or multiwell plates in parallel, work in a timely manner to make sure that the incubation time after the dye loading step will be the same for all dishes or wells.
15. LY-dye solution can be collected and reused. We reuse the dye solution for approximately 10 experiments, when stored in dark and refrigerated. We filter the solution through 0.22 μm syringe filter, if needed.
16. The washing step is very important step because of the reduction of background fluorescence. Even in the absence of a scrape line, some LY can be incorporated into the cells as evidenced by nonspecific background fluorescence. It also binds to cell components after aldehyde fixation [10].
17. The fixation of cells is optional and can be skipped. The cells in CaMg-PBS or medium can also be observed without fixation, but the dye will continue to travel through the cell layers and become overly diffuse to observe.

18. The cells from experimental conditions where the highest and lowest level of GJIC are expected (e.g., negative and positive controls) should be used first to adjust or check the microscope and image acquisition settings. The plates should be positioned so the line or spot of dye-loaded cells will be in the center of the microscope field of vision, and the line also parallel with the horizontal line of image field. Camera exposure time and other image acquisition settings (e.g., excitation source intensity or fluorescence attenuator, camera binning, image brightness, contrast and gamma correction) should be adjusted in a way that LY- or RhD-stained cells can be clearly discriminated from the background, i.e., from the cells whose fluorescence intensity is comparable to all the other cells in regions distant from the cut. However, the background cells should not turn out completely black in the image (too dim images), since such condition might lead to underestimation of GJIC. The used combination of the objective magnification (typically 5–20× objective), digital camera (e.g., C-Mount adapter magnification, size of the imaging sensor), and other image acquisition settings should allow to fit within one image (one field of view) not only all LY-stained cells in the direction perpendicular to the cut, but also part of the background, so to assure most accurate quantification GJIC and to prevent underestimation of communication in the cells from the experimental conditions with the most intense GJIC.
19. Bright field or phase contrast images from the same field of view as LY/RhD fluorescence images can offer additional visual information on the cells, such as the effects of experimental treatments on cell morphology, growth, confluency, and attachment, and also provide additional information to discriminate between the reduction of LY-stained area due to inhibition of GJIC, as compared to reduced dye transfer as a function of subconfluency or cell detachment issues.
20. An alternative method of quantitating GJIC is by counting the rows of fluorescent cells from the scrape line. This method is useful and more appropriate when comparing populations of different cell type, size, and growth state [26].
21. The most frequent problem is the high intensity of background fluorescence, so the cells stained by LY due to the dye transfer cannot be discriminated from the cells in the background. The most common contributions to background fluorescence are as follows: (1) an insufficient rinse of the extracellular dye, (2) treating cells with cytotoxic concentrations of the chemical (an uptake of dye by cells that

were not scraped or near to scrape line indicating disrupted cell membranes or detachment of the cells from the plate during the rinse step), and (3) “overconfluent cells,” i.e., cells have been confluent for more than one day and have started to produce significant extracellular matrix (LY binds to extracellular matrix). Dim images are almost always problem related to the photobleaching of LY solution, especially if it is being recycled and reused. In the short term, this issue can be compensated for by increasing exposure time for fluorescence image acquisition. Fresh LY solutions will usually alleviate this problem.

22. A more simplified version of the SL/DT assay is to load cells with only LY and not the RhD. The results from these experiments typically give FOC values very similar to those that include RhD. However, when measuring the dye fronts, the loaded cells cannot be identified, and thus cannot be subtracted from the calculations resulting in values that are always above zero. This issue can be circumvented by introducing a positive control into the experimental design, i.e., treatment with a known inhibitor with GJIC (such as 12-O-tetradecanoyl-13-phosphol acetate), which will induce complete inhibition of GJIC. The net LY dye transfer can be then calculated by subtracting the average area of LY-stained cells in the positive control from LY-stained areas of all images. Adjusted areas of the experimental treatments can be then compared to the averaged adjusted area of the negative or solvent control:

$$\text{GJIC FOC}_{\text{Treatment}} = \frac{\left(\text{Area}_{\text{Treatment}}^{\text{LY}} - \text{Area}_{\text{Positive control (Averaged)}}^{\text{LY}} \right)}{\left(\text{Area}_{\text{Negative control (Averaged)}}^{\text{LY}} - \text{Area}_{\text{Positive control (Averaged)}}^{\text{LY}} \right)}$$

This approach is suitable only for in vitro models with well characterized GJIC, where complete inhibition of GJIC can be reproducibly induced and reliably recognized. However, this greatly simplifies the assay, particularly at the microscopy step where only one dye needs to be assessed.

Acknowledgements

This work was financially supported by the National Sustainability Programme of the Czech Ministry of Education, Youth and Sports (LO1214) and the RECETOX research infrastructure (LM2015051), and NIEHS grant #R01 ES013268-01A2 to Upham.

References

1. Elfouly MH, Trosko JE, Chang CC (1987) Scrape-loading and dye transfer—a rapid and simple technique to study gap junctional intercellular communication. *Exp Cell Res* 168:422–430
2. Abbaci M, Barberi-Heyob M, Blondel W et al (2008) Advantages and limitations of commonly used methods to assay the molecular permeability of gap junctional intercellular communication. *Biotechniques* 45:33–58
3. Klaunig JE, Shi Y (2009) Assessment of gap junctional intercellular communication. *Curr Protoc Toxicol* Chapter 2, Unit 2 17
4. Trosko JE, Ruch RJ (2002) Gap junctions as targets for cancer chemoprevention and chemotherapy. *Curr Drug Targets* 3:465–482
5. Upham BL (2011) Role of integrative signaling through gap junctions in toxicology. In: Maines MD (ed) *Curr Protoc Toxicol*, vol Chapter 2. p Unit 2.18
6. Vinken M, Doktorova T, Decrock E et al (2009) Gap junctional intercellular communication as a target for liver toxicity and carcinogenicity. *Crit Rev Biochem Mol Biol* 44:201–222
7. Loch-Carusio R, Caldwell V, Cimini M et al (1990) Comparison of assays for gap junctional communication using human embryocarcinoma cells exposed to dieldrin. *Fundam Appl Toxicol* 15:63–74
8. Opsahl H, Rivedal E (2000) Quantitative determination of gap junction intercellular communication by scrape loading and image analysis. *Cell Commun Adhes* 7:367–375
9. Sovadinova I, Babica P, Boke H et al (2015) Phosphatidylcholine specific PLC-induced dysregulation of gap junctions, a robust cellular response to environmental toxicants, and prevention by resveratrol in a rat liver cell model. *PLoS One* 10:e0124454
10. Meda P (2000) Probing the function of connexin channels in primary tissues. *Methods* 20:232–244
11. Trosko JE, Chang CC, Wilson MR et al (2000) Gap junctions and the regulation of cellular functions of stem cells during development and differentiation. *Methods* 20:245–264
12. Dakin K, Zhao Y, Li WH (2005) LAMP, a new imaging assay of gap junctional communication unveils that Ca²⁺ influx inhibits cell coupling. *Nat Methods* 2:55–62
13. Yang S, Li WH (2009) Assaying dynamic cell-cell junctional communication using noninvasive and quantitative fluorescence imaging techniques: LAMP and infrared-LAMP. *Nat Protoc* 4:94–101
14. Sai K, Kanno J, Hasegawa R et al (2000) Prevention of the down-regulation of gap junctional intercellular communication by green tea in the liver of mice fed pentachlorophenol. *Carcinogenesis* 21:1671–1676
15. Upham BL, Park JS, Babica P et al (2009) Structure-activity-dependent regulation of cell communication by perfluorinated fatty acids using in vivo and in vitro model systems. *Environ Health Perspect* 117:545–551
16. Goliger JA, Paul DL (1995) Wounding alters epidermal connexin expression and gap junction-mediated intercellular communication. *Mol Biol Cell* 6:1491–1501
17. McKarns SC, Doolittle DJ (1992) Limitations of the scrape-loading dye transfer technique to quantify inhibition of gap junctional intercellular communication. *Cell Biol Toxicol* 8:89–103
18. Pastor A, Kremer M, Möller T et al (1998) Dye coupling between spinal cord oligodendrocytes: differences in coupling efficiency between gray and white matter. *Glia* 24:108–120
19. Risley MS, Tan IP, Farrell J (2002) Gap junctions with varied permeability properties establish cell-type specific communication pathways in the rat seminiferous epithelium. *Biol Reprod* 67:945–952
20. Bittman K, Becker DL, Cicirata F et al (2002) Connexin expression in homotypic and heterotypic cell coupling in the developing cerebral cortex. *J Comp Neurol* 443:201–212
21. Rouach N, Segal M, Koulakoff A et al (2003) Carbenoxolone blockade of neuronal network activity in culture is not mediated by an action on gap junctions. *J Physiol* 553:729–745
22. Yamasaki H, Naus CC (1996) Role of connexin genes in growth control. *Carcinogenesis* 17:1199–1213
23. El-Sabban ME, Sfeir AJ, Daher MH et al (2003) ECM-induced gap junctional communication enhances mammary epithelial cell differentiation. *J Cell Sci* 116:3531–3541
24. Jongen WM, Fitzgerald DJ, Asamoto M et al (1991) Regulation of connexin 43-mediated gap junctional intercellular communication by Ca²⁺ in mouse epidermal cells is controlled by E-cadherin. *J Cell Biol* 114:545–555
25. Czyn J, Irmer U, Schulz G et al (2000) Gap-junctional coupling measured by flow cytometry. *Exp Cell Res* 255:40–46
26. Vaz-de-Lima BB, Ionta M, Machado-Santelli GA (2008) Changes in cell morphology affect the quantification of intercellular communication. *Micron* 39:631–634

- II.** Upham, B.L.* , Sovadinová, I., **Babica, P.**, 2016. Gap Junctional Intercellular Communication: A Functional Biomarker to Assess Adverse Effects of Toxicants and Toxins, and Health Benefits of Natural Products. *Journal of Visualized Experiments* 118, e54281.

Video Article

Gap Junctional Intercellular Communication: A Functional Biomarker to Assess Adverse Effects of Toxicants and Toxins, and Health Benefits of Natural Products

Brad L. Upham¹, Iva Sovadinová², Pavel Babica²¹Department of Pediatrics & Human Development, Institute for Integrative Toxicology, Michigan State University²RECETOX — Research Centre for Toxic Compounds in the Environment, Faculty of Science, Masaryk UniversityCorrespondence to: Brad L. Upham at Brad.Upham@hc.msu.eduURL: <http://www.jove.com/video/54281>DOI: [doi:10.3791/54281](https://doi.org/10.3791/54281)Keywords: Cellular Biology, Issue 118, gap junctional intercellular communication, scalpel load-fluorescent dye transfer, *in vitro* toxicology, biomarker, cell signaling, signal transduction, cancer, chemoprevention

Date Published: 12/25/2016

Citation: Upham, B.L., Sovadinová, I., Babica, P. Gap Junctional Intercellular Communication: A Functional Biomarker to Assess Adverse Effects of Toxicants and Toxins, and Health Benefits of Natural Products. *J. Vis. Exp.* (118), e54281, doi:10.3791/54281 (2016).

Abstract

This protocol describes a scalpel loading-fluorescent dye transfer (SL-DT) technique that measures intercellular communication through gap junction channels, which is a major intercellular process by which tissue homeostasis is maintained. Interruption of gap junctional intercellular communication (GJIC) by toxicants, toxins, drugs, *etc.* has been linked to numerous adverse health effects. Many genetic-based human diseases have been linked to mutations in gap junction genes. The SL-DT technique is a simple functional assay for the simultaneous assessment of GJIC in a large population of cells. The assay involves pre-loading cells with a fluorescent dye by briefly perturbing the cell membrane with a scalpel blade through a population of cells. The fluorescent dye is then allowed to traverse through gap junction channels to neighboring cells for a designated time. The assay is then terminated by the addition of formalin to the cells. The spread of the fluorescent dye through a population of cells is assessed with an epifluorescence microscope and the images are analyzed with any number of morphometric software packages that are available, including free software packages found on the public domain. This assay has also been adapted for *in vivo* studies using tissue slices from various organs from treated animals. Overall, the SL-DT assay can serve a broad range of *in vitro* pharmacological and toxicological needs, and can be potentially adapted for high throughput set-up systems with automated fluorescence microscopy imaging and analysis to elucidate more samples in a shorter time.

Video Link

The video component of this article can be found at <http://www.jove.com/video/54281/>

Introduction

The overall goal of this method is to provide a simple, comprehensive and relatively inexpensive technique to assess the potential toxicities of compounds. This is an *in vitro* approach that can be used in multiple cell lines. Standard cell biology labs equipped with epifluorescence microscopes can conduct research using this assay.

Our basic knowledge of cell functions has been highly dependent on *in vitro* bioassays, and has become an essential component in toxicological assessments of pharmaceuticals, environmental pollutants, and food born contaminants. Unfortunately, there is no single *in vitro* bioassay system that can comprehensively meet the demands for all toxicological assessments. Many *in vitro* assays are designed and optimized to evaluate as well as assess a specific biochemical or molecular endpoint. These are quite often combined in a high throughput set up to reflect a perturbation of a certain signal transduction pathway, such as estrogen-receptor signaling¹. This strategy has been quite successful, but the extensive number of signal transduction pathways involved in gene expression makes the task of choosing a specific signaling pathway to assess quite complex. High through-put protocols are currently being developed and used to simultaneously measure numerous signaling pathways, which has been one approach to overcome some of the limitations of single assays. However, not all signaling pathways have been successfully incorporated into more comprehensive approaches, plus new signaling pathways are constantly being discovered that further complicates this assessment process. Using extensive numbers of *in vitro* approaches, particularly high through-put systems, for comprehensive toxicological assessments are also very expensive and are not conducive to most single investigator led research projects.

GJIC is a process tightly controlled by changes in voltage, calcium concentration, pH, redox balance, regulated by major intracellular signal transduction pathways and interactions with membrane and cytoskeleton proteins^{2,3}. Thus, inhibition of GJIC can reflect different types of cellular stress, disruption of different cellular functions, or perturbations of different signal transduction pathways. Another approach to overcome the use of limited signal transduction bioassays is to take advantage of the biological phenomena that many, if not most, signal transduction pathways are further modulated by cooperative intercellular signaling systems through gap junction channels⁴⁻⁸. Although intercellular signaling systems are also numerous and under multiple pathway control, the intercellular signaling through gap junction channels is ultimately a function of the channels being opened, partially closed or completely closed. This provides an endpoint that can be easily measured using various *in vitro*

bioassay systems⁷. Considering that the homeostatic set point of a tissue requires open channels, determining the effect of compounds on gap junctional intercellular communication (GJIC) is a more comprehensive approach in determining potential toxic effects of compounds^{4,8}. In essence, this critical biological phenomenon that plays a central role in coordinating multiple signal transduction events controlling gene expression allows for a broad assessment of toxic effects. Thus, bioassays that assess GJIC are an excellent starting point to evaluate the toxic potential of compounds.

The most extensive techniques used to assess GJIC are based on preloading cells with a fluorescent probe and then monitoring the migration of the dye from the loaded cell or cells to adjacent cells. Techniques to preload the dye have involved microinjection⁹, scrape loading¹⁰, and methyl esters of the probes¹¹. The scalpel loading-fluorescent dye transfer (SL-DT) method is a modification of the scrape load - dye transfer assay developed by El Fouly¹⁰. Rather than the more invasive scrape, the scalpel loading method of this report involves a gentle roll of a scalpel with a round blade through a monolayer of cells that minimize invasive damage (**Figure 1**). The advantages of this technique are the toxicological assessment of a population of cells rather than single cells of the microinjection assay. Furthermore, the simplicity of this assay allows for rapid detection of multiple plates in a short time whereas methods using microinjection techniques and techniques that use methyl esters of fluorescent probes are significantly more time consuming and require considerably higher skill level.

Although there is no single method to meet all the needs of studying GJIC; the SL-DT assay is a simple, fairly inexpensive and versatile assay that can meet many of the needs for initial assessments of toxicities of various compounds. Major advantages include: simplicity, no special need for equipment or skills that are required for other methods such as microinjection, fluorescent recovery after photobleaching (FRAP) assay and local activation of molecular fluorescent probe assays, a rapid and simultaneous assessment of GJIC in a large number of cells, conducive to a high throughput set-up with automated fluorescence microscopy imaging and analysis, as well as its adaptability for *in vivo* studies.

Protocol

The protocol for this study was approved by the Animal Care and Utilization Committee of the National Institutes of Health Sciences of Japan, which is where the *in vivo* experiments were done, to assure that the rats were treated humanely and with regard for alleviation of suffering.

1. SL-DT Bioassay

1. Seed 3×10^5 WB-F344 rat liver epithelial cells onto 35 mm diameter culture plates containing Eagles modified medium plus 5% fetal bovine serum, and culture the cells in an incubator at 37 °C, 100% relative humidity (RH), 5% CO₂.
2. Culture the cells until they reach 100% confluence (typically, 2 days) and conduct the desired experimental treatment of the cells as described below.
 1. Conduct Dose Response Experiments
 1. Add 10 µl and 20 µl of a 2 mM stock solution of phenanthrene in 100 % acetonitrile and 4 µl, 6 µl, and 8 µl of a 20 mM stock solution of phenanthrene in 100 % acetonitrile to three plates of cells containing 2 ml of growth medium for each added volume of stock solution.
 2. Add 4 µl, 6 µl, 8 µl, 10 µl, and 20 µl of a 100% solution of acetonitrile to three plates of cells containing 2 ml of growth medium for each added volume of acetonitrile solution to serve as the vehicle control.
 3. Incubate plates for 15 min in an incubator set at 37 °C, 100% RH and 5% CO₂.
 4. Proceed to step 1.3.
 2. Conduct Time Response Experiments
 1. Add 7 µl of a 20 mM stock solution of phenanthrene in 100% acetonitrile to three plates of cells containing 2 ml of growth medium for each time point (*i.e.*, 0, 1, 2, 3, 4, 5, 10 min).
 2. Add 7 µl of 100% acetonitrile to three plates of cells containing 2 ml of growth medium for each time point to serve as the vehicle control.
 3. Incubate plates for each designated time point in an incubator at 37 °C, 100% RH and 5% CO₂.
 4. Proceed to step 1.3.
 3. Conduct Time Recovery Experiments
 1. Add 7 µl of a 20 mM stock solution of phenanthrene in 100% acetonitrile to three plates of cells containing 2 ml of growth medium for 15 min.
 2. Add 7 µl of 100% acetonitrile to three plates of cells containing 2 ml of growth medium for 15 min to serve as the vehicle control.
 3. Decant the medium containing either the phenanthrene or acetonitrile and rinse 3x each with 3 ml of phosphate buffered saline (PBS).
 4. Add 2 ml of fresh growth medium to each plate and incubate for the desired recovery times (*i.e.*, 25, 35, 45, 60, 90, 120, 150, 180, 240, 360 min) in an incubator at 37 °C, 100% RH and 5% CO₂.
 5. Proceed to step 1.3.
 4. Conduct Mechanism Experiments
 1. Add the signal transduction inhibitor, *i.e.*, 5 µl of a 20 mM stock solution of D609 in 100% acetonitrile to three plates of cells containing 2 ml of growth medium for 15 min.
 2. Add 5 µl of 100% acetonitrile to three plates of cells containing 2 ml of growth medium for 15 min to serve as the vehicle control.
 3. Add 7 µl of a 20 mM stock solution of phenanthrene in 100% acetonitrile to three plates of cells containing 2 ml of growth medium plus the D609 for an additional 15 min.
 4. Add 7 µl of 100% acetonitrile to three plates of cells containing 2 ml of growth medium plus the 100% acetonitrile for an additional 15 min to serve as the vehicle control.

5. Proceed to step 1.3.
3. Discard the culture medium by either gently pouring off the medium or by vacuum suction.
Note: Dispose culture medium containing hazardous waste appropriately.
4. Rinse the cells three times each with 3 ml of PBS and either decant or aspirate between rinses.
5. Pipette 1 ml of 1 mg/ml Lucifer Yellow dye dissolved in PBS (LY) into each cell plate.
6. Preload the dye into the cells by gently rolling a #20 surgical steel blade with a rounded edge through a population of cells in three different areas of the plate.
 1. Begin by placing the scalpel perpendicular (90° angle) and 5 mm from the edge of the culture plate, and then roll the scalpel from this perpendicular angle to about an angle of 15° (see **Figure 1**).
Note: This is achieved by pinching the scalpel between the index finger and thumb. Use gravity to allow the scalpel to gently go from the 90° to 15° position (as the rounded blade simply rolls over the cells). This motion will leave a visually noticeable indentation line.
7. Incubate the cells with the LY solution for 3 min at room temperature.
8. Decant or aspirate the LY and rinse three times with 3 ml of PBS to remove all extracellular dye to eliminate extracellular background fluorescence.
9. Add 0.5 ml of 10% phosphate buffered formalin solution to fix the cells.
Note: After fixing in formalin, air dry the cells and store in the dark for up to two years with minimum photobleaching of the LY dye. When required, rehydrate with 10% formalin solution to visualize the fluorescent dye front.
10. View the fixed cells using an epifluorescence microscope equipped with a dichroic cube for excitation/emission peaks of 428/536 nm at a magnification of 200X. Align all plates so that the indentation line is parallel to the horizontal field of vision.
Note: A FITC dichroic cube works well.
 1. Capture the image with a CCD camera and supporting software.
 1. Open the supporting software for the CCD camera and use the settings for auto exposure. Use the "capture" button to digitally acquire the image. Save the image as .tif files using the "Save" button.

2. Adaptation of the SL-DT Assay to Liver Tissue

1. Remove approximately a 2 x 2 cm slice from the left lobe of a liver from a 5 week old, male Fischer 344 rat using dissection scissors and place it on a plastic weigh plate covered with wet gauze¹².
2. Pipette 0.5 ml of a PBS solution containing 1 mg/ml each of lucifer yellow and rhodamine-dextran (RD) onto the surface of the liver slice in the plastic weigh plate.
Note: The RD is a dye that cannot traverse gap junction channels and will mark the cells that were loaded.
3. Make three to five incisions approximately 1 cm long on the surface of the liver slice that has the dye solution in the weigh plate with a sharp blade and then add additional dye sufficient to fill the incisions.
4. Incubate the tissue for 3 min at room temperature on the plastic weigh plate.
5. Rinse three times with 5 ml of PBS.
6. Fix the tissue overnight in 30 ml of 10% phosphate buffered formalin in a 50 ml conical centrifuge tube in the dark at room temperature.
7. The following day, wash the slices with water, trim tissue around the incision with dissecting scissors into 1 x 1 x 0.5 cm³ strips and then use standard techniques to embed the slices in paraffin¹³.
8. Section the slices perpendicular to the incision line to thickness of 5 µm and store the samples in the dark until ready to be imaged using standard sectioning techniques with a microtome¹³.
9. Use an epifluorescence microscope equipped with a CCD digital camera to visualize and capture the images of the fluorescent dye fronts according to section 1.10⁷.

3. Quantifying GJIC

1. Measure the fluorescent dye spread using a morphometric software package (e.g., ImageJ).
 1. Click the "File" tab and then click "open" to open the saved image.
 2. Click on the "Free Hand Tool" in the Tool Bar Tab to trace the outline of the dye front.
 3. Click the "Analyze" tab and then click "Measure".
Note: This will generate an area value in a spread sheet, which can be copied into other spread sheet programs if desired.
2. Using a spreadsheet program, compute the fraction of the control (FOC) by dividing the area of the dye spread in the experimental plate by the area the dye travelled in the control plate using the following equation:

$$\text{Eq. 1: } \frac{A_e}{A_c} = \text{FOC}$$

A_e = area of the dye spread in cells exposed to an experimental variable, such as cells treated with a chemical at a specific dose or time
A_c = area of the dye spread in the control, which are cells treated with the vehicle used to dissolve the chemical of interest

Note: To determine the effect of the vehicle, A_e would be the area of the dye spread in cells treated by the vehicle and A_c would be the area of the dye spread in cells not treated by the vehicle. The effect of the vehicle should preferably be less than 10%.

Representative Results

Interruption of GJIC has been extensively used as a biomarker for identifying toxic compounds at the nongenotoxic, epigenetic level of gene control that induces adverse health effects¹⁴. For example, polycyclic aromatic hydrocarbons (PAHs) are ubiquitous contaminants of the environment but vary in their epigenetic toxicities as a function of their molecular structures¹⁵. The lower molecular weight PAHs are typically found at relatively higher concentrations than the higher molecular weight PAHs in many diverse environments such as contaminated river sediments to that of cigarette smoke^{15,16}. Phenanthrene is an example of a low molecular weight PAH that possess three benzene rings with an angular pocket called the bay region. **Figure 2** is a series of SL-DT images of WB-F344 rat liver epithelial cells treated with increasing doses of phenanthrene. Note the decrease in the migration of the fluorescent dye, Lucifer Yellow, with increasing doses. The areas of the scanned images can be determined as a fraction of the control (FOC). The control for **Figure 2** are cells treated with the solvent that the PAH was dissolved in, namely acetonitrile. Typically SL-DT experiments are done in duplicate or triplicate for each trial with a minimum of three independent trials for each experimental parameter, which would be a dose in this experiment. The FOC values can then be averaged, statistically analyzed, and then graphed (see **Figure 3**).

Similar experiments are also routinely conducted to establish the time for toxicant-induced inhibition of GJIC, and the time period needed to recover from this toxicant-induced inhibition of GJIC after the cells are transferred to toxicant-free medium. **Figure 4** shows both the time response and recovery from inhibition by phenanthrene (Phe). The SL-DT assay can also be used to determine underlying mechanisms by which toxicant and toxins dysregulate GJIC^{4,16}. This is done by pre-incubating cells with a pharmaceutical inhibitor of a selected signaling pathway before the addition of the toxicant or toxin that dysregulates GJIC. If the toxicant or toxin no longer dysregulates GJIC in the presence of a selected pharmaceutical that blocks a signaling pathway, then this pathway is determined to be a regulatory pathway of GJIC, while such pathways can be ruled out if the toxicant continues to dysregulate GJIC. **Figure 5** demonstrates this principal in which 1-methylanthracene (1-MeA), another three ringed PAH that inhibits GJIC, but not in the presence of D609, which is a fairly specific inhibitor of phosphatidylcholine specific phospholipase C (PC-PLC). Thus, PC-PLC is ruled in as a candidate signaling enzyme involved in 1-MeA-induced inhibition of GJIC. The role of PC-PLC has been validated with further experimentation^{4,16}. Overall, the SL-DT assays are quite conducive to begin the process of mapping signaling networks involved in the mechanisms of how toxicants and toxins inhibit (dysregulate) GJIC. This approach can also be used to screen for natural products that can block a toxicant or toxin from dysregulating GJIC. For example, resveratrol, an antioxidant found in high concentrations in red wine and peanut products can prevent 1-MeA from inhibiting GJIC (**Figure 6**).

The SL-DT assay has been adapted to tissue slices from animals, particularly in the liver¹⁷. Perfluorooctanoic acid (PFOA) is an 8-carbon fluorinated fatty acid that is a persistent environmental pollutant known to induce liver cancers^{12,17}. Using the SL-DT technique PFOA was shown to inhibit GJIC in an *in vitro* WB-F344rat liver model system¹⁸. An *in vivo* follow-up study determined that PFOA also inhibited GJIC in the livers of F344 rats treated with PFOA, thus validating the *in vitro* model system^{12,17}. **Figure 7** are fluorescent images from this follow-up experiment showing the dye spread in liver tissues of rats treated with the vehicle and PFOA.

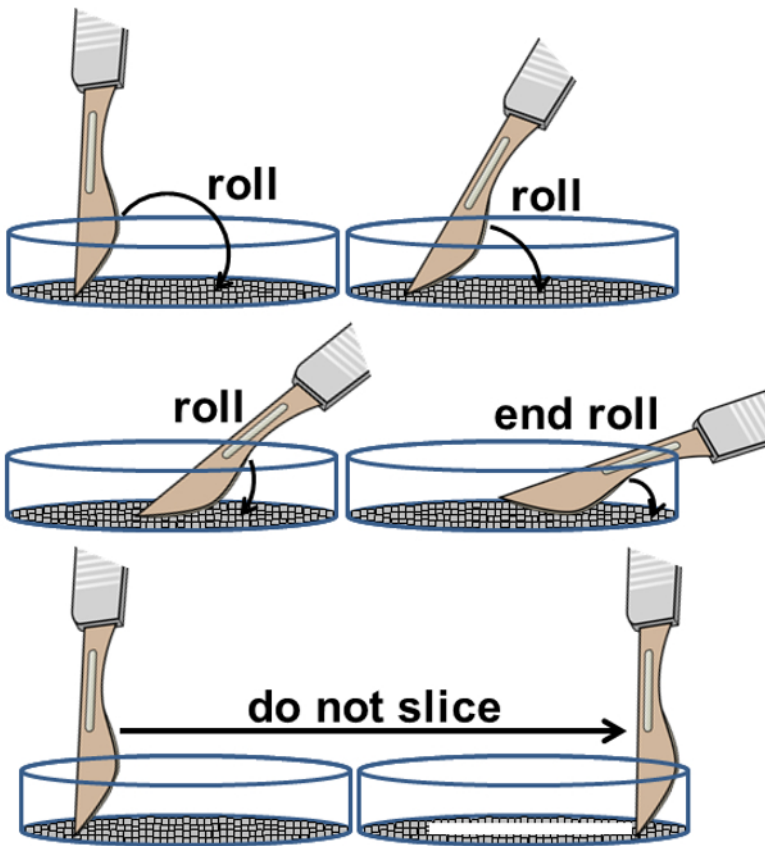


Figure 1: Cartoon image of the scalpel dye loading step. An illustration showing that the scalpel loading process involves rolling the blade rather than horizontally slicing through the cells as to minimize cell damage.

SL-DT Images of WB Cell Treated with Phenanthrene

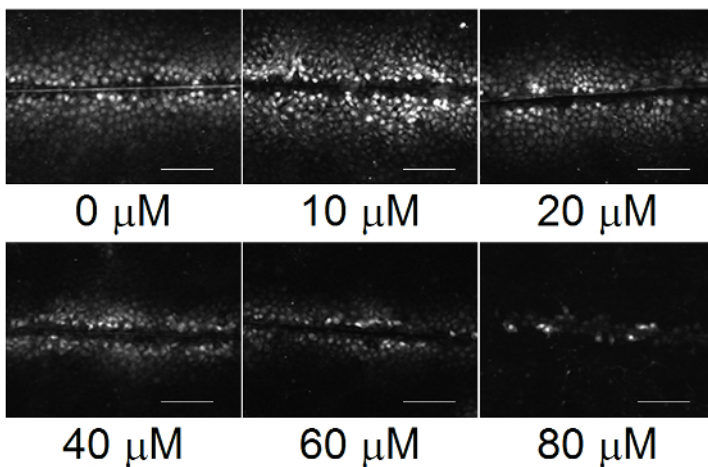


Figure 2: Representative fluorescent microscopic images of the dye spread through gap junctions. WB-F344 rat liver epithelial cells were treated for 15 min with increasing doses of phenanthrene, a prevalent PAH found in the environment. Scale bar = 100 μ m. [Please click here to view a larger version of this figure.](#)

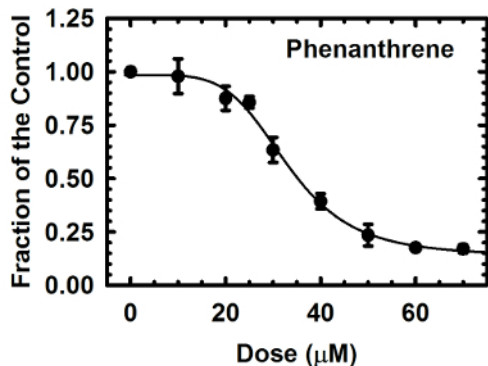


Figure 3: Dose response curve of phenanthrene-treated WB-F344 rat liver epithelial cells. Areas of SL-DT images were computed and then reported as a fraction of the control, which were cells treated with the vehicle (acetonitrile). Each data point is an average of three independent experiments and the error bars are the standard deviations at the 95% confidence limit for each dose after a 15 min exposure time. A four parameter logistic function was used to fit the line through the data points. [Please click here to view a larger version of this figure.](#)

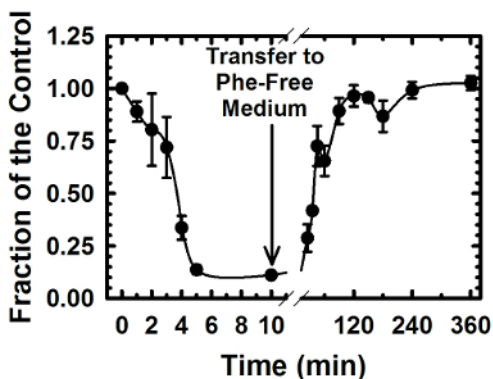


Figure 4: Time and time recovery response curve of phenanthrene-treated WB-F344 rat liver epithelial cells. After complete inhibition of GJIC after 10 min of exposure, the medium containing phenanthrene (Phe) was switched to Phe-Free medium and then the cells were monitored for recovery from inhibition. Areas of SL-DT images were computed and then reported as a fraction of the control, which were cells treated with the vehicle (acetonitrile). Each data point is an average of three independent experiments and the error bars are the standard deviations at the 95% confidence limit. [Please click here to view a larger version of this figure.](#)

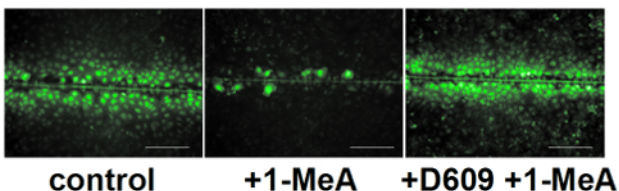


Figure 5: Inhibition of GJIC by 1-methylanthracene is dependent on phosphatidylcholine specific phospholipase C. 1-methylanthracene (1-MeA) is a prevalent PAH found in the environment. The left panel represent cells treated with the vehicle (acetonitrile, 0.35% v/v). The middle panel represents WB-F344 rat liver epithelial cells treated for 15 min with 70 μM 1-MeA. The right panel represent cells pretreated first for 20 min with 50 μM D609, a phosphatidylcholine specific phospholipase C inhibitor, followed by the addition of 70 μM 1-MeA for an additional 15 min. Scale bar = 100 μm . [Please click here to view a larger version of this figure.](#)

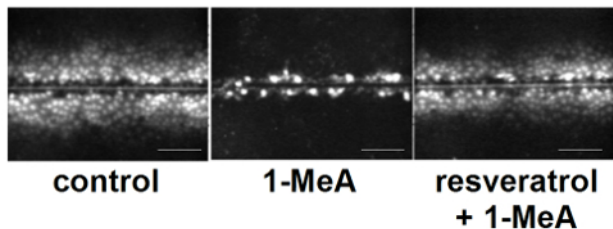


Figure 6: Resveratrol prevented the inhibition of GJIC by 1-methylanthracene. The left panel represent cells treated with the vehicle (acetonitrile, 0.35% v/v). Resveratrol is an antioxidant found in red wine and peanut products. The middle panel represents cells treated for 15 min with 70 μM 1-MeA. The right panel represents cells first pretreated for 20 min with 50 μM resveratrol followed by the addition of 70 μM 1-MeA for an additional 15 min. Scale bar = 100 μm . [Please click here to view a larger version of this figure.](#)

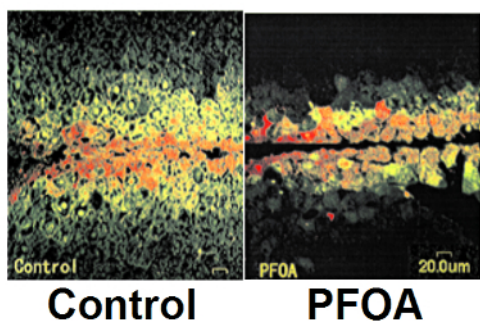


Figure 7: Ex vivo SL-DT assays of GJIC in liver slices from male F-344 rats. The left panel represents a slice of liver tissue from a rat treated with the vehicle control, dimethyl sulfoxide, for 24 hr. The right panel represents a slice of liver tissue from a rat after intraperitoneal administration of 100 mg/kg perfluorooctanoic acid (PFOA) after 24 hr. PFOA, a prevalent environmental contaminant, is a tumor promoting peroxisome proliferator that induces hepatomegaly and demonstrated to block gap junctions using an *in vitro* model. The incision loaded dye was done on liver slices from the vehicle and PFOA treated animals, which were then fixed, trimmed and sectioned. Reproduced from *Environmental Health Perspectives*¹². Scale bar = 20 μm . [Please click here to view a larger version of this figure.](#)

Discussion

The SL-DT assay is a simple and versatile technique in measuring GJIC, but there are several critical concerns that should be accounted for in designing appropriate experimental protocols. For robust measurements of GJIC using the SL-DT assay there must be a good dye spread of the LY through gap junctions of the cells. At minimum, an adequate time should be selected to assure that the dye spreads through eight or more rows of cells from the scalpel loaded cells in both directions. Also, for the ease of measurement of the distance that the dye migrated from the scalpel loaded cells, select a magnification factor that assures the dye spread of the control plates fills 70 to 90% of the field of vision. For the WB-F344 rat liver epithelial cells, three minute incubation with the LY solution is sufficient for the dye front to move beyond four cell rows, and a magnification of 200X is optimum. Cells are grown on 35 mm diameter plates, which is quite amendable to loading the dye into the cells with a scalpel. However, cells can be grown in small wells, but the use of a scalpel is not possible, particularly in 96 well culture plates. For small wells, use a small round-tipped cutting edge that can fit into the well, and again, use a rolling action. This rolling action is a critical step as it is minimally invasive and provides a very clean line of loading that prevents the cells from being torn and creating a large cell-free gap typical of the original scraping method. Alternatively, an acupuncture needle can be used in which a small twist of the needle does a nice job of loading dye into the cells.

Other cell-types can be used in this assay. However, selection of cells and understanding the roles of GJIC in a particular cell type is important in framing appropriate hypotheses and the design of the experiments. The first and most obvious step is to develop cell culture conditions in which functional gap junctions are expressed. In well-differentiated cell types, which perform specific metabolic functions, gap junctions typically play a role in coordinating metabolic pathways between contiguous cells. Well-differentiated cell types have limited, if any, proliferative capacities and the channels probably play a tissue specific metabolic role that often depends on morphology and specific arrangement of cells. For example, cardiac myocytes are elongated cells where gap junctions are predominantly aligned at the intercalated discs, thus using the SL-DT method would require aligning the cells, which can be done in a grooved dish. Thus, careful considerations must be made for each cell type. Studies with neuronal cell cultures typically are not confluent and also require specific contact points, which makes the use of the SL-DT inappropriate and alternative GJIC assays must be used.

In proliferative cell types, such as stem and early progenitor cells, GJIC plays a more critical role in coordinating cell signaling events that control gene expression regulating mitogenic events. The WB-F344 rat liver epithelial cells used in this protocol falls into this category. Gap junction genes are critical during tissue development and maintenance¹⁹⁻²¹. Although gap junction channels are expressed and formed on all cell plasma membrane surfaces, proliferative cells are very sensitive to growth factors, which inhibit GJIC. Critical considerations for proliferative cell-types are usually oriented more to the composition of the media. Growth factors are often in excess, particularly in undefined medium containing fetal bovine serum, and the cells' gap junctions may be in a closed state. The easiest way to establish GJIC in these cells is to reduce or remove the serum levels for 4 to 24 hr before experimentation, although 24 hr would be too long for cells with no serum as they would apoptose. The WB-F344 liver epithelial cells used for the experiments presented in this paper are not overly sensitive to serum with no need to reduce serum levels.

In contrast, experiments using a C10 mouse cell line must be first serum deprived to establish GJIC²². Although serum levels vary between the two cell types, interestingly, the C-10 cells responded very similarly to methyl isomers of anthracene^{22,23}.

Other considerations for quality results include conducting the experiments at non-cytotoxic doses. Cells need to be checked with phase contrast microscopy to determine healthy morphological features expected of the cell type before and after treatment. To assure that the effects of a compound on gap junction function is not due to a general cytotoxic response, cytotoxicity assays for each compound should be done at the same time and dose used in the SL-DT assay. Conducting experiments to determine if an inhibitory effect of a compound on GJIC is reversible is also a good experiment for at least two reasons. Most compounds tested reversibly inhibit GJIC, but if there is no recovery of GJIC, then cytotoxicity might be a factor and further testing would be required. However, if GJIC is restored then the dose and time tested were probably not cytotoxic. There are biological implications for the reversible inhibition of GJIC. The adverse health effects of many environmental and food borne toxicants and toxins is a reversible process. Therefore understanding this reversibility at the molecular level is important. If an unknown compound does not reversibly inhibit GJIC, then the implications for the health of an organism could be quite different from most other agents and needs to be part of the risk calculations.

Determining the dose and time involved in the inhibition of GJIC is an iterative process. To save time and money for the culture supplies, the best approach is to begin at a high dose, which depends on solubility and time (typically an hour, as most inhibition occurs in less than 15 min), and then reduce the time and dose by half in a step wise process until there is no effect. If there is no inhibition at a high dose at one hour, then double the time period in a step wise process. Initial experiments can be done on a single plate. Once the general time estimates and doses are established, then more thorough studies can be efficiently designed with appropriate sample sizes for statistical analyses. One experimental design feature would be to use the dose and time that reach 75 to 100% inhibition. Obviously, the final interpretations of results will be a factor of the above parameters. However, by first determining a biological effect, even if the dose and time may not be relevant *in vivo*, the established doses can play a role in situations of occupational exposures, or to general populations exposed to other factors that also affect GJIC with potential additive or synergistic effects.

The inhibition of GJIC by most compounds typically is not highly variable and two to three replicates (each replicate would be a culture plate or well) is sufficient to generate dose and time response curves. However, if variability is high then more replicates would be needed to get an accurate value for a given dependent variable of one independent trial. Of course, at least three independent trials need to be done for statistical analyses.

The simplicity of this assay and the assessment of significant cell population sizes is an advantage for many applications. This is particularly useful in many toxicological assessments. However, there are limitations of the SL-DT assays, which can depend on several factors. One is whether this technique is appropriate to the cells being studied. This assay would not work well for cells that do not reach high confluency with sporadic contacts throughout the culture plate or well. Alternative techniques, such as microinjection should be considered. Alternatively, the SL-DT assay can be modified. Success in loading single cells has been achieved with an acupuncture needle, which requires a slight twisting action when loading the dye⁷. The spread of dye would be radial in more confluent situations or amorphous through cell culture with sporadic cell contacts. The addition of Rhodamine dextran (RD, 1 mg/ml) to the LY dye solution is recommended for experiments where identifying the loaded cells would be difficult without a marker (such as RD). RD is too large to traverse gap junction channels, thus identifying which cells were loaded. RD can also be used in all SL-DT assay, but the scalpel leaves an indentation on the bottom of the dish identifying where cells are loaded. The SL-DT assay is also not conducive to measuring changes in GJIC between different types of cell as the dye loading would not discriminate between cell types. Again microinjection is the method of choice, but the acupuncture needle method might also work if one can target a specific cell using a microscope.

The metabolic cooperation assay is another method to measure GJIC. This method was one of the first standardized bioassay for GJIC²⁴. In this assay, wild-type Chinese hamster V79 cells (6-thioguanine-sensitive) and 6-thioguanine-resistant cells were co-cultured at high densities in which 6-thioguanine (6-TG) resistant cells do not metabolize 6-TG to a toxic metabolite, thus conferring resistance. Co-culture with the 6-TG sensitive cells results in the transfer of the toxic metabolite through gap junctions resulting in cell death where inhibition of GJIC results in the rescue of 6-TG resistant cells by preventing the transfer of the toxic 6-TG metabolite from the 6-TG sensitive cells. Although an advantage of this assay is that it is minimally invasive, a major disadvantage is that it requires one week for completion, which makes extensive dose and time dependent assessments of toxicants as well as mechanistic studies, *etc.* impractical for assessing many chemicals.

The SL-DT assay is not conducive to mechanistic studies that need to trace the migration of dyes through different cell types, in which microinjection is the preferred method. Alternatively, cells can be preloaded with the methyl ester of fluorescent dyes. The loading of the dye is a function of intracellular methyl esterases that hydrolyze the lipophilic dye into its more hydrophilic form, thus trapping the dye in the cells. This is a less invasive way to preload the fluorescent probe, but the most common way to measure intercellular communication where all cells are preloaded by this method is the FRAP assay¹¹. The advantage of FRAP is again the ability to assess gap junctions in single cells, which is excellent for mechanistic studies. However the disadvantage of FRAP lies in: the inability to measure populations of cells for toxicological assessments, the need for sophisticated and very expensive microscopes/laser cytometers, the need for highly skilled technical expertise, is moderately invasive from the free radicals produced by the laser, and not conducive to high throughput.

More recently another technique has been developed; the local activation of molecular fluorescent probe (LAMP) method²⁵, which is based upon a new generation of caged coumarin-like fluorophores. Similar to the FRAP assay, all cells are preloaded with dyes containing a methyl ester, however, these dyes become fluorescent upon subsequent localized illumination by lasers with a small dose of ultraviolet light, which probably produces significantly lower ROS than FRAP. Again, this assay has the same limitations of the FRAP assay. Other recent advancements for measuring GJIC are the preloading and parachute techniques, which also involve the use of methyl ester-fluorescent dyes. The preloading technique involves suspending the cells preloaded with fluorescent probe together with the unloaded counterparts and are then plated and allowed to form a confluent monolayer. The spread of the dye can then be observed with an epifluorescence microscope²⁶. In the parachute assay, the cells preloaded with the fluorescent probe are overlaid onto a monolayer of unloaded cells, and the spread of the dye is observed with an epifluorescence microscope²⁷. Again, the above techniques are technically more challenging for high throughput analyses, and must be immediately plated at near confluence and requires a time lag for the reattachment of cells.

Overall, the SL-DT assay is a relatively inexpensive, simple and versatile technique that uses equipment, such as CO₂ cell culture incubators, biosafety cabinets and epifluorescence microscope, typically found in most cell culture labs. With minimal experience many plates can be processed in a day, which is conducive for screening compounds for toxicity as well as for natural products that prevent or reverse the effects of toxicants and toxins. Also, adapting this assay for high throughput analyses using robotics, with automated fluorescence microscopy imaging and analysis systems will have the potential to screen large numbers of toxicants and toxins.

Disclosures

The authors have nothing to disclose.

Acknowledgements

Supported by NIEHS grants #R01 ES013268-01A2, and the contents are solely the responsibility of the author and do not necessarily represent the official views of the NIEHS, and supported by CETOCOEN UPgrade project No. CZ.1.05/2.1.00/19.0382.

References

1. Rotroff, D.M. *et al.* Predictive endocrine testing in the 21st century using in vitro assays of estrogen receptor signaling responses. *Environ.Sci.Technol.* **48** (15), 8706-8716 (2014).
2. Axelsen, L.N., Calloe, K., Holstein-Rathlou, N.H., & Nielsen, M.S. Managing the complexity of communication: regulation of gap junctions by post-translational modification. *Front Pharmacol.* **4** 130 (2013).
3. Nielsen, M.S. *et al.* Gap junctions. *Compr.Physiol.* **2** (3), 1981-2035 (2012).
4. Sovadinova, I. *et al.* Phosphatidylcholine specific PLC-induced dysregulation of gap junctions, a robust cellular response to environmental toxicants, and prevention by resveratrol in a rat liver cell model. *PLoS.One.* **10** (5), e0124454 (2015).
5. Trosko, J.E., & Chang, C.C. In: *Biologically Based Methods for Cancer Risk Assessment*. Travis, C.C. ed., Plenum Press, New York, 165-179 (1989).
6. Trosko, J.E. In: *Biomarkers and occupational health: progress and perspectives*. Mendelsohn, M.D., Peeters, J.P., & Normandy, M.J. eds., John Henry Press, Washington D.C., 264-274 (1995).
7. Upham, B.L. Role of integrative signaling through gap junctions in toxicology. *Curr.Protoc.Toxicol.* **47** 2.18:2.18.1-2.18.18 (2011).
8. Vinken, M. *et al.* Connexins and their channels in cell growth and cell death. *Cell.Signal.* **18** (5), 592-600 (2006).
9. Browne, C.L., Wiley, H.S., & Dumont, J.N. Oocyte-follicle cell gap junctions in *Xenopus laevis* and the effects of gonadotropin on their permeability. *Science.* **203** (4376), 182-183 (1979).
10. El-Fouly, M.H., Trosko, J.E., & Chang, C.C. Scrape-loading and dye transfer. A rapid and simple technique to study gap junctional intercellular communication. *Exp.Cell Res.* **168** (2), 422-430 (1987).
11. Wade, M.H., Trosko, J.E., & Schindler, M. A fluorescence photobleaching assay of gap junction-mediated communication between human cells. *Science.* **232** (4749), 525-528 (1986).
12. Upham, B.L. *et al.* Structure-activity-dependent regulation of cell communication by perfluorinated fatty acids using in vivo and in vitro model systems. *Environ.Health Perspect.* **117** (4), 545-551 (2009).
13. Paraffin Processing of Tissue. *Protoplasma-*. Source: [<http://protocolsonline.com/histology/sample-preparation/paraffin-processing-of-tissue/>]. (2012).
14. Trosko, J.E. Gap junctional intercellular communication as a biological "Rosetta stone" in understanding, in a systems biological manner, stem cell behavior, mechanisms of epigenetic toxicology, chemoprevention and chemotherapy. *J.Membr.Biol.* **218** (1-3), 93-100 (2007).
15. Upham, B.L., Weis, L.M., & Trosko, J.E. Modulated gap junctional intercellular communication as a biomarker of PAH epigenetic toxicity: structure-function relationship. *Environ.Health Perspect.* **106** 975-981 (1998).
16. Upham, B.L. *et al.* Tumor promoting properties of a cigarette smoke prevalent polycyclic aromatic hydrocarbon as indicated by the inhibition of gap junctional intercellular communication via phosphatidylcholine-specific phospholipase C. *Cancer Sci.* **99** (4), 696-705 (2008).
17. Sai, K., Kanno, J., Hasegawa, R., Trosko, J.E., & Inoue, T. Prevention of the down-regulation of gap junctional intercellular communication by green tea in the liver of mice fed pentachlorophenol. *Carcinogenesis.* **21** (9), 1671-1676 (2000).
18. Upham, B.L., Deocampo, N.D., Wurl, B., & Trosko, J.E. Inhibition of gap junctional intercellular communication by perfluorinated fatty acids is dependent on the chain length of the fluorinated tail. *Int.J.Cancer.* **78** (4), 491-495 (1998).
19. Trosko, J.E., & Tai, M.H. In: *Infections and inflammation: Impacts on oncogenesis. Impacts on Oncogenesis. Contrib Microbiol.* Dittmar, T., Zaenkar, K.S., & Schmidt, A. eds., S. Karger, Basel, 45-65 (2006).
20. Trosko, J.E. Human stem cells as targets for the aging and diseases of aging processes. *Med.Hypotheses.* **60** (3), 439-447 (2003).
21. Trosko, J.E. In: *Stem Cells and Cancer*. Dittmar, T., & Zaenkar, K. eds., Nova Publishers, New York, 147-188 (2008).
22. Osgood, R.S. *et al.* Polycyclic aromatic hydrocarbon-induced signaling events relevant to inflammation and tumorigenesis in lung cells are dependent on molecular structure. *PLoS.One.* **8** (6), e65150 (2014).
23. Weis, L.M., Rummel, A.M., Masten, S.J., Trosko, J.E., & Upham, B.L. Bay or baylike regions of polycyclic aromatic hydrocarbons were potent inhibitors of gap junctional intercellular communication. *Environ.Health Perspect.* **106** (1), 17-22 (1998).
24. Yotti, L.P., Chang, C.C., & Trosko, J.E. Elimination of metabolic cooperation in Chinese hamster cells by a tumor promoter. *Science.* **206** (4422), 1089-1091 (1979).
25. Zhao, Y. *et al.* New caged coumarin fluorophores with extraordinary uncaging cross sections suitable for biological imaging applications. *J.Am.Chem.Soc.* **126** (14), 4653-4663 (2004).
26. Goldberg, G.S., Bechberger, J.F., & Naus, C.C. A pre-loading method of evaluating gap junctional communication by fluorescent dye transfer. *Biotechniques.* **18** (3), 490-497, (1995).
27. Ziambaras, K., Lecanda, F., Steinberg, T.H., & Civitelli, R. Cyclic stretch enhances gap junctional communication between osteoblastic cells. *J.Bone Miner.Res.* **13** (2), 218-228 (1998).

- III.** Upham, B.L.*, Blaha, L., **Babica, P.**, Park, J.S., Sovadinova, I., Pudrith, C., Rummel, A.M., Weis, L.M., Sai, K., Tithof, P.K., Guzvic, M., Vondracek, J., Machala, M., Trosko, J.E., 2008. Tumor promoting properties of a cigarette smoke prevalent polycyclic aromatic hydrocarbon as indicated by the inhibition of gap junctional intercellular communication via phosphatidylcholine-specific phospholipase C. *Cancer Science* 99, 696–705.

Tumor promoting properties of a cigarette smoke prevalent polycyclic aromatic hydrocarbon as indicated by the inhibition of gap junctional intercellular communication via phosphatidylcholine-specific phospholipase C

Brad L. Upham,^{1,8} Ludek Bláha,^{2,9} Pavel Babica,¹ Joon-Suk Park,¹ Iva Sovadinova,¹ Charles Pudrith,¹ Alisa M. Rummel,¹ Liliane M. Weis,¹ Kimie Sai,^{3,9} Patti K. Tithof,⁴ Miodrag Gužvić,^{5,9} Jan Vondráček,^{6,7} Miroslav Machala⁶ and James E. Trosko¹

¹Department of Pediatrics & Human Development; and the National Food Safety & Toxicology Center, Michigan State University, East Lansing, MI 48824; ²Research Centre for Environmental Chemistry & Ecotoxicology, Kamenice 126/3, 62500 Brno, Czech Republic; ³Division of Biosignaling, National Institute of Health Sciences, 1-18-1 Kamiyoga, Setagaya-ku, Tokyo 158-8501 Japan; ⁴Department of Pathobiology, College of Veterinary Medicine, University of Tennessee, Knoxville, TN 37996-4543, USA; ⁵Laboratory for Radiobiology and Molecular Genetics, Institute of Nuclear Sciences 'Vinca', Belgrade, Serbia and Montenegro; ⁶Veterinary Research Institute, Department of Chemistry and Toxicology, Hudcova 70, 62132 Brno, Czech Republic; ⁷Institute of Biophysics, Kraválovopdská 135 61265 Brno, Czech Republic

(Received October 25, 2007/Revised December 11, 2007/Accepted December 19, 2007/Online publication March 17, 2008)

Inhibition of gap junctional intercellular communication (GJIC) and the activation of intracellular mitogenic pathways are common hallmarks of epithelial derived cancer cells. We previously determined that the 1-methyl and not the 2-methyl isomer of anthracene, which are prominent cigarette smoke components, activated extracellular receptor kinase, and inhibited GJIC in WB-F344 rat liver epithelial cells. Using these same cells, we show that an immediate upstream response to 1-methylanthracene was a rapid (<1 min) release of arachidonic acid. Inhibition of phosphatidylcholine-specific phospholipase C prevented the inhibition of GJIC by 1-methylanthracene. In contrast, inhibition of phosphatidylinositol specific phospholipase C, phospholipase A₂, diacylglycerol lipase, phospholipase D, protein kinase C, and tyrosine protein kinases had no effect on 1-methylanthracene-induced inhibition of GJIC. Inhibition of protein kinase A also prevented inhibition of GJIC by 1-methylanthracene. Direct measurement of phosphatidylcholine-specific phospholipase C and sphingomyelinase indicated that only phosphatidylcholine-specific phospholipase C was activated in response to 1-methylanthracene, while 2-methylanthracene had no effect. 1-methylanthracene also activated p38-mitogen activated protein kinase; however, like extracellular kinase, its activation was not involved in 1-methylanthracene-induced regulation of GJIC, and this activation was independent of phosphatidylcholine-specific phospholipase C. Although mitogen activated protein kinases were activated, Western blot analyzes indicated no change in connexin43 phosphorylation status. Our results indicate that phosphatidylcholine-specific phospholipase C is an important enzyme in the induction of a tumorigenic phenotype, namely the inhibition of GJIC; whereas mitogen activated protein kinases triggered in response to 1-methylanthracene, were not involved in the deregulation of GJIC. (*Cancer Sci* 2008; 99: 696–705)

Considerable toxicological and carcinogenic research on polycyclic aromatic hydrocarbons (PAH) has focused on the genotoxic attributes of these compounds.⁽¹⁾ However, many human diseases, such as cancer, are not solely the consequence of non-reversible mutagenic events, but also include reversible, epigenetic events (altered expression of genes at transcriptional, translational and post-translational levels) that alter the normal phenotype of a cell.⁽²⁾ Thus, there is a need to reassess the toxicity and carcinogenicity of environmental toxicants, including PAH, at the epigenetic level. Rosenkranz *et al.*⁽³⁾ showed that out of a group of 251 chemicals, there was actually

a much stronger correlation of tumorigenicity with the inhibition of gap junctional intercellular communication (GJIC), an epigenetic event, than with mutagenicity. Cell proliferative diseases such as cancer include crucial epigenetic events that ultimately remove quiescent initiated-cells from the growth suppressive control of neighboring cells.^(2,4) Intercellular communication between contiguous cells via protein complexes, known as gap junctions, also alters, epigenetically, the expression of genes and strongly suggests that intercellular signaling can further modulate the intracellular signal transduction pathways.^(5–7)

Cancer cells have been characterized as cells that lose their ability to regulate growth through contact inhibition,⁽⁸⁾ and that lack the ability to terminally differentiate,⁽⁹⁾ which implies a breakdown in one of the communicating mechanisms.⁽²⁾ Alteration of cell-to-cell communication via gap junctions has been implicated in the carcinogenic process and is supported by considerable evidence.^(7,10) Most cancer cells have defective GJIC.⁽¹¹⁾ Chemical tumor promoters and oncogenes inhibit GJIC, while tumor suppressor genes and chemopreventative compounds enhance GJIC.^(10,12) Inactivation of gap junction genes in normal cells result in cancer-like cells,⁽¹³⁾ and gap junction genes transfected into cancer cells restore their normal growth regulation.⁽¹⁰⁾ The knockout of the gap gene connexin (Cx32), in mice that were administered with a single dose of the tumor initiator, diethylnitrosamine (DEN) had a 3.3–12.8 times increase of preneoplastic foci as compared to the DEN-treated wild-type mice. These results indicate that the deletion of Cx32 promoted the carcinogenic effects of diethylnitrosamine.⁽¹⁴⁾ Cx32 knockout mice also exhibit increased levels of radiation and chemical-induced liver and lung tumor formation.^(15,16) Tumor induction utilizing X-ray radiation resulted in a statistically significant increase in overall tumor burden in Cx32-deficient

⁸To whom correspondence should be addressed. E-mail: upham@msu.edu

⁹On leave of absence.

Abbreviations: gap junctional intercellular communication (GJIC), connexin43 (Cx43), mitogen activated protein kinase (MAPK), extracellular receptor kinase (ERK), phosphatidylcholine (PC), phospholipase C (PLC), phosphatidylcholine specific phospholipase C (PC-PLC), phosphatidylinositol specific PLC (PI-PLC), sphingomyelin (SM), sphingomyelinase (SMase), protein kinase A (PKA), protein kinase C (PKC), scrape loading-dye transfer (SL-DT), polycyclic aromatic hydrocarbon (PAH), polycyclic aromatic hydrocarbons (PAHs), 1-methylanthracene (1-MeA), 2-methylanthracene (2-MeA), polychlorinated biphenyls (PCBs), 12-O-tetradecanoylphorbol-13-acetate (TPA), phosphate buffered saline (PBS), hydrogen peroxide (H₂O₂), bovine serum albumin (BSA).

mice compared with wild-type mice due to tumorigenesis in several tissues such as the lung, liver, adrenal, lymph and small intestine.⁽¹⁶⁾ Increased levels of activated mitogen-activated protein kinases (MAPK) were also observed in these Cx32-deficient mouse model systems compared with wild-type counterparts implicating that MAPK-related pathways may be preferentially activated or conversely that tumors harboring activated MAPK pathways may selectively progressed towards more advanced tumor states in the absence of Cx32-mediated GJIC.⁽¹⁶⁾ These results collectively indicate that Cx32 potentially play a tumor suppressive role.

Cell proliferative diseases such as cancer not only require the release of a quiescent cell from growth suppression via down-regulation of GJIC and/or changes in extracellular components (i.e. integrins), but also need to activate mitogenic signaling pathways. The MAPK pathways are the major intracellular signaling mechanisms by which a cell activates, via phosphorylation, transcription factors involved in mitogenesis.⁽¹⁷⁻¹⁹⁾ Four major mitogenic cascade pathways are the following: extracellular receptor kinase (ERK), stress activated protein kinase/Jun N-terminal kinase, p38,⁽¹⁹⁾ and ERK5/big MAPK1.⁽²⁰⁾ The ERK-pathway has been extensively characterized and is the most understood of the MAPK pathways.⁽¹⁹⁾ The relationship between MAPK and GJIC has not been well characterized. The disruption of GJIC by epidermal growth factor, a mitogen, might be mediated in part by the phosphorylation of three serine sites of connexin43 (Cx43) via MAPK.⁽²¹⁾ However the phosphorylation of Cx43 alone is insufficient in the closure of gap junction channels,⁽²²⁾ but phosphorylation does play multiple roles in gap junction function and expression.⁽²³⁾

We have previously reported that PAH with strict structural criteria, specifically the existence of a bay or bay-like region, activate ERK-MAPK and inhibit GJIC.⁽²⁴⁻²⁷⁾ PAH, like polychlorinated biphenyls (PCB), do not regulate GJIC through a MEK-dependent mechanism,^(25,28) which is unlike growth factors and protein kinase C (PKC)-dependent promoters, such as 12-*O*-tetradecanoylphorbol-13-acetate (TPA).⁽²⁹⁾ We previously reported that phosphatidylcholine-specific phospholipase C (PC-PLC) is involved in PCB-induced inhibition of GJIC.⁽²⁸⁾ Thus, we tested the hypothesis that PC-PLC and not MAPK is directly involved in the regulation of GJIC by PAH. We specifically chose 1-methylanathracene (1-MeA) and 2-methylanathracene (2-MeA) for this study for the following reasons. Our previous studies indicated that the 1-methyl and not the 2-methyl isomer of anthracene inhibit GJIC and activate ERK-MAPK,^(24,26,27) which gives us an excellent model system of comparing biological effects of two similar compounds, yet one isomer (2-MeA), can serve as a negative control. These compounds are also environmentally relevant,⁽³⁰⁾ and in particular represent a major component of the PAH fraction of cigarette smoke.⁽³¹⁾ In this report, we demonstrate that 1-MeA inhibited GJIC through a PC-PLC-dependent mechanism, and released arachidonic acid. In addition to activating ERK-MAPK,⁽²⁵⁾ 1-MeA also activated p38-MAPK, yet the phosphorylation patterns of Cx43 were not altered as determined by Western blot analyses. In contrast, the 2-MeA, did not inhibit GJIC, and did not activate ERK, p38 and PC-PLC, nor induced the release of arachidonic acid.

Methods and Materials

Chemicals. The following are the commercial sources for the reagents used in this study: Lucifer Yellow (Molecular Probes, Eugene, OR, USA), sodium dodecyl sulfate (SDS), Tween 20, TRIS, glycine, acrylamide, and TEMED (Bio-Rad Laboratories, Hercules, CA, USA); anthracene, 1-MeA, 2-MeA, 9-MeA, RHC80267, 1-butanol, ET-18-OCH₃, 4',6-diamidino-2-phenylindole (DAPI), *p*-bromophenacylbromide (BPB) and genistein (Sigma Chemical Co., St. Louis, MO, USA); acetonitrile (EM Science, Gibstown,

NJ, USA); PP2 (Calbiochem, LA Jolla, CA, USA); D609 (Tocris Bioscience, Ellisville, MO, USA); H-89, BEL (Biomol International, Plymouth Meeting, PA, USA); AACOCF₃ and MAFP (Cayman Chemical, Ann Arbor, MI, USA), all electrophoresis reagents and the DC protein kit (Bio-Rad laboratories); phospho-specific polyclonal antibodies directed to ERK-1 phosphorylated at Thr 202/Tyr204, and ERK-2 directed to phosphorylated Thr183/Tyr185 (New England Biolabs, Ipswich, MA, USA) and to Cx43 (Zymed Laboratories Inc., San Francisco, CA, USA), GADPH (Chemicon, Temecula, CA, USA), and to α -tubulin (Abcam, Cambridge, MA, USA), phosphospecific polyclonal anti p38 antibody directed to phosphorylated Thr 180/Tyr 182 (Invitrogen/Zymed, Carlsbad, CA, USA). Secondary antibodies used were antirabbit and antimouse Ig-G conjugated with horse radish peroxidase (Amersham, Life Science, Denver CO, USA). The final volume of the exposure medium for each independent culture plate was 2 mL. The concentration of each chemical is indicated in each figure or figure legend and the vehicle for each experiment is equivalent to the volume added with the test compounds.

Cell culture. The WB-F344 rat liver epithelial cell line was obtained from Drs J. W. Grisham and M. S. Tsao of the University of North Carolina (Chapel Hill, NC, USA),⁽³²⁾ and cultured in D-medium (Formula no. 78-5470EF, Gibco Laboratories, Grand Island, NY, USA) on 35 mm tissue culture plates (Corning Inc., Corning, NY, USA), supplemented with 5% fetal bovine serum (Gibco Laboratories), and incubated at 37°C in a humidified atmosphere containing 5% CO₂ and 95% air. Bioassays were conducted with confluent cultures that were obtained after two to three days of growth.

This cell line expresses primarily Cx43 and serves as an *in vitro* cell model system for regenerative epithelial cell types that expresses Cx43. The following are some further attributes of this cell line. They are diploid and non-tumorigenic,⁽³²⁾ and have been extensively characterized for its expressed gap junction genes and functional GJIC using all available techniques in the absence and presence of well-known tumor promoters, growth factors, tumor suppressor genes and oncogenes to modulate GJIC.⁽¹⁰⁾ Intrahepatic transplantation of WB-cells into adult syngenic F344 rats results in the morphological differentiation of these cells into hepatocytes and incorporation into hepatic plates.⁽³³⁾ The pluripotency of these cells was further demonstrated by their differentiation into functional-contracting cardiomyocytes when transplanted into the heart tissue of adult syngenic F344 rats.⁽³⁴⁾

Bioassay of GJIC. The scrape loading-dye transfer (SL-DT) technique was adapted after the method of El-Fouly *et al.*⁽³⁵⁾ The test chemicals were added directly to the cell culture medium from concentrated stock solutions and appropriate solvent controls were run at all times, which did not differ from untreated cells. After treatment, cells were washed with phosphate buffered saline (PBS) followed by the addition of 1 mg/mL of Lucifer Yellow dissolved in PBS. The dye was introduced into the cells with three different scrapes through the monolayer of confluent cells using a surgical steel scalpel blade. The transfer of dye through gap junctions was for three minutes, followed by a thorough rinse with PBS to remove extracellular dye, and then fixed with a 4% formalin solution in PBS. Migration of the dye in the cells was observed at 200X using a Nikon epifluorescence microscope equipped with a Nikon Cool Snap EZ CCD camera and the images digitally acquired using a Nikon NIS-Elements F2.2 imaging system. The fluorescence area of the dye migration from the scrape line was quantified using 'Gel Expert' image analysis program (NucleoTech Corp, San Mateo, CA). The data was reported as a fraction of the dye spread of the vehicle control.

Western blot analysis. Cells were grown in 35 mm diameter tissue culture plates from Corning (Corning, NY) to the same

confluency as the SL-DT assay. The cells treated by the test chemicals were done under the same conditions as those used in the SL-DT assay. The proteins were extracted with 20% SDS solution containing 1 mM phenylmethylsulfonyl fluoride, 100 μ M Na_3VO_4 to the PBS, and 100 nM aprotinin, 1.0 μ M leupeptin and 1.0 μ M antipain, 100 μ M Na_3VO_4 , 5.0 mM NaF. The protein content was determined with the Bio-Rad DC assay kit. The proteins (15 μ g) were separated on 12.5% SDS-PAGE according to the method of Laemmli.⁽³⁶⁾ The proteins were electrophoretically transferred from the gel to polyvinylidene fluoride (PVDF) membranes (Millipore Corp, Bedford, MA, USA). Detection of the Western Blot signals for Cx43, p38 and ERK used enhanced chemiluminescent (ECL) detection kit and HyperFilm™-MP (Amersham, Life Science, Denver, CO, USA), except for p38, we used SuperSignal West Pico Stable Peroxide Solution and Luminol/Enhancer Solution (Pierce, Rockford, IL, USA), film HyBlot™-CL (Denville Scientific, Metuchen, NJ, USA).

Assay of PC-PLC and sphingomyelinase (SMase) activity. Confluent cells in 100 mm plates, serum-deprived for 4 h, were exposed to 1-MeA and 2-MeA at the desired concentrations for 5 and 15 min at 37°C (solvent control did not exceed 0.5% v/v). After exposure, cells were briefly washed with ice-cold PBS, scraped and centrifuged. The pellets (about 2.5×10^6 cells) were lysed for 60 min on ice with 0.6 mL of an ice cold buffer (pH 7.5) containing 50 mM TRIS, 150 mM sodium chloride, 2 mM ethylene diamine tetraacetic acid, 1 mM ethylene glycol tetraacetic acid, 1% v/v, Triton-X, 1 μ g/mL aprotinin and 100 μ g/mL phenylmethylsulfonyl fluoride. We used about 200 μ L of the lysis buffer per plate. The lysed-suspension was centrifuged at 17 000 \times g for 10 min, and the supernatant fraction was collected and stored at -80°C for SMase and PLC activity assays.

SMase and PC-PLC activities were determined using Amplex Red reaction kits (Molecular Probes, Invitrogen, Eugene, OR, USA). The assay according to Zhou *et al.*⁽³⁷⁾ worked as follows. SMase and PC-PLC hydrolytic activities were determined by the exogenous addition of their respective substrates, sphingomyelin (SM) or phosphatidylcholine (PC), to the thawed supernatant fraction. Phosphocholine, the hydrolysis product of either SM/SMase or PC/PC-PLC, was dephosphorylated with alkaline phosphatase to choline, which was further oxidized with choline oxidase and ambient oxygen to betaine aldehyde and hydrogen peroxide (H_2O_2). The H_2O_2 , in the presence of horseradish peroxidase, oxidizes Amplex Red to the fluorescent resorufin. Reaction mixtures contained the buffer, which for SMase determination was 100 mM TRIS HCl and 10 mM magnesium chloride, pH 7.4, and for PC-PLC activity was 50 mM TRIS HCl, 140 mM NaCl, 2 mM CaCl_2 , pH 7.4; plus the substrates (0.5 mM SM or PC, respectively), 0.1 unit/mL choline oxidase, 5 μ M Amplex Red, 4 units/mL alkaline phosphatase, 1 unit/mL horseradish peroxidase. The kinetics of the fluorescence intensity was recorded at 590 nm (excitation at 544 nm) using Gemini microplate fluorescence reader (Molecular Devices, Sunnyvale, CA, USA), at 37°C. The slopes were derived from the initial 10 min of the kinetic reaction.

Assay of Arachidonic acid release. Arachidonic acid-release was measured according to the method of Tithof *et al.*⁽³⁸⁾ Cells were grown to 75% confluency in 35 mm culture dishes and then treated for 24 h with 1.00 μ Ci ^3H -arachidonic acid (specific activity = 180–240 Ci/mM) at normal cell culture conditions. At the end of the labeling period in which the cells have attained 95–100% confluency, the extracellular ^3H -arachidonic acid was removed with three washings of PBS and resuspended in growth medium containing 0.1% bovine serum albumin (BSA) that is arachidonic acid and phospholipid free. The BSA served as a sink for the arachidonic acid released into the medium.⁽³⁸⁾ The incorporation of ^3H -arachidonic acids into the cells was

typically greater than 80%. These cells were treated with the PAH and at the end of the treatment time the culture medium was added to 14 mL of scintillation cocktail and counted for radioactivity in a scintillation counter. The remaining cells were trypsinized and solubilized in 14 mL of scintillation cocktail and counted for radioactivity in a scintillation counter. The data were expressed as a percentage of total cellular radioactivity released into the medium.

Assay of immunostaining of Cx43. WB-F344 cells were cultured to confluency in eight-well chamber slides (Fisher Scientific, Pittsburgh, PA, USA). Subsequently, cells were gently rinsed three times with PBS and fixed with 5% acetic acid in methanol for 10 min. The non-specific binding sites were blocked with 10% goat serum (Zymed, Carlsbad, CA, USA) for 2 h at room temperature (RT). Rabbit polyclonal Cx43 antibody (Zymed, South San Francisco, CA, USA) was diluted 1:150 in 1% BSA +0.1% Tween-20 in PBS at 4°C for 2 h, washed three times with 1% BSA +0.1% Tween-20 in PBS, then incubated with Alexa Fluor 488 goat antirabbit secondary antibody (Molecular Probes, Eugene, OR, USA) for 30 min at RT. Negative controls were prepared by eliminating the primary/secondary antibody. Slides were washed with PBS and counterstained with DAPI for 5 min before finally embedding with Prolong Antifade kit (Molecular Probes). Fluorescent images were obtained using a Nikon Epi-fluorescent microscope equipped with a SPOTRT digital camera (Diagnostic Instruments, Detroit, MI, USA) and analyzed with Spot Advanced analysis software (Diagnostic Instruments).

Results

The structures of 1-MeA and 2-MeA are illustrated in Figure 1(a). Inhibition of GJIC by 1-MeA was dose and time-dependent (Fig. 1b). A shift of the methyl group from the 1 position, which forms a bay-like region, to the 2 position on the anthracene ring, which does not form a bay-like region, renders this isomer of methylanthracene as fairly inactive relative to the inhibition of GJIC up to 3 h, although slight inhibition was seen at 8 h. A slight recovery was observed after a 4 h exposure time to 1-MeA, which was maintained up to 8 h. We previously reported that 1-MeA and not 2-MeA activated ERK-MAPK,⁽²⁵⁾ and the inhibition of GJIC was independent of this MAPK. Similarly, 1-MeA activated p38-MAPK, while 2-MeA did not activate p38 (Fig. 1c). Like the previous data on ERK-MAPK,⁽²⁵⁾ activation occurred after the time period needed to inhibit GJIC, 5 min versus 10 min (Fig. 1b vs Fig. 1c). Figure 1(d) illustrates the data for the densitometry analyzes of the p38 band. Although there was a slight trend of 2-MeA induced phospho-p38, these results were not significant, while the increase of the p38 bands in 1-MeA treated cells were significant (Fig. 1d). Confirmation that the inhibition of GJIC by 1-MeA was p38-independent is indicated in Figure 1(e) where the significant inactivation of p38 with SB202190, a selective inhibitor of p38, did not prevent 1-MeA from inhibiting GJIC.

Changes in the phosphorylation status of the connexin proteins, which make up the gap junction channels, has been implicated in the inhibition of GJIC. Our results indicate that the various isomers of methylanthracene, including 1-, 2- and 9-methylanthracene, did not alter the phosphorylation status of Cx43, the major connexin type in this cell line (Fig. 1f). TPA was used as the positive control for altering the phosphorylation status of Cx43, as indicated in a shift of the bands to higher molecular weights and the disappearance of the P_0 band. The P_0 band is the unphosphorylated form of Cx43 as determined by all bands collapsing to this position after treatment with alkaline phosphatase.⁽³⁹⁾ This lack of an effect on the phosphorylation of Cx43 continued even after the known activation of ERK,⁽²⁵⁾ and p38 (Fig. 1c,d). The densitometry analysis of the three Cx43

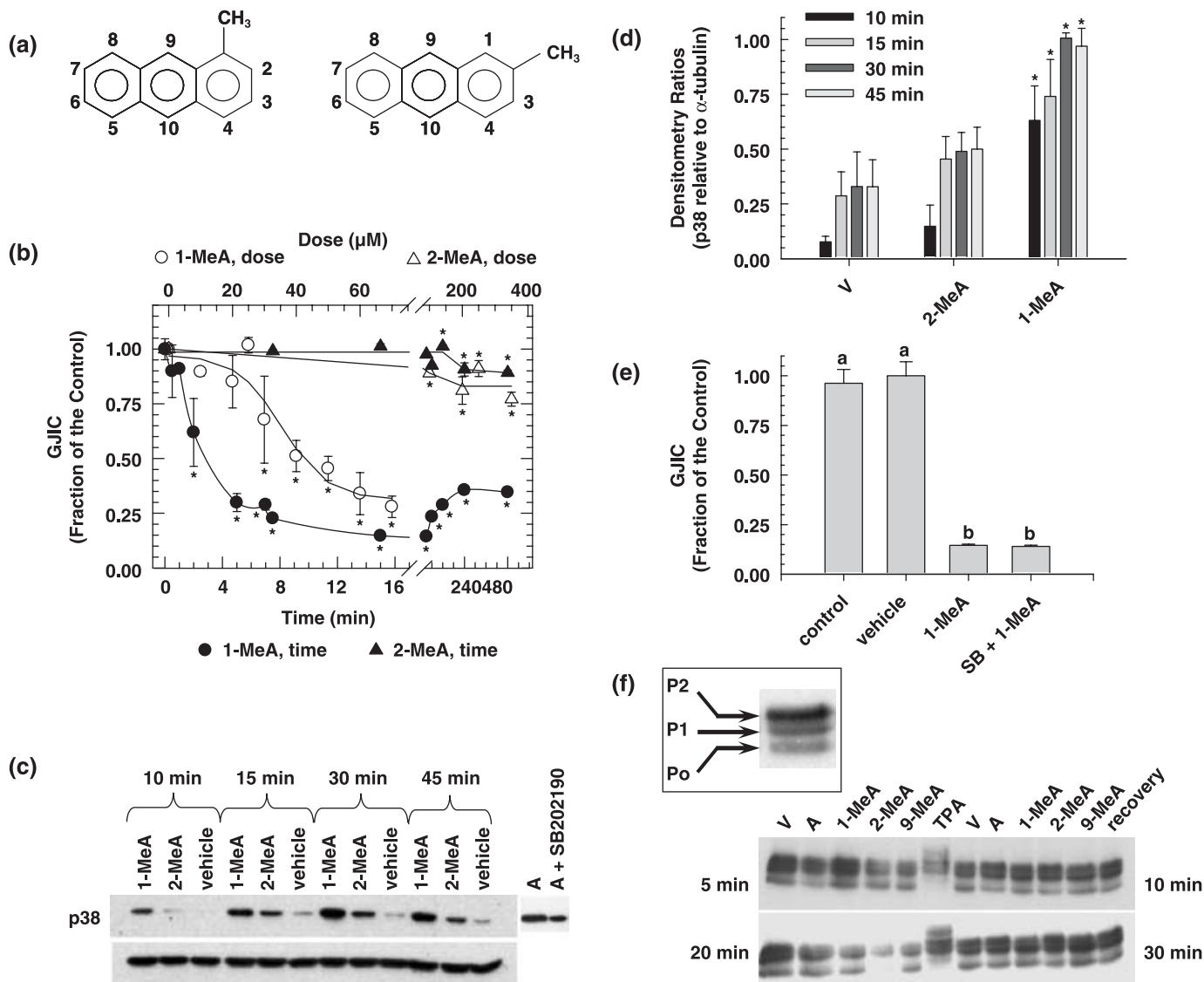


Fig. 1. The effects of 1-methylanthracene (1-MeA) versus 2-methylanthracene (2-MeA) on gap junction biology. (a) Structures of 1-MeA and 2-MeA; (b) Dose and time effect of 1-MeA versus 2-MeA on gap junctional intercellular communication (GJIC) activity. The data for the dose-response were obtained from Rummel *et al.* in which WB-F344 rat liver epithelial cell line were treated with the indicated polycyclic aromatic hydrocarbons (PAH) for 15 min. The dose for the time response data of each PAH was 75 μM , and the WB-F344 rat liver epithelial cell line was used for this and all subsequent experiments. The scrape load-dye transfer assay was used to assess GJIC for both the time and dose-response experiments. Average of the data ($n = 3$) \pm standard deviation at the 95% confidence level. An ANOVA indicated significance at $P < 0.001$ for 1-MeA dose ($F = 29.1$), 1-MeA time ($F = 87.0$), 2-MeA dose ($F = 18.2$), 2-MeA time ($F = 15.9$), and *indicated significance from the vehicle control using a Holm-Sidak posthoc T -test at the $P = 0.05$ level. (c) The effect of 1-MeA versus 2-MeA on the mitogen activated protein kinase, p38, as determined by Western blot analysis of p38 using phospho-specific antibodies (top gel) and the house keeping protein α -tubulin (bottom gel). The proteins were extracted from cells treated with 75 μM of the indicated polycyclic aromatic hydrocarbon. Anisomycin (A) at 0.5 μM and 30 min was used as a positive control. (d) Densitometry analysis of Western blots of p38 from proteins extracted from three independently treated cell culture plates, including the gel presented in (c). The values are the densitometry ratios of the p38 relative to α -tubulin. ANOVAs of the 10 min group ($F = 23.5$, $P < 0.001$), 15 min group ($F = 9.4$, $P = 0.014$), 30 min group ($F = 34.1$, $P < 0.001$), 45 min group ($F = 31.2$, $P < 0.001$), indicated significance between the vehicle, 2-MeA and 1-MeA. *Specifically indicates a difference as compared to the vehicle within each time group at $P = 0.05$ using a Holm-Sidak posthoc T -test at the $P = 0.05$ level. (e) The effect of a p38 inhibitor, SB202190 (4-(4-Fluorophenyl)-2-(4-hydroxyphenyl)-5-(4-pyridyl)-1H-imidazole), were 20 μM and 20 min. The GJIC data are an average of the data ($n = 3$) \pm standard deviation at the 95% confidence level. An ANOVA indicated significance at $P < 0.001$, $F = 285$, and the different letters indicated significance using an all pair multiple comparison-Holm Sidak posthoc T -test at the $P = 0.05$ level. (f) The effect of methylanthracene isomers on the phosphorylation status of connexin43 (Cx43). A Western blot analysis using antiCx43 antibodies was used to identify the phosphorylated states of Cx43. The duration of exposure times to the various PAH and vehicle were 5, 10, 20, and 30 min as indicated in the four quadrants of the figure. The quadrants are separated by the 12-*O*-tetradecanoylphorbol-13-acetate (TPA) data, in which these cells were treated with TPA for 10 min. Lanes TPA = 500 ng/mL, V = vehicle (0.3% v/v acetonitrile), A = 60 μM anthracene, 1-MeA = 60 μM 1-methylanthracene, 2-MeA = 60 μM 2-methylanthracene, 9-MeA = 60 μM 9-methylanthracene, Recovery for top gel = 6 h recovery from cells treated with 60 μM 1-MeA for 30 min, Recovery for bottom gel = 6 h recovery from cells treated with 60 μM 9-MeA for 30 min. The 1st (bottom), 2nd and 3rd bands are typically designated P_0 , P_1 and P_2 as indicated in the boxed inset, and the addition of alkaline phosphatase to the protein samples results in only a P_0 band, using this Western blot analysis protocol. The experiment was done in triplicate and the densitometry analyzes of the data are presented in Table 1.

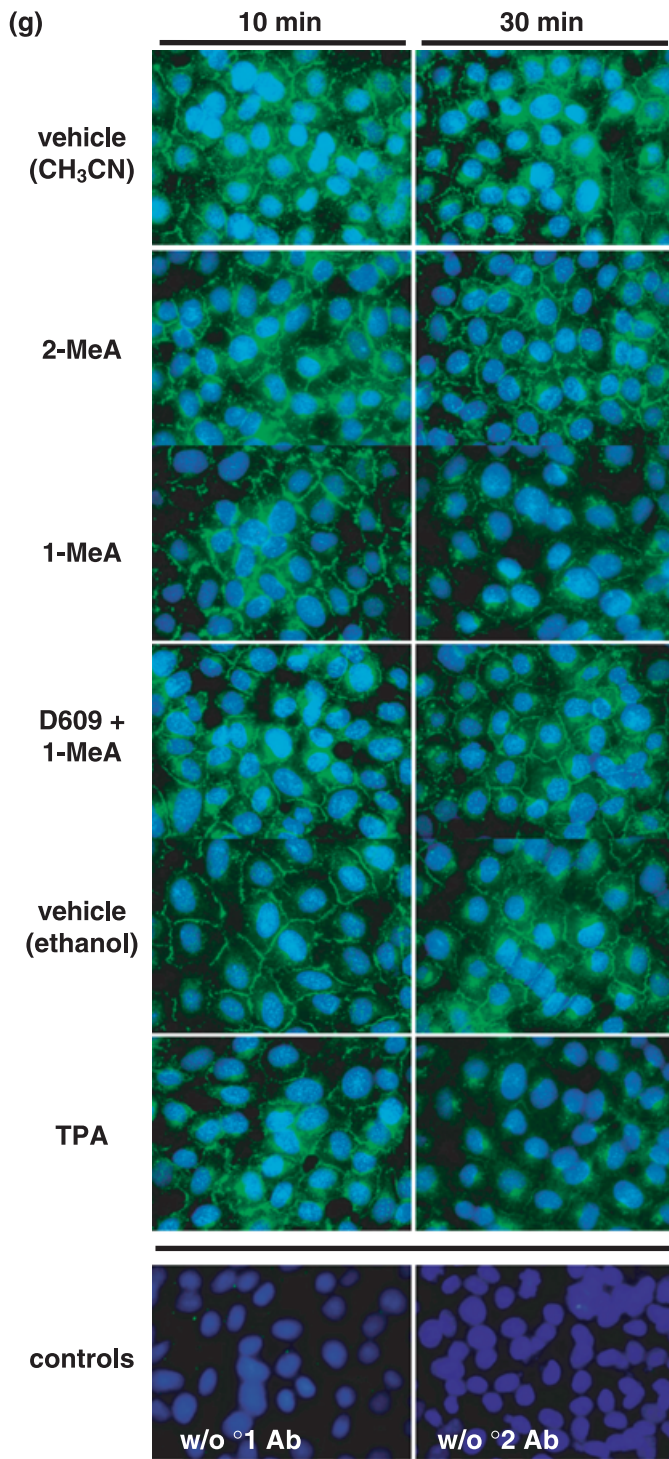


Fig. 1 (continued). (g) Cytological localization of Cx43 in cells treated with 1-MeA, 2-MeA and TPA. The concentrations of 1-MeA and 2-MeA were both 70 μ M, and for TPA 50 ng/mL. The vehicle was 0.3% (v/v) acetonitrile. An antiCx43 antibody was used to label this protein. The magnification of the images was 1000 \times . Ab, antibody; w/o, without.

bands of three independent experiments, including data from Figure 1(f) is presented in Table 1. ANOVA analyzes indicated that there were no significant changes in the ratios of the P₁ and P₂ bands relative to P₀ of all cells treated by the methylated anthracenes, while the TPA treated cells had a significant decrease in the P₀ band relative to P₁ and P₂.

Table 1. Densitometry scans of the phosphorylated (P₁ and P₂) Cx43-bands relative to the unphosphorylated (P₀) band from Western blots of proteins extracted from three different cell treatments in which one blot is presented in Figure 1(f)

Treatment	Densitometry Ratios of P ₁ and P ₂ Relative to P ₀ (FOC)			
	5 min	10 min	20 min	30 min
P₀/P₁				
V	1.00 \pm 0.04	1.00 \pm 0.18	1.00 \pm 0.08	1.00 \pm 0.08
A	0.90 \pm 0.12	0.99 \pm 0.28	0.94 \pm 0.05	0.91 \pm 0.23
1-MeA	1.01 \pm 0.03	1.04 \pm 0.12	1.05 \pm 0.12	0.97 \pm 0.15
2-MeA	0.93 \pm 0.05	1.05 \pm 0.25	0.62 \pm 0.28	0.93 \pm 0.02
9-MeA	1.00 \pm 0.07	1.01 \pm 0.12	0.91 \pm 0.01	1.12 \pm 0.05
TPA	ND	*0.34 \pm 0.16	ND	ND
ANOVA	(1.73, 0.218)	(4.718, 0.013)	(3.468, 0.05)	(1.233, 0.357)
P₀/P₂				
V	1.00 \pm 0.04	1.00 \pm 0.19	1.00 \pm 0.14	1.00 \pm 0.17
A	0.93 \pm 0.13	0.94 \pm 0.28	0.95 \pm 0.13	0.86 \pm 0.22
1-MeA	1.03 \pm 0.06	1.00 \pm 0.13	1.13 \pm 0.07	1.16 \pm 0.25
2-MeA	0.97 \pm 0.16	1.01 \pm 0.26	0.54 \pm 0.25	1.00 \pm 0.24
9-MeA	1.05 \pm 0.09	0.94 \pm 0.08	1.03 \pm 0.15	1.26 \pm 0.33
TPA	ND	*0.27 \pm 0.07	ND	ND
ANOVA	(0.613, 0.663)	(6.584, 0.004)	(2.642, 0.97)	(1.484, 0.278)
(F, P-value)				

*Significant from the vehicle as determined by a Holm-Sidak post hoc test. The ANOVA was conducted on the densitometry data, including the vehicle. The fraction of the control (FOC) is the densitometry value of each treatment divided by the densitometry value of the vehicle within each time group. 1-MeA, 1-methylanthracene; 2-MeA, 2-methylanthracene; 9-MeA, 9-methylanthracene; A, anthracene; Cx43, connexin43; ND, not determined; TPA, 12-O-tetradecanoylphorbol-13-acetate; V, vehicle.

Connexins are commonly internalized into the cytoplasm in response to a tumor promoter such as TPA. Similar to TPA, Cx43 was internalized in response to 1-MeA, but not in response to 2-MeA (Fig. 1g). However, this trafficking event of Cx43 does not occur within 10 min, which is after the inhibition of GJIC by either 1-MeA or TPA. Thus, inhibition of GJIC precedes the trafficking of Cx43. However, inhibition of PC-PLC by D609, a selective inhibitor of PC-PLC, partially prevented the internalization of Cx43.

Phospholipases have been implicated in the regulation of GJIC,⁽²⁸⁾ thus we measured the release of arachidonic acid from the membranes of the cells in response to exposure to the methyl-isomers of anthracene as an indicator of phospholipase activation (Fig. 2a and 2b). The 1-MeA isomer induced the release of arachidonic acid in a time and dose dependent manner, while the 2-MeA isomer had no effect (Fig. 2a and 2b). Significant release of arachidonic acid began at 10 μ M, which is a dose significantly lower than the dose needed to inhibit GJIC. This release of arachidonic acid began within one minute of treatment. Although the dose-response data suggested that the release of arachidonic acid might not be directly involved in the inhibition of GJIC, these data indicated that phospholipases are activated in the same isomer-specific mode and precedes the inhibitory events of GJIC. We have also measured the release of arachidonic acid from WB-F344 cells by a non-radioactive high performance liquid chromatography-fluorescence detection method, which does not require pretreatment with ³[H]-arachidonic acid. Our aim was to confirm that this effect of 1-MeA was not affected by increased levels of arachidonic acid incorporated in the membrane. In this assay, only 1-MeA was active, thus confirming the results of the release of ³[H]-arachidonic acid (data not shown). PLC, which hydrolyzes the polar group of phosphoglycerol lipids, was one class of phospholipases that we investigated for

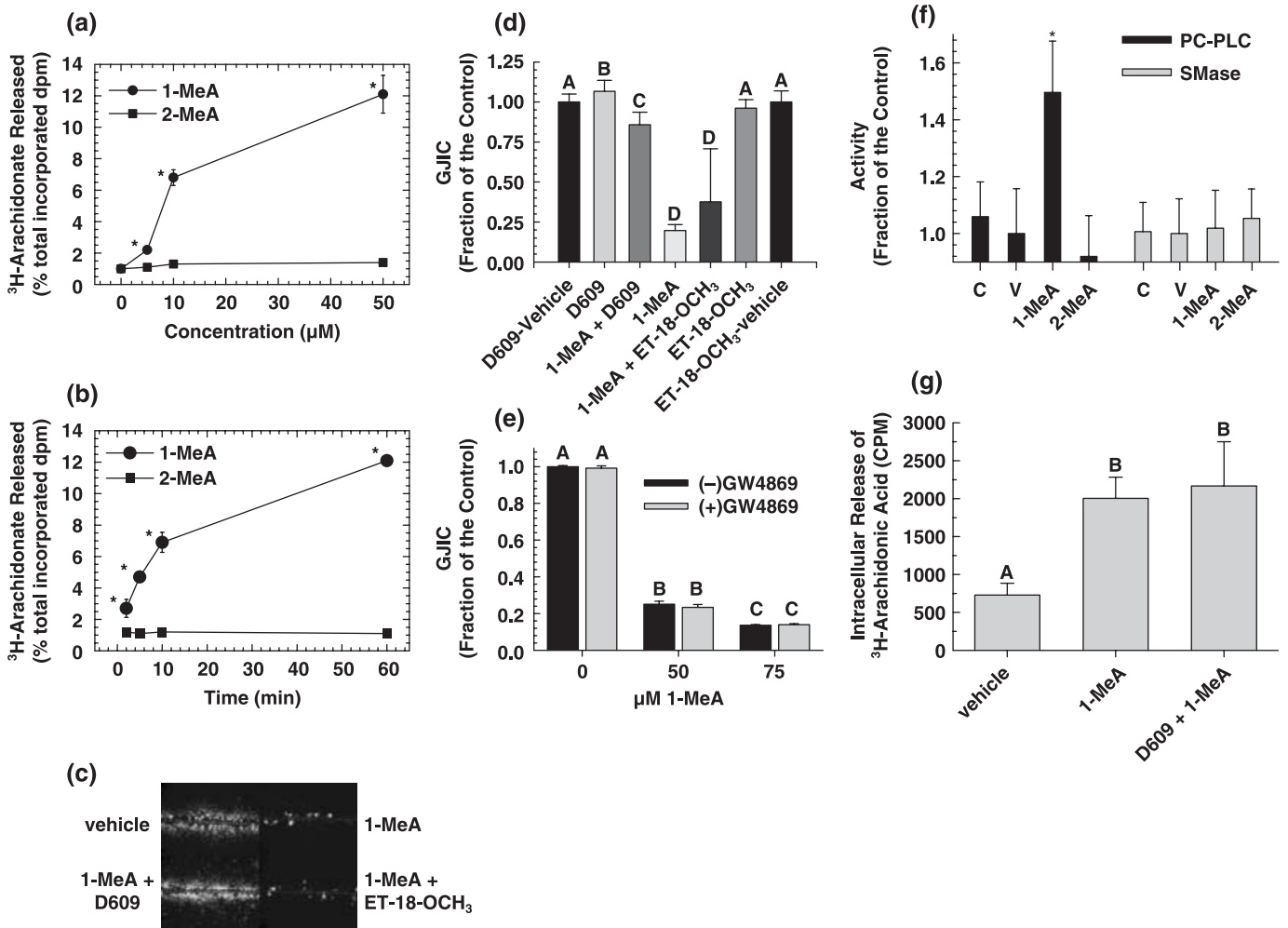


Fig. 2. The role of phospholipid signaling in 1-methylanthracene (1-MeA) versus 2-methylanthracene (2-MeA) induced effects on gap junctional intercellular communication (GJIC). (a) The effect of 1-MeA versus 2-MeA doses on the release of arachidonic acid. (b) The effect of 1-MeA versus 2-MeA exposure times on the release of arachidonic acid. (a,b) 0.1% albumin was added to the medium to inhibit reacylation and metabolism of released ³[H]-arachidonic acid therefore the data reflected cumulative deacylation from membrane phospholipids. At the end of the incubation period, the medium was collected into scintillation cocktail solution and radioactivity determined by scintillation counting of disintegrations per minute (dpm). Radioactivity in the cellular fraction was also determined, and ³[H]-fatty acid release was expressed as a percentage of total cellular radioactivity. The data are an average of at least four independent treatments, and *indicated significant differences paired between 1-MeA and 2-MeA for each dose and time as determined by a two-tailed paired *t*-test at the 95% confidence interval, *P* < 0.001. (c) The effects of phospholipase C (PLC) inhibitors on 1-MeA-induced inhibition of GJIC. The scrape load-dye transfer (SL-DT) assay was used to assess GJIC at 200×. (d) Presents a summary of the averaged data of *n* = 3, including those shown in (c). (c,d), Phosphatidylcholine(PC)- and phosphatidylinositol(PI)-specific-PLC were inhibited by preincubating the cells for 15 min with either 50 μM D609 or 30 μM ET-18-OCH₃, respectively. The inhibitors were left on the cells for an additional 15 min, which was the exposure time of 1-MeA. The dose of 1-MeA was 70 μM. The data are an average of the data (*n* = 3) ± standard deviation at the 95% confidence level. An ANOVA indicated significance at *P* < 0.001, *F* = 420.1, and the different letters (A, B, C and D) indicated significance using an all pair multiple comparison-Holm Sidak posthoc *T*-test at the *P* = 0.05 level. (e) The effect of a sphingomyelinase inhibitor on 1-MeA-induced inhibition of GJIC. The SL-DT assay was used to determine GJIC. The incubation time of 1-MeA was 15 min, and the concentration and preincubation time of the sphingomyelinase inhibitor, GW4869 (N,N'-Bis[4-(4,5-dihydro-1H-imidazol-2-yl)phenyl]-3,3'-p-phenylene-bis-acrylamide dihydrochloride) was 40 μM and 30 min. The results are an average of the data (*n* = 3) ± standard deviation at the 95% confidence level. An ANOVA indicated significance at *P* < 0.001, *F* = 3743.6, and the different letters (A, B and C) indicated significance using an all pair multiple comparison-Holm Sidak posthoc *T*-test at the *P* = 0.05 level. (f) The effects of 1-MeA versus 2-MeA on the activation of either PC-PLC or sphingomyelinase (SMase). An AmplexRed assay system as described in the methods and material section was used to measure the activities of the indicated lipases. The concentration and incubation times of the PAH were 100 μM and 15 min. The results are an average of the data (*n* = 5) ± standard deviation at the 95% confidence level. An ANOVA indicated significance at *P* = 0.003, *F* = 5.153, and the *indicated significance from all other groups using an all pair multiple comparison-Holm Sidak posthoc *T*-test at the *P* = 0.05 level. (g) Intracellular release of ³[H]-arachidonic acid from cells treated with 1-MeA and a phosphatidylcholine-specific PLC inhibitor. The extracellular media was decanted, cells rinsed with phosphate buffered saline and then 1 mL of 0.5% bovine serum albumin in water was added to the cells for 10 min to extract the intracellular arachidonic acid and the radioactivity was determined by scintillation counting of counts per minute (CPM). The results are an average of the data (*n* = 3) ± standard deviation at the 95% confidence level. An ANOVA indicated significance at *P* < 0.001, *F* = 25.2, and the different letters indicated significance using an all pair multiple comparison-Holm Sidak posthoc *T*-test at the *P* = 0.05 level.

involvement in the control of GJIC. Inhibition of phosphatidylinositol specific PLC (PI-PLC) by ET-18-OCH₃, a selective inhibitor of PI-PLC, did not prevent the inhibition of GJIC by 1-MeA (Fig. 2c,d and Table 2), however, inhibition of PC-PLC by

D609, did prevent the inhibition of GJIC by 1-MeA (Fig. 2c,d and Table 2). Similarly, inhibition of PC-PLC with D609 also prevented the internalization of Cx43 in response to 1-MeA treatment (Fig. 1g), a downstream event to the inhibition of GJIC.

Table 2. Modulation of 1-MeA-induced inhibition of GJIC by various inhibitors of phospholipases and protein kinase signaling proteins

¹ Inhibitor	Target signaling protein	² Effect	³ % inhibition of GJIC
None (+1-MeA)	Gap Junction	↓↓↓	100
+D609 (50 μM, 15 min)	PC-PLC	↑↑↑	*10
+H-89 (40 μM, 30 min)	PKA, GPCR	↑↑	*18
+PKI (50 μM, 2 h)	PKA	↑↑↑	*16
+BEL (2.5 μM, 30 min)	iPLA ₂	↑	*74
+BPB (5.0 μM, 20 min)	sPLA ₂	↓↓↓	97
+AACOF3 (10 μM, 30 min)	cPLA ₂ , iPLA ₂	↓↓↓	115
+MAFP (1.25 μM, 30 min)	cPLA ₂ , iPLA ₂	↓↓↓	101
+MJ33 (10 μM, 30 min)	acidic iPLA ₂	↓↓↓	104
+ET-18-OCH ₃ (30 μM, 30 min)	PI-PLC	↓↓↓	90
+1-butanol (0.5% v/v, 15 min)	PLD	↓↓↓	101
+RHC80267 (50 μM, 20 min)	DAG lipase	↓↓↓	97
+GF109203X (20 μM)	PKC (pan-specific)	↓↓↓	100
+PP2 (40–100 μM)	Src	↓↓↓	102
+Genistein (100 μM)	Protein Tyr kinases (pan-specific)	↓↓↓	102

¹Inhibitors were added before the addition of 1-MeA, which was incubated for 15 min at 70 μM, except for the BEL experiment where the time of 1-MeA treatment was 30 min. The inhibitors were added at concentrations and times indicated in the parentheses, and remained in the medium for the duration of the experiment. D609, tricyclodecan-9-yl-xanthate; H-89, N-(2-(4-bromocinnamylamino)ethyl)-5-isoquinolinesulfonamide; BPB, p-bromophenacyl bromide; AACOF3, arachidonyl trifluoromethylketone; PKI, myristoylated PKI (14–22) amide; BEL, bromoenol lactone; MAFP, methyl arachidonyl fluorophosphates; MJ33, 1-hexadecyl-3-(trifluoroethyl)-sn-glycero-2-phosphomethanol; ET-18-OCH₃, 1-O-Octadecyl-2-O-methyl-sn-glycero-3-phosphorylcholine; RHC80267, 1,6-bis-(cyclohexyloximinocarbonylamino)hexane; GF109203X, bisindolylmaleimide I; PP2, 4-amino-5-(4-chloro-phenyl)-7-(t-butyl)pyrazolo[3,4-d]pyrimidine).

²↓↓↓ – complete inhibition of GJIC; ↑, ↑↑ – partial reversal of 1-MeA-induced inhibition of GJIC; ↑↑↑ – complete reversal of 1-MeA-induced inhibition of GJIC.

³An average with *n* = 3, % Inhibition = [(1 – FOC of Inhibitor)/(1 – FOC of vehicle)] × 100.

*Significant as determined by a two-tailed paired *t*-test at the 95% confidence interval, *P* < 0.001 between the (1-MeA) versus (1-MeA + inhibitor) treated cells.

1-MeA, 1-methylanthracene; DAG, diacylglycerol; GJIC, gap junctional intercellular communication; GPCR, G-protein coupled receptor; PC-PLC, phosphatidylcholine specific phospholipase C; PI-PLC, phosphatidylinositol specific phospholipase C; PKA, protein kinase A; PLD, phospholipase D.

The PC-PLC inhibitor used, D609, has also been implicated in the inhibition of SMase. Thus, we inhibited SMase with an inhibitor specific to this enzyme (GW4869), which did not reverse the inhibition of GJIC (Fig. 2e). Further evidence of PC-PLC involvement is indicated by the activation of this specific phospholipase by 1-MeA, while 1-MeA did not increase the activity of SMase (Fig. 2f). These results indicate that D609 probably reversed the 1-MeA-induced inhibition of GJIC by acting upon PC-PLC and not SMase. However, D609 did not reverse the effects of 1-MeA induced release of arachidonic acid (Fig. 2g). This suggests that the release of arachidonic acid was not dependent on PC-PLC but rather from another phospholipase. Western blot analyzes of ERK and p38 (Fig. 3a,b) demonstrated that D609 did not reverse the activation of these MAPKs in response to 1-MeA. Densitometry analyzes of the bands were normalized to the house keeping protein glyceraldehyde 3-phosphate dehydrogenase and *t*-tests were conducted comparing (1-MeA) versus (1-MeA + D609) for each of the MAPK bands.

Inhibitors of other signal transduction proteins were also preincubated with the cells before the addition of 1-MeA (Table 2). Most significant, was inhibition of protein kinase A (PKA) where a 72–84% recovery was observed with the following inhibitors H89 and PKI, respectively. Several inhibitors of PLA₂ were used against the various PLA₂ isoforms; particularly sPLA₂ (p-bromophenacyl bromide), cPLA₂ (AACOF3 and MAFP), iPLA₂ (bromoenol lactone [BEL] and MAFPP) and acidic iPLA₂ (MJ33). BEL was the only PLA₂ inhibitor that partially reversed (26%) 1-MeA-induced closure of gap junctions, while all other PLA₂ inhibitors had no significant effect, which suggests that the small BEL effect was not specific to PLA₂. Inhibitors of diacylglycerol (DAG) lipases, PLA₂, PI-PLC, phospholipase D (PLD), sphingomyelinase, PKC, Src kinases, and protein tyrosine kinases did not prevent the inhibition of GJIC by 1-MeA (Table 2).

Discussion

The mechanisms by which exogenous and endogenous chemicals modulate GJIC have only been recently explored. There are examples of modulation of GJIC at all three levels of control: transcriptional, translational and post-translational.⁽⁴⁰⁾ Phosphorylation of gap junction proteins has been the most extensively studied post-translational modification of gap junctions.⁽⁴⁰⁾ Compounds, such as phorbol esters, which activate PKC are also known to inhibit GJIC and cause a hyperphosphorylation of gap junction proteins via a Mek-dependent mechanism.⁽⁴⁰⁾ The hyperphosphorylation of gap junction proteins can be detected by Western blot analysis using 1-dimensional gel systems in which shifts in the electrophoretic bands can be readily observed.⁽⁴¹⁾ However, phosphorylation alone has been shown to be insufficient in the regulation of GJIC.⁽²²⁾ Apparently, non-phosphorylating mechanisms are also involved in the control of GJIC,⁽⁴⁰⁾ which is evidently how 1-MeA is regulating gap junctions. Our Western blot results clearly indicated that the activation of MAPKs, such as ERK and p38, does not necessarily result in the hyperphosphorylation of Cx43, even though Cx43 has known consensus sequences for ERK-MAPK.⁽²³⁾ We previously demonstrated that the addition of a Mek inhibitor does not prevent the closure of gap junction channels,^(25,28) and in this report, we similarly showed that inhibition of p38 did not reverse the effects of 1-MeA on GJIC. Thus, activation of MAPKs, although typically required in cell proliferation and is always accompanied with inhibition of GJIC, does not always result in their direct control of gap junction function.

Lipid signaling has been implicated in the control of GJIC.⁽⁴²⁾ Lipid metabolites, such as arachidonic acid, are known to inhibit GJIC.^(43,44) Therefore, we explored the potential role of phospholipases. The release of arachidonic acid was significantly

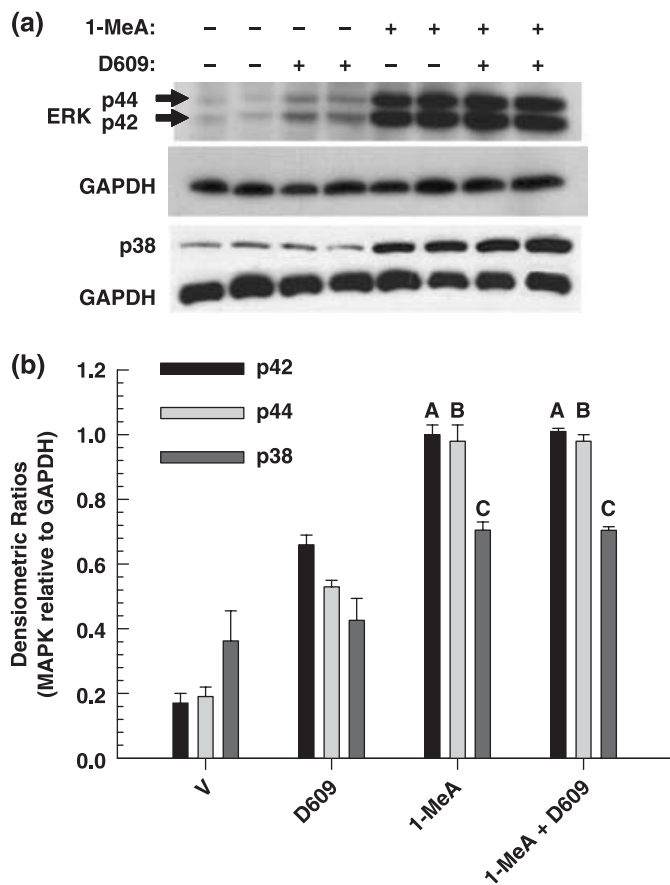


Fig. 3. The effect of a phosphatidyl choline specific phospholipase C (PC-PLC) inhibitor on 1-methylanthracene (1-MeA)-induced activation of extracellular receptor kinase (ERK) and p38. (a) The activation of ERK and p38 was determined by Western blot analysis using phosphospecific antibodies. (b) The densitometry analyzes of the three independent Western blot experiments including those shown in (a) of the mitogen activated protein kinase (MAPK) bands relative to the house keeping protein, GAPDH. (a,b) The dose and time of 1-MeA was 75 μ M and 30 min. The PC-PLC inhibitor, 50 μ M of D609, was added 20 min prior to 1-MeA and remained on the cells for an additional 30 min after the 1-MeA was added. The D609 control was 50 min. The first two lanes was the vehicle. Using a two-tailed *t*-test, the letter A in (b) indicates no significant difference in the p42 band between the 1-MeA and 1-MeA + D609 treatment ($t = -0.548$, $P = 0.613$). Similarly, the letter B indicated no difference in the p44 band ($t = -0.000$, $P = 1.000$) and the letter C indicated no difference in the p38 band ($t = -0.0418$, $P = 0.969$) between the 1-MeA and 1-MeA + D609 treatment.

detected within 2 min indicating that phospholipases are immediately activated in response to 1-MeA. The employment of a consortium of phospholipase inhibitors indicated that PC-PLC was involved in 1-MeA-induced inhibition of GJIC. Inhibition of PC-PLC by the inhibitor, D609, has also been implicated in the inhibition of sphingomyelinase SMase, but our results showed that a more specific SMase inhibitor did not prevent inhibition of GJIC by 1-MeA, and the activation of PC-PLC and not SMase by 1-MeA strongly suggested that PC-PLC was the key regulator of GJIC in response to 1-MeA. However, PC-PLC was involved in neither the release of arachidonic acid nor the activation of ERK and p38 MAPKs indicating that other phospholipases are involved in these two important signaling events. Apparently 1-MeA either initiated a general activator or repressed a general inhibitor of phospholipases. In contrast to PI-PLC, the function of PC-PLC in tumorigenesis has not been extensively studied, yet there are reports indicating that

PC-PLC does play a very significant role in cancer.⁽⁴⁵⁾ Our results implicate that one significant role PC-PLC in cancer could be the potential regulation of GJIC by environmental agents such as certain polycyclic aromatic hydrocarbons known to be prevalent in cigarette smoke.

Although PC-PLC was an essential component of the signaling pathway controlling GJIC, this phospholipase was not involved in arachidonic acid release indicating that other phospholipases were activated. However, inhibition of other phospholipases such as PI-PLC, various PLA₂ isozymes, PLD and diacylglycerol lipase did not prevent the inhibition of GJIC by 1-MeA indicating that these lipid signaling enzymes were not regulating GJIC. In addition, inhibition of Src kinases and PKC, both common signaling enzymes, also did not prevent the inhibition of GJIC by 1-MeA. The concentrations and times used for these inhibitors of signaling enzymes were similar to those reported in literature where an inhibitor-induced effect was observed, but there is always the possibility of a false negative. However, the use of several PLA₂ inhibitors strongly suggested that this class of signal transduction enzymes were not involved in the regulation of GJIC. When cells were pre-incubated with a PKA inhibitor, H89, a 72% recovery from 1-MeA-induced inhibition of GJIC was seen, indicating a potential role of the cAMP dependent kinase, PKA, in the regulation of GJIC. Although H89 is known to inhibit at least eight other kinases such as MAPKAP-K1b, S6K1, MSK1, KB α , SGK, ROCK II, AMPK and CHK 1,⁽⁴⁶⁾ further experiments with the cell permeable specific inhibitor of PKA, myristoylated PKI (14–22) amide, also indicated the role of PKA in the down-regulation of GJIC after exposure to 1-MeA (84% recovery of GJIC). Another class of compounds, PCB, also inhibit GJIC through a PC-PLC dependent mechanism, but 1-MeA, unlike the PCB did not involve Src or DAG lipase.⁽²⁸⁾

Most research on PAH toxicity has focused on the mutagenic and DNA damaging properties of the higher molecular weight compounds but clearly the lower molecular weight-PAH are capable of inducing biological effects relevant to tumor promotion. We previously reported the effects of 41 different PAH on GJIC including 16 with five or more rings.^(24,27,47,48) Most of these PAH, including the high molecular weight PAH, inhibited GJIC with varying potencies, but the potencies of the lower molecular weight PAH (four rings or less) tended to be much stronger if they contained a bay or bay-like region.^(6,24,27) The low molecular weight PAH also tend to be the most abundant in the environment.

One example is cigarette smoke, where the low molecular weight fractions, particularly the three- and four-ringed PAH predominate in which the methylated anthracenes and phenanthrenes are 62 times higher than benzo(a)pyrene and benzo(e)pyrene.⁽³¹⁾ Considering that the fraction of cigarette smoke containing the three- and four-ringed-PAH is highly cocarcinogenic when applied to the skin of mice treated with benzo(a)pyrene,⁽⁴⁹⁾ and that cigarette smoke is a strong promoter and weak complete carcinogen,^(50–53) suggest that this fraction could significantly contribute to cancer. Ten to 15 years after giving up smoking, the ex-smoker faces the same low risk of developing cancer of the upper digestive tract, the lung, the pancreas, and the urinary tract as the non-smoker.⁽⁵⁴⁾ This fact strongly implicates that cigarette smoke contributes to the non-genotoxic and reversible phases of cancer. Contribution of cigarette smoke to the non-genotoxic phase of cancer is particularly important. Early work on the carcinogenicity of cigarette smoke condensates strongly indicated that the neutral fractions, which contained primarily PAHs were the most carcinogenic fractions, but that the concentrations of the most prominent complete carcinogens, that is benzo(a)pyrene, was far too low to account, by themselves, for the carcinogenic activity of the condensates.^(50,55) In addition, we have shown that the 1-MeA, but not the 2-MeA, inhibited GJIC

and prevented the induction of differentiation of normal human pancreatic cells using an *in vitro* system at non-cytotoxic doses.⁽⁵⁶⁾ Cigarette smoking has been one of the suspected risk factors for pancreatic cancer. Furthermore, the much less studied area of cocarcinogenesis is a closer fit to the extended exposure of human smoking than the complete carcinogenic nature of selected PAH from cigarette smoke condensates.⁽⁵⁰⁾ Therefore, understanding the biological effects of these three- and four-ringed PAH, which are very prevalent in cigarette smoke and possess cocarcinogenic activity, on cell signaling pathways relevant to the epigenetic, non-genotoxic phase of cancer is important. In particular, functional GJIC offers a very central signaling system to assess risk.

The homeostasis of a tissue requires functional GJIC. Although, the transient closure of gap junction channels during proliferation is a normal response to mitogens, the chronic inhibition of GJIC by repeated exposures to toxicants, toxins, or cytokines released during compensatory hyperplasia could contribute to cancer. Chronic inhibition of GJIC has been correlated with enhanced proliferation, and inhibition of apoptosis and differentiation. Determining the effect of PAH on key signaling and gene expression events would provide invaluable mechanistically based information on the epigenetic toxicity of these compounds, thereby aiding in the development of preventative strategies of controlling human diseases such as cancer.

References

- Baird WM. Carcinogenic polycyclic aromatic hydrocarbon-DNA adducts and mechanism of action. *Environ Mol Mutagenesis* 2005; **45**: 106–14.
- Trosko JE, Upham BL. The emperor wears no clothes in the field of carcinogen risk assessment: ignored concepts in cancer risk assessment. *Mutagenesis* 2005; **20**: 81–92.
- Rosenkranz M, Rosenkranz HS, Klopman G. Intercellular communication, tumor promotion and non-genotoxic carcinogenesis: relationships based upon structural considerations. *Mutat Res* 1997; **381**: 171–88.
- Fagotto F. Cell contact-dependent signaling. *Developmental-Biology* 1996; **180**: 445–54.
- Upham BL, Trosko JE. A paradigm shift in the understanding of oxidative stress and its implications to exposure of low-level ionizing radiation. *Acta Med Nagasakiensis* 2006; **50**: 63–8.
- Upham BL, Weis LM, Trosko JE. Modulated gap junctional intercellular communication as a biomarker of PAH epigenetic toxicity: structure-function relationship. *Environ Health Perspect* 1998; **106**: 975–81.
- Yamasaki H, Krutovskikh V, Mesnil M, Tanaka T, Zaidan DM, Omori Y. Role of connexin (gap junction) genes in cell growth control and carcinogenesis. *C R Acad Sci III* 1999; **322**: 151–9.
- Borek C, Sachs L. The difference in contact inhibition of cell replication between normal cells and cells transformed by different carcinogens. *Proc Natl Acad Sci USA* 1966; **56**: 1705–11.
- Potter VR. Phenotypic diversity in experimental hepatomas: The concept of partially blocked ontogeny. *Br J Cancer* 1978; **38**: 1–23.
- Trosko JE, Ruch RJ. Gap junctions as targets for cancer chemoprevention and chemotherapy. *Curr Drug Targets* 2002; **3**: 465–82.
- Yamasaki H, Naus CCG. Role of connexin genes in growth control. *Carcinogenesis* 1996; **17**: 1199–213.
- King TJ. Connexins as targets for cancer chemoprevention and chemotherapy. *Biochimica Biophys Acta* 2005; **1719**: 146–60.
- Ruch RJ, Guan X, Sigler K. Inhibition of gap junctional intercellular communication and enhancement of growth in BALB/c 3T3 cells treated with connexin43 antisense oligonucleotides. *Mol Carcinog* 1995; **14**: 269–74.
- Evert M. Morphology and morphometric investigation of hepatocellular preneoplastic lesions and neoplasms in connexin32-deficient mice. *Carcinogenesis* 2002; **23**: 697–703.
- King TJ. Deficiency in the gap junction protein connexin32 alters p27Kip1 tumor suppression and MAPK activation in a tissue-specific manner. *Oncogene* 2005; **24**: 1718–26.
- King TJ. Mice deficient for the gap junction protein Connexin32 exhibit increased radiation-induced tumorigenesis associated with elevated mitogen-activated protein kinase (p44/Erk1, p42/Erk2) activation. *Carcinogenesis* 2004; **25**: 669–80.

Conclusion

Inhibition of GJIC and the activation of intracellular mitogenic pathways are characteristic of epithelial derived cancer cells. Our results indicate that PC-PLC is an important signaling enzyme needed for the inhibition of GJIC in response to a cigarette smoke relevant polycyclic aromatic hydrocarbon. This report clearly indicates that specific phospholipid signaling is involved in the regulation of GJIC, and that, in addition to reported Mek-dependent regulation of GJIC, the regulation of GJIC can be Mek-independent even though this MAPK pathway is activated. Thus, not all tumor promoters inhibit GJIC through the same signaling pathway, and this implicates that chemoprevention strategies relative to up-regulating GJIC activity probably can not be universally effective.

Acknowledgments

This research was supported by National Institute of Environmental Health Sciences (NIEHS) grants #R01 ES013268-01A2 to Upham and it's contents are solely the responsibility of the authors and do not necessarily represent the official views of the NIEHS; and #5D43 TW00641-10 Fogarty International Center, National Institutes of Health, USA, to the Institute of International Health at Michigan State University for the funding of M. Gužviã; and Czech Science Foundation (grant no. 524/05/0595) and the Czech Ministry of Agriculture (No. MZE0002716201) to M. Machala and J. Vondráček.

- Wright JH, Munar E, Jameson DR *et al*. Mitogen-activated protein kinase activity is required for the G(2)/M transition of the cell cycle in mammalian fibroblasts. *Proc Natl Acad Sci USA* 1999; **96**: 11335–40.
- Seger R, Krebs EG. The MAPK signaling cascade. *FASEB J* 1995; **9**: 726–35.
- Denhardt DT. Signal-transducing protein phosphorylation cascades mediated by Ras/Rho proteins in the mammalian cell: the potential for multiplex signalling. *Biochem J* 1996; **318**: 729–47.
- Fukuhara S, Marinissen MJ, Chiariello M, Gutkind JS. Signaling from G protein-coupled receptors to ERK5/Big MAPK 1 involves Galpha q and Galpha 12/13 families of heterotrimeric G proteins. Evidence for the existence of a novel Ras and Rho-independent pathway. *J Biol Chem* 2000; **275**: 21730–6.
- Warn CB, Lampe PD, Kurata WE *et al*. Characterization of the mitogen-activated protein kinase phosphorylation sites on the connexin-43 gap junction protein. *J Biol Chem* 1996; **271**: 3779–86.
- Hossain MZ, Jagdale AB, Ao P, Boynton AL. Mitogen-activated protein kinase and phosphorylation of connexin43 are not sufficient for the disruption of gap junctional communication by platelet-derived growth factor and tetradecanoylphorbol acetate. *J Cell Physiol* 1999; **179**: 87–96.
- Lampe PD. The effects of connexin phosphorylation on gap junctional communication. *Int J Biochem Cell Biol* 2004; **36**: 1171–86.
- Bláha L, Kapplová P, Vondráček J, Upham B, Machala M. Inhibition of gap-junctional intercellular communication by environmentally occurring polycyclic aromatic hydrocarbons. *Toxicol Sci* 2002; **65**: 43–51.
- Rummel AM, Trosko JE, Wilson MR, Upham BL. Polycyclic aromatic hydrocarbons with bay-like regions inhibited gap junctional intercellular communication and stimulated MAPK activity. *Toxicol Sci* 1999; **49**: 232–40.
- Upham BL, Weis LM, Rummel AM, Masten SJ, Trosko JE. The effects of anthracene and methylated anthracenes on gap junctional intercellular communication in rat liver epithelial cells. *Fundam Appl Toxicol* 1996; **34**: 260–4.
- Weis LM, Rummel AM, Masten SJ, Trosko JE, Upham BL. Bay or baylike regions of polycyclic aromatic hydrocarbons were potent inhibitors of Gap junctional intercellular communication. *Environ Health Perspect* 1998; **106**: 17–22.
- Machala M, Bláha L, Vondráček J, Trosko JE, Scott J, Upham BL. Inhibition of gap junctional intercellular communication by noncoplanar polychlorinated biphenyls. inhibitory potencies and screening for potential mode(s) of action. *Toxicol Sci* 2003; **76**: 102–11.
- Rivedal E, Opsahl H. Role of PKC and MAP kinase in EGF- and TPA-induced connexin43 phosphorylation and inhibition of gap junction intercellular communication in rat liver epithelial cells. *Carcinogenesis* 2001; **22**: 1543–50.
- Vondráček J, Švihálková-Šindlerová L, Pěnčíková K *et al*. Concentrations of

- methylated naphthalenes, anthracenes, and phenathrenes occurring in Czech river sediments and their effects on toxic events associated with carcinogenesis in rat liver cells. *Environ Toxicol Chem* 2007; **26**: 2308–16.
- 31 Severson RF, Snook ME, Higman HC, Chortyk OT, Akin FJ. Isolation, identification, and quantification of polynuclear aromatic hydrocarbons in tobacco smoke. In: Freudenthal RI, Jones PW, eds. *Carcinogenesis-a Comprehensive Survey. Vol. 1. Polynuclear Aromatic Hydrocarbons: Chemistry, Metabolism, and Carcinogenesis*. New York (NY): Raven Press, 1976: 253–70.
 - 32 Tsao MS, Smith JD, Nelson KG, Grisham JW. A diploid epithelial cell line from normal adult rat liver with phenotypic properties of 'oval' cells. *Exp Cell Res* 1984; **154**: 38–52.
 - 33 Coleman WB, Wennerberg AE, Smith GJ, Grisham JW. Regulation of the differentiation of diploid and some aneuploid rat liver epithelial (stemlike) cells by the hepatic microenvironment. *Am J Pathol* 1993; **142**: 1373–82.
 - 34 Malouf NN, Coleman WB, Grisham JW *et al*. Adult-derived stem cells from the liver become myocytes in the heart in vivo. *Am J Pathol* 2001; **158**: 1929–35.
 - 35 El-Fouly MH, Trosko JE, Chang CC. Scrape-loading and dye transfer. A rapid and simple technique to study gap junctional intercellular communication. *Exp Cell Res* 1987; **168**: 422–30.
 - 36 Laemmli UK. Cleavage of structural proteins during the assembly of the head of bacteriophage T4. *Nature* 1970; **227**: 680–5.
 - 37 Zhou M, Diwu Z, Panchuk Voloshina N, Haugland RP. A stable nonfluorescent derivative of resorufin for the fluorometric determination of trace hydrogen peroxide: applications in detecting the activity of phagocyte NADPH oxidase and other oxidases. *Anal Biochem* 1997; **253**: 162–8.
 - 38 Tithof PK, Schiamberg E, Peters-Golden M, Ganey PE. Phospholipase A2 is involved in the mechanism of activation of neutrophils by polychlorinated biphenyls. *Environ Health Perspect* 1996; **104**: 52–8.
 - 39 Trosko JE, Chang CC, Wilson MR, Upham B, Hayashi T, Wade M. Gap junctions and the regulation of cellular functions of stem cells during development and differentiation. *Methods* 2000; **20**: 245–64.
 - 40 Saez JC, Berthoud VM, Moreno AP, Spray DC. Gap junctions. Multiplicity of controls in differentiated and undifferentiated cells and possible functional implications. *Adv Second Messenger Phosphoprotein Res* 1993; **27**: 163–98.
 - 41 Matesic DF, Rupp HL, Bonney WJ, Ruch RJ, Trosko JE. Changes in gap-junction permeability, phosphorylation, and number mediated by phorbol ester and non-phorbol-ester tumor promoters in rat liver epithelial cells. *Mol Carcinog* 1994; **10**: 226–36.
 - 42 Aylsworth CF. Effects of fatty acids on gap junctional communication: possible role in tumor promotion by dietary fat. *Lipids* 1987; **22**: 445–54.
 - 43 Lazrak A. Ca-mediated and independent effects of arachidonic acid on gap junctions and Ca-independent effects of oleic acid and halothane. *Biophysical-Journal* 1994; **67**: 1052–9.
 - 44 Gainer HS. Diacylglycerol inhibits gap junctional communication in cultured epidermal cells: evidence for a role of protein kinase C. *Biochem Biophys Res Commun* 1985; **126**: 1109–13.
 - 45 Cheng J, Weber JD, Baldassare JJ, Raben DM. Ablation of Go alpha-subunit results in a transformed phenotype and constitutively active phosphatidylcholine-specific phospholipase C. *J Biol Chem* 1997; **272**: 17312–9.
 - 46 Lochner A, Moolman JA. The many faces of H89: a review. *Cardiovasc Drug Rev* 2006; **24**: 261–74.
 - 47 Ghoshal S, Weber WJ, Rummel AM, Trosko JE, Upham BL. Epigenetic toxicity of a mixture of polycyclic aromatic hydrocarbons on gap junctional intercellular communication before and after biodegradation. *Environ Sci Technol* 1999; **33**: 1044–50.
 - 48 Upham BL, Masten SJ, Lockwood BR, Trosko JE. Nongenotoxic effects of polycyclic aromatic hydrocarbons and their ozonation by-products on the intercellular communication of rat liver epithelial cells. *Fundam Appl Toxicol* 1994; **23**: 470–5.
 - 49 Hoffmann D, Schmeltz SS, Hecht SS, Wynder EL. Tobacco carcinogenesis. In: Gelboin HV, Ts'o PO, eds. *Polycyclic Aromatic Hydrocarbons and Cancer. Vol. 1. Environment, Chemistry, and Metabolism*. New York, NY: Academic Press, Inc., 1978: 85–117.
 - 50 Rubin H. Selective clonal expansion and microenvironmental permissiveness in tobacco carcinogenesis. *Oncogene* 2002; **21**: 7392–411.
 - 51 Van Duuren BL, Sivak A, Langseth L. The tumor-promoting activity of tobacco leaf extract and whole cigarette tar. *Br J Cancer* 1967; **21**: 460–3.
 - 52 Van Duuren BL, Sivak A, Katz C, Melchionne S. Cigarette smoke carcinogenesis: importance of tumor promoters. *J Natl Cancer Inst* 1971; **47**: 235–40.
 - 53 Bock FG. Tumor promoters in tobacco and cigarette-smoke condensate. *J Natl Cancer Inst* 1972; **48**: 1849–53.
 - 54 Wynder EL, Hoffmann D. Tobacco and tobacco smoke. *Semin Oncol* 1976; **3**: 5–15.
 - 55 Hoffmann D, Hoffmann I, El Bayoumy K. The less harmful cigarette: a controversial issue. a tribute to Ernst L. *Wynder Chem Res Toxicol* 2001; **14**: 767–90.
 - 56 Tai MH, Upham BL, Olson LK, Tsao MS, Reed DN Jr, Trosko JE. Cigarette smoke components inhibited intercellular communication and differentiation in human pancreatic ductal epithelial cells. *Int J Cancer* 2007; **120**: 1855–62.

IV. Sovadinová, I., **Babica, P.**, Boke, H., Kumar, E., Wilke, A., Park, J.-S., Trosko, J.E., Upham, B.L.*, 2015. Phosphatidylcholine specific PLC-induced dysregulation of gap junctions, a robust cellular response to environmental toxicants, and prevention by resveratrol. *PLoS One* 10, e0124454.

RESEARCH ARTICLE

Phosphatidylcholine Specific PLC-Induced Dysregulation of Gap Junctions, a Robust Cellular Response to Environmental Toxicants, and Prevention by Resveratrol in a Rat Liver Cell Model

Iva Sovadinova^{1,2}, Pavel Babica^{1,3}, Hatice Böke¹, Esha Kumar¹, Andrew Wilke¹, Joon-Suk Park^{1,4}, James E. Trosko¹, Brad L. Upham^{1*}

1 Department of Pediatrics & Human Development; Center for Integrative Toxicology; and the Food Safety & Toxicology Center, Michigan State University, East Lansing, Michigan, 48824, United States of America, **2** Research Centre for Toxic Compounds in the Environment—RECETOX, Masaryk University, Kamenice 5, CZ62500, Brno, Czech Republic, **3** Department of Experimental Phycology and Ecotoxicology, Institute of Botany ASCR, Lidická 25/27, CZ60200, Brno, Czech Republic, **4** Laboratory Animal Center, Daegu-Gyeongbuk Medical Innovation Foundation, Daegu, Korea

* upham@msu.edu



OPEN ACCESS

Citation: Sovadinova I, Babica P, Böke H, Kumar E, Wilke A, Park J-S, et al. (2015) Phosphatidylcholine Specific PLC-Induced Dysregulation of Gap Junctions, a Robust Cellular Response to Environmental Toxicants, and Prevention by Resveratrol in a Rat Liver Cell Model. PLoS ONE 10 (5): e0124454. doi:10.1371/journal.pone.0124454

Academic Editor: Rajesh Agarwal, University of Colorado Denver, UNITED STATES

Received: April 28, 2014

Accepted: March 10, 2015

Published: May 29, 2015

Copyright: © 2015 Sovadinova et al. This is an open access article distributed under the terms of the [Creative Commons Attribution License](https://creativecommons.org/licenses/by/4.0/), which permits unrestricted use, distribution, and reproduction in any medium, provided the original author and source are credited.

Data Availability Statement: All relevant data are within the paper and its Supporting Information file.

Funding: This work received financial support from National Institute of Environmental Health Sciences (<https://www.niehs.nih.gov/>) grants #R01 ES013268-01A2 to BLU and this paper's contents are solely the responsibility of the authors and do not necessarily represent the official views of the NIEHS. This work also received support from Czech Ministry of Youth, Education and Sports (<http://www.msmt.cz/?lang=2>) grant #LH12034 "CHEMOPREV" to PB.

Abstract

Dysregulation of gap junctional intercellular communication (GJIC) has been associated with different pathologies, including cancer; however, molecular mechanisms regulating GJIC are not fully understood. Mitogen Activated Protein Kinase (MAPK)-dependent mechanisms of GJIC-dysregulation have been well-established, however recent discoveries have implicated phosphatidylcholine-specific phospholipase C (PC-PLC) in the regulation of GJIC. What is not known is how prevalent these two signaling mechanisms are in toxicant/toxin-induced dysregulation of GJIC, and do toxicants/toxins work through either signaling mechanisms or both, or through alternative signaling mechanisms. Different chemical toxicants were used to assess whether they dysregulate GJIC *via* MEK or PC-PLC, or both Mek and PC-PLC, or through other signaling pathways, using a pluripotent rat liver epithelial oval-cell line, WB-F344. Epidermal growth factor, 12-O-tetradecanoylphorbol-13-acetate, thrombin receptor activating peptide-6 and lindane regulated GJIC through a MEK1/2-dependent mechanism that was independent of PC-PLC; whereas PAHs, DDT, PCB 153, dicumylperoxide and perfluorodecanoic acid inhibited GJIC through PC-PLC independent of Mek. Dysregulation of GJIC by perfluorooctanoic acid and R59022 required both MEK1/2 and PC-PLC; while benzoylperoxide, arachidonic acid, 18 β -glycyrrhetic acid, perfluorooctane sulfonic acid, 1-monolaurin, pentachlorophenol and alachlor required neither MEK1/2 nor PC-PLC. Resveratrol prevented dysregulation of GJIC by toxicants that acted either through MEK1/2 or PC-PLC. Except for alachlor, resveratrol did not prevent dysregulation of GJIC by toxicants that worked through PC-PLC-independent and MEK1/2-independent pathways, which indicated at least two other, yet unidentified, pathways that are involved in the regulation of GJIC. In conclusion: the dysregulation of GJIC is a

Competing Interests: The authors have declared that no competing interests exist.

contributing factor to the cancer process; however the underlying mechanisms by which gap junction channels are closed by toxicants vary. Thus, accurate assessments of risk posed by toxic agents, and the role of dietary phytochemicals play in preventing or reversing the effects of these agents must take into account the specific mechanisms involved in the cancer process.

Introduction

Gap junctional intercellular communication (GJIC) represents a key regulatory mechanism for the maintenance of tissue homeostasis, regulation of cell growth, differentiation and death [1,2]. Gap junctional channels are formed between adjacent cells by proteins termed, connexins, and allow direct cell-to-cell flux of small (<1–1.5 kDa) hydrophilic molecules, such as metabolites, nutrients, ions or second messengers [3,4]. Chronic impairment of GJIC caused by oncogene activation, endogenous cell-death-induced compensatory release of growth factors or by exposure to tumorigenic xenobiotics is strongly linked to the promoting phase of cancer [5,6]. Conversely, tumor suppressor genes and chemopreventive agents are known to reverse the inhibitory effects of tumor promoters or oncogenes, and restore cell-cell communication [7,8].

A number of chemicals are known to rapidly dysregulate GJIC, including a model tumor promoter, 12-O-tetradecanoylphorbol-13-acetate (TPA), biological toxins, organic solvents, environmental pollutants, pesticides, pharmaceuticals, peroxides, metals and others [9]. Despite numerous studies reporting modulation of GJIC by chemicals and endogenous or exogenous ligands, the underlying intracellular mechanisms responsible for rapid inhibition of connexin-based cell-cell communication have not been fully elucidated.

Regulation of GJIC through the phosphorylation of connexins has been the most extensively studied mechanism of GJIC regulation. Connexin43, the most studied connexin in phosphorylation studies, was identified as a substrate for many kinases, including mitogen activated protein kinases (MAPKs), protein kinase A (PKA), protein kinase C (PKC), casein kinase 1, Src-kinase or Akt [10–12]. Activation of MEK1/2, which is a MAPK-kinase, is considered to be a mechanism by which TPA and epidermal growth factor (EGF) dysregulates GJIC [13,14].

Recently, phospholipase-dependent mechanisms have been reported in the control of connexin43-based GJIC. Toxicants, such as PCB153 or dicumylperoxide (diCuOOH) or 1-methylanthracene (1-MeA), dysregulated GJIC through a phosphatidylcholine-specific phospholipase C (PC-PLC) mechanism [15–17]. Phosphatidylinositol-specific phospholipase C (PI-PLC) does not play a role in either PCB153 or 1-MeA induced dysregulation of GJIC [15,17], while the involvement of PI-PLC was not determined for diCuOOH. Unlike PI-PLC, the function of PC-PLC in tumorigenesis has not been extensively studied, yet there are reports indicating that PC-PLC plays a very significant role in cancer [18]. Questions that arise are: What is the prevalence PC-PLC in toxicant-induced dysregulation of GJIC? Is PC-PLC involved in the dysregulation of GJIC by toxicants known to inhibit GJIC through Mek, or are Mek-dependent and PC-PLC-dependent inhibition of GJIC by toxicants unique mechanisms that are always independent of each other? Are these two mechanisms prevalent in toxicant-induced dysregulation of GJIC or do toxicants more commonly dysregulate GJIC through other, yet to be determined mechanisms?

In this report, we addressed these questions by determining if the dysregulation of connexin43-based GJIC in Fischer F344 rat liver epithelial cells (WB-F344), exposed to a selected set

(25 compounds) of growth-regulating compounds, signal pathway modulators, environmental toxicants and potential tumor promoters (Fig 1), was mediated through either PC-PLC or MEK1/2, or both of these signaling proteins, or through other unidentified mechanisms. Several of these toxicants are known to dysregulate GJIC through either Mek or PC-PLC, but no study has yet to determine if these toxicants work through either one of both of these mechanisms, while the role of Mek and PC-PLC for many of the other GJIC-dysregulating toxicants are yet unknown.

The prevention of cancers through diet, and potentially by botanical supplements, is considered an important strategy in the control of this set of chronic diseases. Chemopreventive agents are known to prevent tumor promoters from dysregulating GJIC. Thus, another question that arises is: do anti-carcinogenic compounds prevent tumor promoters from dysregulating GJIC through Mek- and PC-PLC-dependent mechanisms or through general antioxidative mechanisms. For these experiments, we chose resveratrol, which is an antioxidant found in red wine and is associated with reduced rates of cardiovascular diseases and cancer [19]. Our results indicated that PC-PLC-dependent dysregulation of GJIC was a prevalent toxic mechanism and that there were at least two other mechanisms in addition to Mek and PC-PLC. Resveratrol prevented the dysregulation of GJIC by toxicants through Mek and PC-PLC but not through a third mechanism.

Materials & Methods

Chemicals

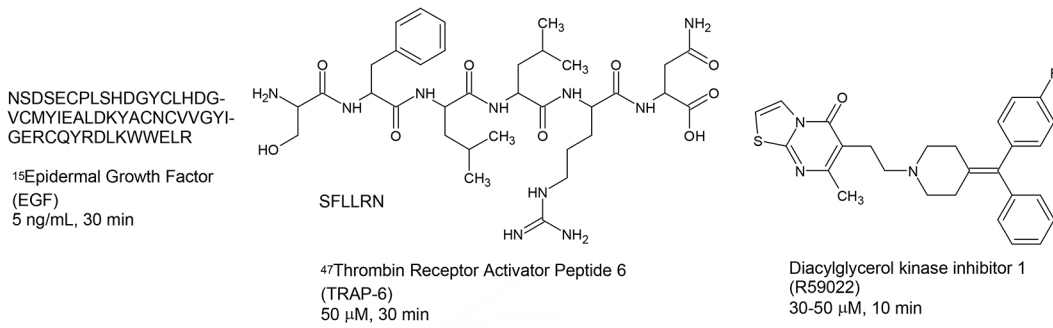
The chemicals used in this study were obtained from the following sources: resveratrol from CTMedChem (Bronx, NY); U0126 and D609 from Tocris Bioscience (Ellisville, MO); alachlor and lindane from Chem Service (West Chester, PA); arachidonic acid from Cayman Chemical (Ann Arbor, MI); 1-monolaurin (Lauricidin[®]) from Med-Chem Laboratories (Galena, IL); TPA from Biomol International (Plymouth Meeting, PA); 1-methylanthracene, 1-methylfluorene, benzoylperoxide (Luperox[®] A98), 18- β -glycyrrhetic acid, dicumylperoxide, EGF, fluoranthene, fluorene, Lucifer Yellow CH dilithium salt (MW 457.25), pentachlorophenol, perfluorodecanoic acid (PFDA), perfluorooctane sulfonic acid (PFOSA), phenanthrene, pyrene and thrombin receptor activator peptide 6 (TRAP-6) from Sigma-Aldrich (St. Louis, MO); 9,10-dimethylanthracene, 1-methylpyrene, PFOA and 2,2',4,4',5,5'-hexachlorobiphenyl (PCB153) from Fluka (Buchs, Switzerland); 4,4'-(2,2,2-trichloroethane-1,1-diyl)bis(chlorobenzene) (DDT) from Supelco (Bellefonte, PA); R59022 from Calbiochem (La Jolla, CA); acetonitrile, dimethylsulfoxide (DMSO), ethanol and formaldehyde from Mallinckrodt Baker (Phillipsburg NJ).

Cell line/Cell culture

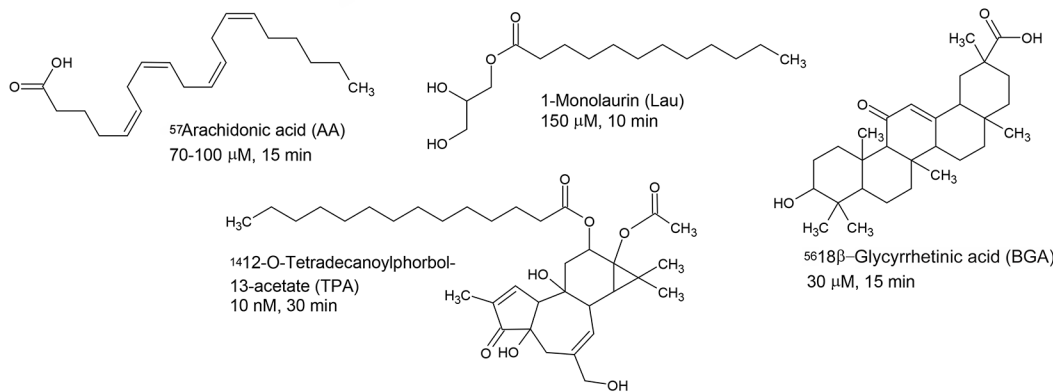
The WB-F344 rat liver epithelial cell line was obtained from Drs. J. W. Grisham and M. S. Tsao of the University of North Carolina (Chapel Hill, NC) [20]. Cells were grown in D-medium formulated from commercially purchased modified Eagle's minimum essential medium (Formula No. 78-5470EF, Gibco Laboratories, Grand Island, NY) supplemented with 5% fetal bovine serum (Gibco Laboratories) and 10 μ g/ml gentamicin (Gibco Laboratories). Cells were cultured on 35 mm diameter tissue culture plates (Corning Inc., Corning, NY) at 37°C in a humidified atmosphere containing 5% CO₂ and 95% air. Bioassays were conducted with confluent cultures that were obtained after two to three days of growth.

This cell line derived from F344 rats was used for the following reasons. These WB-cells are diploid and non-tumorigenic [20] and have been extensively characterized for its expressed gap junction genes, namely connexin43, and functional GJIC using all available techniques in

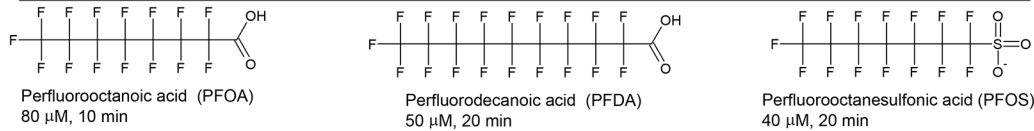
Growth factors and signal pathway modulators



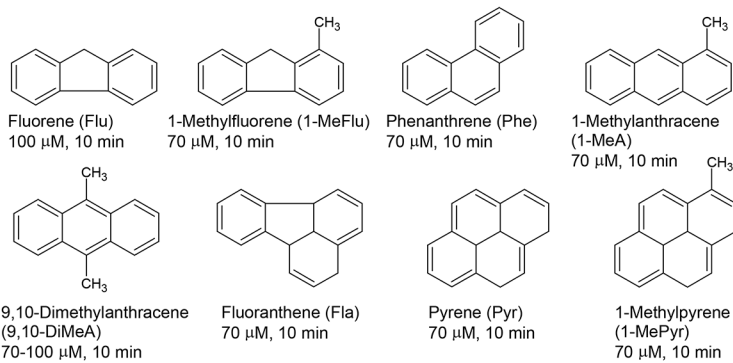
Lipid compounds



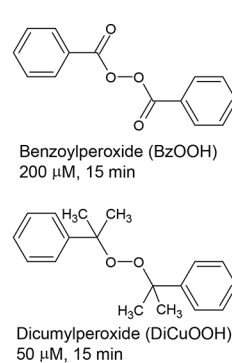
⁴⁵Fluorinated acids



^{28,30}Polycyclic aromatic hydrocarbons



¹⁶Organic peroxides



Organochlorine compounds

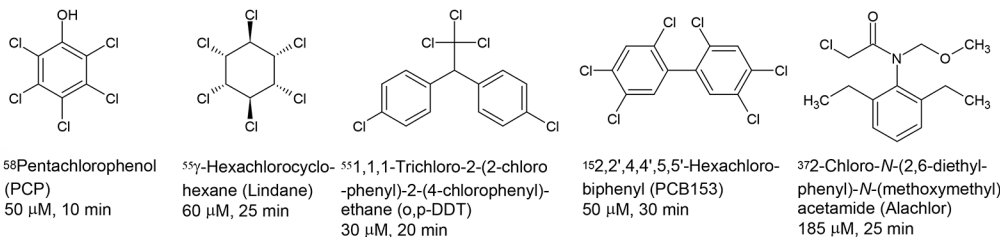


Fig 1. Structures, abbreviations, experimental doses and times of studied dysregulators of gap junctional intercellular communication. Superscript numbers of the following: [14–16,30,37,41,45,47,55–58] identify the references reporting a dysregulation of GJIC by these chemical in WB-F344 cells, with exception of Ref. 47, which used Rat-1 cells and Ref. 57, which used rat derived astrocytes.

doi:10.1371/journal.pone.0124454.g001

the absence and presence of well-known tumor promoters, growth factors, tumor suppressor genes and oncogenes to modulate GJIC [21]. WB-F344 cells are pluripotent, capable of differentiation into hepatocytes [22] and functional-contracting cardiomyocytes [23] and represent an ideal model for studying tumor promotion under the paradigm of stem-cell theory of cancer [24,25].

Experimental design

Confluent WB-F344 cells grown on 35 mm dishes were first pretreated either with a PC-PLC inhibitor, D609 (50 μ M, 20 min), a MEK1/2 inhibitor, U0126 (20 μ M, 30 min), or resveratrol (100 μ M, 15 min). After the pretreatment, the tested GJIC-dysregulator or vehicle was added to the dish for a specific incubation time and followed by a scalpel loading-dye transfer assay (note that the signal pathway inhibitor or resveratrol remained in the cell culture medium during the incubation period with the GJIC-dysregulator). The exposure regimes necessary to induce almost complete inhibition of GJIC (FOC < 0.2–0.4) were determined in separate concentration- and time-response experiments (data not shown). The lowest concentration of GJIC-dysregulator and the shortest exposure time sufficient to significantly dysregulate GJIC were chosen and they are summarized in Fig 1. The tested chemicals at the applied doses were not cytotoxic after 1 h exposure as evaluated by Neutral Red uptake assay (data not shown), except the treatment with benzoylperoxide (200 μ M) which induced about 50% decrease of Neutral Red uptake after 15 min exposure. The cytotoxic effects of benzoylperoxide are prevented by N-acetyl-L-(+)-cysteine (NAC) [16], therefore the experiments with benzoylperoxide were carried out with or without a 15 min pretreatment with 1 mM NAC prior to the addition of a toxicant to the cells.

To assure that the cells were responding to GJIC-dysregulators in a reproducible manner and that the signal-pathway inhibitors and resveratrol were able to induce significant effects, a system of positive controls (1-methylanthracene, D609 + 1-methylanthracene, resveratrol + 1-methylanthracene, EGF, and U0126 + EGF) was included in each experimental design besides the negative controls (vehicle, signal-pathway inhibitors or resveratrol without the GJIC-dysregulator). At least three independent experiments were conducted, each on a different day and cell population.

Bioassay of GJIC

A scalpel loading-dye transfer (SL-DT) technique was adapted after the method of El-Fouly *et al.* [26]. After treatment with the chemicals, cells were washed with phosphate buffered saline containing 0.1 g/L calcium chloride and 0.1 g/L magnesium chloride (CaMgPBS) followed by the addition of 1 mg/ml of Lucifer-Yellow dissolved in CaMgPBS. The dye was introduced into the cells with three different lines of scalpel-based dye injection through the monolayer of confluent cells using a surgical steel scalpel blade. The transfer of dye through gap junctions was for three minutes, followed by a thorough rinse with CaMgPBS to remove extracellular dye, and then fixed with a 4% formalin solution in PBS. Migration of the dye in the cells was observed at 200X using a Nikon epifluorescence microscope equipped with a Nikon Cool Snap EZ CCD camera and the images digitally acquired using a Nikon NIS-Elements F2.2 imaging system. The fluorescence area of the dye migration from the scalpel line was quantified using

‘ImageJ’ image analysis program (National Institute of Health, Bethesda, MD). The data were reported as a fraction of the dye spread in the vehicle control (Fraction of the Control, FOC).

Data and statistical analysis

The values were reported as an average \pm S.D. from at least three independent SL-DT experiments. A one-way ANOVA and Dunnett’s post hoc test was computed using SigmaStat (SPSS Inc., Chicago, IL) to determine significance of differences ($P < 0.05$) between a given dysregulator of GJIC and the following groups: (D609 + dysregulator), (U0126 + dysregulator), (resveratrol + dysregulator). The differences in the effects of D609, U0126 and resveratrol on the collection of all GJIC-dysregulators were further summarized in a principal component analysis (PCA) using Statistica for Windows 7.1 (StatSoft, Tulsa, OK, USA) and the results were presented in the component score plot of individual GJIC-dysregulators.

Results

A mechanistic survey was conducted on 25 chemicals dysregulating GJIC (Fig 1) to determine if they interrupted gap junction function through MEK1/2, PC-PLC, and if the antioxidant, resveratrol, protected gap junction function from the GJIC-dysregulating effects of the tested toxicants. Structures of these toxicants are listed in Fig 1. GJIC was measured by SL-DT bioassay in a WB-F344 rat liver epithelial cells pre-incubated with an inhibitor of PC-PLC or MEK1/2, or resveratrol, followed by the addition of a GJIC-dysregulating chemical.

All GJIC-dysregulators tested under the used exposure regimes induced statistically significant inhibition of GJIC with FOC values varying between 0.2–0.40 (Figs 2–5) when compared to the vehicle control (ANOVA, Dunnett’s post hoc test, $P < 0.05$). The pretreatment of the cells with NAC resulted in a slight increase (about 11%) of GJIC in cells treated with benzoylperoxide (compare Figs 4 and 5). The levels of GJIC were measured in cells, first pretreated with either a signal pathway inhibitors or resveratrol, and then treated with a GJIC-dysregulator. These results were compared to the cells exposed only to the tested GJIC-dysregulator and significance of differences was evaluated by ANOVA and Dunnett’s post hoc test at $P < 0.05$. Toxicants whose effects on GJIC were significantly attenuated by a PC-PLC inhibitor, D609, but not by MEK1/2 inhibitor, were fluorene, 1-methylfluorene, fluoranthene, phenanthrene, 1-methylanthracene, 9,10-dimethylanthracene, pyrene, 1-methylpyrene, PFDA, dicumylperoxide, PCB-153 and DDT (Fig 2A and 2B). With the exception of PFDA, D609 resulted in restoring GJIC to 0.70–0.96 FOC. D609 restored PFDA-induced dysregulation of GJIC only partially, by 24% (from 0.22 to 0.46 FOC).

Chemicals that were significantly prevented from GJIC-dysregulation by a MEK1/2 inhibitor, U0126, but not by a PC-PLC inhibitor, were TPA, EGF and lindane (Fig 3). The GJIC was restored to 0.70–0.98 FOC by pretreatment with U0126. The GJIC-dysregulating effects of PFOA, (NAC + benzoylperoxide), diacylglycerol kinase inhibitor I (R59022), and TRAP-6 were attenuated to a different extent (0.44–1.05 FOC) by both, PC-PLC and MEK1/2 inhibitors, D609 and U0126, respectively (Fig 4). Neither PC-PLC nor MEK1/2 inhibitor altered dysregulation of GJIC induced by PFOSA, BzOOH, arachidonic acid, 1-monolaurin, 18- β -glycyrrhetic acid, pentachlorophenol, and alachlor (Fig 5), and the level of GJIC remained between 0.23–0.37 FOC.

Resveratrol effectively prevented the dysregulation of GJIC by all toxicants that worked through either a PC-PLC- (Fig 2A and 2B), MEK1/2- (Fig 3), or both PC-PLC and MEK1/2-dependent pathway (Fig 4), except for PFDA (Fig 2B) and benzoylperoxide in the cells pretreated with NAC (Fig 4). Resveratrol also prevented the dysregulation of GJIC by alachlor, but all other compounds that dysregulated GJIC through a PC-PLC-independent and

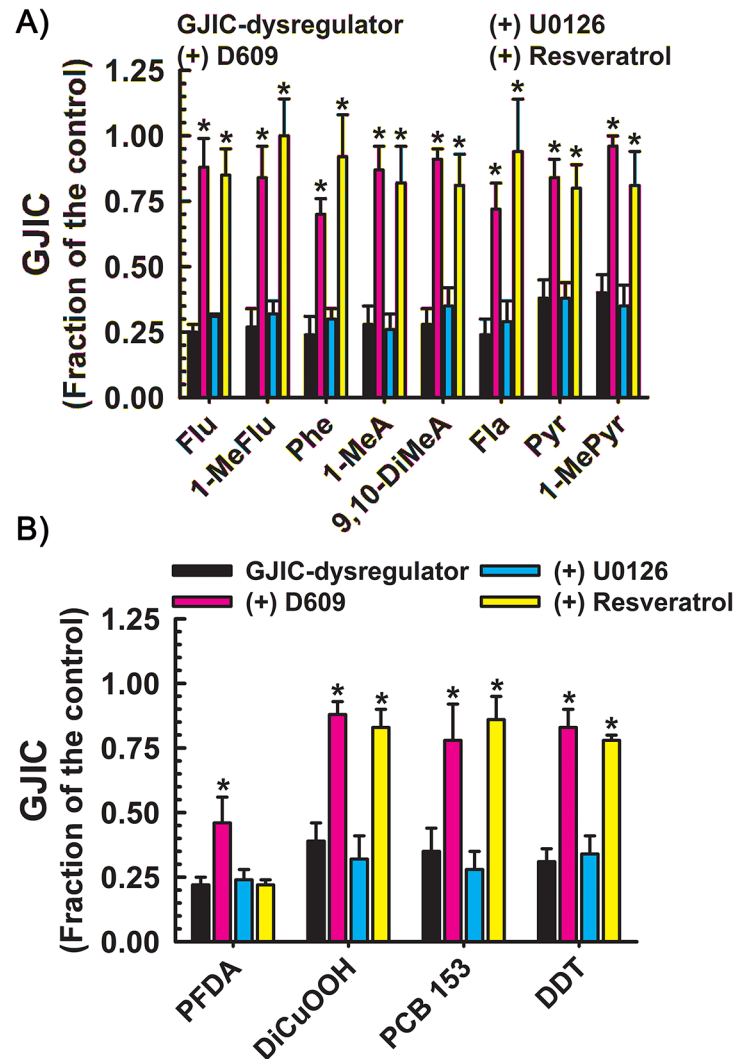


Fig 2. Dysregulation of GJIC through PC-PLC. The following compounds inhibited GJIC through PC-PLC: (a) Through the following PAHs: Flu (100 μ M, 10 min), 1-MeFlu (70 μ M, 10 min), Phe (70 μ M, 10 min), 1-MeA (70 μ M, 10 min), 9,10-DiMeA (100 μ M, 10 min), Fla (70 μ M, 10 min), Pyr (70 μ M, 10 min) and 1-MePyr (70 μ M, 10 min); (b) Other toxicants: PFDA (50 μ M, 20 min), DiCuOOH (50 μ M, 15 min), PCB 153 (50 μ M, 30 min), and DDT (30 μ M, 20 min). The cells were treated with inhibitors of PC-PLC (D609, 50 μ M, 20 min) or MEK1/2 (U0126, 20 μ M, 30 min), or resveratrol (100 μ M, 15 min) before addition of GJIC-dysregulator. At least three independent experiments were averaged \pm SD. An ANOVA was conducted for each GJIC-dysregulator followed by a Dunnett's post-hoc test to determine significance (at $P < 0.05$ as indicated by an *) from cells treated with only the GJIC-dysregulator. The F-values for Flu, 1-MeFlu, Phe, 1-MeA, 9,10-DiMeA, Fla, Pyr and 1-MeP were 71.8 ($P < 0.001$), 75.6 ($P < 0.001$), 57.7 ($P < 0.001$), 737.3 ($P < 0.001$), 74.2 ($P < 0.001$), 58.4 ($P < 0.001$), 67.4 ($P < 0.001$) and 50.5 ($P < 0.001$), respectively. The F-values for PFDA, DiCuOOH, PCB 153, and DDT were 13.1 ($P = 0.002$), 51.2 ($P < 0.001$), 38.3 ($P < 0.001$) and 87.5 ($P < 0.001$), respectively.

doi:10.1371/journal.pone.0124454.g002

MEK1/2-independent mechanism were unaffected by resveratrol (Fig 5). Resveratrol alone had no affect on GJIC nor did it reverse the inhibitory effects of GJIC if added after the addition of the dysregulator (data not shown).

A principal component analysis (PCA) was conducted on all data using four variables of FOC values from experiments with (1) dysregulator, (2) D609 + dysregulator, (3) U0126 + dysregulator or (4) resveratrol + dysregulator). The first two principal components in the component score plot of individual dysregulators of GJIC explained 74% of the variance (Fig 6). The

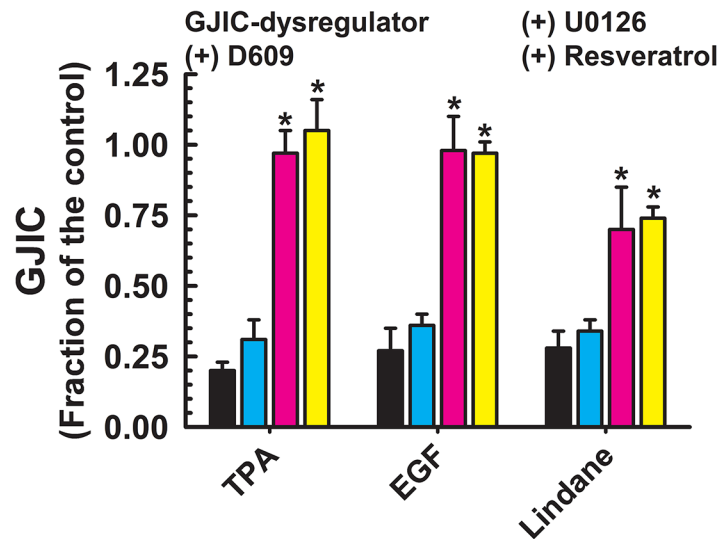


Fig 3. Dysregulation of GJIC through MEK1/2. The following compounds inhibited GJIC through MEK1/2: TPA (10 nM, 30 min), EGF (5 ng/ml, 30 min), TRAP-6 (50 μ M, 30 min) and lindane (60 μ M, 25 min). The cells were treated with inhibitors of MEK1/2 (U0126, 20 μ M, 30 min) or PC-PLC (D609, 50 μ M, 20 min), or resveratrol (100 μ M, 15 min) before addition of GJIC-dysregulator. At least three independent experiments were averaged \pm SD. An ANOVA was conducted for each GJIC-dysregulator followed by a Dunnett's post-hoc test to determine significance (at $P < 0.05$ as indicated by an *) from cells treated with only the GJIC-dysregulator. The F-values for TPA, EGF, TRAP-6 and lindane were 156.563 ($P < 0.001$), 750.742 ($P < 0.001$), 135.648 ($P < 0.001$) and 36.717 ($P < 0.001$), respectively.

doi:10.1371/journal.pone.0124454.g003

four different symbols represent GJIC-dysregulators as grouped in the Figs 1–4 based on the effects of D609 and U0126 (PC-PLC-dependent chemicals, MEK1/2-dependent chemicals, both PC-PLC and MEK1/2-dependent chemicals, PC-PLC- and MEK1/2-independent chemicals). The PCA plot indicated a cluster of all PC-PLC-dependent GJIC-dysregulators except PFDA, and also for PC-PLC- and MEK1/2-independent GJIC-dysregulators except for alachlor. MEK1/2-dependent GJIC-dysregulators, TPA and EGF clustered together, but another MEK1/2-dependent chemical, lindane, showed to be an outlier from this cluster. PC-PLC and MEK1/2-dependent chemicals were both scattered in the plot, with PFOA and R59022 closer to the PC-PLC-dependent group, but TRAP-6 was in proximity to the MEK1/2 dependent group.

Discussion

Intercellular communication *via* opened-gap junction channels is critical in maintaining the homeostasis of a tissue. Although transient closure of gap junctions in response to a growth factor or cytokine is normal, chronic closure of the channels by persistent exposure to xenobiotics, cytokines and growth factors interrupts tissue homeostasis and is characteristic of the hyperproliferative states of growth and development diseases, such as cancer [6,9,27]. The mechanisms involved in the regulation of gap junction channels are not fully understood, but MEK1/2 and PC-PLC are key signal transduction proteins known to be involved. The role of PC-PLC in the regulation of GJIC has only been recently determined [15–17] for a very limited number of compounds, namely 1-methylantracene, dicumylperoxide and PCB-153. Thus, the prominence of PC-PLC in toxicant-induced inhibition of GJIC is not known. Our results indicated that the dysregulation of GJIC through a PC-PLC-dependent mechanism is a robust response of an oval-like rat liver epithelial cell line to many toxicants. Of the 25 compounds

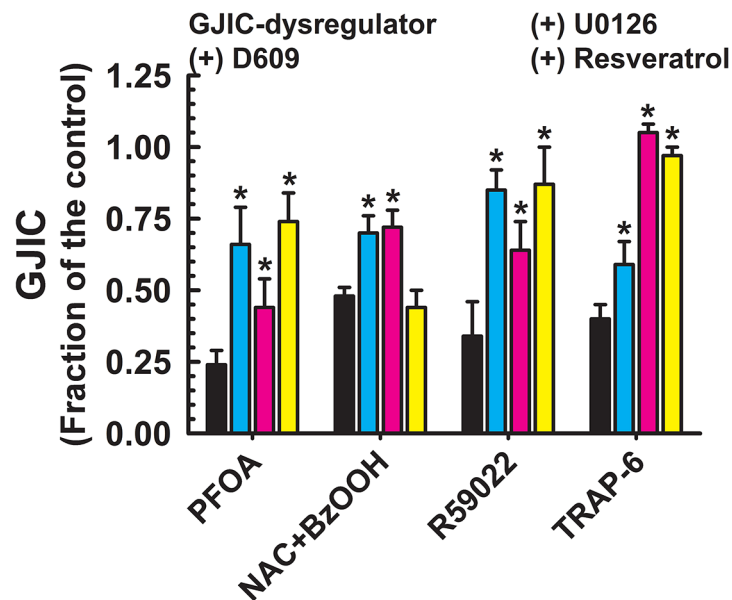


Fig 4. Dysregulation of GJIC through both MEK1/2 and PC-PLC. The following compounds inhibited GJIC through both MEK1/2 and PC-PLC: PFOA (80 μ M, 10 min), NAC+BzOOH (cells were treated with 1 mM NAC for 15 min prior the addition of 200 μ M BzOOH for 15 min), and R59022 (30–50 μ M, 10 min). The cells were treated with inhibitors of PC-PLC (D609, 50 μ M, 20 min) or MEK1/2 (U0126, 20 μ M, 30 min), or resveratrol (100 μ M, 15 min) before addition of GJIC-dysregulator. At least three independent experiments were averaged \pm SD. An ANOVA was conducted for each GJIC-dysregulator followed by a Dunnett's post-hoc test to determine significance (at $P < 0.05$ as indicated by an *) from cells treated with only the GJIC-dysregulator. The F-values for PFOA and R59022 were 27.0 ($P < 0.001$), 28.2 ($P < 0.001$) and 20.9 ($P < 0.001$), respectively.

doi:10.1371/journal.pone.0124454.g004

tested, 15 of them likely required PC-PLC in the dysregulation of GJIC, and three of these compounds also required MEK1/2.

Eight of these 25 compounds were low molecular weight polycyclic aromatic hydrocarbons (PAHs). Although the lower molecular weight PAHs are the most prominent PAHs found in the environment, these PAHs, which have two to four aromatic rings, have been largely ignored by the research community in assessing adverse health effects due to their lack of genotoxicity [8,17,27]. However, lower molecular weight-PAHs are biologically active and known to induce signaling pathways that control gene expression. Thus, these low molecular weight PAH-compounds must be considered as “epigenetic toxicants” [27]. In particular, low molecular weight-PAHs were shown to be effective inhibitors of GJIC, and the GJIC-inhibitory properties were strongly linked to the existence of a bay or bay-like regions on the PAH [27–30], which also correlated with the induction of arachidonic acid release and activation of MAPKs [17,31]. Mixtures of PAHs exhibit an additive effect on the inhibition of GJIC suggesting a common mechanism of action [32]. The PAHs tested in this study (9,10-dimethylanthracene, fluorene, 1-methylfluorene, fluoranthene, phenanthrene, pyrene, 1-methylpyrene) all inhibited GJIC through a resveratrol sensitive, PC-PLC-dependent mechanism that was independent of MEK1/2 activation, which is consistent with a common-mechanism hypothesis.

Dysregulation of GJIC through a PC-PLC-dependent mechanism was not unique to the PAHs, but also to several other very prominent environmental toxicants (PCB153 and PFDA), pesticide (DDT) and the oxidant (dicumylperoxide). Similar to lower molecular weight PAHs, the effects of these toxicants on GJIC were also prevented by pretreatment with resveratrol. With the exception of PFDA, inhibition of PC-PLC by D609 almost completely prevented

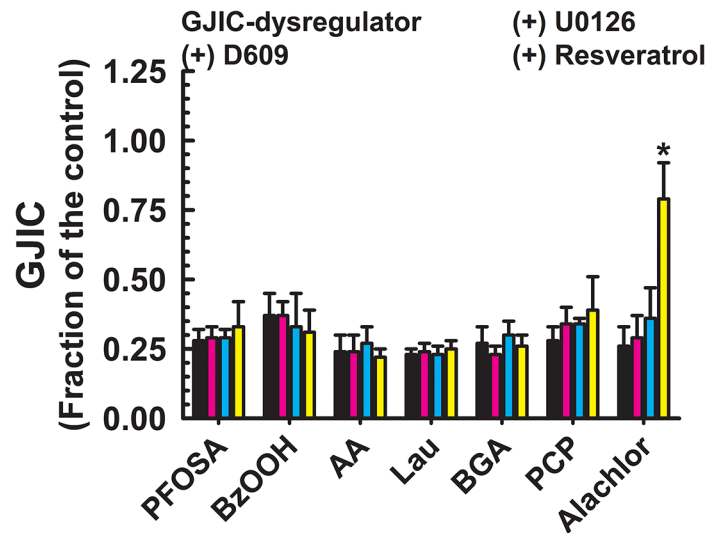


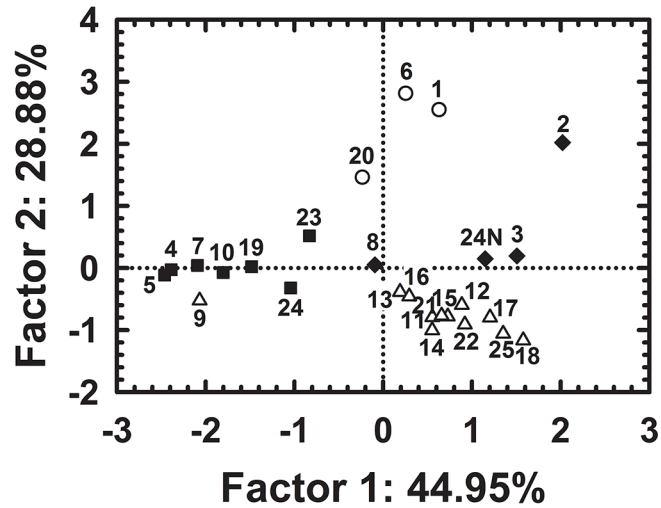
Fig 5. Dysregulation of GJIC through signaling pathways other than MEK1/2 or PC-PLC. The following compounds inhibited GJIC neither through MEK1/2 nor PC-PLC: PFOSA (40 μ M, 20 min), BzOOH (200 μ M, 15 min), AA (70–100 μ M, 15 min), Lau (150 μ M, 10 min), BGA (30 μ M, 15 min), PCP (50 μ M, 10 min) and Alachlor (185 μ M, 25 min). The cells were treated with inhibitors of PC-PLC (D609, 50 μ M, 20 min) or MEK1/2 (U0126, 20 μ M, 30 min), or resveratrol (100 μ M, 15 min) before addition of GJIC-dysregulator. At least three independent experiments were averaged \pm SD. An ANOVA was conducted for each GJIC-dysregulator followed by a Dunnett's post-hoc test to determine significance (at $P < 0.05$ as indicated by an *) from cells treated with only the GJIC-dysregulator. The F-values for PFOSA, BzOOH, AA, Lau, BGA, PCP and alachlor were 1.0 ($P = 0.426$), 0.6 ($P = 0.628$), 0.7 ($P = 0.565$), 0.6 ($P = 0.617$), 2.1 ($P = 0.131$), 1.9 ($P = 0.162$) and 58.6 ($P < 0.001$), respectively.

doi:10.1371/journal.pone.0124454.g005

toxicant-induced dysregulation of GJIC (0.78–0.88 FOC), but PFDA-induced dysregulation of GJIC was only partially prevented by D609 (0.46 FOC). Correspondingly, the PCA analysis placed PFDA out of the cluster of PC-PLC-dependent chemicals and close to the cluster of toxicants that were dependent on neither PC-PLC- nor MEK1/2.

Ligands of the receptor tyrosine kinase-Raf-pathway, such as EGF, or PKC-activators, such as TPA, result in MEK1/2-dependent inhibition of GJIC [14,33,34], and is the most studied mechanism of GJIC-dysregulation. EGF and TPA also induce the phosphorylation of connexin43 [10,13,35,36]. Our results confirm published data indicating that EGF and TPA dysregulate GJIC through MEK1/2, but our current results indicated that PC-PLC was not involved. Although lindane is known to dysregulate GJIC [37], this is the first time implicating MEK1/2 as the underlying mechanism of lindane inhibition of GJIC. The importance of these findings is that these compounds dysregulated GJIC specifically through MEK1/2 and not through PC-PLC. Thus, PC-PLC and MEK1/2 regulation of GJIC are two separate intracellular signaling mechanisms regulating GJIC.

Although MEK1/2 appears to be a GJIC-regulatory pathway, the activation of MEK1/2 alone is not necessarily sufficient for the dysregulation of GJIC [38]. Most of the chemicals investigated in this study are also reported to activate the MAPK/ERK pathway in different cell types, including WB-F344 cells: TRAP-6 [39], arachidonic acid [40], PFOA, [41], 1-methylanthracene [17,31], pentachlorophenol [42], lindane [43], DDT [44], PCB153 [15], benzoylperoxide and dicumylperoxide [16]; yet, not all of these compounds dysregulate GJIC through a MEK1/2-ERK-dependent pathway (See Figs 2 and 5). As noted above, connexin43 has known phosphorylation sites specific to MAPKs, but the activation of MEK1/2, ERK1/2 and p38 by 1-MeA did not alter the phosphorylation status of Connexin43 as detected by Western blots



Data point description:

Data #	Toxicant	Data #	Toxicant	Data #	Toxicant	Data #	Toxicant	Data #	Toxicant
1	EGF	6	TPA	11	Flu	16	Fla	21	DDT
2	TRAP-6	7	BGA	12	1-MeFLU	17	Pyr	22	PCB 153
3	R50022	8	PFOA	13	Phe	18	1-MePyr	23	Alachlor
4	AA	9	PFDA	14	1-MeA	19	PCP	24	BzOOH
5	Lau	10	PFOSA	15	9,10-DiMeA	20	Lindane	24N	NAC+BzOOH
								25	DiCuOOH

Fig 6. Component score plot from principal component analysis showing distribution of different GJIC-dysregulators based on their effects on GJIC and alteration of these effects by D609, U0126 or resveratrol. Symbols represent different groups of GJIC-dysregulators: (triangles = PC-PLC-dependent compound, (circles = MEK1/2-dependent compounds), (diamonds = both PC-PLC- and MEK1/2-dependent compounds), (squares = neither PC-PLC- nor MEK1/2-dependent compounds).

doi:10.1371/journal.pone.0124454.g006

[17,31]. Collectively, these results indicate that the dysregulation of GJIC by MEK1/2-dependent pathway requires another essential cell signaling protein.

Two compounds, PFOA and the diacylglycerol kinase inhibitor I, R59022, inhibited GJIC that depended, in part on both PC-PLC and MEK1/2. PFOA has been shown to activate MAPK/ERK [41] and inhibit GJIC [45]. Additionally, the inhibition of diacylglycerol kinase by R59022 results in an accumulation of diacylglycerol and activation of PKC [46], and we may speculate that possible PKC-dependent activation of MAPK/ERK pathway could explain the effects of MEK1/2 inhibitor on GJIC-dysregulation induced by R59022. However, these two chemicals were also PC-PLC- and resveratrol-dependent, which indicates that these toxicants can dysregulate gap junction function through multiple pathways. TRAP-6 clearly dysregulated GJIC through a MEK1/2 mechanism, but was partially dependent on PC-PLC-inhibitor as indicated by a 19% increase in GJIC by pretreatment with D609, however this small D609 effect did not remove this toxicant from the cluster of MEK-dependent compounds in the PCA plot. Interestingly, TRAP-6 was previously reported to dysregulate connexin43-mediated GJIC in Rat-1 fibroblasts through a PI-PLC-induced decrease of membrane phosphatidylinositol 4,5-bisphosphate, a mechanism most likely not-involving MAPK pathway [47].

Another significant result was that 7 of the 25 compounds tested inhibited GJIC through mechanisms independent of either PC-PLC or MEK1/2. These compounds included PFOSA, benzoylperoxide, arachidonic acid, 1-monolaurin, 18β-glycyrrhetic acid, pentachlorophenol, and alachlor. Except for alachlor, resveratrol did not prevent the dysregulation of GJIC. These results clearly indicate at least two other mechanism are involved in the closure of gap junction

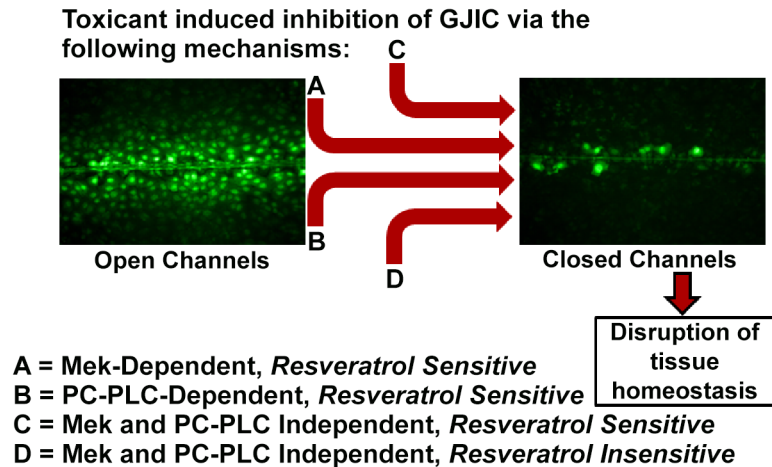


Fig 7. Summary of toxicant-dependent regulatory pathways of GJIC. Each of the four pathways are designated as **A**, Mek-dependent and resveratrol sensitive, **B**, Phosphatidylcholine-specific phospholipase C (PC-PLC) and resveratrol sensitive, **C**, Mek and PC-PLC independent and resveratrol sensitive, and **D**, Mek and PC-PLC independent and resveratrol insensitive.

doi:10.1371/journal.pone.0124454.g007

channels in that one of these mechanisms was independent of MEK1/2, PC-PLC and resveratrol, and the other dependent on resveratrol. Possible candidates might include PKA, PKC, Akt or p38 [10–12,48], phospholipases [47] and redox-dependent regulatory mechanisms [49].

The identification of underlying mechanisms regulating GJIC is important in determining more accurate assessments on adverse health effects of environmental toxicants, as well as developing potential preventive health strategies. Ingestion of natural compounds found in dietary food or supplements is one major approach in developing more effective prevention strategies to the adverse health effects of exposures to environmental toxicants. Due to numerous reports in the prevention of cardiovascular diseases, cancer, and the aging processes in several organisms, resveratrol is one compound that has received considerable attention in the research field [19]. Several reports have demonstrated resveratrol can modulate toxic effects of epigenetic compounds on GJIC [50,51]. Our results indicated that resveratrol prevented compounds from inhibiting GJIC through PC-PLC and MEK1/2. Possibly these two pathways are redox sensitive, which are specific to resveratrol. NAC, also an antioxidant, did not prevent BzOOH-induced dysregulation of GJIC [16]. NAC also did not prevent 1-MeA-induced dysregulation of GJIC (data not shown). Although we used higher concentrations of resveratrol for our mechanistic studies, we previously showed that *in vitro* concentrations of resveratrol as low as 25 μM significantly prevented inhibition of GJIC by dicumylperoxide indicating physiologic significance [16], particularly if other food- or supplement-based antioxidative compounds can exhibit similar activities. These results suggest that populations exposed to toxicants that dysregulate GJIC through PC-PLC- and MEK-dependent mechanisms could potentially benefit from dietary intake of resveratrol and similar compounds in the prevention of diseases that depend on the dysregulation of GJIC.

Conclusions

The disruption of tissue homeostasis by compounds through the dysregulation of intercellular communication through gap junctions poses potential health risks. The dysregulation of GJIC occurs through multiple pathways (Fig 7), and the identification of these pathways within tissue types will be useful in the assessment of risks and benefits of toxicants and

chemopreventive compounds. Considering that the liver is a major target for environmental toxicants, the use of the rat liver oval cell type is a good *in vitro* model system to begin an assessment of the underlying mechanisms involved in regulating GJIC. These cells are bipotent in hepatic tissue, capable of differentiation into hepatocytes and biliary duct cells [22], and represent an ideal *in vitro* model for studying tumor promotion in liver under the paradigm of stem-cell theory of cancer [24,25]. Our results indicate at least four different pathways are regulating GJIC (Fig 7), two of which depend on either PC-PLC or MEK1/2. The recently discovered PC-PLC-dependent mechanism was a robust and prevalent response of epithelial cells to environmental toxicants. Of the 25 compounds tested, 15 of them required PC-PLC in the dysregulation of GJIC, while three of these compounds also required MEK1/2. The function of PC-PLC in tumorigenesis has not been extensively studied, yet, there are reports indicating that PC-PLC plays a very significant role in cancer [18,52]. PC-PLC has also been specifically linked to the regulation of cellular differentiation [53] and apoptosis [54], which are processes strongly associated with tumor promotion. Furthermore, resveratrol effectively prevented the dysregulation of GJIC that worked through either MEK1/2 or PC-PLC indicating the potential to prevent an adverse effect of a toxicant through compounds that can be attained through diet. However, preventive effects by such compounds are apparently not universal considering that not all GJIC-regulatory mechanisms are equally affected by a chemopreventive agent, such as resveratrol (Fig 7). These results, which are relevant to liver tissue, also demonstrate an important conceptual way of integrating extra- intra- and gap junctional inter-cellular communication mechanisms to maintain tissue homeostasis.

Supporting Information

S1 Dataset.
(XLSX)

Acknowledgments

We would like to thank Ms. Lindsay Goodall for her excellent contribution of maintaining cultures of cells for these experiments.

Author Contributions

Conceived and designed the experiments: IS PB JSP JET BLU. Performed the experiments: IS PB HB EK AW JSP BLU. Analyzed the data: IS PB HB EK AW JSP BLU. Contributed reagents/materials/analysis tools: PB BLU JET. Wrote the paper: IS PB BLU.

References

1. Chipman JK, Mally A, Edwards GO. Disruption of gap junctions in toxicity and carcinogenicity. *Toxicol Sci.* 2003; 71: 146–153. PMID: [12563100](#)
2. Vinken M, Vanhaecke T, Papeleu P, Snykers S, Henkens T, Rogiers V. Connexins and their channels in cell growth and cell death. *Cell Signal.* 2006; 18: 592–600. PMID: [16183253](#)
3. Goldberg GS, Lampe PD, Nicholson BJ. Selective transfer of endogenous metabolites through gap junctions composed of different connexins. *Nat Cell Biol.* 1999; 1: 457–459. PMID: [10559992](#)
4. Mehta PP. Introduction: a tribute to cell-to-cell channels. *J Membr Biol.* 2007; 217: 5–12. PMID: [17876494](#)
5. Trosko JE, Chang CC, Upham BL. Modulation of gap-junctional communication by 'epigenetic' toxicants: a shared mechanism in teratogenesis, carcinogenesis, atherogenesis, immunomodulation, reproductive and neurotoxicities. In: Wilson SH, Suk A, editors. *Biomarkers of environmental associated disease*; Boca Raton: Lewis Publishers;2002 pp. 445–454.

6. Yamasaki H, Omori Y, Zaidan DM, Mironov N, Mesnil M, Krutovskikh V. Genetic and epigenetic changes of intercellular communication genes during multistage carcinogenesis. *Cancer Detect Prev*. 1999; 23: 273–279. PMID: [10403898](#)
7. Trosko JE, Ruch RJ. Gap junctions as targets for cancer chemoprevention and chemotherapy. *Curr Drug Targets*. 2002; 3: 465–482. PMID: [12448698](#)
8. Trosko JE, Upham BL. The emperor wears no clothes in the field of carcinogen risk assessment: ignored concepts in cancer risk assessment. *Mutagenesis*. 2005; 20: 81–92. PMID: [15784692](#)
9. Vinken M, Doktorova T, Decrock E, Leybaert L, Vanhaecke T, Rogiers V. Gap junctional intercellular communication as a target for liver toxicity and carcinogenicity. *Crit Rev Biochem Mol Biol*. 2009; 44: 201–222. doi: [10.1080/10409230903061215](#) PMID: [19635038](#)
10. Laird DW. Connexin phosphorylation as a regulatory event linked to gap junction internalization and degradation. *Biochim Biophys Acta-Biomembranes*. 2005; 1711: 172–182. PMID: [15955302](#)
11. Park DJ, Wallick CJ, Martyn KD, Lau AF, Jin C, Warn-Cramer BJ. Akt phosphorylates connexin43 on Ser373, a "Mode-1" binding site for 14-3-3. *Cell Communication and Adhesion*. 2007; 14: 211–226. PMID: [18163231](#)
12. Solan JL, Lampe PD. Connexin43 phosphorylation: structural changes and biological effects. *Biochem J*. 2009; 419: 261–272. doi: [10.1042/BJ20082319](#) PMID: [19309313](#)
13. Rivedal E, Opsahl H. Role of PKC and MAP kinase in EGF- and TPA-induced connexin43 phosphorylation and inhibition of gap junction intercellular communication in rat liver epithelial cells. *Carcinogenesis*. 2001; 22: 1543–1550. PMID: [11532878](#)
14. Ruch RJ, Trosko JE, Madhukar BV. Inhibition of connexin43 gap junctional intercellular communication by TPA requires ERK activation. *J Cell Biochem*. 2001; 83: 163–169. PMID: [11500965](#)
15. Machala M, Blaha L, Vondracek J, Trosko JE, Scott J, Upham BL. Inhibition of gap junctional intercellular communication by noncoplanar polychlorinated biphenyls: Inhibitory potencies and screening for potential mode(s) of action. *Toxicol Sci*. 2003; 76: 102–111. PMID: [12915713](#)
16. Upham BL, Guzvic M, Scott J, Carbone JM, Blaha L, Coe C, et al. Inhibition of gap junctional intercellular communication and activation of mitogen-activated protein kinase by tumor-promoting organic peroxides and protection by resveratrol. *Nutr Cancer*. 2007; 57: 38–47. PMID: [17516861](#)
17. Upham BL, Blaha L, Babica P, Park JS, Sovadinova I, Pudrith C, et al. Tumor promoting properties of a cigarette smoke prevalent polycyclic aromatic hydrocarbon as indicated by the inhibition of gap junctional intercellular communication via phosphatidylcholine-specific phospholipase C. *Cancer Sci*. 2008; 99: 696–705. doi: [10.1111/j.1349-7006.2008.00752.x](#) PMID: [18377422](#)
18. Cheng J, Weber JD, Baldassare JJ, Raben DM. Ablation of Go alpha-subunit results in a transformed phenotype and constitutively active phosphatidylcholine-specific phospholipase C. *J Biol Chem*. 1997; 272: 17312–17319. PMID: [9211868](#)
19. Pervaiz S, Holme AL. Resveratrol: Its Biologic Targets and Functional Activity. *Antioxidants & Redox Signaling*. 2009; 11: 2851–2897.
20. Tsao MS, Smith JD, Nelson KG, Grisham JW. A diploid epithelial cell line from normal adult rat liver with phenotypic properties of 'oval' cells. *Exp Cell Res*. 1984; 154: 38–52. PMID: [6468534](#)
21. Trosko JE, Chang CC. Epigenetic-toxicology induced modulated gap junctional intercellular communication in carcinogenesis. In: Vanden-Heuvel JP, Perdeu GH, Mattes WB, Greenlee WF, editors. *Comprehensive Toxicology*, Vol. xiv; Amsterdam: Elsevier Science;2002 pp. 409–419.
22. Coleman WB, Wennerberg AE, Smith GJ, Grisham JW. Regulation of the differentiation of diploid and some aneuploid rat liver epithelial (stemlike) cells by the hepatic microenvironment. *Am J Pathol*. 1993; 142: 1373–1382. PMID: [8494041](#)
23. Malouf NN, Coleman WB, Grisham JW, Lininger RA, Madden VJ, Sproul M, et al. Adult-derived stem cells from the liver become myocytes in the heart in vivo. *Am J Pathol*. 2001; 158: 1929–1935. PMID: [11395367](#)
24. Trosko JE. Human adult stem cells as targets for cancer stem cells: Evolution; Oct-4 gene, and cell to cell communication. In: Dittmar T, Zaenkar K, editors. *Stem Cells and Cancer*; New York: Nova Publishers;2008.
25. Trosko JE. Cancer Stem Cells and Cancer Nonstem Cells: From Adult Stem Cells or from Reprogramming of Differentiated Somatic Cells. *Vet Pathol*. 2009; 46: 176–193. doi: [10.1354/vp.46-2-176](#) PMID: [19261629](#)
26. El-Fouly MH, Trosko JE, Chang CC. Scrape-loading and dye transfer. A rapid and simple technique to study gap junctional intercellular communication. *Exp Cell Res*. 1987; 168: 422–430. PMID: [2433137](#)
27. Upham BL, Weis LM, Trosko JE. Modulated gap junctional intercellular communication as a biomarker of PAH epigenetic toxicity: structure-function relationship. *Environ Health Perspect*. 1998; 106: 975–981. PMID: [9703481](#)

28. Blaha L, Kapplova P, Vondracek J, Upham B, Machala M. Inhibition of gap-junctional intercellular communication by environmentally occurring polycyclic aromatic hydrocarbons. *Toxicol Sci.* 2002; 65: 43–51. PMID: [11752684](#)
29. Upham BL, Weis LM, Rummel AM, Masten SJ, Trosko JE. The effects of anthracene and methylated anthracenes on gap junctional intercellular communication in rat liver epithelial cells. *Fundam Appl Toxicol.* 1996; 34: 260–264. PMID: [8954755](#)
30. Weis LM, Rummel AM, Masten SJ, Trosko JE, Upham BL. Bay or baylike regions of polycyclic aromatic hydrocarbons were potent inhibitors of Gap junctional intercellular communication. *Environ Health Perspect.* 1998; 106: 17–22. PMID: [9417772](#)
31. Rummel AM, Trosko JE, Wilson MR, Upham BL. Polycyclic aromatic hydrocarbons with bay-like regions inhibited gap junctional intercellular communication and stimulated MAPK activity. *Toxicol Sci.* 1999; 49: 232–240. PMID: [10416268](#)
32. Ghoshal S, Weber WJ, Rummel AM, Trosko JE, Upham BL. Epigenetic toxicity of a mixture of polycyclic aromatic hydrocarbons on gap junctional intercellular communication before and after biodegradation. *Environmental Science and Technology.* 1999; 33: 1044–1050.
33. Cameron SJ, Malik S, Akaike M, Lerner-Marmarosh N, Yan C, Lee JD, et al. Regulation of epidermal growth factor-induced connexin 43 gap junction communication by big mitogen-activated protein kinase1/ERK5 but not ERK1/2 kinase activation. *J Biol Chem.* 2003; 278: 18682–18688. PMID: [12637502](#)
34. Sirnes S, Kjenseth A, Leithe E, Rivedal E. Interplay between PKC and the MAP kinase pathway in Connexin43 phosphorylation and inhibition of gap junction intercellular communication. *Biochem Biophys Res Commun.* 2009; 382: 41–45. doi: [10.1016/j.bbrc.2009.02.141](#) PMID: [19258009](#)
35. Warn-Cramer BJ. Regulation of gap junctions by tyrosine protein kinases. *Biochimica-et-biophysica-acta.* 2004; 1662: 81–95. PMID: [15033580](#)
36. Rivedal E, Leithe E. Connexin43 synthesis, phosphorylation, and degradation in regulation of transient inhibition of gap junction intercellular communication by the phorbol ester TPA in rat liver epithelial cells. *Exp Cell Res.* 2005; 302: 143–152. PMID: [15561096](#)
37. Upham BL, Boddy B, Xing X, Trosko JE, Masten SJ. Non-genotoxic effects of selected pesticides and their disinfection by-products on gap junctional intercellular communication. *Ozone Science and Engineering.* 1997; 19: 351–369.
38. Hossain MZ, Jagdale AB, Ao P, Boynton AL. Mitogen-activated protein kinase and phosphorylation of connexin43 are not sufficient for the disruption of gap junctional communication by platelet-derived growth factor and tetradecanoylphorbol acetate. *J Cell Physiol.* 1999; 179: 87–96. PMID: [10082136](#)
39. Luttrell LM, Daaka Y, DellaRocca GJ, Lefkowitz RJ. G protein-coupled receptors mediate two functionally distinct pathways of tyrosine phosphorylation in rat 1a fibroblasts—Shc phosphorylation and receptor endocytosis correlate with activation of Erk kinases. *J Biol Chem.* 1997; 272: 31648–31656. PMID: [9395506](#)
40. Rao GN, Baas AS, Glasgow WC, Eling TE, Runge MS, Alexander RW. Activation of Mitogen-Activated Protein-Kinases by Arachidonic-Acid and Its Metabolites in Vascular Smooth-Muscle Cells. *J Biol Chem.* 1994; 269: 32586–32591. PMID: [7798262](#)
41. Upham BL, Park JS, Babica P, Sovadinova I, Rummel AM, Trosko JE, et al. Structure-activity-dependent regulation of cell communication by perfluorinated fatty acids using in vivo and in vitro model systems. *Environ Health Perspect.* 2009; 117: 545–551. doi: [10.1289/ehp.11728](#) PMID: [19440492](#)
42. Corcelle E, Djerbi N, Mari M, Nebout M, Fiorini C, Fenichel P, et al. Control of the autophagy maturation step by the MAPK ERK and p38: lessons from environmental carcinogens. *Autophagy.* 2007; 3: 57–59. PMID: [17102581](#)
43. Mograbi B, Corcelle E, Defamie N, Samson M, Nebout M, Segretain D, et al. Aberrant Connexin 43 endocytosis by the carcinogen lindane involves activation of the ERK/mitogen-activated protein kinase pathway. *Carcinogenesis.* 2003; 24: 1415–1423. PMID: [12807735](#)
44. Han EH, Kim JY, Kim HK, Hwang YP, Jeong HG. o,p'-DDT induces cyclooxygenase-2 gene expression in murine macrophages: Role of AP-1 and CRE promoter elements and PI3-kinase/Akt/MAPK signaling pathways. *Toxicol Appl Pharmacol.* 2008; 233: 333–342. doi: [10.1016/j.taap.2008.09.003](#) PMID: [18840457](#)
45. Upham BL, Deocampo ND, Wurl B, Trosko JE. Inhibition of gap junctional intercellular communication by perfluorinated fatty acids is dependent on the chain length of the fluorinated tail. *Int J Cancer.* 1998; 78: 491–495. PMID: [9797139](#)
46. Matowe WC, Ginsberg J. Effects of the diacylglycerol kinase inhibitor, R59022, on TSH-stimulated iodide organification in porcine thyroid cells. *Pharmacology.* 1996; 53: 376–383. PMID: [9032802](#)

47. van Zeijl L, Ponsioen B, Giepmans BNG, Ariaens A, Postma FR, Várnai P, et al. Regulation of connexin43 gap junctional communication by phosphatidylinositol 4,5-bisphosphate. *J Cell Biol.* 2007; 177: 881–891. PMID: [17535964](#)
48. Ogawa T, Hayashi T, Kyoizumi S, Kusunoki Y, Nakachi K, MacPhee DG, et al. Anisomycin downregulates gap-junctional intercellular communication via the p38 MAP-kinase pathway. *J Cell Sci.* 2004; 117: 2087–2096. PMID: [15054109](#)
49. Upham BL, Trosko JE. Oxidative-dependent integration of signal transduction with intercellular gap junctional communication in the control of gene expression. *Antioxid Redox Signal.* 2008; 11: 297–307.
50. Kim JH, Choi SH, Kim J, Lee BK, Lee KW, Lee HJ. Differential regulation of the hydrogen-peroxide-induced inhibition of gap-junction intercellular communication by resveratrol and butylated hydroxyanisole. *Mutat Res.* 2009; 671: 40–44. doi: [10.1016/j.mrfmmm.2009.08.011](#) PMID: [19720069](#)
51. Nielsen M, Ruch RJ, Vang O. Resveratrol reverses tumor-promoter-induced inhibition of gap-junctional intercellular communication. *Biochem Biophys Res Commun.* 2000; 275: 804–809. PMID: [10973802](#)
52. Spadaro F, Ramoni C, Mezzanzanica D, Miotti S, Alberti P, Cecchetti S, et al. Phosphatidylcholine-specific phospholipase C activation in epithelial ovarian cancer cells. *Cancer Res.* 2008; 68: 6541–6549. doi: [10.1158/0008-5472.CAN-07-6763](#) PMID: [18701477](#)
53. Wang N, Sun C, Huo S, Zhang Y, Zhao J, Zhang S, et al. Cooperation of phosphatidylcholine-specific phospholipase C and basic fibroblast growth factor in the neural differentiation of mesenchymal stem cells in vitro. *International Journal of Biochemistry & Cell Biology.* 2008; 40: 294–306.
54. Liu X, Zhao QT, Araki S, Zhang SL, Miao JY. Contrasting effects of phosphatidylinositol- and phosphatidylcholine-specific phospholipase C on apoptosis in cultured endothelial cells. *Endothelium-Journal of Endothelial Cell Research.* 2006; 13: 205–211. PMID: [16840176](#)
55. Guan X, Ruch RJ. Gap junction endocytosis and lysosomal degradation of connexin43-P2 in WB-F344 rat liver epithelial cells treated with DDT and lindane. *Carcinogenesis.* 1996; 17: 1791–1798. PMID: [8824497](#)
56. Guan X, Wilson S, Schlender KK, Ruch RJ. Gap-junction disassembly and connexin 43 dephosphorylation induced by 18 beta-glycyrrhetic acid. *Mol Carcinog.* 1996; 16: 157–164. PMID: [8688151](#)
57. Martinez AD, Saez JC. Arachidonic acid-induced dye uncoupling in rat cortical astrocytes is mediated by arachidonic acid byproducts. *Brain Res.* 1999; 816: 411–423. PMID: [9878857](#)
58. Sai K, Upham BL, Kang KS, Hasegawa R, Inoue T, Trosko JE. Inhibitory effect of pentachlorophenol on gap junctional intercellular communication in rat liver epithelial cells in vitro. *Cancer Lett.* 1998; 130: 9–17. PMID: [9751251](#)

V. **Babica, P.***, Zurabian, R., Kumar, E.R., Chopra, R., Mianecky, M.J., Park, J.-S., Jaša, L., Trosko, J.E., Upham, B.L., 2016. Methoxychlor and vinclozolin induce rapid changes in intercellular and intracellular signaling in liver progenitor cells. *Toxicological Sciences* 153, 174–185.

Methoxychlor and Vinclozolin Induce Rapid Changes in Intercellular and Intracellular Signaling in Liver Progenitor Cells

Pavel Babica,^{*,†,‡,1} Rimma Zurabian,^{‡,§} Esha R. Kumar,[‡] Rajus Chopra,[‡] Maxwell J. Miannecki,[‡] Joon-Suk Park,^{‡,¶} Libor Jaša,^{*,†} James E. Trosko,[‡] and Brad L. Upham[‡]

*Department of Experimental Phycology and Ecotoxicology, Institute of Botany, Brno 60200, Czech Republic; [†]RECETOX, Faculty of Science, Masaryk University, Brno 62500, Czech Republic; [‡]Department of Pediatrics and Human Development, and Institute for Integrative Toxicology, Michigan State University, East Lansing, Michigan 48824; [§]Department of Microbiology and Parasitology, Faculty of Medicine, National Autonomous University of Mexico, CdMx, 04510, Mexico; and [¶]Laboratory Animal Center, Daegu-Gyeongbuk Medical Innovation Foundation, Daegu, Korea

¹To whom correspondence should be addressed at Department of Experimental Phycology and Ecotoxicology, Institute of Botany, Lidicka 25/27, Brno 60200, Czech Republic. Fax: +420 541 126 231. E-mail: pavel.babica@centrum.cz.

ABSTRACT

Methoxychlor (MXC) and vinclozolin (VIN) are well-recognized endocrine disrupting chemicals known to alter epigenetic regulations and transgenerational inheritance; however, non-endocrine disruption endpoints are also important. Thus, we determined the effects of MXC and VIN on the dysregulation of gap junctional intercellular communication (GJIC) and activation of mitogen-activated protein kinases (MAPKs) in WB-F344 rat liver epithelial cells. Both chemicals induced a rapid dysregulation of GJIC at non-cytotoxic doses, with 30 min EC₅₀ values for GJIC inhibition being 10 μM for MXC and 126 μM for VIN. MXC inhibited GJIC for at least 24 h, while VIN effects were transient and GJIC recovered after 4 h. VIN induced rapid hyperphosphorylation and internalization of gap junction protein connexin43, and both chemicals also activated MAPK ERK1/2 and p38. Effects on GJIC were not prevented by MEK1/2 inhibitor, but by an inhibitor of phosphatidylcholine-specific phospholipase C (PC-PLC), resveratrol, and in the case of VIN, also, by a p38 inhibitor. Estrogen (ER) and androgen receptor (AR) modulators (estradiol, ICI 182,780, HPTE, testosterone, flutamide, VIN M2) did not attenuate MXC or VIN effects on GJIC. Our data also indicate that the effects were elicited by the parental compounds of MXC and VIN. Our study provides new evidence that MXC and VIN dysregulate GJIC via mechanisms involving rapid activation of PC-PLC occurring independently of ER- or AR-dependent genomic signaling. Such alterations of rapid intercellular and intracellular signaling events involved in regulations of gene expression, tissue development, function and homeostasis, could also contribute to transgenerational epigenetic effects of endocrine disruptors.

Key words: gap junctional intercellular communication; endocrine disruptors; mitogen-activated protein kinases; phosphatidylcholine-specific phospholipase C; epigenetic toxicity; non-genomic signaling.

Methoxychlor (MXC) and vinclozolin (VIN) represent well-recognized environmental endocrine disrupting compounds (EDCs). Xenoestrogenic MXC and antiandrogenic VIN have been demonstrated to induce adverse effects on development and

function of both male and female reproductive system, neuro-endocrine, and immune system, and to alter reproductive and social behavior (Manikkam *et al.*, 2014; van Ravenzwaay *et al.*, 2013). These chemicals affect not only prenatally or postnatally

exposed organisms, but also alter epigenetic programming of germ cells and transmit their adverse effects from the exposed (grand)parental generations to unexposed offspring (Anway *et al.*, 2005; Skinner, 2014).

As for many other EDCs, interactions with nuclear sex hormone receptors and their ligand-dependent transcription factor activity (so-called genomic signaling mechanism) have been implicated as the principal molecular mechanism responsible for endocrine disrupting activity of MXC and VIN (Manikkam *et al.*, 2014; Ozgyin *et al.*, 2015; van Ravenzwaay *et al.*, 2013). Although MXC is a weak estrogen receptor (ER) agonist, its hydroxylated metabolites, such as HPTE (2,2-bis-(p-hydroxyphenyl)-1,1,1-trichloroethane), are potent ER α agonists and weak antagonists to both ER β and androgen receptor (AR) (Gaido *et al.*, 2000). VIN and its major metabolites, M1 and M2, are potent antagonists of AR, and moderate agonists to progesterone and ERs (Molina-Molina *et al.*, 2006). However, there is increasing evidence that endogenous hormones, as well as environmental EDCs, can also act via mechanisms of non-genomic signaling, which are independent of ligand-dependent transactivation function of nuclear receptors (Trevino *et al.*, 2015; Watson *et al.*, 2014; Wong and Walker, 2013). Non-genomic signaling mechanisms altered by EDCs include rapid modulations of ion levels or activities of ion channels, protein kinases, phospholipases, or adenylate cyclase. Coincidentally, alternations of these signaling events and pathways have been also implicated in dysregulation of gap junctional intercellular communication (GJIC) between coupled cells, which was a phenomenon initially recognized as an important mechanism in the concept of 'epigenetic toxicology' (Trosko *et al.*, 1993, 1998). Exchange of various ions, nutrients, secondary messengers or microRNAs through gap junctional connexin channels represents a key mechanism required for coordination of signal transduction pathways and control of gene expression within a tissue, which is essential for proper tissue development, function and regeneration (Trosko, 2011). GJIC is a process strictly regulated via transcriptional, translational, post-translational and epigenetic mechanisms (Axelsen *et al.*, 2013; Vinken *et al.*, 2009a,b). These non-endocrine dependent mechanisms might be involved in VIN and MXC induced increases in liver hypertrophy and hepatocellular carcinomas in various rodent model systems (HSDB, 2010; Reuber, 1980).

Many EDCs, such as bisphenol A, DDT, lindane or phthalates, were found to induce rapid dysregulation of GJIC, with their effects shown to be structure-dependent and mediated via mechanisms including activation of specific kinases or phospholipases (Sovadinova *et al.*, 2015; Vinken *et al.*, 2009b). These data indicate that dysregulation of GJIC could be the key cellular process altered by EDCs via mechanisms independent on genomic signaling, which might contribute to their disruptive effects on epigenetic regulations, developmental programming, tissue development, and homeostasis.

Although MXC and VIN are being intensively investigated as prototypical EDCs in order to understand their mechanisms of endocrine disruption, epigenetic regulation and transgenerational inheritance (Manikkam *et al.*, 2014; Ozgyin *et al.*, 2015; Skinner, 2014), and even though rapid alterations of cellular signaling are being increasingly recognized as an important mechanism contributing to the adverse effects of EDCs (Trevino *et al.*, 2015; Watson *et al.*, 2014; Wong and Walker, 2013), there is only limited information about effects of MXC and VIN on rapid intercellular and intracellular signaling events, such as GJIC or mitogen-activated protein kinases (MAPKs).

Thus, we used MXC and VIN as model EDCs to investigate their rapid effects on GJIC and related signal transduction pathways. These effects, which are relevant for transcriptional and epigenetic control of gene expression and normal cell behavior (Trosko, 2011), were studied in a rat liver epithelial cell line WB-F344. This cell line is a well-established *in vitro* model for assessment of GJIC and mechanistic studies in responses to environmental contaminants (Sovadinova *et al.*, 2015; Upham *et al.*, 2007, 2008), which has been validated by *in vivo* studies (Sai *et al.*, 2000; Upham *et al.*, 2009) and matches the most extensively used rodent model system, F344 rats, in the National Toxicology Program. Both of these EDCs exhibited dose, time and mechanistic differences on GJIC, MAPKs, and phospholipase C, which were elicited by the parental compounds and occurred independently of ER- or AR-mediated genomic mechanisms. We also determined that resveratrol, a natural chemopreventive and phytoestrogenic agent, prevented MXC- and VIN-induced dysregulation of GJIC.

MATERIALS AND METHODS

Chemicals. 1,1,1-Trichloro-2,2-bis(4-hydroxyphenyl)ethane (HPTE), 1-methylanthracene (1-MeA), 12-O-tetradecanoylphorbol-13-acetate (TPA), 17 β -estradiol (E2), anisomycin, epidermal growth factor (EGF), flutamide, ICI 182 780, MXC, SB202190, resveratrol, testosterone and VIN were purchased from Sigma-Aldrich Chemical (St Louis, Missouri). D609 and U0126 were obtained from Tocris Bioscience (Ellisville, Missouri), and 3',5'-dichloro-2-hydroxy-2-methylbut-3-enamide (VIN M2) from Cayman Chemical (Ann Arbor, Michigan). Acetonitrile and acetic acid were provided by EMD Chemicals (Gibbstown, New Jersey), acetic acid, ammonium fluoride, ethanol, dimethyl sulfoxide (DMSO) and methanol were purchased from Sigma-Aldrich. Milli-Q water was produced using Milli-Q Synthesis device (EMD Millipore, Billerica, Massachusetts). Anisomycin, E2, flutamide, ICI 182,780, MXC, HPTE, resveratrol, testosterone, U0126, VIN and VIN M2 were dissolved in acetonitrile, SB202190 in DMSO, TPA in ethanol, EGF in phosphate buffered saline (PBS), and D609 in Milli-Q water.

Cell culture. The normal, non-tumorigenic, diploid WB-F344 rat liver epithelial cell line was obtained from Drs. Grisham and Tsao, University of North Carolina (Tsao *et al.*, 1984). These stem-like cells share many characteristics with oval cells and hepatocyte progenitor cells present in the normal adult rat liver (Coleman *et al.*, 1997; Tsao *et al.*, 1984). The cells were grown in a modified Eagle's Minimum Essential Medium prepared according to (Kao *et al.*, 1997) from powdered formula (Gibco 78-5470EF, Life Technologies, Grand Island, New York), and supplemented with 1 g/l sodium bicarbonate, 7.635 g/l sodium chloride, 1 mM sodium pyruvate (Sigma-Aldrich), 5% (v/v) fetal bovine serum and 10 μ g/ml of gentamicin (Life Technologies). Cells were routinely cultured in 75 cm² tissue culture flasks (Costar, Cambridge, Massachusetts) in humidified 5% CO₂ atmosphere at 37 °C, and routinely passaged every other day.

Experimental setup. All experiments were done with confluent cultures obtained after seeding the cells at the density of 20–40 $\times 10^3$ cell/cm² and 48 or 72 h of growth. For immunostaining, WB-F344 cells were seeded onto sterile round glass cover slips (Fisher Scientific, Vernon Hills, Illinois) placed into 12-well plates (Costar). For other bioassays, the cells were grown on 35 mm-diameter tissue culture Petri dishes (Costar). The tested chemicals were pipetted from the stock solution and added directly to the cell cultures and then incubated for desired

exposure time. In experiments with signaling enzyme inhibitors, resveratrol, and ER or AR modulators, the cells were first pretreated with the chemical of interest, and then exposed to a GJIC-inhibitor or vehicle. Concentrations and incubation times of signaling enzyme inhibitors were based on previous publications (Ogawa *et al.*, 2004; Sovadinova *et al.*, 2015) and efficiency of these pretreatments was verified by positive controls with model chemicals known to dysregulate GJIC by a mechanism dependent on a given pathway: EGF was used as a positive control for U0126 (MEK1/2 inhibitor), anisomycin for SB202190 (p38 inhibitor), 1-MeA for D609 (PC-PLC inhibitor) and resveratrol. Pretreatments with ER agonist (E2, HPTE), ER antagonists (ICI 182 780), AR agonist (testosterone) and AR antagonists (flutamide, VIN M2) were done using concentrations ranging from 1 to 250 μM and 30 or 120 min incubation time.

In all experiments, the concentration of organic solvents did not exceed 1% (v/v) and corresponding vehicle controls were included in each experiment.

Cell viability assay. Exposed cells were washed with PBS and incubated for 1 h with 150 $\mu\text{g}/\text{ml}$ neutral red. After incubation, the cells were rinsed with PBS and neutral red was extracted by 1% glacial acetic acid in 50% ethanol. Neutral red uptake was quantified by absorbance measurement at 540 nm (reference wavelength = 690 nm) using a Beckman DU 7400 spectrophotometer (Beckman Instruments, Schaumburg, Illinois). Each experiment was carried out in duplicates and repeated at least 3 times independently.

Bioassay of GJIC. The scalpel loading-dye transfer (SL-DT) technique was adapted after the method of (El Fouly *et al.*, 1987) and done according to previously published protocol (Upham, 2011). Briefly, the exposed cells were washed with calcium- and magnesium-supplemented PBS (CaMg-PBS). Lucifer yellow CH dilithium salt (Sigma-Aldrich, 1 mg/ml in CaMg-PBS) was added to the cells and the dye introduced to the monolayer by 3 parallel cuts with a surgical scalpel blade. After 3 min, the cells were rinsed with CaMg-PBS and fixed with a 4% formaldehyde solution in PBS. Microscopic images were taken with 20 \times objective using a Nikon microscope equipped with Nikon Cool Snap EZ CCD camera (Nikon Instruments, Melville, New York). The extent of GJIC was evaluated using ImageJ as a function of the area of the cells stained with lucifer yellow dye. The fluorescence area from the positive control treated with 1-MeA (70 μM , 10 min) inducing complete inhibition of GJIC (Upham *et al.*, 2008) was subtracted from each treatment. Each experiment was repeated at least 3 times independently.

Western blot analysis. Western blots were done according to previously published protocol (Trosko *et al.*, 2000). All chemicals (eg ammonium persulfate, sodium dodecyl sulfate, Tween 20, Tris, glycine, acrylamide, and tetramethylethylenediamine, 2 \times SDS loading buffer) were purchased from Bio-Rad Laboratories (Hercules, California), unless otherwise specified. As optimized and used previously (Upham *et al.*, 2009), the cells were placed in a serum-free cell culture medium for 4 h prior the addition of the tested chemicals to minimize basal activity of MAPKs (Pirkmajer and Chibalin, 2011). TPA (50 nM, 30 min) was used as a positive control to induce MAPK ERK1/2 and Cx43 phosphorylation, 1-MeA (70 μM , 30 min) was used as a positive control for MAPK ERK1/2 and p38 activation (Upham *et al.*, 2008). After exposure, the cells were rinsed with PBS and the proteins extracted with 20% SDS (v/v) containing protease and phosphatase inhibitors (Trosko *et al.*, 2000). Cell lysates were homogenized using an

ultrasonic probe (BioLogics, Manassas, Virginia), and protein concentrations were determined using the DC protein kit (Bio-Rad). Proteins (15 μg) were separated using SDS-PAGE on 12.5% polyacrylamide gels and then electrophoretically-transferred onto Immobilon-P membrane (EMD Millipore) using Mini Protean apparatus (Bio-Rad). Membranes were blocked with 5% non-fat dry milk (w/v) in Tris-buffered saline with 0.1% Tween 20 (v/v), and then incubated overnight at 4 $^{\circ}\text{C}$ with a primary antibody diluted with the blocking solution.

Following antibodies and dilutions were used: 1:2000 diluted rabbit polyclonal antibodies against phosphorylated p38 (Life Technologies, Cat. No. 36-8500), phosphorylated ERK1/2 (Cell Signaling Technology, Danver, Massachusetts, Cat. No. 9101S), total p38 (Cell Signaling Technology, Cat. No. 9212) and total ERK1/2 (Cell Signaling Technology, Cat. No. 9102), 1:1000 diluted rabbit polyclonal antibodies against ER α (Santa Cruz Biotechnology, Dallas, Texas, Cat. No. sc-542) and AR (Santa Cruz Biotechnology, Cat. No. sc-816), 1:1000 diluted mouse monoclonal antibody against Cx43 (BD Transduction Lab, Franklin Lakes, New Jersey, Cat. No. C13720), 1:5000 diluted mouse monoclonal antibody against GAPDH (EMD Millipore, Cat. No. MAB374) and rabbit polyclonal antibody against α -tubulin (Abcam, Cambridge, UK, Cat. No. AB15246). After the washing step, membranes were incubated with 1:1000 diluted secondary antibodies for 2 h at room temperature: horse radish peroxidase-conjugated anti-rabbit (Cat. No. NA934) or anti-mouse (Cat. No. NA931) IgG antibodies obtained from GE Life Sciences (Arlington Heights, Illinois). Western blot signals were detected using HyGLO Chemiluminescent HRP reagents and HyBlot CL film (Denville Scientific, South Plainfield, New Jersey). All MXC and VIN treatments for MAPK and Cx43 detection were done in duplicate, and the time-response experiment was repeated 2 times independently. Cell lysates from mouse Leydig TM3 cell line, mouse Sertoli TM4 cell line, hER-transfected human cervical adenocarcinoma cell line HeLa-9903, and AIZ-AR cell line (derived from AR-expressing human prostate carcinoma epithelial cell line 22Rv1) were used as positive controls for ER α or AR detection.

Immunocytochemistry. The cells were rinsed with ice cold PBS and fixed with 5% acetic acid in methanol (v/v) at -20°C for 20 min. The non-specific binding sites were blocked with 10% normal goat serum (Life Technologies) for 1 h at room temperature. The cells were incubated overnight at 4 $^{\circ}\text{C}$ with mouse monoclonal anti-Cx43 antibody (BD Transduction Lab, Cat. No. C13720) diluted 1:200 with 1% bovine serum albumin (w/v, BSA, Sigma-Aldrich) in PBS-0.1% Tween 20 (v/v, PBST). After wash with PBST, the cells were incubated for 1 h at room temperature with secondary Cy3-conjugated monoclonal anti-mouse IgG antibody (Jackson ImmunoResearch Lab., West Grove, PA, Cat. No. 115-165-100) diluted 1:1000 in 1% BSA-PBST. After wash with PBST and nuclear counterstaining (5 min with 0.1 $\mu\text{g}/\text{ml}$ DAPI, Sigma-Aldrich), the cover slips were mounted using ProLong Antifade reagent (Life Technologies). TPA (50 nM) was used as a positive control inducing Cx43 translocation and internalization (Upham *et al.*, 2008). Negative controls for non-specific antibody binding were prepared using non-treated cells subjected to the same staining procedure without either the primary or the secondary antibody incubation. Fluorescent images were obtained with a Nikon Epi-fluorescent microscope using an 100 \times oil immersion objective and a SPOT RT digital camera (Diagnostic Instruments, Sterling Heights, Michigan).

LC-MS/MS analysis of HPTE and VIN M2. Volume of cell culture media in 35 mm dishes containing confluent cultures of WB-F344 cells was adjusted to 1 ml and then 25 μM of MXC or 250 μM of VIN was added. The dishes were incubated for 10 min up to 24 h in the CO_2 incubator. Method recovery was determined in experiments with the addition of 25 μM of HPTE or 250 μM of VIN M2 followed by brief incubation (<1 min). After incubation, 250 μl of acetonitrile was added to each dish, the cells were extracted using ultrasonic probe for 1 min, and the extracts were collected and filtered through 0.45 μm PVDF syringe filter. HPTE and VIN M2 were analyzed with Agilent 1260 Infinity (Agilent Technologies Inc.) using Agilent Poroshell 120 EC-C18 ($2.1 \times 10 \text{ mm}$, 2.7 μm) column and Guard column ($2.1 \times 5 \text{ mm}$, 2.7 μm). The injection volume was 5 μl and the flow rate was set to 0.3 ml/min. The mobile phase (A) was 0.2 mM ammonium fluoride in water, and the mobile phase (B) was acetonitrile. Gradient conditions were 90% of (A), ramped using a linear gradient to 33.5% (A) over 5 min, then ramped to 0% of (A) from 5 to 6 min and held until 11 min. Under these conditions, the retention time was 6.5 and 7.1 min for HPTE and VIN M2, respectively.

An Agilent 6406 triple quadrupole mass spectrometer with an electrospray ionization source was used in a negative mode: a nitrogen gas at temperature 150 $^\circ\text{C}$ and flow 5 l/min, nebulizer pressure 45 psi, a sheath nitrogen gas at temperature 250 $^\circ\text{C}$ and flow 11 l/min, capillary voltage 3500 V and nozzle voltage 500 V. The dwelling time of each compound was 200 ms. The HPTE (precursor at m/z 314.9) was fragmented using collision energies of 1 V to produce characteristic fragment ions at m/z 279.1 and 243.2. The VIN M2 (precursor at m/z 258) was fragmented using collision energies of 9 and 33 V to produce characteristic fragment ions at m/z 160 and 35. Recovery of the method from the cell culture was 72% for HPTE and 74% for M2, method limit of detection was 1.6 nM for HPTE and 1 nM for VIN M2.

Statistical analyses. Quantitative data from all bioassays (SLDT, neutral red uptake, Western blot densitometry) were compared with the vehicle or negative control from the corresponding experiment and reported as the fraction of the control (FOC). Data from independently repeated experiments were combined and used for all statistical analyses and comparisons. One-way ANOVA followed by Dunnett's post-hoc test was used for comparing data passing normality (Shapiro-Wilk's test) and equal variance tests, whereas Kruskal-Wallis ANOVA on ranks followed by Dunn's test was used for comparing data with unequal variances and/or non-normal distribution. *P*-values lower than .05 were considered as statistically significant. Curve-fitting was done using non-linear, 4-parameter sigmoidal regression model ($f = y_0 + a/(1 + \exp(-(x-x_0)/b))$). All calculations were done in SigmaPlot (Systat Software, San Jose, California).

RESULTS

Effects of MXC and VIN on GJIC

Effects of MXC and VIN on GJIC were first investigated after a 30 min exposure of WB-F344 cells to varying concentrations of the chemicals. Statistically significant inhibition of GJIC was observed at concentrations of MXC $\geq 5 \mu\text{M}$, with concentrations above 20 μM causing almost complete inhibition of GJIC (Figure 1A). The effective concentration that caused 50% inhibition of GJIC (EC_{50}) for MXC-induced inhibition of GJIC was estimated using nonlinear regression to be 9.5 μM . VIN induced slight, but statistically significant, inhibition of GJIC at 50 μM , with the

effects becoming more pronounced with increasing concentration of VIN and resulting into nearly complete inhibition of GJIC after exposure to concentrations $\geq 200 \mu\text{M}$ (Figure 1A). Estimated EC_{50} value for GJIC inhibition by 30 min treatment with VIN was 126 μM .

Concentrations of MXC and VIN shown to induce complete inhibition of GJIC (100%, EC_{100}) after 30 min exposure, ie, 25 μM methoxychlor and 250 μM VIN, were then used to investigate time-dependent effects on GJIC during 1 min–24 h interval (Figure 1B). An observable reduction of GJIC by both chemicals was seen within a 1 min exposure, which was most apparent in the case of VIN, where the GJIC level decreased by approximately 40%. Time required for 50% inhibition of GJIC was estimated using nonlinear regression to be 4.2 min for 25 μM MXC, and 1.4 min for 250 μM VIN. For both chemicals, complete inhibition of GJIC was observed after 10 min (Figures 1B and 5A). However, GJIC remained inhibited up to 24 h of exposure to MXC, whereas the inhibitory effects of VIN on GJIC were only transient. After VIN treatment, the inhibition of GJIC was observed during the initial 120 min incubation with the chemical, then followed by restoration of cell-to-cell communication during 4–24 h even in the continuous presence of the chemical in the medium (Figure 1B). GJIC was restored to 50% of the control approximately after 3 h of VIN treatment.

The ability of cells to recover from the inhibition GJIC by MXC or VIN was determined by measuring GJIC after a 30 min pulsed-treatment with either MXC (25 μM) or VIN (250 μM), followed by the cell transfer into toxicant-free medium. Treatment with toxicants resulted in complete inhibition of GJIC, as apparent from the 0 min time point in the Figure 1C, where no time for recovery was allowed. For MXC, significant recovery of communication began after 120 min in toxicant-free medium. The recovery half-time for MXC was estimated to be 168 min. Near normal levels of GJIC (75%) began after 5 h and remained at this level up to 24 h of recovery time (Figure 1C). Recovery from VIN-induced inhibition of GJIC was observed within 5 min after the transfer to toxicant-free medium with a recovery half-time estimated to be 8.1 min. After 60 min, recovery from VIN-induced inhibition of GJIC was 100% and was not significantly different from the control, untreated cells (Figure 1C).

Effects of MXC and VIN on Cell Viability

The concentrations of MXC and VIN needed to induce inhibition of GJIC were not lethally cytotoxic nor did they reduce cell viability, as evaluated using the neutral red uptake assay (Supplementary Figure S1). Statistically significant reduction of the cell viability was observed only after prolonged incubations with 50 μM MXC or 400–500 μM VIN, which represent concentrations 8–10 times higher than concentrations causing significant reduction of GJIC levels, and 2 times higher than concentrations required to induce complete inhibition of GJIC (Figure 1A). Furthermore, the ability to recover from inhibition of GJIC after a pulsed treatment also indicates these compounds are not lethal to the cells.

Transformation of MXC and VIN in the Cell Cultures

Concentrations of HPTE and VIN M2, the major metabolites of MXC and VIN, were analyzed in the cultures of WB-F344 cells exposed to 25 μM MXC or 250 μM VIN for 10 min to 24 h. Throughout the experiment, HPTE was not detected using a sensitive LC-MS/MS method (Figure 1D). A gradual increase of concentrations of VIN metabolite M2 was observed. Within the first 10 min of exposure, concentrations of M2 increased from non-detectable levels to 4 μM (1.5% of the nominal concentration of

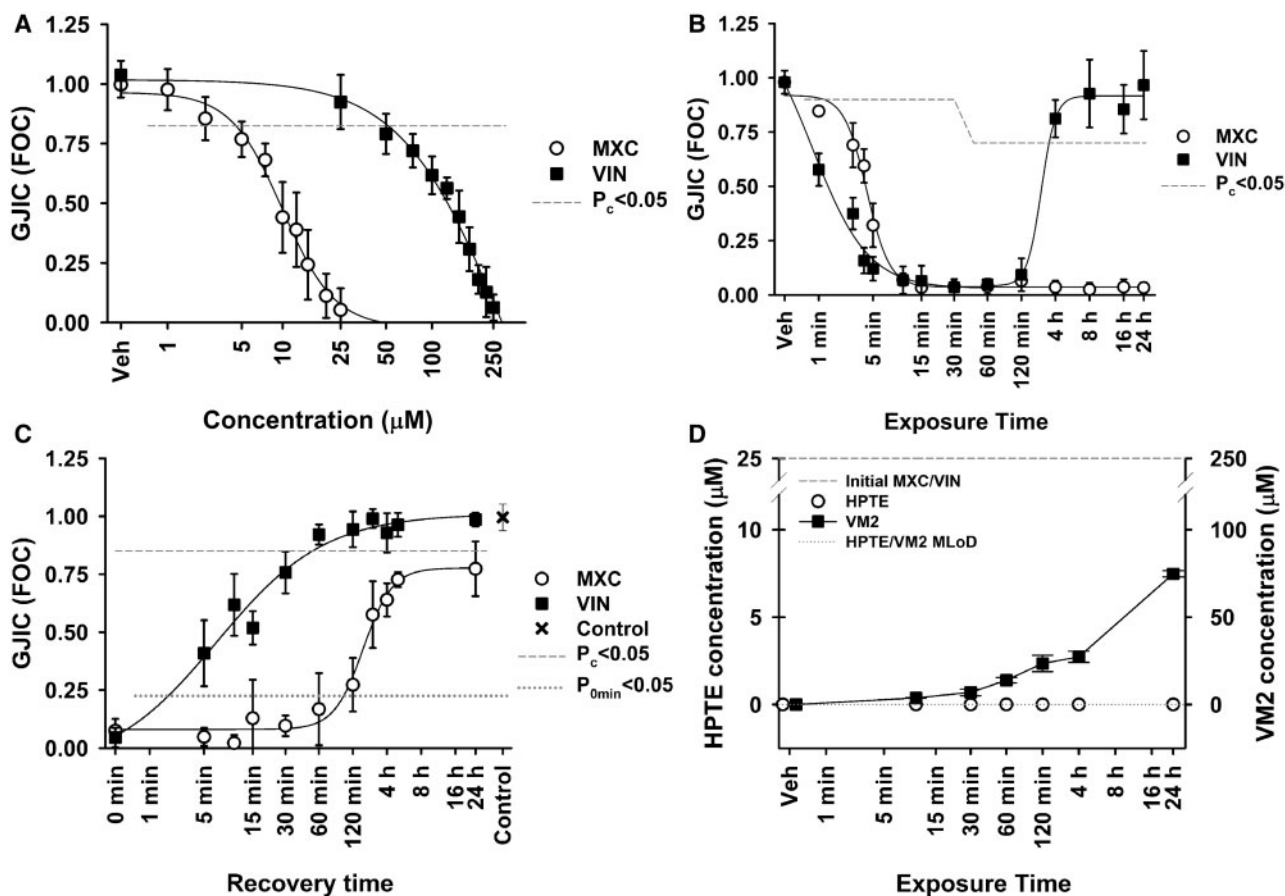


FIG. 1. Effects of MXC and VIN on GJIC in WB-F344 cells and transformation of the toxicants in the cell culture system. **A**, Concentration-dependent effects of MXC (1–50 μM) and VIN (25–250 μM) after 30 min of exposure, **B**, Time-dependent effects of MXC (25 μM) and VIN (250 μM) after 1 min–24 h exposure, **C**, Recovery of GJIC from inhibition induced by 30 min treatment with MXC (25 μM) or VIN (250 μM) followed by removal of the exposure medium and incubation (0 min–24 h) in MXC-free or VIN-free cell culture medium prior the evaluation of GJIC. GJIC was evaluated using SL-DT assay, the effects of the chemicals were compared with the dye transfer in the negative control and expressed as FOC. Data represent means ± SD from at least 3 independent experiments. Data points below the dash line were significantly different from the vehicle (Veh) control ($P_c < 0.05$), whereas data points above the dotted line in the recovery experiment were significantly different from GJIC level in the cells exposed for 30 min to MXC or VIN with no recovery time ($P_{0min} < 0.05$). ANOVA followed by Dunnett's post hoc test was used for statistical comparisons. **D**, Analysis of MXC metabolite HPTE and VIN metabolite M2 (VM2) in WB-F344 cultures exposed to MXC (25 μM) or VIN (250 μM). Data represent means ± SD from measurements in duplicate. MLOD indicates the method limit of detection.

the parental compound). The concentrations of VIN M2 continued to further increase to 14 μM (5.6%) after 60 min, 27 μM (11%) after 240 min, and reach 75 μM (30% of the nominal) after 24 h incubation (Figure 1D). Although concentrations of VIN M2 seems to represent only a small fraction of the nominal concentration of VIN, the real extent of VIN transformation was probably much greater, as concentrations of VIN M1 were reported to be even 5–6 times higher than concentrations of M2 formed by spontaneous VIN hydrolysis during incubation in a culture medium without cells (Bursztyka et al., 2008).

Role of ERs and ARs in GJIC Inhibition Induced by MXC and VIN

Results of Western blotting indicated an expression of ERα or its isoforms in WB-F344 cell line (Supplementary Figure S2). However, effects of ER agonist E2 and ER antagonist ICI 182 780 were not found to dramatically reduce GJIC within 30 min to 24 h exposures to concentrations between 1 and 250 μM (Figs. 2A and B). HPTE, a MXC metabolite and also ERα agonist and ERβ antagonist, reduced GJIC communication (Figure 2C), but its effects were less pronounced and manifested after longer exposure times (6 h) than comparable or even lower concentrations of MXC (Figs. 1A

and B). Higher concentrations of HPTE (>100 μM) were associated with cytotoxic effects and thus not evaluated. Pretreatment with these modulators of ER (1–100 or 250 μM for 30–120 min) did not attenuate rapid inhibition of GJIC induced by 10 min treatment with MXC (Supplementary Figure S3).

In WB-F344 cells, there was no detectable expression of AR (Supplementary Figure S2). Testosterone, a natural AR ligand, did not significantly reduce GJIC (1–250 μM, 30 min–24 h, Figure 2D). Similar treatments with flutamide, an AR antagonist, resulted in a partial inhibition of GJIC after 120 min–6 h treatment with a concentration of 250 μM, which was associated with a cytotoxic effect occurring after 24 h exposure (Figure 2E). VIN metabolite M2, a potent antagonist of AR was capable to inhibit GJIC, although its effects appeared to be less potent and manifested more slowly than in the case of VIN (Figure 2F). Similarly to VIN, the inhibitory effects observed after 30 min with 100 μM M2 seemed to be only transient, whereas the effects of 250 μM treatment rather progressed over the time (Figure 2F). Pretreatments of WB-F344 cells with 1–250 μM testosterone, flutamide or M2 for 30–120 min did not prevent VIN-induced dysregulation of GJIC (Supplementary Figure S4).

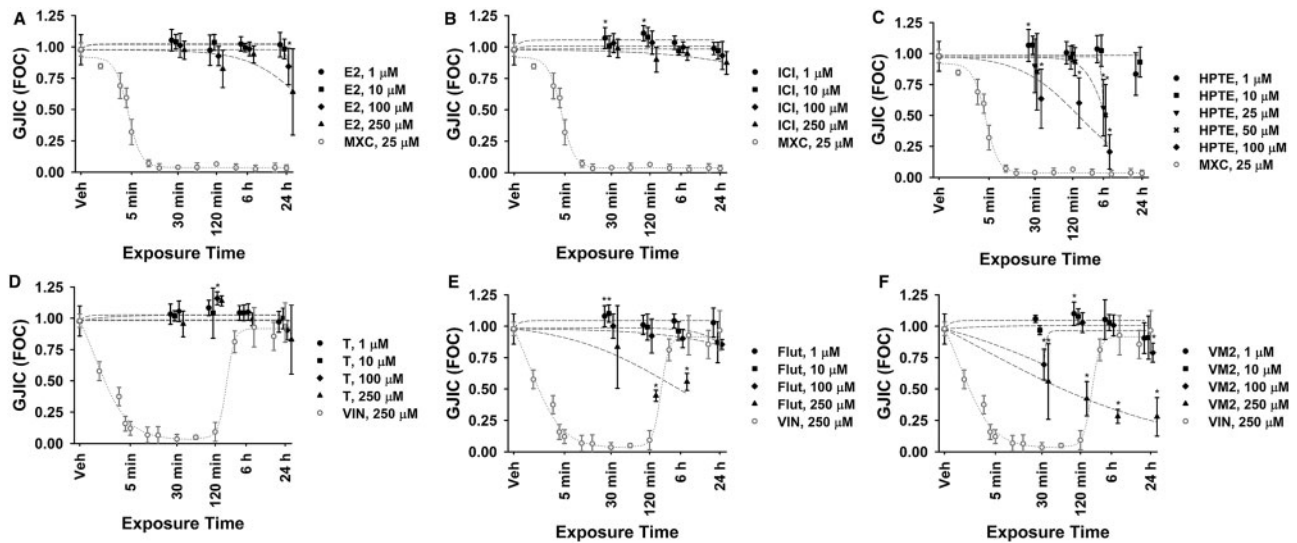


FIG. 2. Effects of ER and AR modulators on GJIC in WB-F344 cells. The cells were treated with (A) an ER agonist 17 β -estradiol (E2), (B) an ER antagonist ICI 182 780 (ICI), (C) an ER α /ER β agonist/antagonist HPTE (a MXC metabolite), (D) an AR agonist testosterone (T), and AR antagonists (E) Flutamide (Flut) and (F) VIN M2 (VM2, a VIN metabolite) for 30 min–24 h and GJIC was evaluated using SL-DT assay. The effects of the chemicals were compared with the dye transfer in the negative control and expressed as FOC. Time course of MXC (25 μ M) or VIN (250 μ M) induced inhibition of GJIC is shown for comparison. Data represent means \pm SD from at least 3 independent experiments. Asterisks indicate FOC values significantly different from the vehicle control (Kruskal-Wallis ANOVA on Ranks followed by Dunn's comparison method, $P < .05$).

Effects of MXC and VIN on the Gap Junction Protein Cx43

Because of the observed inhibition of GJIC by MXC and VIN, the effects of the chemicals on phosphorylation and cellular localization of gap junctional protein Cx43 were also examined. Western blots images showed that MXC (25 μ M) did not alter ratio of the 3 major Cx43 bands, P0, P1, P2, during the first 60 min of the exposure (Figs. 3A and B). Only after 120 min, MXC decreased the intensity of P2-band, i.e. the band corresponding to the hyperphosphorylated Cx43. Exposure to 25 μ M MXC for 10–30 min, which was shown to completely inhibit GJIC (Figure 1) did not affect intracellular localization of Cx43, since there were no apparent changes of immunostained Cx43 plaques in plasma membranes of exposed WB-F344 cells (Figure 3D). Cx43-band pattern was not altered after a 5 min exposure to 250 μ M VIN, but 10–30 min incubation with VIN resulted into hyperphosphorylation of Cx43, as indicated by simultaneous decrease in the intensity of nonphosphorylated Cx43 P0-band and increase in the intensity of hyperphosphorylated P2-band (Figs. 3A and C). These effects were similar to the effects of tumor promoting phorbol ester, TPA, which was used as a positive control. After 60 min exposure to VIN, Cx43 bands were restored to the pattern resembling the vehicle control, and then followed by a disappearance of the P2-band after 120 min. Unlike MXC, VIN caused a decrease of the number and intensity of membrane-associated Cx43 immunostained plaques which was similar to the effects of TPA (Figure 3D).

Effects of MXC and VIN on MAPK ERK1/2 and p38

Since MAPKs were implicated in the control of GJIC level and phosphorylation of Cx43, changes in activity of MAPK ERK1/2 and p38 were also investigated in response to MXC and VIN in WB-F344 cells. In concentration-response experiment, both MXC and VIN were found to increase the amount of phosphorylated ERK1/2 and p38 after a 30 min exposure time, with the most pronounced effects observed at concentrations corresponding to those required for complete inhibition of GJIC, ie, 25 μ M MXC and 250 μ M VIN (Supplementary Figure S5). Time-course experiments

revealed that ERK1/2 and p38 phosphorylation gradually increased during the exposure to 25 μ M MXC, becoming significantly activated after \geq 10–15 min and peaking between 30 and 60 min, but remaining significantly upregulated after 120 min (Figs. 4A and B). In contrast, VIN induced significant activation of both ERK1/2 and p38 within 5 min (Figs. 4C and D), which is the same time interval for the inhibition of GJIC (Figure 1B). The VIN-induced activation of ERK1/2 and p38 was sustained up to 60 min and then decreased close to the control level at 120 min (Figs. 4C and D). The levels of total (phosphorylated plus nonphosphorylated) ERK1/2 and p38, as well as α -tubulin, did not change significantly during the investigated exposure periods, indicating that the observed changes in the amount of phosphorylated MAPKs were caused by increased activation/phosphorylation, and not by an increase in MAPK gene expression via genomic mechanisms.

Mechanisms of GJIC Inhibition Induced by MXC and VIN

Finally, it was examined whether the effects of MXC and VIN on GJIC were mediated through the activation of ERK1/2, p38 or phosphatidylcholine-specific phospholipase C (PC-PLC), and also whether the inhibition of GJIC induced by a 10 min exposure to MXC (20–25 μ M) or VIN (200–250 μ M) can be prevented by resveratrol. Pretreatment of WB-F344 cells with MEK1/2 inhibitor, U0126, had no apparent effect on the downregulation of GJIC induced by either MXC or VIN (Figure 5), although U0126 effectively prevented ERK1/2-dependent inhibition of GJIC by the EGF, which was used as a positive control (Supplementary Figure S6).

Pretreatment with SB202190, an inhibitor of p38, partially attenuated the inhibition of GJIC elicited by 20 μ M MXC, but these effects diminished at 25 μ M (Figs. 5A and B). The effects of VIN on GJIC were completely prevented by pretreatment with SB202190, (Figs. 5A and C). Experiments with p38-dependent inhibitor of GJIC, anisomycin, confirmed that effective doses of SB202190 were achieved (Supplementary Figure S6).

For both MXC and VIN, inhibition of GJIC was prevented by pretreatment with PC-PLC inhibitor, D609, which maintained

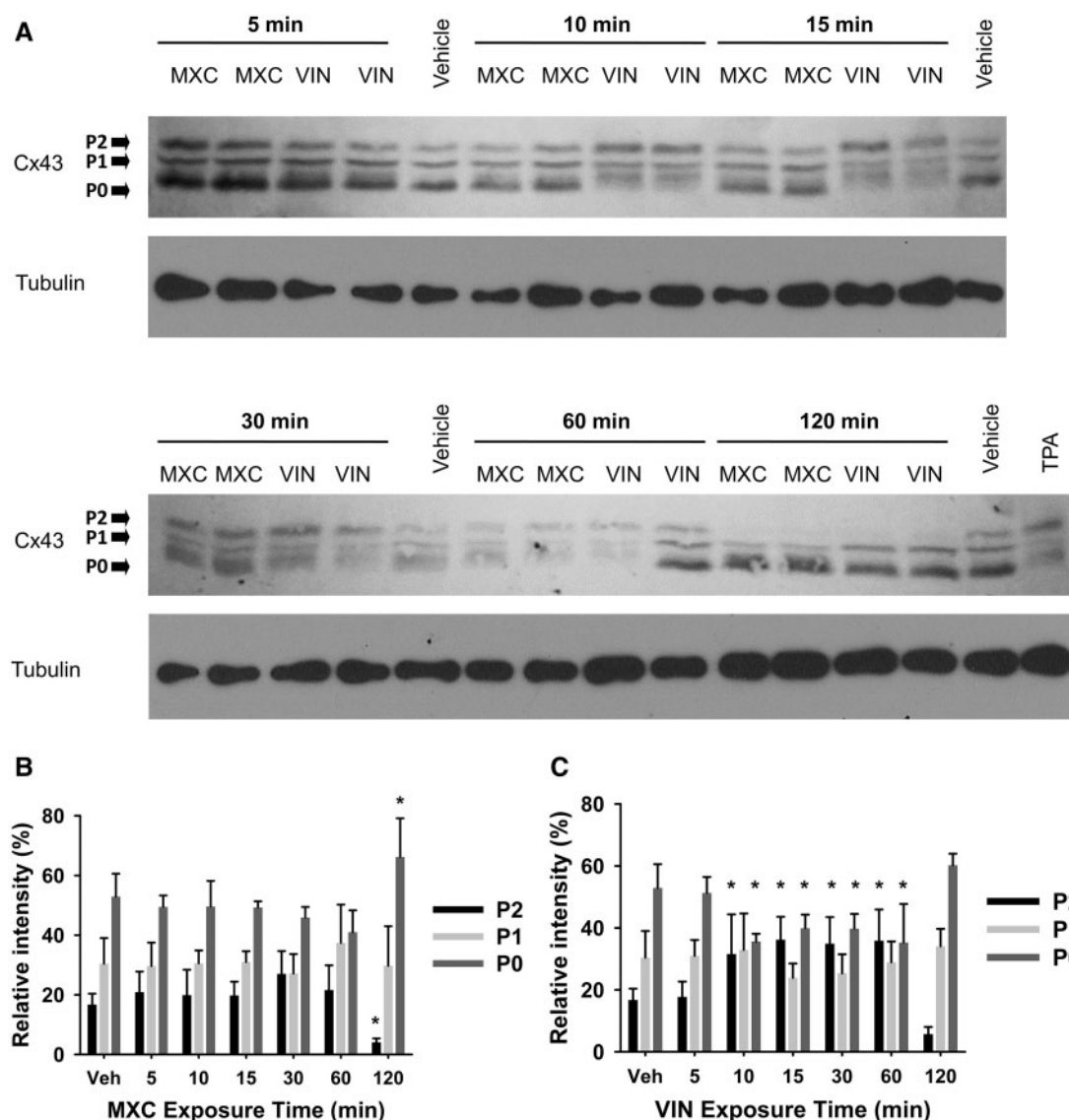


FIG. 3. Effects of MXC and VIN on gap junctional protein connexin43 (Cx43) in WB-F344 cells. A, Effects of MXC (25 μ M) or VIN (250 μ M) on phosphorylation status of Cx43 were detected after 5–120 min using Western blot analysis, where differences in Cx43 phosphorylation lead to differences in the protein electrophoretic mobility and to appearance of 3 major Cx43 bands labeled as P0, P1 and P2. TPA treatment (50 nM, 30 min) known to induce hyperphosphorylation of Cx43 characterized by increase of P2 band intensity was used as a positive control. Effects of MXC (B) and VIN (C) on changes in proportion of 3 Cx43 bands (P0, P1, P2) relative (%) to total Cx43 intensity in Western blot analysis. Data represent means \pm SD (n = 4). Asterisks indicate values significantly different from the vehicle (Veh) control (ANOVA followed by Dunnett's post hoc test, $P < .05$).

GJIC at levels not significantly different from the control after the addition of the studied chemicals (Figure 5). The effects of MXC and VIN on GJIC were also blocked by 15 min pretreatment of WB-F344 cells with resveratrol (Figure 5), which was similar to the effects of resveratrol on another PC-PLC-dependent inhibitor of GJIC, 1-MeA (Supplementary Figure S6).

DISCUSSION

The rapid inhibition of GJIC in response to MXC or VIN is comparable with the effects reported for several other EDCs. In fact, recognized EDCs, such as lindane, chlordane, and DDT, represent the environmental toxicants which were for the first time identified to inhibit GJIC (Tsushimoto et al., 1983). MXC was initially reported to inhibit GJIC in primary bovine oviductal cells after 1–5 h exposure to concentrations ≥ 16 –32 μ M (Tiemann and

Pohland, 1999). Even more rapid and pronounced inhibition of GJIC by MXC (30-min EC_{50} = 9.5 μ M, 50% inhibition achieved within 5 min) was observed in this study, which is comparable to several other chlorinated compounds known to inhibit GJIC in WB-F344 cells within 5–60 min exposures to concentrations between 10 and 100 μ M (Guan et al., 1995; Machala et al., 2003; Matesic et al., 1994; Ruch et al., 1994). GJIC dysregulation by VIN has not been previously reported. Effective concentrations of VIN for inhibition of GJIC (30-min EC_{50} = 126 μ M) are comparable with the chemicals like alachlor, perfluoroheptanoic acid, benzoylperoxide, or lipidic compounds, which required higher concentrations (>100 μ M) to rapidly induce >50% inhibitory effect (Sovadinova et al., 2015; Upham et al., 1998, 2007). Also, endogenous or synthetic estrogens and androgens were found to affect GJIC and connexins not only via classical genomic mechanism (Ren et al., 2013), but also via rapid actions of non-genomic

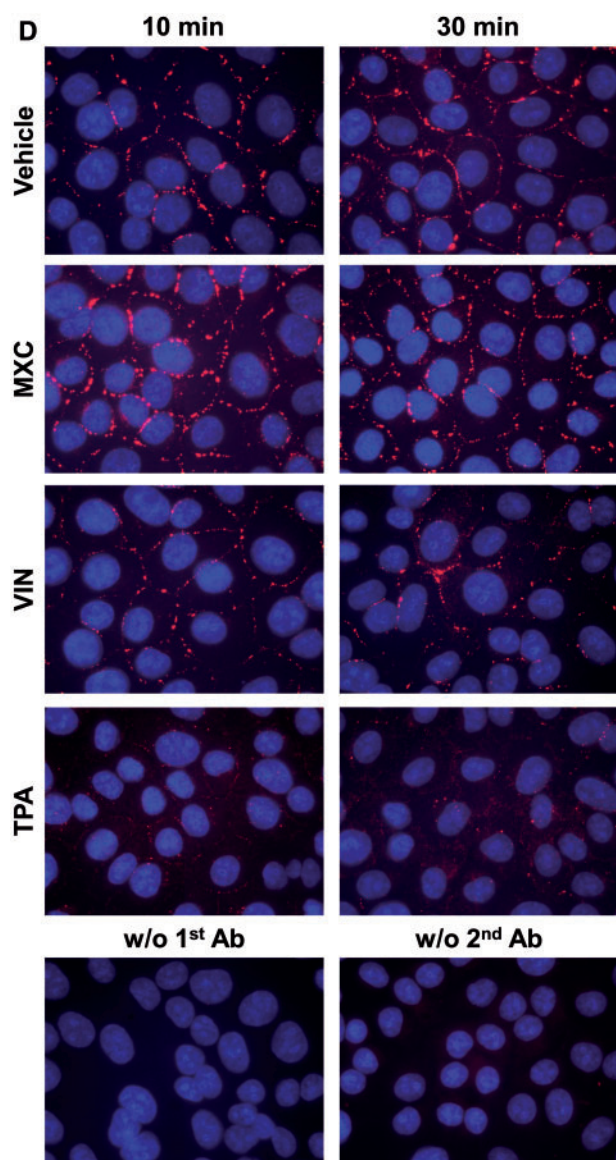


FIG. 3. continued

D, Immunocytochemistry of Cx43 in the cells treated for 10 or 30 min with MXC (25 μ M) or VIN (250 μ M). TPA treatment (50 nM, 30 min) known to induce internalization of Cx34 was used as a positive control. Images were acquired using 100 \times oil immersion objective. Controls for non-specific antibody binding were also done using control cells incubated either without primary (w/o 1st Ab) or secondary (w/o second Ab) antibody. The images are representative of 2 independent experiments with the treatments done in duplicates.

signaling (Iwase et al., 2006; Lyng et al., 2000; Pluciennik et al., 1996). GJIC thus represents a cellular event possibly altered by hormones and EDCs via different mechanisms, which might be chemical-, as well as cell type-specific (Osgood et al., 2013; Sovadinova et al., 2015). The immediate cell responses to MXC and VIN observed in this study, such as inhibition of GJIC and phosphorylation of MAPKs and Cx43, were most likely mediated by rapid mechanisms independent of ER or AR genomic signaling. WB-F344 cells have been reported to express weakly ER α but not ER β (Tanabe et al., 2012), which corresponds to the results of our Western blot analysis. These cells could therefore be susceptible to ER α -agonistic actions of MXC or its major metabolite HPTE (Gaido et al., 2000). HPTE indeed reduced GJIC, however,

only after prolonged exposures, which indicates possibly slower nuclear receptor-dependent genomic action different from the rapid inhibitory mechanism of MXC. Moreover, transformation of MXC to HPTE was not observed in our study, most likely due to progenitor characteristics of the cell line associated with its low biotransformation capacity. Finally, neither ER agonists (E2, HPTE) nor ER antagonist (ICI 182,780) induced rapid dysregulation of GJIC or attenuated effects of MXC. Taken together, these findings strongly suggest that the rapid effects of MXC on cell signaling were mediated by the parental compound and independent of HPTE- and ER α -dependent signaling.

Antagonistic interactions of VIN and its metabolites with AR are crucial for their mode of action (van Ravenzwaay et al., 2013). However, we did not detect expression of AR in WB-F344 cells, thus the rapid effects of VIN were probably induced by a mechanism independent of AR. This is also supported by the observation that a pretreatment of WB-F344 cells with modulators of AR (testosterone, flutamide, and VIN M2) did not prevent dysregulation of GJIC by VIN.

The effects of VIN on GJIC and phosphorylation of MAPKs and Cx43 occurred more rapidly (≤ 10 min) than the gradual transformation of VIN in the cell culture, as indicated by formation of M2 suggesting that the initial VIN effects were induced by the parental compound rather than its metabolites.

VIN effects had a transient character, which is similar to the transient inhibition of GJIC induced by TPA, EGF (Rivedal and Opsahl, 2001), lindane (Caruso et al., 2005), phenobarbital (Ruch and Klaunig, 1988) and other hepatic peroxisome proliferators (Cruciani et al., 1997). Restoration of GJIC, decrease in MAPK activity and Cx43 phosphorylation in this study coincided with the steady increase of M2 concentrations in the cell culture medium during the experiment, indicating an ongoing transformation of VIN into possibly less active products. In addition to M2, even greater amounts of M1 can be expected to form, as it was reported that after 120 min incubation of VIN in the cell culture medium, about 20% of total VIN hydrolyzes into M2 while 80% is converted into M1 (Bursztyka et al., 2008). Interestingly, M2 metabolite was found in our study to induce an inhibition of GJIC, which did not seem to have a transient character. It is possible that, while conversion to presumably M1 or some other metabolite(s) reduced VIN effects, M2 might retain similar effects as the parental chemical but was not formed in a quantity sufficient to sustain GJIC inhibition.

Rapid inhibition of GJIC by MXC and VIN in WB-F344 cells was apparently elicited by the parental chemicals and via mechanisms independent of ER or AR signaling. Since the parental compounds of MXC and VIN can be found in the blood and tissues of human populations (Freire et al., 2013; Wickerham et al., 2012), their effects and underlying mechanisms might be toxicologically relevant. These mechanisms probably include rapid activation of MAPK ERK1/2 or p38 observed in our study after 5–10 min exposure. Our findings on activation of MAPKs by VIN are supported by a recent study, which reported rapid and transient (1–15 min) activation of ERK1/2 and Akt kinases in VIN-treated porcine granulosa cells (Wartalski et al., 2016). For MXC, MAPKs activation was implicated in the responses of macrophages exposed for 18–24 h (Kim et al., 2005), whereas rapid (10 min) activation of ERK1/2 and p38 was observed in MCF-7 cells exposed to HPTE (Li et al., 2006). Our study thus provides one of the first observations that MAPKs can be activated also by the parental chemicals via rapid signaling mechanisms. Although MAPKs have been implicated in the regulation of GJIC via Cx43 phosphorylation (Axelsen et al., 2013), Cx43 phosphorylation followed by its internalization was observed only for VIN

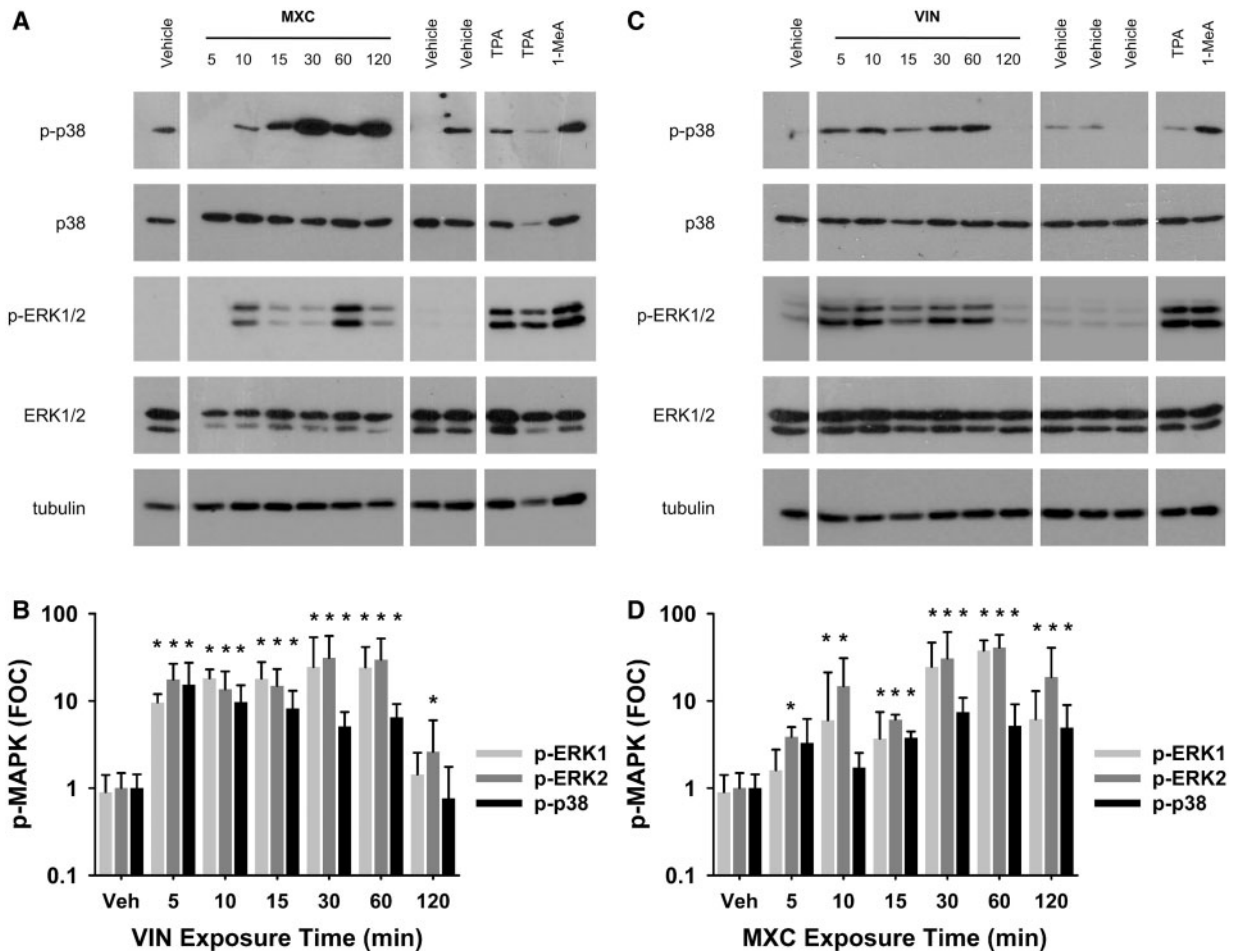


FIG. 4. Effects of MXC and VIN on activity of MAPK- ERK1/2 and MAPK-p38 in WB-F344 cells. The cells were treated with 25 μ M MXC or 250 μ M VIN and activity of MAPKs was determined using Western blotting and antibodies directed against phosphorylated (activated) ERK1/2 (p-ERK1/2) or p38 (p-p38). TPA (50 nM, 30 min) and 1-methylthiathracene (1-MeA, 70 μ M, 10 min) treatments were used as positive controls for MAPK activation. The blot images (A, C) are representative of 2 independent experiments with the treatments done in duplicates. Densitometric analysis (B, D) presents intensities of p-MAPKs bands adjusted according to the intensity of the corresponding non-phosphorylated MAPK band and then related to the vehicle control (Veh) to calculate FOC. Data represent means \pm SD (n=4). Asterisks indicate values significantly different from the vehicle control (Kruskal-Wallis ANOVA on Ranks followed by Dunn's comparison method, $P < .05$).

but not MXC. Moreover, neither MXC - nor VIN -induced inhibition of GJIC was prevented by a MEK1/2 inhibitor, which indicates that dysregulation of GJIC by these 2 chemicals did not occur via classical ERK1/2-dependent mechanism reported for TPA, EGF, or lindane (Sovadinova *et al.*, 2015).

The dysregulation of GJIC by VIN was attenuated by an inhibitor of p38, which is mechanistically similar to effects induced by 1-MeA in lung but not liver epithelial cells (Osgood *et al.*, 2013; Upham *et al.*, 2008), or by anisomycin in WB-F344 cells (Ogawa *et al.*, 2004). Interestingly, the effects of MXC and VIN on GJIC were prevented by an inhibitor of PC-PLC. This signal transduction enzyme was implicated in downregulation of GJIC in response to various toxicants, including DDT, PCB153, dicumylperoxide, perfluorooctanoic acid, or polycyclic aromatic hydrocarbons (Sovadinova *et al.*, 2015). However, our study might be one of the rare reports suggesting activation of phospholipases in response to MXC (Cheng *et al.*, 2012; Tseng *et al.*, 2011), and possibly the first one demonstrating the key role of rapid phospholipase activation in cell responses to VIN exposure. Future studies should address the signaling events upstream and downstream of PC-PLC activation and their role in the mechanisms of GJIC inhibition and MAPK activation.

Similar to the other PC-PLC-dependent inhibitors of GJIC (Sovadinova *et al.*, 2015), MXC and VIN actions were effectively prevented by a dietary phytoalexin, resveratrol. Preventive effects were induced by a short pretreatment with resveratrol, which suggests that this phytoestrogen can also rapidly modulate signal transductions interfering with signaling pathways responsible for dysregulation of GJIC in response to MXC or VIN. Since PC-PLC represents a shared mechanism among a large group of resveratrol-sensitive inhibitors of GJIC, these data indicate that PC-PLC might be a possible novel target of rapid non-genomic actions of resveratrol as well as EDCs.

SUMMARY

In this study, we provide the first report that the parental compounds of prototypical EDCs, MXC, and VIN, can rapidly inhibit GJIC and activate ERK1/2, p38 and PC-PLC independently of ER or AR signaling. Alterations of these cellular events known to be critically important for control of gene expression and epigenetic regulations were manifested in a model epithelial cell line expressing Cx43, which represents the major connexin protein responsible for the maintenance of GJIC and tissue homeostasis

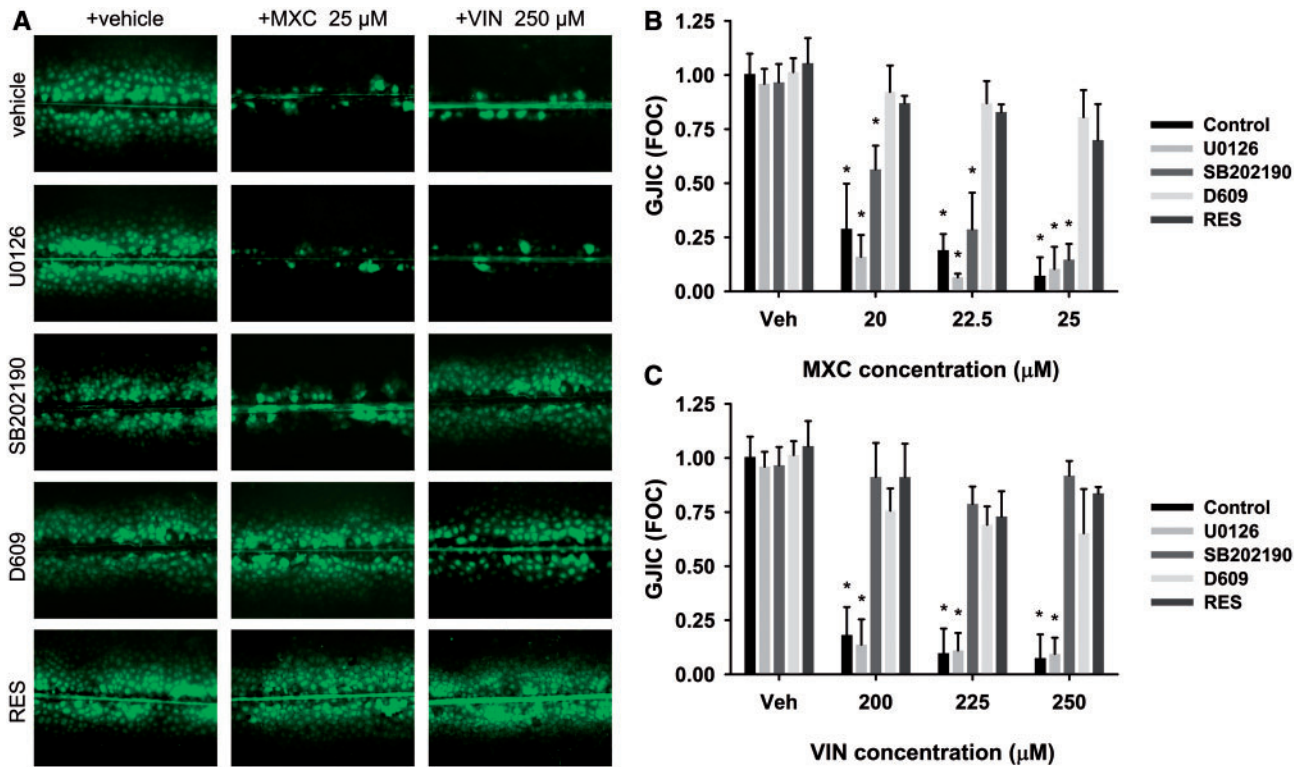


FIG. 5. Effects of signal pathway inhibitors and resveratrol on inhibition of GJIC induced by MXC and VIN in WB-F344 cells. The cells were pretreated with MEK1/2 inhibitor, U0126 (20 μ M, 30 min), p38 inhibitor SB202190 (25 μ M, 30 min), phosphatidylcholine-specific phospholipase C inhibitor D609 (50 μ M, 20 min), or with resveratrol (100 μ M, 15 min), then exposed to MXC (20–25 μ M, 10 min) or VIN (200–250 μ M, 10 min). **A**, Representative images from SL-DT assay used for evaluation of GJIC. The effects of the chemicals were compared with the dye transfer in the negative control and expressed as FOC for both GJIC inhibitors, **(B)** MXC and **(C)** VIN. Data represent means \pm SD from at least 3 independent experiments. Asterisks indicate values significantly different from the vehicle (Veh) control (Kruskal-Wallis ANOVA on Ranks followed by Dunn's comparison method, $P < .05$).

in many different cell types, tissues and organs. Cx43 expressing cells include, for example, cells from male and female reproductive organs, such as cumulus and granulosa cells of ovarian follicles or somatic testicular Leydig or Sertoli cells, which are known to be critical for gametogenesis, sex hormone production and reproduction (Kidder and Cyr, 2016; Winterhager and Kidder, 2015). Future *in vitro* and *in vivo* studies should therefore address the possible roles of these rapid intercellular and intracellular signaling events in the mechanisms of endocrine disruption, epigenetic dysregulations and transgenerational epigenetic inheritance induced by MXC, VIN, or other EDCs. Epigenetic effects elicited in the key cell populations, such as organ-specific (somatic, adult) stem cells, during the critical developmental phases could also represent the mechanism responsible for the developmental origin of adult chronic diseases (Barker, 2004), and further studies should consider testing this hypothesis (Trosko, 2011).

SUPPLEMENTARY DATA

Supplementary data are available online at <http://toxsci.oxfordjournals.org/>.

ACKNOWLEDGEMENTS

We would like to thank Ms Lindsay Goodall for her excellent contribution of maintaining cultures of cells for these experiments.

FUNDING

This work was supported by the Czech Ministry of Education, Youth and Sports (LH12034 to P.B., LO1214 and LM2015051 to RECETOX); National Institute of Environmental Health Sciences (R01 ES013268-01A2 to B.L.U.), and Universidad Nacional Autónoma de México (PASPA-UNAM 2009-2010 to R.Z.).

REFERENCES

- Anway, M. D., Cupp, A. S., Uzumcu, M., and Skinner, M. K. (2005). Epigenetic transgenerational actions of endocrine disruptors and male fertility. *Science* **308**, 1466–1469.
- Axelsen, L. N., Calloe, K., Holstein-Rathlou, N. H., and Nielsen, M. S. (2013). Managing the complexity of communication: Regulation of gap junctions by post-translational modification. *Front. Pharmacol.* **4**, 130.
- Barker, D. J. (2004). The developmental origins of adult disease. *J. Am. Coll. Nutr.* **23**, 588S–595S.
- Bursztyka, J., Debrauwer, L., Perdu, E., Jouanin, I., Jaeg, J. P., and Cravedi, J. P. (2008). Biotransformation of vinclozolin in rat precision-cut liver slices: Comparison with *in vivo* metabolic pattern. *J. Agric. Food Chem.* **56**, 4832–4839.
- Caruso, R. L., Upham, B. L., Harris, C., and Trosko, J. E. (2005). Biphasic lindane-induced oxidation of glutathione and inhibition of gap junctions in myometrial cells. *Toxicol. Sci.* **86**, 417–426.
- Cheng, H. H., Lu, Y. C., Lu, T., Cheng, J. S., Mar, G. Y., Fang, Y. C., Chai, K. L., and Jan, C. R. (2012). Effect of methoxychlor on

- Ca(2+) movement and viability in MDCK renal tubular cells. *Basic Clin. Pharmacol. Toxicol.* **111**, 224–231.
- Coleman, W. B., McCullough, K. D., Esch, G. L., Faris, R. A., Hixson, D. C., Smith, G. J., and Grisham, J. W. (1997). Evaluation of the differentiation potential of WB-F344 rat liver epithelial stem-like cells in vivo - Differentiation to hepatocytes after transplantation into dipeptidylpeptidase-IV-deficient rat liver. *Am. J. Pathol.* **151**, 353–359.
- Cruciani, V. R., Mikalsen, S. O., Vasseur, P., and Sanner, T. (1997). Effects of peroxisome proliferators and 12-O-tetradecanoyl phorbol-13-acetate on intercellular communication and connexin43 in two hamster fibroblast systems. *Int. J. Cancer* **73**, 240–248.
- El Fouly, M. H., Trosko, J. E., and Chang, C. C. (1987). Scrape-loading and dye transfer - a rapid and simple technique to study gap junctional intercellular communication. *Exp. Cell. Res.* **168**, 422–430.
- Freire, C., Koifman, R. J., Sarcinelli, P. N., Simoes Rosa, A. C., Clapauch, R., and Koifman, S. (2013). Long-term exposure to organochlorine pesticides and thyroid status in adults in a heavily contaminated area in Brazil. *Environ. Res.* **127**, 7–15. 10.1016/j.envres.2013.09.001.
- Gaido, K. W., Maness, S. C., McDonnell, D. P., Dehal, S. S., Kupfer, D., and Safe, S. (2000). Interaction of methoxychlor and related compounds with estrogen receptor alpha and beta, and androgen receptor: Structure-activity studies. *Mol. Pharmacol.* **58**, 852–858.
- Guan, X. J., Bonney, W. J., and Ruch, R. J. (1995). Changes in gap junction permeability, gap junction number, and connexin43 expression in lindane-treated rat-liver epithelial-cells. *Toxicol. Appl. Pharmacol.* **130**, 79–86.
- Hazardous Substances Data Bank [Internet]. Bethesda (MD): National Library of Medicine (US); [Last Revision Date 2010, Jan 27]. Vinclozolin; Hazardous Substances Databank Number: 6747. Available from <http://toxnet.nlm.nih.gov/cgi-bin/sis/htmlgen?HSDB>. Accessed July 4, 2016.
- Iwase, Y., Fukata, H., and Mori, C. (2006). Estrogenic compounds inhibit gap junctional intercellular communication in mouse Leydig TM3 cells. *Toxicol. Appl. Pharmacol.* **212**, 237–246.
- Kao, C. Y., Oakley, C. S., Welsch, C. W., and Chang, C. C. (1997). Growth requirements and neoplastic transformation of two types of normal human breast epithelial cells derived from reduction mammoplasty. *In Vitro Cell. Dev. Biol. Anim.* **33**, 282–288.
- Kidder, G. M., and Cyr, D. G. (2016). Roles of connexins in testis development and spermatogenesis. *Semin. Cell Dev. Biol.* **50**, 22–30. 10.1016/j.semcdb.2015.12.019.
- Kim, J. Y., Oh, K. N., Han, E. H., Kim, D. H., Jeong, T. C., Lee, E. S., and Jeong, H. G. (2005). Methoxychlor-induced inducible nitric oxide synthase and proinflammatory cytokines expression in macrophages via NF-kappa B, ERK, and p38 mitogen-activated protein kinases. *Biochem. Biophys. Res. Commun.* **333**, 1234–1240.
- Li, X., Zhang, S., and Safe, S. (2006). Activation of kinase pathways in MCF-7 cells by 17beta-estradiol and structurally diverse estrogenic compounds. *J. Steroid Biochem. Mol. Biol.* **98**, 122–132.
- Lyng, F. M., Jones, G. R., and Rommerts, F. F. G. (2000). Rapid androgen actions on calcium signaling in rat sertoli cells and two human prostatic cell lines: similar biphasic responses between 1 picomolar and 100 nanomolar concentrations. *Biol. Reprod.* **63**, 736–747.
- Machala, M., Blaha, L., Vondracek, J., Trosko, J. E., Scott, J., and Upham, B. L. (2003). Inhibition of gap junctional intercellular communication by noncoplanar polychlorinated biphenyls: Inhibitory potencies and screening for potential mode(s) of action. *Toxicol. Sci.* **76**, 102–111.
- Manikkam, M., Haque, M. M., Guerrero-Bosagna, C., Nilsson, E. E., and Skinner, M. K. (2014). Pesticide methoxychlor promotes the epigenetic transgenerational inheritance of adult-onset disease through the female germline. *PLOS One* **9**, e102091.
- Matesic, D. F., Rupp, H. L., Bonney, W. J., Ruch, R. J., and Trosko, J. E. (1994). Changes in gap-junction permeability, phosphorylation, and number mediated by phorbol ester and non-phorbol-ester tumor promoters in rat-liver epithelial-cells. *Mol. Carcinog.* **10**, 226–236.
- Molina-Molina, J. M., Hillenweck, A., Jouanin, I., Zalko, D., Cravedi, J. P., Fernandez, M. F., Pillon, A., Nicolas, J. C., Olea, N., and Balaguer, P. (2006). Steroid receptor profiling of vinclozolin and its primary metabolites. *Toxicol. Appl. Pharmacol.* **216**, 44–54.
- Ogawa, T., Hayashi, T., Kyoizumi, S., Kusunoki, Y., Nakachi, K., MacPhee, D. G., Trosko, J. E., Kataoka, K., and Yorioka, N. (2004). Anisomycin downregulates gap-junctional intercellular communication via the p38 MAP-kinase pathway. *J. Cell. Sci.* **117**, 2087–2096.
- Osgood, R. S., Upham, B. L., Hill, T., Helms, K. L., Velmurugan, K., Babica, P., and Bauer, A. K. (2013). Polycyclic aromatic hydrocarbon-induced signaling events relevant to inflammation and tumorigenesis in lung cells are dependent on molecular structure. *PLOS One* **8**, e65150.
- Ozgyin, L., Erdos, E., Bojcsuk, D., and Balint, B. L. (2015). Nuclear receptors in transgenerational epigenetic inheritance. *Prog. Biophys. Mol. Biol.* **118**, 34–43.
- Pirkmajer, S., and Chibalin, A. V. (2011). Serum starvation: Caveat emptor. *Am. J. Physiol. Cell. Physiol.* **301**, C272–C279. 10.1152/ajpcell.00091.2011.
- Pluciennik, F., Verrecchia, F., Bastide, B., Herve, J. C., Joffre, M., and Deleze, J. (1996). Reversible interruption of gap junctional communication by testosterone propionate in cultured sertoli cells and cardiac myocytes. *J. Membr. Biol.* **149**, 169–177.
- Ren, J., Wang, X. H., Wang, G. C., and Wu, J. H. (2013). 17 beta Estradiol regulation of connexin 43-based gap junction and mechanosensitivity through classical estrogen receptor pathway in osteocyte-like MLO-Y4 cells. *Bone* **53**, 587–596.
- Reuber, M. D. (1980). Carcinogenicity and toxicity of methoxychlor. *Environ. Health Perspect.* **36**, 205–219.
- Rivedal, E., and Opsahl, H. (2001). Role of PKC and MAP kinase in EGF- and TPA-induced connexin43 phosphorylation and inhibition of gap junction intercellular communication in rat liver epithelial cells. *Carcinogenesis* **22**, 1543–1550.
- Ruch, R. J., Bonney, W. J., Sigler, K., Guan, X. J., Matesic, D., Schafer, L. D., Dupont, E., and Trosko, J. E. (1994). Loss of gap-junctions from DDT-treated rat-liver epithelial-cells. *Carcinogenesis* **15**, 301–306.
- Ruch, R. J., and Klaunig, J. E. (1988). Kinetics of phenobarbital inhibition of intercellular communication in mouse hepatocytes. *Cancer Res.* **48**, 2519–2523.
- Sai, K., Kanno, J., Hasegawa, R., Trosko, J. E., and Inoue, T. (2000). Prevention of the down-regulation of gap junctional intercellular communication by green tea in the liver of mice fed pentachlorophenol. *Carcinogenesis* **21**, 1671–1676.
- Skinner, M. K. (2014). Environmental stress and epigenetic transgenerational inheritance. *BMC Med.* **12**, 153.
- Sovadinova, I., Babica, P., Boke, H., Kumar, E., Wilke, A., Park, J. S., Trosko, J. E., and Upham, B. L. (2015). Phosphatidylcholine specific PLC-induced dysregulation of gap junctions, a robust

- cellular response to environmental toxicants, and prevention by resveratrol. *PLoS One* **10**, e0124454.
- Tanabe, E., Shibata, A., Inoue, S., Kitayoshi, M., Fukushima, N., and Tsujiuchi, T. (2012). Regulation of cell motile activity through the different induction of LPA receptors by estrogens in liver epithelial WB-F344 cells. *Biochem. Biophys. Res. Commun.* **428**, 105–109.
- Tiemann, U., and Pohland, R. (1999). Inhibitory effects of organochlorine pesticides on intercellular transfer of Lucifer Yellow in cultured bovine oviductal cells. *Reprod. Toxicol.* **13**, 123–130.
- Trevino, L. S., Wang, Q., and Walker, C. L. (2015). Hypothesis: Activation of rapid signaling by environmental estrogens and epigenetic reprogramming in breast cancer. *Reprod. Toxicol.* **54**, 136–140.
- Trosko, J. E. (2011). The gap junction as a “Biological Rosetta Stone”: Implications of evolution, stem cells to homeostatic regulation of health and disease in the Barker hypothesis. *J. Cell. Commun. Signal.* **5**, 53–66.
- Trosko, J. E., Chang, C. C., Upham, B., and Wilson, M. (1998). Epigenetic toxicology as toxicant-induced changes in intracellular signalling leading to altered gap junctional intercellular communication. *Toxicol. Lett.* **102-103**, 71–78.
- Trosko, J. E., Chang, C. C., Wilson, M. R., Upham, B., Hayashi, T., and Wade, M. (2000). Gap junctions and the regulation of cellular functions of stem cells during development and differentiation. *Methods* **20**, 245–264.
- Trosko, J. E., Madhukar, B. V., and Chang, C. C. (1993). Endogenous and exogenous modulation of gap junctional intercellular communication - toxicological and pharmacological implications. *Life Sci.* **53**, 1–19.
- Tsao, M. S., Smith, J. D., Nelson, K. G., and Grisham, J. W. (1984). A diploid epithelial-cell line from normal adult-rat liver with phenotypic properties of oval cells. *Exp. Cell. Res.* **154**, 38–52.
- Tseng, L. L., Shu, S. S., Kuo, C. C., Chou, C. T., Hsieh, Y. D., Chu, S. T., Chi, C. C., Liang, W. Z., Ho, C. M., and Jan, C. R. (2011). Effect of methoxychlor on Ca²⁺ handling and viability in OC2 human oral cancer cells. *Basic Clin. Pharmacol. Toxicol.* **108**, 341–348.
- Tsushimoto, G., Chang, C. C., Trosko, J. E., and Matsumura, F. (1983). Cyto-toxic, mutagenic, and cell-cell communication Inhibitory properties of DDT, lindane, and chlordane on Chinese-Hamster cells-in vitro. *Arch. Environ. Contam. Toxicol.* **12**, 721–730.
- Upham, B. L. (2011). Role of integrative signaling through gap junctions in toxicology. *Curr. Protoc. Toxicol.* **47**, 1–18.
- Upham, B. L., Blaha, L., Babica, P., Park, J. S., Sovadinova, I., Pudrith, C., Rummel, A. M., Weis, L. M., Sai, K., Tithof, P. K., et al. (2008). Tumor promoting properties of a cigarette smoke prevalent polycyclic aromatic hydrocarbon as indicated by the inhibition of gap junctional intercellular communication via phosphatidylcholine-specific phospholipase C. *Cancer Sci.* **99**, 696–705.
- Upham, B. L., Deocampo, N. D., Wurl, B., and Trosko, J. E. (1998). Inhibition of gap junctional intercellular communication by perfluorinated fatty acids is dependent on the chain length of the fluorinated tail. *Int. J. Cancer* **78**, 491–495.
- Upham, B. L., Guzvic, M., Scott, J., Carbone, J. M., Blaha, L., Coe, C., Li, L. L., Rummel, A. M., and Trosko, J. E. (2007). Inhibition of gap junctional intercellular communication and activation of mitogen-activated protein kinase by tumor-promoting organic peroxides and protection by resveratrol. *Nutr. Cancer* **57**, 38–47.
- Upham, B. L., Park, J. S., Babica, P., Sovadinova, I., Rummel, A. M., Trosko, J. E., Hirose, A., Hasegawa, R., Kanno, J., and Sai, K. (2009). Structure-activity-dependent regulation of cell communication by perfluorinated fatty acids using in vivo and in vitro model systems. *Environ. Health Perspect.* **117**, 545–551.
- van Ravenzwaay, B., Kolle, S. N., Ramirez, T., and Kamp, H. G. (2013). Vinclozolin: A case study on the identification of endocrine active substances in the past and a future perspective. *Toxicol. Lett.* **223**, 271–279.
- Vinken, M., De Rop, E., Decrock, E., De Vuyst, E., Leybaert, L., Vanhaecke, T., and Rogiers, V. (2009a). Epigenetic regulation of gap junctional intercellular communication: More than a way to keep cells quiet? *Biochim. Biophys. Acta-Rev. Cancer* **1795**, 53–61.
- Vinken, M., Doktorova, T., Decrock, E., Leybaert, L., Vanhaecke, T., and Rogiers, V. (2009b). Gap junctional intercellular communication as a target for liver toxicity and carcinogenicity. *Crit. Rev. Biochem. Mol. Biol.* **44**, 201–222.
- Wartalski, K., Knet-Seweryn, M., Hoja-Lukowicz, D., Tabarowski, Z., and Duda, M. (2016). Androgen receptor-mediated nongenomic effects of vinclozolin on porcine ovarian follicles and isolated granulosa cells: Vinclozolin and non-genomic effects in porcine ovarian follicles. *Acta Histochem.* **118**, 377–386.
- Watson, C. S., Hu, G. Z., and Paulucci-Holthausen, A. A. (2014). Rapid actions of xenoestrogens disrupt normal estrogenic signaling. *Steroids* **81**, 36–42.
- Wickerham, E. L., Lozoff, B., Shao, J., Kaciroti, N., Xia, Y., and Meeker, J. D. (2012). Reduced birth weight in relation to pesticide mixtures detected in cord blood of full-term infants. *Environ. Int.* **47**, 80–85. 10.1016/j.envint.2012.06.007.
- Winterhager, E., and Kidder, G. M. (2015). Gap junction connexins in female reproductive organs: Implications for women’s reproductive health. *Hum. Reprod. Update* **21**, 340–352. 10.1093/humupd/dmv007.
- Wong, R. L. Y., and Walker, C. L. (2013). Molecular pathways: Environmental estrogens activate nongenomic signaling to developmentally reprogram the epigenome. *Clin. Cancer Res.* **19**, 3732–3737.

VI. Osgood, R.S., Upham, B.L., Hill, T., Helms, K.L., Velmurugan, K., **Babica, P.**, Bauer, A.K.*, 2013. Polycyclic aromatic hydrocarbon-induced signaling events relevant to inflammation and tumorigenesis in lung cells are dependent on molecular structure. *PLoS One* 8, e65150.

Polycyclic Aromatic Hydrocarbon-Induced Signaling Events Relevant to Inflammation and Tumorigenesis in Lung Cells Are Dependent on Molecular Structure

Ross S. Osgood¹, Brad L. Upham³, Thomas Hill III², Katherine L. Helms³, Kalpana Velmurugan², Pavel Babica³, Alison K. Bauer^{2*}

1 Department of Pharmaceutical Sciences, University of Colorado Anschutz Medical Center, Aurora, Colorado, United States of America, **2** Department of Environmental and Occupational Health, University of Colorado Anschutz Medical Center, Aurora, Colorado, United States of America, **3** Department of Pediatrics and Human Development, Michigan State University, East Lansing, Michigan, United States of America

Abstract

Polycyclic aromatic hydrocarbons (PAHs) are ubiquitous environmental and occupational toxicants, which are a major human health concern in the U.S. and abroad. Previous research has focused on the genotoxic events caused by high molecular weight PAHs, but not on non-genotoxic events elicited by low molecular weight PAHs. We used an isomeric pair of low molecular weight PAHs, namely 1-Methylanthracene (1-MeA) and 2-Methylanthracene (2-MeA), in which only 1-MeA possessed a bay-like region, and hypothesized that 1-MeA, but not 2-MeA, would affect non-genotoxic endpoints relevant to tumor promotion in murine C10 lung cells, a non-tumorigenic type II alveolar pneumocyte and progenitor cell type of lung adenocarcinoma. The non-genotoxic endpoints assessed were dysregulation of gap junction intercellular communication function and changes in the major pulmonary connexin protein, connexin 43, using fluorescent redistribution and immunoblots, activation of mitogen activated protein kinases (MAPK) using phosphospecific MAPK antibodies for immunoblots, and induction of inflammatory genes using quantitative RT-PCR. 2-MeA had no effect on any of the endpoints, but 1-MeA dysregulated gap junctional communication in a dose and time dependent manner, reduced connexin 43 protein expression, and altered membrane localization. 1-MeA also activated ERK1/2 and p38 MAP kinases. Inflammatory genes, such as cyclooxygenase 2, and chemokine ligand 2 (macrophage chemoattractant 2), were also upregulated in response to 1-MeA only. These results indicate a possible structure-activity relationship of these low molecular weight PAHs relevant to non-genotoxic endpoints of the promoting aspects of cancer. Therefore, our novel findings may improve the ability to predict outcomes for future studies with additional toxicants and mixtures, identify novel targets for biomarkers and chemotherapeutics, and have possible implications for future risk assessment for these PAHs.

Citation: Osgood RS, Upham BL, Hill T III, Helms KL, Velmurugan K, et al. (2013) Polycyclic Aromatic Hydrocarbon-Induced Signaling Events Relevant to Inflammation and Tumorigenesis in Lung Cells Are Dependent on Molecular Structure. PLoS ONE 8(6): e65150. doi:10.1371/journal.pone.0065150

Editor: Fernando Rodrigues-Lima, University Paris Diderot-Paris 7, France

Received: February 8, 2013; **Accepted:** April 23, 2013; **Published:** June 3, 2013

Copyright: © 2013 Osgood et al. This is an open-access article distributed under the terms of the Creative Commons Attribution License, which permits unrestricted use, distribution, and reproduction in any medium, provided the original author and source are credited.

Funding: This work was funded by intramural Colorado School of Public Health, CU funds (A.K.B.), NIEHS ES013268-01A2 (B.L.U.), and the Department of Pharmaceutical Sciences Toxicology Graduate Program (RSO). The funders had no role in study design, data collection and analysis, decision to publish, or preparation of the manuscript.

Competing Interests: The authors have declared that no competing interests exist.

* E-mail: Alison.bauer@ucdenver.edu

Introduction

Polycyclic aromatic hydrocarbons (PAHs) are ubiquitous environmental toxicants found in air, water, plants, soil, and sediment in many countries. Occupational exposures to PAH are due to diesel exhaust, mining activities, and oil production. While genotoxic effects of PAHs have been extensively studied, diseases such as cancer are the consequence of reversible, non-genotoxic events, i.e. tumor promotion as well as irreversible mutagenic events [1–3]. High molecular weight (HMW) PAHs, such as benzo[a]pyrene (BaP), tend to elicit genotoxic effects while the lower molecular weight (LMW) PAHs have little to no observed carcinogenic initiation or genotoxic activity [4–6]. The two-four ring LMW PAHs are the most abundant PAHs in sidestream smoke or environmental tobacco smoke (ETS), reaching levels >5,500 ng/cigarette, however, little is known about these PAHs and their potential as cancer promoters. While secondhand smoke

exposure has greatly decreased in the U.S., except in apartment dwellings [7], other countries, such as China, Korea, Japan, India, Russia, Poland, and Egypt are still dealing with the effects of ETS, including childhood and adult asthma, chronic obstructive pulmonary disease (COPD), and cancer, as well as other associated etiologies such as reproductive health issues [8–10]. Both *in vivo* and *in vitro* evidence in several cell types suggests that these non-genotoxic PAHs can modulate mechanisms involved in pulmonary diseases, such as MAP kinases (MAPK), inflammatory signaling, and influence understudied signaling events such as gap junctional intercellular communication (GJIC) [11,12].

Alveolar type II pneumocyte is an epithelial cell type involved in many pulmonary diseases, such as asthma [13] and COPD [14], and is a progenitor cell for lung adenocarcinoma (AC) in humans and mice, which is the most common type of lung cancer in both smokers and non-smokers [15,16]. Non-tumorigenic C10 cells used in these studies were derived from type II cells in a BALB/c

mouse and have been well characterized for basal and stimulated phenotypes [17–20], including contact growth inhibition.

Some of the mechanisms involved in pulmonary diseases, such as idiopathic pulmonary fibrosis (IPF) and cancer, include activation of mitogenic signal transduction pathways, dysregulation of GJIC [21], and induction of inflammation pathways [1–3,22–24], which likely interact to elicit the observed effects (eg. promotion of initiated cells during carcinogenesis). Gap junctions, composed of connexins, are intercellular channels that allow for molecular communication between neighboring cells that are often inhibited by tumor promoters [3], however very little is known about their function in other pulmonary diseases. In a study that evaluated 251 chemicals, a stronger significant correlation was observed between tumorigenicity and GJIC than with that observed with mutagenicity, suggesting that GJIC is a valid marker for promotion [24]. Tobacco smoke condensates and specific LMW PAHs in cigarettes, such as 1-Methylantracene (1-MeA), as well as 12-O-tetradecanoylphorbol-13-acetate (TPA), a classic tumor promoter in several organs, have induced significant GJIC dysregulation in a liver cell line (WB-F44) [25–27]. Connexin 43 (Cx43) is the primary connexin expressed in alveolar type II and bronchiolar Clara cells [28,29], and its expression is significantly reduced in mouse C10 cells treated with the lung tumor promoter, butylated hydroxytoluene (BHT) [28]. *Cx43*^{-/-} mice also have significantly increased urethane-induced lung tumor susceptibility [30], further suggesting a role for gap junctions in pulmonary carcinogenesis and other pulmonary diseases.

MAPK pathways are also activated in response to PAHs in liver and smooth muscle cells [11,31]. In mouse alveolar type II cell lines (C10 and E10), ERK1/2 MAPK inhibition lead to decreased cell proliferation and in mouse lung, tumor regression and restored apoptosis [19,32]. In addition, multiple *in vivo* and *in vitro* studies have linked inflammatory pathways upstream and downstream of MAPK with lung disease mechanisms for fibrosis [33], COPD [34], and cancer (ie. tumor promotion) [3,23,35–40]. For example, Mcp-1(Ccl2), a known macrophage chemoattractant secreted in lungs by pulmonary epithelial cells, has been reported to affect MAPK activation [39].

The PAH isomers herein, 1- and 2-MeA, have been shown to have disparate effects on the dysregulation of GJIC, activation of MAPK and induction of arachidonic acid release in WB-F44 rat liver cells [25]. The active GJIC inhibitor, 1-MeA, contains a bay-like structural region while the inactive isomer 2-MeA, does not (Fig. 1) [25,41,42]. These structural differences exist among other isomeric PAHs [43] and produced similar isomeric disparities in gap junction dysregulation as well as induction of apoptosis in a human monocyte cell line [44]. We hypothesized that the active PAH (1-MeA) would also inhibit GJIC, activate MAPKs, and induce inflammatory cytokines and chemokines, in a mouse type II cell line in contrast to its isomer (2-MeA).

Materials and Methods

Materials and Reagents

Reagents were purchased from Crescent Chemical (1-MeA; purity 99.5%) and Sigma Aldrich (St. Louis, MO; 2-MeA, purity 97%; acetonitrile, lucifer yellow, 12-O-tetradecanoylphorbol-13-acetate (TPA)). Stock solutions for PAHs and TPA were prepared by dissolving the compounds in acetonitrile or DMSO, respectively, which were also used as the vehicle controls. TEMED (USA) and acrylamide (China) were both purchased from BioRad (Hercules, CA). The p38 inhibitors (SB203580 and SB202190), ERK1/2 inhibitor (FR180204) and the MEK inhibitor (U0126)

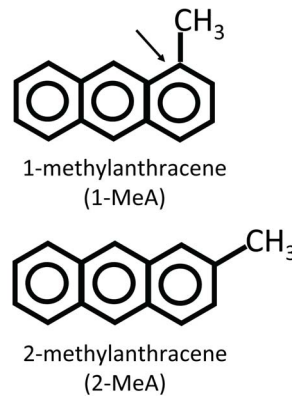


Figure 1. Structures of 1- and 2-methylantracene. An arrow indicates the bay-like region of 1-MeA.
doi:10.1371/journal.pone.0065150.g001

were purchased from Tocris Bioscience (Bristol, UK). All other reagents were purchased from Sigma Aldrich.

Cell Line Maintenance and Treatment with PAHs

The C10 mouse cell line was obtained from Dr. Lori Dwyer Nield (University of Colorado, Aurora, CO) [18]. C10 cells are cultured in CMRL 1066 (Gibco, Invitrogen, Grand Island, NY) with 10% FBS and 1% glutamate. Cells were grown in 35 mm tissue culture dishes for the scrape load-dye transfer (SL/DT) assays and 60 mm plates for the protein and RNA extractions in a humidified atmosphere at 37°C with 5% CO₂ and 95% air. At confluence (2–3 days), serum deprivation was initiated for 24 h prior to experimental treatments. After serum deprivation, PAHs or vehicle (CH₃CN) were applied directly to the plates without media change from a concentrated stock solution for all experiments.

Scrape-load/dye-transfer (SL/DT) Assay

The SL/DT assay was conducted following the method of Upham [45]. Three cuts in the monolayer of cells were made with a steel scalpel in the presence of lucifer yellow (1 mg/ml of PBS) and allowed to transfer through the cells for three minutes. The cells were then fixed with 4% formalin and the dye spread was visualized with an Eclipse Ti-S microscope. Images were collected with a DS-QiMc camera (Nikon; Melville, NY) at a magnification of 100X. The images were quantified using ImageJ software (<http://imagej.nih.gov/ij/>) by measuring the area of dye spread of the PAH treated plates relative to the CH₃CN vehicle. TPA was used as a positive control for all studies; the dose was determined in previous studies (50 nM, 60 min) [46]. For the MAPK-inhibitor studies, U0126, SB203580, and SB202190 were applied separately 1 h prior to treatment with 1-MeA; doses used were previously published [19,25,47]. Cytotoxicity assays were performed on confluent cells after 24 h serum deprivation followed by treatment with vehicle control or PAHs for 30 min, 1.5 h, and 6 h time points. The CellTiter 96 AQueous One Solution Cell Viability assay was then performed as described by the manufacturer and measured at 490 nm (MTS assay, Promega, Madison, WI).

Protein Extraction and Immunoblots

Cells were exposed to PAH at set intervals of 15 min to 4 h, and then extracted with 20% SDS containing protease inhibitor (Protease Inhibitor Cocktail 100X, Sigma) and phosphatase inhibitor (Halt Phosphatase Inhibitor Cocktail 100X, Thermo

Scientific). The BioRad DC protein assay was used to quantify protein. 15 μ g of protein were separated on a 12.5% SDS page gel and transferred to polyvinylidene fluoride (PVDF) membrane (Millipore, Billerica, MA). Primary antibodies were incubated with the membranes overnight at 4°C, similar to Rondini et al. (2010) [39] : anti-mouse Cx43 from Millipore (monoclonal, 1:7,500 dilution) and anti-rabbit from Cell Signaling for pP38, ERK1/2 and MAPKAPK-2 (1:500 dilution, Cat# 9215S), total P38 (1:1,000 dilution, Cat# 9212), pERK1/2 (1:1,000, Cat# 4370S), and total ERK1/2 (1:1,000, Cat#4695) pMAPKAPK-2 (1:1,000, Cat# 3007) and total MAPKAPK-2 (1:1,000, Cat# 3042). Secondary antibody conjugated with HRP was used (Pierce Goat anti-Rabbit for pP38, total P38, pERK1/2, and total ERK1/2 all at a dilution of 1:7500 and for Cx43 goat anti mouse IgG-HRP from Santa Cruz at 1:1000) and a tertiary antibody for pP38 with Streptavidin-HRP from ThermoScientific at 1:25,000. Supersignal West Dura chemiluminescent detection was used for all proteins of interest. All immunoblots were quantified by densitometry using the BioRad Quantity One Software.

Immunostaining

Cells were grown on cover slips in a 12 well plate for 2 days and serum deprived for 24 hours before treatment. Following treatment, the cells were washed three times with PBS and fixed with warm 4% paraformaldehyde for 30 minutes. The cells were then washed again three times with PBS, permeabilized, and blocked with 5% BSA with 0.2% Triton X-100 in PBS for 90 minutes. After 90 minutes, primary antibody for Cx43 (Transduction Laboratories, monoclonal 1:200, Cat# C13720) was applied and incubated at 4° overnight. The following day the cells were washed with PBS and secondary antibody was applied for 90 minutes (Alexa Fluor 488 goat anti-mouse, monoclonal 1:250, Invitrogen). The plate was again washed, coated with Prolong Gold antifade reagent containing DAPI (Invitrogen), allowed to dry overnight before it was sealed, and viewed on a confocal microscope (Nikon D-Eclipse C1, 1000X).

RNA Isolation and Quantitative Reverse Transcriptase-polymerase Chain Reaction (qRT-PCR)

RNA isolation was performed following the manufacturer's instructions using the Nucleospin RNA II kit (Macherey-Nagel, Duren, Germany). An aliquot (1 μ g) of total lung RNA was reverse transcribed as previously published [48,49]. The cDNA was amplified in a 20 μ l volume containing gene-specific primers labeled with SYBR Green master mix (Kappa Biosystems; Woburn, MA) using an Eppendorf Mastercycler ep Realplex (Eppendorf, Hauppauge, NY). *Ccl2* (*Mcp-1*) (For) 5'-GTCAC-CAAGCTCAAGAGAGA-3', (Rev) 5'-GTCACCTCTACAG AAGTGCT-3'; *Ptgs2* (*Cox-2*), (For) 5'-ATTGGTGGAGAGGTG-TATCC-3', (Rev) 5'-ACACTCTGTTGTGC TCCCGAA-3'; *Tnf* (For) 5'-ACGGCATGGATCTCAAAGAC-3', *Tnf* (Rev) 5'-AGATAGCAAATCGGCTGACG-3'. The relative quantification of gene expression was calculated from the threshold cycle (C_T) values for each sample and normalized in relation to the expression of 18S rRNA [50] using the comparative C_T method.

Statistical Analysis

Data were expressed as the group mean \pm standard error of the mean (SEM). Two-way ANOVA was used to evaluate the effects of treatment (vehicle, 1-MeA, 2-MeA) and concentration or time. The Student-Newman-Keuls test was used for a *posteriori* comparisons of means ($p < 0.05$). All of the statistical analyses were

performed using SigmaStat 3.0 software program (SPSS Science Inc., Chicago, IL).

Results

GJIC in Response to LMW PAHs

Little cytotoxicity was observed in the C10 cells in response to either vehicle, 1- or 2-MeA treatments (Fig. 2) at doses between 25–150 μ M for several time points (30 min, 1.5 and 6 h), thus all subsequent experiments on cell signaling were conducted at these non-cytotoxic doses and times. The CH₃CN vehicle had no effect on GJIC and the positive control (TPA) demonstrated dysregulation of GJIC in C10 cells (Fig. 3C). 1-MeA was shown to inhibit GJIC in a concentration dependent manner in which the most significant change in the dysregulation of GJIC occurred between 10 and 25 μ M with a maximum inhibition observed between 50–100 μ M. Exposure to 2-MeA did not dysregulate GJIC, even at high concentrations (Fig. 3A). To assure robust responses for the other experiments, we chose a mid-value of 75 μ M for maximum inhibition. Significant dose and treatment effects were observed for 1-MeA compared to the control or 2-MeA treatment ($p < 0.05$). A time course experiment indicated that 1-MeA significantly and rapidly inhibited GJIC, by 15 to 30 minutes, and continued to inhibit through the 6 h time point; while 2-MeA (200 μ M) did not inhibit GJIC at any of the time points (Fig. 3B). Figure 3D depicts examples of the fluorescent images of the SL-DT assay lucifer yellow dye spread following treatment of the C10 cells with 1-MeA, 2-MeA, and TPA. Since 1-MeA was shown to inhibit GJIC quickly and effectively at a concentration of 75 μ M, we investigated whether this effect was reversible after removal of 1-MeA and replacement with serum free media. Significant recovery of GJIC began after 30 min, however was not completely restored 4 h later (Fig. 3E).

MAP Kinase (MAPK) Activation

The activity of MAP kinase was assessed over a time course of 15 min to 4 h using immunoblotting techniques of the phosphorylated (activated) forms of ERK and p38 (Fig. 4 and 5). Phosphorylated ERK1/2 (pERK1/2) was significantly increased at 1–4 h by 1-MeA while 2-MeA and the vehicle control (Cntl) had no effect on the activation of pERK1/2 (Fig. 4). Phosphorylated P38 (pP38) also rapidly increased following exposure to 1-MeA, but not to exposure with 2-MeA or the vehicle (Fig. 5). The

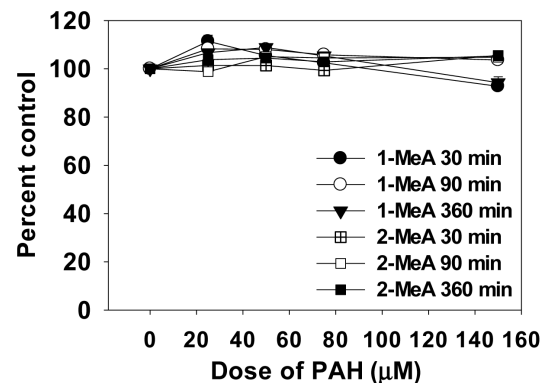


Figure 2. Cytotoxicity is not observed in response to 1 or 2-MeA in the C10 cells. The MTS assay observed no toxic levels of either PAH between 25–150 μ M for 30 min, 1.5, or 6 h time points in the C10 cells. Mean \pm SEM presented with $n = 3$ per study, replicated twice.

doi:10.1371/journal.pone.0065150.g002

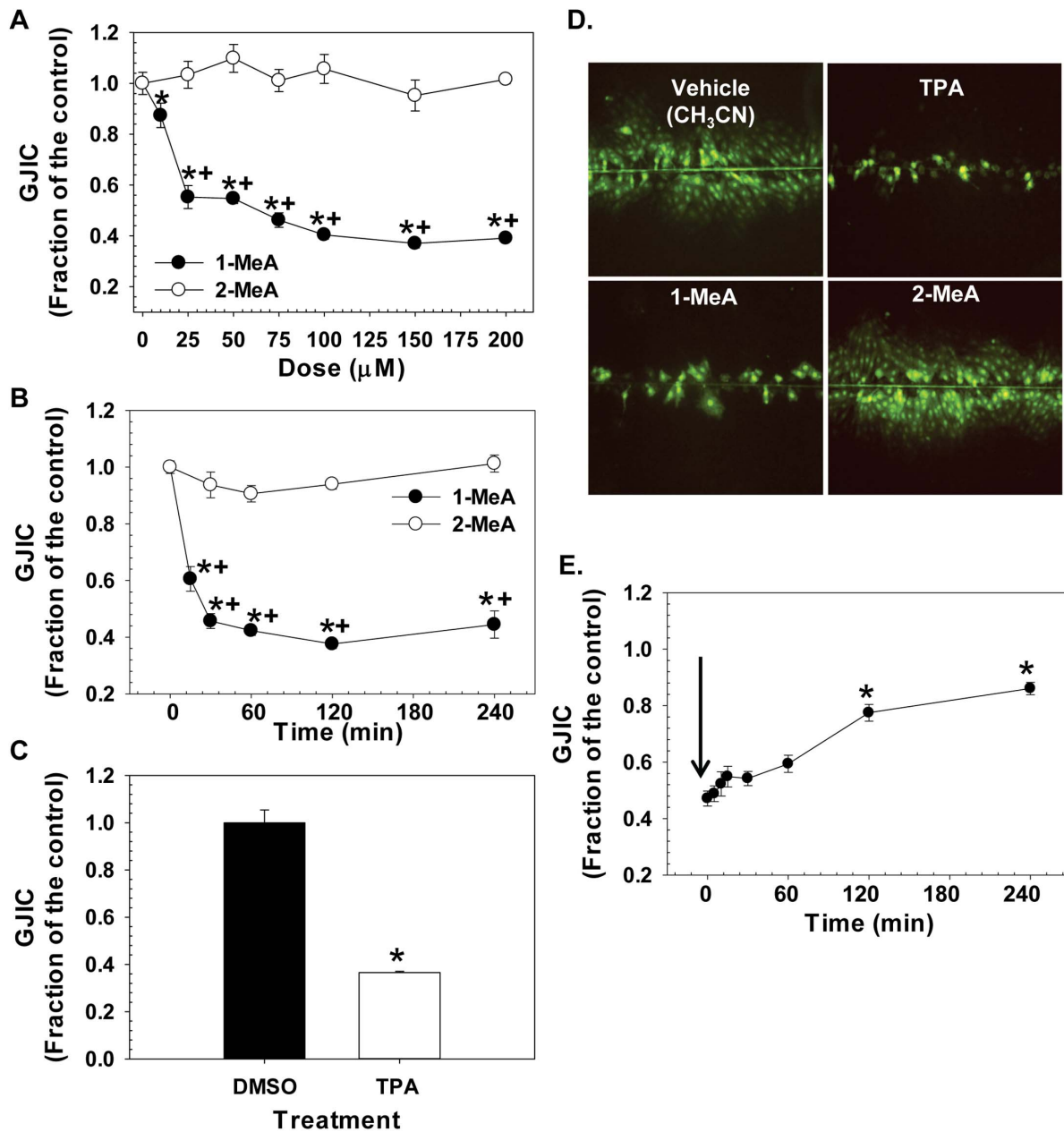


Figure 3. Dose response, time course, and recovery studies following treatment with 1- and 2-MeA. (A) Dose response for 1 and 2-MeA from 0–200 μM. Acetonitrile (CH₃CN) is the vehicle control for the PAHs for all studies. (B) Time course following treatment with 1 and 2-MeA from 0–4 h. 1-MeA (75 μM) and 2-MeA (200 μM). (C) TPA positive control (50 nM, 60 min) for GJIC dysregulation in C10 cells. DMSO is the vehicle control for the TPA. Mean ± SEM presented in A–C with n=3 per study, replicated 3 times. 1-MeA, 1-methylanthracene; 2-MeA, 2-methylanthracene. *p<0.05 compared to control; *p<0.05 compared to 2-MeA treated cells at the same concentration or time point. (D) Depiction of SL/DT assay after 30 min incubation with vehicle control (CH₃CN), TPA (50 nM), 1-MeA, and 2-MeA treatment both at 75 μM demonstrating the lucifer yellow dye incorporation into the C10 cells that are communicating via gap junctions. DAPI was used for nuclear staining. Magnification at 100X. (E) Time to recovery for reversal of GJIC dysregulation in C10 cells following a 30 min treatment with 1-MeA. Black arrow indicates the removal of 1-MeA and replacement with serum-free media. Some recovery was observed approximately 1 h following removal of 1-MeA and continued through 4 h, although complete recovery was not seen. Mean ± SEM presented with n=3 per study, replicated 3 times. *p<0.05 compared to C10 cells at 0 time point which is 30 min following 1-MeA treatment. doi:10.1371/journal.pone.0065150.g003

phosphorylation of P38 occurred within 15 min of exposure to 1-MeA, peaked at 1 h, and persisted through 4 h. Significant differences were observed for both pERK1/2 and pP38 after normalization to total ERK and total P38 in response to 1-MeA for both treatment and time, but not to 2-MeA or control treatments (Fig. 4B and 5B). TPA was used as a positive control for

pERK1/2 and pP38 in these studies, as observed in part C of Figures 4 and 5. Twenty-five and 50 μM doses of 1-MeA were also used to demonstrate increased activation of ERK1/2 at lower doses (Fig. S1).

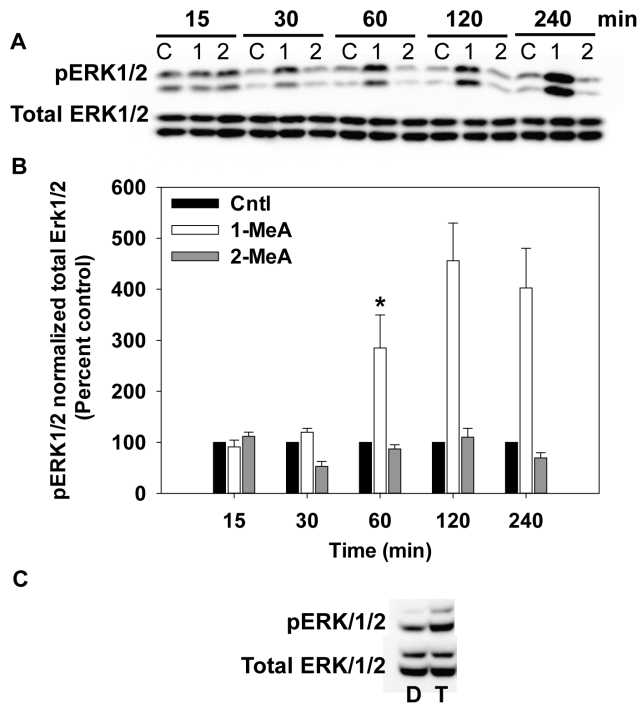


Figure 4. Phospho-ERK1/2 MAPK activation following treatment with 1- but not 2- MeA. (A) Immunoblot for pERK1/2 and total ERK for 15 min to 4 h of treatment. (B) Densitometric analysis of pERK1/2 normalized to total ERK, represented as percent control. Concentrations used: 75 μ M 1-MeA and 75 μ M 2-MeA. Mean \pm SEM presented with $n=3$ per study, replicated 3 times. 1-MeA, 1-methylanthracene; 2-MeA, 2-methylanthracene; Cntl, CH₃CN vehicle control. * $p<0.05$ compared to control; † $p<0.05$ compared to 2-MeA treated cells at the same time point. (C) Positive control using T, TPA (50 nM, 60 min) or D, DMSO (negative control) for activation of ERK1/2. doi:10.1371/journal.pone.0065150.g004

Cx43 Expression

Immunoblot analyses were used to assess the relative protein levels and phosphorylation status of Cx43, the major gap junction protein of these pulmonary cells. The same time course was used for Cx43 as the MAPK (15 min–4 h). As observed with previous endpoints, CH₃CN control had no effect on Cx43 protein expression levels, similar to the lack of effect on GJIC or MAPK activation (Fig. 6). There were no significant changes in the ratios of the three forms of Cx43 at 15 and 30 min, which indicate no change in phosphorylation of the connexins and are within the time period of 1-MeA-induced dysregulation of GJIC. However, 1-MeA did significantly reduce total Cx43 expression at the 2 and 4 h time points as compared to either the vehicle or 2-MeA exposure (Fig. 6). In contrast, TPA induced a hyperphosphorylation of the connexins as indicated by a mobility shift to higher molecular weights (Fig. 6C). This latter result indicated that Cx43 in lung cells are capable of phosphorylation changes, yet the 1-MeA had no effect on the phosphorylation status as determined by the lack of mobility shifts in immunoblots.

Cx43 immunostaining demonstrated punctate staining on the cell membrane in the vehicle or 2-MeA treated C10 cells at both 30 min and 4 h time points, however, in the 1-MeA exposed cells, the punctate staining decreased in the plasma membranes, became more apparent in the cytoplasm after 30 min, and almost completely disappeared by 4 h (Fig. 7). These events occurred after the dysregulation of GJIC and are similar to that observed

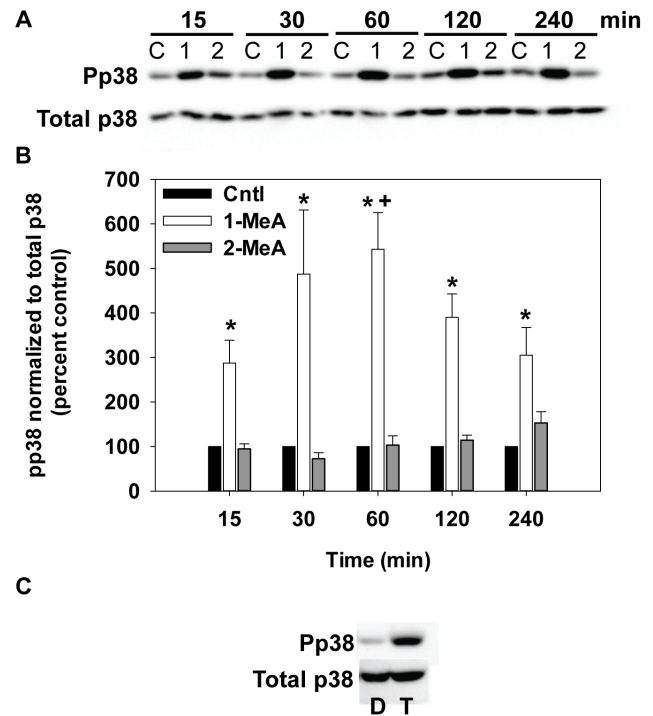


Figure 5. Phosphop38 (pP38) MAPK activation following treatment with 1- but not 2- MeA. (A) Immunoblot for pP38 and total p38 for 15 min to 4 h of treatment. (B) Densitometric analysis of pP38 normalized to total p38, represented as percent control. Concentrations used: 75 μ M 1-MeA and 75 μ M 2-MeA. Mean \pm SEM presented with $n=3$ per study, replicated 3 times. 1-MeA, 1-methylanthracene; 2-MeA, 2-methylanthracene; Cntl, CH₃CN vehicle control. * $p<0.05$ compared to control; † $p<0.05$ compared to 2-MeA treated cells at the same time point. (C) Positive control using T, TPA (50 nM, 60 min) or D, DMSO (negative control) for activation of P38. doi:10.1371/journal.pone.0065150.g005

with TPA in which dysfunctional GJIC lead to the connexins being re trafficked to the cytosolic cell compartments (Fig. 7).

Role of MAPK in the Dysregulation of GJIC

Because the activation of P38 and ERK1/2 in response to 1-MeA occurred at time points when GJIC was also inhibited, we determined the effects of ERK1/2 and P38 dysregulation on GJIC activity. We pre-incubated the cells with either a MEK-inhibitor (U0126; inhibits upstream of ERK1/2), a specific ERK1/2 inhibitor (FR180204; inhibits ERK1 and 2) or a specific inhibitor of p38 (SB203580) and then assessed the effects of 1-MeA on GJIC. Inhibition of P38 prevented the dysregulation of GJIC by 1-MeA, while inhibition of the MEK pathway using U0126 and ERK1/2 using FR180204, had no effect on the dysregulation of GJIC elicited by 1-MeA (Fig. 8). An additional P38 inhibitor (SB202190, 20 μ M, [25]) was also used to reverse 1-MeA-induced dysregulation of GJIC and confirmed the SB203580 results (data not shown). Immunoblots of MAPKAPK-2, a known substrate for P38 [51] were done to demonstrate inhibition of P38, since SB203580 inhibits p38 activity, but not necessarily phosphorylation [47] (see Fig. S2A). pERK1/2 immunoblots also demonstrated inhibition of pERK with both U0126 and FR180204, although, FR180204 only partially inhibited ERK (Fig. S2B). These results indicate 1-MeA-induced dysregulation of GJIC depended, in part, on the p38, but not the ERK1/2 MAPK pathway. TPA-induced dysregulation of GJIC was prevented by U0126, the MEK

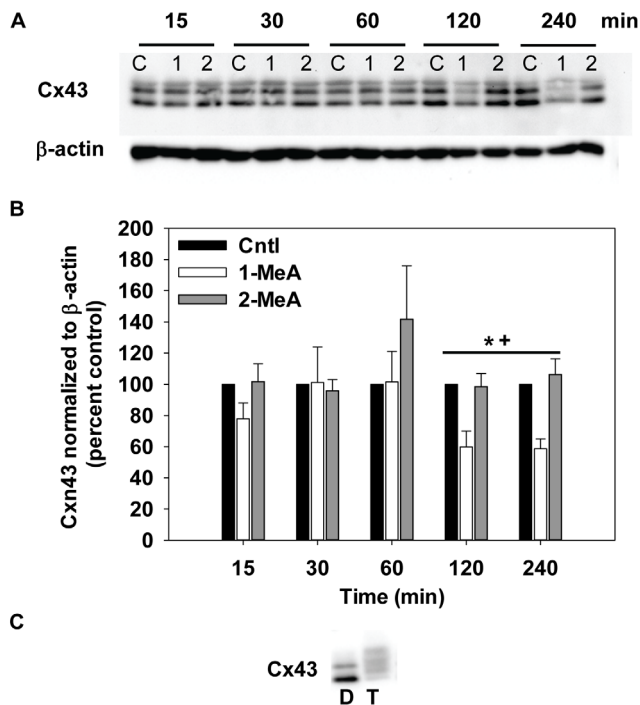


Figure 6. Decreases in Cx43 protein expression following 1-MeA treatment but not 2-MeA treatment. (A) Immunoblot of Cx43 for 15 min to 4 h after treatment. (B) Densitometric analysis of Cx43 normalized to β -actin, represented as percent control. Concentrations used: 75 μ M 1-MeA and 75 μ M 2-MeA. Mean \pm SEM presented with $n=3$ per study, replicated 3 times. 1-MeA, 1-methylanthracene; 2-MeA, 2-methylanthracene; Cntl, CH₃CN vehicle control. * $p<0.05$ compared to control; + $p<0.05$ compared to 2-MeA treated cells at the same time point. (C) Positive control using T (TPA; 50 nM, 60 min) or D (DMSO; negative control) for activation of Cx43. doi:10.1371/journal.pone.0065150.g006

inhibitor, which supports previous findings on the involvement of ERK1/2 MAPK in gap junction regulation with TPA [52].

Inflammatory Pathways Downstream of MAPK

RNA expression for several pathways downstream of the MAPKs, among other pathways, was analyzed via qPCR for 2–6 h following 1- or 2-MeA treatments compared to vehicle treated cells at each time point (Fig. 9). *Ccl2* (*Mcp-1*; Fig. 9A) gene expression significantly increased at 4 h and was increased at 6 h following 1-MeA treatment, but was not observed in 2-MeA or vehicle treatments. *Cox2* (*Ptgs2*; Fig. 9B) expression was also highly elevated (between 18–80-fold; $P<0.05$) at 2, 4 and 6 h time points compared to either 2-MeA or control treatments. *Cox-2* expression was slightly elevated at 2 h in the 2-MeA treatment group. *Tnf* (Fig. 9 C) was also significantly elevated at 2 h in both 1- and 2-MeA compared to the vehicle treatment and remained significantly elevated only in the 1-MeA treatment at 4 h. However, by 6 h, repression of *Tnf* was observed in the 1- and 2-MeA treatment groups, suggesting feedback regulation of *Tnf* after the initial increase.

Discussion

These novel studies address the effects of low molecular weight PAHs (1 and 2-MeA) on alveolar type II cells and identified several markers of downstream signaling pathways that were modulated in response to 1-MeA, but not 2-MeA. GJIC was dysregulated and

MAPKs were activated (P38, pERK1/2) as an early response to the active PAH (1-MeA), but not to 2-MeA, suggesting a structure-activity relationship underlies the efficacy of responses. Longer-term effects included a decrease in the protein levels of Cx43, relocalization of Cx43 from the plasma membrane to the cytoplasm, and the induction of specific inflammatory mediators (*Mcp-1*, *Cox-2*, and *Tnf*). The rapid onset of GJIC dysregulation in our model at time points that coincide with observed increases in pP38 suggests an interaction between the MAPK pathways and regulation of gap junctions. Our finding that inhibition of P38 almost completely blocked the 1-MeA-induced dysregulation of gap junctions, indicates that the regulation of GJIC was, in fact, P38-dependent. In response to 1-MeA, the activation of pERK1/2 was subsequent (30 min) to the dysregulation of GJIC (<15 min), and the inhibition of MEK or ERK1/2 with U0126 or FR180204, respectively, did not prevent the dysregulation of GJIC, which indicates that the ERK1/2 pathway was not involved in 1-MeA-induced dysregulation of GJIC. Cx43 protein levels decreased several hours after the dysregulation of GJIC, although the Cx43 staining at 30 min (Fig. 7) indicated early removal of Cx43 from the plasma membrane of treated cells, consistent with Cx43 trafficking. However, we cannot rule out the possibility that other connexins are involved in this 1-MeA-induced response. Alveolar type II cells can also express Cx26, Cx32, Cx37, and Cx46 and some can heterodimerize, although the concept of mixed gap junction channels remains controversial [29].

Gap Junctions and the Lung

Gap junctions have important roles in many normal physiological processes in the CNS, kidney, liver, heart, and lung, [29,53,54], and when channel resistance increases, impairment of function can lead to pathological states. In some lung diseases, such as acute lung injury, deficient communication between cells could be a causal mechanism. In lung fibroblasts isolated from idiopathic pulmonary fibrosis patients (IPF), gap junction activity and Cx43 expression was significantly decreased compared to controls [21], however the importance of decreased fibroblast communication in fibrosis is not clear.

Changes in the phosphorylation status of the connexin proteins have been implicated in the dysregulation of GJIC [55–58]. Our results indicate that 1-MeA did not alter the phosphorylation status of Cx43. TPA was used as the positive control for hyperphosphorylation of Cx43, as indicated in a shift of the bands to higher molecular weights and the disappearance of the bottom band (unphosphorylated Cx43) (Fig. 6C). The lack of an effect on the phosphorylation of Cx43 by 1-MeA persisted after the activation of ERK1/2 and p38, similar to findings for 1-MeA treated rat liver cells [25,43] and p38 [25]. Although Cx43 has consensus sequences for MAPKs [59,60], these results indicate that other signaling factors, which were not activated in response to 1-MeA, are also required to phosphorylate Cx43. The phosphorylation of Cx43 by TPA is known to be dependent on protein kinase C and ERK1/2 [61]. Alternatively, our results did show a decrease in all Cx43 bands that was consistent with our immunostaining experiments in which Cx43 localized to the cytoplasm, and displayed an overall decrease to near disappearance over our time course (Fig. 7).

PAHs

The structural differences between 1- and 2-MeA while minor in appearance, elicit completely different responses in the C10 cells due to the lack of a bay-like region in the 2-MeA structure compared to the 1-MeA structure. Similar differences were

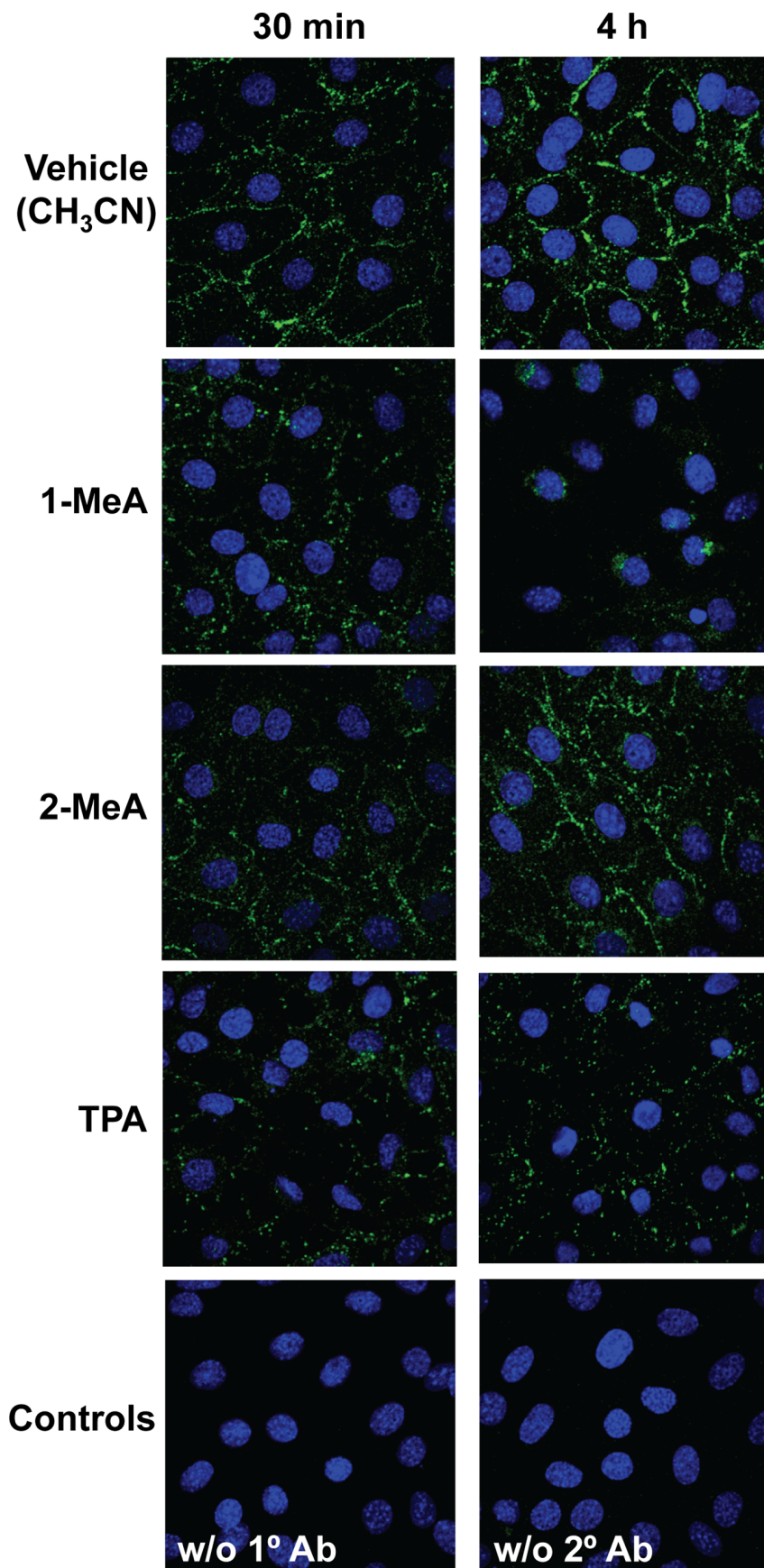


Figure 7. Reduced C10 cell Cx43 immunostaining in response to 1-MeA, but not 2-MeA treatment. Cells were treated with acetonitrile vehicle (CH₃CN), 1-MeA (75 μ M), 2-MeA (75 μ M), TPA (50 nM, 60 min) as a positive control, and two negative controls, one without (w/o) primary antibody and one without (w/o) secondary antibody. Two time points were assessed, 30 min and 4 h to observe changes at several time points known to inhibit gap junctions. Magnification was at 1000X using a Nikon D-Eclipse C1 confocal microscope. Experiments were repeated twice. doi:10.1371/journal.pone.0065150.g007

observed in other cell types, such as liver and pancreas [25,62], thus these structural differences are not unique to lung.

Doses for these studies were chosen based on several studies demonstrating levels of LMW PAHs in sidestream smoke (ETS) were > mainstream smoke (3186–5695 ng/cigarette) [63,64]. At the low end of the range, 20 cigarettes/pack \times 3186 ng/cigar-

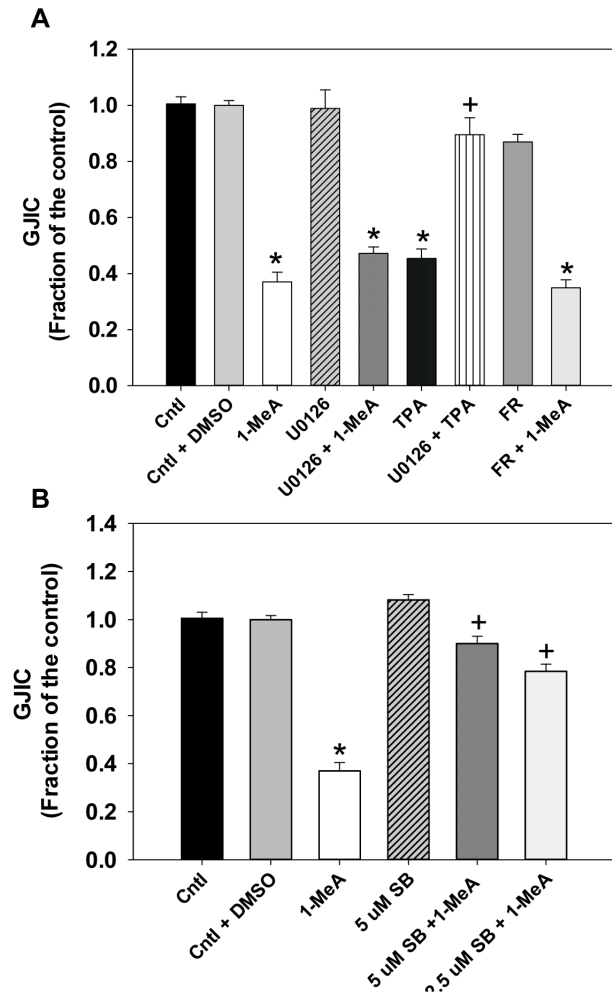


Figure 8. Reversal of 1-MeA-induced GJIC dysregulation using a p38 MAPK inhibitor. (A) U0126 (20 μ M) and FR180204 (5 μ M) were used to inhibit MEK or ERK1/2, respectively, prior to exposure to 1-MeA for 30 min. SL/DT assays were then done following 1-MeA treatment. TPA was also used as a positive control. Cntl, acetonitrile control; 1-MeA, 1-methylanthracene (75 μ M, 30 min); U0126 alone (20 μ M, 1 h prior); U0126+1-MeA, U0126 prior to incubation with 1-MeA; TPA (50 nM, 1 h), TPA alone; U0126+ TPA, U0126 prior to incubation with TPA; FR, FR180204 alone (5 μ M, 1 h prior); FR +1-MeA, FR180204 prior to incubation with 1-MeA. Mean \pm SEM presented with n = 3 per study, replicated 3 times. *p < 0.05 compared to control; +p < 0.05 compared to TPA treated cells. (B) SB203580 (2.5, 5 μ M) was used to inhibit p38 1 h prior to exposure to 1-MeA for 30 min. SL/DT assays were then done following 1-MeA treatment. SB, SB203580 (2.5 or 5 μ M, 1 h); SB +1-MeA, SB203580 prior to incubation with 1-MeA. *p < 0.05 compared to control; +p < 0.05 compared to 1-MeA treated cells. doi:10.1371/journal.pone.0065150.g008

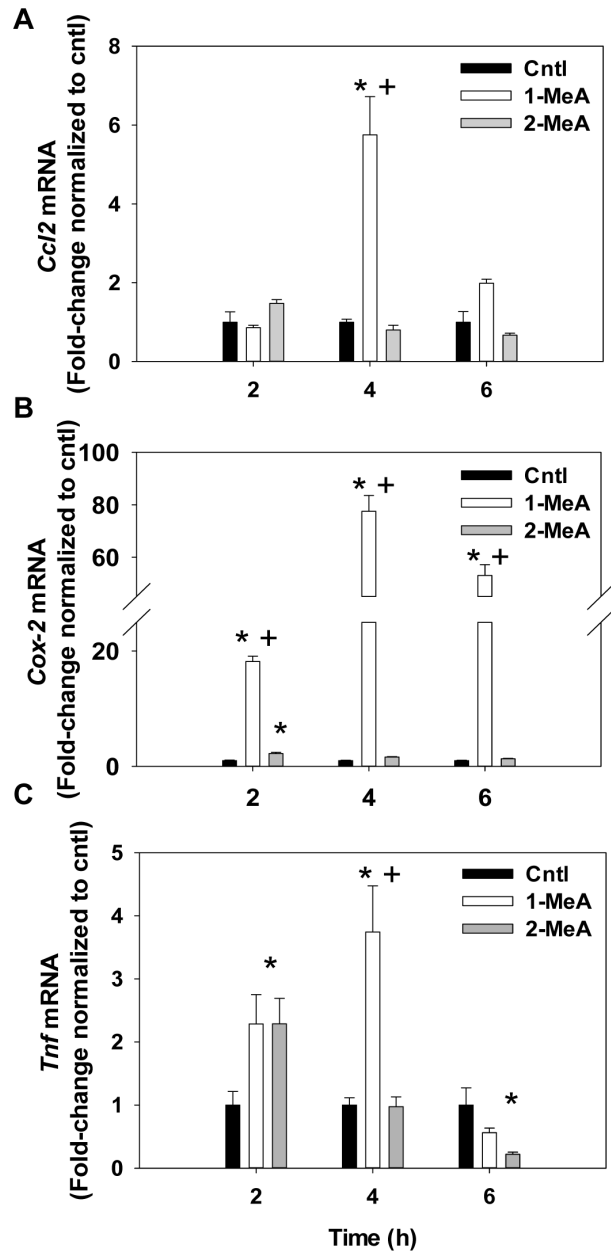


Figure 9. Inflammatory pathways downstream of MAPKs and dysregulation of GJIC are influenced by 1-MeA. (A) *Ccl2*, or *Mcp-1*, mRNA expression in response to 1-MeA, 2-MeA, or control treated cells. (B) *Ptgs2*, or *Cox2*, mRNA expression in response to 1-MeA, 2-MeA, or control treated cells. (C) *Tnf* mRNA expression in response to 1-MeA, 2-MeA, or control treated cells. Concentrations used: 1-MeA, (75 μ M) and 2-MeA (75 μ M). For each gene, mean and SEM are presented; n = 3 per treatment, repeated twice. Genes are first normalized to 18S followed by normalization to acetonitrile control per time point. Cntl = control acetonitrile; 1-MeA, 1-methylanthracene; 2-MeA, 2-methylanthracene; *Ccl2*, chemokine (CC-motif) ligand 2; *Mcp-1*, monocyte chemoattractant 2; *Cox-2*, cyclooxygenase 1; *Ptgs2*, prostaglandin-endoperoxide synthase 2; *Tnf*, tumor necrosis factor α . doi:10.1371/journal.pone.0065150.g009

ette \times 7d/wk = \sim 0.45 mg/wk for the PAH mixture released as ETS. Our dose range is 0.03–0.04 mg/study per individual PAH, however, doses for future studies in mixtures will likely be lower, due to contributing effects [65]. These doses and PAHs were chosen to identify any differences in the phenotypes assessed between an active and inactive isomer, however, we are typically exposed to mixtures of multiple PAHs and not single PAHs. For example, coal tar pitch contains many PAHs [66], both LWM, such as methylanthracenes, and high MW PAHs, and recently was shown to induce promoting characteristics in lung cells [67]. Furthermore, a mixture of PAHs commonly found in coal tar and creosote products demonstrated that dysregulation of GJIC by these PAHs were additive [65], thus there is a definite cumulative effect by many of the PAHs indicating that doses should be based on total PAH content.

MAPK Activation and Gap Junctions

TPA, a classic tumor promoter in most cell types, dysregulates gap junctions through several mechanisms, including MAPKs (P38 and ERK1/2) via the activation of PKC [61,68,69]. Thus, some MAPK pathways are known to mediate the regulation of GJIC in several cell types [61,70]. ERK1/2 also dysregulates gap junctions in other classic non-genotoxic carcinogen models, such as perfluoroalkanoates [71]. However, the activation of ERK1/2 by 1-MeA was not involved in 1-MeA-induced dysregulation of GJIC in the lung cells used in this study, while P38 was involved. This suggests that ERK1/2 is independent of GJIC dysregulation, but is still activated by treatment with 1-MeA, while P38 is linked to GJIC shown by return of normal GJIC by inhibition of P38. Activation of P38 and ERK1/2 by 1-MeA is most likely through an indirect mechanism, eg. activation of receptors or G-proteins.

Gap Junction and MAPK Involvement in Regulating the Pulmonary Microenvironment

In most lung diseases, the pulmonary microenvironment is critical in regulating the inflammation and adverse effects that occur, such as fibrosis and carcinogenesis. Inflammation is an important element of tumorigenesis, at all stages, and is typically considered downstream of earlier triggering events, such as dysregulation of gap junctions and activation of MAPKs [23,72,73].

P38 can induce M α p-1 (Ccl2) in endothelial cells [74,75], and induce other chemokines, such as IL-8, in lung epithelial cells [76]. Cx43 decreased M α p-1 expression in glioblastoma cells which lead to decreased proliferation, suggesting that a reduction in gap junction function lead to increased M α p-1 [77]. Ccl2 (M α p-1) is routinely used as a marker in our *in vivo* promotion models, such as BHT and vanadium pentoxide (V $_2$ O $_5$) [39,50], because it is secreted by the pulmonary epithelial cells as a chemoattractant for both macrophages and lymphocytes into the lung. Macrophage infiltration plays a pivotal role during promotion in these *in vivo* models and an *in vivo* pilot study using fluoranthene, another LMW PAH, demonstrated increased numbers of bronchoalveolar lavage macrophages in the lungs compared to controls (unpublished data, A.K. Bauer). V $_2$ O $_5$ -induced promotion also leads to increases in both ERK1/2 and P38 MAPK activation [39]. Thus, in our *in vitro* model, we show that M α p-1 is increased following MAPK activation (P38 and ERK1/2), and gap junction dysregulation, all evidence for 1-MeA's potential to contribute to the early signaling events involved in promoting lung cancer.

P38 is also considered the major MAPK involved in TNF-induction [78,79]. Interestingly, TNF can also induce MAPK [80], particularly P38, thus, a positive feed-forward mechanism may be involved in regulating this pathway. In addition, TNF can inhibit

gap junctions in fibroblasts [81] and repress Cx43 expression in keratinocytes [82], thus supporting a possible link between pro-inflammatory cytokine expression and regulation of gap junctions.

In rat liver cells (WB F344) and human coronary artery endothelial cells, arachidonic acid (AA) is released in response to 1-MeA, but not 2-MeA [25,83]. Since Cox-2 is downstream of AA and cytosolic phospholipase A $_2$ (cPLA $_2$) [23], we determined the possible involvement of the Cox-2 pathway in our model. Prostaglandin E $_2$ (PGE $_2$) and prostaglandin I $_2$ (PGI $_2$) production, both downstream of Cox-2, are ERK1/2-dependent in response to TNF and interferon (IFN) γ stimulation in C10 cells as well as nitric oxide production and inducible nitric oxide synthase (iNOS) expression [17,19]. Preliminary data from our lab demonstrated that both p38 and ERK1/2 regulate Cox-2 gene expression in 1-MeA treated C10 cells (data not shown).

Conclusion

Although the most abundant PAHs in the environment are the LMW PAHs, research on PAHs has focused primarily on the mutagenic and DNA damaging properties of the higher molecular weight compounds, however, evidence supports the LMW PAHs ability to induce molecular events relevant to lung injury, inflammation, and tumor promotion. We previously reported the effects of 41 different PAHs on GJIC in rat liver cell lines [41,42,65,84] where most of these PAHs, including the high molecular weight PAHs, dysregulated GJIC with varying potencies [41,42]. However, the potencies of the LMW PAHs (4 rings or less) tended to be much stronger if they contained a bay or bay-like region [11,41,42].

Our results extend this research into a lung derived cell model system in which the PAH containing a bay-like structure was biologically active and the PAH lacking these structures was inactive, consistent with the liver model cell systems. Considering that the lung is the major organ of exposure to PAHs in the environment, these novel results suggest that the LMW, non-genotoxic PAHs could contribute to the lung injury and promotion process, thus posing a potential human health risk as well as linking LMW PAH-induced effects with proinflammatory responses, which was also dependent on the PAH possessing a bay-like structure. The role of inflammation in all stages of cancer, fibrosis, COPD, and many other pulmonary diseases further demonstrates the importance of this link between PAH exposure, early signaling and inflammatory mediator involvement [85–88].

Collectively, this study provides the first assessment of the effects of these LMW PAHs on pulmonary cells that may lead to predictive outcomes for future identification of complex mixture effects, as well as identify novel targets for potential biomarkers, develop innovative chemopreventive strategies, and impact future risk assessment for these PAHs in lung and other cancers, such as liver, pancreas, and breast.

Supporting Information

Figure S1 pERK1/2 at several doses of 1-MeA demonstrating increased ERK1/2 activation. C10 cells were exposed to 25 and 50 μ M 1-MeA for 2 h and compared to DMSO vehicle control treated cells (0 μ M). Densitometry of the immunoblot is presented with mean \pm SEM. *P<0.05 for 1-MeA treated cells compared to DMSO alone. (TIF)

Figure S2 Confirmation of inhibition of p38 and ERK1/2 activity following inhibitor incubation using immunoblots. (A) A MAPKAPK-2 immunoblot in C10 cells demonstrating inhibition of phosphorylation of MAPKAPK-2, a known

substrate of p38, compare lane 3 to lane 5 and 6. Lane 1, control, acetonitrile; lane 2, control+DMSO; lane 3, 1-MeA (75 μ M); lane 4, control+SB203580 inhibitor (5 μ M); lane 5, SB203580 (5 μ M) inhibitor +1-MeA; lane 6, SB203580 (2.5 μ M) inhibitor +1-MeA. Total MAPKAPK-2 is seen below the phosphorylated immunoblot demonstrating equal amounts of total in each sample. (B) pERK1/2 immunoblot following treatment with FR180204 (5 μ M) or U0126 (20 μ M) prior to treatment with 75 μ M 1-MeA demonstrating inhibition of ERK phosphorylation in lanes 5 and 6 compared to 3. Lane 1, control, acetonitrile; lane 2, control+DMSO; lane 3, 1-MeA (75 μ M); lane 4, con-

trol+FR180204 (5 μ M); lane 5 FR180204 (5 μ M) +1-MeA; lane 6, U0126 (20 μ M) +1-MeA. (TIF)

Author Contributions

Conceived and designed the experiments: AKB RO PB BLU. Performed the experiments: RO AKB TH KLH KV. Analyzed the data: AKB RO BLU PB. Contributed reagents/materials/analysis tools: AKB BLU. Wrote the paper: RO AKB BLU.

References

- Hazleton WD, Clements MS, Moolgavkar SH (2005) Multistage carcinogenesis and lung cancer mortality in three cohorts. *Cancer Epidemiol Biomarkers Prev* 14: 1171–1181.
- Klaunig JE, Kamendulis LM, Xu Y (2000) Epigenetic mechanisms of chemical carcinogenesis. *Hum Exp Toxicol* 19: 543–555.
- Trosko JE (2001) Commentary: is the concept of “tumor promotion” a useful paradigm? *Mol Carcinog* 30: 131–137.
- ATSDR (2005) Toxicology profile for polyaromatic hydrocarbons. Boca Raton, FL: CRC Press.
- Palitti F, Cozzi R, Fiore M, Palombo F, Polcaro C, et al. (1986) An in vitro and in vivo study on mutagenic activity of fluoranthene: comparison between cytogenetic studies and HPLC analysis. *Mutat Res* 174: 125–130.
- Roszinsky-Kocher G, Basler A, Rohrborn G (1979) Mutagenicity of polycyclic hydrocarbons. V. Induction of sister-chromatid exchanges in vivo. *Mutat Res* 66: 65–67.
- Wilson KM, Klein JD, Blumkin AK, Gottlieb M, Winickoff JP (2011) Tobacco-smoke exposure in children who live in multiunit housing. *Pediatrics* 127: 85–92.
- Centers for Disease C, Prevention (2012) Current tobacco use and secondhand smoke exposure among women of reproductive age - 14 countries, 2008–2010. *MMWR Morb Mortal Wkly Rep* 61: 877–882.
- He Y, Jiang B, Li LS, Li LS, Ko L, et al. (2012) Secondhand smoke exposure predicted chronic obstructive pulmonary disease and other tobacco related mortality in a 17-years cohort study in China. *Chest*.
- Miller RL, Garfinkel R, Horton M, Camann D, Perera FP, et al. (2004) Polycyclic aromatic hydrocarbons, environmental tobacco smoke, and respiratory symptoms in an inner-city birth cohort. *Chest* 126: 1071–1078.
- Upham BL, Weis LM, Trosko JE (1998) Modulated gap junctional intercellular communication as a biomarker of PAH epigenetic toxicity: structure-function relationship. *Environ Health Perspect* 106 Suppl 4: 975–981.
- Warshawsky D, Barkley W, Bingham E (1993) Factors affecting carcinogenic potential of mixtures. *Fundam Appl Toxicol* 20: 376–382.
- Lloyd CM, Saglani S (2010) Asthma and allergy: the emerging epithelium. *Nat Med* 16: 273–274.
- Fujino N, Ota C, Takahashi T, Suzuki T, Suzuki S, et al. (2012) Gene expression profiles of alveolar type II cells of chronic obstructive pulmonary disease: a case-control study. *BMJ Open* 2.
- Schottenfeld D (2000) Etiology and Epidemiology of Lung Cancer. In: Pass HI, Mitchell JB, Johnson DH, Turrisi AT, Minna JD, editors. *Lung Cancer-Principles and Practice*. 2nd ed. Philadelphia: Lippincott Williams and Wilkins. 367–388.
- American Cancer Society (2012) What is non-small cell lung cancer? In: American Cancer Society Inc., editor. Available: <http://www.cancer.org/cancer/lungcancer-non-smallcell/index>. Accessed 16 December, 2012.
- Dwyer-Nield LD, Srebernak MC, Barrett BS, Ahn J, Cospser P, et al. (2005) Cytokines differentially regulate the synthesis of prostanoid and nitric oxide mediators in tumorigenic versus non-tumorigenic mouse lung epithelial cell lines. *Carcinogenesis* 26: 1196–1206.
- Malkinson AM, Dwyer-Nield LD, Rice PL, Dinsdale D (1997) Mouse lung epithelial cell lines—tools for the study of differentiation and the neoplastic phenotype. *Toxicology* 123: 53–100.
- Rice PL, Barrett BS, Fritz JM, Srebernak MC, Kiskey LR, et al. (2010) Regulation of cytokine-induced prostanoid and nitric oxide synthesis by extracellular signal-regulated kinase 1/2 in lung epithelial cells. *Exp Lung Res* 36: 558–571.
- Thompson DC, Porter SE, Bauer AK, Das KC, Ou B, et al. (1998) Cytokine-induced nitric oxide formation in normal but not in neoplastic murine lung epithelial cell lines. *Am J Physiol* 274: L922–932.
- Trovato-Salinaro A, Trovato-Salinaro E, Failla M, Mastruzzo C, Tomaselli V, et al. (2006) Altered intercellular communication in lung fibroblast cultures from patients with idiopathic pulmonary fibrosis. *Respir Res* 7: 122.
- Bauer AK, Malkinson AM, Kleiberger SR (2004) Susceptibility to neoplastic and non-neoplastic pulmonary diseases in mice: genetic similarities. *Am J Physiol Lung Cell Mol Physiol* 287: L685–703.
- Bauer AK, Rondini EA (2009) Review paper: the role of inflammation in mouse pulmonary neoplasia. *Vet Pathol* 46: 369–390.
- Rosenkranz M, Rosenkranz HS, Klopman G (1997) Intercellular communication, tumor promotion and non-genotoxic carcinogenesis: relationships based upon structural considerations. *Mutat Res* 381: 171–188.
- Upham BL, Blaha L, Babica P, Park JS, Sovadinova I, et al. (2008) Tumor promoting properties of a cigarette smoke prevalent polycyclic aromatic hydrocarbon as indicated by the inhibition of gap junctional intercellular communication via phosphatidylcholine-specific phospholipase C. *Cancer Sci* 99: 696–705.
- Upham BL, Weis LM, Rummel AM, Masten SJ, Trosko JE (1996) The effects of anthracene and methylated anthracenes on gap junctional intercellular communication in rat liver epithelial cells. *Fundam Appl Toxicol* 34: 260–264.
- Vang O, Wallin H, Autrup H (1995) Inhibition of intercellular communication by condensates of high and low tar cigarettes. *Arch Toxicol* 69: 415–420.
- Guan X, Hardenbrook J, Fernstrom MJ, Chaudhuri R, Malkinson AM, et al. (1995) Down-regulation by butylated hydroxytoluene of the number and function of gap junctions in epithelial cell lines derived from mouse lung and rat liver. *Carcinogenesis* 16: 2575–2582.
- Johnson LN, Koval M (2009) Cross-talk between pulmonary injury, oxidant stress, and gap junctional communication. *Antioxid Redox Signal* 11: 355–367.
- Avanzo JL, Mesnil M, Hernandez-Blazquez FJ, Mackowiak, II, Mori CM, et al. (2004) Increased susceptibility to urethane-induced lung tumors in mice with decreased expression of connexin43. *Carcinogenesis* 25: 1973–1982.
- Yan Z, Subbaramaiah K, Camilli T, Zhang F, Tanabe T, et al. (2000) Benzo[a]pyrene induces the transcription of cyclooxygenase-2 in vascular smooth muscle cells. Evidence for the involvement of extracellular signal-regulated kinase and NF-kappaB. *J Biol Chem* 275: 4949–4955.
- Ji H, Wang Z, Perera SA, Li D, Liang MC, et al. (2007) Mutations in BRAF and KRAS converge on activation of the mitogen-activated protein kinase pathway in lung cancer mouse models. *Cancer Res* 67: 4933–4939.
- Walters DM, Antao-Menezes A, Ingram JL, Rice AB, Nyska A, et al. (2005) Susceptibility of signal transducer and activator of transcription-1-deficient mice to pulmonary fibrogenesis. *Am J Pathol* 167: 1221–1229.
- Moghaddam SJ, Ochoa CE, Sethi S, Dickey BF (2011) Nontypeable Haemophilus influenzae in chronic obstructive pulmonary disease and lung cancer. *Int J Chron Obstruct Pulmon Dis* 6: 113–123.
- Bernert H, Sekikawa K, Radcliffe RA, Iraqi F, You M, et al. (2003) Tnfa and Il-10 deficiencies have contrasting effects on lung tumor susceptibility: gender-dependent modulation of IL-10 haploinsufficiency. *Mol Carcinog* 38: 117–123.
- Duperron C (1997) Chemopreventive efficacies of aspirin and sulindac against lung tumorigenesis in A/J mice. *Carcinogenesis* 18: 1001–1006.
- Kiskey LR, Barrett BS, Bauer AK, Dwyer-Nield LD, Barthel B, et al. (2002) Genetic ablation of inducible nitric oxide synthase decreases mouse lung tumorigenesis. *Cancer Res* 62: 6850–6856.
- Meyer AM, Dwyer-Nield LD, Hurteau G, Keith RL, Ouyang Y, et al. (2006) Attenuation of the pulmonary inflammatory response following butylated hydroxytoluene treatment of cytosolic phospholipase A2 null mice. *Am J Physiol Lung Cell Mol Physiol* 290: L1260–1266.
- Rondini EA, Walters DM, Bauer AK (2010) Vanadium pentoxide induces pulmonary inflammation and tumor promotion in a strain-dependent manner. *Part Fibre Toxicol* 7: 9.
- Wattenberg LW, Estensen RD (1997) Studies of chemopreventive effects of budenoside on benzo[a]pyrene-induced neoplasia of the lung of female A/J mice. *Carcinogenesis* 18: 2015–2017.
- Blaha L, Kapplova P, Vondracek J, Upham B, Machala M (2002) Inhibition of gap-junctional intercellular communication by environmentally occurring polycyclic aromatic hydrocarbons. *Toxicol Sci* 65: 43–51.
- Weis LM, Rummel AM, Masten SJ, Trosko JE, Upham BL (1998) Bay or baylike regions of polycyclic aromatic hydrocarbons were potent inhibitors of gap junctional intercellular communication. *Environ Health Perspect* 106: 17–22.
- Rummel AM, Trosko JE, Wilson MR, Upham BL (1999) Polycyclic aromatic hydrocarbons with bay-like regions inhibited gap junctional intercellular communication and stimulated MAPK activity. *Toxicol Sci* 49: 232–240.
- Wan B, Sayler GS, Schultz TW (2006) Structure-activity relationships for flow cytometric data of smaller polycyclic aromatic hydrocarbons. *SAR QSAR Environ Res* 17: 597–605.

45. Upham BL (2011) Role of integrative signaling through gap junctions in toxicology. *Curr Protoc Toxicol* Chapter 2: Unit2 18.
46. Chaudhuri R, Sigler K, Dupont E, Trosko JE, Malkinson AM, et al. (1993) Gap junctional intercellular communication in mouse lung epithelial cell lines: effects of cell transformation and tumor promoters. *Cancer Lett* 71: 11–18.
47. Tong Q, Zheng L, Dodd-o J, Langer J, Wang D, et al. (2006) Hypoxia-induced mitogenic factor modulates surfactant protein B and C expression in mouse lung. *Am J Respir Cell Mol Biol* 34: 28–38.
48. Cho HY, Jedlicka AE, Reddy SP, Kensler TW, Yamamoto M, et al. (2002) Role of NRF2 in protection against hyperoxic lung injury in mice. *Am J Respir Cell Mol Biol* 26: 175–182.
49. Bauer AK, Cho HY, Miller-Degraff L, Walker C, Helms K, et al. (2011) Targeted deletion of Nrf2 reduces urethane-induced lung tumor development in mice. *PLoS One* 6: e26590.
50. Bauer AK, Fostel J, Degraff LM, Rondini EA, Walker C, et al. (2009) Transcriptomic analysis of pathways regulated by toll-like receptor 4 in a murine model of chronic pulmonary inflammation and carcinogenesis. *Mol Cancer* 8: 107.
51. Ben-Levy R, Leighton IA, Doza YN, Attwood P, Morrice N, et al. (1995) Identification of novel phosphorylation sites required for activation of MAPKAP kinase-2. *EMBO J* 14: 5920–5930.
52. Ruch RJ, Trosko JE, Madhukar BV (2001) Inhibition of connexin43 gap junctional intercellular communication by TPA requires ERK activation. *J Cell Biochem* 83: 163–169.
53. Eugenin EA, Basilio D, Saez JC, Orellana JA, Raine CS, et al. (2012) The role of gap junction channels during physiologic and pathologic conditions of the human central nervous system. *J Neuroimmune Pharmacol* 7: 499–518.
54. Sorensen CM, Holstein-Rathlou NH (2012) Cell-cell communication in the kidney microcirculation. *Microcirculation* 19: 451–460.
55. Abdelmohsen K, Gerber PA, von Montfort C, Sies H, Klotz LO (2003) Epidermal growth factor receptor is a common mediator of quinone-induced signaling leading to phosphorylation of connexin-43: role of glutathione and tyrosine phosphatases. *J Biol Chem* 278: 38360–38367.
56. Guan X, Wilson S, Schlender KK, Ruch RJ (1996) Gap-junction disassembly and connexin 43 dephosphorylation induced by 18 beta-glycyrrhetic acid. *Mol Carcinog* 16: 157–164.
57. Husoy T, Cruciani V, Sanner T, Mikalsen SO (2001) Phosphorylation of connexin43 and inhibition of gap junctional communication in 12-O-tetradecanoylphorbol-13-acetate-exposed R6 fibroblasts: minor role of protein kinase C beta 1 and mu. *Carcinogenesis* 22: 221–231.
58. Musil LS, Goodenough DA (1991) Biochemical analysis of connexin43 intracellular transport, phosphorylation, and assembly into gap junctional plaques. *J Cell Biol* 115: 1357–1374.
59. Lampe PD, Lau AF (2004) The effects of connexin phosphorylation on gap junctional communication. *Int J Biochem Cell Biol* 36: 1171–1186.
60. Warn-Cramer BJ, Lampe PD, Kurata WE, Kanemitsu MY, Loo LW, et al. (1996) Characterization of the mitogen-activated protein kinase phosphorylation sites on the connexin-43 gap junction protein. *J Biol Chem* 271: 3779–3786.
61. Rivedal E, Opsahl H (2001) Role of PKC and MAP kinase in EGF- and TPA-induced connexin43 phosphorylation and inhibition of gap junction intercellular communication in rat liver epithelial cells. *Carcinogenesis* 22: 1543–1550.
62. Tai MH, Upham BL, Olson LK, Tsao MS, Reed DN, Jr., et al. (2007) Cigarette smoke components inhibited intercellular communication and differentiation in human pancreatic ductal epithelial cells. *Int J Cancer* 120: 1855–1862.
63. Lee HL, Hsieh DP, Li LA (2010) Polycyclic aromatic hydrocarbons in cigarette sidestream smoke particulates from a Taiwanese brand and their carcinogenic relevance. *Chemosphere* 10.1016/j.chemosphere.2010.09.045.
64. Moir D, Rickert WS, Levasseur G, Larose Y, Maertens R, et al. (2008) A comparison of mainstream and sidestream marijuana and tobacco cigarette smoke produced under two machine smoking conditions. *Chem Res Toxicol* 21: 494–502.
65. Ghoshal B, Weber WJ, Rummel AM, Trosko JE, Upham BL (1999) Epigenetic Toxicity of a Mixture of Polycyclic Aromatic Hydrocarbon on Gap Junctional Intercellular Communication Before and After Biodegradation. *Environment Science Technology* 33: 1044–1050.
66. Services USDoHaH (2002) Toxicological profile for wood, creosote, coal tar creosote, coal tar, coal tar pitch, and coal tar pitch volatiles. Atlanta, GA. 225–227 p.
67. Feng F, Wu Y, Zhang S, Liu Y, Qin L, et al. (2012) Macrophages Facilitate Coal Tar Pitch Extract-Induced Tumorigenic Transformation of Human Bronchial Epithelial Cells Mediated by NF-kappaB. *PLoS One* 7: e51690.
68. Pahujaa M, Anikin M, Goldberg GS (2007) Phosphorylation of connexin43 induced by Src: regulation of gap junctional communication between transformed cells. *Exp Cell Res* 313: 4083–4090.
69. Woodruff ML, Chaban VV, Worley CM, Dirksen ER (1999) PKC role in mechanically induced Ca²⁺ waves and ATP-induced Ca²⁺ oscillations in airway epithelial cells. *Am J Physiol* 276: L669–678.
70. Yang SR, Cho SD, Ahn NS, Jung JW, Park JS, et al. (2005) Role of gap junctional intercellular communication (GJIC) through p38 and ERK1/2 pathway in the differentiation of rat neuronal stem cells. *J Vet Med Sci* 67: 291–294.
71. Upham BL, Park JS, Babica P, Sovadinova I, Rummel AM, et al. (2009) Structure-activity-dependent regulation of cell communication by perfluorinated fatty acids using in vivo and in vitro model systems. *Environ Health Perspect* 117: 545–551.
72. Cohen BH, Diamond EL, Graves CG, Kreiss P, Levy DA, et al. (1977) A common familial component in lung cancer and chronic obstructive pulmonary disease. *Lancet* 2: 523–526.
73. Wu AH, Fontham ET, Reynolds P, Greenberg RS, Buffler P, et al. (1995) Previous lung disease and risk of lung cancer among lifetime nonsmoking women in the United States. *Am J Epidemiol* 141: 1023–1032.
74. Marin V, Farnarier C, Gres S, Kaplanski S, Su MS, et al. (2001) The p38 mitogen-activated protein kinase pathway plays a critical role in thrombin-induced endothelial chemokine production and leukocyte recruitment. *Blood* 98: 667–673.
75. Sung FL, Slow YL, Wang G, Lynn EG, O K (2001) Homocysteine stimulates the expression of monocyte chemoattractant protein-1 in endothelial cells leading to enhanced monocyte chemotaxis. *Mol Cell Biochem* 216: 121–128.
76. Schmeck B, Zahlten J, Moog K, van Laak V, Huber S, et al. (2004) Streptococcus pneumoniae-induced p38 MAPK-dependent phosphorylation of RelA at the interleukin-8 promoter. *J Biol Chem* 279: 53241–53247.
77. Huang R, Lin Y, Wang CC, Gano J, Lin B, et al. (2002) Connexin 43 suppresses human glioblastoma cell growth by down-regulation of monocyte chemotactic protein 1, as discovered using protein array technology. *Cancer Res* 62: 2806–2812.
78. Brook M, Sully G, Clark AR, Saklatvala J (2000) Regulation of tumour necrosis factor alpha mRNA stability by the mitogen-activated protein kinase p38 signalling cascade. *FEBS Lett* 483: 57–61.
79. Lee JC, Laydon JT, McDonnell PC, Gallagher TF, Kumar S, et al. (1994) A protein kinase involved in the regulation of inflammatory cytokine biosynthesis. *Nature* 372: 739–746.
80. Kim EK, Choi EJ (2010) Pathological roles of MAPK signaling pathways in human diseases. *Biochim Biophys Acta* 1802: 396–405.
81. Ito S, Hyodo T, Hasegawa H, Yuan H, Hamaguchi M, et al. (2010) PI3K/Akt signaling is involved in the disruption of gap junctional communication caused by v-Src and TNF-alpha. *Biochem Biophys Res Commun* 400: 230–235.
82. Tacheau C, Laboureaux J, Mauviel A, Verrecchia F (2008) TNF-alpha represses connexin43 expression in HaCat keratinocytes via activation of JNK signaling. *J Cell Physiol* 216: 438–444.
83. Tithof PK, Elgayyar M, Cho Y, Guan W, Fisher AB, et al. (2002) Polycyclic aromatic hydrocarbons present in cigarette smoke cause endothelial cell apoptosis by a phospholipase A2-dependent mechanism. *FASEB J* 16: 1463–1464.
84. Upham BL, Masten SJ, Lockwood BR, Trosko JE (1994) Nongenotoxic effects of polycyclic aromatic hydrocarbons and their oxygenation by-products on the intercellular communication of rat liver epithelial cells. *Fundam Appl Toxicol* 23: 470–475.
85. Allavena P, Mantovani A (2012) Immunology in the clinic review series: focus on cancer: tumour-associated macrophages: undisputed stars of the inflammatory tumour microenvironment. *Clin Exp Immunol* 167: 195–205.
86. Guadagni F, Ferroni P, Palmirotta R, Portarena I, Formica V, et al. (2007) Review. TNF/VEGF cross-talk in chronic inflammation-related cancer initiation and progression: an early target in anticancer therapeutic strategy. *In Vivo* 21: 147–161.
87. Smith LA, Paszkiewicz GM, Hutson AD, Pauly JL (2010) Inflammatory response of lung macrophages and epithelial cells to tobacco smoke: a literature review of ex vivo investigations. *Immunol Res* 46: 94–126.
88. Van Laere S, Limame R, Van Marck EA, Vermeulen PB, Dirix LY (2010) Is there a role for mammary stem cells in inflammatory breast carcinoma?: a review of evidence from cell line, animal model, and human tissue sample experiments. *Cancer* 116: 2794–2805.

VII. Upham, B.L.*, Park, J.-S., **Babica, P.**, Sovadinova, I., Rummel, A.M., Trosko, J.E., Hirose, A., Hasegawa, R., Kanno, J., Sai, K., 2009. Structure-activity-dependent regulation of cell communication by perfluorinated fatty acids using in vivo and in vitro model systems. *Environmental Health Perspectives* 117, 545–551.

Structure-Activity-Dependent Regulation of Cell Communication by Perfluorinated Fatty Acids using *in Vivo* and *in Vitro* Model Systems

Brad L. Upham,¹ Joon-Suk Park,¹ Pavel Babica,¹ Iva Sovadinova,¹ Alisa M. Rummel,¹ James E. Trosko,¹ Akihiko Hirose,² Ryuichi Hasegawa,^{2*} Jun Kanno,³ and Kimie Sai^{3**}

¹Department of Pediatrics and Human Development, National Food Safety and Toxicology Center, Michigan State University, East Lansing, Michigan, USA; ²Division of Risk Assessment, and ³Division of Cellular and Molecular Toxicology, National Institute of Health Sciences, Tokyo, Japan

BACKGROUND: Perfluoroalkanoates, [e.g., perfluorooctanoate (PFOA)], are known peroxisome proliferators that induce hepatomegaly and hepatocarcinogenesis in rodents, and are classic nongenotoxic carcinogens that inhibit *in vitro* gap-junctional intercellular communication (GJIC). This inhibition of GJIC is known to be a function of perfluorinated carbon lengths ranging from 7 to 10.

OBJECTIVES: The aim of this study was to determine if the inhibition of GJIC by PFOA but not perfluoropentanoate (PFPeA) observed in F344 rat liver cells *in vitro* also occurs in F344 rats *in vivo* and to determine mechanisms of PFOA dysregulation of GJIC using *in vitro* assay systems.

METHODS: We used an incision load/dye transfer technique to assess GJIC in livers of rats exposed to PFOA and PFPeA. We used *in vitro* assays with inhibitors of cell signaling enzymes and antioxidants known to regulate GJIC to identify which enzymes regulated PFOA-induced inhibition of GJIC.

RESULTS: PFOA inhibited GJIC and induced hepatomegaly in rat livers, whereas PFPeA had no effect on either end point. Serum biochemistry of liver enzymes indicated no cytotoxic response to these compounds. *In vitro* analysis of mitogen-activated protein kinase (MAPK) indicated that PFOA, but not PFPeA, can activate the extracellular receptor kinase (ERK). Inhibition of GJIC, *in vitro*, by PFOA depended on the activation of both ERK and phosphatidylcholine-specific phospholipase C (PC-PLC) in the dysregulation of GJIC in an oxidative-dependent mechanism.

CONCLUSIONS: The *in vitro* analysis of GJIC, an epigenetic marker of tumor promoters, can also predict the *in vivo* activity of PFOA, which dysregulated GJIC via ERK and PC-PLC.

KEY WORDS: extracellular receptor kinase, gap-junctional intercellular communication, mitogen-activated protein kinase, perfluorooctanoate, perfluoropentanoate, phosphatidylcholine-specific-phospholipase C, tumor promotion. *Environ Health Perspect* 117:545–551 (2009). doi:10.1289/ehp.11728 available via <http://dx.doi.org/> [Online 23 October 2008]

Research on the environmental fate and toxicology of halogenated compounds has focused primarily on brominated and chlorinated organics, whereas fluorinated organics received less attention, partly because of the perception that these compounds, which are quite chemically inert, were also biologically inert (Key et al. 1997). However, perfluorinated fatty acids (PFFAs), such as perfluorooctanoate (PFOA) and perfluorooctane sulfonate (PFOS), are found in the environment and have been detected in the blood of animals throughout the world, including the seals of remote arctic regions, indicating widespread distribution (Kannan 2001; Tao 2006; Van de Vijver 2005). Significant levels of PFOA and PFOS have also been detected in the serum of humans, but there is evidence of a significant decline in body burdens of PFOS and PFOA over the last 5–10 years (Calafat et al. 2007). The values from the first National Health and Nutrition Examination Survey (NHANES) conducted from 1999 to 2000 reported geometric means of 30.4 µg PFOS/L and 5.4 µg PFOA/L, and the second NHANES conducted between 2003 and 2004 reported geometric means of 20.7 µg PFOS/L and 3.9 µg PFOA/L (Calafat et al. 2007). Contamination of the environment is not limited to PFOA and PFOS but also

includes short-chain perfluorinated alkanates, such as perfluorobutyrate, perfluoropentanoate (PFPeA), perfluorohexanoate, and perfluoroheptanoate (Skutlarek et al. 2006).

The acute toxicities of PFOA and PFOS in rodent systems are low (Hekster 2003; Kudo and Kawashima 2003). After the absorption of PFOA into the body, it is predominantly distributed in the liver and plasma and, to a lesser extent, the kidney and lungs (Kudo and Kawashima 2003). Thus, the chronic and short-term effects of PFOA in rats are found largely in the liver (Kennedy et al. 2004) and immune system (DeWitt et al. 2008). Peroxisome proliferation in rodent livers is one of the major responses to PFOA, along with subsequent interferences with normal metabolism of fatty acids and cholesterol, and the induction of hepatocellular hypertrophy (Kennedy et al. 2004). Peroxisome-proliferating chemicals are classic nongenotoxic tumor promoters in rodent liver tissue (Cattley et al. 1995), and like other peroxisome proliferators, PFOA has also been shown to strongly promote tumors in rodent livers (Abdellatif et al. 1991). However, peroxisome-proliferating compounds might not be strong tumor promoters in human livers because of species differences in the response to peroxisome proliferators *in vivo*,

with rodents more responsive than primates (Klaunig et al. 2003).

Although the underlying mechanisms of tumor promotion might vary, such as the induction of peroxisome proliferation, tumorigenic cells have long been characterized as cells that lose their ability to regulate growth through contact inhibition (Borek and Sachs 1966) and lack the ability to terminally differentiate (Potter 1978), which implies a breakdown in one of the communicating mechanisms (Trosko and Upham 2005). Tumorigenic cells can be benign, leading to the compression of surrounding tissues, or have the potential to acquire genetic mutations that lead to a malignant state where the cancerous cells can invade surrounding tissues. Alteration of cell-to-cell communication via gap junctions has been implicated in the tumorigenic process and is supported by considerable evidence (Trosko and Ruch 2002).

Inhibition of gap-junctional intercellular communication (GJIC) appears to be a necessary, albeit insufficient, step of tumorigenesis and is therefore a common response of cells to tumor promoters, oncogenes, growth factors, and nongenotoxic carcinogens such as peroxisome proliferators (Trosko and Ruch 1998; Trosko and Upham 2005). Although GJIC is modulated by multiple signaling pathways, simple bioassays of intercellular communication can be used to assess dysregulation of gap junctions regardless of the upstream effectors.

Address correspondence to B.L. Upham, Michigan State University, 243 National Food Safety and Toxicology Center, East Lansing, MI 48824 USA. Telephone: (517) 884-2051. Fax: (517) 432-6340. E-mail: upham@msu.edu

*Current address: Division of Medical Safety Science, National Institute of Health Sciences, Tokyo, Japan.

**Current address: Division of Functional Biochemistry and Genomics, National Institute of Health Sciences, Tokyo, Japan.

This research was supported by National Institute of Environmental Health Sciences (NIEHS) grant R01 ES013268-01A2 to B.L.U. and by a Grant-in-Aid for Science Research from the Ministry of Education, Science, Sports, and Culture of Japan (11694334).

The contents of this article are solely the responsibility of the authors and do not necessarily represent the official views of the NIEHS.

The authors declare they have no competing financial interests.

Received 23 May 2008; accepted 23 October 2008.

Thus, GJIC is an excellent biomarker first to assess the potential tumorigenicity of chemicals and then to use as a cell signaling end point to determine the early molecular events induced by these chemicals.

Cell proliferative diseases, such as cancer, not only require the release of a quiescent cell from growth suppression via down-regulation of GJIC and/or changes in extracellular components (i.e., integrins), but also need to activate mitogenic signaling pathways. The mitogen-activated protein kinase (MAPK) pathways are the major intracellular signaling mechanisms by which a cell activates, via phosphorylation, transcription factors involved in mitogenesis (Denhardt 1996). The extracellular receptor kinase (ERK) pathway has been extensively characterized, is the most understood of the MAPK pathways (Denhardt 1996), and is a key pathway of carcinogenesis (Roberts and Der 2007).

In the present study, we extended our *in vitro* studies with F344 rat liver epithelial cells, which determined that PFOA, but not PFPeA, inhibited GJIC (Upham et al. 1998), to an *in vivo* study using F344 rats exposed to PFOA, PFPeA, or phenobarbital (PB), a known tumor promoter, to determine GJIC in liver tissue. We also continued our *in vitro* studies of PFOA versus PFPeA in determining differential effects of these compounds on MAPK, specifically ERK, and further determined that the mechanism of PFOA-induced inhibition of GJIC depends on redox activity, ERK, and phosphatidylcholine-specific phospholipase C (PC-PLC).

Materials and Methods

Chemicals. We purchased PFOA (purity > 90%) and PFPeA (purity = 97%), for the data presented in Figures 1–3 and 4A, from Fluka Chemie AG (Buchs, Switzerland), and because of unavailability from Fluka, we purchased PFOA for the data presented in Figures 4B, 5, and 6 from Aldrich Chemical Company Inc. (Milwaukee, WI, USA), with a purity of 96%. The purity values were

obtained from the commercial sources. The ratios of linear versus branched isomers in our samples were undetermined. The stock solutions were prepared by dissolving the powder in the solvent: acetonitrile for the *in vitro* assays and dimethyl sulfoxide (DMSO) for the *in vivo* studies; we also used these solvents as the vehicle controls. We purchased Lucifer yellow (LY) from Molecular Probes (Eugene, OR, USA); sodium dodecyl sulfate, Tween 20, Tris, glycine, acrylamide, tetramethylethylenediamine (TEMED) and DC protein kit from Bio-Rad Laboratories (Hercules, CA, USA); DMSO, rhodamine-dextran (RhD; molecular weight, 10,000 Da), dithiothreitol (DTT), *N*-acetylcysteine (Nac), L-ascorbate-2-phosphate (Asc-2-P) sesquimagnesium salt hydrate, and PB from Sigma-Aldrich Chemical Company (St. Louis, MO, USA); D609 and U0126, from Tocris Bioscience (Ellisville, MO, USA); resveratrol from CTMedChem (Bronx, NY, USA); acetonitrile, from EM Science (Gibbstown, NJ, USA); polyclonal antibodies directed to phospho-ERK, from New England Biolabs (Ipswich, MA, USA); and mouse polyclonal antibody directed to glyceraldehyde 3-phosphate dehydrogenase (GAPDH), from Chemicon (Temecula, CA, USA).

In vivo study. Animal treatment. The protocol for this study was approved by the Animal Care and Utilization Committee of the National Institutes of Health Sciences of Japan to assure that the rats were treated humanely and with regard for alleviation of suffering. Male Fischer-344 (F344) rats, 5 weeks old, were purchased from Charles River Japan (Kanagawa, Japan) and housed in plastic cages (five rats/cage). Male F-344 rats were chosen to match the *in vitro* studies that used liver epithelial cells isolated from male F-344 rats. The rats were kept under conditions of controlled temperature ($23 \pm 2^\circ\text{C}$), humidity ($55 \pm 5\%$), and lighting (12/12-hr dark/light cycle) and given CRF-12 basal diet (Oriental Yeast Co., Tokyo, Japan) and tap water *ad libitum*.

We used the rats in the experiments after 1 week of acclimation. Eighty rats were divided into four groups and twenty rats per group were treated with a single intraperitoneal (i.p.) administration of 100 mg/kg PFOA, 100 mg/kg PFPeA, 100 mg/kg PB, or only vehicle (DMSO). Four rats per group were killed under anesthesia at 1, 3, 6, 12, and 24 hr after administration. Another 16 rats were divided into four groups and four rats of each group were given powder diet containing PFOA, PFPeA, PB, or basal powder diet only (control), and then killed after 1 week. The diets were prepared by blending each chemical into the basal powder diet at final concentrations of 0.02% for PFOA and PFPeA and 0.05% for PB. We determined the weight of the rats at the beginning and end of the experiment, and the food consumption on days 3 and 7 of the experiment. Based on the average weight of the rats and the average food consumed per day, the estimated daily doses of chemical exposures for PFOA, PFPeA, and PB were 37.9, 32.3, and 93.3 mg/day/kg, respectively.

Diethyl ether was used to euthanize the rats. Before sacrifice, blood was collected from the orbital venous plexus under anesthesia with diethyl ether and prepared for measuring serum aspartate aminotransferase (sAST), serum alanine aminotransferase (sALT), and serum alkaline phosphatase (sALP). Determination of sAST, sALT, and sALP was carried out with a Hitachi automatic Analyzer 7150 (Hitachi, Ltd., Tokyo, Japan) using commercially available GOP, GPT and ALP diagnostic reagents (Wako Pure Chemical Industries, Ltd., Tokyo, Japan). After opening the abdominal cavity, we excised the liver and immediately used one part of the liver for the incision loading/dye transfer (IL/DT). Our preliminary study confirmed that the anesthetic and the vehicle, DMSO, under our experimental conditions did not affect *in vivo* GJIC.

Bioassay of GJIC (IL/DT). We assayed *ex vivo* GJIC in the liver by the IL/DT method described previously (Sai et al. 2000). A part of the left lobe of the liver was put on a plastic

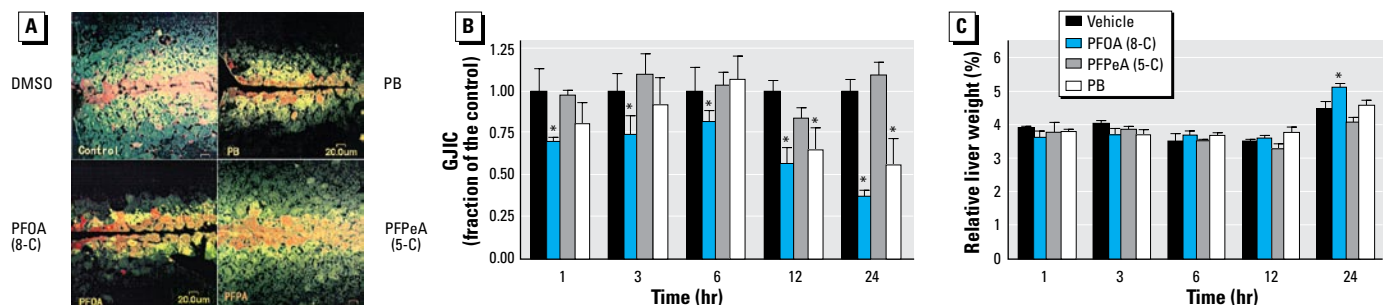


Figure 1. Analysis of *in vivo* effects of PFOA and PFPeA on GJIC in the liver tissue using IL/DT technique. Abbreviations: 5-C, five carbon; 8-C, eight carbon. (A) A fluorescent image of an IL/DT analysis of GJIC in the liver tissue of rats at 24 hr after a single i.p. administration of DMSO (vehicle), PB, PFOA, or PFPeA. Bar = 20 μm . (B) Mean \pm SD of the IL/DT data from rats treated with DMSO, PB, PFOA, or PFPeA for the acute exposure group. (C) Mean \pm SD relative liver weight from rats treated with DMSO, PB, PFOA, and PFPeA for the acute exposure group.

* $p < 0.05$ compared with vehicle, determined by one-way ANOVA for each time group followed by Dunnett's post hoc test.

plate covered with wet gauze. A mixture of fluorescent dyes containing 0.5 mg/mL LY and 0.5 mg/mL RhD in phosphate-buffered saline (PBS) was dropped on the tissue's surface. Three to four incisions were made on the surface of each specimen with a sharp blade. Excess amount of dye mixture was additionally put into the incisions and kept there for 3 min at room temperature. After incubation, the tissue was washed with PBS three times and fixed in 10% phosphate-buffered formalin overnight. Slices were washed with water and processed for embedding in paraffin. Five μ m sections for GJIC analysis were prepared by cutting the paraffin block perpendicular to the incision line. Areas stained with LY alone or with RhD were detected by the emission of fluorescence using a confocal microscope (Fluoview, Olympus, Tokyo, Japan). We counted the number of cells stained with LY alone and normalized this number by dividing by the incision length. At least three incision sites per specimen were randomly chosen for the analysis, and the mean value was used as data from one animal. The values were expressed as a fraction of the control.

In vitro study. Cell culture. We obtained the WB-F344 rat liver epithelial cell line from J.W. Grisham and M.S. Tsao of the University of North Carolina at Chapel Hill, Chapel Hill, NC, USA (Tsao et al. 1984). Cells were cultured in D-medium (formula 78-5470EF, Gibco Laboratories, Grand Island, NY, USA), supplemented with 5% fetal bovine serum (Gibco Laboratories), and incubated at 37°C in a humidified atmosphere containing 5% CO₂ and 95% air. The cells were grown in 35-mm tissue culture plates (Corning Inc., Corning, NY, USA) and the culture medium was changed every other day. Bioassays were conducted with confluent cultures that were obtained after 2–3 days of growth.

These WB cells are diploid and nontumorigenic (Tsao et al. 1984) and have been extensively characterized for GJIC in the absence and presence of well-known tumor promoters, growth factors, tumor suppressor genes, and oncogenes (Trosko and Ruch 1998). Intrahepatic transplantation of WB cells, which are liver bipolar stem cells, into adult syngenic F344 rats results in the morphologic differentiation of these cells into hepatocytes and incorporation into hepatic plates (Coleman et al. 1993).

Bioassay of GJIC (scrape load/dye transfer). The scrape loading/dye transfer (SL/DT) technique was adapted after the method of Upham et al. (1998). The test chemicals were added directly to the cell culture medium from concentrated stock solutions. The migration of the dye through gap junctions was visualized with a Nikon Eclipse TE3000 phase contrast/fluorescent microscope and the images were digitally captured with Nikon EZ Cool Snap charge-coupled device camera (Nikon Inc., Nikon, Japan). GJIC was assessed by comparing the distance the dye traveled in the chemically treated cells with the distance the dye traveled in the vehicle controls, which was measured using the Gel-Expert imaging software (Nucleotech, San

Mateo, CA, USA). We report GJIC as a fraction of the control. Based on previous results (Upham et al. 1996, 1998), 1-methylantracene as well as PFOA were used as positive controls of inhibition of GJIC, whereas acetonitrile at vehicle concentrations was used as a negative control. The vehicles used for the *in vitro* assays, acetonitrile and PBS, had no effect on GJIC. We performed all experiments at least in triplicate and report the results as means \pm SD at the 95% confidence interval.

Western blot analysis. Cells were grown in 35-mm-diameter Corning tissue culture plates to the same confluency as the SL/DT assay. The cells were depleted of serum 5 hr before addition of PFFAs to synchronize the cells into G₀ to minimize background ERK levels. This does not alter the effect on GJIC in the F344 WB cells, as previously determined (Rummel et al. 1999). The proteins were extracted with 20% sodium dodecyl sulfate (SDS) solution containing 1 mM phenylmethylsulfonyl fluoride, 100 μ M Na₃VO₄, 100 nM aprotinin, 1.0 μ M leupeptin, 1.0 μ M antipain, and 5.0 mM NaF. The protein content was determined with the Bio-Rad DC assay kit. The proteins were separated on 12.5% SDS–polyacrylamide gel electrophoresis according to the method of Laemmli

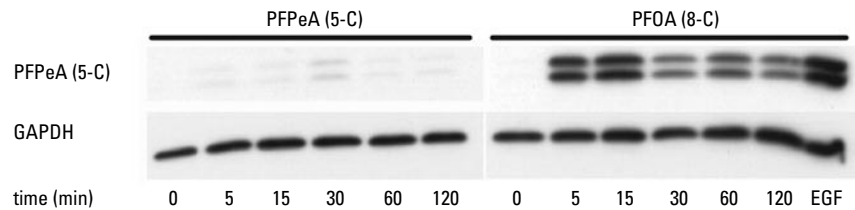


Figure 3. Activation of ERK-MAPK by PFOA, but not by PFPeA, in F344 WB rat liver epithelial cells determined by Western blots: Top panel probed with a phosphorylated ERK specific antibody and the bottom panel probed with a GAPDH specific antibody. The concentrations of PFPeA and PFOA were 100 μ M. The concentration and time of incubation for epidermal growth factor (EGF) was 20.0 ng/mL and 15 min.

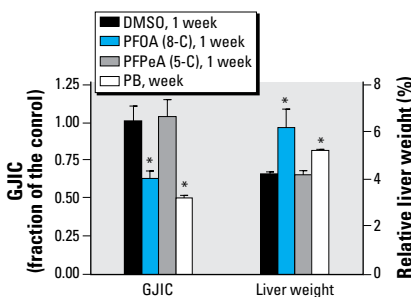


Figure 2. The long-term effects (1 week) of PB, PFOA, and PFPeA on GJIC and RLW (mean \pm SD). Abbreviations: 5-C, five carbon; 8-C, eight carbon. A one-way ANOVA was done for the GJIC data and a Kruskal-Wallis one-way ANOVA was done for the RLW data because these data failed the normality test.

* $p < 0.05$ compared with vehicle (DMSO); significant effects determined by ANOVA or Kruskal-Wallis ANOVA for each group was followed with a Dunnett's post hoc test at $p < 0.05$.

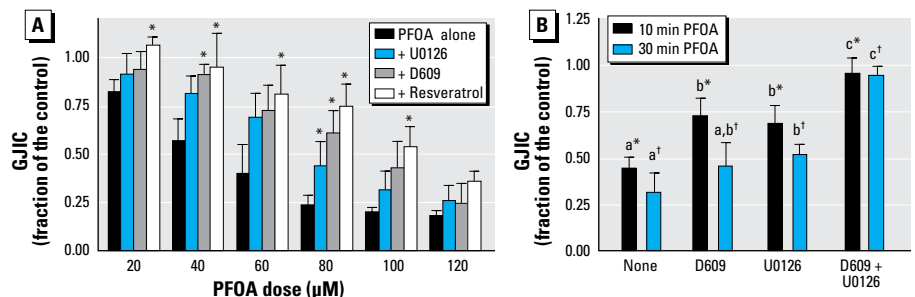


Figure 4. (A) Prevention of PFOA-induced inhibition of GJIC by inhibitors of MEK and PC-PLC and resveratrol at various doses of PFOA (mean \pm SD). The concentrations and times of preincubation of U0126, D609, and resveratrol were 20 μ M/30 min, 50 μ M/20 min, and 100 μ M/15 min, respectively. A one-way ANOVA was done for each dose group. *Significant at $p < 0.05$ using the Dunnett's post hoc test that compared each inhibitor treatment with that of PFOA alone. (B) The interactive effect of MEK and PC-PLC inhibitors on reversing PFOA-induced inhibition of GJIC at 10 and 30 min (mean \pm SD). The concentrations and times of preincubation of U0126 and D609 were 20 μ M/30 min and 50 μ M/20 min, respectively. A one-way ANOVA indicated significance at $p < 0.05$ for each time group. The Tukey pairwise-comparison post hoc test was used to determine statistical differences, as indicated by different letters, between the inhibitor treatments for each time group. The lettered asterisks represent the 10-min group and lettered daggers represent the 30-min group.

(1970). Fifteen micrograms protein was loaded onto the gels and electrophoretically transferred from the gel to polyvinyl difluoride membranes (Millipore Corp., Bedford, MA, USA). Phosphorylated ERK 1 and ERK 2 were detected with a 1:2,000 dilution of anti-phospho-ERK polyclonal antibodies, and GAPDH was detected with a 1:10,000 dilution of anti-GAPDH polyclonal antibodies, that were incubated sequentially with the membranes, each for 2 hr. The protein–primary antibody complex was probed with a 1:1,000 dilution of horseradish peroxidase–conjugated anti-rabbit or anti-mouse antibodies (Amersham Life Science Products, Arlington Heights, IL, USA) for 1 hr. The ERK and GAPDH protein bands were detected using the Super Signal chemiluminescence detection kit (Pierce Corp., Arlington Heights, IL, USA), enhanced chemiluminescence (ECL) detection kit, and ECL Hyperfilm–MP (Amersham Life Science Products, Denver, CO, USA).

Statistics. For the *in vivo* studies, the value of each group was expressed as the mean \pm SD of data derived from four rats. The *in vitro* assays were done in at least triplicate and expressed as a fraction of the control. The significance of differences in all results was evaluated with either a one-way analysis of variance (ANOVA) or, if the data set failed the normality test, a Kruskal–Wallis one-way ANOVA on ranked means. Normality assumption testing was done with the Kolmogorov–Smirnov test and equal variance assumption testing with the Levene median test. If ANOVA or Kruskal–Wallis ANOVA rejected the null hypothesis, then the results that were compared with a designated control used Dunnett’s multiple-comparison post hoc tests or Tukey’s post hoc test for pairwise multiple comparisons.

Results

In vivo results. The *in vivo* results of PFOA and PFPeA were compared with PB, a known liver tumor promoter. We used two different dosing schemes: an acute 24-hr exposure via i.p. administration and a longer-term (1 week) dietary exposure. An ANOVA indicated that

PFOA, PFPeA, and PB had no statistically significant effect on body weights of the rats (data not shown). Liver injury was assessed using the biomarkers sALT, sAST, sALP, and the results for both dosing schemes are presented in Table 1. At day 7, there were no significant differences between the rats treated with PFOA, PFPeA, and PB for all three of the selected liver enzymes, indicating no long-term liver injury. After 1 day, we found a small, biologically insignificant, but statistically significant increase in sAST, with the data exhibiting high variability.

To assess the *in vivo* effects of these compounds on GJIC in the liver tissue, we used an IL/DT technique. Figure 1A shows the incorporation of the fluorescent dye into the liver cells and subsequent distribution of the fluorescent dye through the gap junctions of the tissue. RhD, which is a large-molecular-weight dye that does not traverse gap junctions, is color-coded red. LY, which does travel through gap junction channels, is color-coded for yellow for high intensity to green for lower intensity. We measured and averaged the distances traveled by the gap-junction–permeable dye and show them in Figure 1B (acute exposure) and Figure 2 (long-term exposure). PFOA and PB but not PFPeA inhibited *in vivo* GJIC in the liver tissues of rats treated either acutely or chronically. Significant inhibition of GJIC by PFOA was observed after 1 hr, and continued to inhibit GJIC until 24 hr in the acutely treated rats. Significant inhibition of GJIC did not begin until after 12 hr of treatment with PB in this group of rats.

In the acute dose regimen (Figure 1C), a significant increase in the relative weight of livers from rats treated with PFOA was observed at 24 hr. Similarly, rats chronically exposed to PFOA and PB for 1 week had significant increases in relative liver weight (RLW; Figure 2). The livers of animals treated either acutely or chronically with PFPeA did not significantly increase in relative weights compared with rats fed the vehicle (Figures 1C, 2).

In vitro results. Considering that the *in vitro* results of PFOA and PFPeA effects on gap junctions correlated with their effects

on gap junctions *in vivo*, we did further *in vitro* analyses of PFOA to determine underlying mechanisms involved in the dysregulation of GJIC. PFOA, which inhibits GJIC, also activated ERK as determined by Western blot analysis of the phosphorylated, activated form of ERK (Figure 3). In contrast, the non-GJIC inhibitory PFPeA did not activate ERK (Figure 3). Activation of ERK was within 5 min in cells treated with PFOA, which correlates with the time of inhibition of GJIC, indicating a potential link. Preincubation of the cells with an MEK inhibitor, U0126, partially but significantly prevented the inhibition of GJIC by PFOA (Figure 4A). Preincubation of the cells with the PC-PLC inhibitor D609 also partially but significantly prevented the inhibition of GJIC by PFOA (Figure 4A). The significant contribution of PC-PLC and MEK in PFOA-induced inhibition of GJIC diminished after the maximum inhibitory dose of 80 μ M to a nonsignificant involvement at the higher dose of 120 μ M (Figure 4A), indicating further that mechanisms other than MEK and PC-PLC are also involved.

Gap junctions are known to be redox sensitive, so we conducted several experiments with various antioxidants. Resveratrol significantly reversed the inhibitory effect on GJIC and was possibly inhibiting both MEK and PC-PLC (Figure 4A). Additional experiments were performed to look at the combinatorial effect of pretreating cells with both D609 and U0126. The combination of both of these inhibitors of signal transduction enzymes resulted in the prevention of GJIC inhibition by PFOA, and the combinatorial effect was significantly greater than cells treated with either inhibitor alone as determined by a Tukey post hoc multiple-comparison test (Figure 4B). These results collectively indicate that PFOA-induced regulation of GJIC is a function of both of these signaling enzymes.

Further experiments were performed with DTT, Nac, and Asc-2-P (Figure 5). DTT

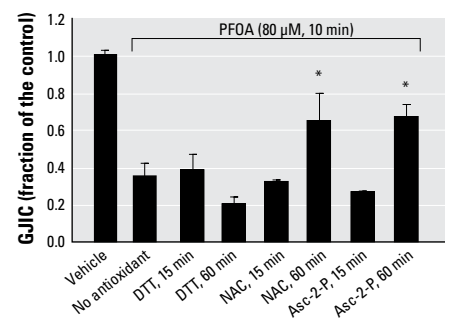


Figure 5. Prevention of PFOA-induced inhibition of GJIC by various antioxidants (mean \pm SD). The concentrations of PFOA, DTT, Nac, and Asc-2-P were 80 μ M, 10 mM, 100 μ M, and 100 μ M, respectively. * $p < 0.05$ by ANOVA and Dunnett’s post hoc test comparing each antioxidant treatment with that of PFOA alone (no antioxidant).

Table 1. The effect of PFOA, PFPeA, and PB on the levels of various biomarkers of liver injury in F344 rats.

Exposure, time, enzyme	Enzyme activity (mU/mL)			
	DMSO (vehicle)	PFOA	PFPeA	PB
Acute (24 hr)				
sALT	51.5 \pm 3.2	138.6 \pm 126.4	56.3 \pm 13.2	54.5 \pm 4.1
sAST	98.8 \pm 8.8	232 \pm 169.8*	113.0 \pm 17.6	100.6 \pm 15.1
sALP	1672.8 \pm 90.0	1521.8 \pm 220.2	1495.0 \pm 233.8	1561.0 \pm 115.2
Longer-term (1 week)				
sALT	39.3 \pm 2.0	41.2 \pm 1.9	39.8 \pm 3.0	39.7 \pm 2.6
sAST	71.2 \pm 10.0	70.4 \pm 4.3	73.9 \pm 10.7	76.1 \pm 9.4
sALP	1488.8 \pm 62.9	1394.5 \pm 59.4	1449.5 \pm 36.6	1349.3 \pm 53.0

To determine significant effects, we performed a one-way ANOVA for sALP (1 day), sALP (1 week), and sALT (1 week) and a Kruskal–Wallis one-way ANOVA on ranks for sAST (1 day), sAST (1 week), and sALT (1 day). Any significant effects determined by ANOVA were followed by a Dunnett’s post hoc test, with DMSO designated as the control.

* $p < 0.05$.

and Nac in the absence of PFOA had no statistically (ANOVA) significant effect on GJIC at both 15 and 60 min (data not shown). Asc-2-P had a small, < 10% effect (ANOVA, Tukey) on GJIC in the absence of PFOA at 15 min but not 60 min (data not shown). Asc-2-P and Nac both prevented the inhibition of GJIC by PFOA within a 60-min preincubation time, but not DTT, implicating redox-sensitive proteins that probably do not involve thiol oxidations. Preincubation of Asc-2-P and Nac for 15 min did not reverse the effect of PFOA on GJIC. The oxidative nature of PFOA was not cytotoxic, as indicated after 2 days of growing cells after the log-phase of growth with 80 μ M PFOA, resulting in no visual abnormalities in the morphology of the cells and complete restoration of GJIC after the cells were transferred to fresh medium for 5 hr containing no PFOA (Figure 6).

Discussion

Understanding the biological effects of the environmentally prevalent PFFAs on cell signaling pathways relevant to the epigenetic, nongenotoxic phase of cancer is important. In particular, GJIC offers a very central signaling system to assess risk (Trosko and Upham 2005). Although the transient closure of gap junction channels during proliferation is a normal response to mitogens, the chronic inhibition of GJIC by toxicants and toxins or by cytokines released during compensatory hyperplasia could lead to pathologic states (Trosko and Upham 2005; Upham and Trosko 2006). Thus, we conducted two dosing schemes, one a short term of 24 hr following an i.p. injection of PFOA, PFPeA, or PB, and another a longer-term study where the rats were dosed with these compounds through their daily feedings for 1 week. We previously demonstrated that inhibition of GJIC using *in vitro* model systems by perfluoroalkyl carboxylates and sulfonates depended on the chain length, where PFFAs with 7–10 carbons inhibited GJIC, and PFFAs with 2–6 carbons did not (Hu et al. 2002; Upham et al. 1998). To determine if chain length of PFFAs would exhibit similar effects on GJIC in a living organism, we treated F344 rats with PFOA, an eight-carbon PFFA, and PFPeA, a five-carbon PFFA, and determined GJIC in the liver tissue using an *ex vivo* IL/DT assay.

The liver is the primary target of PFOA (Kudo and Kawashima 2003), which is known to induce hepatocellular tumors in rodent model systems (Abdellatif et al. 1991; Kennedy et al. 2004). Similar to our *in vitro* results (Hu et al. 2002; Upham et al. 1998), PFOA decreased GJIC activity in the liver compared with the rats treated with the vehicle (control) for both the acute and long-term dosing schemes. In contrast, PFPeA-treated rats did not have altered GJIC in

the livers compared with the control rats for both dosing schemes, which is also consistent with our *in vitro* observations. Another possible reason for the lack of an *in vivo* response by PFPeA could be a consequence of a greater elimination rate that is typical of PFFAs with shorter chain lengths (Chang et al. 2008; Ohmori et al. 2003). Although we did not measure the elimination rates of PFPeA in our experiments, the half-life of perfluorobutyrate is 9.2 hr (oral) and 6.4 hr (intravenous) in Sprague-Dawley rats (Chang et al. 2008). These half-lives are similar to that of PB in Sprague-Dawley rats, which is 8–9 hr. Considering that PB inhibited GJIC and induced hepatomegaly in the livers of the rats used in our experiments, and PFPeA did not inhibit GJIC using an *in vitro* assay system, we would expect that the noninhibitory effects of PFPeA on GJIC *in vivo* would not result from its increased rate of elimination. Further experiments are needed to confirm such a conclusion.

We previously published data that indicated the treatment of Sprague-Dawley rats with PFOS resulted in a decrease in GJIC activity in the liver tissue; thus, PFOA and PFOS have similar activities (Hu et al. 2002). The following are additional reports demonstrating that tumor promoters, known to inhibit GJIC *in vitro*, also inhibited GJIC *in vivo*: pentachlorophenol (Sai et al. 2000), 2-acetylaminofluorene (Krutovskikh et al. 1991), PB (Kolaja et al. 2000; Krutovskikh 1995), polychlorinated biphenyls (Kolaja et al. 2000; Krutovskikh 1995), pregnenolone-16 α -carbonitrile (Kolaja et al. 2000), cadmium (Jeong et al. 2000), clofibrate, and DDT (Krutovskikh 1995). Another interesting report on the *in vivo* effects of chemicals on GJIC is the treatment of rats with the antioxidants lycopene and alpha and beta carotene. High doses of these antioxidants resulted in a decrease in GJIC activity, whereas rats exposed to low doses exhibited an increase in GJIC (Krutovskikh et al. 1997). Although *in vivo* assessment of intercellular communication has been limited in both the number of studies and choice of organ, namely, the liver, these results, including those presented in this report, nevertheless suggest that the *in vitro* rat liver epithelial cell assay system is a good predictor of the *in vivo* effects of chemicals on gap junctions in the liver tissues of rodents.

PFOA and PB induced hepatomegaly, whereas PFPeA had no effect. These results are similar to those previously published indicating that PFOA, but not perfluorobutyrate, affected RLWs in F344 rats (Takagi et al. 1991). Although not causally linked, hepatomegaly has been correlated with the promotion of liver tumors by many peroxisome proliferator-activated receptor α agonists, including PFOA (Takagi et al. 1992). The

null effect of PFPeA on GJIC and hepatomegaly suggest that PFPeA would not be a tumor promoter; however, two-stage (initiation and promotion) carcinogenesis studies would be needed to confirm this conclusion. Tissue necrosis is known to induce compensatory hyperplasia that leads to increased liver weights, but this is unlikely the cause of hepatomegaly in the PFOA- and PB-treated rats, considering that no visual damage of the liver was seen in the histologic sections (data not shown) and there was no increase in serum enzymes.

Tissue homeostasis in multicellular organisms depends on functional GJIC, and the disruption of intercellular communication has been linked to many diseases (Trosko and Upham 2005). PFOA clearly interrupted GJIC in the liver tissues of rats, but further experiments would need to be done in other species. PFOS also inhibited GJIC in rat liver tissue as well as *in vitro* systems that included dolphin kidney cells (Hu et al. 2002). Thus, the potential for cross-species effects of PFOA on GJIC implicates a health risk to multicellular organisms. Future experiments, particularly with human cell lines, will aid in determining differences in the sensitivity of various organisms to the effects of PFOS and PFOA on GJIC and allow for more accurate assessment of risks these compounds pose to humans and wildlife.

Considering that *in vitro* analyses of PFFA, using rat liver epithelial cells, accurately predicted the *in vivo* effects on GJIC for various PFFAs, we did further *in vitro* analyses of PFPeA- and PFOA-treated rat liver epithelial cells to determine potential signaling mechanisms involved in PFOA-induced regulation of GJIC. Connexin 43 (Cx43) is a

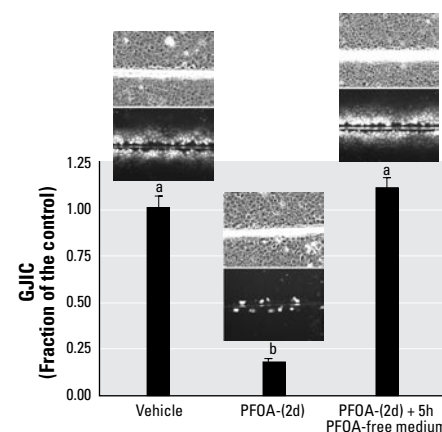


Figure 6. The effects of an extended incubation of cells with PFOA (80 μ M, 2 days) and transfer of cells to PFOA-free medium (5 hr) on cell morphology and GJIC (mean + SD). Each phase-contrast and fluorescent photomicrograph represents one of the three replicates of each treatment group (magnification, 200 \times). Different letters indicate significance at $p < 0.05$ using ANOVA and Tukey post hoc test with a pairwise comparison.

phosphoprotein, and the phosphorylation of the carboxy terminus by protein kinases, such as protein kinase C (PKC), Src, and MAPKs, in the regulation of GJIC has been well documented (Solan and Lampe 2005). Although phosphorylation of gap junctions is known to regulate the function, assembly, internalization, and degradation of this protein complex, the alteration of connexin phosphorylation by protein kinases, such as MAPKs, does not necessarily dysregulate gap junction function (Hossain et al. 1999), nor does the activation of protein kinases (i.e., MAPK) alter the phosphorylation status of connexins (Upham et al. 2008).

This was also true for PFOA, which clearly activated ERK-MAPK (Figure 3) but did not induce a change in the phosphorylation pattern of Cx43 as previously determined by Western blot analysis (Upham et al. 1998). Whether or not gap junctions are phosphorylated, several compounds (i.e., growth factors, lindane, lysophosphatidic acid, 12-*O*-tetradecanoylphorbol-13-acetate, and cannabinoids) are known to inhibit GJIC through a MEK-dependent pathway (Komatsu et al. 2006; Mograbi et al. 2003; Rivedal and Opsahl 2001; Upham et al. 2003). Although many compounds activate MAPKs, such as p38 and ERK, the mechanism of inhibiting GJIC by many of these compounds is independent from these MAPKs (Machala et al. 2003; Upham et al. 2008).

Our results indicated that PFOA activated ERK in F344 WB rat liver epithelial cells within 5 min, and this time period is within the interval required for the inhibition of GJIC by PFOA in this cell line. PFPeA, which does not inhibit GJIC in this cell line (Upham et al. 1998), also did not activate ERK. Preincubation of these cells with an MEK inhibitor, U0126, partially prevented PFOA from inhibiting GJIC, indicating that PFOA-induced modulation of GJIC was not solely dependent on the ERK pathway.

Recently, PC-PLC has been implicated in the dysregulation of GJIC in response to toxicants that regulate GJIC through an MEK-independent mechanism (Machala et al. 2003; Upham et al. 2008). Preincubation of F344 WB cells with the PC-PLC inhibitor D609 also partially prevented PFOA from inhibiting GJIC. These results suggest that PFOA is regulating GJIC through multiple cellular mechanisms. This becomes more apparent as the dose of PFOA is increased resulting in the inhibition of GJIC at a high dose of 120 μ M that depended on neither PC-PLC nor MEK. However, maximum inhibition of GJIC by PFOA, which was around 80 μ M, was very dependent on the activity of both MEK and PC-PLC. This was further apparent from the experiment where cells were pretreated with a combination of both D609 and

U0126, resulting in almost complete recovery of GJIC. The activation of ERK and PC-PLC will not only control gap junction function but is known to alter gene expression, leading to various pathologies, including cancer. The function of PC-PLC in tumorigenesis has not been extensively studied, yet there are significant reports indicating that PC-PLC does play a very significant role in cancer (Cheng et al. 1997). The ERK pathway has been extensively characterized and is the most understood of the MAPK pathways (Denhardt 1996) and is a key pathway of carcinogenesis (Roberts and Der 2007).

PFOA, but not perfluorobutyrate, is known to induce oxidative stress in the livers of rats, as indicated by 8-hydroxydeoxyguanosine formation (Takagi et al. 1991), and redox mechanisms are known to commonly play a role in gap junction function (Upham and Trosko 2009). These oxidative signaling effects could be site-directed redox regulations of specific regulatory proteins or from general oxidative effects (Upham and Trosko 2008). Recently, we reported that the antioxidant resveratrol prevented inhibition of GJIC by dicumylperoxide but not by benzoylperoxide (Upham et al. 2007). Dicumylperoxide, but not benzoylperoxide, inhibits GJIC through a PC-PLC-dependent mechanism (Upham et al. 2007). Similar to dicumylperoxide, we showed that resveratrol prevented inhibition of GJIC by PFOA to a greater level than either D609 or U0126 alone, but similar to the level of GJIC recovery seen when cells were pretreated with both D609 and U0126. These results indicate the possibility that PFOA dysregulates GJIC through both MEK and PC-PLC and that protection of GJIC by resveratrol is potentially through oxidative signaling events controlling both MEK and PC-PLC. Beyond the implication of redox mechanisms of the resveratrol experiment, this antioxidant is regularly consumed by humans and is found in high concentrations in red wine and peanut products (Sobolev and Cole 1999; Wang et al. 2002), and thus may have some relevance to the health of humans that may be exposed to environmental toxicants, such as PFOA. Chemopreventive effects of resveratrol are known to inhibit initiation, promotion, and progression of tumors (Signorelli and Ghidoni 2005). Thus, resveratrol could potentially contribute to a protective effect in humans exposed to PFOA by significantly blocking PFOA from inhibiting GJIC.

The addition of Asc-2-P or Nac partially reversed the inhibitory effects of PFOA on GJIC, similar to that of resveratrol. In contrast, DTT did not prevent PFOA from inhibiting GJIC, indicating that the oxidative events controlling PC-PLC and Mek are not thiol based. The exposure of F344 WB cells to PFOA for 2 days showed no adverse effects

on cell morphology, and they communicated normally after PFOA was removed from the medium (Figure 6), which implicates that the PFOA-induced oxidative events are not killing the cells. These results suggest that general oxidative processes are involved in PFOA-induced inhibition of GJIC and that health benefits could potentially be attained by the consumption of many antioxidant rich foods, particularly in individuals deficient in antioxidants. Moreover, the reversible properties of PFOA-induced inhibition of GJIC are consistent with the known reversible nature of tumor promoters in two-stage carcinogenesis model systems (Trosko and Upham 2005). These results also indicate that reversing the effect of PFOA on GJIC after a simple washing of the treated cells with PBS demonstrates that PFOA is not covalently or tightly bound to the cell. The effect of PFOA on GJIC was probably not a consequence of directly interacting with the gap junction proteins because the inhibition of MAPK and PC-PLC both prevented the GJIC effect. Possibly PFOA interacted with these two proteins or interacted with a signaling protein or receptor even further upstream.

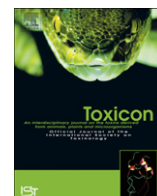
In conclusion, the *in vitro* assay system used to assess the effects of PFOA and PFPeA on GJIC predicted the *in vivo* results of GJIC from rats treated with these compounds. GJIC plays a vital role in maintaining tissue homeostasis, and disruption of gap junction function can lead to diseased states such as tumorigenesis. These results are similar to other tumor-promoting compounds tested in both an *in vitro* and *in vivo* assay system. Although there are several mechanisms by which environmental compounds might promote an initiated cell, such as through peroxisome proliferator activated receptors or protein kinase C, the disruption of normal intercellular communication is an essential event of multiple tumorigenic mechanisms (Trosko and Upham 2005) and serves as a central biomarker to assess the epigenetic toxicity of contaminants (Rosenkranz et al. 1997; Trosko and Upham 2005), as well as to assess the potential anti-tumorigenic health benefits of nutrition based food products (Trosko and Upham 2005).

REFERENCES

- Abdellatif AG, Preat V, Taper HS, Roberfroid M. 1991. The modulation of rat liver carcinogenesis by perfluorooctanoic acid, a peroxisome proliferator. *Toxicol Appl Pharmacol* 111(3):530–537.
- Borek C, Sachs L. 1966. The difference in contact inhibition of cell replication between normal cells and cells transformed by different carcinogens. *Proc Natl Acad Sci USA* 56(1705):1705–1711.
- Calafat AM, Wong LY, Kuklennyk Z, Reidy JA, Needham LL. 2007. Polyfluoroalkyl chemicals in the U.S. population: data from the National Health and Nutrition Examination Survey (NHANES) 2003–2004 and comparisons with NHANES 1999–2000. *Environ Health Perspect* 115:1596–1602.
- Cattley RC, Miller RT, Corton JC. 1995. Peroxisome proliferators: potential role of altered hepatocyte growth and

- differentiation in tumor development. *Prog Clin Biol Res* 391:295–303.
- Chang SC, Das K, Ehresman DJ, Ellefson ME, Gorman GS, Hart JA, et al. 2008. Comparative pharmacokinetics of perfluorobutyrate in rats, mice, monkeys, and humans and relevance to human exposure via drinking water. *Toxicol Sci* 104(1):40–53.
- Cheng J, Weber JD, Baldassare JJ, Raben DM. 1997. Ablation of Go alpha-subunit results in a transformed phenotype and constitutively active phosphatidylcholine-specific phospholipase C. *J Biol Chem* 272(28):17312–17319.
- Coleman WB, Wennerberg AE, Smith GJ, Grisham JW. 1993. Regulation of the differentiation of diploid and some aneuploid rat liver epithelial (stemlike) cells by the hepatic microenvironment. *Am J Pathol* 142(5):1373–1382.
- Denhardt DT. 1996. Signal-transducing protein phosphorylation cascades mediated by Ras/Rho proteins in the mammalian cell: the potential for multiplex signalling. *Biochem J* 318(pt 3):729–747.
- DeWitt JC, Copeland CB, Strynar MJ, Luebke RW. 2008. Perfluorooctanoic acid-induced immunomodulation in adult C57BL/6J or C57BL/6N female mice. *Environ Health Perspect* 116:645–650.
- Hekster FM. 2003. Environmental and toxicity effects of perfluoroalkylated substances. *Rev Environ Contam Toxicol* 79:99–121.
- Hossain MZ, Jagdale AB, Ao P, Boynton AL. 1999. Mitogen-activated protein kinase and phosphorylation of connexin43 are not sufficient for the disruption of gap junctional communication by platelet-derived growth factor and tetradecanoylphorbol acetate. *J Cell Physiol* 179(1):87–96.
- Hu W, Jones PD, Upham BL, Trosko JE, Lau C, Giesy JP. 2002. Inhibition of gap junctional intercellular communication by perfluorinated compounds in rat liver and dolphin kidney epithelial cell lines in vitro and Sprague-Dawley rats in vivo. *Toxicol Sci* 68(2):429–436.
- Jeong SH, Habeebu SSM, Klaassen CD. 2000. Cadmium decreases gap junctional intercellular communication in mouse liver. *Toxicol Sci* 57(1):156–166.
- Kannan K. 2001. Accumulation of perfluorooctane sulfonate in marine mammals. *Environ Sci Technol* 35(8):1593–1598.
- Kennedy GL, Butenhoff JL, Olsen GW, O'Connor JC, Seacat AM, Perkins RG, et al. 2004. The toxicology of perfluorooctanoate. *Crit Rev Toxicol* 34(4):351–384.
- Key BD, Howell RD, Criddle CS. 1997. Fluorinated organics in the biosphere. *Environ Sci Technol* 31:2445–2454.
- Klaunig JE, Babich MA, Baetcke KP, Cook JC, Corton JC, David RM, et al. 2003. PPARalpha agonist-induced rodent tumors: modes of action and human relevance. *Crit Rev Toxicol* 33(6):655–780.
- Kolaja KL, Engelken DT, Klaassen CD. 2000. Inhibition of gap-junctional-intercellular communication in intact rat liver by nongenotoxic hepatocarcinogens. *Toxicology* 146(1):15–22.
- Komatsu J, Yamano S, Kuwahara A, Tokumura A, Irahara M. 2006. The signaling pathways linking to lysophosphatidic acid-promoted meiotic maturation in mice. *Life Sci* 79(5):506–511.
- Krutovskikh VA. 1995. Inhibition of rat liver gap junction intercellular communication by tumor-promoting agents in vivo. Association with aberrant localization of connexin proteins. *Lab Invest* 72(5):571–577.
- Krutovskikh V, Asamoto M, Takasuka N, Murakoshi M, Nishino H, Tsuda H. 1997. Differential dose-dependent effects of alpha-, beta-carotenes and lycopene on gap-junctional intercellular communication in rat liver in vivo. *Jpn J Cancer Res* 88(12):1121–1124.
- Krutovskikh VA, Oyama M, Yamasaki H. 1991. Sequential changes of gap-junctional intercellular communications during multistage rat liver carcinogenesis: direct measurement of communication in vivo. *Carcinogenesis* 12(9):1701–1706.
- Kudo N, Kawashima Y. 2003. Toxicity and toxicokinetics of perfluorooctanoic acid in humans and animals. *J Toxicol Sci* 28(2):49–57.
- Laemmli UK. 1970. Cleavage of structural proteins during the assembly of the head of bacteriophage T4. *Nature* 227:680–685.
- Machala M, Blaha L, Vondracek J, Trosko JE, Scott J, Upham BL. 2003. Inhibition of gap junctional intercellular communication by noncoplanar polychlorinated biphenyls: inhibitory potencies and screening for potential mode(s) of action. *Toxicol Sci* 76(1):102–111.
- Mograb B, Corcelle E, Defamie N, Samson M, Nebout M, Segretain D, et al. 2003. Aberrant connexin 43 endocytosis by the carcinogen lindane involves activation of the ERK/mitogen-activated protein kinase pathway. *Carcinogenesis* 24(8):1415–1423.
- Ohmori K, Kudo N, Katayama K, Kawashima Y. 2003. Comparison of the toxicokinetics between perfluorocarboxylic acids with different carbon chain length. *Toxicology* 184(2–3):135–140.
- Potter VR. 1978. Phenotypic diversity in experimental hepatomas: the concept of partially blocked ontogeny. *Br J Cancer* 38(1):1–23.
- Rivedal E, Opsahl H. 2001. Role of PKC and MAP kinase in EGF- and TPA-induced connexin43 phosphorylation and inhibition of gap junction intercellular communication in rat liver epithelial cells. *Carcinogenesis* 22(9):1543–1550.
- Roberts PJ, Der CJ. 2007. Targeting the Raf-MEK-ERK mitogen-activated protein kinase cascade for the treatment of cancer. *Oncogene* 26(22):3291–3310.
- Rosenkranz M, Rosenkranz HS, Klopman G. 1997. Intercellular communication, tumor promotion and non-genotoxic carcinogenesis: relationships based upon structural considerations. *Mutat Res* 381(2):171–188.
- Rummel AM, Trosko JE, Wilson MR, Upham BL. 1999. Polycyclic aromatic hydrocarbons with bay-like regions inhibited gap junctional intercellular communication and stimulated MAPK activity. *Toxicol Sci* 49(2):232–240.
- Sai K, Kanno J, Hasegawa R, Trosko JE, Inoue T. 2000. Prevention of the down-regulation of gap junctional intercellular communication by green tea in the liver of mice fed pentachlorophenol. *Carcinogenesis* 21(9):1671–1676.
- Signorelli P, Ghidoni R. 2005. Resveratrol as an anticancer nutrient: molecular basis, open questions and promises. *J Nutr Biochem* 16(8):449–466.
- Skutlarek D, Exner M, Farber H. 2006. Perfluorinated surfactants in surface and drinking waters. *Environ Sci Pollut Res Int* 13(5):299–307.
- Sobolev VS, Cole RJ. 1999. trans-resveratrol content in commercial peanuts and peanut products. *J Agric Food Chem* 47(4):1435–1439.
- Solan JL, Lampe PD. 2005. Connexin phosphorylation as a regulatory event linked to gap junction channel assembly. *Biochim Biophys Acta* 1711(2):154–163.
- Takagi A, Sai K, Umemura T, Hasegawa R, Kurokawa Y. 1991. Short-term exposure to the peroxisome proliferators, perfluorooctanoic acid and perfluorodecanoic acid, causes significant increase of 8-hydroxydeoxyguanosine in liver DNA of rats. *Cancer Lett* 57(1):55–60.
- Takagi A, Sai K, Umemura T, Hasegawa R, Kurokawa Y. 1992. Hepatomegaly is an early biomarker for hepatocarcinogenesis induced by peroxisome proliferators. *J Environ Pathol Toxicol Oncol* 11:145–149.
- Tao L. 2006. Perfluorooctanesulfonate and related fluorochemicals in albatrosses, elephant seals, penguins, and polar skuas from the Southern Ocean. *Environ Sci Technol* 40(24):7642–7648.
- Trosko JE, Ruch RJ. 1998. Cell-cell communication in carcinogenesis. *Front Biosci* 3:208–236.
- Trosko JE, Ruch RJ. 2002. Gap junctions as targets for cancer chemoprevention and chemotherapy. *Curr Drug Targets* 3(6):465–482.
- Trosko JE, Upham BL. 2005. The emperor wears no clothes in the field of carcinogen risk assessment: ignored concepts in cancer risk assessment. *Mutagenesis* 20(2):81–92.
- Tsao MS, Smith JD, Nelson KG, Grisham JW. 1984. A diploid epithelial cell line from normal adult rat liver with phenotypic properties of "oval" cells. *Exp Cell Res* 154(1):38–52.
- Upham BL, Blaha L, Babica P, Park JS, Sovadinova I, Pudrith C, et al. 2008. Tumor promoting properties of a cigarette smoke prevalent polycyclic aromatic hydrocarbon as indicated by the inhibition of gap junctional intercellular communication via phosphatidylcholine-specific phospholipase C. *Cancer Sci* 99(4):696–705.
- Upham BL, Deocampo ND, Wurl B, Trosko JE. 1998. Inhibition of gap junctional intercellular communication by perfluorinated fatty acids is dependent on the chain length of the fluorinated tail. *Int J Cancer* 78(4):491–495.
- Upham BL, Guzvic M, Scott J, Carbone JM, Blaha L, Coe C, et al. 2007. Inhibition of gap junctional intercellular communication and activation of mitogen-activated protein kinase by tumor-promoting organic peroxides and protection by resveratrol. *Nutr Cancer* 57(1):38–47.
- Upham BL, Rummel AM, Carbone JM, Trosko JE, Ouyang Y, Crawford RB, et al. 2003. Cannabinoids inhibit gap junctional intercellular communication and activate ERK in a rat liver epithelial cell line. *Int J Cancer* 104(1):12–18.
- Upham BL, Trosko JE. 2006. A paradigm shift in the understanding of oxidative stress and its implications to exposure of low-level ionizing radiation. *Acta Med Nagasaki* 50:63–68.
- Upham BL, Trosko JE. 2009. Oxidative-dependent integration of signal transduction with intercellular gap junctional communication in the control of gene expression. *Antioxid Redox Signal* 11(2):297–307.
- Upham BL, Weis LM, Rummel AM, Masten SA, Trosko JE. 1996. The effects of anthracene and methylated anthracenes on gap junctional intercellular communication in rat liver epithelial cells. *Fundam Appl Toxicol* 34(2):260–264.
- Van de Vijver KI. 2005. Tissue distribution of perfluorinated chemicals in harbor seals (*Phoca vitulina*) from the Dutch Wadden Sea. *Environ Sci Technol* 39(18):6978–6984.
- Wang Y, Catana F, Yang Y, Roderick R, van Breemen RB. 2002. An LC-MS method for analyzing total resveratrol in grape juice, cranberry juice, and in wine. *J Agric Food Chem* 50(3):431–435.

VIII. Bláha, L., **Babica, P.***, Hilscherová, K., Upham, B.L., , 2010. Inhibition of gap-junctional intercellular communication and activation of mitogen-activated protein kinases by cyanobacterial extracts - Indications of novel tumor-promoting cyanotoxins? *Toxicon* 55, 126–134.



Inhibition of gap-junctional intercellular communication and activation of mitogen-activated protein kinases by cyanobacterial extracts – Indications of novel tumor-promoting cyanotoxins?

Luděk Bláha^{a,b}, Pavel Babica^{a,c,d,*}, Klára Hilscherová^{a,b}, Brad L. Upham^{c,d}

^a Institute of Botany, Academy of Sciences, Lidická 25/27, CZ65720 Brno, Czech Republic

^b Masaryk University, Faculty of Science, RECETOX, Kamenice 3, CZ62500 Brno, Czech Republic

^c Michigan State University, Department of Pediatrics & Human Development, East Lansing, MI 48824, USA

^d Michigan State University, Center for Integrated Toxicology, East Lansing, MI 48824, USA

ARTICLE INFO

Article history:

Received 18 March 2009

Received in revised form 9 July 2009

Accepted 13 July 2009

Available online 18 July 2009

Keywords:

Liver tumor promotion

Gap-junctional intercellular communication

Mitogen-activated protein kinases

Microcystin

Cylindrospermopsin

Cyanobacteria

ABSTRACT

Toxicity and liver tumor promotion of cyanotoxins microcystins have been extensively studied. However, recent studies document that other metabolites present in the complex cyanobacterial water blooms may also have adverse health effects. In this study we used rat liver epithelial stem-like cells (WB-F344) to examine the effects of cyanobacterial extracts on two established markers of tumor promotion, inhibition of gap-junctional intercellular communication (GJIC) and activation of mitogen-activated protein kinases (MAPKs) – ERK1/2. Extracts of cyanobacteria (laboratory cultures of *Microcystis aeruginosa* and *Aphanizomenon flos-aquae* and water blooms dominated by these species) inhibited GJIC and activated MAPKs in a dose-dependent manner (effective concentrations ranging 0.5–5 mg d.w./mL). Effects were independent of the microcystin content and the strongest responses were elicited by the extracts of *Aphanizomenon* sp. Neither pure microcystin-LR nor cylindrospermopsin inhibited GJIC or activated MAPKs. Modulations of GJIC and MAPKs appeared to be specific to cyanobacterial extracts since extracts from green alga *Chlamydomonas reinhardtii*, heterotrophic bacterium *Klebsiella terrigena*, and isolated bacterial lipopolysaccharides had no comparable effects. Our study provides the first evidence on the existence of unknown cyanobacterial toxic metabolites that affect *in vitro* biomarkers of tumor promotion, i.e. inhibition of GJIC and activation of MAPKs.

© 2009 Elsevier Ltd. All rights reserved.

1. Introduction

Cyanobacteria are an important component of aquatic as well as terrestrial ecosystems and they are known to produce numerous bioactive compounds. Various human activities resulted in the eutrophication of waters with occurrence of massive water blooms dominated by cyanobacteria. Consequent production of toxic metabolites

(cyanotoxins) has become a health and ecological problem worldwide (Carmichael, 2001). The increased prevalence of hepatocellular or colorectal cancer associated with consumption of drinking water contaminated with cyanobacterial blooms as reported in China (Yu, 1995; Zhou et al., 2002) is considered to be one of the most severe chronic consequences of cyanobacterial bloom development and cyanotoxin production. One major class of cyanotoxins are the cyclic heptapeptides, microcystins, which are known to induce hepatotoxic and liver tumor-promoting activities that has attracted broad scientific and regulatory attention (Chorus and Bartram, 1999; Codd et al., 2005). Although the toxicity and ecotoxicity of microcystins have been

* Corresponding author. Institute of Botany, Academy of Sciences, Lidická 25/27, CZ65720 Brno, Czech Republic. Tel.: +420 53050 6742; fax: +420 54112 6231.

E-mail address: pavel.babica@centrum.cz (P. Babica).

investigated in detail, several recent studies indicate that cyanobacterial water blooms also contain many unidentified components that may evoke toxic effects that could be more pronounced than those of microcystins or other chemically characterized cyanotoxins (Pietsch et al., 2001; Buryškova et al., 2006).

Cyanotoxins act via multiple mechanisms resulting in various adverse *in vivo* effects. For example, microcystins and nodularins are known inhibitors of regulatory protein phosphatases 1 and 2A, a mechanism considered the most important for their *in vivo* toxicities, such as acute liver necroses or chronic liver tumor promotions (Nishiwaki-Matsushima et al., 1992; Ohta et al., 1994). Although phosphatases have been implicated in the cancer process and microcystin-LR has been recently classified by the International Agency for Research on Cancer as “possibly carcinogenic to humans” (group 2B) (Grosse et al., 2006), other mechanisms also play important roles in cancer. In particular, the downregulation of gap-junctional intercellular communication (GJIC) and the activation of mitogen-activated protein kinases (MAPKs), specifically extracellular receptor kinases 1 and 2 (ERK 1 and ERK 2), have been strongly linked to the tumor-promoting phase of cancer (Trosko and Ruch, 2002; Trosko and Upham, 2005). GJIC is an important mechanism controlling homeostasis in normal tissue, and its malfunction promotes a growth of transformed cells (King, 2004). Most cancer cells are known to be defective in GJIC, chemical tumor promoters and oncogenes inhibit GJIC, while tumor suppressor genes and chemopreventive compounds enhance GJIC (Trosko and Ruch, 2002; Trosko and Upham, 2005). MAPK pathways are the major intracellular signaling mechanisms by which a cell activates transcription factors involved in the cell proliferation (Denhardt, 1996; Wright et al., 1999), and a subclass of MAPKs, extracellular receptor kinases (ERKs), has been extensively characterized (Denhardt, 1996). Both parameters, i.e. downregulation of GJIC and activation of MAPKs by chemicals, were recognized as important *in vitro* biomarkers of *in vivo* tumor-promoting potencies of carcinogenic chemicals (Rosenkrantz et al., 2000).

In this study, we focused on potencies of toxic cyanobacteria to modulate GJIC (using a scrape loading-dye transfer assay) and to activate ERK1/2 (determination of phosphorylated ERK1/2 by Western blotting) in rat liver epithelial WB-F344 cells, which is a normal diploid, non-tumorigenic and pluripotent (stem-like) cell line (Tsao et al., 1984). This cell line has been thoroughly characterized for its expressed gap junction genes, and extensively used for studying the effects of tumor promoters, growth factors, tumor suppressor genes and oncogenes on GJIC (Trosko and Ruch, 2002). To discriminate between cyanobacteria-specific and non-specific effects; we assessed different cyanobacterial metabolites and extracts including pure microcystin-LR, cylindrospermopsin, extracts from laboratory cultures of the most prevalent cyanobacteria (*Microcystis aeruginosa* and *Aphanizomenon flos-aquae*), extracts from a series of complex natural water blooms (dominated by *M. aeruginosa*, *A. flos-aquae*, *Woronichinia naegeliana* or *Planktothrix aghardii*), and we compared these results to those obtained from the extracts of a heterotrophic bacterium *Klebsiella terrigena* or

a eukaryotic green alga *Chlamydomonas reinhardtii*, and a lipopolysaccharide (LPS) isolated from bacterium *Salmonella typhimurium*. In summary, the data indicated the presence of yet unknown non-microcystin tumor-promoting metabolites specific to cyanobacteria that modulated GJIC and MAPKs.

2. Material and methods

2.1. Chemicals

Microcystin-LR and cylindrospermopsin were obtained from Alexis Biochemicals (Läufelfingen, Switzerland), lipopolysaccharides (LPS) from *Salmonella enterica* serotype *typhimurium* and epidermal growth factor (EGF) were from Sigma-Aldrich (St. Louis, MO).

2.2. Microorganisms

Laboratory cultures of cyanobacteria *M. aeruginosa* PCC 7806 and *A. flos-aquae* CCALA008 and green alga *C. reinhardtii* UTEX 2246 were obtained from the Culture Collection of Algal Laboratory (Institute of Botany, Czech Academy of Sciences, Třeboň, Czech Republic). Organisms were grown at 22 °C under continuous light (cool white fluorescent tubes, 3000 lux) in cultivation medium with following composition: mixture of Zehnder medium (Schlosser, 1994), Bristol (modified Bold) medium (Stein, 1975) and distilled water (1:1:2, v/v). Cultures were aerated with ambient air sterilized by 0.22 µm filter. Bacterium *K. terrigena* CCM 3568 was obtained from the Czech Collection of Microorganisms (Masaryk University, Brno, Czech Republic), cultured in beef-peptone B1 medium at 30 °C for 3–4 days under sterile conditions. Biomasses of laboratory cultures of cyanobacteria, bacterium and green alga were harvested by centrifugation at 2500 × g for 10 min and then lyophilized. Natural cyanobacterial water blooms were collected with plankton net (20 µm) from reservoirs in the Czech Republic (Table 1) and lyophilized.

2.3. Extract preparations

Dry microorganism biomasses were homogenized in methanol (equivalents of 200 mg d.w./1 mL), sonicated (ultrasonic probe Bandelin Sonopuls HD2070, Bandelin Electronics, Berlin, Germany), decanted by centrifugation (14,000 × g, 10 min) and extracts evaporated under vacuum. Desired concentrations were prepared prior to testing by diluting in 50% methanol. Concentrations were expressed as dry weight of extracted biomass per volume (mg d.w./mL).

2.4. Analyses of microcystins

Microcystin content in samples was analyzed according to established methods (Babica et al., 2006), using HPLC Agilent 1100 Series coupled with photodiode array detector (Agilent Technologies, Waldbronn, Germany). Microcystins were separated on a Supelcosil ABZ+ Plus column (150 × 4.6 mm, 5 µm, Supelco, Bellefonte, PA) at 30 °C. Mobile phases were water and acetonitrile, both containing

Table 1

Characterization of the studied samples with concentrations of microcystins (MCs) and effects on gap-junctional intercellular communication after 15 min (GJIC).

Samples (cultures/locality & date)	Description/dominant species	Content of microcystins (MCs $\mu\text{g/g}$ d.w.)	Inhibition of GJIC (IC_{50} , mg d.w./mL)
<i>Microcystis aeruginosa</i> PCC 7806	Laboratory culture – cyanobacteria	1946 $\mu\text{g/g}$ d.w.(MC-LR 1240, unidentified MC 706)	3.5 (2.2–4.8) ^a
<i>Aphanizomenon flos-aquae</i> CCALA008	Laboratory culture – cyanobacteria	ND ^b	3.3 (2.1–4.5)
<i>Chlamydomonas reinhardtii</i> UTEX 2246	Laboratory culture – green alga	ND	>12.5
<i>Klebsiella terrigena</i> CCM 3568	Laboratory culture – heterotrophic bacteria	ND	>12.5
Loudilka (04/10/2004)	Water bloom – <i>Microcystis aeruginosa</i> (98%)	3662 $\mu\text{g/g}$ d.w.(MC-LR 1361, MC-YR 289, MC-RR 2012)	4.4 (2.7–5.1)
Dolní Heřmanice (24/8/2004)	Water bloom – <i>Aphanizomenon flos-aquae</i> (95%)	ND	0.8 (0.4–1.2)
Dubice (08/09/2004)	Water bloom – <i>Planktothrix agardhii</i> (95%)	2602 $\mu\text{g/g}$ d.w.(unidentified MCs)	2.1 (1.7–2.6)
Stanovice (13/09/2004)	Water bloom – <i>Woronichinia naegaliana</i> (75%), <i>Microcystis</i> sp.(25%)	ND	7.8 (6.7–8.5)

^a 95% confidence interval for IC_{50} in parentheses.

^b ND – not detected (reliable detection limit of the method was 1 $\mu\text{g/g}$ d.w.).

0.1% (v/v) trifluoroacetic acid. Chromatographic separation was achieved at a flow rate 1 mL/min using a linear gradient starting at 20% aqueous acetonitrile increasing to 59% over the next 30 min. UV spectra were recorded from 200 to 300 nm and chromatograms were evaluated at 238 nm. Microcystins were identified by comparison of UV spectra and retention time with standards of microcystin-LR, -LF, -LW, -RR (Alexis Biochemicals) or microcystin-YR (Sigma–Aldrich). Microcystins were quantified using microcystin-LR as standard. Reliable detection limit of the method for the individual microcystin variants was 1 $\mu\text{g/g}$ d.w.

2.5. Cell culture

The WB-F344 rat liver epithelial cell line was obtained from Drs. J.W. Grisham and M.S. Tsao of the University of North Carolina (Chapel Hill, NC) (Tsao et al., 1984), and cultured in D-medium (Formula No. 78-5470EF, GIBCO Laboratories, Grand Island, NY) on 35 mm tissue culture plates (Corning Inc., Corning, NY), supplemented with 5% fetal bovine serum (GIBCO Laboratories), and incubated at 37 °C in a humidified atmosphere containing 5% CO_2 and 95% air. Bioassays were conducted with confluent cultures obtained after two or three days of growth.

2.6. Bioassay of GJIC

The scrape loading-dye transfer (SL-DT) technique was adapted after the method of El-Fouly et al. (1987). The test samples were added directly to the cell culture medium from concentrated stock solutions. Appropriate solvent controls (maximum 3% methanol, v/v, in the case of cyanobacterial extracts) were run in each experiment and did not induce responses significantly different from non-treated control. After the exposure (15, 30 and 120 min), cells were washed with phosphate buffered saline (PBS) followed by the addition of 1 mg/mL of Lucifer-Yellow (Sigma–Aldrich) dissolved in PBS. The dye was introduced into the cells with three scrapes through the monolayer of confluent cells using a surgical steel scalpel blade. The transfer of dye through gap junction channels was allowed for 3 min, followed by a thorough rinse of cells with PBS to

remove extracellular dye, and then fixation with a 4% formaldehyde solution in PBS. Migration of the dye in the cells was observed at 200-times magnification using a Nikon epifluorescence microscope equipped with a Nikon Cool Snap EZ CCD camera and the images were acquired by Nikon NIS-Elements F2.2 imaging system. The fluorescence area of the dye migration from the scrape line was quantified using 'Gel Expert' image analysis program (Nucleo-Tech Corp, San Mateo, CA). The results were expressed as fraction of the solvent control. To evaluate time-dependent effects and recovery (known to vary among tumor promoters acting via different mechanisms), the cells were exposed for 30 min, washed with PBS and samples were replaced with the fresh serum-free culture medium for another 90 min. Each SL-DT experiment was performed three times independently.

2.7. Western blot analysis

Confluent cells were incubated in serum-free medium for 4–5 h before an experiment and then exposed to the test samples for 30, 60 and 120 min under the same conditions as those used in the SL-DT assay. Cells exposed to EGF (5 ng/mL) for 30 min were used as a positive control for ERK1/2 activation. Appropriate solvent controls (maximum 1.25% methanol, v/v, in the case of cyanobacterial extracts) were run in each experiment and did not induce responses significantly different from non-treated control. The proteins from the cells were extracted with 20% SDS solution containing 1 mM phenylmethylsulfonyl fluoride, 100 μM Na_3VO_4 , 100 nM aprotinin, 1.0 μM leupeptin and 1.0 μM antipain. The proteins (15 μg , determined by the DC protein kit Bio-Rad Laboratories Inc., Hercules, CA) were separated by 12.5% SDS-PAGE (Bio-Rad Laboratories Inc.) and then electrophoretically transferred from the gel to PVDF membranes (Millipore Corp., Billerica, MA). To visualize activated, i.e. phosphorylated ERK1/2, we used phospho-specific polyclonal antibodies directed to ERK 1 phosphorylated at Thr202/Tyr204, and ERK 2 directed to phosphorylated Thr185/Tyr187 (New England Biolabs, Ipswich, MA). Levels of glyceraldehyde 3-phosphate dehydrogenase (GAPDH) as a housekeeping protein were determined with mouse anti-GAPDH antibody

(Chemicon; currently Millipore). Secondary anti-rabbit or anti-mouse IgG conjugated with horse radish peroxidase, ECL detection kit and HyperFilm™-MP (Amersham Life Science, Denver, CO) were used for detection of signals for ERK1/2 and GAPDH. Each Western blotting experiment was repeated twice independently.

2.8. Data analysis

The mean values \pm standard deviations from three independent experiments were evaluated by one-way ANOVA followed by Dunnett's post hoc test. *P* values less than 0.05 were considered statistically significant. The IC_{50} values and 95% confidence intervals were calculated using non-linear regression. Calculations were performed in Statistica 8.0 (StatSoft, Tulsa, OK, USA).

3. Results

Potencies of extracts from cyanobacteria, a bacterium and a green alga to inhibit GJIC in WB-F344 cells are shown in Fig. 1 and Table 1. After short 15 or 30 min exposures, extracts of cyanobacteria (both laboratory cultures and water blooms) significantly inhibited GJIC in a dose-dependent manner with IC_{50} values ranging from 0.8 to 7.8 mg d.w./mL (Fig. 1 and Table 1). The effects of cyanobacterial extracts on GJIC decreased in the following order: *A. flos-aquae* (bloom) > *P. aghardii* (bloom) > *A. flos-aquae* (culture) \sim *M. aeruginosa* (culture) > *M. aeruginosa* (bloom) > *W. naegeliana* (bloom). To the contrary, weak or no inhibitory effects on GJIC were observed in cells exposed to extracts of the heterotrophic bacterium *K. terrigena* or the green alga *C. reinhardtii* (Fig. 1A and Table 1). The highest concentration of microcystins was found in the water bloom of *M. aeruginosa*, followed by the bloom sample of *P. aghardii* and the laboratory culture of *M. aeruginosa*, but no microcystins were detected in the samples extracted from *A. flos-aquae*, which were extracts that induced strong inhibition of GJIC. These results indicate that inhibition of GJIC was independent of microcystin content (Table 1 and Fig. 2). In addition, purified LPS, microcystin-LR and cylindrospermopsin did not inhibit GJIC in WB-F344 cells (Fig. 2).

Time-responses of GJIC varied among cyanobacterial samples (Fig. 2). Unlike the extracts from the blooms where GJIC was inhibited for the first 30 min followed by a complete recovery from inhibition at 120 min, the extracts from laboratory cultures of both *M. aeruginosa* and *A. flos-aquae* continued inhibiting GJIC throughout the 120 min exposure period. An additional experiment was done in which the cells were exposed to the extracts for 30 min and then rinsed with PBS and incubated for an additional 90 min in fresh serum-free medium containing no extracts (Fig. 2). Again, inhibition of GJIC was maintained for the total 120 min time period in cells that were exposed to the extracts from the cyanobacterial cultures but not the blooms.

Extracts from both *M. aeruginosa* and *A. flos-aquae* cyanobacteria (cultures and water blooms) induced phosphorylation of ERK1/2 (Fig. 3A). The most pronounced effects were observed at both *A. flos-aquae* samples, where

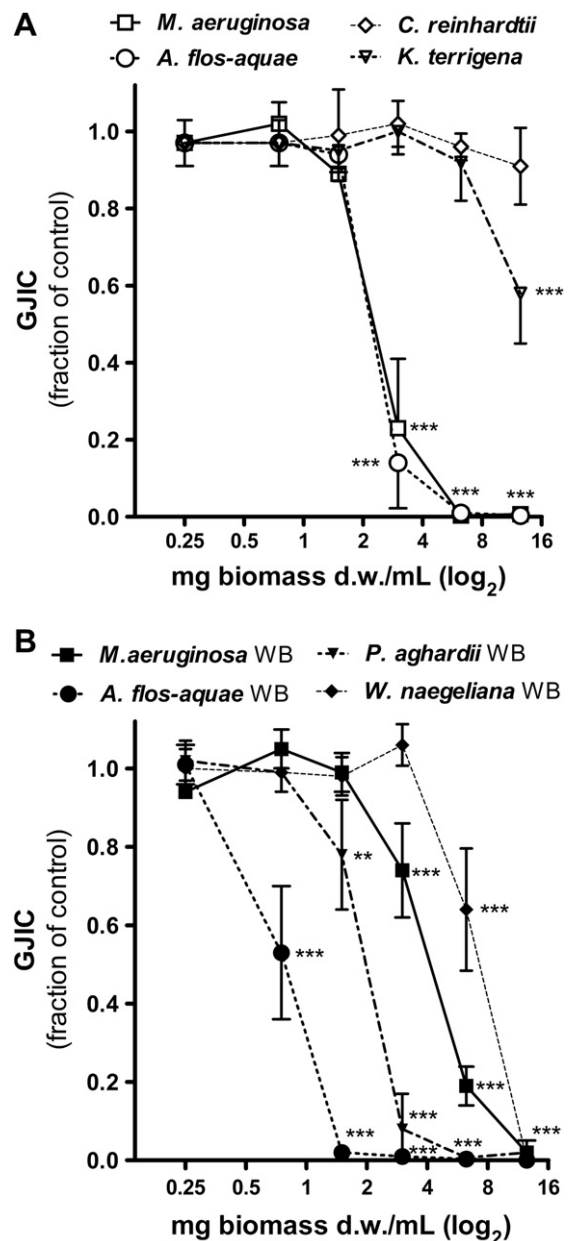


Fig. 1. Effects of tested samples (0.25–12.5 mg d.w./mL) on gap-junctional intercellular communication (GJIC) in WB-F344 cells after 30 min exposure. A – effects of laboratory cultures of cyanobacteria, bacterium and green alga; B – effects of water bloom (WB) samples dominated by various cyanobacterial species. Data are means \pm standard deviations of three independent experiments. Significant differences from the solvent control are indicated at $0.001 \leq P < 0.01$ (**) or $P < 0.001$ (***) as determined by one-way ANOVA followed by Dunnett's post hoc test.

phosphorylation and activation of ERK1/2 was sustained during the entire 30–120 min exposure periods, whereas the activation induced by *M. aeruginosa* extracts was weaker and diminished after incubation for 120 min (Fig. 3A). Neither extracts from bacterium *K. terrigena*, alga *C. reinhardtii* (Fig. 3B), isolated bacterial LPS, microcystin-LR nor cylindrospermopsin (Fig. 3C) induced significant effects on the activation of ERK1/2.

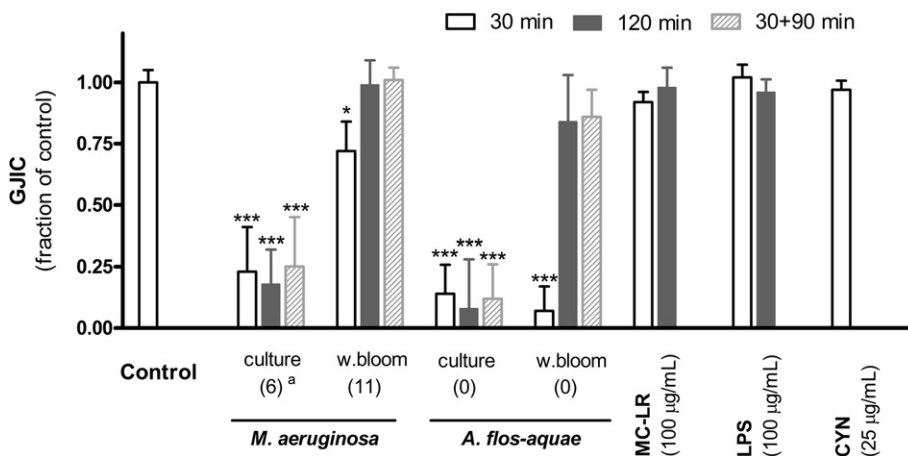


Fig. 2. Modulation of GJIC by cyanobacterial samples (3 mg d.w./mL of laboratory cultures and water blooms of *M. aeruginosa* and *A. flos-aquae*) after 30 or 120 min continual exposure or after 30 min incubation with the sample followed by 90 min incubation in fresh serum-free medium (30 + 90 min). For comparison, presented are also effects of 100 µg/mL of microcystin-LR (MC-LR), *Salmonella* lipopolysaccharide (LPS) and 25 µg/mL of cylindrospermopsin (CYN). Data are means ± standard deviations of three independent experiments. Significant differences from the solvent control are indicated at $0.01 \leq P < 0.05$ (*) or $P < 0.001$ (***) as determined by one-way ANOVA followed by Dunnett's post hoc test. ^aValues in parentheses at cyanobacterial samples indicate actual concentrations of microcystins in tested samples (µg/mL).

4. Discussion

This is the first study documenting the effects of extracts from toxic cyanobacteria on the downregulation of GJIC and activation of ERK1/2, which are two important *in vitro* biomarkers of tumor promotion. We focused in detail on *Microcystis* sp., as this is the most often studied and reported taxa dominating cyanobacterial blooms in North America and Europe, including Czech Republic (Codd et al., 2005; Blahova et al., 2007). *Microcystis* strains are also potent producers of the most studied cyanobacterial toxins – microcystins (Chorus and Bartram, 1999). Previous toxicological research focused mostly on microcystins, which might elevate MAPK activities by inhibiting protein phosphatase 2A (MacKintosh et al., 1990), which is the phosphatase that deactivates MAPKs (Junttila et al., 2008), or via induction of oxidative stress (Dietrich and Hoeger, 2005), which is also known to regulate MAPK activity (McCubrey et al., 2006). For instance, microcystin-LR was reported to activate MAPKs ERK1/2, SAP/JNK and p38 in HEK293 cells transfected with OATP1B3 transporter (Komatsu et al., 2007). Gene expression of JNK and p38 was also upregulated at the mRNA-level in the microcystin-LR-transformed and conditionally immortalized normal human colorectal crypt epithelial cell line NCC (Zhu et al., 2005). However, in our study there were no apparent effects on GJIC and MAPKs related to the microcystin content in cyanobacterial biomass (Table 1, Figs. 2 and 3). Pure microcystin-LR also did not affect GJIC (Fig. 2) or ERK1/2 (Fig. 3C), even in concentration much higher (100 µg/mL) than were the actual concentrations of microcystins in the tested dilutions of cyanobacterial extracts (≤ 46 µg/mL). One of the explanations could be possible absence of OATP-transporters in WB-F344 cells used in our experiments but this issue remains to be studied in detail.

Our study showed that the effects of cyanobacterial samples on the inhibition of GJIC and activation of ERK1/2

did not correlate with microcystin concentrations, and the strongest responses were induced by extracts of *Aphanizomenon* sp. samples that did not contain microcystins (Figs. 1–3, Table 1). These results are important considering that a toxicity of the water blooms dominated by *Microcystis*, *Planktothrix* or *Anabaena* sp. has been extensively studied because of their ability to produce microcystins (Codd et al., 2005), and less attention has been paid to the possible hazards of other cyanobacteria that do not produce microcystins such as *Aphanizomenon* sp. Regulations concerning cyanobacterial toxins has revolved around the determination of microcystin content. *Aphanizomenon* sp. may be of concern due to the possible production of hepatotoxic and potentially carcinogenic cylindrospermopsin (Rucker et al., 2007; Blahova et al., 2008). Since we did not analyze cylindrospermopsin content in the tested samples, we can only speculate about concentrations of cylindrospermopsin in *A. flos-aquae* extracts. Concentrations of this cyanotoxin in *Aphanizomenon* sp. biomass are known to range from several tens µg/g d.w. in water blooms (Fastner et al., 2007; Blahova et al., 2009) to 5000–6600 µg/g d.w. in isolated cultures (Bacsi et al., 2006; Preussel et al., 2006). If cylindrospermopsin content in our *A. flos-aquae* samples had been at the higher level reported from the literature (5000 µg/g d.w.), then the cyanobacterial extract at the dose 2.5 mg of d.w./mL (which induced significant effects on both GJIC and ERK1/2) would have contained cylindrospermopsin at concentration 12.5 µg/mL. However, pure cylindrospermopsin in concentration 25 µg/mL affected neither GJIC nor ERK1/2 activities (Figs. 2 and 3C). Moreover, extracts of *M. aeruginosa* or *P. aghardii* inhibited GJIC (Fig. 1), and *M. aeruginosa* also activated ERK1/2 (Fig. 3A,C), although these species are not known to produce cylindrospermopsin (Codd et al., 2005). Thus, the strong effects of cyanobacterial extracts on GJIC and ERK1/2 were probably microcystin- and cylindrospermopsin-independent, which indicates the existence and presence

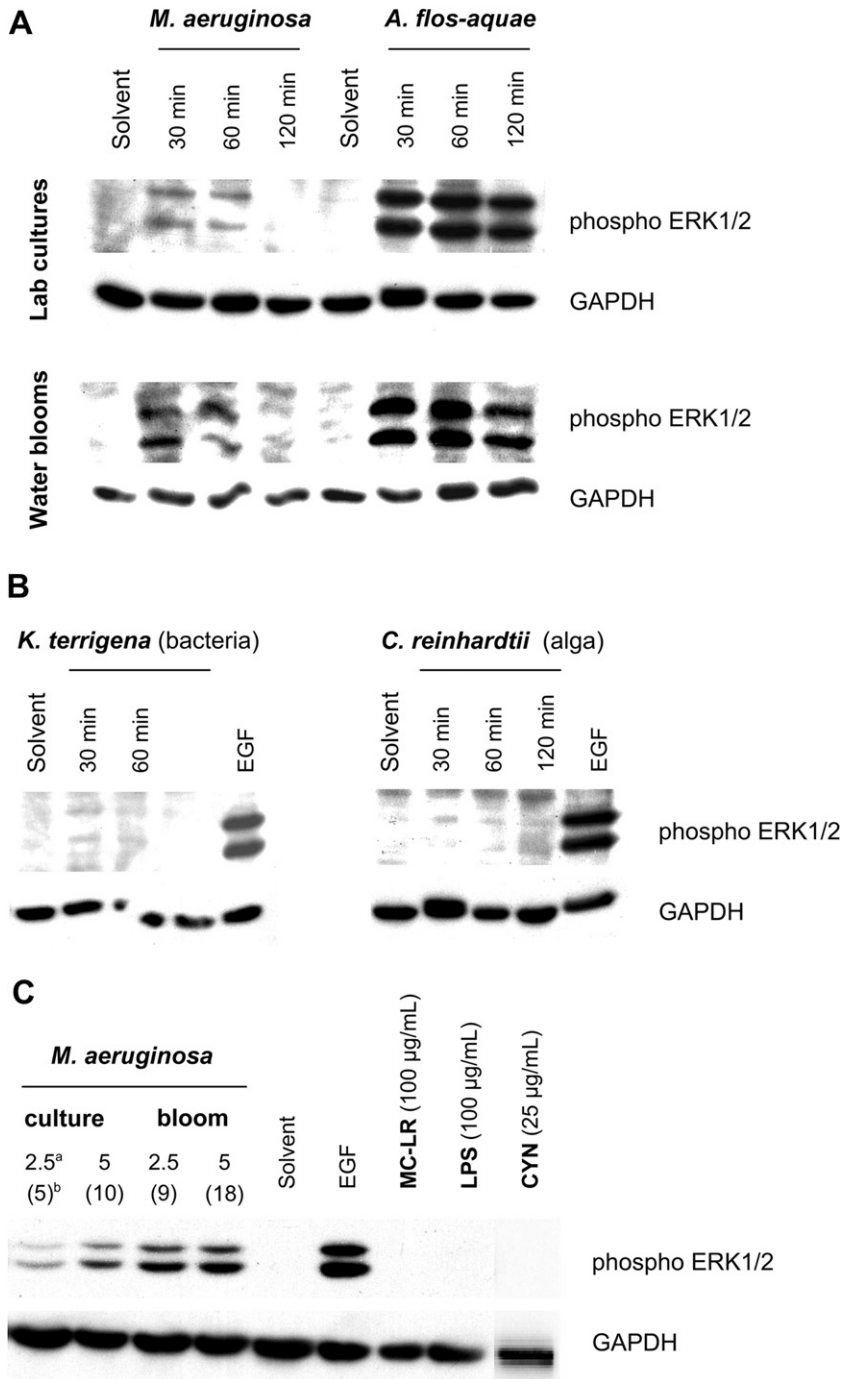


Fig. 3. Activation of a subclass of mitogen-activated protein kinases (MAPKs) – extracellular receptor kinases 1 and 2 (ERK1/2) by tested samples as determined by Western blotting (glyceraldehyde 3-phosphate dehydrogenase, GAPDH, was assayed as a housekeeping protein). EGF (5 ng/mL, 30 min) was used as a positive control. A – time-dependent effects of extracts from water blooms and laboratory cultures of cyanobacteria *M. aeruginosa* (2.5 mg d.w./mL) and *A. flos-aquae* (0.75 mg d.w./mL). B – effects of extracts of bacterium *K. terrigena* and alga *C. reinhardtii* (2.5 mg d.w./mL both) C – no effects (30 min exposures) of microcystin-LR (MC-LR), *Salmonella* lipopolysaccharide (LPS) and cylindrospermopsin (CYN) compared with the effects of *M. aeruginosa* (2.5 and 5 mg d.w./mL). ^aConcentration of cyanobacterial extract (mg d.w./mL). ^bValues in parentheses indicate actual concentrations of microcystins in tested samples (µg/mL).

of unidentified toxins that could potentially contribute to tumor promotion.

Apparently, these not-yet-identified substances may induce tumor promotion-related effects in other types of liver cells independent from differentiated hepatocytes,

which are the primary targets for known cyanobacterial hepatotoxins such as microcystins and cylindrospermopsin. WB-F344 stem-like cell line used in our study have the characteristics of oval cells, which have been implicated as the target cell type in liver cancer (Sell, 1993; Ruch and

Trosko, 1999) and their proliferation is often seen in the early stages of diseased states that lead to cancer not only in rodents but also humans (Roskams et al., 1998; Lowes et al., 1999). Also, the effects of cyanobacterial extracts on GJIC and ERK1/2 in WB-F344 cells are very similar to the effects of many well-recognized nongenotoxic carcinogens and tumor promoters such as phorbol esters (Madhukar et al., 1996), polycyclic aromatic hydrocarbons (Blaha et al., 2002), polychlorinated biphenyls, PCBs (Kang et al., 1996; Machala et al., 2003), organochlorine pesticides (Trosko et al., 1987; Upham et al., 1997; Sai et al., 1998; Masten et al., 2001), perfluorinated fatty acids (Upham et al., 1998a) or organic peroxides (Upham et al., 2007). Thus, our results suggest not only an existence of so far uncharacterized tumor-promoting chemicals of cyanobacterial origin and an involvement of GJIC and MAPK activation in cyanobacteria-associated tumor promotion, but also a possible role of adult stem or stem-like cells in cyanobacteria-induced carcinogenesis.

Interestingly, there were significant differences in the time-dependent effects on GJIC between cyanobacterial extracts from water blooms and laboratory cultures (Fig. 2). Rapid inhibition of GJIC followed by almost complete recovery of communication after prolonged exposures was observed from the water bloom extracts of both *M. aeruginosa* and *A. flos-aquae*, even in the case of continual incubation with the extracts. These results are similar to those of EGF or tumor-promoting phorbol ester, where the inhibition of GJIC has a transient character (Madhukar et al., 1996; Rivedal and Opsahl, 2001). On the contrary, the inhibition of GJIC by extracts from laboratory cultures persisted for at least 2 h. Persistent inhibition of GJIC was reported from experiments with PCB 153 (Machala et al., 2003) or perfluorooctanoic acid (Upham et al., 2009), where intercellular communication was not restored even after 24-h or longer incubation in the presence of inhibiting factor. However, inhibition of GJIC by extracts from laboratory cultures continued for 90 min after the cells were transferred to toxin-free medium, although the removal of GJIC inhibitor usually results in recovery of communication. For instance, GJIC is completely restored within periods ranging from 30 min for fluorinated fatty acids (Upham et al., 1998a) to 2 h for polycyclic aromatic hydrocarbons (Upham et al., 1998b), pesticides (Masten et al., 2001) or organic peroxides (Upham et al., 2007), and partial but significant recovery of GJIC occurs actually in 60 min or less. Since tested concentrations of extracts (based on the dry weight of biomass) were similar for all samples, it seems that the active compound(s) and/or their concentrations had to be different between laboratory cultures and bloom samples considering that there were significant differences in both dose and time responses, and particularly in the ability to recover from the inhibition of GJIC. Moreover, the effects of cyanobacterial extracts on GJIC did not always correlate with the effects on ERK1/2. Both extracts from cultures of *A. flos-aquae* and *M. aeruginosa* inhibited GJIC with similar potencies (Fig. 1A), but *A. flos-aquae* extract induced more pronounced activation of ERK1/2 (Fig. 3A). Also, *M. aeruginosa* bloom extract was a weaker inhibitor of GJIC (Fig. 1) but stronger activator of ERK1/2 (Fig. 3A,C) than the extract from *M. aeruginosa* culture. In the case of *A. flos-*

aquae, both bloom and culture extract elicited similar activation of ERK1/2 (Fig. 3A), but the extract from water bloom inhibited GJIC more significantly than the extract from the culture (Fig. 1). It is therefore possible that the effects on GJIC and ERK1/2 could be elicited by different compounds of cyanobacterial origin or that they could be synergistically/antagonistically modulated by other bioactive chemicals present in cyanobacterial extracts.

To explore the selectivity of the *in vitro* tumor-promoting effects of cyanobacteria, we compared these results to the extracts from a model eukaryotic green alga, *C. reinhardtii*, and from a heterotrophic gram-negative bacterium, *K. terrigena*. Cyanobacteria belong among gram-negative bacteria by the composition of the cell wall containing lipopolysaccharides (Papageorgiou et al., 2004; Bernardova et al., 2008). LPS have been reported to activate ERKs in some cell types (Schumann et al., 1996; Watters et al., 2002), but no such effects were observed in our experiments with the rat liver epithelial WB-F344 cells, even when we used LPS isolated from *S. typhimurium*, a serotype producing LPS known to induce significant biological responses. Both pure LPS and bacterial extracts caused only weak and temporal downregulations of GJIC that were not accompanied by activations of ERK1/2 (Figs. 1–3). Considering also no effects of green algal extracts (Figs. 1A and 3B), our results indicate that observed effects are really specific to metabolites present dominantly in cyanobacterial cells.

In summary, cyanobacteria seem to produce specific metabolites that modulate two important *in vitro* biomarkers of tumor promotion, i.e. inhibition of GJIC and activation of ERK1/2. Our study demonstrates significant effects especially for the *Aphanizomenon* extracts and we have confirmed that these effects were independent of microcystins and cylindrospermopsin. Tumor promoting and/or carcinogenic effects of cyanobacterial blooms therefore should not be simply attributed to known tumor promoters like microcystins or potential human carcinogens like cylindrospermopsin. Further efforts should focus on the identification and chemical characterization of biologically active compounds, determination of the biochemical effectors that are upstream and downstream of ERKs and GJIC, and linking these molecular signaling events with cellular responses such as proliferation or apoptosis.

Acknowledgements

The research is supported by the Czech Science Foundation grant No. GACR 524/08/0496 to Blaha; and by NIEHS grant #R01 ES013268-01A2 to Upham and its content is solely the responsibility of the authors and does not necessarily represent the official views of the NIEHS; and by the Center of Water Science at Michigan State University.

Conflict of interest

The authors declare that there are no conflicts of interest.

References

- Babica, P., Kohoutek, J., Blaha, L., Adamovsky, O., Marsalek, B., 2006. Evaluation of extraction approaches linked to ELISA and HPLC for analyses of microcystin-LR, -RR and -YR in freshwater sediments with different organic material contents. *Analytical and Bioanalytical Chemistry* 285 (8), 1545–1551.
- Bacsi, I., Vasas, G., Suranyi, G., Hamvas, M., Mathe, C., Toth, E., Grigorszy, I., Gaspar, A., Toth, S., Borbely, G., 2006. Alteration of cylindrospermopsin production in sulfate- or phosphate-starved cyanobacterium *Aphanizomenon ovalisporum*. *FEMS Microbiology Letters* 259 (2), 303–310.
- Bernardova, K., Babica, P., Marsalek, B., Blaha, L., 2008. Isolation and endotoxin activities of lipopolysaccharides from cyanobacterial cultures and complex water blooms and comparison with effects of heterotrophic bacteria and green alga. *Journal of Applied Toxicology* 28 (1), 72–77.
- Blaha, L., Kapplova, P., Vondracek, J., Upham, B.L., Machala, M., 2002. Inhibition of gap-junctional intercellular communication by environmentally occurring polycyclic aromatic hydrocarbons. *Toxicological Sciences* 65 (1), 43–51.
- Blahova, L., Babica, P., Marsalkova, E., Marsalek, B., Blaha, L., 2007. Concentrations and seasonal trends of extracellular microcystins in freshwaters of the Czech Republic results of the national monitoring program. *Clean – Soil, Air, Water* 35 (4), 348–354.
- Blahova, L., Babica, P., Adamovsky, O., Kohoutek, J., Marsalek, B., Blaha, L., 2008. Analyses of cyanobacterial toxins (microcystins, cylindrospermopsin) in the reservoirs of the Czech Republic and evaluation of health risks. *Environmental Chemistry Letters* 6 (4), 223–227.
- Blahova, L., Oravec, M., Marsalek, B., Sejnohova, L., Simek, Z., Blaha, L., 2009. The first occurrence of the cyanobacterial alkaloid toxin cylindrospermopsin in the Czech Republic as determined by immunochemical and LC/MS methods. *Toxicol* 53 (5), 519–524.
- Buryskova, B., Hilscherova, K., Babica, P., Vrskova, D., Marsalek, B., Blaha, L., 2006. Toxicity of complex cyanobacterial samples and their fractions in *Xenopus laevis* embryos and the role of microcystins. *Aquatic Toxicology* 80 (4), 346–354.
- Carmichael, W.W., 2001. Health effects of toxin-producing cyanobacteria: “The CyanoHABs”. *Human and Ecological Risk Assessment* 7 (5), 1393–1407.
- Chorus, I., Bartram, J. (Eds.), 1999. *Toxic Cyanobacteria in Water: a Guide to Their Public Health Consequences, Monitoring and Management*. E&FN Spon, London, p. 432.
- Codd, G.A., Morrison, L.F., Metcalf, J.S., 2005. Cyanobacterial toxins: risk management for health protection. *Toxicology and Applied Pharmacology* 203 (3), 264–272.
- Denhardt, D.T., 1996. Signal-transducing protein phosphorylation cascades mediated by Ras/Rho proteins in the mammalian cell: the potential for multiplex signalling. *Biochemical Journal* 318 (Pt 3), 729–747.
- Dietrich, D., Hoeger, S., 2005. Guidance values for microcystins in water and cyanobacterial supplement products (blue-green algal supplements): a reasonable or misguided approach? *Toxicology and Applied Pharmacology* 203 (3), 273–289.
- El-Fouly, M.H., Trosko, J.E., Chang, C.C., 1987. Scrape-loading and dye transfer: a rapid and simple technique to study gap junctional intercellular communication. *Experimental Cell Research* 168 (2), 422–430.
- Fastner, J., Rucker, J., Stuken, A., Preussel, K., Nixdorf, B., Chorus, I., Kohler, A., Wiedner, C., 2007. Occurrence of the cyanobacterial toxin cylindrospermopsin in northeast Germany. *Environmental Toxicology* 22 (1), 26–32.
- Grosse, Y., Baan, R., Straif, K., Secretan, B., El Ghissassi, F., Coglian, V., 2006. Carcinogenicity of nitrate, nitrite, and cyanobacterial peptide toxins. *Lancet Oncology* 7 (8), 628–629.
- Junttila, M.R., Li, S.P., Westermarck, J., 2008. Phosphatase-mediated crosstalk between MAPK signalling pathways in the regulation of cell survival. *FASEB Journal* 22 (4), 954–965.
- Kang, K.S., Wilson, M.R., Hayashi, T., Chang, C.C., Trosko, J.E., 1996. Inhibition of gap junctional intercellular communication in normal human breast epithelial cells after treatment with pesticides, PCBs, and PBBs, alone or in mixtures. *Environmental Health Perspectives* 104 (2), 192–200.
- King, T.J., 2004. Mice deficient for the gap junction protein Connexin32 exhibit increased radiation-induced tumorigenesis associated with elevated mitogen-activated protein kinase (p44/Erk1, p42/Erk2) activation. *Carcinogenesis* 25 (5), 669–680.
- Komatsu, M., Furukawa, T., Ikeda, R., Takumi, S., Nong, Q., Aoyama, K., Akiyama, S.I., Keppler, D., Takeuchi, T., 2007. Involvement of mitogen-activated protein kinase signaling pathways in microcystin-LR-induced apoptosis after its selective uptake mediated by OATP1B1 and OATP1B3. *Toxicological Sciences* 97 (2), 407–416.
- Lowes, K.N., Brennan, B.A., Yeoh, G.C., Olynyk, J.K., 1999. Oval cell numbers in human chronic liver diseases are directly related to disease severity. *American Journal of Pathology* 154 (2), 537–541.
- Machala, M., Blaha, L., Vondracek, J., Trosko, J.E., Scott, J., Upham, B.L., 2003. Inhibition of gap junctional intercellular communication by noncoplanar polychlorinated biphenyls: inhibitory potencies and screening for potential mode(s) of action. *Toxicological Sciences* 76 (1), 102–111.
- MacKintosh, C., Beattie, K., Klumpp, S., Cohen, C., Codd, G.A., 1990. Cyanobacterial microcystin-LR is a potent and specific inhibitor of protein phosphatases 1 and 2A from both mammals and higher plants. *FEBS Letters* 264 (2), 187–192.
- Madhukar, B.V., de Feijter-Rupp, H.L., Trosko, J.E., 1996. Pulse treatment with the tumor promoter TPA delays the onset of desensitization response and prolongs the inhibitory effect on gap junctional intercellular communication of a rat liver epithelial cell line WB F-344. *Cancer Letters* 106 (1), 117–123.
- Masten, S.J., Tian, M., Upham, B.L., Trosko, J.E., 2001. Effect of selected pesticides and their ozonation by-products on gap junctional intercellular communication using rat liver epithelial cell lines. *Chemosphere* 44 (3), 457–465.
- McCubrey, J.A., LaHair, M.M., Franklin, R.A., 2006. Reactive oxygen species-induced activation of the MAP kinase signaling pathways. *Antioxidants & Redox Signaling* 8 (9–10), 1775–1789.
- Nishiwaki-Matsushima, R., Ohta, T., Nishiwaki, S., Suganuma, M., Kohyama, K., Ishikawa, T., Carmichael, W.W., Fujiki, H., 1992. Liver tumor promotion by the cyanobacterial cyclic peptide toxin microcystin-LR. *Journal of Cancer Research and Clinical Oncology* 118 (6), 420–424.
- Ohta, T., Sueoka, E., Iida, N., Komori, A., Suganuma, M., Nishiwaki, R., Tatematsu, M., Kim, S.J., Carmichael, W.W., Fujiki, H., 1994. Nodularin, a potent inhibitor of protein phosphatase-1 and phosphatase-2A, is a new environmental carcinogen in male F344 rat-liver. *Cancer Research* 54 (24), 6402–6406.
- Papageorgiou, J., Linke, T.A., Kapralos, C., Nicholson, B.C., Steffensen, D.A., 2004. Extraction of cyanobacterial endotoxin. *Environmental Toxicology* 19 (1), 82–87.
- Pietsch, C., Wiegand, C., Ame, M.V., Nicklisch, A., Wunderlin, D., Pflugmacher, S., 2001. The effects of a cyanobacterial crude extract on different aquatic organisms: evidence for cyanobacterial toxin modulating factors. *Environmental Toxicology* 16 (6), 535–542.
- Preussel, K., Stuken, A., Wiedner, C., Chorus, I., Fastner, J., 2006. First report on cylindrospermopsin producing *Aphanizomenon flos-aquae* (cyanobacteria) isolated from two German lakes. *Toxicol* 47 (2), 156–162.
- Rivedal, E., Opsahl, H., 2001. Role of PKC and MAP kinase in EGF- and TPA-induced connexin43 phosphorylation and inhibition of gap junction intercellular communication in rat liver epithelial cells. *Carcinogenesis* 22 (9), 1543–1550.
- Rosenkrantz, H.S., Pollack, N., Cunningham, A.R., 2000. Exploring the relationship between the inhibition of gap junctional intercellular communication and other biological phenomena. *Carcinogenesis* 21 (5), 1007–1011.
- Roskams, T., De Vos, R., Van Eyken, P., Myazaki, H., Van Damme, B., Desmet, V., 1998. Hepatic OV-6 expression in human liver disease and rat experiments: evidence for hepatic progenitor cells in man. *Journal of Hepatology* 29 (3), 455–463.
- Ruch, R.J., Trosko, J.E., 1999. The role of oval cells and gap junctional intercellular communication in hepatocarcinogenesis. *Anticancer Research* 19 (6A), 4831–4838.
- Rucker, J., Stuken, A., Nixdorf, B., Fastner, J., Chorus, I., Wiedner, C., 2007. Concentrations of particulate and dissolved cylindrospermopsin in 21 *Aphanizomenon*-dominated temperate lakes. *Toxicol* 50 (6), 800–809.
- Sai, K., Upham, B.L., Kang, K.S., Hasegawa, R., Inoue, T., Trosko, J.E., 1998. Inhibitory effect of pentachlorophenol on gap junctional intercellular communication in rat liver epithelial cells in vitro. *Cancer Letters* 130 (1–2), 9–17.
- Schlosser, U.G., 1994. SAG – Sammlung von Algenkulturen at the University of Göttingen – catalog of strains 1994. *Botanica Acta* 107 (3), 113–186.
- Schumann, R., Pfeil, D., Lamping, N., Kirschning, C., Scherzinger, G., Schlag, P., Karawajew, L., Herrmann, F., 1996. Lipopolysaccharide induces the rapid tyrosine phosphorylation of the mitogen-activated protein kinases erk-1 and p38 in cultured human vascular endothelial cells requiring the presence of soluble CD14. *Blood* 87 (7), 2805–2814.

- Sell, S., 1993. The role of determined stem-cells in the cellular lineage of hepatocellular-carcinoma. *International Journal of Developmental Biology* 37 (1), 189–201.
- Stein, J., 1975. *Handbook of Phycological Methods: Culture Methods and Growth Measurements*. Cambridge University Press, Cambridge, 477 pp.
- Trosko, J.E., Jone, C., Chang, C.C., 1987. Inhibition of gap junctional-mediated intercellular communication *in vitro* by aldrin, dieldrin, and toxaphene: a possible cellular mechanism for their tumor-promoting and neurotoxic effects. *Molecular Toxicology* 1 (1), 83–93.
- Trosko, J.E., Ruch, R.J., 2002. Gap junctions as targets for cancer chemoprevention and chemotherapy. *Current Drug Targets* 3 (6), 465–482.
- Trosko, J.E., Upham, B.L., 2005. The emperor wears no clothes in the field of carcinogen risk assessment: ignored concepts in cancer risk assessment. *Mutagenesis* 20 (2), 81–92.
- Tsao, M.S., Smith, J.D., Nelson, K.G., Grisham, J.W., 1984. A diploid epithelial cell line from normal adult rat liver with phenotypic properties of 'oval' cells. *Experimental Cell Research* 154 (1), 38–52.
- Upham, B.L., Boddy, B., Xing, X.S., Trosko, J.E., Masten, S.J., 1997. Non-genotoxic effects of selected pesticides and their disinfection by-products on gap junctional intercellular communication. *Ozone Science & Engineering* 19 (4), 351–369.
- Upham, B.L., Deocampo, N.D., Wurl, B., Trosko, J.E., 1998a. Inhibition of gap junctional intercellular communication by perfluorinated fatty acids is dependent on the chain length of the fluorinated tail. *International Journal of Cancer* 78 (4), 491–495.
- Upham, B.L., Weis, L.M., Trosko, J.E., 1998b. Modulated gap junctional intercellular communication as a biomarker of PAH epigenetic toxicity: structure–function relationship. *Environmental Health Perspectives* 106 (4), 975–981.
- Upham, B.L., Guzvic, M., Scott, J., Carbone, J.M., Blaha, L., Coe, C., Li, L.L., Rummel, A.M., Trosko, J.E., 2007. Inhibition of gap junctional intercellular communication and activation of mitogen-activated protein kinase by tumor-promoting organic peroxides and protection by resveratrol. *Nutrition and Cancer* 57 (1), 38–47.
- Upham, B.L., Park, J.-S., Babica, P., Sovadinova, I., Rummel, A.M., Trosko, J.E., Hirose, A., Hasegawa, R., Kanno, J., Sai, K., 2009. Structure–activity-dependent regulation of cell communication by perfluorinated fatty acids using *in vivo* and *in vitro* model systems. *Environmental Health Perspectives* 117 (4), 545–551.
- Watters, J., Sommer, J., Pfeiffer, Z., Prabhu, U., Guerra, A., Bertics, P., 2002. A differential role for the mitogen-activated protein kinases in lipopolysaccharide signaling – the MEK/ERK pathway is not essential for nitric oxide and interleukin 10 production. *Journal of Biological Chemistry* 277 (11), 9077–9087.
- Wright, J.H., Munar, E., Jameson, D.R., Andreassen, P.R., Margolis, R.L., Seger, R., Krebs, E., 1999. Mitogen-activated protein kinase activity is required for the G(2)/M transition of the cell cycle in mammalian fibroblasts. *Proceedings of the National Academy of Sciences USA* 96 (20), 11335–11340.
- Yu, S.Z., 1995. Primary prevention of hepatocellular carcinoma. *Journal of Gastroenterology and Hepatology* 10 (6), 674–682.
- Zhou, L., Yu, H., Chen, K., 2002. Relationship between microcystin in drinking water and colorectal cancer. *Biomedical and Environmental Sciences* 15 (2), 166–171.
- Zhu, Y.L., Zhong, X., Zheng, S., Ge, Z., Du, Q., Zhang, S.Z., 2005. Transformation of immortalized colorectal crypt cells by microcystin involving constitutive activation of Akt and MAPK cascade. *Carcinogenesis* 26 (7), 1207–1214.

IX. Nováková, K., **Babica, P.***, Adamovský, O., Bláha, L., 2011. Modulation of gap-junctional intercellular communication by a series of cyanobacterial samples from nature and laboratory cultures. *Toxicon* 58, 76–84.



Contents lists available at ScienceDirect

Toxicon

journal homepage: www.elsevier.com/locate/toxicon

Modulation of gap-junctional intercellular communication by a series of cyanobacterial samples from nature and laboratory cultures

Kateřina Nováková^{a,b}, Pavel Babica^{a,*}, Ondřej Adamovský^b, Luděk Bláha^{a,b}

^a Institute of Botany, Academy of Sciences of the Czech Republic, Lidická 25/27, Brno CZ60200, Czech Republic

^b Research Centre for Toxic Compounds in the Environment, RECETOX, Faculty of Science, Masaryk University, Kamenice 3, Brno CZ62500, Czech Republic

ARTICLE INFO

Article history:

Received 17 January 2011
Received in revised form 7 May 2011
Accepted 10 May 2011
Available online 18 May 2011

Keywords:

Gap-junctional intercellular communication (GJIC)
Exudate
Biomass
Cyanobacteria
Tumor promotion

ABSTRACT

Cyanobacterial extracts have been recently shown to alter two *in vitro* biomarkers of tumor promotion, namely to cause inhibition of gap-junctional intercellular communication (GJIC) and activation of mitogen-activated protein kinases (Blaha et al., 2010a). In the present study, we investigated GJIC-inhibitory potencies of 10 laboratory strains representing common water bloom-forming cyanobacteria (*Anabaena*, *Aphanizomenon*, *Cylindrospermopsis*, *Microcystis* and *Planktothrix*) and six natural water bloom samples (dominated by *Aphanizomenon* sp. or *Microcystis*). The most pronounced inhibitions of GJIC in a model rat liver epithelial cell line WB-F344 were caused by methanolic extracts of *Anabaena flos-aquae* UTEX 1444, *Aphanizomenon flos-aquae* SAG 31.87, *Aphanizomenon gracile* RCX 06, *Microcystis aeruginosa* PCC 7806, *Cylindrospermopsis raciborskii* SAG 1.97, *Planktothrix agardhii* CICALA 159 and SAG 32.79, whereas weaker effects were induced by *Aphanizomenon klebahnii* CICALA 009 and no inhibition was induced by extracts of *Aph. flos-aquae* PCC 7905 and *Aph. gracile* SAG 31.79. Exudates of the laboratory cultured strains concentrated by solid phase extraction also induced species-specific inhibitory effects, but they did not necessarily correlate with the inhibitory potencies of extracts from the corresponding species. Interestingly, the GJIC-inhibitory effects may not be restricted to cyanobacteria, since exudates of two green alga species also affected GJIC, although their extracts caused no effects. The extracts from different natural water blooms inhibited GJIC with different potencies without apparent relation to bloom-species composition. Since the observed effects on GJIC did not correlate with the content of cyanotoxins microcystins and cylindrospermopsin in the tested samples, they were most likely induced by unknown compound(s). Our results indicate that putative tumor promoting compound(s) could be associated with different species of bloom-forming cyanobacteria, but their production is probably species- and strain-specific.

© 2011 Elsevier Ltd. All rights reserved.

1. Introduction

Cyanobacteria are known producers of toxic compounds, which have been linked to tumor promotion and chemical carcinogenesis (Blaha et al., 2010b). The most

intensively studied cyanotoxin, microcystin-LR, is a potent inhibitor of eukaryotic regulatory enzymes protein serine/threonine phosphatases PP1 and PP2A, and its tumor promoting activity has been demonstrated in both *in vitro* and *in vivo* experiments (Humpage and Falconer, 1999; Ito et al., 1997; Nishiwaki-Matsushima et al., 1992). Moreover, a chronic exposure of human populations to drinking water contaminated with microcystins is being discussed as a factor increasing the prevalence of liver or colorectal cancer (Fleming et al., 2002; Svircev et al., 2009; Yu, 1995;

* Corresponding author. Tel.: +420 530 506 743; fax: +420 541 126 231.
E-mail addresses: bartova@recetox.muni.cz (K. Nováková), pavel.babica@centrum.cz (P. Babica), adamovsky@recetox.muni.cz (O. Adamovský), blaha@recetox.muni.cz (L. Bláha).

Zhou et al., 2002). Another cyanotoxin implicated in carcinogenesis is cylindrospermopsin, which irreversibly inhibits proteosynthesis and has been shown to induce genotoxic effects *in vitro* (Humpage et al., 2000, 2005) and *in vivo* (Shen et al., 2002), increase morphological transformation *in vitro* (Maire et al., 2010), and initiate tumors *in vivo* (Falconer and Humpage, 2001).

Besides well-recognized cyanotoxins, cyanobacteria are capable of producing wide range of structurally diverse secondary metabolites (Welker and von Dohren, 2006), and there is cumulating evidence that cyanobacterial metabolites other than microcystins or cylindrospermopsin are significantly contributing to toxicity of cyanobacteria (Berry et al., 2009; Falconer, 2007). Interestingly, we have demonstrated recently that compounds present in cyanobacterial extracts but different from microcystins and cylindrospermopsin might elicit cellular responses known to be involved in the tumor promotion step of cancer (Blaha et al., 2010a). Specifically, biomass extracts of *Aphanizomenon flos-aquae* and *Microcystis aeruginosa* inhibited gap-junctional intercellular communication (GJIC) and activated mitogen-activated protein kinases (MAPKs) ERK1/2 in a pluripotent rat liver epithelial cell WB-F344. These effects were potently induced with cyanobacterial extracts but to much weaker extent with bacterial and green algal extracts (Blaha et al., 2010a).

Direct communication between cells through gap junctions constitutes a key regulatory system maintaining homeostatic balance of cell differentiation, proliferation, and death at the tissue level. Downregulation of GJIC is a common response of the cells to growth factors, oncogene activation or tumor promoters (Trosko, 2007; Trosko and Upham, 2005), including various environmental contaminants such as polycyclic aromatic hydrocarbons, polychlorinated biphenyls or organochlorine pesticides (Vinken et al., 2009). Although inhibition of GJIC may be a necessary step in the removal of a quiescent cell from the growth suppression, other epigenetic events such as the actual activation of a mitogenic-signaling pathway are also required (Trosko and Upham, 2005). Indeed, tumor promoters and chemicals inhibiting GJIC often activate MAPKs (Machala et al., 2003; Ruch et al., 2001; Rummel et al., 1999; Upham et al., 2009), another intracellular signaling mechanism regulating cell proliferation, differentiation, survival and adhesion (Alberts et al., 2002). Inhibition of GJIC and activation of MAPKs thus seem to be critical and central signaling events in the cell proliferative phases of human diseases, such as cancer, and they are considered as important *in vitro* biomarkers of tumor promoting potential (Upham et al., 2009).

Our recent study indicated that tumor promotion might be a process affected by cyanobacterial metabolites (Blaha et al., 2010a). However, not only the character of compound(s) responsible for the observed remains unknown, but so far there is limited knowledge whether GJIC-inhibitory effects are associated with particular cyanobacterial genera or strains and how often they can be detected in natural water blooms. It cannot also be ruled out that the observed effects on GJIC are result of general cell response to a mixture of chemicals present in complex cyanobacterial extracts (Palikova et al., 2007). Also it should

be taken into account that natural cyanobacterial blooms may bioaccumulate other toxic compounds from water (Awasthi and Rai, 2004; Wang et al., 1998) or may be associated with bacteria contributing to their toxicity (Bernardova et al., 2008). Thus, samples with higher purity and lower complexity (such as fractionated extracts or exudates of laboratory cultures) could represent better material for more detailed investigation of the tumor promoting activity and characterization of the causative agents.

Therefore, the goal of the present study was to bring new information on the occurrence of GJIC-inhibitory effects among different cyanobacterial strains and natural water bloom samples. The focus of our study on laboratory cultured cyanobacteria aimed to eliminate eventual effects of non-cyanobacterial compounds potentially present in natural water bloom samples, and to investigate the specificity of the observed effects to cyanobacteria by comparing effects of cyanobacterial and green algal extracts. Our study also aimed to identify the strains inducing the strongest responses, which may become promising candidates for future isolation and chemical characterization of the putative GJIC-inhibiting compound(s). In order to obtain less complex material than biomass extracts, effects of partially purified and concentrated exudates (i.e. growth-spent media) of corresponding laboratory cultured strains were also investigated.

2. Materials and methods

2.1. Cyanobacterial strains and culture conditions

The list, identification and source of investigated cyanobacterial and algal strains as well as their production of cyanobacterial toxins microcystin and cylindrospermopsin are given in Table 1. All strains were cultivated in the mixture of Zehnder medium (Schlosser, 1994), Bristol (modified Bold) medium (Stein, 1973) and distilled water in the ratio 1:1:2 (v/v/v). The exception was *Aph. flos-aquae* PCC 7905 cultured in the nitrogen low BG11 medium (medium composition according to recommendation of Pasteur Institute). Organisms were grown for 14 days at 22 ± 2 °C under continuous light (cool white fluorescent tubes, 3000 lux) and aeration with air filtered through 0.22 µm filter (Labicom, Olomouc, Czech Republic). The cultivations were started with the 20% (v/v) of the inoculum with optical density 0.3 at 680 nm.

2.2. Biomass extract preparation

Biomasses of laboratory strains of the cyanobacteria and algae (Table 1) were collected by centrifugation (2880×g, 10 min, 25 °C) and freeze-dried. Supernatants were further processed to prepare exudate samples (see below). Biomasses of natural water blooms (Table 1) were collected and concentrated by plankton net (20 µm) and freeze-dried. Freeze-dried biomasses (100 mg) were twice reconstituted in 3 ml of 50% methanol and sonicated on ice (Bandelin Sonopuls HD2070, Berlin, Germany) for 5 minutes. After the sonication, samples were centrifuged

Table 1

List of strains and natural water blooms used in our study, their cyanotoxin content, and effects of extracts and exudates on GJIC. CCALA – Culture Collection of Autotrophic Organisms, Institute of Botany, Academy of Sciences of the Czech Republic; RCX – RECETOX Culture Collection of Cyanobacteria and Algae; SAG – Sammlung von Algenkulturen Goettingen; UTEX – The Culture Collection of Algae at the University of Texas at Austin; PCC – Pasteur Culture Collection of Cyanobacteria; MCs – microcystins; CYN – cylindrospermopsin; n.d. – not detected; n.a. – not analysed. Reported GJIC modulations were observed after exposure to 4 mg d.w./ml for extracts of laboratory strains and 10 mg d.w./ml for natural water bloom extracts.

Species	Source ^a	Cyanotoxin concentration (µg/g d.w.) ^b		GJIC after 30 min exposure (FOC) ^c		Total organic carbon (g/l)
		MCs	CYN	Extract (4 or 10 mg d.w./ml)	Exudate (50×)	Exudate (50×)
Non-treated control	–	–	–	1.00 ± 0.01	1.00 ± 0.10	
Cyanobacteria (Nostocales)						
<i>Anabaena flos-aquae</i>	UTEX 1444	n.d.	n.d.	0.02 ± 0.01 (0.84)	0.97 ± 0.11 (>100)	3.26
<i>Aphanizomenon flos-aquae</i>	PCC 7905	n.d.	3100 (29.8 µM)	0.93 ± 0.13	0.23 ± 0.09	1.79
<i>Aph. flos-aquae</i>	SAG 31.87	n.d.	n.d.	0.01 ± 0.00	0.28 ± 0.06	3.42
<i>Aphanizomenon gracile</i>	RCX 06 ^d	n.d.	n.d.	0.02 ± 0.00 (1.05)	0.98 ± 0.19 (>100)	3.23
<i>Aph. gracile</i>	SAG 31.79	n.d.	n.d.	0.97 ± 0.18	0.45 ± 0.09	3.29
<i>Aphanizomenon klebahnii</i>	CCALA 009	n.d.	n.d.	0.54 ± 0.08	0.49 ± 0.07	3.14
<i>Cylindrospermopsis raciborskii</i>	SAG 1.97	n.d.	n.d.	0.00 ± 0.00 (1.55)	0.11 ± 0.01 (31.75)	3.22
Cyanobacteria (Chroococcales)						
<i>Microcystis aeruginosa</i>	PCC 7806	2500 (10 µM)	n.d.	0.20 ± 0.05 (1.38)	0.54 ± 0.09 (51.1)	3.52
Cyanobacteria (Oscillatoriales)						
<i>Planktothrix agardhii</i>	CCALA 159	170 (0.7 µM)	n.d.	0.02 ± 0.00 (1.70)	0.97 ± 0.19 (>100)	4.51
<i>P. agardhii</i>	SAG 32.79	200 (0.8 µM)	n.d.	0.01 ± 0.01	0.99 ± 0.16	3.24
Green algae (Sphaeropleales)						
<i>Desmodesmus quadricauda</i>	CCALA 463	n.d.	n.d.	0.98 ± 0.20	0.02 ± 0.00	2.13
Green algae (Chlorellales)						
<i>Chlorella kessleri</i>	CCALA 253	n.d.	n.d.	0.96 ± 0.15	0.43 ± 0.10	2.88
Natural water blooms ^e						
<i>Aph. flos-aquae</i> (80%)	Dehtár, 26.6.2007	8.5 (0.1 µM)	n.a.	0.43 ± 0.04	n.a.	n.a.
<i>Aph. flos-aquae</i> (80%)	Křižanovice, 3.9.2007	445 (4.5 µM)	n.a.	0.18 ± 0.02 (3.28)	n.a.	n.a.
<i>Aph. gracile</i> (80%)	Letovice–Křetínka, 18.9.2007	417 (4.2 µM)	n.a.	0.01 ± 0.03 (2.03)	n.a.	n.a.
<i>Aph. klebahnii</i> (80%)	Dehtár, 29.8.2007	n.d.	n.a.	0.65 ± 0.04	n.a.	n.a.
<i>Aph. klebahnii</i> (30%) and <i>Anabaena</i> sp. (50%)	Opatovický, 26.6.2007	n.d.	n.a.	0.30 ± 0.08	n.a.	n.a.
<i>Microcystis</i> sp. (70%)	Lednice – Zámecký rybník, 27.8.2007	1832 (18.4 µM)	n.a.	0.31 ± 0.05 (6.04)	n.a.	n.a.

^a Culture collection ID for laboratory cultured strains or sampling site and date for natural water blooms.

^b Concentration of cyanotoxins in biomass (method limit of detection was 5 µg/g d.w. for microcystins and 10 ng/g d.w. for cylindrospermopsin). Concentrations of cyanotoxins in the experiments with extracts are given in parentheses.

^c Data are means of fraction of the solvent control (FOC) from three independent experiments ± standard deviations. Where available, IC50 values are given in parentheses.

^d This species originates from CCALA (strain 008), but has been long-term cultivated at RECETOX.

^e Percentage given in parentheses represents relative abundance of the species.

(2880×g, 10 min, 4 °C), collected supernatants were evaporated to dryness and redissolved in 50% methanol to reach the concentration equivalent to 400 mg d.w./ml for laboratory strains and 250 mg d.w./ml for natural water bloom samples.

2.3. Exudate preparation

Growth-spent media were separated from the cyanobacterial cells (biomass) by centrifugation (2880×g, 10 min, 25 °C) and filtered through 0.6 µm glass fiber filter (Fisher Scientific, Pardubice, Czech Republic). Organic compounds present in the media were concentrated by solid phase extraction (SPE) using two columns connected in the tandem: Oasis HLB column (Waters, Milford, MA, USA) and Carbograff column (Alltech, Deerfield, Illinois USA). SPE

columns were eluted by 100% methanol and eluates evaporated to dryness. Residual material was redissolved in 100% methanol to reach the final volume that corresponded to 2000-times concentrated original media and sonicated for 5 min. Concentrations of total organic carbon (TOC) of exudates were measured by a LiquiTOC II analyzer (ELEMENTAR Analysensysteme, Hanau, Germany) using high temperature catalytic oxidation detection method.

2.4. Cyanotoxin analyses

Microcystins were analysed by HPLC Agilent 1100 Series coupled with PDA detector (Agilent Technologies, Waldbronn, Germany) using C18 Supelcosil ABZ+Plus column, 150 × 4.6 mm, 5 µm (Supelco, Bellefonte, PA, USA), and gradient elution with acetonitrile (Babica et al., 2006).

Microcystins were identified by comparing the UV spectra and retention times with standards of microcystin-LR, -YR, -RR, -LW, -LF (Enzo Life Sciences, Lausen, Switzerland) and quantified using external calibrations (method limit of detection was 5 µg/g d.w. for microcystin). For cylindrospermopsin analyses, the extracts were reconstituted in Milli-Q water and analysed by the Agilent 1200 system coupled to 6410 Triple-Quad mass spectrometer with the electrospray interface. Separation was achieved on C18 Supelcosil ABZ+Plus column at 35 °C using a gradient elution with methanol acidified with 5 mM ammonium acetate. The mass spectrometer was operated in a multiple reaction monitoring mode (MRM) by monitoring the cylindrospermopsin transition ions m/z 416.2 ($M + H^+$) to 194.2 and m/z 416.2 to 176.1 for 25 ms dwell time. Identification and quantification was achieved using the product ions (194.2 and 176.1 transition) based on external calibration of cylindrospermopsin standard (Enzo Life Sciences, Lausen, Switzerland). Method limit of detection was 10 ng/g d.w. (Blahova et al., 2009).

2.5. Cell culture

The WB-F344 rat liver epithelial cell line was isolated by Drs. J.W. Grisham and M.S. Tsao of the University of North Carolina (Chapel Hill, NC) (Tsao et al., 1984). The cells (passage number between 6 and 26) were cultured in DMEM/Ham's F-12 supplemented with 5% fetal bovine serum (PAA, Pasching, Austria) at 37 °C in a humidified atmosphere containing 5% CO₂. For experiments, the cells were seeded at density 35×10^3 cell/cm² on 24-well tissue culture plates (TPP, Trasadingen, Switzerland). The bioassays for GJIC were conducted with confluent cell cultures obtained after two or three days of growth.

2.6. Gap-junctional intercellular communication (GJIC) assay

GJIC was assessed by scrape loading-dye transfer technique adapted from Elfouly et al. (1987). The samples were added directly to the cell culture medium from the concentrated stock solutions. Appropriate solvent controls (methanol) were tested in each experiment and did not induce any responses significantly different from the non-treated control (final methanol concentration in the well did not exceed 2.5%). After the exposure (5, 15 or 30 min), cells were washed with phosphate-buffered saline (PBS) and Lucifer Yellow dye (1 mg/ml of PBS; Sigma–Aldrich) was added. This membrane non-permeable dye was introduced into the cells with 10 scrapes through the monolayer of confluent cells using a surgical steel scalpel blade. The transfer of the dye through gap junction channels was allowed for 3 min, followed by a thorough rinse of the cells with PBS to remove extracellular dye. Cells were fixed using a 4% formaldehyde solution, and the dye transfer through the cell monolayer was observed at 100× magnification using a Zeiss OBSERVER.Z1 epifluorescence microscope equipped with a Zeiss AxioCam HRc camera. The image of the whole scrape was acquired by AxioVision software and quantified using the image analysis program created by Mr. Zdenek Kuna using MATLAB. Each experiment was performed three times independently in two replicates. Images

were acquired from 6 scrapes for each replicate. The results were expressed as a fraction of the dye spread in the solvent control (fraction of the control, FOC).

2.7. Statistical evaluations

The mean values ± standard deviations from three independent experiments were evaluated by one-way ANOVA followed by Dunnett's post hoc test. *P* values less than 0.05 were considered statistically significant. The IC₅₀ values and 95% confidence intervals were calculated using non-linear regression.

3. Results and discussion

In the first set of experiments, we investigated concentration-dependent effects of five cyanobacterial strains representing common bloom-forming species (*Anabaena flos-aquae* UTEX 1444, *Aphanizomenon gracile* RCX 06, *M. aeruginosa* PCC 7806, *Cylindrospermopsis raciborskii* SAG 1.97, *Planktothrix agardhii* CICALA 159) and also three natural water bloom samples dominated by *Aph. flos-aquae* (Křižanovice), *Aph. gracile* and *Microcystis* sp. The selected exposure period 30 min was previously demonstrated to be sufficient to achieve complete inhibition of GJIC by various chemicals as well as by cyanobacterial extracts in our cellular model (Blaha et al., 2010a; Machala et al., 2003).

After 30 min exposure, all studied extracts of laboratory strains significantly downregulated GJIC with the effective concentrations within the range of 1–4 mg d.w./ml (Fig. 1A). Although the extract of *A. flos-aquae* UTEX 1444 inhibited GJIC most potently, the observed differences in concentration-dependent GJIC inhibition between different strains were rather minor (IC₅₀ values ranged between 0.84 and 1.70 mg d.w./ml) and extracts of all five strains inhibited GJIC at concentrations ≥4 mg d.w./ml almost completely (FOC < 0.20). These data are in a good agreement with the original results reporting similar effective concentrations for extracts of *Aph. flos-aquae* var. *gracile* CICALA 008 and *M. aeruginosa* PCC 7806 (Blaha et al., 2010a). The effects of exudates on GJIC were much less uniform than the effects of extracts prepared from corresponding cyanobacterial strains (Fig. 1B), despite the similar levels of TOC present in all five exudates (Table 1). The strongest inhibition of GJIC was induced by exudate of *C. raciborskii* SAG 1.97 with IC₅₀ value corresponding to 31.75-times concentrated exudate, followed by *M. aeruginosa* PCC 7806 with IC₅₀ value corresponding to 51.10-times concentrated exudate. The exudates of the other three strains did not affect GJIC at the experimental concentration range.

Extracts of natural water blooms differed in their GJIC-inhibitory potencies (Fig. 1C). The extract of *Aph. gracile* bloom was the most potent of the three tested samples and inhibited GJIC with efficiency similar to the extract of *A. flos-aquae* UTEX 1444 or *Aph. gracile* RCX 06 (IC₅₀ 2.03 mg d.w./ml). Inhibition of GJIC induced by the extract of *Aph. flos-aquae* bloom from water reservoir Křižanovice was less effective (IC₅₀ 3.28 mg d.w./ml) but still close to the responses elicited by the extracts of laboratory cultured strains, whereas inhibitory effects of *Microcystis* sp. bloom

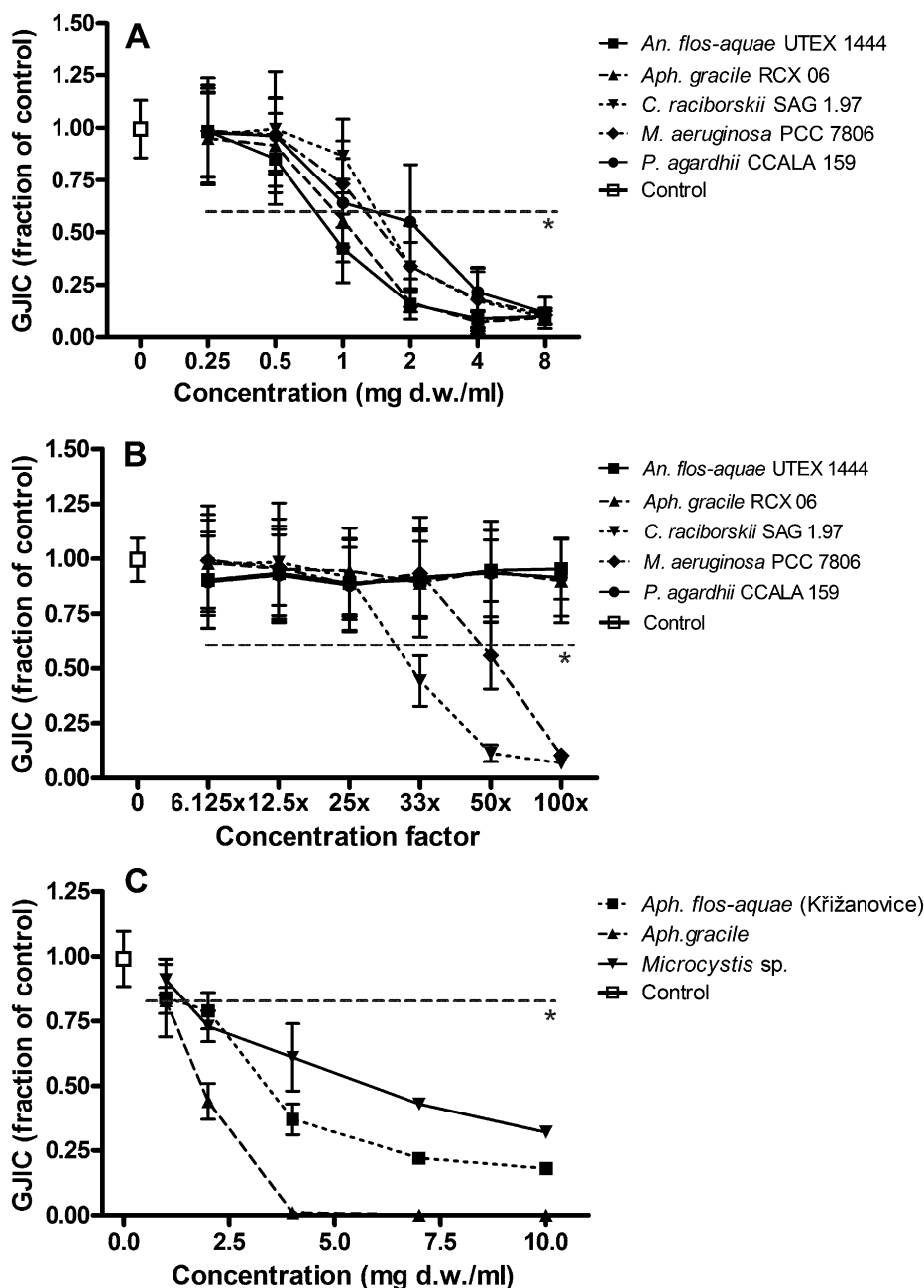


Fig. 1. Concentration-dependent inhibition of gap-junctional intercellular communication (GJIC) in WB-F344 cells caused by laboratory cultured strains or natural water blooms after 30 min exposure. (A) Effects of laboratory cultured strain extracts. (B) Effects of laboratory cultured strain exudates. (C) Effects of natural water bloom extracts. Data are means \pm standard deviations of three independent experiments. *Mean values below the grey line were significantly different from control (ANOVA, $P < 0.050$, Dunnett's test).

extract were weaker (IC₅₀ 6.04 mg d.w./ml). These findings correspond to the results of Blaha et al. (2010a), who also reported greater differences between GJIC-inhibitory potencies of different water bloom extracts, with *Aphanizomenon* sp. bloom extract inducing stronger inhibition of GJIC and activation of MAPKs than *Microcystis* sp. bloom extract (Blaha et al., 2010a).

In the second set of experiments, time-response of GJIC inhibition induced by the same five laboratory cultured strains of cyanobacteria (*A. flos-aquae* UTEX 1444, *Aph. gracile* RCX 06, *M. aeruginosa* PCC 7806, *C. raciborskii* SAG 1.97, *P. agardhii* CCALA 159) was investigated. Since some chemicals (e.g. fluorinated fatty acids) were shown to

completely inhibit GJIC even within 5 min of exposure (Upham et al., 1998), the cells were exposed to cyanobacterial samples for 5, 15 and 30 min. At the tested concentration (4 mg d.w./ml), the extracts rapidly inhibited GJIC and the observed effects became more pronounced with increasing exposure time (Fig. 2A). The time-course experiments revealed more remarkable differences between the studied extracts and clearly showed that *A. flos-aquae* UTEX 1444 extract induced the strongest effect when complete inhibition of GJIC occurred already after 5 min exposure (FOC 0.12), whereas 15–30 min exposure was required by the extracts of the other strains to close GJIC. The effects of exudates of laboratory strains were also

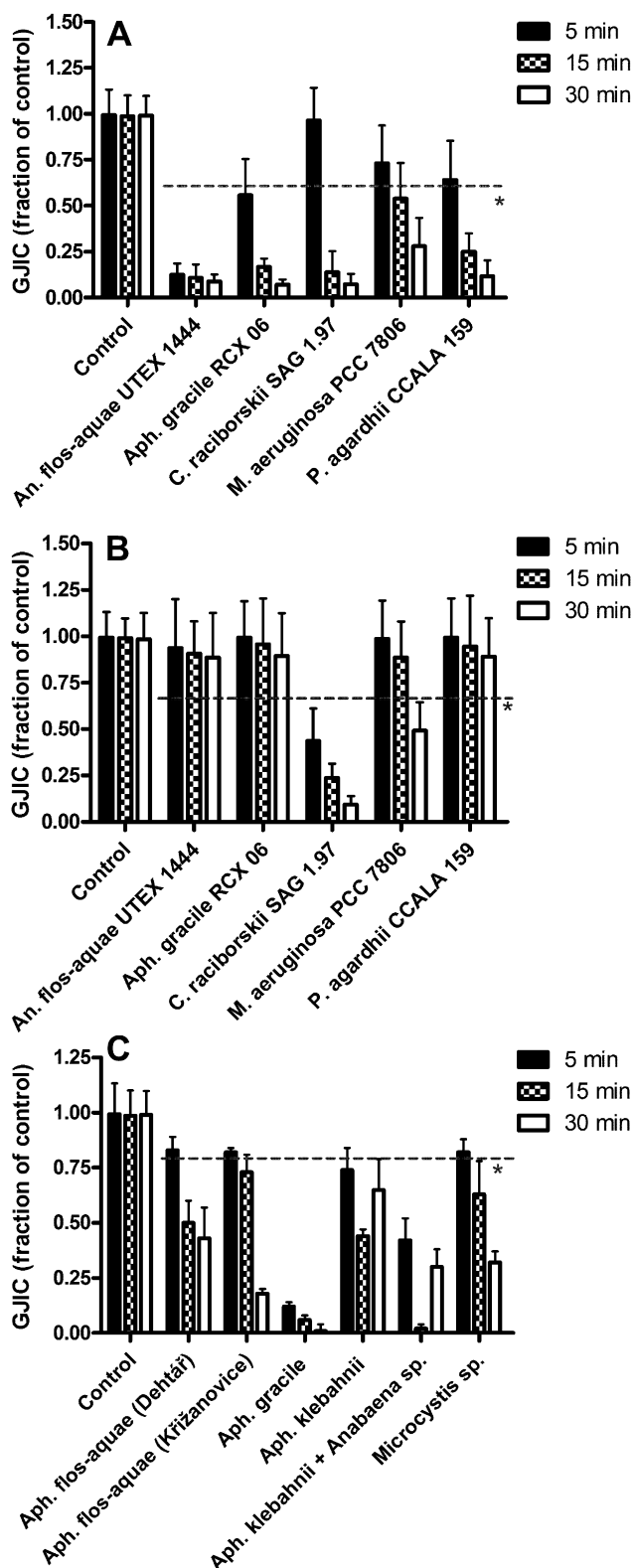


Fig. 2. Time-course inhibition of gap-junctional intercellular communication (GJIC) in WB-F344 cells caused by laboratory cultured strains and natural water blooms after different exposure times (5, 15 and 30 min). (A) Effects of laboratory strain extracts (4 mg d.w./ml). (B) Effects of laboratory strain exudates (50-times concentrated in comparison to the original growth-spent mediums). (C) Effects of natural water bloom extracts (10 mg d.w./ml). Data are means \pm standard deviations of three independent experiments. *Mean values below the grey line were significantly different from control (ANOVA, $P < 0.050$, Dunnett's test).

time-progressive, but only *M. aeruginosa* PCC 7806 and *C. raciborskii* SAG 1.97 induced significant inhibition of GJIC within the experimental exposure regimes (Fig 2B), which corresponds well to the results of concentration–response experiments.

Since recent study of Blaha et al. (2010a) as well as our present results indicate that extracts of *Aphanizomenon* sp. and *Anabaena* sp. might be the most potent inhibitors of GJIC and therefore the samples of our particular interest, three additional extracts of complex water blooms dominated by *Aph. flos-aquae* (Dehtár), *Aph. klebahnii*, and *Aph. klebahnii* + *Anabaena* sp. were included into the time-response experiments. Higher experimental concentrations (10 mg d.w./ml) were used in these experiments with respect to weaker inhibitory potencies observed in some bloom samples. The experiments confirmed that extract of *Aph. gracile*, which inhibited GJIC almost completely after 5 min (FOC 0.12), was the most potent water bloom sample in our study (Fig. 2C). The effects of *Aph. flos-aquae* (Křížanovice and Dehtár) extracts and *Microcystis* sp. extract were less pronounced but progressing with exposure time, with maximum inhibition achieved after 30 min exposure. However, notably different time-course of inhibition was observed in the extracts of *Aph. klebahnii* bloom or *Aph. klebahnii* + *Anabaena* sp. bloom, which caused the maximum inhibition of GJIC after 15 min exposure (FOC 0.44 or 0.02) followed by restoration of communication after 30 min (FOC 0.65 or 0.30) (Fig. 2C). The observed differences in the time-responses may indicate that different extracts inhibited GJIC by different compound(s) with variable mode of action. For example, cells do not restore GJIC during exposure to polychlorinated biphenyl PCB 153, a chemical inhibiting communication by a different mechanism than tumor promoting phorbol ester or epidermal growth factor (Machala et al., 2003), which are known to downregulate GJIC only transiently (Rivedal and Opsahl, 2001).

The last part of our study focused on additional laboratory strains of cyanobacteria, namely *Aph. flos-aquae* PCC 7905, *Aph. flos-aquae* SAG 31.87, *Aph. gracile* SAG 31.79, *Aph. klebahnii* CCALA 009 and *P. agardhii* SAG 32.79. Based on the results from dose- and time-response experiments (Figs. 1 and 2), the effects of 30 min exposure to a single concentration of extracts (4 mg d.w./ml) and exudates (50-times concentrated) were studied. The results obtained from all 10 cyanobacterial strains under the study are compiled in the Table 1. Extracts of seven laboratory cultured strains inhibited GJIC completely, which suggests that the GJIC-inhibitory effects are in fact being induced by some compound(s) produced by cyanobacteria and not caused by other pollutants possibly bioaccumulated or biosorbed by cyanobacterial biomass, as it could be assumed in the case of natural water bloom samples. However, our experiments revealed apparent differences in GJIC-inhibitory potencies of various strains. The extract of *Aph. klebahnii* CCALA 009 induced only a partial inhibition at the tested concentration (FOC 0.54), and no effects on GJIC were elicited by extracts of *Aph. flos-aquae* PCC 7905 and *Aph. gracile* SAG 31.79. Also, the extracts of green algae *Desmodesmus quadricauda* CCALA 463 and *Chlorella kessleri* CCALA 253 did not affect GJIC. Considering the presence of such species-specific or strain-specific differences in GJIC-inhibitory potencies, it seems

that the effects were caused by unknown bioactive chemical(s) produced in particular strains rather than a result of general cell response to a complex mixture of cyanobacterial or algal primary and secondary metabolites. Moreover, GJIC was inhibited also by exudates concentrated and partially purified by SPE, which represent less complex mixture containing mostly organic compounds. No correlation between TOC concentrations in different exudates and their effects on GJIC was observed. Most exudates contained similar levels of TOC corresponding to 58–70 mg/L in non-concentrated samples, even though they inhibited GJIC to different extents (Table 1). The exudate of *P. agardhii* CCALA 159 with the highest concentration of TOC (90 mg/L in non-concentrated sample) did not cause inhibition of GJIC, whereas exudates of *Aph. flos-aquae* PCC7905 and *D. quadricauda* CCALA 463 containing the lowest TOC levels (36 and 43 mg/L in non-concentrated samples) were among the samples inducing the most profound inhibition of GJIC (FOC 0.23 and 0.02). These results suggest that metabolic activity and total amount of organic compounds extracellularly released during cyanobacteria or algae cultivation might have been similar, but production and release of causative agents of GJIC inhibition differed between species and strains.

Interestingly, the effects of exudates did neither correlate with tumor promoting activity of extracts of corresponding cyanobacterial strains (Table 1) and various scenarios were observed in our study: (A) GJIC was inhibited by both extract and exudate (*C. raciborskii* SAG 1.97, *Aph. flos-aquae* SAG 31.87, *Aph. klebahnii* CCALA 009, *M. aeruginosa* PCC 7806); (B) only the extracts but not the exudates downregulated GJIC (*A. flos-aquae* UTEX 1444, *Aph. gracile* RCX 06, *P. agardhii* CCALA 159, *P. agardhii* SAG 32.79); and (C) GJIC was inhibited only by the exudate and not by the extract (*Aph. flos-aquae* PCC 7905, *Aph. gracile* SAG 31.79). To our knowledge, there is only limited number of studies that investigated and compared effects of metabolites extracted from cyanobacterial cells and produced extracellularly. For example Bártová et al. (2010) reported that extract and exudate of *M. aeruginosa* PCC7806 induced quantitatively different oxidative stress-related responses in a green alga, even though the experimental concentrations of extract and exudate were adjusted to the same level of microcystin equivalents. The absence of such adjustment in the present study along with different growth characteristics of the studied strains could affect production and extracellular release of putative bioactive metabolites. This could then explain the lack of clear relationship between toxicities of extracts and exudates observed in our study. However, the possibility that different agents were responsible for the effects of extracts and exudates cannot be excluded. The importance of future toxicological and chemical characterization of exudates is stressed out by the finding that also exudates of the two green algae, *D. quadricauda* CCALA 463 and *C. kesslerii* CCALA 253, downregulated GJIC, although their extracts had no effect (Table 1). These two green algal species represent environmentally common genera of planktonic green algae (Reynolds, 2006) and therefore were chosen as relevant species for comparison with common species of planktonic cyanobacteria, however, more representative

information on distribution of GJIC-inhibitory potencies and chemicals among green algae should be obtained by screening of more species in future studies.

Our study also demonstrated that the ability to inhibit GJIC can be found across different cyanobacterial orders and genera (Nostocales – *Anabaena*, *Aphanizomenon*, *Cylindrospermopsis*; Chroococcales – *Microcystis*; Oscillatoriales – *Planktothrix*) and also in the exudates of green algae, but the inhibitory potencies may substantially differ between the strains. This was most obvious between the extracts of *Aph. flos-aquae* PCC 7905 and *Aph. flos-aquae* SAG 31.87, or between extracts and exudates of *Aph. gracile* RCX 06 and *Aph. gracile* SAG 31.79. These observations correspond well to the fact that the main classes of cyanobacterial oligopeptides (aeruginosins, anabaenopeptins, cyanopeptolines, microcystins, microviridins, microginins and cyclamides) as well as other cyanotoxins (anatoxins, saxitoxins, cylindrospermopsins) can be found in phylogenetically distant cyanobacterial genera, yet the actual spectrum of bioactive metabolites produced by morphologically indistinguishable strains of the same species or morphotype can be different depending on the presence and activity of genes responsible for biosynthesis of these metabolites (Pearson et al., 2010; Welker and von Dohren, 2006). Similarly to the cyanotoxin production and toxicity of cyanobacterial samples, it seems that GJIC-inhibitory potencies also cannot be reliably predicted from morphological species identification.

Although the chemical(s) responsible for GJIC-inhibitory effects of cyanobacterial extracts in our *in vitro* model have not been characterized yet, they were most likely different from microcystins and cylindrospermopsin. Blaha et al. (2010a) reported no modulation of GJIC in WB-F344 cells after exposure to microcystin-LR (100 µM) or cylindrospermopsin (60 µM) and it has been proposed that eventual lack of expression of respective organic anion transport proteins required for microcystin uptake and toxicity OATPs could be responsible for the absence of microcystin effects in WB-F344 cells, since most cell lines *in vitro* do not express OATPs (Blaha et al., 2010a). These findings are strongly supported by our study, where GJIC-inhibitory potencies of the tested samples did not correlate with the content of microcystins or cylindrospermopsin in the studied samples and significant inhibitions of GJIC were elicited by the strains that did not produce these toxins in our study, such as *A. flos-aquae* UTEX 1444, *Aph. flos-aquae* SAG 31.87, *Aph. gracile* RCX 06 and SAG 31.79, *Aph. klebahnii* CCALA 009 or *C. raciborskii* SAG 1.97 (Table 1). Apparently, WB-F344 cells may be a target of GJIC-inhibiting chemicals different from microcystins and cylindrospermopsin. Inhibition of GJIC in WB-F344 cells might be of particular importance, since these normal liver epithelial cells possess characteristics of so-called oval cells, which have been recognized to have an important role in liver tumor promotion and hepatocarcinogenesis (Ruch and Trosko, 1999).

4. Conclusion

Although the research of carcinogenic and tumor promoting effects of cyanobacteria have mostly focused on

microcystins or cylindrospermopsin so far, cyanobacteria seem to produce a range of other but not-yet-identified metabolites with potential tumor promoting effects. We demonstrated that extracts as well as exudates of different cyanobacterial strains as well as extracts of natural water bloom samples inhibit GJIC in a model *in vitro* system. Inhibition of GJIC was caused by most of tested cyanobacteria with extracts of *A. flos-aquae* UTEX 1444, *Aph. flos-aquae* SAG 31.87, *Aph. gracile* RCX 06, *M. aeruginosa* PCC 7806, *C. raciborskii* SAG 1.97, *P. agardhii* CCALA 159 and SAG 32.79 being the most potent inhibitors, whereas green algal extracts did not alter GJIC. However, exudates of green algae downregulated GJIC to similar extent as several cyanobacterial exudates. Interestingly, inhibition of GJIC caused by both samples (extract and exudate) was reported only for few investigated strains, namely *Aph. flos-aquae* SAG 31.87, *Aph. klebahnii* CCALA 009, *C. raciborskii* SAG 1.97 and *M. aeruginosa* PCC 7806.

The data shows that the ability to inhibit GJIC is common among different cyanobacterial species and bloom samples, but may differ significantly between different strains. Identification and characterization of these bioactive compound(s) using approaches of the effect-directed analysis (EDA) is the subject of our ongoing research.

Acknowledgement

The research was supported by the Czech Science Foundation grant No. GACR 524/08/0496, Czech Ministry of Education project INCHEMIBIOL (MSM0021622412) and by the CETOCOEN project from the European Regional Development Fund (No. CZ.1.05/2.1.00/01.0001).

Conflict of interest statement

The authors declare that there is no conflict of interest.

Ethical statement

The authors hereby declare that this manuscript has never been published/submitted for the publication elsewhere. All authors have approved the final version of the article.

References

- Alberts, B., Johnson, A., Lewis, J., Raff, M., Roberts, K., Walter, P., 2002. *Molecular Biology of the Cell*, fourth ed. Garland Science, New York.
- Awasthi, M., Rai, L.C., 2004. Adsorption of nickel, zinc and cadmium by immobilized green algae and cyanobacteria: a comparative study. *Annals of Microbiology* 54, 257–267.
- Babica, P., Kohoutek, J., Blaha, L., Adamovsky, O., Marsalek, B., 2006. Evaluation of extraction approaches linked to ELISA and HPLC for analyses of microcystin-LR, -RR and -YR in freshwater sediments with different organic material contents. *Analytical and Bioanalytical Chemistry* 385, 1545–1551.
- Bártová, K., Hilscherová, K., Babica, P., Maršálek, B., Blaha, L., 2010. Effects of microcystin and complex cyanobacterial samples on the growth and oxidative stress parameters in green alga *Pseudokirchneriella subcapitata* and comparison with the model oxidative stressor-herbicide paraquat. *Environmental Toxicology*. doi:10.1002/tox.20601.
- Bernardova, K., Babica, P., Marsalek, B., Blaha, L., 2008. Isolation and endotoxin activities of lipopolysaccharides from cyanobacterial cultures and complex water blooms and comparison with the effects of heterotrophic bacteria and green alga. *Journal of Applied Toxicology* 28, 72–77.
- Berry, J.P., Gibbs, P.D.L., Schmale, M.C., Saker, M.L., 2009. Toxicity of cylindrospermopsin, and other apparent metabolites from *Cylindrospermopsis raciborskii* and *Aphanizomenon ovalisporum*, to the zebrafish (*Danio rerio*) embryo. *Toxicol* 53, 289–299.
- Blaha, L., Babica, P., Hilscherova, K., Upham, B.L., 2010a. Inhibition of gap-junctional intercellular communication and activation of mitogen-activated protein kinases by cyanobacterial extracts – indications of novel tumor-promoting cyanotoxins? *Toxicol* 55, 126–134.
- Blaha, L., Babica, P., Maršálek, B., 2010b. Toxins produced in cyanobacterial water blooms – toxicity and risks. *Interdisciplinary Toxicology* 2, 36–41.
- Blahova, L., Oravec, M., Marsalek, B., Sejnohova, L., Simek, Z., Blaha, L., 2009. The first occurrence of the cyanobacterial alkaloid toxin cylindrospermopsin in the Czech Republic as determined by immunochemical and LC/MS methods. *Toxicol* 53, 519–524.
- Elfouly, M.H., Trosko, J.E., Chang, C.C., 1987. Scrape-loading and dye transfer – a rapid and simple technique to study gap junctional intercellular communication. *Experimental Cell Research* 168, 422–430.
- Falconer, I.R., 2007. Cyanobacterial toxins present in *Microcystis aeruginosa* extracts – more than microcystins! *Toxicol* 50, 585–588.
- Falconer, I.R., Humpage, A.R., 2001. Preliminary evidence for *in vivo* tumour initiation by oral administration of extracts of the blue-green alga *Cylindrospermopsis raciborskii* containing the toxin cylindrospermopsin. *Environmental Toxicology* 16, 192–195.
- Fleming, L.E., Rivero, C., Burns, J., Williams, C., Bean, J.A., Shea, K.A., Stinn, J., 2002. Blue green algal (cyanobacterial) toxins, surface drinking water, and liver cancer in Florida. *Harmful Algae* 1, 157–168.
- Humpage, A.R., Falconer, I.R., 1999. Microcystin-LR and liver tumor promotion: effects on cytokinesis, ploidy, and apoptosis in cultured hepatocytes. *Environmental Toxicology* 14, 61–75.
- Humpage, A.R., Fenech, M., Thomas, P., Falconer, I.R., 2000. Micronucleus induction and chromosome loss in transformed human white cells indicate clastogenic and aneugenic action of the cyanobacterial toxin, cylindrospermopsin. *Mutation Research/Genetic Toxicology and Environmental Mutagenesis* 472, 155–161.
- Humpage, A.R., Fontaine, F., Frosco, S., Burcham, P., Falconer, I.R., 2005. Cylindrospermopsin genotoxicity and cytotoxicity: role of cytochrome P-450 and oxidative stress. *Journal of Toxicology and Environmental Health-Part a-Current Issues* 68, 739–753.
- Ito, E., Kondo, F., Terao, K., Harada, K.-I., 1997. Neoplastic nodular formation in mouse liver induced by repeated intraperitoneal injections of microcystin-LR. *Toxicol* 35, 1453–1457.
- Machala, M., Blaha, L., Vondracek, J., Trosko, J.E., Scott, J., Upham, B.L., 2003. Inhibition of gap junctional intercellular communication by noncoplanar polychlorinated biphenyls: inhibitory potencies and screening for potential mode(s) of action. *Toxicological Sciences* 76, 102–111.
- Maire, M.A., Bazin, E., Fessard, V., Rast, C., Humpage, A.R., Vasseur, P., 2010. Morphological cell transformation of Syrian hamster embryo (SHE) cells by the cyanotoxin, cylindrospermopsin. *Toxicol* 55, 1317–1322.
- Nishiwaki-Matsushima, R., Ohta, T., Nishiwaki, S., Suganuma, M., Kohyama, K., Ishikawa, T., Carmichael, W.W., Fujiki, H., 1992. Liver-tumor promotion by the cyanobacterial cyclic peptide toxin microcystin-Lr. *Journal of Cancer Research and Clinical Oncology* 118, 420–424.
- Palikova, M., Krejci, R., Hilscherova, K., Buryskova, B., Babica, P., Navratil, S., Kopp, R., Blaha, L., 2007. Effects of different oxygen saturation on activity of complex biomass and aqueous crude extract of cyanobacteria during embryonal development in carp (*Cyprinus carpio* L.). *Acta Veterinaria Brno* 76, 291–299.
- Pearson, L., Mihali, T., Moffitt, M., Kellmann, R., Neilan, B., 2010. On the chemistry, toxicology and genetics of the cyanobacterial toxins, microcystin, nodularin, saxitoxin and cylindrospermopsin. *Marine Drugs* 8, 1650–1680.
- Reynolds, C.S., 2006. *Ecology of Phytoplankton*. Cambridge University Press, Cambridge, UK, 507 pp.
- Rivedal, E., Opsahl, H., 2001. Role of PKC and MAP kinase in EGF- and TPA-induced connexin43 phosphorylation and inhibition of gap junction intercellular communication in rat liver epithelial cells. *Carcinogenesis* 22, 1543–1550.
- Ruch, R.J., Trosko, J.E., 1999. The role of oval cells and gap junctional intercellular communication in hepatocarcinogenesis. *Anticancer Research* 19 (6A), 4831–4838.
- Ruch, R.J., Trosko, J.E., Madhukar, B.V., 2001. Inhibition of connexin43 gap junctional intercellular communication by TPA requires ERK activation. *Journal of Cellular Biochemistry* 83, 163–169.
- Rummel, A.M., Trosko, J.E., Wilson, M.R., Upham, B.L., 1999. Polycyclic aromatic hydrocarbons with bay-like regions inhibited gap junctional intercellular communication and stimulated MAPK activity. *Toxicological Sciences* 49, 232–240.

- Shen, X., Lam, P.K.S., Shaw, G.R., Wickramasinghe, W., 2002. Genotoxicity investigation of a cyanobacterial toxin, cylindrospermopsin. *Toxicol* 40, 1499–1501.
- Schlosser, U.G., 1994. *Sag – Sammlung-Von-Algenkulturen at the University-of-Gottingen – catalog of strains 1994*. *Botanica Acta* 107, 113–186.
- Stein, J., 1973. *Handbook of Phycological Methods. Culture Methods and Growth Measurements*. Cambridge University Press, Cambridge.
- Svircev, Z., Krstic, S., Miladinov-Mikov, M., Baltic, V., Vidovic, M., 2009. Freshwater cyanobacterial blooms and primary liver cancer epidemiological studies in Serbia. *Journal of Environmental Science and Health Part C – Environmental Carcinogenesis & Ecotoxicology Reviews* 27, 36–55.
- Trosko, J.E., 2007. Gap junctional intercellular communication as a biological “Rosetta stone” in understanding, in a systems biological manner, stem cell behavior, mechanisms of epigenetic toxicology, chemoprevention and chemotherapy. *Journal of Membrane Biology* 218, 93–100.
- Trosko, J.E., Upham, B.L., 2005. The emperor wears no clothes in the field of carcinogen risk assessment: ignored concepts in cancer risk assessment. *Mutagenesis* 20, 81–92.
- Tsao, M.S., Smith, J.D., Nelson, K.G., Grisham, J.W., 1984. A diploid epithelial-cell line from normal adult-rat liver with phenotypic properties of oval cells. *Experimental Cell Research* 154, 38–52.
- Upham, B.L., Deocampo, N.D., Wurl, B., Trosko, J.E., 1998. Inhibition of gap junctional intercellular communication by perfluorinated fatty acids is dependent on the chain length of the fluorinated tail. *International Journal of Cancer* 78 (4), 491–495.
- Upham, B.L., Park, J.S., Babica, P., Sovadinova, I., Rummel, A.M., Trosko, J.E., Hirose, A., Hasegawa, R., Kanno, J., Sai, K., 2009. Structure–activity–dependent regulation of cell communication by perfluorinated fatty acids using in vivo and in vitro model systems. *Environmental Health Perspectives* 117, 545–551.
- Vinken, M., Doktorova, T., Decrock, E., Leybaert, L., Vanhaecke, T., Rogiers, V., 2009. Gap junctional intercellular communication as a target for liver toxicity and carcinogenicity. *Critical Reviews in Biochemistry and Molecular Biology* 44, 201–222.
- Wang, T.C., Weissman, J.C., Ramesh, G., Varadarajan, R., Benemann, J.R., 1998. Heavy metal binding and removal by Phormidium. *Bulletin of Environmental Contamination and Toxicology* 60, 739–744.
- Welker, M., von Dohren, H., 2006. Cyanobacterial peptides – nature's own combinatorial biosynthesis. *Fems Microbiology Reviews* 30, 530–563.
- Yu, S.Z., 1995. Primary prevention of hepatocellular-carcinoma. *Journal of Gastroenterology and Hepatology* 10, 674–682.
- Zhou, L., Yu, H., Chen, K., 2002. Relationship between microcystin in drinking water and colorectal cancer. *Biomedical and Environmental Sciences* 15, 166–171.

X. Nováková, K., Bláha, L., **Babica, P***, 2012. Tumor promoting effects of cyanobacterial extracts are potentiated by anthropogenic contaminants – Evidence from in vitro study. *Chemosphere* 89, 30–37.



Contents lists available at SciVerse ScienceDirect

Chemosphere

journal homepage: www.elsevier.com/locate/chemosphere

Tumor promoting effects of cyanobacterial extracts are potentiated by anthropogenic contaminants – Evidence from *in vitro* study

Kateřina Nováková^b, Luděk Bláha^{a,b}, Pavel Babica^{a,b,*}

^aInstitute of Botany, Czech Academy of Sciences, Lidická 25/27, Brno CZ60200, Czech Republic

^bResearch Centre for Toxic Compounds in the Environment, RECETOX, Faculty of Science, Masaryk University, Kamenice 3, Brno CZ62500, Czech Republic

ARTICLE INFO

Article history:

Received 2 February 2012

Received in revised form 22 March 2012

Accepted 4 April 2012

Available online 8 May 2012

Keywords:

Cyanobacteria

Cylindrospermopsin

Gap junctional intercellular communication

Polychlorinated biphenyls

Polycyclic aromatic hydrocarbons

Synergistic effects

ABSTRACT

Inhibition of gap junctional intercellular communication (GJIC) is affiliated with tumor promotion process and it has been employed as an *in vitro* biomarker for evaluation of tumor promoting effects of chemicals. In the present study we investigated combined effects of anthropogenic environmental contaminants 2,2',4,4',5,5'-hexachlorobiphenyl (PCB 153) and fluoranthene, cyanotoxins microcystin-LR and cylindrospermopsin, and extracts of laboratory cultures of cyanobacteria *Aphanizomenon gracile* and *Cylindrospermopsis raciborskii*, on GJIC in the rat liver epithelial cell line WB-F344. Binary mixtures of PCB 153 with fluoranthene and the mixtures of the two cyanobacterial strains elicited simple additive effects on GJIC after 30 min exposure, whereas microcystin-LR and cylindrospermopsin neither inhibited GJIC nor altered effects of PCB 153 or fluoranthene. However, synergistic effects were observed in the cells exposed to binary mixtures of anthropogenic contaminants (PCB 153 or fluoranthene) and cyanobacterial extracts. The synergistic effects were especially pronounced after prolonged (6–24 h) co-exposure to fluoranthene and *A. gracile* extract, when mixture caused nearly complete GJIC inhibition, while none of the individual components caused any downregulation of GJIC at the same concentration and exposure time. The effects of cyanobacterial extracts were independent of microcystin-LR or cylindrospermopsin, which were not detected in cyanobacterial biomass. It provides further evidence on the presence of unknown tumor promoting metabolites in cyanobacteria. Clear potentiation of the GJIC inhibition observed in the mixtures of two anthropogenic contaminants and cyanobacteria highlight the importance of combined toxic effects of chemicals in complex environmental mixtures.

© 2012 Elsevier Ltd. All rights reserved.

1. Introduction

Many external and environmental factors are contributing to carcinogenesis such as diet, cigarette smoking and betel chewing, alcohol drinking, radiation or infection (Wogan et al., 2004). Contamination of the air, food or water by toxic compounds may also increase a risk of developing cancer, and various anthropogenic contaminants are classified as carcinogens, including representa-

Abbreviations: CYN, cylindrospermopsin; FLU, fluoranthene; DDT, dichlorodiphenyltrichloroethane; ERK, extracellular-signal-regulated kinase; GJIC, gap junctional intercellular communication; IARC, International Agency for Research on Cancer; MAPK, mitogen-activated protein kinase; MC-LR, microcystin-LR; PAHs, polycyclic aromatic hydrocarbons; PCB 153, 2,2',4,4',5,5'-hexachlorobiphenyl; PCBs, polychlorinated biphenyls; PCDD/Fs, polychlorinated dibenzodioxins and polychlorinated dibenzofurans; SL-DT, scrape loading-dye transfer.

* Corresponding author at: Institute of Botany, Czech Academy of Sciences, Lidická 25/27, Brno CZ60200, Czech Republic. Tel.: +420 530 506 748; fax: +420 541 126 231.

E-mail addresses: novakova@recetox.muni.cz (K. Nováková), blaha@recetox.muni.cz (L. Bláha), pavel.babica@centrum.cz (P. Babica).

tives of polycyclic aromatic hydrocarbons (PAHs), polychlorinated dibenzodioxins and polychlorinated dibenzofurans (PCDD/Fs), polychlorinated biphenyls (PCBs) as well as some complex mixtures containing these chemicals (Baan et al., 2009). Currently, PCB 126 and benzo[a]pyrene as well as some PAH-related exposures are recognized as carcinogenic to human (IARC Group 1), whereas PCB-mixtures and some other PAHs are classified as probable or possible human carcinogens (IARC Groups 2A or 2B) (Straif et al., 2005; Baan et al., 2009).

Besides the man-made chemicals, massive proliferations of toxic cyanobacteria resulting from nutrient pollution of surface and coastal marine waters represent another global environmental problem, since cyanobacteria produce a wide range of bioactive and toxic chemicals (van Apeldoorn et al., 2007). Toxic cyanobacteria have been associated with increased prevalence of cancer and the most prevalent and studied cyanotoxin, microcystin-LR (MC-LR), is currently classified as a possible human carcinogen (IARC Group 2B) (Svircev et al., 2010). Carcinogenic effects of another emergent cyanotoxin, cylindrospermopsin (CYN), are being investigated and discussed (Zegura et al., 2011).

Processes and mechanisms underlying the chemical carcinogenesis are still not completely understood but it is now well accepted that development of cancer is a multistep process (Vineis et al., 2010). Traditionally, mutations and genotoxicity of chemicals were extensively studied but various non-genotoxic mechanisms were shown to play a crucial role in the process of cancer development (Hernandez et al., 2009; Ziech et al., 2010). Disruption of the tissue homeostasis mediated by gap junctional intercellular communication (GJIC) represents an important non-genotoxic mechanism associated with tumor promotion and cancer (Trosko, 2007). Downregulation of GJIC caused by chemicals *in vitro* can serve as a potent biomarker of tumor promotion and its assessment provides good predictions of *in vivo* tumor promoting potencies of chemicals (Rosenkranz et al., 2000; Upham et al., 2009).

Number of studies demonstrated inhibition of GJIC caused by various classes of chemicals including known tumor promoters and carcinogens such as phorbol ester, polycyclic aromatic hydrocarbons or organochlorine compounds such as polychlorinated biphenyls (Vinken et al., 2009). More recently, we have shown that also cyanobacterial extracts inhibit GJIC (Blaha et al., 2010; Novakova et al., 2011) but the effects could not be related to known cyanotoxins such as MC-LR and CYN. Rather, other unknown toxic metabolite(s) produced by cyanobacteria are responsible for the observed toxicity *in vitro* (Blaha et al., 2010; Novakova et al., 2011).

Since organisms including humans are typically exposed to multi-component chemical mixtures from the environment and food, the issue of mixture toxicity is being intensively addressed in toxicological and ecotoxicological research (McCarty and Borgert, 2006a,b; Syberg et al., 2009). Toxic effects of cyanotoxins have been often examined in mixtures due to frequent use of complex cyanobacterial extracts in many studies, but information on cyanotoxin effects in combination with other environmental contaminants is limited. Interestingly, there is a recent evidence that exposures to toxic cyanobacteria may enhance effects of other non-cyanobacterial toxicants and stressors, such as heavy metals or viral infection (Pikula et al., 2010), or pesticides (Cerbin et al., 2010).

The objective of the present study was to evaluate *in vitro* tumor promoting potencies of mixtures containing two known inhibitors of GJIC, anthropogenic environmental contaminants fluoranthene (FLU) and hexachlorobiphenyl PCB 153, in mixtures with cyanobacterial extracts of *Aphanizomenon gracile* or *Cylindrospermopsis raciborskii* or pure cyanotoxins, MC-LR and CYN.

2. Materials and methods

2.1. Chemicals

2,2',4,4',5,5'-hexachlorobiphenyl (PCB 153) was purchased from Dr. Ehrenstorfer (Augsburg, Germany). Fluoranthene (FLU), cylindrospermopsin (CYN) and lucifer yellow were supplied by Sigma–Aldrich (Prague, Czech Republic). Cyanotoxin microcystin-LR (MC-LR) was provided by Enzo Life Sciences (Lausen, Switzerland).

2.2. Cyanobacterial strains and culture conditions

Cyanobacterial culture of *Aphanizomenon gracile* RCX 06 was obtained from the RECETOX Culture Collection of Cyanobacteria and Algae, Czech Republic. This species originates from the Culture Collection of Autotrophic Organisms, Institute of Botany, Academy of Sciences of the Czech Republic (CCALA strain 008), but has been long-term cultivated at RECETOX laboratories and its properties differ from the original strain. Cyanobacterium *Cylindrospermopsis raciborskii* SAG 1.97 was purchased from the Goettingen University Collection of Cyanobacteria (Goettingen, Germany). Both microor-

ganisms were cultured in the mixture of Zehnder medium (Schlosser, 1994), Bristol (modified Bold) medium (Stein, 1973) and distilled water in the ratio 1:1:2 (v/v/v). Organisms were grown at 22 °C ± 2 °C under continuous light (cool white fluorescent tubes, 3000 lux) and aerated with sterilized air by passing through 0.22 µm filter (Labicom, Olomouc, Czech Republic).

2.3. Biomass extract preparation

Biomasses produced by cyanobacterial cultures were collected by the centrifugation (2880g, 10 min, 25 °C) and freeze-dried. 500 mg of lyophilized biomasses were reconstituted in 100 mL of 50% methanol and sonicated on ice (Bandelin Sonopuls HD2070, Berlin, Germany). After sonication samples were centrifuged (2880g, 10 min, and 25 °C), supernatants were collected, freeze-dried reconstituted in 0.5 mL of 50% methanol to reach concentration 1000 mg d.w. mL⁻¹ and sonicated on ice.

2.4. Cell culture

The WB-F344 rat liver epithelial cell line was originally isolated by Drs. J.W. Grisham and M.S. Tsao of the University of North Carolina (Chapel Hill, NC) (Tsao et al., 1984). Cells were grown in DMEM/Haŕns F-12 with L-Glutamine supplemented with 5% fetal bovine serum (PAA, Pasching, Austria). Cells were cultured in 24-well microplates (TPP, Trasadingen, Switzerland) at 37 °C in a humidified atmosphere containing 5% CO₂ and 95% air. Bioassays were conducted with confluent cultures obtained after 2–3 d of growth.

2.5. Experimental design

Interactions of mixtures cyanobacterial samples or cyanotoxins with model anthropogenic contaminants (FLU and PCB 153) were evaluated by using GJIC *in vitro* assay in several experimental settings in order to characterize:

- (1) Concentration-dependent effects of individual chemicals (PCB 153, FLU, MC-LR or CYN) or cyanobacterial extracts (*A. gracile* or *C. raciborskii*) on GJIC after 30 min exposure.
- (2) Effects of binary mixtures of PCB 153 (5, 10, 30 µM) or FLU (20, 30, 40 µM) and pure cyanotoxins (100 µM MC-LR or 60 µM CYN) on GJIC after 30 min exposure.
- (3) Effects of binary mixtures of PCB 153 (10, 20 and 30 µM) or FLU (30, 40 and 60 µM) with cyanobacterial extracts of *A. gracile* or *C. raciborskii* (1, 2 and 3 mg d.w. mL⁻¹) on GJIC after 30 min exposure
- (4) Effects of single compounds, cyanobacterial extract or their binary mixtures (FLU or PCB 153 mixed with *A. gracile* extract) on GJIC after prolonged exposures (1 h, 6 h and 24 h).

Cyanobacterial strains used in this study were selected because of their common occurrence in cyanobacterial water blooms and their potent inhibitory effects on GJIC demonstrated in previous studies (Blaha et al., 2010; Novakova et al., 2011). These strains were also reported to produce neither MCs nor CYN (Novakova et al., 2011; Stepankova et al., 2011), which was further confirmed in our study by HPLC-DAD and LC-MS analyses (method limit of detection was 5 µg g d.w.⁻¹ for MCs and 10 ng g d.w.⁻¹ for CYN, data not shown). The absence of MCs and CYN production allowed to study unknown tumor promoting compounds in binary mixture experiments with controlled dosing of other cyanotoxins or anthropogenic contaminants previously linked to cancer. In order to recognize eventual additive, synergistic or antagonistic effects, concentrations of chemicals or extracts inducing none or only

partial inhibition of GJIC (to 20–80% of the solvent control) were included in the design of binary mixture experiments. Exposure durations (30 min–24 h) reflected previous studies with different GJIC inhibiting compounds in WB-F344 cells (Weis et al., 1998; Blaha et al., 2002, 2010; Machala et al., 2003).

2.6. Gap-junctional intercellular communication (GJIC) assay

The scrape loading-dye transfer (SL-DT) technique was adapted after the method of (Elfouly et al., 1987). The test samples were added directly to the cell culture medium from concentrated stock solutions. Appropriate solvent controls (0.25% methanol, v/v, in the case of cyanobacterial extracts) were run in each experiment and did not induce responses significantly different from non-treated control. After the exposure, cells were washed with phosphate buffered saline (PBS) followed by the addition of 1 mg mL⁻¹ of lucifer yellow dissolved in PBS. The dye was introduced into the cells with five scrapes through the monolayer of confluent cells using a surgical steel scalpel blade. The transfer of dye through gap junction channels was allowed for 3 min, followed by a thorough rinse of cells with PBS to remove extracellular dye, and then fixation with a 4% formaldehyde solution in PBS. Migration of the dye in the cells was observed at 200-times magnification using a Zeiss OBSERVER.Z1 epifluorescence microscope equipped with an AxioCam HRC camera (Zeiss) and the images were acquired by AxioVision image analysis software. The fluorescence area of the dye migration from the scrape line was quantified using image analysis program created by Zdeněk Kuna and based on MATLAB software. Each SL-DT experiment was performed at least three times independently.

2.7. Data analysis and statistics

The results were expressed as fraction of the solvent control. Combined data from at least three independent experiments were evaluated by one-way ANOVA followed by Dunnett's post hoc test comparing experimental treatments with the corresponding solvent control. Effects of binary mixtures were predicted from the effect of individual compounds or extracts using the simple effect-addition model (Andersen et al., 2009). Predicted and observed effects were then compared by Student's *t*-test. *P* values less than 0.05 were considered statistically significant.

3. Results

Concentration–response curves for 30 min exposure were obtained for individual organic contaminants and cyanobacterial extracts in SL-DT assay (Fig. 1). GJIC was completely or almost completely inhibited after 30 min exposure to >20 μM PCB 153, >60 μM FLU, >2.5 mg d.w. mL⁻¹ of *A. gracile* or *C. raciborskii* extract. The tested concentration range of MC-LR (≤100 μM) or CYN (≤60 μM) did not affect GJIC after 30 min exposure.

The effects of tested chemicals and extracts on GJIC were further studied in binary mixture experiments. Neither pure MC-LR (100 μM) nor CYN (60 μM) modulated inhibition of GJIC caused by 30 min exposure to PCB 153 (5–30 μM) or FLU (20–40 μM), and there were no significant differences (one-way ANOVA, *P* < 0.05) between effects of binary mixtures and treatments with PCB 153 or FLU alone (Fig. 2). Simultaneous exposure to PCB 153 (10 μM) and FLU (30–60 μM) induced clearly additive response (Fig. 3A), as indicated by no significant difference (Student's *t*-test, *P* < 0.05) between observed GJIC inhibition and values predicted by the effect-addition model. Similarly, binary mixtures of *A. gracile* (1 mg d.w. mL⁻¹) and *C. raciborskii* extract (1–3 mg d.w. mL⁻¹) caused additive inhibition of GJIC (Fig. 3B).

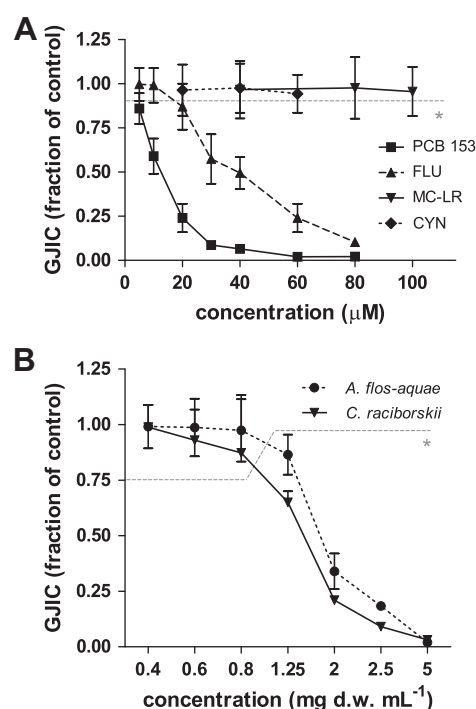


Fig. 1. Gap-junctional intercellular communication (GJIC) in WB-F344 cells after 30 min exposure to individual chemicals or extracts: (A) fluoranthene, PCB 153, microcystin-LR and cylindrospermopsin and (B) cyanobacterial extracts of *A. gracile* and *C. raciborskii*. FLU = fluoranthene, MC-LR = microcystin-LR, CYN = cylindrospermopsin. Data are means ± standard deviations of independent experiments. *Values below gray dashed line were significantly different from solvent control (ANOVA followed by Dunnett's post hoc test, *P* < 0.05).

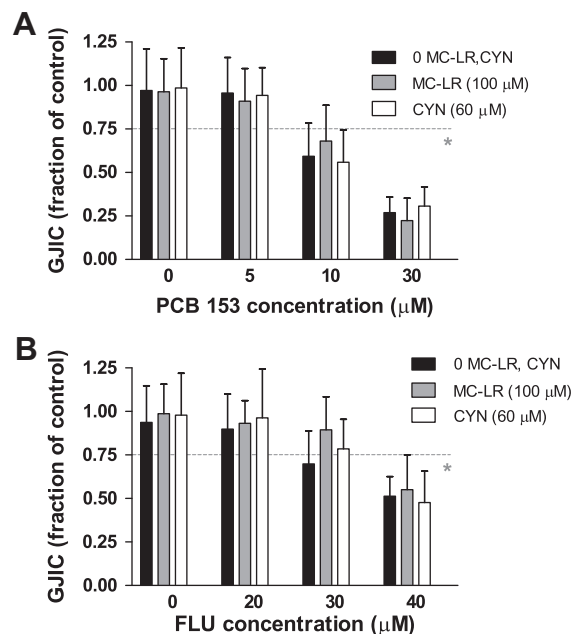


Fig. 2. Gap-junctional intercellular communication (GJIC) in WB-F344 cells after exposure to binary mixtures of anthropogenic contaminants and cyanotoxins: (A) PCB 153 (5–30 μM) and microcystin-LR or cylindrospermopsin and (B) fluoranthene (20–40 μM) and microcystin-LR or cylindrospermopsin. FLU = fluoranthene, MC-LR = microcystin-LR, CYN = cylindrospermopsin. Data are means ± standard deviations of independent experiments. *Values below grey dashed line were significantly different from solvent control (ANOVA followed by Dunnett's post hoc test, *P* < 0.05).

However, exposure of WB-F344 cells to PCB 153 or FLU in mixture with cyanobacterial extract of *A. gracile* or *C. raciborskii*

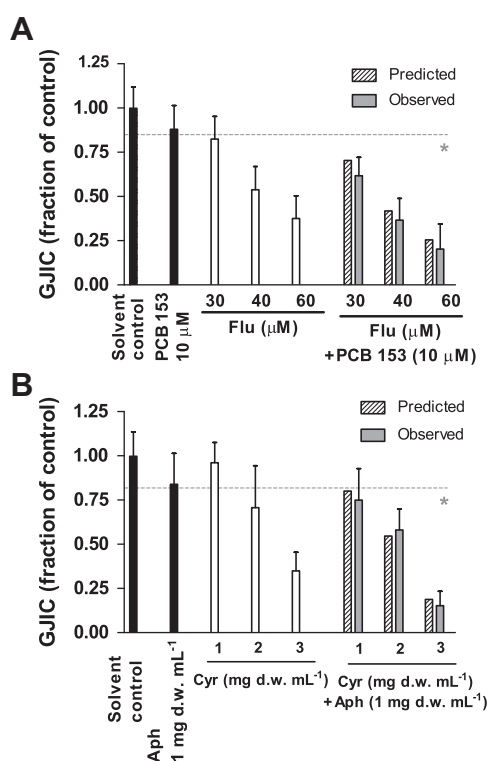


Fig. 3. Gap-junctional intercellular communication (GJIC) in WB-F344 cells after 30 min exposure to binary mixtures of anthropogenic contaminants and cyanobacterial extracts: (A) binary mixture of fluoranthene (30–60 μM) and PCB 153 (10 μM) and (B) binary mixture of cyanobacterial extracts of *A. gracile* (1 mg d.w. mL⁻¹) and *C. raciborskii* (1–3 mg d.w. mL⁻¹). FLU = fluoranthene, MC-LR = microcystin-LR, CYN = cylindrospermopsin, Aph = *A. gracile* extract, Cyr = *C. raciborskii* extract. "Predicted"- predicted additive effects of binary mixtures calculated by simple effect-additive model; "Observed"- observed effects of binary mixtures. Data are means \pm standard deviations of independent experiments. *Values below grey dashed line were significantly different from solvent control (ANOVA followed by Dunnett's post hoc test, $P < 0.05$).

resulted in a significant synergistic effect on GJIC. The observed levels of GJIC communication were significantly lower than values predicted from the effect-addition model in all tested combinations, i.e. PCB 153 + *A. gracile* (Fig. 4A), PCB 153 + *C. raciborskii* (Fig. 4B), FLU + *A. gracile* (Fig. 4C) and FLU + *C. raciborskii* (Fig. 4D). The strong synergism is illustrated by the fact that concentrations of PCB 153, FLU or cyanobacterial extracts not inhibiting GJIC when added to the cells separately (10 μM , 30 μM or 1 mg d.w. mL⁻¹, respectively) induced complete or nearly complete inhibition in the cells exposed to these concentrations of anthropogenic contaminants and cyanobacterial extracts in binary mixtures.

Inhibition of GJIC induced by PCB 153, FLU, extract of *A. gracile* and *C. raciborskii*, and binary mixtures of anthropogenic contaminants and cyanobacterial extracts was examined also after prolonged exposures (1, 6 and 24 h). Whereas GJIC remained inhibited by PCB 153 (30 μM) throughout 24 h of exposure, the inhibitory effects of FLU (40 μM) and both cyanobacterial extracts (2.5 mg d.w. mL⁻¹) decreased with the increasing exposure time (Fig. 5), which indicates a transient character of GJIC inhibition induced by FLU and cyanobacterial extracts. After 6 h incubation with FLU or cyanobacterial extracts, the extent of GJIC was similar to the GJIC level in the control, although a partial downregulation of GJIC was observed in the cells exposed to cyanobacterial extracts for 24 h.

Prolonged exposure to mixtures of *A. gracile* extract (2 mg d.w. mL⁻¹) and PCB 153 (10–30 μM) or FLU (20–60 μM) also

resulted in strong synergistic effects (Fig. 6). Most notably, neither cyanobacterial extract (2 mg d.w. mL⁻¹) nor PCB 153 (10 μM) downregulated GJIC after 6 or 24 h when tested separately, whereas their binary mixture caused significant inhibition of GJIC (Fig. 6A). Similarly, rapid inhibition of GJIC induced by FLU (60 μM) or *A. gracile* extract (2 mg d.w. mL⁻¹) was observed (Fig. 1), but the communication restored when the exposure to FLU or cyanobacterial extract continued for 6 or 24 h (Figs. 5 and 6B). However, no such recovery of GJIC was observed when the cells were exposed to 60 μM Flu and 2 mg d.w. mL⁻¹ *A. gracile* simultaneously (Fig. 6B).

4. Discussion

Many environmental contaminants have been implicated in chemical carcinogenesis and associated with cancer in laboratory and epidemiological studies, including several representatives of PCBs and PAHs, mixtures containing these chemicals and also related exposures (Straif et al., 2005; Baan et al., 2009). Considerable research effort focused on specific mechanisms of carcinogenic or tumor promoting properties of PCBs and PAHs. Alteration of aryl hydrocarbon receptor (AhR)-dependent signaling by coplanar PCBs (Van den Berg et al., 2006), and genotoxicity of some PAHs (Xue and Warshawsky, 2005) have been recognized as the important mechanisms responsible for their carcinogenic effects (Baan et al., 2009). However, toxicity and tumor promoting activity have been reported also for non-coplanar PCBs with no AhR binding activity, such as PCB 153 (Knerer and Schrenk, 2006; Brown et al., 2007; Glauert et al., 2008;). Similarly, tumorigenicity of FLU was demonstrated in rodents (Busby et al., 1984; Wang and Busby, 1993; Lavoie et al., 1994), although FLU is not genotoxic *in vivo* (Stocker et al., 1996) or in human cell line *in vitro* (Durant et al., 1996). These data suggest that mechanisms other than "dioxin-like" toxicity and genotoxicity may contribute to cancer development induced by different PCBs, PAHs and their mixtures. Interestingly, both PCB 153 and FLU have been recently shown to induce *in vitro* inhibition of GJIC in WB-F344 cell line (Weis et al., 1998; Blaha et al., 2002; Machala et al., 2003), indicating that inhibition of GJIC could be involved in tumor promotional or carcinogenic effects of PCBs and PAHs, including those with low AhR-binding activity or genotoxicity.

PCB 153 and FLU were therefore selected as toxicologically relevant environmental contaminants for our study evaluating their mixture-effects on GJIC in WB-F344 cell line.

Various types of cancers have also been associated with another group of toxic compounds – cyanobacterial metabolites (Svircev et al., 2010; Zegura et al., 2011). Recently, we have shown that natural metabolites present in the cell extracts and extracellular material of toxic bloom-forming cyanobacteria also modulate GJIC, and the effects were not related to known toxins such as MCs or CYN (Blaha et al., 2010; Novakova et al., 2011). So far, modulations of GJIC have been studied only by isolated compounds from different groups (i.e. PAHs or PCBs or cyanobacteria) but their widespread occurrence and also the potential of cyanobacterial blooms to accumulate anthropogenic contaminants (Koelmans et al., 1995; Al-Hasan et al., 2001) motivated the present work, which investigated the hypothesis about mixture effects of different compounds on GJIC.

Since most cancers (>85%) are derived from epithelial tissue cells (Cancer Research UK), and connexin43 is a common gap junctional protein expressed in epithelium (Laird, 2006), the employed rat liver epithelial cells WB-F344 expressing connexin43 represent relevant *in vitro* model system for studying connexin43-dependent mechanisms of tumor promotion and cancer. Moreover, WB-F344 cells possess characteristics of liver oval cells (Couchie et al.,

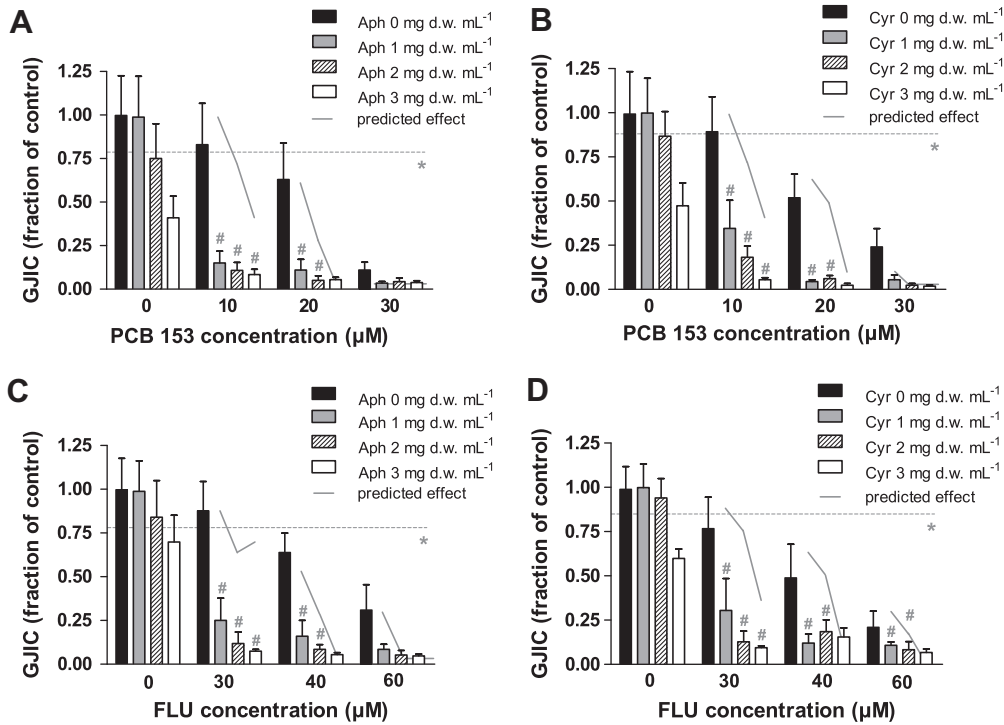


Fig. 4. Gap-junctional intercellular communication (GJIC) in WB-F344 cells after 30 min exposure to binary mixtures: (A) PCB 153 (10–30 μM) with *A. gracile* extract (1–3 mg d.w. mL^{-1}), (B) PCB 153 (10–30 μM) with *C. raciborskii* extract (1–3 mg d.w. mL^{-1}), (C) fluoranthene (30–60 μM) with *A. gracile* extract (1–3 mg d.w. mL^{-1}), and (D) fluoranthene (30–60 μM) with *C. raciborskii* extract (1–3 mg d.w. mL^{-1}). FLU = fluoranthene, Aph = *A. gracile* extract, Cyr = *C. raciborskii* extract. Solid grey lines express predicted effects calculated according to effect–additive model. Data are means \pm standard deviations of independent experiments. *Values below grey dashed line were significantly different from solvent control (ANOVA followed by Dunnett's post hoc test, $P < 0.05$). # Indicates values significantly different from the effect-addition model (Student's *t*-test, $P < 0.05$).

2002) whose increased proliferation has been associated with diseased states that lead to cancer not only in rodents but also in humans (Roskams et al., 1998; Lowes et al., 1999). It has been demonstrated that tumor promoters known to inhibit GJIC in WB-F344 cell line also inhibited GJIC in rodents *in vivo*: PCBs (Krutovskikh et al., 1995; Kolaja et al., 2000), DDT (Krutovskikh et al., 1995), pentachlorophenol (Sai et al., 2000), cadmium (Jeong et al., 2000) and perfluorooctanoic acid (Upham et al., 2009). These studies indicate that *in vitro* evaluation of GJIC in WB-F344 cell line is a

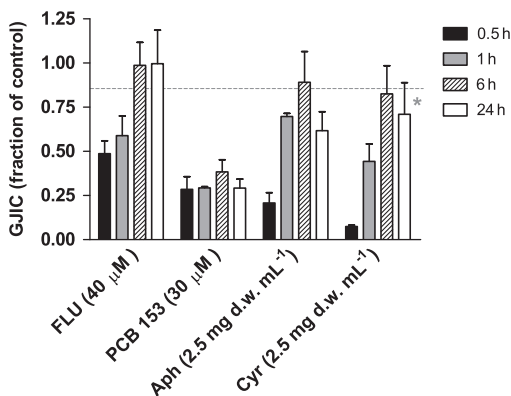


Fig. 5. Effects on gap-junctional intercellular communication (GJIC) in WB-F344 cells of individual chemicals or extracts in time-course experiment (0.5, 1, 6 and 24 h). FLU = fluoranthene, Aph = *A. gracile* extract, Cyr = *C. raciborskii* extract. Data are means \pm standard deviations of independent experiments. *Values below grey dashed line were significantly different from solvent control (ANOVA followed by Dunnett's post hoc test, $P < 0.05$).

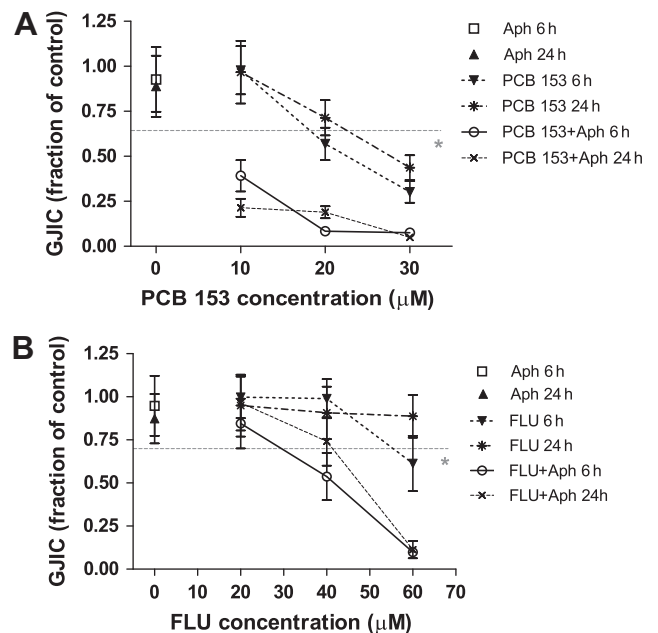


Fig. 6. Gap-junctional intercellular communication (GJIC) in WB-F344 cells after 6 h and 24 h exposure to binary mixtures of anthropogenic contaminants and cyanobacterial extracts: (A) binary mixture of PCB 153 (10–30 μM) and *A. gracile* extract (2 mg d.w. mL^{-1}) and (B) binary mixture of fluoranthene (20–60 μM) and *A. gracile* extract (2 mg d.w. mL^{-1}). FLU = fluoranthene, Aph = *A. gracile* extract, Cyr = *C. raciborskii* extract. Data are means \pm standard deviations of independent experiments. *Values below grey dashed line were significantly different from solvent control (ANOVA followed by Dunnett's post hoc test, $P < 0.05$).

relevant assay for predicting *in vivo* effects of chemicals on gap junctions and tumor promoting effects in the liver tissues of rodents (Upham et al., 2009).

Our study confirmed the original findings on GJIC-inhibiting activity of PCB 153 and FLU (Weis et al., 1998; Blaha et al., 2002; Machala et al., 2003), and provided novel information on the additivity of inhibitory effects of these chemicals. The additive character of the effects suggest that both PCB 153 and FLU downregulate GJIC via similar mechanism, by affecting the same molecular targets. This hypothesis is further supported by similarities in the response of WB-F344 cells to PCB 153 and 1-methylanthracene, another PAH which shares with FLU specific structural features (presence of the bay/bay-like region) and most likely also a mechanism of GJIC inhibition (Weis et al., 1998). Both PCB 153 and 1-methylanthracene not only inhibit GJIC, but also activate MAPKs ERK1/2 and induce release of arachidonic acid (Machala et al., 2003; Umannova et al., 2008; Upham et al., 2008). Moreover, inhibition of GJIC induced by PCB 153 and 1-methylanthracene is prevented by D609, an inhibitor of phosphatidylcholine-specific phospholipase C (PC-PLC), and by H89, a protein kinase A (PKA) inhibitor (Machala et al., 2003; Upham et al., 2008). These data, supported by the additivity of effects observed in the present study, suggest that PCB 153 and PAHs might downregulate GJIC by a common mechanism involving activation of PC-PLC and/or PKA. However, PCB 153 and FLU differed in the time-course of GJIC inhibition. Although GJIC remained inhibited in the presence of PCB 153 throughout the 24 h exposure, the inhibitory effect of FLU occurring after 30 min exposure became less pronounced with increasing exposure time and nearly normal communication was restored after 6 h. Differences in biotransformation kinetic of PCB 153 and FLU or different toxicities of biotransformation products of the two chemicals, are possible explanations which should be addressed by future research.

Consumption of drinking water contaminated with cyanobacterial toxins has been linked to increased prevalence of liver and colorectal cancer (Svircev et al., 2010; Zegura et al., 2011). MC-LR is recognized tumor promoter known to inhibit eukaryotic protein serine/threonine phosphatases PP1 and PP2A, induce oxidative DNA damage, alter cellular signaling and processes involved in regulation of cell cycle, DNA repair, apoptosis, and promote *in vivo* growth of tumors (Svircev et al., 2010). CYN is another prominent cyanotoxin, whose possible carcinogenic effects have been indicated. CYN is irreversible inhibitor of proteosynthesis, induces genotoxic effects *in vitro* and *in vivo* and there is a preliminary evidence for its *in vivo* tumor initiating effects (Zegura et al., 2011). However, a number of studies clearly demonstrated that toxicity of cyanobacterial extracts cannot be always attributed to the known cyanotoxins and that other bioactive compounds from cyanobacteria may be responsible for some observed effects (Falconer, 2007). These effects include also rapid inhibition of GJIC and activation of MAPK ERK1/2 in WB-F344 cells induced by various cyanobacterial extracts regardless microcystin or cylindrospermopsin content (Blaha et al., 2010; Novakova et al., 2011). In the present study, neither MC-LR nor CYN inhibited GJIC in WB-F344 after 30 min exposure, and the lack of effects was further demonstrated in experiments with binary mixtures, where toxins did not modulate inhibitory effects of anthropogenic contaminants PCB 153 or FLU. No observable effects on GJIC attributable to MC-LR and CYN might be simply a consequence of GJIC not being a cellular and molecular target for these cyanotoxins. However, the absence of effects in WB-F344 cells could also be a result of the limited cellular uptake of microcystin, which strongly depends on the expression of respective organic anion transport proteins (Fischer et al., 2010). Similarly, recent study reported that also cylindrospermopsin uptake might be limited in some cell lines resulting in their lower sensitivity to the toxin (Froschio et al., 2009).

Although pure cyanotoxins did not affect GJIC, the extracts of *A. gracile* and *C. raciborskii* inhibited GJIC in concentration-dependent manner, with effective concentrations similar to those previously reported for several laboratory cultures of cyanobacteria *Anabaena flos-aquae*, *Aphanizomenon flos-aquae*, *Microcystis aeruginosa* or *Planktothrix agardhii* (Blaha et al., 2010; Novakova et al., 2011). The concentrations of cyanobacterial extracts or cyanotoxins applied in our study were in similar range (mg d.w. mL⁻¹ or micromolar) as effective concentrations reported for various evaluated endpoints in several *in vitro* studies with different permanent cell lines (Stepankova et al., 2011; Zegura et al., 2011). The absence of detectable amounts of MC-LR or CYN in the extracts investigated in the present study further supports findings that these cyanotoxins are less important toxic agent with respect to GJIC, and that unknown metabolites might alter either different cell populations or molecular mechanisms than MC-LR or CYN and contribute to tumor promotion.

The effects of cyanobacteria on GJIC were additive when the cells were exposed to the extracts of *A. gracile* and *C. raciborskii* simultaneously, similarly to the binary mixtures of PCB 153 and FLU. It may indicate that both extracts inhibited GJIC via the same mechanism and possibly that the same compound(s) were responsible for the inhibitory activity of both extracts. Isolation and characterization of these compound(s) as well as identification of their mode of action need to be addressed by future research.

The most remarkable result of our study is the effect of anthropogenic contaminants in binary mixtures with cyanobacterial extracts, where strong synergistic effects on GJIC were observed in all tested combinations and exposure times. Mixture toxicity of various environmental contaminants is being intensively studied, but most studies are dealing with mixtures of chemicals sharing some general similarity or mechanism of action, whereas experiments with mixtures containing widely divergent components (e.g., organics vs. metals) or chemicals in a combination with non-chemical stressors are much less common (McCarty and Borgert, 2006a). Interestingly, synergistic effects have been reported for mixtures of PAHs and metals (Feng et al., 2003; Lau and Chiu, 2006; Fleeger et al., 2007; Silva et al., 2009), PAHs and PCBs (Wassenberg and Di Giulio, 2004), PCBs and organometals (Jensen et al., 2000; Andersen et al., 2009) or PCBs and various endocrine disruptors (Benachour et al., 2007). Recent studies also demonstrated synergistic effects among various cyanobacterial metabolites such as portoamide A and B (Leao et al., 2010), lobocyclamides A and B (MacMillan et al., 2002) or laxaphycins A and B (Bonnard et al., 2007), but mixture effects of toxic cyanobacteria or cyanotoxins and other environmental contaminants have been so far only rarely investigated. A recent *in vivo* study with Japanese quails showed synergistic toxicity between toxic cyanobacterium *Microcystis*, heavy metal – lead, and viral infection (Pikula et al., 2010). Potentiation of effects of toxic cyanobacterium *Microcystis* and pesticide carbaryl in daphnids has been also reported (Cerbin et al., 2010). Our study thus provides additional evidence on specific toxic interactions between cyanobacterial metabolites and environmental anthropogenic contaminants. It should be noted that both cyanobacterial extracts were complex mixtures of cyanobacterial metabolites and we cannot neglect potential interferences and interactions among the components of these original samples. Nevertheless, clear potentiation of GJIC inhibition observed in mixtures of anthropogenic contaminants (PCB 153 or FLU) and toxic cyanobacteria highlight the importance of studying effects of complex samples, which correspond to naturally occurring situation. The inhibition of GJIC independent of the content of MC-LR and CYN further suggests an existence of unknown cyanobacterial metabolites with tumor promoting activity, which may act synergistically with recognized environmental tumor promoters and toxins.

Acknowledgements

This work was supported by the Czech Science Foundation (GACR 524/08/0496), by the CETOCOEN Project from the European Regional Development Fund (Z.1.05/2.1.00/01.0001), and by the SoMoPro Project No. 2SGA2858 (funded from the European Community within the Seventh Framework Programme (FP/2007–2013) under the Grant Agreement No. 229603 and co-funded by the South Moravian Region).

References

- Al-Hasan, R.H., Khanafer, M., Eliyas, M., Radwan, S.S., 2001. Hydrocarbon accumulation by picocyanobacteria from the Arabian Gulf. *J. Appl. Microbiol.* 91, 533–540.
- Andersen, I.S., Voie, O.A., Fonnum, F., Mariussen, E., 2009. Effects of methyl mercury in combination with polychlorinated biphenyls and brominated flame retardants on the uptake of glutamate in rat brain synaptosomes: a mathematical approach for the study of mixtures. *Toxicol. Sci.* 112, 175–184.
- Baan, R., Grosse, Y., Straif, K., Secretan, B., El Ghissassi, F., Bouvard, V., Benbrahim-Tallaa, L., Guha, N., Freeman, C., Galichet, L., Coglian, V., 2009. Special report: policy a review of human carcinogens – Part F: chemical agents and related occupations. *Lancet Oncol.* 10, 1143–1144.
- Benachour, N., Moslemi, S., Sipahutar, H., Serralini, G.E., 2007. Cytotoxic effects and aromatase inhibition by xenobiotic endocrine disruptors alone and in combination. *Toxicol. Appl. Pharmacol.* 222, 129–140.
- Blaha, L., Babica, P., Hilscherova, K., Upham, B.L., 2010. Inhibition of gap-junctional intercellular communication and activation of mitogen-activated protein kinases by cyanobacterial extracts – Indications of novel tumor-promoting cyanotoxins? *Toxicol. Sci.* 116, 126–134.
- Blaha, L., Kapplova, P., Vondracek, J., Upham, B., Machala, M., 2002. Inhibition of gap-junctional intercellular communication by environmentally occurring polycyclic aromatic hydrocarbons. *Toxicol. Sci.* 65, 43–51.
- Bonnard, I., Rolland, M., Salmon, J.M., Debiton, E., Barthomeuf, C., Banaigs, B., 2007. Total structure and inhibition of tumor cell proliferation of laxaphycins. *J. Med. Chem.* 50, 1266–1279.
- Brown, J.F., Mayes, B.A., Silkworth, J.B., Hamilton, S.B., 2007. Polychlorinated biphenyls-modulated tumorigenesis in Sprague-Dawley rats: correlation with mixed function oxidase activities and superoxide (O₂⁻(center dot-)) formation potentials and implied mode of action. *Toxicol. Sci.* 98, 375–394.
- Busby, W.F., Goldman, M.E., Newberne, P.M., Wogan, G.N., 1984. Tumorigenicity of fluoranthene in a newborn mouse lung adenoma bioassay. *Carcinogenesis* 5, 1311–1316.
- Cerbin, S., Kraak, M.H.S., de Voogt, P., Visser, P.M., Van Donk, E., 2010. Combined and single effects of pesticide carbaryl and toxic *Microcystis aeruginosa* on the life history of *Daphnia pulex*. *Hydrobiologia* 643, 129–138.
- Cancer Research UK, 2011. Types of Cells and Cancer. <<http://www.cancerhelp.cancerresearchuk.org/about-cancer/what-is-cancer/cells/types-of-cells-and-cancer>> (accessed 16.01.12).
- Couchie, D., Holic, N., Chobert, M.N., Corlu, A., Laperche, Y., 2002. In vitro differentiation of WB-F344 rat liver epithelial cells into the biliary lineage. *Differentiation* 69, 209–215.
- Durant, J.L., Busby, W.F., Lafleur, A.L., Penman, B.W., Crespi, C.L., 1996. Human cell mutagenicity of oxygenated, nitrated and unsubstituted polycyclic aromatic hydrocarbons associated with urban aerosols. *Mutat. Res.* 371, 123–157.
- Elfouly, M.H., Trosko, J.E., Chang, C.C., 1987. Scrape-loading and dye transfer – a rapid and simple technique to study gap junctional intercellular communication. *Exp. Cell Biol.* 168, 422–430.
- Falconer, I.R., 2007. Cyanobacterial toxins present in *Microcystis aeruginosa* extracts – more than microcystins! *Toxicol. Sci.* 100, 585–588.
- Feng, Z.H., Hu, W.W., Rom, W.N., Costa, M., Tang, M.S., 2003. Chromium(VI) exposure enhances polycyclic aromatic hydrocarbon-DNA binding at the p53 gene in human lung cells. *Carcinogenesis* 24, 771–778.
- Fischer, A., Hoeger, S.J., Stemmer, K., Feurstein, D.J., Knobeloch, D., Nussler, A., Dietrich, D.R., 2010. The role of organic anion transporting polypeptides (OATPs/SLCOs) in the toxicity of different microcystin congeners in vitro: a comparison of primary human hepatocytes and OATP-transfected HEK293 cells. *Toxicol. Appl. Pharmacol.* 245, 9–20.
- Fleeger, J.W., Gust, K.A., Marlborough, S.J., Tita, G., 2007. Mixtures of metals and polynuclear aromatic hydrocarbons elicit complex, nonadditive toxicological interactions in meiobenthic copepods. *Environ. Toxicol. Chem.* 26, 1677–1685.
- Frosio, S.M., Cannon, E., Lau, H.M., Humpage, A.R., 2009. Limited uptake of the cyanobacterial toxin cylindrospermopsin by Vero cells. *Toxicol. Sci.* 110, 862–868.
- Glauert, H.P., Tharappel, J.C., Lu, Z., Stemm, D., Banerjee, S., Chan, L.S., Lee, E.Y., Lehmler, H.J., Robertson, L.W., Spear, B.T., 2008. Role of oxidative stress in the promoting activities of PCBs. *Environ. Toxicol. Pharm.* 25, 247–250.
- Hernandez, L.G., van Steeg, H., Luijten, M., van Benthem, J., 2009. Mechanisms of non-genotoxic carcinogens and importance of a weight of evidence approach. *Mutat. Res.* 682, 94–109.
- Jensen, K.G., Wiberg, K., Klasson-Wehler, E., Onfelt, A., 2000. Induction of aberrant mitosis with PCBs: particular efficiency of 2,3,3',4,4'-pentachlorobiphenyl and synergism with triphenyltin. *Mutagenesis* 15, 9–15.
- Jeong, S.H., Habeebu, S.S.M., Klaassen, C.D., 2000. Cadmium decreases gap junctional intercellular communication in mouse liver. *Toxicol. Sci.* 57, 156–166.
- Kner, S., Schrenk, D., 2006. Carcinogenicity of “non-dioxinlike” polychlorinated biphenyls. *Crit. Rev. Toxicol.* 36, 663–694.
- Koelmans, A.A., Anzion, S.P.M., Lijklema, L., 1995. Dynamics of organic micropollutant biosorption to cyanobacteria and detritus. *Environ. Sci. Technol.* 29, 933–940.
- Kolaja, K.L., Engelken, D.T., Klaassen, C.D., 2000. Inhibition of gap-junctional intercellular communication in intact rat liver by nongenotoxic hepatocarcinogens. *Toxicology* 146, 15–22.
- Krutovskikh, V.A., Mesnil, M., Mazzoleni, G., Yamasaki, H., 1995. Inhibition of rat-liver gap junction intercellular communication by tumor-promoting agents in vivo – Association with aberrant localization of connexin proteins. *Lab. Invest.* 72, 571–577.
- Laird, D.W., 2006. Life cycle of connexins in health and disease. *Biochem. J.* 394, 527–543.
- Lau, A.T.Y., Chiu, J.F., 2006. Proteomic and biochemical analyses of in vitro carcinogen-induced lung cell transformation: synergism between arsenic and benzo[a]pyrene. *Proteomics* 6, 1619–1630.
- Lavoie, E.J., Cai, Z.W., Meschter, C.L., Weyand, E.H., 1994. Tumorigenic activity of fluoranthene, 2-methylfluoranthene and 3-methylfluoranthene in newborn Cd-1 mice. *Carcinogenesis* 15, 2131–2135.
- Leao, P.N., Pereira, A.R., Liu, W.T., Ng, J., Pevzner, P.A., Dorrestein, P.C., König, G.M., Vasconcelos, V.M., Gerwick, W.H., 2010. Synergistic allelochemicals from a freshwater cyanobacterium. *Proc. Natl. Acad. Sci. USA* 107, 11183–11188.
- Lowes, K.N., Brennan, B.A., Yeoh, G.C., Olynyk, J.K., 1999. Oval cell numbers in human chronic liver diseases are directly related to disease severity. *Am. J. Pathol.* 154, 537–541.
- Machala, M., Blaha, L., Vondracek, J., Trosko, J.E., Scott, J., Upham, B.L., 2003. Inhibition of gap junctional intercellular communication by noncoplanar polychlorinated biphenyls: Inhibitory potencies and screening for potential mode(s) of action. *Toxicol. Sci.* 76, 102–111.
- MacMillan, J.B., Ernst-Russell, M.A., de Ropp, J.S., Molinski, T.F., 2002. Lobocyclamides A–C, lipopeptides from a cryptic cyanobacterial mat containing *Lyngbya confervoides*. *J. Org. Chem.* 67, 8210–8215.
- McCarty, L.S., Borgert, C.J., 2006a. Review of the toxicity of chemical mixtures containing at least one organochlorine. *Regul. Toxicol. Pharmacol.* 45, 104–118.
- McCarty, L.S., Borgert, C.J., 2006b. Review of the toxicity of chemical mixtures: theory, policy, and regulatory practice. *Regul. Toxicol. Pharmacol.* 45, 119–143.
- Novakova, K., Babica, P., Adamovsky, O., Blaha, L., 2011. Modulation of gap-junctional intercellular communication by a series of cyanobacterial samples from nature and laboratory cultures. *Toxicol. Sci.* 116, 76–84.
- Pikula, J., Bandouchova, H., Hilscherova, K., Paskova, V., Sedlackova, J., Adamovsky, O., Knotkova, Z., Lany, P., Machat, J., Marsalek, B., Novotny, L., Pohanka, M., Vitula, F., 2010. Combined exposure to cyanobacterial biomass, lead and the Newcastle virus enhances avian toxicity. *Sci. Total. Environ.* 408, 4984–4992.
- Rosenkranz, H.S., Pollack, N., Cunningham, A.R., 2000. Exploring the relationship between the inhibition of gap junctional intercellular communication and other biological phenomena. *Carcinogenesis* 21, 1007–1011.
- Roskams, T., De Vos, R., Van Eyken, P., Myazaki, H., Van Damme, B., Desmet, V., 1998. Hepatic OV-6 expression in human liver disease and rat experiments: evidence for hepatic progenitor cells in man. *J. Hepatol.* 29, 455–463.
- Sai, K., Kanno, J., Hasegawa, R., Trosko, J.E., Inoue, T., 2000. Prevention of the down-regulation of gap junctional intercellular communication by green tea in the liver of mice fed pentachlorophenol. *Carcinogenesis* 21, 1671–1676.
- Schlosser, U.G., 1994. Sag – Sammlung-Von-Algenkulturen at the University-of-Göttingen – Catalog of Strains 1994. *Bot. Acta* 107, 113–186.
- Silva, S.J., Carman, K.R., Fleeger, J.W., Marshall, T., Marlborough, S.J., 2009. Effects of phenanthrene- and metal-contaminated sediment on the feeding activity of the harpacticoid copepod, *Schizopera knabeni*. *Arch. Environ. Contam. Toxicol.* 56, 434–441.
- Stein, J., 1973. Handbook of Physiological methods. Culture methods and growth measurements. Cambridge University Press, Cambridge.
- Stepankova, T., Ambrozova, L., Blaha, L., Giesy, J.P., Hilscherova, K., 2011. In vitro modulation of intracellular receptor signaling and cytotoxicity induced by extracts of cyanobacteria, complex water blooms and their fractions. *Aquat. Toxicol.* 105 (3–4), 497–507.
- Stocker, K.J., Howard, W.R., Statham, J., Proudlock, R.J., 1996. Assessment of the potential in vivo genotoxicity of fluoranthene. *Mutagenesis* 11, 493–496.
- Straif, K., Baan, R., Grosse, Y., Secretan, B., El Ghissassi, F., Coglian, V., 2005. Carcinogenicity of polycyclic aromatic hydrocarbons. *Lancet Oncol.* 6, 931–932.
- Svircev, Z., Baltic, V., Gantar, M., Jukovic, M., Stojanovic, D., Baltic, M., 2010. Molecular aspects of microcystin-induced hepatotoxicity and hepatocarcinogenesis. *J. Environ. Sci. Health C Environ. Carcinog. Ecotoxicol. Rev.* 28, 39–59.
- Syberg, K., Jensen, T.S., Cedergreen, N., Rank, J., 2009. On the use of mixture toxicity assessment in reach and the water framework directive: a review. *Human Ecol. Risk Assess.* 15, 1257–1272.
- Trosko, J.E., 2007. Gap junctional intercellular communication as a biological “Rosetta stone” in understanding, in a systems biological manner, stem cell behavior, mechanisms of epigenetic toxicology, chemoprevention and chemotherapy. *J. Membr. Biol.* 218, 93–100.
- Tsao, M.S., Smith, J.D., Nelson, K.G., Grisham, J.W., 1984. A diploid epithelial-cell line from normal adult-rat liver with phenotypic properties of oval cells. *Exp. Cell Biol.* 154, 38–52.

- Umannova, L., Neca, J., Andryšik, Z., Vondracek, J., Upham, B.L., Trosko, J.E., Hofmanova, J., Kozubik, A., Machala, M., 2008. Non-dioxin-like polychlorinated biphenyls induce a release of arachidonic acid in liver epithelial cells: A partial role of cytosolic phospholipase A(2) and extracellular signal-regulated kinases 1/2 signalling. *Toxicology* 247, 55–60.
- Upham, B.L., Blaha, L., Babica, P., Park, J.S., Sovadinova, I., Pudrith, C., Rummel, A.M., Weis, L.M., Sai, K., Tithof, P.K., Guzvic, M., Vondracek, J., Machala, M., Trosko, J.E., 2008. Tumor promoting properties of a cigarette smoke prevalent polycyclic aromatic hydrocarbon as indicated by the inhibition of gap junctional intercellular communication via phosphatidylcholine-specific phospholipase C. *Cancer Sci.* 99, 696–705.
- Upham, B.L., Park, J.S., Babica, P., Sovadinova, I., Rummel, A.M., Trosko, J.E., Hirose, A., Hasegawa, R., Kanno, J., Sai, K., 2009. Structure-activity-dependent regulation of cell communication by perfluorinated fatty acids using in vivo and in vitro model systems. *Environ. Health Perspect.* 117, 545–551.
- van Apeldoorn, M.E., van Egmond, H.P., Speijers, G.J.A., Bakker, G.J.I., 2007. Toxins of cyanobacteria. *Mol. Nutr. Food Res.* 51, 7–60.
- Van den Berg, M., Birnbaum, L.S., Denison, M., De Vito, M., Farland, W., Feeley, M., Fiedler, H., Hakansson, H., Hanberg, A., Haws, L., Rose, M., Safe, S., Schrenk, D., Tohyama, C., Tritscher, A., Tuomisto, J., Tysklind, M., Walker, N., Peterson, R.E., 2006. The 2005 World Health Organization reevaluation of human and mammalian toxic equivalency factors for dioxins and dioxin-like compounds. *Toxicol. Sci.* 93, 223–241.
- Vineis, P., Schatzkin, A., Potter, J.D., 2010. Models of carcinogenesis: an overview. *Carcinogenesis* 31, 1703–1709.
- Vinken, M., Doktorova, T., Decrock, E., Leybaert, L., Vanhaecke, T., Rogiers, V., 2009. Gap junctional intercellular communication as a target for liver toxicity and carcinogenicity. *Crit. Rev. Biochem. Mol. Biol.* 44, 201–222.
- Wang, J.S., Busby, W.F., 1993. Induction of lung and liver-tumors by fluoranthene in a preweanling Cd-1 mouse bioassay. *Carcinogenesis* 14, 1871–1874.
- Wassenberg, D.M., Di Giulio, R.T., 2004. Synergistic embryotoxicity of polycyclic aromatic hydrocarbon aryl hydrocarbon receptor Agonists with cytochrome P4501A inhibitors in *Fundulus heteroclitus*. *Environ. Health Perspect.* 112, 1658–1664.
- Weis, L.M., Rummel, A.M., Masten, S.J., Trosko, J.E., Upham, B.L., 1998. Bay or baylike regions of polycyclic aromatic hydrocarbons were potent inhibitors of gap junctional intercellular communication. *Environ. Health Perspect.* 106, 17–22.
- Wogan, G.N., Hecht, S.S., Felton, J.S., Conney, A.H., Loeb, L.A., 2004. Environmental and chemical carcinogenesis. *Semin. Cancer Biol.* 14, 473–486.
- Xue, W.L., Warshawsky, D., 2005. Metabolic activation of polycyclic and heterocyclic aromatic hydrocarbons and DNA damage: a review. *Toxicol. Appl. Pharmacol.* 206, 73–93.
- Zegura, B., Straser, A., Filipic, M., 2011. Genotoxicity and potential carcinogenicity of cyanobacterial toxins – a review. *Mutat. Res.* 727, 16–41.
- Ziech, D., Franco, R., Pappa, A., Malamou-Mitsi, V., Georgakila, S., Georgakilas, A.G., Panayiotidis, M.I., 2010. The role of epigenetics in environmental and occupational carcinogenesis. *Chem. Biol. Interact.* 188, 340–349.

- XI.** Sovadinová, I.*, **Babica, P.**, Adamovský, O., Alpatova, A., Tarabara, V., Upham, B., Bláha, L., 2017. Chlorination and ozonation differentially reduced the microcystin content and tumour promoting activity of a complex cyanobacterial extract. *Advances in Oceanography and Limnology* 8, 107–120.

Chlorination and ozonation differentially reduced the microcystin content and tumour promoting activity of a complex cyanobacterial extract

Iva Sovadinová,^{1,2*} Pavel Babica,^{1,2,3} Ondřej Adamovský,^{1,2} Alla Alpatova,^{4,5} Volodymyr Tarabara,⁴ Brad Luther Upham,² Luděk Bláha¹

¹RECETOX - Research Centre for Toxic Compounds in the Environment, Faculty of Science, Masaryk University, Kamenice 753/5, 62500 Brno, Czech Republic; ²Department of Pediatrics and Human Development, and Institute for Integrative Toxicology, Michigan State University, 1129 Farm Lane, East Lansing, MI 48824, USA; ³Department of Experimental Phycology and Ecotoxicology, Institute of Botany, Czech Academy of Sciences, Lidická 25/27, 60200 Brno, Czech Republic; ⁴Department of Civil and Environmental Engineering, Michigan State University, 428 S. Shaw Lane, East Lansing, MI 48824, USA; ⁵Civil and Environmental Engineering, University of Alberta, AB T6G 2E1 Edmonton, Canada

*Corresponding author: sovadinova@recetox.muni.cz

ABSTRACT

Despite intensive research and management efforts in the past decades, cyanobacterial blooms and their toxins, such as microcystins (MCs), continue to represent a major ecological and health problem in fresh waters throughout the world. Our objective was to compare the efficacy of two commonly used drinking water treatment technologies, chlorination and ozonation, in removing MCs and in reducing tumour promotion-related effects of cyanobacteria, such as inhibition of gap junctional intercellular communication (GJIC) and activation of mitogen activated protein kinases (MAPKs) in a rat liver epithelial stem-like cell line (WB-F344). This combined chemical and bioassay approach demonstrated that ozone effectively removed all MCs from an extract of a globally important bloom-forming cyanobacterium, *Microcystis* sp. Ozone also significantly reduced the overall tumour promotional potency of the cyanobacterial extract, as indicated by a substantial reduction in the ability of the extract to inhibit GJIC and activate extracellular receptor kinase 1/2 (ERK1/2). Although comparable reduction of total organic carbon was achieved by ozone and chlorine treatment, chlorination was much less effective in removing MCs and reducing the effects on GJIC. Chlorination had a biphasic effect with an observed decrease of extract-induced activation of ERK1/2 at the lower chlorine doses; whereas at high doses of chlorine the by-products of chlorination actually induced the activation of ERK1/2. The extracts induced p38 activation, and chlorination was not effective in reversing this effect, while ozone did reverse this effect, albeit not as much as the activation of ERK1/2. Thus, ozone was effective in reducing the toxicity of cyanobacterial extracts while chlorination was not only lacking efficacy, but at high doses of chlorination further produced by-products that were equally toxic as the untreated samples. Our study indicates the value of using an effect-based approach to assess the efficacy of water treatment systems in removing toxins, and more specifically demonstrates that ozone was more effective at reducing the toxic potential of cyanobacterial-contaminated water.

Key words: Cyanobacteria; water treatment; toxicity; chlorination; ozonation; microcystin.

Received: 11 October 2016. **Accepted:** 14 February 2017.

INTRODUCTION

Despite intensive research identifying causes, consequences and possible preventive measures of cyanobacterial mass proliferations, cyanobacterial blooms represent a major problem in fresh waters throughout the world. The adverse consequences include water quality degradation, accumulation and microbial decay of bloom biomass followed by lowering of oxygen content in water (Wiegand and Pflugmacher, 2005). In addition, a wide spectrum of toxins and secondary metabolites produced by cyanobacteria have been shown to adversely affect aquatic organisms (Codd *et al.*, 2005; Zanchett and Oliveira-Filho, 2013), livestock (McGorum *et al.*, 2015) and human health (Kuiper-Goodman *et al.*, 1999; Zanchett and Oliveira-Filho, 2013).

While different cyanobacterial taxa can contribute to the formation of dense cyanobacterial water blooms depending on geographical and ecological conditions, *Microcystis* sp. represents cosmopolitan and pervasive cyanobacterial genera, which is frequently reported to dominate water blooms in freshwaters of all continents except Antarctica (Harke *et al.*, 2016). *Microcystis* species (such as *Microcystis aeruginosa*) are also among the prominent producers of the most broadly studied cyanobacterial toxins microcystins (MCs) (Bláha *et al.*, 2009). MCs are known liver tumour promoters (Nishiwaki-Matsushima *et al.*, 1992), with the most common structural variant microcystin-LR (MC-LR) being classified by the International Agency for Research on Cancer as a possible human carcinogen (IARC2B) (Grosse *et al.*, 2006). MCs have been shown to act via inhibition of serine/threonine protein phos-

phatases (PPs) (Campos and Vasconcelos, 2010) and induction of oxidative stress followed by damage to cellular macromolecules (Mathe *et al.*, 2016). Chronic exposures to cyanobacteria and their toxins – *e.g.*, via contaminated drinking water – have been associated with increased occurrence of liver and colorectal cancer (Yu, 1995; Zhou *et al.*, 2002; Svircev *et al.*, 2009). Other (often yet unidentified) compounds produced by complex cyanobacterial blooms can also induce or contribute to different adverse effects (Oberemm *et al.*, 1997; Berry *et al.*, 2009) including tumour promotion (Bláha *et al.*, 2010).

Occurrence of toxic cyanobacteria in surface water presents a challenge to drinking water treatment facilities. Preventive measures as well as various water treatment technologies used to minimize human health risks caused by cyanobacteria and their toxins have been recently summarized and critically discussed (Westrick *et al.*, 2010; Merel *et al.*, 2013; Roegner *et al.*, 2014; Hiskia *et al.*, 2016; Ibelings *et al.*, 2016). The available approaches able to remove MCs to different extents include coagulation-flocculation-sedimentation, standard oxidation and disinfection by chlorine or permanganate, ozonation and UV disinfection, sorption by activated carbon, nano- and ultrafiltration, and advanced oxidation processes (AOP) (Westrick *et al.*, 2010; Merel *et al.*, 2013; Roegner *et al.*, 2014). Different drinking water treatment technologies are applied in different countries and contexts, and evaluation of their treatment efficiency should focus on i) removal of targeted priority pollutants (*e.g.*, MCs in case of cyanobacterial toxins) to comply with current treatment goals; as well as ii) removal of other potentially harmful and toxic components of the complex material which may not be fully chemically characterized; and iii) formation of new harmful metabolites/toxic by-products during the application of the water treatment technology (Upham *et al.*, 1994; Upham *et al.*, 1995; Prasse *et al.*, 2015).

To address these different aspects of drinking water treatment, complementary chemical and biological tools (*i.e.* instrumental analyses and bioassays) should be included in the monitoring plans (Maier *et al.*, 2015). This ongoing effort can be highlighted by current implementation of the effect-based tools into the monitoring guidelines for water quality assessment (Wernersson *et al.*, 2014), which combines several bioassays targeting different toxic modes of action (MoAs) to provide additional information to classical chemical analyses and thus a more integrative view.

Gap junctional intercellular communication (GJIC) plays a fundamental role in maintaining tissue homeostasis, and provides an excellent biological endpoint to assess potential adverse health effects of many anthropogenic toxicants and natural toxins (Vinken *et al.*, 2009). GJIC is a critical cellular process for the coordination of different intra-, extra-, and inter-cellular signalling pathways re-

quired for proper cell behaviour, tissue development, tissue function and maintenance of tissue homeostasis. Most chemical carcinogens and tumour promoters inhibit GJIC in *in vitro* assays, and demonstrated to be a representative marker of tumour promoting potency (Rosenkranz *et al.*, 1997). Recently cyanobacterial extracts and exudates were determined to be potent *in vitro* inhibitors of GJIC (Bláha *et al.*, 2010; Novakova *et al.*, 2011). Inhibition of GJIC by these extracts were independent of the well-recognized tumour promoting cyanotoxins, MCs or cylindrospermopsin, indicating the existence of not-yet-identified toxic compounds (Novakova *et al.*, 2013). Aquatic contaminants, such as polycyclic aromatic hydrocarbons (PAHs) or polychlorinated biphenyls synergistically potentiated the inhibitory effects of cyanobacterial extracts on GJIC (Novakova *et al.*, 2012), which further highlights the need to bioassay these mixtures for adverse effects in the complex assessment of drinking water quality, and efficacy of treatment technologies.

In fact, *in vitro* assessment of GJIC has been successfully used along with chemical analysis as a principal bioassay to study tumour promoting activity of water chlorination by-products (Hakulinen *et al.*, 2004; Nishikawa *et al.*, 2006). Similarly, GJIC assay has been applied to evaluate the efficiency of removing different anthropogenic contaminants and their toxic by-products with ozone, such as polycyclic aromatic hydrocarbons (Upham *et al.*, 1994; Upham *et al.*, 1995; Herner *et al.*, 2001; Luster-Teasley *et al.*, 2002; Luster-Teasley *et al.*, 2005) and various pesticides (Upham *et al.*, 1997; Masten *et al.*, 2001; Wu *et al.*, 2007). The *in vitro* bioassays used in these studies to assess GJIC were based on the scrape-load dye transfer (SL-DT) technique (El-Fouly *et al.*, 1987). This SL-DT assay provides fast (minutes of exposure) and integrative responses, which reflect dysregulations of different cell processes and multiple signalling pathways controlling GJIC (Upham *et al.*, 2016). Dysregulation of GJIC is an epigenetic, phenotypic marker for determining tumour promotional activity, which contrasts and complements the more commonly used genotoxic and specific nuclear receptor transactivation assays (Leusch and Snyder, 2015). GJIC can be assessed *in vitro* using diverse non-tumorigenic cells, with a rat liver epithelial cell line, WB-F344, being one of the most widely used GJIC model for the assessment of tumour promoting activity, as well as determining chemopreventive effects of chemicals (Upham *et al.*, 1998; Sovadinova *et al.*, 2015; Babica *et al.*, 2016b). To further validate tumorigenic activity, compounds that dysregulate GJIC are often tested for effects on signal transduction pathways implicated in neoplastic transformation, such as mitogen-activated protein kinases (MAPK-ERK1/2 and MAPK-p38) (Upham *et al.*, 2008; Osgood *et al.*, 2014; Babica *et al.*, 2016a).

Our objective was to evaluate and compare the effi-

cacy of two broadly used drinking water treatment oxidation technologies, namely chlorination and ozonation, on the removal of known cyanotoxin MC concentrations as well as on changes in biological effects that are independent of the MC content (*i.e.*, removal of overall cytotoxicity and tumour promotional potency). We used a natural bloom sample that was dominated by the cosmopolitan and environmentally relevant bloom-forming cyanobacteria *M. aeruginosa*. Extracts were prepared and characterized for content of MC, total organic carbon (TOC) concentration, initial cytotoxicity, effect on GJIC and modulation of signalling kinases (MAPKs). These cyanobacterial extracts were treated by chlorine or ozone, and evaluated for the changes in the toxin content, TOC, and *in vitro* cytotoxicity and tumour promoting activity.

METHODS

Cyanobacterial sample

The sample of toxic cyanobacterial water bloom was collected from a lake located within the campus of Michigan State University (East Lansing, MI, USA; 42°40'50.09"N, 84°29'14.27"W) in September 2008 using a 20 µm plankton net. The bloom was dominated by *Microcystis* species: *M. aeruginosa* (>50% of the cell counts) accompanied by *M. flos-aquae* (~20%) and *M. ichthyoblabe* (~20%). The biomass was freeze-dried and 38 g of dry weight (DW) was extracted by 20 min sonication (Fisher Sonic Dismembrator Model 300; Fisher Scientific, Pittsburgh, PA, USA) while stirring on ice with 566 mL of 50% methanol (*i.e.*, 66.7 g DW L⁻¹ equivalent). The samples were centrifuged at 31,000 × g and the supernatant fraction was collected and dried using a vacuum evaporator. The dry extract was dissolved in 47.2 mL of MilliQ water (MilliQ Synthesis A10; Millipore, Billerica, MA, USA) to obtain the final concentrated extract corresponding to 800 g DW of original biomass per one liter of water.

Chlorination and ozonation

The extract was aliquoted into 4 mL fractions to be treated by chlorination or ozonation as summarized in Tab. 1. Chlorination was carried out with sodium hypochlorite (NaOCl) in a phosphate buffer (0.5 M K₂HPO₄-0.293 M NaOH, pH 7.0±0.2) according to the Method 5710C (Clesceri *et al.*, 1998). The sample was treated for 30 min to 24 h with NaOCl at different concentrations of free chlorine (7 to 1000 mg L⁻¹) corresponding to contact time (CT) values 0.21×10³, 7×10³, 50×10³ and 1440×10³ mg min L⁻¹. The oxidation reaction was stopped by addition of 10% w/v of NaHSO₃. Vehicle controls were prepared from MilliQ water equally treated with chlorine and quenched. No residual chlorine was present in the vehicle controls after the quenching. To increase the weight ratio of chlorine to dry

weight of the extract (or TOC or MC concentration), the concentration of the original biomass was also diluted four- and eight times (*i.e.*, "1/4" or "1/8") before the chlorination step with 500 mg L⁻¹ of chlorine for 100 min.

The original extract dissolved in MilliQ water was ozonated for 30 min using a commercial ozone generator (OZ2PCS-V; Ozotech, Yreka, CA, USA) at the concentration of O₃ (gas)=5.0 mg L⁻¹ with a gas flow rate of one L min⁻¹ and temperature of 20.0±0.5°C to maximize ozone dissolution.

Microcystin analysis

The concentrations of MCs in the original biomass as well as in the samples after the chlorination and ozonation treatment were analysed by HPLC-UV/DAD following the procedure described earlier (Babica *et al.*, 2006). Toxins were identified based on their retention times and characteristic UV absorption spectra and quantified using the calibration curves of standards of MC-RR, -YR, -LR, -LW, -LF, and nodularin. An example of the HPLC chromatograph of the cyanobacterial extract recorded at 238 nm is in Supplementary Fig. 1.

TOC analysis

TOC of the extract before and after chlorination and ozonation was determined using LiquiTOC analyzer (Elementar Analysensysteme, Hanau, Germany) where measurements were made by high temperature oxidation of the carbon (850-900°C) and detection of CO₂ by an NDIR photometer.

Bioassays

WB-F344 rat liver non-tumorigenic stem-like cells (Tsao *et al.*, 1984) were cultured in D-media (Kao *et al.*, 1997) with 5% v/v of fetal bovine serum (Gibco, Life Technologies, Grand Island, NY, USA) at 37°C and 5% CO₂. Cells were cultured to full confluence for 48 h in 35 mm tissue culture dishes (Costar; Cambridge, MA, USA). These confluent cells were used for the various time and dose related experiments. The vehicle controls were water chlorinated or ozonated using the same conditions as applied for studied samples. A sample or vehicle was added directly to the cell culture medium in the dish and gently mixed. Non-treated cells were used as negative controls. The final concentrations of extracts in the bioassays were expressed as the original weight of dry biomass used for extract preparation per unit volume (g DW L⁻¹). Viability/cytotoxicity was tested after 30-min and 24-h exposures using the neutral red assay as reported before (Babica *et al.*, 2016b). The method determines viable cells capable of neutral red inclusion into lysosomes (Borenfreund and Puerner, 1985). Viability was expressed as the fraction of negative (non-treated) control (FOC).

Tab. 1. Conditions of chlorination and ozonation of the studied cyanobacterial extract.

Abbreviation	Treatment type and CT value (mg min L ⁻¹)	Dose of Cl or O ₃ (mg L ⁻¹)	Treatment duration	Total MC (µg g ⁻¹ DW) ^o	MC-LR (µg g ⁻¹ DW) ^o	TOC (µg g ⁻¹ DW) ^o	24-h Cell viability IC ₅₀ (95%CI) LOEC (g DW L ⁻¹)	30-min GJIC IC ₅₀ (95%CI) LOEC (g DW L ⁻¹)	30-min ERK1/2 LOEC (g DW L ⁻¹)	30-min p38 LOEC (g DW L ⁻¹)
NT	no treatment	--	--	517 (0.52-12.41) [§]	411 (0.41-9.86) [§]	104,761 (105-2514) [§]	11.6 [#] (10.2-13.1) 12	7.8 [#] (7.0 to 8.7) 8	8	4
Cl(7-30)	Chlorination 0.21×10 ³	7	30 min	559 (0.56-13.42)	443 (0.44-10.63)	114,761 (114-2739)	14.8 (12.6-17.3) 12	10.0 (9.3-10.7) 8	8	4
Cl(70-100)	Chlorination 7×10 ³	70	100 min	447 (0.45-10.74)	352 (0.35-8.44)	88,355 (88-2121)	14.3 (12.2-16.5) 12	10.7 ^{***} (9.7-11.8) 8	16	4
Cl(500-100)	Chlorination 50×10 ³	500	100 min	467 (0.47-11.20)	371 (0.37-8.91)	86,895 (87-2085)	9.1 (6.9-12.2) 12	12.6 ^{***} (11.2-14.1) 8	16	4
½ Cl(500-100) [§]	Chlorination 50×10 ³	500	100 min	346 (0.35-8.31)	275 (0.28-6.60)	77,229 (77-1853)	10.4 (7.1-15.4) 12	9.6 (8.4-11.0) 8	8	4
½ Cl(500-100) [§]	Chlorination 50×10 ³	500	100 min	412 (0.41-9.88)	331 (0.33-7.94)	81,193 (81-1949)	7.0 (7.0-15.5) 12	8.1 (6.7-9.7) 8	n.a.	n.a.
Cl(1000-24h)	Chlorination 1440×10 ³	1000	24 h	367 (0.37-8.81)	295 (0.29-7.07)	78,754 (79-1890)	12.3 (9.7-15.7) 12	12.7 ^{***} (10.7-15.0) 12	16	4
O ₃	Ozonation	5 [°]	30 min	n.d.	n.d.	70,622 (71-1695)	>24 >24	>24 24	>16	4

CT values: the concentration of free chlorine multiplied by the contact time with the sample being disinfected; it is expressed in units of mg min L⁻¹. ^oThe concentration is calculated per g DW of original biomass before methanol extraction. [#] Plain text represents IC₅₀ values with 95% confidence intervals in parentheses, italicized numbers show LOEC values. [§] Values in parentheses indicate the range of actual MC and TOC concentrations (mg L⁻¹) in the experiments (calculated for the range of tested concentrations of 1-24 g DW L⁻¹). ^{*}Significantly different than IC₅₀ value of NT extract (Student's *t*-test, P<0.05). [°]Before chlorination, the concentration of original biomass was diluted four (¼) or eight times (⅛). ^{°°}Gas flow rate of 1 L min⁻¹ for 30 min; n.d., not detected; minimal detection limit (MDL) for an individual MC variant=1.3 µg g⁻¹ DW; n.a., not analysed.

Tumour promotion assay based on GJIC assessment used only the concentrations that were determined to be noncytotoxic using the neutral red assay. Cells were exposed for 30 min to the tested samples or corresponding vehicle. Treatment with 1-methylanthracene (70 μM , 30 min) was used as a positive control inducing complete inhibition of GJIC. GJIC was assessed using modified SL-DT technique (El-Fouly *et al.*, 1987; Babica *et al.*, 2016c; Upham *et al.*, 2016). The migration of the dye through gap junctions was visualized with a Nikon Eclipse TE3000 phase contrast/fluorescent microscope and the images digitally captured with Nikon EZ Cool Snap CCD camera (Nikon Instruments, Melville, NY, USA), where three representative images were acquired from each dish. The area of dye transfer was measured for each image using ImageJ (<https://imagej.nih.gov/ij/>). The measured areas were adjusted by subtracting an area of the dye transfer in the positive control with completely inhibited GJIC. Adjusted areas from each image were compared with an averaged adjusted area of the negative control and expressed as FOC.

Activation of regulatory kinases MAPK ERK1/2 and p38 after a 30 min exposure to the sample was determined by Western blotting. Western blot analyses were done as reported previously (Babica *et al.*, 2016a). Briefly, the proteins were extracted with 20% SDS solution containing inhibitors of proteases and phosphatases, and the protein concentration of the cell lysates was determined with DC assay kit (Bio-Rad, Hercules, CA, USA). The proteins (20 μg per lane) were separated on 12.5% SDS-PAGE (Laemmli, 1970) and then electrophoretically transferred to a 0.45 μm PVDF membrane (Millipore). To visualize activated, *i.e.* phosphorylated ERKs and p38, we used rabbit phospho-specific polyclonal antibodies directed to ERK-1 phosphorylated at Thr 202/Tyr204, and ERK-2 phosphorylated at Thr185/Tyr187 (Cell Signaling #9101S, Danvers, MA, USA) and directed to p38 phosphorylated at Thr180/Tyr182 (Zymed #36-8500, San Francisco, CA, USA), and secondary donkey anti-rabbit IgG conjugated with horse radish peroxidase (Amersham Bioscience #NA934V, Life Science, Denver, CO, USA). Levels of glyceraldehyde 3-phosphate dehydrogenase (GAPDH) was used as a housekeeping protein, and determined with mouse anti-GAPDH antibodies (Chemicon #MAB374, Millipore) and secondary sheep anti-mouse IgG conjugated with horse radish peroxidase (Amersham Bioscience #NA931V; Life Science). The ERK, p38 and GAPDH protein bands were detected using the ECL SuperSignal West Pico Chemiluminescence detection kit (Pierce, Arlington Heights, IL, USA) and Bio-Rad Image Analyzer.

Data analyses and statistics

At least three independent experiments were done for each treatment (except for Western blot analyses), and the mean \pm standard deviations from independent experi-

ments were calculated. IC_{50} concentrations causing 50% inhibition of the studied effects and their 95% confidence intervals were derived using non-linear regression in GraphPad (GraphPad software Inc., La Jolla, CA, USA). One-way Analysis of Variance (ANOVA) followed by Dunnett's *post-hoc* test was used to identify treatments significantly different from the control. Differences between IC_{50} values were assessed by Student's *t*-test. P-values less than 0.05 were considered statistically significant.

RESULTS

The original biomass contained 517 μg of total MC per g of DW with MC-LR being the dominant variant (411 $\mu\text{g g}^{-1}$ DW, 79%, Tab. 1). The other variants present included MC-RR (2%), MC-LW (2%), MC-LF (3%) and two other structurally unidentified MC variants (14%). The total MC concentration in the original extract (corresponding to 800 g biomass DW L^{-1}) was 414 mg L^{-1} (MC-LR concentration: 329 mg L^{-1}). TOC concentration in the non-treated extract of 800 g biomass DW L^{-1} was 83.81 g L^{-1} , which represents 105 mg of extractable total organic carbon per g of biomass DW.

Ozonation of cyanobacterial samples had direct effects on the concentrations of organic matter in the biomass. As shown in Tab. 1, the 30-min treatment with ozone caused complete degradation of MCs and 33% reduction of TOC compared to non-treated extract. The chlorination with low dose of chlorine (7 mg L^{-1}) for short time (30 min) had no effect on MC and TOC concentrations. The higher doses (70 to 1000 mg L^{-1}) of chlorine and longer treatments (100 min to 24 h) were more effective in reducing MC levels (by 10 to 33%), and this reduction was dependent on chlorine concentrations and treatment times. There was no observed shift in the proportion of individual MC congeners with the MC-LR being the dominant variant. TOC degradation by chlorine (by 16 to 25%) correlated well with MC degradation. The increase of the weight ratio of chlorine to original biomass by diluting non-treated extract before chlorination (Tab. 1, variants $\frac{1}{4}$ or $\frac{1}{8}$ Cl(500-100)) slightly improved reduction of MC and TOC amount, when the results were adjusted by the corresponding dilution factor and then compared to the non-diluted extract chlorinated under the same conditions (Cl(500-100)).

The original extract (non-treated, NT) showed no significant cytotoxic effects on WB-F344 during 30-min exposure within the range of concentrations tested (up to 24 g DW L^{-1} ; negative data not shown). After longer exposure time (24 h), the sample significantly decreased viability of WB-F344 cells (Fig. 1A) with the calculated $\text{IC}_{50}=11.6$ g DW L^{-1} (Tab. 1). The lowest observed effect concentration (LOEC) inducing statistically significant reduction of the cell viability was 12 g DW L^{-1} (Fig. 1A).

The effects of the NT extract on GJIC in WB-F344 cells after 30-min exposure are shown in Fig. 2A. The sample had pronounced inhibitory effects on GJIC, which were concentration-dependent with the calculated $IC_{50}=7.8$ g DW L⁻¹ (Tab. 1). LOEC concentration of NT extract for

inhibition of intercellular communication was 8 g DW L⁻¹ (containing 4.1 mg L⁻¹ MCs) (Fig. 2A). The tumour promotional activity of the NT sample indicated by its effect on GJIC was also confirmed by additional experiments assessing phosphorylation of signalling protein

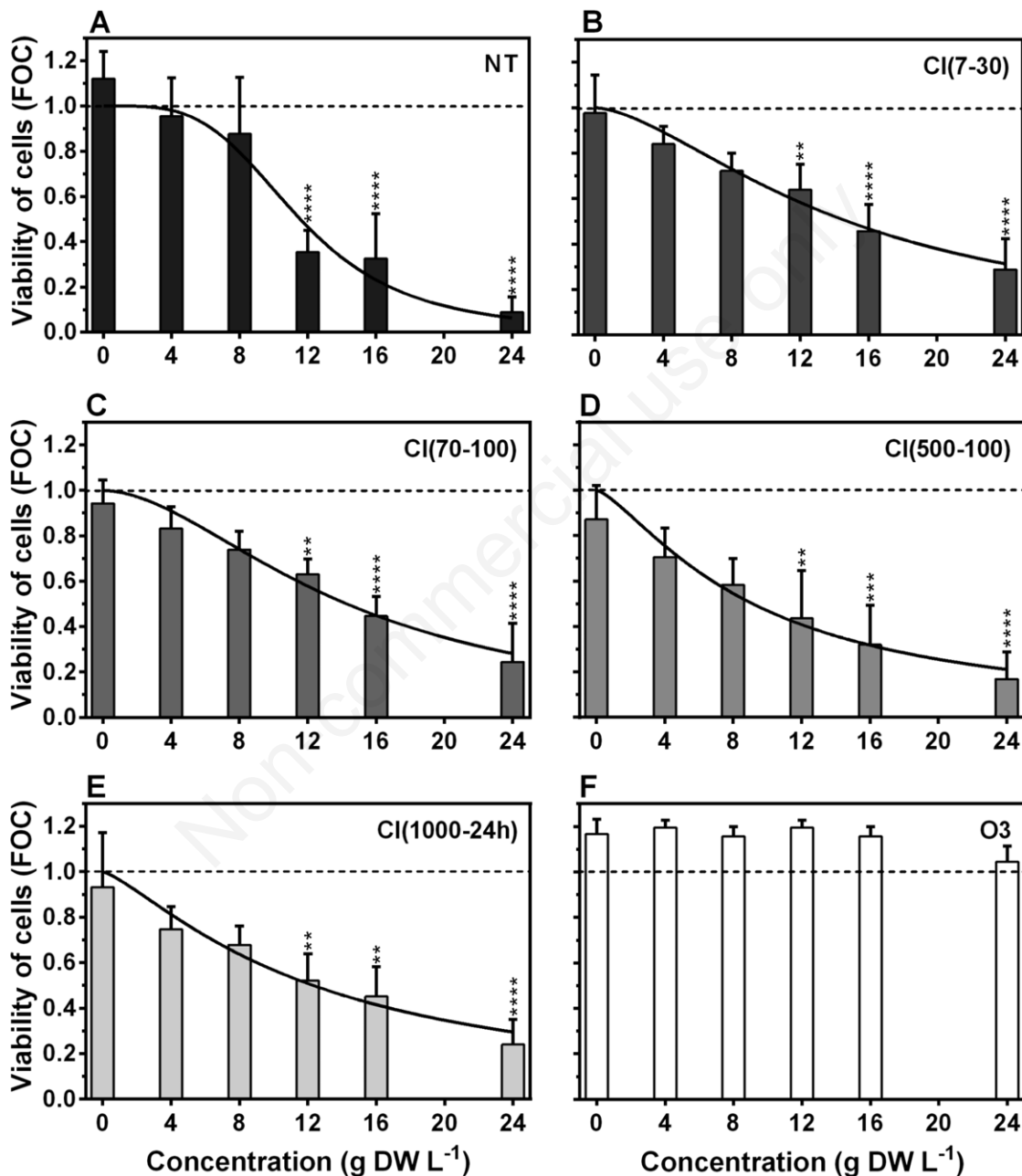


Fig. 1. The effect of chlorination (B-E) and ozonation (F) of the tested cyanobacterial extract on viability in WB-F344 cells after 24-h exposure to 6 different concentrations (4-24 g DW L⁻¹). Data are fractions of controls (FOC) as means \pm standard deviations of independent repetitions of the experiment ($n \geq 3$). Significant differences from the vehicle control (A) are indicated by asterisks (one-way ANOVA followed by Dunnett's *post-hoc* test; * $P \leq 0.05$; ** $P \leq 0.01$; *** $P \leq 0.001$; **** $P \leq 0.0001$). NT, original non-treated extract; CI, chlorinated extracts (in parentheses - free Cl concentrations 7, 70, 500 and 1000 mg L⁻¹; treatment durations 30 min, 100 min, 24 h); O3, ozonated extract (30 min, the flow rate of 1 L min⁻¹ with 5 g O₃ m⁻³).

kinases in WB-F344 cells (MAPK-ERK 1/2 and p38, Fig. 3A). Rapid and clear concentration-dependent activation of both MAPKs was observed after 30-min exposure. The LOEC values for hyperphosphorylation of MAPK- ERK 1/2 and p38 were 8 or 4 g DW L⁻¹ of the NT extract, respectively, with maximal effects observed at the highest tested concentration of 16 g DW L⁻¹ (Fig. 3A).

Ozonation and chlorination of the original sample had a pronounced effect on the biological activity. The cytotoxic effect was completely eliminated by the ozonation of the extract (Fig. 1F). At the same time, none of the chlorination experimental protocols had any significant effect on cytotoxicity of the original NT extract (Figs. 1B-E), with the estimated IC₅₀ values ranging between 9.1 and 14.8 g DW L⁻¹ and not being significantly different (P<0.05) from the IC₅₀ value for the NT extract (Tab. 1). Also, the LOEC values for viability of cells exposed to chlorinated extracts remained at 12 g DW L⁻¹. Interestingly, slight but non-significant increase of IC₅₀ values was associated with lower rather than higher chlorine doses. The increase of weight ratio of chlorine to the original biomass by diluting non-treated extract before chlorination did not decrease the cytotoxicity with the IC₅₀ values of 10.4 g DW L⁻¹ for ¼ Cl(500-100) and 7.0 g DW L⁻¹ for ⅛ Cl(500-100) (Tab. 1, Supplementary Fig. 2). The corresponding vehicle controls for these chlorination conditions caused 20 to 30% significant decrease in WB-F344 cell viability when compared to non-treated control (Supplementary Fig. 2).

The ozone application was also highly potent in eliminating tumour promotional activity of the original NT extract, as shown in Fig. 2F. After 30-min ozonation, the LOEC value for GJIC inhibition was 24 g DW L⁻¹, *i.e.* three times higher than in NT extract. GJIC was reduced only by 30% at 24 g DW L⁻¹ concentration (Fig. 2F), while nearly 100% inhibition of GJIC was observed at 16 to 24 g DW L⁻¹ of NT extract (Fig. 2A).

In contrast, the chlorination treatments had much less pronounced effects on the inhibition of GJIC, with the IC₅₀ values of the chlorinated extracts ranging between 10.0-12.7 g DW L⁻¹. Although these IC₅₀ values were relatively similar to the IC₅₀ estimated for NT extract, they were significantly higher except for the lowest free chlorine doses and shortest treatment (P<0.05), and their increase depended on the chlorine dose- and treatment duration (Tab. 1). When the weight-ratio of chlorine to the original biomass was increased by diluting the non-treated extract before chlorination (Supplementary Fig. 3), there was no observable decrease in the dysregulation of GJIC induced as compared to the original NT extract, with the IC₅₀ values after chlorination being 8.1 to 9.6 g DW L⁻¹ (Tab. 1, Supplementary Fig. 2). Both ozone and chlorine treatments significantly attenuated the activation of MAPK ERK1/2 induced by NT extract (Fig. 3). Ozona-

tion was more effective, when no activations of the ERK1/2 kinase were observed at concentrations between 4 to 16 g DW L⁻¹. Chlorination also resulted in reduced levels of MAPK ERK1/2 activation (Fig. 3, Tab. 1). The protective effects had biphasic character, when initially increased but then became less apparent with an increase in chlorine dose and chlorination time (Fig. 3, Tab. 1). The effects of both ozone and chlorine treatments on the activation of p38 MAPK were much less pronounced when compared to MAPK ERK1/2, and activation of p38 was still apparent for the ozonated extract as well as most of the chlorinated extracts even at the lowest experimental concentration of 4 g DW L⁻¹ (Fig. 3).

DISCUSSION

Adverse effects of toxic cyanobacteria on human health remain a major issue for both researchers and water managers. Our study confirmed that rapid inhibitions of GJIC and activations of MAPK-ERK1/2 might be a common effect induced by bloom-forming cyanobacteria. The effective concentration for 30-min GJIC inhibition (IC₅₀=8 g DW L⁻¹) was similar to previously reported values for other extracts from natural blooms dominated by *Microcystis* sp. (IC₅₀=4 or 6 g DW L⁻¹, respectively) (Bláha *et al.*, 2010; Novakova *et al.*, 2011). Modulation of these cellular events by chemicals *in vitro* are considered to be relevant biomarkers of tumour promoting potency *in vivo*, as was demonstrated *e.g.* for tumour promoting phorbol esters like TPA (Madhukar *et al.*, 1996), organochlorine pesticides (Trosko *et al.*, 1987), PCBs (Kang *et al.*, 1996), low molecular weight PAHs (Bláha *et al.*, 2002), clofibrate, phenobarbital, perfluorooctanoic acid, or organic peroxides (Upham *et al.*, 2007; Upham *et al.*, 2009; Vinken *et al.*, 2009). MCs and other cyanotoxins like cylindrospermopsin have been shown to modulate development of tumours (Nishiwaki-Matsushima *et al.*, 1992; Falconer and Humpage, 2005; Svircev *et al.*, 2010; Zegura *et al.*, 2011; de la Cruz *et al.*, 2013). However, neither MC-LR nor cylindrospermopsin had any direct effect on rapid inhibition of GJIC or activation of MAPK ERK 1/2 indicating that other metabolites in cyanobacteria might be responsible for their GJIC-dependent tumour promoting activity (Bláha *et al.*, 2010; Novakova *et al.*, 2011). However, these metabolites have not been identified yet.

In addition, our present study demonstrates, for the first time, a rapid activation of another MAPK-p38 by cyanobacterial environmental extract in the cell line WB-F344, which possesses characteristics of liver progenitor cells (Babica *et al.*, 2016a, b). MAPK-p38 is a critical participant in cellular stress responses and has a key role in inflammation, as well as in tissue homeostasis, by controlling cell proliferation, differentiation, death, survival and the

migration of specific cell types (DiDonato *et al.*, 2012). In contrast to MAPK-ERK1/2, which are activated by mitogens or growth factors, MAPK-p38 is activated by environmental and genotoxic stresses including hypoxia, UV, ROS, hyperosmolarity, and heat shock, and its activation

has been linked to protein phosphatase 2 (PP2A) (Nebreda and Porras, 2000; Wagner and Nebreda, 2009). Indeed, MC-LR, a known PP2A inhibitor, has been previously reported to activate MAPKs ERK1/2, p38 or JNK in rodent liver *in vivo* and also in experiments with various cell lines

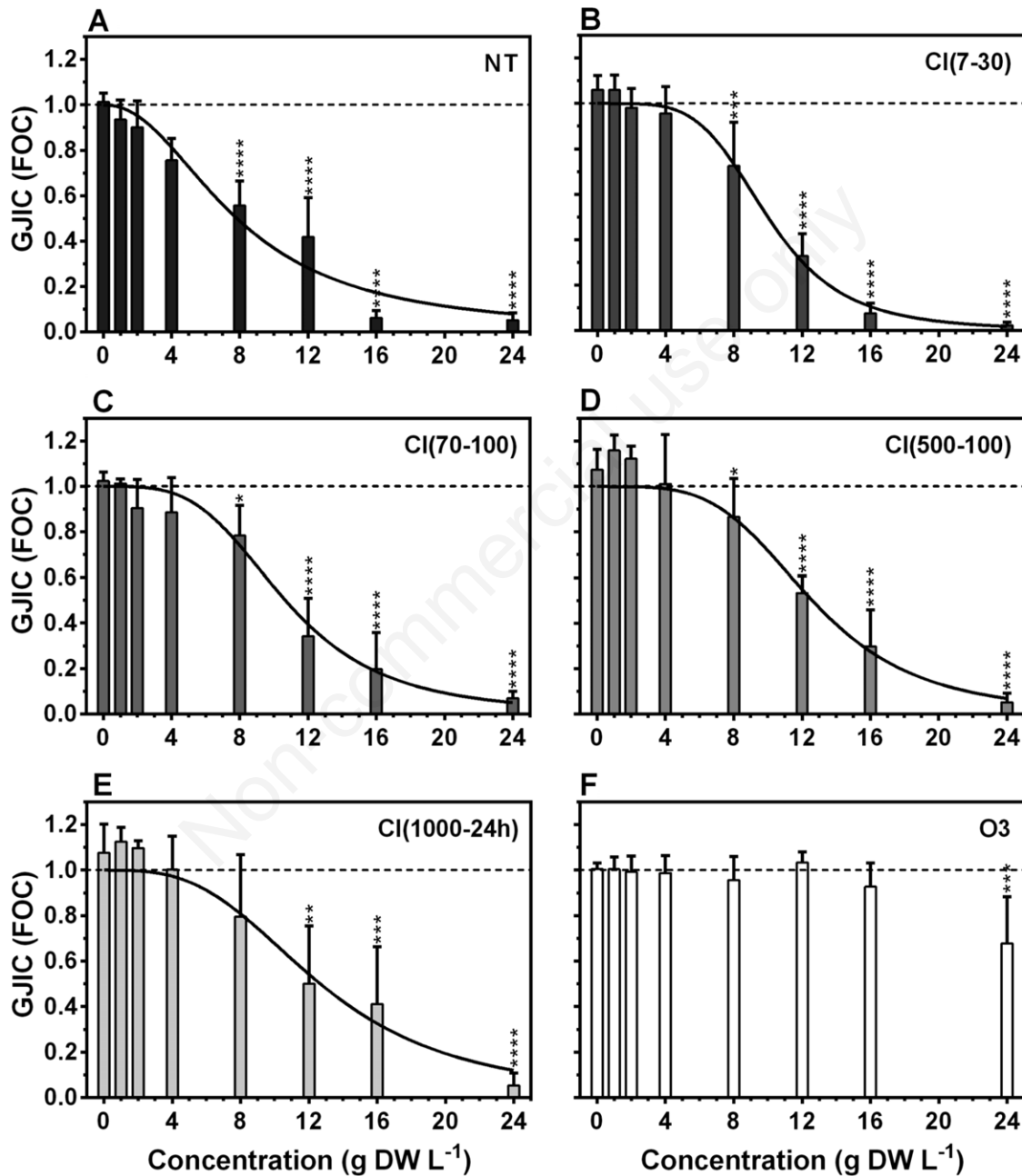


Fig. 2. The effect of chlorination (B-E and ozonation (F) of the tested cyanobacterial extract on gap-junctional intercellular communication (GJIC) in WB-F344 cells after 30-min exposure to 6 different concentrations (1-24 g DW L⁻¹). Data are fractions of controls (FOC) as means ± standard deviations of independent repetitions of the experiment (n≥3). Significant differences from the NT extract (A) are indicated by asterisks (one-way ANOVA followed by Dunnett's post hoc test; *P≤0.05; **P≤0.01; ***P≤0.001; ****P≤0.0001). NT, original non-treated extract; CI, chlorinated extracts (in parentheses - free Cl concentrations 7, 70, 500 and 1000 mg L⁻¹; treatment durations 30 min, 100 min, 24 h); O3, ozonated extract (30 min, the flow rate of 1 L min⁻¹ with 5 g O₃ m⁻³).

in vitro. However, MC-LR effects on MAPKs seem to be dependent on the kinase type, a cell type, and probably also exposure times and concentrations. Depending on the study, MC-LR was found to activate ERK1/2 but not p38 (Dias *et al.*, 2010; Zhang *et al.*, 2013; Adamovsky *et al.*, 2015), p38 but not ERK1/2 (Meng *et al.*, 2011; Lezcano *et al.*, 2012), and both ERK1/2 and p38 (Komatsu *et al.*, 2007; Daily *et al.*, 2010; Sun *et al.*, 2011; Chen *et al.*, 2012; Liu *et al.*, 2016; Wang *et al.*, 2017). The effective concentrations of MC-LR in these studies were typically between 1 and 10 μM ($\sim 1\text{--}10\text{ mg L}^{-1}$).

In the present study, cytotoxicity, GJIC and MAPKs were affected by the cyanobacterial extract diluted to 4–12 g DW L^{-1} containing MCs with concentrations between 2 and 6 mg L^{-1} , which corresponds to 2 to 6 μM range and is quite comparable with the other *in vitro* studies reporting MAPK activation by MCs. However, we previously demonstrated that tumour promoting events, such as rapid GJIC inhibition and MAPK ERK1/2 activation in rat liver progenitor cells, are induced by other cyanobacterial metabolites but not MC-LR or cylindrospermopsin (Bláha *et al.*, 2010). Our results suggest that MAPK p38 can also be activated by transformation or degradation products of MCs, other compounds of cyanobacterial origin and/or their transformation or degradation products, since p38 was activated not only by MC-containing non-treated cyanobacterial extract, but also by ozonated extract without detectable levels of MCs. These findings suggest that progenitor cells, in comparison with differentiated hepatocytes, might be less prone to the effects of MCs, possibly due to limited expression of key proteins involved in MCs uptake and metabolism, such as organic-anion transporting polypeptides (OATPs). Nevertheless, progenitor cells can be apparently a target of other compounds present in cyanobacterial biomass, which are capable to induce toxic and tumour promoting effects in this specific population of liver cells (Bláha *et al.*, 2010) known to play a critical role in the maintenance of liver tissue homeostasis, liver regeneration and hepatocarcinogenesis (Canovas-Jorda *et al.*, 2014).

The evidence supporting the existence of other components of cyanobacterial biomass contributing to the tumour promoting and toxic effects of complex cyanobacterial samples emphasize the need for effect-based evaluation of the efficacy of water treatment technologies in addition to chemical analyses. Different physicochemical purification processes employed in DWTPs may have different efficacies in removing the target contaminant, such as well recognized toxicants (such as MCs) vs. elimination of the overall toxicity. Our results demonstrate that ozone effectively and rapidly removes the MC fraction of the complex cyanobacterial samples. Although the highest chlorine dose resulted in a decrease of TOC that was comparable to the ozone treatment, re-

active chlorine was not as effective compared to ozone in removal of MCs. Similarly, removal of cytotoxicity and overall epigenetic toxicity of the studied sample by ozonation appeared to be much more effective than chlorination, although ozone had a less pronounced effect in decreasing p38 activation as compared to ERK1/2 and GJIC.

With regard to chlorine the literature demonstrate that its application removes MCs but the efficiency of removal decreases with increases in pH and dissolved organic material along with formation of less effective oxidant ClO^- (Merel *et al.*, 2010). Several studies agreed that 0.5 mg of residual chlorine per liter should efficiently remove pure MCs in distilled water during 5–30 min (depending on MC concentration) at pH lower than 8 (Nicholson *et al.*, 1994; Newcombe and Nicholson, 2004; Acero *et al.*, 2005). Similar scenarios are also expected at DWTP at environmentally relevant concentrations of MCs (Merel *et al.*, 2009).

Several previous studies using PP-inhibition as a biomarker of toxicity as well as other bioassays reported a decrease in MC concentration and toxicity after chlorination of cyanobacterial samples (Nicholson *et al.*, 1994; Tsuji *et al.*, 1997; Rodriguez *et al.*, 2008; Merel *et al.*, 2010). For example, the chlorination of *M. aeruginosa* extract (16 mg DW L^{-1}) with the dose of 1 mg L^{-1} chlorine and contact time of 30 min (CT value=30) effectively removed 95% of MCs (initial concentration: 192 $\mu\text{g L}^{-1}$) and completely eliminated the acute toxicity of this extract in a mouse bioassay (Nicholson *et al.*, 1994). Interestingly, our study showed that chlorination of cyanobacterial extract was less effective. The dose of 7 mg of chlorine per liter for 30 min at pH 7.2 did not decrease MCs nor TOC concentrations. Higher doses and longer treatment times removed up to 10–30% of the original MCs and TOC levels, and caused only moderate reduction of toxicity (cytotoxicity, GJIC inhibition and MAPK activations). Chlorination apparently removed some compounds responsible for the inhibition of GJIC and activation of ERK1/2 as reflected by the slight, yet statistically significant, increase in respective IC_{50} or LOEC values, and had only a minor effect on cytotoxicity and p38 activation. The lower effectiveness of chlorination observed in our study could be explained by the interactions of chlorine with the relatively higher concentrations of organic matter, which might have reduced the effectiveness of the oxidation process due to the competition between the toxins and the dissolved organic carbon reacting with the oxidant (Rodriguez *et al.*, 2008).

An important problem associated with the chlorine application is the formation of by-products such as halogenated organic compounds, especially in the presence of high amounts of organic matter. These by-products can have toxic or potential carcinogenic potencies (Neale *et al.*, 2012); and also for MCs, chlorine was shown to cause substitutions and modifications of the toxic Adda moiety

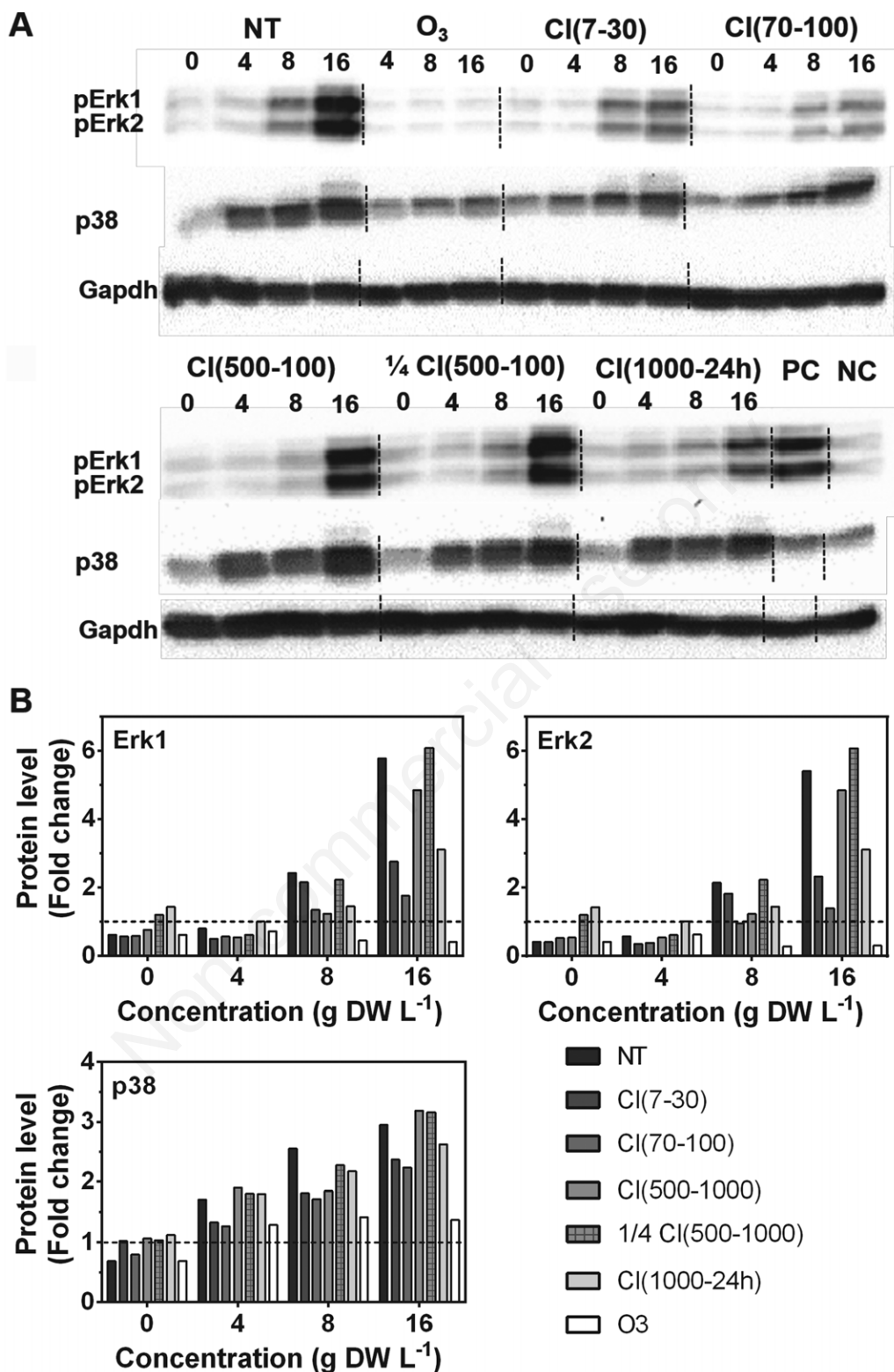


Fig. 3. Activation of mitogen-activated protein kinases (MAPKs) by studied samples after 30-min exposure to 3 different concentrations (4-16 g DW L⁻¹). Phosphorylation of extracellular receptor kinases 1 and 2 (ERK1/2) and p38 was determined by Western blotting (A). The bar graphs (B) show values from the densitometric image analysis normalized to negative control (NC=1). NT, original non-treated extract; CI, chlorinated extracts (in parentheses - free CI concentrations 7, 70, 500 and 1000 mg L⁻¹; treatment durations 30 min, 100 min, 24 h), O₃ - ozonated extract (30 min, the flow rate of 1 L min⁻¹ with 5 g O₃ m⁻³); NC, negative control (no treatment of the cells); PC, positive control for ERK1/2 activation (12-O-tetradecanoyl phorbol-13-acetate, 10 nM, 30 min).

(Tsuji *et al.*, 1997; Merel *et al.*, 2009). In addition, *de novo* formation of chlorinated by-products with potencies to affect GJIC and activate intracellular signalling (Hakulinen *et al.*, 2004; Nishikawa *et al.*, 2006) should also be considered, and could be related to the weak efficiency in removal of GJIC inhibitions and MAPK activations during the chlorination as observed in the present study. Possible toxicity of chlorinated by-products could also explain the observed biphasic effect, when lower doses of chlorine were slightly more effective in the elimination of cytotoxicity and MAPKs activation than the higher doses, although concentrations of TOC and MCs were slightly but progressively reduced with increasing chlorine dose and treatment time.

We demonstrated that ozonation completely removed MCs, substantial fractions of TOC and protected against cytotoxicity, GJIC inhibition or activation of ERK1/2. These findings are in agreement with similar studies, which documented complete MC removal (5 mg L^{-1}) by $2 \text{ mg L}^{-1} \text{ O}_3$ within 2 min (Al Momani and Jarrah, 2010). Further improvements in kinetics could be achieved by increased O_3 doses and temperature, and decreased pH (Al Momani and Jarrah, 2010; Shawwa and Smith, 2001). Naturally, organic matter negatively reduces the efficiency of ozonation, but under realistic DWTP situations of levels as low as 0.05 mg L^{-1} of residual O_3 assures MC removal (Newcombe and Nicholson, 2004; Brooke *et al.*, 2006). Despite a high amount of organic material in our sample that also competes with toxins for ozone, ozonation was highly effective in MC reduction and elimination of toxicity even after short treatment.

A high efficiency of oxidation of MC is known to be mediated by hydroxyl radicals attacking conjugated diene structure in MC followed by the cleavage of the Adda side chain (responsible for PPase inhibition) and ultimately opening of the peptide ring (Al Momani and Jarrah, 2010; Miao *et al.*, 2010). Biological assessments using PP-inhibition assay or mouse test confirmed elimination of the toxicity along with the described structural changes of MC (Brooke *et al.*, 2006; Miao *et al.*, 2010). Although ozone was quite efficient in removal of cytotoxic, GJIC inhibiting and ERK1/2 activating compounds in our study, it had only a partial effect on the removal of p38 activating components. This might indicate that p38 is not involved in GJIC inhibition and its activation was caused by metabolites with different modes of actions (Wagner and Nebreda, 2009). With respect to the critical role of p38 in cellular responses to different types of stress and also in controlling the proliferation, differentiation, survival, migration and inflammatory responses of specific cell types, further research should address interactions of cyanobacterial metabolites with this signalling pathway and evaluate its relevance as a biomarker of environmental and genotoxic stress induced by

cyanobacteria. Interestingly, activation of p38 was found to be the most sensitive endpoint in this study, where the increased levels of p38 phosphorylation were observed after 30-min exposure to the non-treated extract at concentration of 4 g DW L^{-1} , whereas significant inhibition of GJIC and activation of ERK1/2 occurred at concentrations 8 g DW L^{-1} and higher, and significant reduction of cell viability required 24-h exposure to 12 g DW L^{-1} . Inhibition of GJIC and activation of MAPKs was induced by lower concentrations and after shorter exposures than the cytotoxic effects, which indicates that these cell signalling events were altered via rapid non-genotoxic and non-cytotoxic mechanisms. *In vitro* evaluation of GJIC and MAPKs thus represent a simple and sensitive bioassay for assessment of 'epigenetic toxicity' and tumour promoting potential of complex cyanobacterial extracts, which is also suitable for effect-based studies focusing on the elimination of these hazardous properties of contaminated water.

CONCLUSIONS

Ozonation of an extract of a *Microcystis* water bloom sample was shown to be a very effective method in the complete removal of MCs, as well as the substantial elimination of the overall cytotoxicity and tumour promotional potency. On the contrary, chlorination experiments, despite high doses and long exposures, were much less effective, and potentially led to the formation of by-products, which could add to the observed toxic effects. Our study also demonstrated strong activations of p38 MAPK by cyanobacterial samples, which were not effectively removed by chlorination and only partially by ozonation. With respect to the role of p38 in inflammation as well as maintenance of tissue homeostasis, further research should address interactions of cyanobacterial samples with this biomarker of cellular stress and evaluate its environmental relevance. In agreement with several recent reports, the study also demonstrates the need to enforce effect-based (bioassay) tools into the assessment of water quality and monitoring the efficacy of water treatment systems.

ACKNOWLEDGMENTS

Supported by the Czech Science Foundation project GA15-12408S; the Czech Republic Ministry of Education, Youth and Sports infrastructure projects No. LO1214 and LM2015051; long-term research development project RVO 67985939; and by National Institute of Environmental Health Sciences (NIEHS) grant #R01 ES013268-01A2 to Upham. We would like to thank Dr. Ondřej Mikeš for the help with TOC analysis.

REFERENCES

- Acero JL, Rodriguez E, Meriluoto J, 2005. Kinetics of reactions between chlorine and the cyanobacterial toxins microcystins. *Water Res.* 39:1628-1638.
- Adamovsky O, Moosova Z, Pekarova M, Basu A, Babica P, Svihalkova Sindlerova L, Kubala L, Blaha L, 2015. Immunomodulatory potency of microcystin, an important water-polluting cyanobacterial toxin. *Environ. Sci. Technol.* 49:12457-12464.
- Al Momani FA, Jarrah N, 2010. Treatment and kinetic study of cyanobacterial toxin by ozone. *J. Environ. Sci. Health A Tox. Hazard. Subst. Environ. Eng.* 45:719-731.
- Babica P, Kohoutek J, Blaha L, Adamovsky O, Marsalek B, 2006. Evaluation of extraction approaches linked to ELISA and HPLC for analyses of microcystin-LR, -RR and -YR in freshwater sediments with different organic material contents. *Anal. Bioanal. Chem.* 385:1545-1551.
- Babica P, Zurabian R, Kumar ER, Chopra R, Mianeci MJ, Park JS, Jasa L, Trosko JE, Upham BL, 2016a. Methoxychlor and vinclozolin induce rapid changes in intercellular and intracellular signaling in liver progenitor cells. *Toxicol. Sci.* 153:174-185.
- Babica P, Ctverackova L, Lencesova Z, Trosko JE, Upham BL, 2016b. Chemopreventive agents attenuate rapid inhibition of gap junctional intercellular communication induced by environmental toxicants. *Nutr. Cancer* 68: 827-837.
- Babica P, Sovadinova I, Upham BL, 2016c. Scrape loading / dye transfer, p. 133-144. In: M. Vinken and S. Johnstone (eds.), *Methods in molecular biology*. 1437. Gap Junction Protocols. Springer.
- Berry JP, Gibbs PDL, Schmale MC, Saker ML, 2009. Toxicity of cylindrospermopsin, and other apparent metabolites from *Cylindrospermopsis raciborskii* and *Aphanizomenon ovalisporum*, to the zebrafish (*Danio rerio*) embryo. *Toxicol* 53 289-299.
- Bláha L, Kapplová P, Vondráček J, Upham B, Machala M, 2002. Inhibition of gap-junctional intercellular communication by environmentally occurring polycyclic aromatic hydrocarbons. *Toxicol. Sci.* 6543-51.
- Bláha L, Babica P, Maršálek B, 2009. Toxins produced in cyanobacterial water blooms – toxicity and risks. *Interdiscip. Toxicol.* 2:36-41.
- Bláha L, Babica P, Hilscherová K, Upham BL, 2010. Inhibition of gap-junctional intercellular communication and activation of mitogen-activated protein kinases by cyanobacterial extracts - indications of novel tumor promoting cyanotoxins? *Toxicol* 55:126-134.
- Borenfreund E, Puermer JA, 1985. Toxicity determined in vitro by morphological alterations and neutral red absorption. *Toxicol. Lett.* 24:119-124.
- Brooke S, Newcombe G, Nicholson B, Klass G, 2006. Decrease in toxicity of microcystins LA and LR in drinking water by ozonation. *Toxicol* 48:1054-1059.
- Campos A, Vasconcelos V, 2010. Molecular mechanisms of microcystin toxicity in animal cells. *Int. J. Mol. Sci.* 11:268-287.
- Canovas-Jorda D, Louise J, Pistollato F, Zagoura D, Bremer S, 2014. Regenerative toxicology: the role of stem cells in the development of chronic toxicities. *Expert Opin. Drug Metab. Toxicol.* 10:39-50.
- Chen DN, Zeng J, Wang F, Zheng W, Tu WW, Zhao JS, Xu J, 2012. Hyperphosphorylation of intermediate filament proteins is involved in microcystin-LR-induced toxicity in HL7702 cells. *Toxicol. Lett.* 214:192-199.
- Clesceri LS, Greenberg AE, Eaton AD. 1998. Standard methods for examinations of water and wastewater. 20th edition, American Public Health Association, Washington DC: 1496 pp.
- Codd GA, Lindsay J, Young FM, Morrison LF, Metcalf JS. 2005. Cyanobacterial toxins, p. 1-23. In: J. Huisman, H. C. P. Matthijs and P. M. Visser (eds.), *Harmful cyanobacteria*. Springer.
- Daily A, Monks NR, Leggas M, Moscow JA, 2010. Abrogation of microcystin cytotoxicity by MAP kinase inhibitors and N-acetyl cysteine is confounded by OATPIB1 uptake activity inhibition. *Toxicol* 55:827-837.
- de la Cruz AA, Hiskia A, Kaloudis T, Chernoff N, Hill D, Antoniou MG, He X, Loftin K, O'Shea K, Zhao C, Pelaez M, Han C, Lynch TJ, Dionysiou DD, 2013. A review on cylindrospermopsin: the global occurrence, detection, toxicity and degradation of a potent cyanotoxin. *Environ. Sci. Proc. Imp.* 15:1979-2003.
- Dias E, Matos P, Pereira P, Batoreu MC, Silva MJ, Jordan P, 2010. Microcystin-LR activates the ERK1/2 kinases and stimulates the proliferation of the monkey kidney-derived cell line Vero-E6. *Toxicol. In Vitro* 24:1689-1695.
- DiDonato JA, Mercurio F, Karin M, 2012. NF-kappaB and the link between inflammation and cancer. *Immunol. Rev.* 246:379-400.
- El-Fouly MH, Trosko JE, Chang C-C, 1987. Scrape-loading and dye transfer. *Exp. Cell Res.* 168:422-430.
- Falconer IR, Humpage AR, 2005. Health risk assessment of cyanobacterial (blue-green algal) toxins in drinking water. *Int. J. Environ. Res. Public Health.* 2:43-50.
- Grosse Y, Baan R, Straif K, Secretan B, El Ghissassi F, Coglianò V, 2006. Carcinogenicity of nitrate, nitrite, and cyanobacterial peptide toxins. *Lancet Oncol.* 7:628-629.
- Hakulinen P, Maki-Paakkanen J, Naarala J, Kronberg L, Komulainen H, 2004. Potent inhibition of gap junctional intercellular communication by 3-chloro-4-(dichloromethyl)-5-hydroxy-2(5H)-furanone (MX) in BALB/c 3T3 cells. *Toxicol. Lett.* 151:439-449.
- Harke MJ, Steffen MM, Gobler CJ, Otten TG, Wilhelm SW, Wood SA, Paerl HW, 2016. A review of the global ecology, genomics, and biogeography of the toxic cyanobacterium, *Microcystis* spp. *Harmful Algae* 54:4-20.
- Herner HA, Trosko JE, Masten SJ, 2001. The epigenetic toxicity of pyrene and related ozonation byproducts containing an aldehyde functional group. *Environ. Sci. Technol.* 35: 3576-3583.
- Hiskia A, Dionysiou DD, Antoniou M, Kaloudis T, 2016. *Water Treatment for purification from cyanobacteria and cyanotoxins*. 1st ed. Wiley-Blackwell: 272 pp.
- Ibelings BW, Bormans M, Fastner J, Visser PM, 2016. CYANOCOST special issue on cyanobacterial blooms: synopsis - a critical review of the management options for their prevention, control and mitigation. *Aquat. Ecol.* 50:595-605.
- Kang KS, Wilson MR, Hayashi T, Chang CC, Trosko JE, 1996. Inhibition of gap junctional intercellular communication in normal human breast epithelial cells after treatment with pesticides, PCBs, and PBBs, alone or in mixtures. *Environ. Health Perspect.* 104:192-200.
- Kao CY, Oakley CS, Welsch CW, Chang CC, 1997. Growth requirements and neoplastic transformation of two types of normal human breast epithelial cells derived from reduction mammoplasty. *In vitro cellular & developmental biology. Animal* 33:282-288.

- Komatsu M, Furukawa T, Ikeda R, Takumi S, Nong Q, Aoyama K, Akiyama S, Keppler D, Takeuchi T, 2007. Involvement of mitogen-activated protein kinase signaling pathways in microcystin-LR-induced apoptosis after its selective uptake mediated by OATP1B1 and OATP1B3. *Toxicol. Sci.* 97: 407-416.
- Kuiper-Goodman T, Falconer I, Fitzgerald J. 1999. Human Health Aspects, p. 113-153. In: I. Chorus and J. Bartram (eds.), *Toxic cyanobacteria in water: A guide to their public health consequences, monitoring and management*. World Health Organization, Geneva, Switzerland.
- Laemmli UK, 1970. Cleavage of structural proteins during the assembly of the head of bacteriophage T4. *Nature* 227:680-685.
- Leusch FDL, Snyder SA, 2015. Bioanalytical tools: half a century of application for potable reuse. *Environmental Science: Water Res. Technol.* 1:606-621.
- Lezcano N, Sedan D, Lucotti I, Giannuzzi L, Vittone L, Andrinolo D, Mundina-Weilenmann C, 2012. Subchronic microcystin-LR exposure increased hepatic apoptosis and induced compensatory mechanisms in mice. *J. Biochem. Mol. Toxic.* 26:131-138.
- Liu J, Wang B, Huang P, Wang H, Xu K, Wang X, Xu L, Guo Z, 2016. Microcystin-LR promotes cell proliferation in the mice liver by activating Akt and p38/ERK/JNK cascades. *Chemosphere* 163:14-21.
- Luster-Teasley SL, Yao JJ, Herner HH, Trosko JE, Masten SJ, 2002. Ozonation of chrysene: evaluation of byproduct mixtures and identification of toxic constituent. *Environ. Sci. Technol.* 36:869-876.
- Luster-Teasley SL, Ganey PE, DiOrio M, Ward JS, Maleczka RE, Jr., Trosko JE, Masten SJ, 2005. Effect of byproducts from the ozonation of pyrene: biphenyl-2,2',6,6'-tetracarbaldehyde and biphenyl-2,2',6,6'-tetracarboxylic acid on gap junction intercellular communication and neutrophil function. *Environ. Toxicol. Chem.* 24:733-740.
- Madhukar BV, de Feijter Rupp HL, Trosko JE, 1996. Pulse treatment with the tumor promoter TPA delays the onset of desensitization response and prolongs the inhibitory effect on gap junctional intercellular communication of a rat liver epithelial cell line WB F-344. *Cancer Lett.* 106:117-123.
- Maier D, Blaha L, Giesy JP, Henneberg A, Kohler HR, Kuch B, Osterauer R, Peschke K, Richter D, Scheurer M, Triebkorn R, 2015. Biological plausibility as a tool to associate analytical data for micropollutants and effect potentials in wastewater, surface water, and sediments with effects in fishes. *Water Res.* 72:127-144.
- Masten SJ, Tian M, Upham BL, Trosko JE, 2001. Effect of selected pesticides and their ozonation by-products on gap junctional intercellular communication using rat liver epithelial cell lines. *Chemosphere* 44:457-465.
- Máthé C, Beyer D, M-Hamvas M, Vasas G, 2016. The effects of microcystins (cyanobacterial heptapeptides) on the eukaryotic cytoskeletal system. *Mini Rev. Med. Chem.* 16:1063-1077.
- McGorum BC, Pirie RS, Glendinning L, McLachlan G, Metcalf JS, Banack SA, Cox PA, Codd GA, 2015. Grazing livestock are exposed to terrestrial cyanobacteria. *Vet. Res.* 46:1-10.
- Meng G, Sun Y, Fu W, Guo Z, Xu L, 2011. Microcystin-LR induces cytoskeleton system reorganization through hyperphosphorylation of tau and HSP27 via PP2A inhibition and subsequent activation of the p38 MAPK signaling pathway in neuroendocrine (PC12) cells. *Toxicology* 290:218-229.
- Merel S, LeBot B, Clément M, Seux R, Thomas O, 2009. Ms identification of microcystin-LR chlorination by-products. *Chemosphere* 74:832-839.
- Merel S, Clément M, Thomas O, 2010. State of the art on cyanotoxins in water and their behaviour towards chlorine. *Toxicol.* 55:677-691.
- Merel S, Walker D, Chicana R, Snyder S, Baurès E, Thomas O, 2013. State of knowledge and concerns on cyanobacterial blooms and cyanotoxins. *Environ. Int.* 59:303-327.
- Miao H-F, Qin F, Tao G-J, Tao W-Y, Ruan W-Q, 2010. Detoxification and degradation of microcystin-LR and -RR by ozonation. *Chemosphere* 79:355-361.
- Moreira C, Azevedo J, Antunes A, Vasconcelos V, 2013. *Cylindrospermopsis*: occurrence, methods of detection and toxicology. *J. Appl. Microbiol.* 114:605-620.
- Mowe MAD, Mitrovic SM, Lim RP, Furey A, Yeo DCJ, 2014. Tropical cyanobacterial blooms: a review of prevalence, problem taxa, toxins and influencing environmental factors. *J. Limnol.* 74:1005.
- Neale PA, Antony A, Bartkow ME, Farre MJ, Heitz A, Kristiana I, Tang JY, Escher BI, 2012. Bioanalytical assessment of the formation of disinfection byproducts in a drinking water treatment plant. *Environ. Sci. Technol.* 46:10317-10325.
- Nebreda AR, Porras A, 2000. p38 MAP kinases: beyond the stress response. *Trends Biochem. Sci.* 25:257-260.
- Newcombe G, Nicholson B, 2004. Water treatment options for dissolved cyanotoxins. *J. Water Supply Res. Technol.* 53:227-239.
- Nicholson BC, Rositano J, Burch MD, 1994. Destruction of cyanobacterial peptide hepatotoxins by chlorine and chloramine. *Water Res.* 28:1297-1303.
- Nishikawa A, Sai K, Okazaki K, Son HY, Kanki K, Nakajima M, Kinai N, Nohmi T, Trosko JE, Inoue T, Hirose M, 2006. MX, a by-product of water chlorination, lacks in vivo genotoxicity in gpt delta mice but inhibits gap junctional intercellular communication in rat WB cells. *Environ. Mol. Mutagen.* 47:48-55.
- Nishiwaki-Matsushima R, Ohta T, Nishiwaki S, Suganuma M, Kohyama K, Ishikawa T, Carmichael WW, Fujiki H, 1992. Liver tumor promotion by the cyanobacterial cyclic peptide toxin microcystin-LR. *J. Cancer Res. Clin. Oncol.* 118:420-424.
- Novakova K, Babica P, Adamovsky O, Blaha L, 2011. Modulation of gap-junctional intercellular communication by a series of cyanobacterial samples from nature and laboratory cultures. *Toxicol.* 58:76-84.
- Novakova K, Blaha L, Babica P, 2012. Tumor promoting effects of cyanobacterial extracts are potentiated by anthropogenic contaminants-evidence from in vitro study. *Chemosphere* 89:30-37.
- Novakova K, Kohoutek J, Adamovsky O, Brack W, Krauss M, Blaha L, 2013. Novel metabolites in cyanobacterium *Cylindrospermopsis raciborskii* with potencies to inhibit gap junctional intercellular communication. *J. Hazard. Mater.* 262:571-579.
- Oberemm A, Fastner J, Steinberg CEW, 1997. Effects of microcystin-LR and cyanobacterial crude extracts on embryo-larval development of zebrafish (*Danio rerio*). *Water Res.* 31:2918-2921.
- Osgood RS, Upham BL, Hill T, Helms KL, Velmurugan K, Babica P, Bauer AK, 2014. Polycyclic aromatic hydrocarbon-induced signaling events relevant to inflammation and tumorigenesis in lung cells are dependent on molecular structure. *PLoS One* 8:e65150.

- Prasse C, Stalter D, Schulte-Oehlmann U, Oehlmann J, Ternes TA, 2015. Spoilt for choice: A critical review on the chemical and biological assessment of current wastewater treatment technologies. *Water Res.* 87:237-270.
- Rodriguez EM, Acero JL, Spool L, Meriluoto J, 2008. Oxidation of MC-LR and -RR with chlorine and potassium permanganate: Toxicity of the reaction products. *Water Res.* 42: 1744-1752.
- Roegner AF, Brena B, González-Sapienza G, Puschner B, 2014. Microcystins in potable surface waters: toxic effects and removal strategies. *J. Appl. Toxicol.* 34:441-457.
- Rosenkranz M, Rosenkranz HS, Klopman G, 1997. Intercellular communication, tumor promotion and non-genotoxic carcinogenesis: relationships based upon structural considerations. *Mutat. Res.* 381:171-188.
- Shawwa AR, Smith DW, 2001. Kinetics of microcystin-LR oxidation by ozone. *Ozone Sci. Eng.* 23:161-170.
- Sovadinova I, Babica P, Boke H, Kumar E, Wilke A, Park JS, Trosko JE, Upham BL, 2015. Phosphatidylcholine specific PLC-induced dysregulation of gap junctions, a robust cellular response to environmental toxicants, and prevention by resveratrol in a rat liver cell model. *PLoS One* 10:e0124454.
- Sun Y, Meng GM, Guo ZL, Xu LH, 2011. Regulation of heat shock protein 27 phosphorylation during microcystin-LR-induced cytoskeletal reorganization in a human liver cell line. *Toxicol. Lett.* 207:270-277.
- Svircev Z, Krstic S, Miladinov-Mikov M, Baltic V, Vidovic M, 2009. Freshwater cyanobacterial blooms and primary liver cancer epidemiological studies in Serbia. *J. Environ. Sci. Health C Environ. Carcinog. Ecotoxicol. Rev.* 27:36-55.
- Svircev Z, Baltic V, Gantar M, Jukovic M, Stojanovic D, Baltic M, 2010. Molecular aspects of microcystin-induced hepatotoxicity and hepatocarcinogenesis. *J. Environ. Sci. Health C Environ. Carcinog. Ecotoxicol. Rev.* 28:39-59.
- Trosko JE, Jone C, Chang CC, 1987. Inhibition of gap junctional-mediated intercellular communication in vitro by aldrin, dieldrin and toxaphene: a possible cellular mechanism for their tumor-promoting and neurotoxic effects. *Mol. Toxicol.* 1:83-94.
- Tsao MS, Smith JD, Nelson KG, Grisham JW, 1984. A diploid epithelial cell line from normal adult rat liver with phenotypic properties of 'oval' cells. *Exp. Cell Res.* 154:38-52.
- Tsuji K, Watanuki T, Kondo F, Watanabe MF, Nakazawa H, Suzuki M, Uchida H, Harada K-I, 1997. Stability of Microcystins from cyanobacteria - iv. effect of chlorination on decomposition. *Toxicol.* 35:1033-1041.
- Upham B, Masten SJ, Lockwood BR, Trosko JE, 1994. Nongenotoxic effects of polycyclic aromatic hydrocarbons and their ozonation by-products on the intercellular communication of rat liver epithelial cells. *Fundam. Appl. Toxicol.* 23 470-475.
- Upham BL, Yao JJ, Trosko JE, Masten SJ, 1995. Determination of the efficacy of ozone treatment systems using a gap junction intercellular communication bioassay. *Environ. Sci. Technol.* 29:2923-2928.
- Upham BL, Boddy B, Xing X, Trosko JE, Masten SJ, 1997. Non-genotoxic effects of selected pesticides and their disinfection by-products on gap junctional intercellular communication. *Ozone: Sci. Eng.* 19:351-369.
- Upham BL, Weis LM, Trosko JE, 1998. Modulated gap junctional intercellular communication as a biomarker of PAH epigenetic toxicity: structure-function relationship. *Environ. Health Perspect.* 106(Suppl 4):975-981.
- Upham BL, Guzvic M, Scott J, Carbone JM, Blaha L, Coe C, Li LL, Rummel AM, Trosko JE, 2007. Inhibition of gap junctional intercellular communication and activation of mitogen-activated protein kinase by tumor-promoting organic peroxides and protection by resveratrol. *Nutr. Cancer* 57:38-47.
- Upham BL, Blaha L, Babica P, Park JS, Sovadinova I, Pudrith C, Rummel AM, Weis LM, Sai K, Tithof PK, Guzvic M, Vondracek J, Machala M, Trosko JE, 2008. Tumor promoting properties of a cigarette smoke prevalent polycyclic aromatic hydrocarbon as indicated by the inhibition of gap junctional intercellular communication via phosphatidylcholine-specific phospholipase C. *Cancer Sci.* 99:696-705.
- Upham BL, Park JS, Babica P, Sovadinova I, Rummel AM, Trosko JE, Hirose A, Hasegawa R, Kanno J, Sai K, 2009. Structure-activity-dependent regulation of cell communication by perfluorinated fatty acids using in vivo and in vitro model systems. *Environ. Health Perspect.* 117:545-551.
- Upham BL, Sovadinova I, Babica P, 2016. Gap junctional intercellular communication: a functional biomarker to assess adverse effects of toxicants and toxins, and health benefits of natural products. *J. Vis. Exp.* 118:e54281.
- Vinken M, Doktorova T, Decrock E, Leybaert L, Vanhaecke T, Rogiers V, 2009. Gap junctional intercellular communication as a target for liver toxicity and carcinogenicity. *Crit. Rev. Biochem. Mol. Biol.* 44:201-222.
- Wagner EF, Nebreda AR, 2009. Signal integration by JNK and p38 MAPK pathways in cancer development. *Nat. Rev. Cancer* 9:537-549.
- Wang B, Liu J, Huang P, Xu K, Wang H, Wang X, Guo Z, Xu L, 2017. Protein phosphatase 2A inhibition and subsequent cytoskeleton reorganization contributes to cell migration caused by microcystin-LR in human laryngeal epithelial cells (Hep-2). *Environ. Toxicol.* 32:890-903.
- Wernersson A, Maggi C, Carere M, 2014. Technical report on aquatic effect-based monitoring tools. Office for Official Publications of the European Communities.
- Westrick JA, Szlag DC, Southwell BJ, Sinclair J, 2010. A review of cyanobacteria and cyanotoxins removal/inactivation in drinking water treatment. *Anal. Bioanal. Chem.* 397:705-1714.
- Wiegand C, Pflugmacher S, 2005. Ecotoxicological effects of selected cyanobacterial secondary metabolites a short review. *Toxicol. Appl. Pharmacol.* 203:201-218.
- Wu J, Lin L, Luan T, Chan Gilbert YS, Lan C, 2007. Effects of organophosphorus pesticides and their ozonation byproducts on gap junctional intercellular communication in rat liver cell line. *Food Chem. Toxicol.* 45:2057-2063.
- Yu SZ, 1995. Primary prevention of hepatocellular carcinoma. *J. Gastroenterol. Hepatol.* 10:674-682.
- Zanchett G, Oliveira-Filho E, 2013. Cyanobacteria and cyanotoxins: From impacts on aquatic ecosystems and human health to anticarcinogenic effects. *Toxins* 5:1896.
- Zegura B, Straser A, Filipic M, 2011. Genotoxicity and potential carcinogenicity of cyanobacterial toxins - a review. *Mutat. Res.* 727:16-41.
- Zhang J, Chen J, Xia Z, 2013. Microcystin-LR exhibits immunomodulatory role in mouse primary hepatocytes through activation of the NF-kappaB and MAPK signaling pathways. *Toxicol. Sci.* 136:86-96.
- Zhou L, Yu H, Chen K, 2002. Relationship between microcystin in drinking water and colorectal cancer. *Biomed. Environ. Sci.* 15 166-171.

XII. Babica, P.*, Čtveráčková, L., Lenčešová, Z., Trosko, J.E., Upham, B.L., 2016. Chemopreventive Agents Attenuate Rapid Inhibition of Gap Junctional Intercellular Communication Induced by Environmental Toxicants. *Nutrition and Cancer* 68, 827–837.

Chemopreventive Agents Attenuate Rapid Inhibition of Gap Junctional Intercellular Communication Induced by Environmental Toxicants

Pavel Babica^{a,b}, Lucie Čtveráčková^{a,b}, Zuzana Lenčešová^{a,b}, James E. Trosko^c, and Brad L. Upham^c

^aDepartment of Experimental Phycology and Ecotoxicology, Institute of Botany of the ASCR, Brno, Czech Republic; ^bRECETOX – Research Centre for Toxic Compounds in the Environment, Faculty of Science, Masaryk University, Brno, Czech Republic; ^cDepartment of Pediatrics and Human Development & Institute for Integrative Toxicology, Michigan State University, Michigan, USA

ABSTRACT

Altered gap junctional intercellular communication (GJIC) has been associated with chemical carcinogenesis, where both chemical tumor promoters and chemopreventive agents (CPAs) are known to conversely modulate GJIC. The aim of this study was to investigate whether attenuation of chemically inhibited GJIC represents a common outcome induced by different CPAs, which could be effectively evaluated using in vitro methods. Rat liver epithelial cells WB-F344 were pretreated with a CPA for either 30 min or 24 h, and then exposed to GJIC-inhibiting concentration of a selected tumor promoter or environmental toxicant [12-O-tetradecanoylphorbol-13-acetate (TPA), lindane, fluoranthene, 1,1,1-trichloro-2,2-bis(4-chlorophenyl)ethane (DDT), perfluorooctanoic acid (PFOA), or pentachlorophenol]. Out of nine CPAs tested, quercetin and silibinin elicited the most pronounced effects, preventing the dysregulation of GJIC by all the GJIC inhibitors, but DDT. Metformin and curcumin attenuated the effects of three GJIC inhibitors, whereas the other CPAs prevented the effects of two (diallyl sulfide, emodin) or one (indole-3-carbinol, thymoquinone) GJIC inhibitor. Significant attenuation of chemically induced inhibition of GJIC was observed in 27 (50%) out of 54 possible combinations of nine CPAs and six GJIC inhibitors. Our data demonstrate that in vitro evaluation of GJIC can be used as an effective screening tool for identification of chemicals with potential chemopreventive activity.

ARTICLE HISTORY

Received 13 August 2015
Accepted 8 February 2016

Introduction

Chemical exposure to environmental and food-borne contaminants has been commonly linked to the etiology of cancers (1). The underlying cellular processes, known to be critical for cancer development, are DNA alterations by genotoxic mechanisms during the initiation stage of cancer, or alterations of signal transduction pathways and gene expression patterns by nongenotoxic or epigenetic mechanisms, leading primarily to an increase in cell proliferation, inhibition of differentiation, inhibition of apoptosis, and inflammatory responses associated with tumor promotion and progression stages of cancer (2,3).

Conversely, chemical compounds can also counteract these carcinogenic processes, and thus function as cancer chemopreventive agents (CPAs), that is, natural or synthetic chemicals which inhibit, suppress, or reverse the development and progression of cancer (4). Phytochemicals and other natural products are important sources of CPAs, capable of targeting the different stages of the multistep carcinogenic process (5–7). Dietary intake of phytochemicals, thus, represents an important approach

to minimizing cancer risks in healthy individuals, mostly by preventing the tumor-initiating and promoting phases of cancer. The application of phytochemicals in the form of dietary supplements or pharmacological agents can be used for individuals with a high risk of cancer to prevent early phases of cancer, or even for patients in the late stages of cancer to aid chemopreventive, chemoprotective, and chemoquiescent effects in chemotherapy during cancer treatment and at the postcancer stage (5). In the effort to identify novel CPAs and to understand the mechanisms of their chemopreventive activity, plant-derived products and compounds are typically evaluated for their ability to modulate DNA repair, detoxification, free-radical scavenging, carcinogen metabolism, proliferation, angiogenesis, apoptosis, differentiation, inflammation, and immune responses, that is, alterations of biochemical and cellular processes connected to acquisition of phenotypic traits characteristic for cancer or transformed cells, so-called hallmarks of cancer (5–7).

CONTACT Pavel Babica  pavel.babica@centrum.cz  Department of Experimental Phycology and Ecotoxicology, Institute of Botany, Lidická 25/27, Brno, 60200, Czech Republic.

 Supplemental data for this article can be accessed at www.tandfonline.com/hnuc.

© 2016 Taylor & Francis Group, LLC

In addition to the traditionally recognized hallmarks of cancer, abnormal gap junctional intercellular communication (GJIC) has been documented as another phenotypic hallmark of cancer (8). GJIC facilitates direct exchange of essential signaling molecules and metabolites between adjacent cells, coordinates electrotonic and metabolic events in tissues, and provides the key mechanism of homeostatic regulation (8,9). Since cancer can be viewed as a disorder of homeostatic regulation, it is consistent with observations that GJIC is dysregulated in vivo or in vitro in response to oncogene activation, exposures to growth factors, or chemical tumor promoters (10–14). In different cancer or oncogene-transformed cell lines, CPAs have been reported to increase expression of gap junctional proteins connexin and/or enhance GJIC, which is typically accompanied by suppression of other phenotypic traits characteristic for cancer cells (9). Various plant-derived products and compounds were also found to prevent inhibition of GJIC, which was induced in normally communicating cells by tumor-promoting chemicals, such as hydrogen peroxide or model tumor promoters like 12-*O*-tetradecanoylphorbol-13-acetate (TPA) (9). CPAs, like quercetin, resveratrol, green tea, or tomato/grape seed extracts, were also reported to prevent inhibition of GJIC caused by several environmental toxicants, such as pentachlorophenol (15), pesticides (16–19), dimethylnitrosamine (20), mercury (21,22), organic peroxides (23), and perfluorooctanoic acid (PFOA) (24).

Thus, prevention of chemically induced inhibition of GJIC might represent an important mechanism contributing to the chemopreventive effects of CPAs. Modulation of GJIC might be relevant, especially during the tumor promotion phase of cancer, where the tumor-promoting activity of environmental and food toxicants could be counteracted by co-exposure to CPAs from diet or dietary supplements and reduce the risks of cancer. In vitro evaluation of the ability of chemicals to prevent inhibition of GJIC could then be a very effective approach for rapid identification of agents with biological activities relevant for cancer chemoprevention and suppression. However, there is a lack of studies systematically looking at the effects of different CPAs on GJIC inhibition induced by different environmental toxicants in vitro (9). Therefore, the aim of this study was to investigate whether chemicals with known chemopreventive activity, but limited knowledge regarding their effects on GJIC, would be able to prevent inhibition of GJIC induced in vitro by tumor promoters and environmental toxicants.

We investigated nine commercially available chemicals previously implicated in cancer chemoprevention (5–7): polyphenols, quercetin, silibinin, and curcumin;

simple phenol, indole-3-carbinol; quinones, thymoquinone, and emodin; unsaturated aromatic carboxylic acid, cinnamic acid; organosulfur compound, diallyl sulfide; and an antidiabetic drug, biguanide metformin. These selected CPAs were evaluated for their ability to prevent inhibition of GJIC induced in vitro in rat liver epithelial cells, WB-F344, by six different tumor promoters and/or environmental toxicants with different mechanism of GJIC inhibition (25): TPA, lindane, 1,1,1-trichloro-2,2-bis(4-chlorophenyl)ethane (DDT), fluoranthene, PFOA, and pentachlorophenol. Results of this study suggest that the attenuation of chemically induced inhibition of GJIC represents a typical but signal transduction pathway-specific effect of CPAs, which could be easily evaluated in vitro and utilized as an effective screening tool for identification of chemicals with chemopreventive activity.

Materials and methods

Chemicals

All chemicals, including all GJIC inhibitors (i.e., TPA, DDT, fluoranthene, lindane, pentachlorophenol, and PFOA) and CPAs (cinnamic acid, curcumin, diallyl sulfide, emodin, indole-3-carbinol, metformin, quercetin, silibinin, and thymoquinone), lucifer yellow, neutral red (NR), dimethylsulfoxide (DMSO), glucose, formaldehyde, inorganic salts for preparation of phosphate-buffered saline [PBS and PBS supplemented with 0.68 mM calcium chloride and 0.49 mM magnesium chloride (CaMgPBS)] and culture medium preparation were purchased from Sigma-Aldrich (St. Louis, MO, USA). Acetonitrile, acetic acid, and ethanol were obtained from Lachner (Neratovice, Czech Republic). Stock solutions of GJIC inhibitors were prepared in acetonitrile except TPA, which was dissolved in ethanol. CPAs were dissolved in DMSO. All aqueous solutions were prepared using Milli-Q water produced with a Millipore Synergy water production device (Merck Millipore, Billerica, MA, USA).

Cell culture

WB-F344 rat liver epithelial nontumorigenic cells were obtained from Drs. Grisham and Tsao, University of North Carolina (26). The cells were grown in a so-called CCD medium (C. C. Chang's D-medium) developed by C. C. Chang (27). CCD medium was prepared from Eagle's Minimum Essential Medium (MEM) (Formula M3024, Sigma-Aldrich) supplemented with 1 g/l sodium bicarbonate, 7.635 g/l sodium chloride, 1 mM sodium pyruvate (Gibco, Life Technologies, Carlsbad, CA, USA), 2 mM L-glutamine (Gibco), with concentrations of all

vitamins and essential amino acids increased 1.5 times by addition of Gibco's MEM vitamin solution and MEM essential amino acids solution, and concentrations of all nonessential amino acids were increased two times by addition of Gibco's MEM nonessential amino acids solution. All components were dissolved in Milli-Q water, and the medium was sterilized by filtration through a polyethersulfone filter with a pore size $0.1\ \mu\text{m}$ (VWR Int., Radnor, PA, USA) and then supplemented with 5% (vol/vol) fetal bovine serum (Biochrom S0615, Merck Millipore). The cells were routinely cultured in $75\ \text{cm}^2$ tissue culture flasks (TPP, Trasadingen, Switzerland) in a humidified 5% CO_2 atmosphere at 37 C, and passaged every other day using trypsin-ethylenediaminetetraacetic acid (Life Technologies) for cell detachment.

GJIC evaluation

WB-F344 cells were seeded at a density of $20\text{--}40 \times 10^3$ cell/ cm^2 on 35-mm-diameter tissue culture Petri dishes (Sterilin, Newport, UK) and cultured for 48 or 72 h to reach complete confluence before the addition of the chemical. Confluent cultures were exposed to the selected CPA or DMSO for 30 min or 24 h, followed directly by the addition of a tumor promoter, environmental toxicant, or corresponding solvent (acetonitrile or ethanol) for 15 min. In addition to solvent controls, a negative control of cells not treated with any chemical was included in each experiment to account for solvent effects, where solvent concentrations did not exceed 1% (vol/vol). All chemicals selected as inhibitors of GJIC were previously shown to induce rapid dysregulation of cell-cell communication, and their effects on GJIC occurring within 10–30 min of exposure were shown to be mediated via different signal transduction mechanisms: TPA and lindane inhibited GJIC via mitogen-activated protein kinase-extracellular receptor kinase 1/2 (MAPK-ERK1/2)-dependent mechanism, fluoranthene, and DDT through a phosphatidylcholine-specific phospholipase C (PC-PLC)-dependent mechanism, PFOA through a mixed, both ERK1/2 and PC-PLC-dependent mechanism, and pentachlorophenol via mechanism independent of ERK1/2 and PC-PLC (25). In order to evaluate the ability of CPAs to target the specific signal transduction pathway implicated in the mechanism of rapid dysregulation of GJIC induced by a given inhibitor, we focused on the attenuation of GJIC after 15 min of exposure to a GJIC inhibitor. The scalpel loading-dye transfer (SL-DT) technique used for the evaluation of GJIC was adapted after the scrape-loading method (28) and carried out according to the previously published protocol (29). Briefly, the

exposed cells were washed three times with CaMgPBS. Then 1 mg/ml of lucifer yellow dilithium salt diluted in CaMgPBS was added to the cells. By gently pressing the surgical scalpel blade against the dish bottom, the lucifer yellow was introduced into the cell monolayer (three parallel scalpel injections were made per dish). The dye was allowed to diffuse through gap junctions for 3 min, followed by a thorough rinse of cells with CaMgPBS and a fixation step with a 4% (vol/vol) formaldehyde solution in PBS. A representative microscopic image of the lucifer yellow dye transfer was taken from each cut at $200\times$ magnification using an Olympus IX51 microscope equipped with DP72 CCD camera (Olympus, Hamburg, Germany). The extent of GJIC was evaluated using ImageJ (version 1.50e) software as an area of the cells stained with lucifer yellow dye. The average fluorescence area in the positive control treated with $70\ \mu\text{M}$ fluoranthene for 15 min was subtracted from each treatment. The adjusted areas of individual treatments were compared with the adjusted area of the vehicle control and expressed as a percentage of GJIC in vehicle control (% control). Each experiment was repeated at least three times independently.

Cell viability assay

WB-F344 cells were seeded onto 96-well microplates (TPP) at the same seeding densities as for GJIC evaluation and cultured for 48–72 h to reach confluence. The selected CPAs or DMSO (max. 1%, vol/vol) were then added to the cells and incubated for 1 or 24 h. The effects of chemicals on cell viability were evaluated using the NR uptake assay. A solution of $150\ \mu\text{g/ml}$ NR dye, that is, 3-amino-7-(dimethylamino)-2-methylphenazine hydrochloride, in a serum-free culture medium was prepared, equilibrated in a CO_2 incubator, and filtered through a $0.22\ \mu\text{m}$ polyethersulfone syringe filter (Merck Millipore). Cells were rinsed twice with PBS, NR solution was added, and the cells were incubated for 1 h in a CO_2 incubator to allow dye uptake. After incubation, the cells were rinsed three times with PBS to remove extracellular NR. Intracellular NR was extracted from the cells by the addition of 1% glacial acetic acid in 50% ethanol. After 15 min of incubation on an orbital shaker, the absorbance was measured at 540 nm (reference wavelength = 690 nm) using a TECAN Genios spectrophotometer (TECAN, Männedorf, Switzerland). After subtraction of the blank value, NR dye uptake in an individual treatment was compared with negative control and expressed as percentage of viability. Each experiment was carried out in triplicate and repeated at least three times independently.

Results

Selection of CPA concentration for experiments with GJIC inhibitors

In the first set of experiments, effects of the selected CPAs on viability of WB-F344 cells was evaluated (Figure 1) along with their effects on GJIC (Figure S1). This was done to establish a suitable concentration that was neither cytotoxic nor inhibitory of GJIC. Curcumin, emodin, and thymoquinone induced the most pronounced cytotoxic effects, when a significant decrease of cell viability was elicited after a 1 h exposure to concentrations of $>50 \mu\text{M}$, with even more pronounced effects observed after 24 h exposure (Figure 1B, D, I). Emodin and curcumin also inhibited GJIC (Figure S1A). Concentrations of $1 \mu\text{M}$ curcumin and $10 \mu\text{M}$ of emodin and thymoquinone were found to be both nontoxic (Figure 1B, D, I) and noninhibitory of GJIC (Figure S1B) up to a 24 h exposure and thus selected for experiments with the GJIC inhibitors. Quercetin and silibinin at $100 \mu\text{M}$ concentration reduced neither cell viability (Figure 1G, H) nor GJIC (Figure S1B) after 1 h exposure, and were used for a 30 min pretreatment. However, a $100 \mu\text{M}$ concentration of silibinin and quercetin was cytotoxic after 24 h exposure, which was manifested by silibinin-induced decrease of the NR dye uptake (Figure 1H) and quercetin-induced increase of cell membrane permeability leading to extensive cell staining with lucifer yellow in SL-DT assays (data not shown). Concentrations of $50 \mu\text{M}$ silibinin and $25 \mu\text{M}$ quercetin were found to be noncytotoxic and used for 24 h cell pretreatment. Similarly to quercetin, indole-3-carbinol did not decrease NR dye uptake (Figure 1E), but at concentrations $>25 \mu\text{M}$ it increased permeability of the cell membrane for lucifer yellow in SL-DT assay (data not shown). Indole-3-carbinol at a concentration of $10 \mu\text{M}$ was not observed to induce any effect in SL-DT assay (Figure S1B) and thus selected for further experiments. Cinnamic acid, diallyl sulfide, and metformin did not affect cell viability (Figure 1A, C, F) or GJIC at concentrations up to 5 mM. The final concentrations of these CPAs were selected in preliminary experiments with GJIC inhibitor lindane (data not shown). The final summary of concentrations of CPAs used for experiments with GJIC inhibitors is given in Table 1.

Selection of GJIC inhibitor concentration

The selected tumor promoters and environmental toxicants rapidly inhibited GJIC within 15 min exposure (Figure S2). The lowest concentrations of GJIC inhibitors sufficient to repeatedly induce nearly complete inhibition

of GJIC ($<20\%$) were used for experiments with CPAs, as indicated in Figure S2 and summarized in Table 1.

Effects of CPAs on chemically induced inhibition of GJIC

Median GJIC levels in the cells treated with a GJIC inhibitor alone were compared with median GJIC levels in the cells first pretreated with CPAs and then treated with the GJIC inhibitor. The observed differences (ΔGJIC) ranged from slightly negative or positive values ($\Delta\text{GJIC} <10\%$), indicating none or only a weak effect, up to 78%, which corresponds to almost complete prevention of GJIC inhibition (Table 1). Out of the 54 different combinations of nine CPAs with six GJIC inhibitors, at least mild ($\Delta\text{GJIC} >10\%$) and statistically significant ($P \leq 0.05$) attenuation of GJIC inhibition by CPA pretreatment was observed for 24 unique combinations of a specific CPA and GJIC inhibitor. Such a significant preventive effect was observed for 20 different pairs of CPA-GJIC inhibitor in the case of 30 min pretreatment with a CPA, and for 11 different pairs in the case of 24 h pretreatment (Table 1).

CPAs elicited the most pronounced effects on inhibition of GJIC induced by lindane, when all CPAs significantly attenuated effects of lindane after 30 min pretreatment (Figure 2A). However, these preventive effects became less frequent and pronounced with prolonged time of CPA pretreatment, where only quercetin and silibinin induced significant effects, but weaker than the 30 min pretreatment (Figure 2A). Quercetin and silibinin were also the only CPAs showing significant effects on TPA-induced inhibition of GJIC, again with more pronounced effects observed after a 30 min pretreatment in comparison with the 24 h incubation with CPA (Figure 2B). A similar pattern was observed for PFOA, where attenuation of GJIC inhibition by quercetin, silibinin, and also curcumin was apparent only in the 30 min pretreatment, but neither CPA elicited significant effects after a 24 h pretreatment (Figure 2C).

Also inhibition of GJIC induced by pentachlorophenol was prevented more efficiently by a 30 min pretreatment with curcumin and metformin, whereas the effects of quercetin and silibinin were comparable for both 30 min and 24 h pretreatment (Figure 2D).

A different pattern was observed in experiments with fluoranthene and DDT, where attenuation of GJIC inhibition was more frequent when the cells were exposed to CPAs for 24 h (Figure 2E, F). Effects of fluoranthene on GJIC were prevented by a 24 h pretreatment with curcumin, diallyl sulfide, emodin, quercetin, and silibinin, whereas a 30 min pretreatment modulated fluoranthene-induced inhibition of GJIC only with quercetin and silibinin (Figure 2E). Similarly, GJIC inhibition by DDT

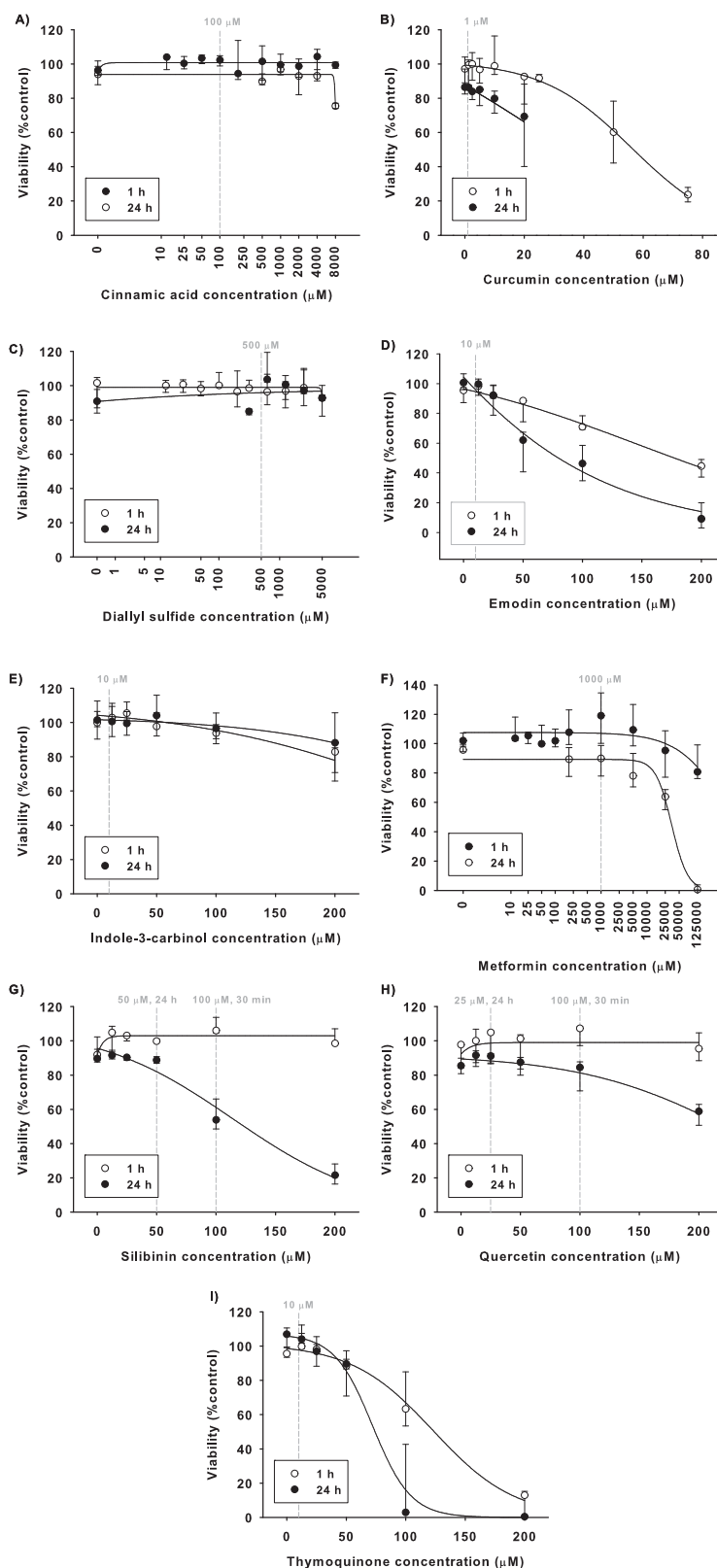


Figure 1. Effects of chemopreventive agents (CPAs) on viability of WB-F344 cells. WB-F344 cells were treated for 1 or 24 h with CPAs: (A) Cinnamic acid, (B) Curcumin, (C) Diallyl sulfide, (D) Emodin, (E) Indole-3-carbinol, (F) Metformin, (G) Silibinin, (H) Quercetin, and (I) Thymoquinone. The cell viability was evaluated using the neutral red uptake assay and the results were expressed as % of the negative control. Data represent medians (circles) with interquartile ranges (error bars) of at least three independent experiments. Sigmoidal regression was used to plot the concentration-response curves. Dashed vertical lines indicate concentrations selected for experiments with GJIC inhibitors.

Table 1. Difference between GJIC level in WB-F344 cells treated and nontreated with a CPA before the addition of a GJIC inhibitor (Δ GJIC).

Chemical	Concentration (μ M)	Pretreatment time	Δ GJIC ^{a,b} = M[GJIC _{(w/o CPA)+(GJIC inhibitor)] - M[GJIC_{(w/o CPA)+(GJIC inhibitor)}]}											
			-GJIC inhibitor (15 min)					+GJIC inhibitor (15 min)						
			ERK1/2-dependent ^c		ERK1/2 and PC-PLC-dependent		ERK1/2 and PC-PLC-independent		Fluoranthene (50 μ M)		DDT (25 μ M)			
			Lindane (70 μ M)	TPA (7.5 nM)	PFOA (100 μ M)	Pentachlorophenol (70 μ M)	Fluoranthene (50 μ M)	DDT (25 μ M)						
Cinnamic acid	100	30 min	47 (***P = 0.001) ^d	9 (P = 0.244)	3 (P = 0.116)	4 (P = 0.725)	1 (P = 0.66)	-1 (P = 0.608)						
Curcumin	1		38 (**P = 0.004)	1 (P = 0.525)	34 (**P = 0.002)	15 (P = 0.05)	-1 (P = 0.367)	0 (P = 0.788)						
Diallyl sulfide	500		47 (***P = 0.001)	-3 (P = 0.169)	6 (P = 0.19)	4 (P = 0.34)	5 (P = 0.159)	0 (P = 0.606)						
Emodin	10		27 (***P = 0.001)	3 (P = 0.672)	-2 (P = 0.489)	-7 (P = 0.063)	-1 (P = 0.705)	3 (P = 0.36)						
Indole-3-carbinol	10		41 (***P < 0.001)	10 (P = 0.194)	-1 (P = 0.584)	-3 (P = 0.58)	0 (P = 1)	2 (P = 0.909)						
Metformin	1000		27 (**P = 0.004)	-2 (P = 0.672)	6 (P = 0.328)	14 (P = 0.031)	8 (P = 0.075)	0 (P = 0.492)						
Quercetin	100		69 (***P < 0.001)	27 (**P = 0.008)	43 (***P < 0.001)	29 (***P = 0.008)	19 (***P = 0.009)	0 (P = 0.762)						
Silibinin	100		78 (***P = 0.001)	25 (P = 0.011)	58 (***P = 0.001)	19 (P = 0.05)	26 (***P = 0.002)	1 (P = 0.34)						
Thymoquinone	10		48 (***P < 0.001)	4 (P = 0.823)	5 (P = 0.171)	8 (P = 0.097)	0 (P = 0.982)	0 (P = 0.775)						
Cinnamic acid	100	24 h	-6 (P = 0.351)	-1 (P = 0.525)	-3 (P = 0.133)	-7 (P = 0.119)	1 (P = 0.279)	11 (P = 0.012)						
Curcumin	1		4 (P = 0.601)	1 (P = 0.832)	1 (P = 0.685)	-3 (P = 0.802)	7 (P = 0.013)	0 (P = 0.689)						
Diallyl sulfide	500		1 (P = 0.599)	2 (P = 1)	-2 (P = 0.353)	-7 (P = 0.031)	7 (P = 0.039)	30 (***P = 0.005)						
Emodin	10		3 (P = 0.501)	2 (P = 0.112)	6 (P = 0.121)	4 (P = 0.88)	17 (***P = 0.007)	2 (P = 0.541)						
Indole-3-carbinol	10		-2 (P = 0.57)	-1 (P = 1)	5 (P = 0.617)	6 (P = 0.58)	4 (P = 0.132)	9 (P = 0.457)						
Metformin	1000		2 (P = 0.699)	6 (P = 0.138)	0 (P = 0.867)	5 (P = 0.898)	9 (P = 0.066)	26 (***P = 0.005)						
Quercetin	25		42 (***P = 0.001)	15 (P = 0.015)	3 (P = 0.263)	39 (***P = 0.006)	38 (***P = 0.002)	5 (P = 0.039)						
Silibinin	50		26 (P = 0.028)	6 (P = 0.044)	-2 (P = 0.584)	13 (***P = 0.01)	24 (***P = 0.002)	1 (P = 0.391)						
Thymoquinone	10		-9 (P = 0.285)	-3 (P = 0.459)	8 (P = 0.121)	4 (P = 0.802)	0 (P = 0.33)	9 (P = 0.423)						

CPA, chemopreventive agent; GJIC, gap junctional intercellular communication; TPA, 12-O-tetradecanoyl-phorbol-13-acetate; DDT, 1,1,1-trichloro-2,2-bis(4-chlorophenyl)ethane; PFOA, perfluorooctanoic acid.

^a Δ GJIC was calculated as a difference between a median (M) value of GJIC (%control) obtained from experiments with a selected CPA and a given GJIC inhibitor, where the cells were pretreated for 30 min or 24 h with a selected CPA and then treated with GJIC inhibitor, that is, (M[GJIC_{(w/o CPA)+(GJIC inhibitor)]), and a median value from experiments with a given GJIC inhibitor, where the cells were not pretreated with CPA, that is, (M[GJIC_{(w/o CPA)+}}

(GJIC inhibitor)]).

^bShading indicates intensity of GJIC attenuation: none or weak effect (Δ GJIC \leq 10%), mild effect (Δ GJIC > 10 and \leq 25%), moderate effect (Δ GJIC > 25 and \leq 50%), strong effect (Δ GJIC > 50%).^cMechanism of GJIC inhibition, <comp: ensure to maintain the proper shading throughout table>^dSignificance of differences between GJIC in the cells treated and nontreated with a CPA before the addition of a GJIC inhibitor was determined by Mann-Whitney U-test, P values are given in parentheses and labeled with asterisks*P \leq 0.05 **P \leq 0.01 ***P \leq 0.001.

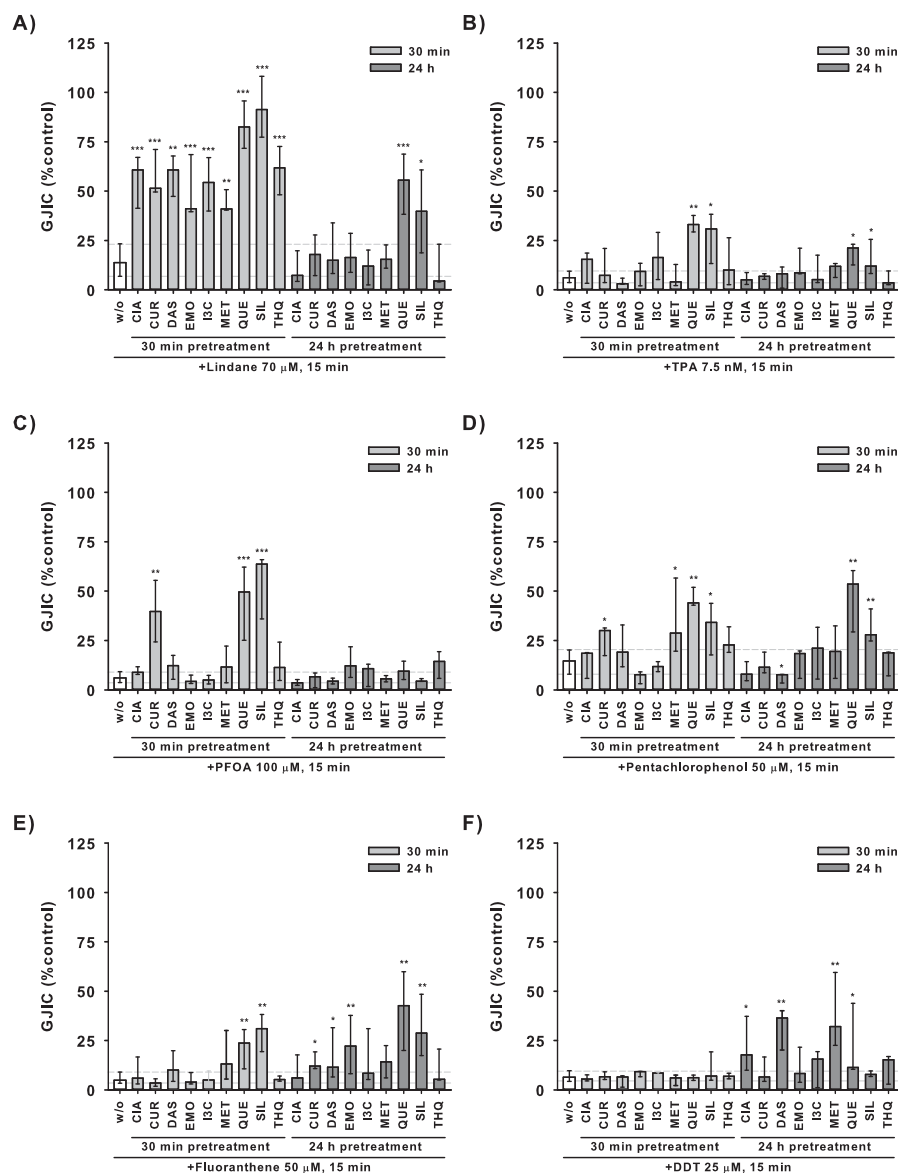


Figure 2. Effects of chemopreventive agents (CPAs) on chemically-induced inhibition of gap junctional intercellular communication (GJIC) in WB-F344 cells. WB-F344 cells were either not pretreated (w/o) or pretreated with different CPAs for 30 min or 24 h, then treated with an inhibitor of GJIC for 15 min: (A) Lindane, (B) TPA = 12-O-tetradecanoyl-phorbol-13-acetate, (C) PFOA = perfluorooctanoic acid, (D) Pentachlorophenol, (E) Fluoranthene, (F) DDT = 1,1,1-trichloro-2,2-bis(4-chlorophenyl)ethane. Concentrations of CPAs were 100 μ M for cinnamic acid (CIA), 1 μ M for curcumin, 500 μ M for diallyl sulfide (DAS), 10 μ M for emodin (EMO), indole-3-carbinol (I3C), 1000 μ M for metformin (MET), 100 μ M (30 min) or 25 μ M (24 h) for quercetin (QUE), 100 μ M (30 min) or 50 μ M (24 h) for silibinin (SIL), 10 μ M for thymoquinone (THQ). GJIC was evaluated using scalpel loading-dye transfer assay and expressed as % of the vehicle control. Data represent medians (bars) and interquartile ranges (error bars) of at least three independent experiments. Dashed horizontal lines indicate interquartile range of the treatment with GJIC inhibitor only (w/o). Values significantly different from the treatment with GJIC inhibitor only are labeled by asterisks (Mann-Whitney test, * $P \leq 0.05$, ** $P \leq 0.01$, *** $P \leq 0.001$).

was prevented by a 24 h pretreatment with cinnamic acid, diallyl sulfide, metformin, and weakly by quercetin, while DDT effects were not altered by any CPA after a 30 min pretreatment (Figure 2F).

When comparing effects of individual CPAs, quercetin and silibinin were found to attenuate the effects of all GJIC inhibitors by more than 10% (Table 1), with the exception of DDT, where only quercetin effects were

observed (Table 1, Figure 2F). Curcumin and metformin each prevented GJIC inhibition induced by three different chemicals (Table 1). Pretreatment for 30 min with either curcumin or metformin prevented GJIC inhibition induced by either lindane or pentachlorophenol (Figure 2A, D). In addition, a 30 min pretreatment with curcumin significantly blocked GJIC inhibition induced by PFOA (Figure 2C), whereas a 24 h pretreatment with

metformin altered DDT-induced inhibition of GJIC (Figure 2F). Cinnamic acid, diallyl sulfide, and emodin prevented effects of two GJIC inhibitors. In addition to the effects of these CPAs in experiments with lindane (30 min pretreatment, Figure 2A), cinnamic acid and diallyl sulfide also attenuated GJIC inhibition induced by DDT (24 h pretreatment, Figure 2F), whereas a 24 h pretreatment with emodin prevented GJIC inhibition induced by fluoranthene (Figure 2E). Indole-3-carbinol and thymoquinone elicited effects only against lindane-induced inhibition of GJIC after a 30 min pretreatment (Table 1, Figure 2A).

Discussion

Altered connexin expression and function have been found to play a critical role in carcinogenesis, where chronic inhibition of GJIC seem to represent an essential step required for tumor promotion and progression of initiated cells (9–13). Chronic exposure to environmental toxicants inducing the inhibition of GJIC probably represents a very important process involved in the tumor promotion phase of cancer (1,14), whereas prevention of GJIC inhibition seems to be crucial for preventing chemically induced tumor promotion (15,30) and might be one of the key mechanisms contributing to the potential chemopreventive activity of CPAs. In fact, various plant-derived products and compounds were reported to prevent inhibition of GJIC induced by model tumor promoters (e.g., hydrogen peroxide, TPA, butylated hydroxytoluene, or phenobarbital), but the effects of CPAs on the inhibition of GJIC elicited by environmentally relevant toxicants are much less understood (9).

From the set of CPAs evaluated in this study, attenuation of GJIC inhibition induced by hydrogen peroxide or TPA has been reported only for quercetin (16,31,32), indole-3-carbinol (33), and curcumin derivatives (34), whereas curcumin did not prevent TPA-induced inhibition of GJIC (35). Quercetin was also found to prevent inhibition of GJIC induced by DDT (16), but the ability of these CPAs to attenuate the effects of other GJIC inhibitors represent a novel finding of this study.

The other investigated CPAs, cinnamic acid, diallyl sulfide, emodin, silibinin, and thymoquinone represent phytochemicals well-recognized for their antioxidative and chemopreventive activity (5–7), but there is a lack of information on their possible effects on connexins or GJIC. Similarly, a widely used antidiabetic drug, metformin, which is structurally related to French lilac biguanides, has been recently implicated in cancer chemoprevention (36,37), but its effects on chemically induced inhibition of GJIC by environmental toxicants have not been specifically addressed so far. Our study

thus provides the very first information that prevention of the chemically induced inhibition of GJIC could be involved in the chemopreventive effects of these CPAs. Importantly, these effects relevant to cancer chemoprevention were elicited in rat liver epithelial cells, which possess characteristics of oval cells, that is, multipotent progenitors of hepatocytes and biliary duct cells, known to play a crucial role in hepatocarcinogenesis (12,13,38). Thus, CPAs can not only revert or suppress the phenotype of a cell which has already progressed into a neoplastic or malignant stage, but they can also directly counteract chemically induced tumor-promoting events such as the inhibition of GJIC in the not-yet-tumorigenic precursors of cancer cells. Such mechanisms relevant for environmental and food toxicant-induced tumor-promoting events are especially interesting from the whole chemoprevention perspective, since tumor promotion represents the rate-limiting step of carcinogenesis, which can be probably most effectively targeted via dietary intake of CPAs.

In summary, all CPAs investigated in this study were found to attenuate inhibition of GJIC induced by one or more environmental toxicants. Statistically significant effect on GJIC was observed in 50% of the evaluated combinations of CPA pretreatment/GJIC inhibitor treatment. These results indicate that *in vitro* evaluation of phytochemical or natural product effects on chemically induced inhibition of GJIC can be used as an effective tool suitable for *in vitro* screening for novel compounds with chemopreventive activity. The effects of CPAs were elicited by concentrations which were lower by factor of 2 or higher than the lowest concentration found to decrease cell viability or induce morphological or membrane-permeability changes in WB-F344 cells. Thus, the observed effects of CPAs were most likely mediated by modulations of specific biochemical and signaling events, rather than by eventual cytotoxic stress reaction to CPAs, which might possibly interfere with the action of GJIC inhibitors. Indeed, our experiments revealed that attenuation of chemically induced inhibition of GJIC does not seem to be a general activity shared by all different CPAs, since there were substantial qualitative and quantitative differences in the ability of individual CPAs to attenuate the effects of different chemicals inhibiting GJIC through different mechanisms.

Antioxidative activity has been implicated as the principal mechanism responsible for prevention of hydrogen peroxide-dependent inhibition of GJIC by different CPAs (31,39–41). Such activity could explain also the observed attenuation of lindane-induced inhibition of GJIC in this study, since all investigated CPAs have been associated with antioxidative activity and with reduction of oxidative stress. Moreover,

lindane was found to inhibit GJIC via the MAPK-ERK1/2 pathway activated through a redox-dependent mechanism (25,42,43). However, despite sharing a similar ERK1/2-dependent mechanism of GJIC inhibition with lindane (25,44), the effects of TPA on GJIC are most likely not dependent on formation of free radicals (45,46). Therefore, a different mechanism was probably responsible for the preventive effects of quercetin and silibinin. PFOA inhibits GJIC through MAPK-ERK1/2 and PC-PLC-dependent pathways and antioxidants including resveratrol, *N*-acetylcysteine, and 2-ascorbic acid prevent this inhibition (24,25).

Such an implication of the redox-dependent mechanism of GJIC inhibition suggested that the investigated CPAs would prevent PFOA-induced inhibition of GJIC due to their antioxidative activity, as observed in lindane-induced inhibition of GJIC. However, only three CPAs, namely quercetin, silibinin, and curcumin, prevented inhibition of GJIC by PFOA. Thus, these effects could be due to modulations of specific mechanisms of redox signaling regulating GJIC rather than due to non-specific antioxidative activities. Since the effects of CPAs on ERK1/2-dependent or codependent inhibitors of GJIC, that is, TPA, lindane, and PFOA, were manifested already after 30 min pretreatment with a CPA, this indicates that attenuation of GJIC inhibition was mediated via rapid biochemical and molecular mechanisms, probably involving not only modulations of redox signaling or oxidative stress, but also interactions of CPAs with cellular receptors or signal transduction enzymes controlling GJIC. Such rapid mechanisms could be responsible for the effects of metformin and curcumin on GJIC dysregulation caused by pentachlorophenol, which inhibits GJIC via a mechanism independent of ERK1/2 and PC-PLC activity (25). Significant effects observed after 30 min pretreatment with CPAs usually had a transient character and became less pronounced or diminished with prolonged 24 h incubation with a CPA.

However, significant effects of quercetin and silibinin on GJIC inhibition induced by pentachlorophenol or fluoranthene, a PC-PLC-dependent inhibitor of GJIC (25), remained similar or became even more pronounced with an increase of the pretreatment time with a CPA at 24 h. The mechanisms underlying chemopreventive effects, manifested after 24 h incubation with a CPA, included probably more permanent modulations of processes and signal transduction pathways responsible for GJIC dysregulation, possibly involving altered expression of genes involved in gap junction assembly and GJIC control. Moreover, one needs to consider metabolism, transformation, or degradation of the tested compounds during the incubation, since transformation products of

CPAs might elicit different activities or target different biochemical and molecular events than the parental compounds, and eventually become responsible for the observed differences between 30 min and 24 h pretreatments with CPAs. Therefore, future studies should focus on further characterization of pharmacokinetics and pharmacodynamics of the individual CPAs in relation to their effects on GJIC. Interestingly, 24 h pretreatment with CPAs induced more pronounced attenuation of GJIC in comparison with 30 min pretreatment almost exclusively in the case of GJIC inhibition elicited by ERK1/2-independent but PC-PLC-dependent inhibitors, namely DDT and fluoranthene (25). GJIC dysregulation induced by these toxicants was most effectively attenuated by 24 h pretreatment with cinnamic acid, diallyl sulfide, emodin, metformin, quercetin, or silibinin. Since the same CPAs were observed to attenuate also ERK1/2-dependent inhibitors, but more effectively after a 30 min pretreatment, it indicates that the same CPA can protect GJIC inhibition induced via multiple mechanisms. These observations support the previous findings of Sovadinova et al. from experiments with resveratrol (25), and strongly suggest that attenuation of chemically induced inhibition of GJIC is probably a very specific outcome depending on CPA-induced biochemical and molecular events and their specific interactions and cross-talks with signal transduction pathways dysregulating GJIC in response to a GJIC inhibitor. Finally, these studies demonstrate that there will be few, if any, “universal” CPAs against all cancers. However, in vitro assessment of CPA effects on chemically induced inhibition of GJIC can provide mechanistic clues to their chemopreventive effects, and thus represents a possible tool not only for rapid identification of novel chemopreventive compounds, but also for further characterization of mechanisms responsible for their chemopreventive activity.

Funding

This research was supported by the Czech Ministry of Education grant #LH12034, and by NIEHS grant #R01 ES013268-01A2 to Upham. The RECETOX research infrastructure was supported by the projects of the Czech Ministry of Education #LO1214 and #LM2015051.

References

1. Persano L, Zagoura D, Louise J, and Pistollato F: Role of environmental chemicals, processed food derivatives and nutrients in the induction of carcinogenesis. *Stem Cells Dev*, 2015.
2. Oliveira PA, Colaco A, Chaves R, Guedes-Pinto H, and De-La-Cruz LF, et al.: Chemical carcinogenesis. *Anais Da Academia Brasileira De Ciencias* 79, 593–616, 2007.

3. Cohen SM and Arnold LL: Chemical Carcinogenesis. *Toxicol Sciences* **120**, S76–S92, 2011.
4. Sporn MB, Dunlop NM, Newton DL, and Smith JM: Prevention of chemical carcinogenesis by vitamin-a and its synthetic analogs (Retinoids). *Fed Proc* **35**, 1332–1338, 1976.
5. Mehta RG, Murillo G, Naithani R, and Peng XJ: Cancer chemoprevention by natural products: How far have we come? *Pharma Res* **27**, 950–961, 2011.
6. Shu LM, Cheung KL, Khor TO, Chen C, and Kong AN: Phytochemicals: cancer chemoprevention and suppression of tumor onset and metastasis. *Cancer Metastasis Rev* **29**, 483–502, 2010.
7. Gonzalez-Vallinas M, Gonzalez-Castejon M, Rodriguez-Casado A, and Ramirez de Molina A: Dietary phytochemicals in cancer prevention and therapy: a complementary approach with promising perspectives. *Nutr Rev* **71**, 585–599, 2013.
8. Trosko JE, Chang CC, Upham BL, and Tai MH: Ignored hallmarks of carcinogenesis: Stem cells and cell-cell communication. *Ann N Y Acad Sci* **1028**, 192–201, 2004.
9. Leone A, Longo C, and Trosko JE: The chemopreventive role of dietary phytochemicals through gap junctional intercellular communication. *Phytochem Rev* 2012. doi: 10.1007/s11101-012-9235-7.
10. Trosko JE and Chang CC: Mechanism of up-regulated gap junctional intercellular communication during chemoprevention and chemotherapy of cancer. *Mutat Res Fund Mol Mech Mut* **480**, 219–229, 2001.
11. Trosko JE and Ruch RJ: Gap junctions as targets for cancer chemoprevention and chemotherapy. *Current Drug Targets* **3**, 465–482, 2002.
12. Trosko JE, Chang CC, Upham BL, and Tai MH: The role of human adult stem cells and cell-cell communication in cancer chemoprevention and chemotherapy strategies. *Mutat Res Fund Mol Mech Mut* **591**, 187–197, 2005.
13. Trosko JE: The role of stem cells and gap junctions as targets for cancer chemoprevention and chemotherapy. *Biomed Pharmacother* **59**, S326–S331, 2005.
14. Vinken M, Doktorova T, Decrock E, Leybaert L, and Vanhaecke T, et al.: Gap junctional intercellular communication as a target for liver toxicity and carcinogenicity. *Crit Rev Biochem Mol Biol* **44**, 201–222, 2009.
15. Sai K, Kanno J, Hasegawa R, Trosko JE, and Inoue T: Prevention of the down-regulation of gap junctional intercellular communication by green tea in the liver of mice fed pentachlorophenol. *Carcinogenesis* **21**, 1671–1676, 2000.
16. Warngard L, Flodstrom S, Ljungquist S, and Ahlborg UG: Interaction between quercetin, TPA and DDT in the V79 metabolic cooperation assay. *Carcinogenesis* **8**, 1201–1205, 1987.
17. Sigler K, Ruch RJ: Enhancement of gap junctional intercellular communication in tumor promoter-treated cells by components of green tea. *Cancer Lett* **69**, 15–19, 1993.
18. Matesic DF, Blommel ML, Sunman JA, Cutler SJ, and Cutler HG: Prevention of organochlorine-induced inhibition of gap junctional communication by chaetoglobosin K in astrocytes. *Cell Biol Toxicol* **17**, 395–408, 2001.
19. Ruch RJ, Cheng SJ and Klauunig JE: Prevention of cytotoxicity and inhibition of intercellular communication by antioxidant catechins isolated from Chinese green tea. *Carcinogenesis* **10**, 1003–1008, 1989.
20. Takahashi H, Nomata K, Mori K, Matsuo M, and Miyaguchi T, et al.: The preventive effect of green tea on the gap junction intercellular communication in renal epithelial cells treated with a renal carcinogen. *Anticancer Res* **24**, 3757–3762, 2004.
21. Zefferino R, Leone A, Piccaluga S, Cincione R, and Ambrosi L: Mercury modulates interplay between IL-1beta, TNF-alpha, and gap junctional intercellular communication in keratinocytes: mitigation by lycopene. *J Immunotoxicol* **5**, 353–560, 2008.
22. Leone A, Zefferino R, Longo C, Leo L, and Zacheo G: Supercritical CO₂-extracted tomato oleoresins enhance gap junction intercellular communications and recover from mercury chloride inhibition in keratinocytes. *J Agric Food Chem* **58**, 4769–4778, 2010.
23. Upham BL, Guzvic M, Scott J, Carbone JM, and Blaha L, et al.: Inhibition of gap junctional intercellular communication and activation of mitogen-activated protein kinase by tumor-promoting organic peroxides and protection by resveratrol. *Nutr Cancer* **57**, 38–47, 2007.
24. Upham BL, Park J-S, Babica P, Sovadinova I, and Rummel AM, et al.: Structure-activity-dependent regulation of cell communication by perfluorinated fatty acids using in vivo and in vitro model systems. *Environ Health Perspect* **117**, 545–551, 2009.
25. Sovadinova I, Babica P, Boke H, Kumar E, and Wilke A, et al.: Phosphatidylcholine specific PLC-induced dysregulation of gap junctions, a robust cellular response to environmental toxicants, and prevention by resveratrol. *PLOS One* **10**, e0124454, 2015.
26. Tsao MS, Smith JD, Nelson KG, and Grisham JW: A diploid epithelial-cell line from normal adult-rat liver with phenotypic properties of oval cells. *Exp Cell Res* **154**, 38–52, 1984.
27. Kao CY, Oakley CS, Welsch CW, and Chang CC: Growth requirements and neoplastic transformation of two types of normal human breast epithelial cells derived from reduction mammoplasty. *In Vitro Cell Dev Biol Anim* **33**, 282–288, 1997.
28. El Fouly MH, Trosko JE, Chang CC: Scrape-loading and dye transfer – a rapid and simple technique to study gap junctional intercellular communication. *Exp Cell Res* **168**, 422–430, 1987.
29. Upham BL: Role of integrative signaling through gap junctions in toxicology. *Curr Protoc Toxicol* **47**, 1–18, 2011.
30. Choung YH, Choi SJ, Joo JS, Lee JB, and Lee HK, et al.: Green tea prevents down-regulation of gap junction intercellular communication in human keratinocytes treated with PMA. *Eur Arch Otorhinolaryngol* **268**, 885–892, 2011.
31. Lee DE, Shin BJ, Hur HJ, Kim JH, and Kim J, et al.: Quercetin, the active phenolic component in kiwifruit, prevents hydrogen peroxide-induced inhibition of gap-junction intercellular communication. *Br J Nutr* **104**, 164–70, 2010.
32. Kim YJ, Seo SG, Choi K, Kim JE, and Kang H, et al.: Recovery effect of onion peel extract against H₂O₂-induced inhibition of gap-junctional intercellular communication is mediated through quercetin. *J Food Sci* **79**, H1011–H1017, 2014.
33. Hwang JW, Jung JW, Lee YS, and Kang KS: Indole-3-Carbinol Prevents H₂O₂-Induced Inhibition of Gap Junctional Intercellular Communication by Inactivation of PKB/Akt. *J Vet Med Sci* **70**, 1057–1063, 2008.

34. Li Y, Fu Z, Chen X, Han R: Effects of curcumin derivatives on the GJIC of normal and tumor cells. *Zhongguo Yi Xue Ke Xue Yuan Xue Bao* **18**, 111–115, 1996.
35. Pasti G, Kertai P, and Adany R: Curcumin does not alter the phorbol ester effect on cell-cell transfer of lucifer yellow CH. *Carcinogenesis* **16**, 1229–1231, 1995.
36. Jung JW, Park SB, Lee SJ, Seo MS, and Trosko JE, et al.: Metformin represses self-renewal of the human breast carcinoma stem Cells via inhibition of estrogen receptor-mediated OCT4 expression. *PLOS One* **6**, 2011.
37. Anisimov VN: Do metformin a real anticarcinogen? A critical reappraisal of experimental data. *Ann Transl Med* **2**, 60, 2014.
38. Canovas-Jorda D, Louise J, Pistollato F, Zagoura D, and Bremer S: Regenerative toxicology: the role of stem cells in the development of chronic toxicities. *Expert Opin Drug Metab Toxicol* **10**, 39–50, 2014.
39. Lee DE, Kang NJ, Lee KM, Lee BK, and Kim JH, et al.: Cocoa polyphenols attenuate hydrogen peroxide-induced inhibition of gap-junction intercellular communication by blocking phosphorylation of connexin 43 via the MEK/ERK signaling pathway. *J Nutr Biochem* **21**, 680–686, 2010.
40. Kim JH, Lee BK, Lee KW, and Lee HJ: Resveratrol counteracts gallic acid-induced down-regulation of gap-junction intercellular communication. *J Nutr Biochem* **20**, 149–154, 2009.
41. Kim JH, Choi SH, Kim J, Lee BK, and Lee KW, et al.: Differential regulation of the hydrogen-peroxide-induced inhibition of gap-junction intercellular communication by resveratrol and butylated hydroxyanisole. *Mutat Res* **671**, 40–44, 2009.
42. Loch-Carusio R, Upham BL, Harris C, and Trosko JE: Divergent roles for glutathione in lindane-induced acute and delayed-onset inhibition of rat myometrial gap junctions. *Toxicol Sci* **85**, 694–702, 2005.
43. Upham BL and Trosko JE: Oxidative-dependent integration of signal transduction with intercellular gap junctional communication in the control of gene expression. *Antioxid Redox Signal* **11**, 297–307, 2009.
44. Ruch RJ, Trosko JE, and Madhukar BV: Inhibition of connexin43 gap junctional intercellular communication by TPA requires ERK activation. *J Cell Biochem* **83**, 163–169, 2001.
45. Hasler CM, Frick MA, Bennink MR, and Trosko JE: TPA-induced inhibition of gap junctional intercellular communication is not mediated through free radicals. *Toxicol Appl Pharmacol* **103**, 389–398, 1990.
46. Upham BL, Kang KS, Cho HY, and Trosko JE: Hydrogen peroxide inhibits gap junctional intercellular communication in glutathione sufficient but not glutathione deficient cells. *Carcinogenesis* **18**, 37–42, 1997.

XIII. Alpatova, A.L., Shan, W., **Babica, P.**, Upham, B.L., Rogensues, A.R., Masten, S.J., Drown, E., Mohanty, A.K., Alocilja, E.C., Tarabara, V. V.*, 2010. Single-walled carbon nanotubes dispersed in aqueous media via non-covalent functionalization: Effect of dispersant on the stability, cytotoxicity, and epigenetic toxicity of nanotube suspensions. *Water Research* 44, 505–520.

Available at www.sciencedirect.comjournal homepage: www.elsevier.com/locate/watres

Single-walled carbon nanotubes dispersed in aqueous media via non-covalent functionalization: Effect of dispersant on the stability, cytotoxicity, and epigenetic toxicity of nanotube suspensions

Alla L. Alpatova^a, Wenqian Shan^a, Pavel Babica^b, Brad L. Upham^{b,c}, Adam R. Rogensues^a, Susan J. Masten^a, Edward Drown^{d,1}, Amar K. Mohanty^{d,2}, Evangelyn C. Alocilja^e, Volodymyr V. Tarabara^{a,*}

^aDepartment of Civil and Environmental Engineering, Michigan State University, East Lansing, MI 48824, USA

^bCenter for Integrative Toxicology, Michigan State University, East Lansing, MI 48824, USA

^cDepartment of Pediatrics and Human Development, Michigan State University, East Lansing, MI 48824, USA

^dSchool of Packaging, Michigan State University, East Lansing, MI 48824, USA

^eDepartment of Biosystems and Agricultural Engineering, Michigan State University, East Lansing, MI 48824, USA

ARTICLE INFO

Article history:

Received 2 June 2009

Received in revised form

14 September 2009

Accepted 17 September 2009

Available online 30 September 2009

Keywords:

Single-walled carbon nanotubes

Dispersion

Non-covalent functionalization

Cytotoxicity

Epigenetic toxicity

ABSTRACT

As the range of applications for carbon nanotubes (CNTs) rapidly expands, understanding the effect of CNTs on prokaryotic and eukaryotic cell systems has become an important research priority, especially in light of recent reports of the facile dispersion of CNTs in a variety of aqueous systems including natural water. In this study, single-walled carbon nanotubes (SWCNTs) were dispersed in water using a range of natural (gum arabic, amylose, Suwannee River natural organic matter) and synthetic (polyvinyl pyrrolidone, Triton X-100) dispersing agents (dispersants) that attach to the CNT surface non-covalently via different physiosorption mechanisms. The charge and the average effective hydrodynamic diameter of suspended SWCNTs as well as the concentration of exfoliated SWCNTs in the dispersion were found to remain relatively stable over a period of 4 weeks. The cytotoxicity of suspended SWCNTs was assessed as a function of dispersant type and exposure time (up to 48 h) using general viability bioassay with *Escherichia coli* and using neutral red dye uptake (NDU) bioassay with WB-F344 rat liver epithelia cells. In the *E. coli* viability bioassays, three types of growth media with different organic loadings and salt contents were evaluated. When the dispersant itself was non-toxic, no losses of *E. coli* and WB-F344 viability were observed. The cell viability was affected only by SWCNTs dispersed using Triton X-100, which was cytotoxic in SWCNT-free (control) solution. The epigenetic toxicity of dispersed CNTs was evaluated using gap junction intercellular communication (GJIC) bioassay applied to WB-F344 rat liver epithelial cells. With all SWCNT suspensions except those where SWCNTs were dispersed using Triton X-100 (wherein GJIC could not be measured because the sample was cytotoxic), no inhibition of GJIC in the presence of SWCNTs was observed. These results suggest a strong dependence of the toxicity of

* Corresponding author. Tel.: +517 432 1755; fax: +517 355 0250.

E-mail address: tarabara@msu.edu (V.V. Tarabara).

¹ Present address: Department of Chemical Engineering and Materials Science, Michigan State University, East Lansing, MI 48824, USA.

² Present address: Department of Plant Agriculture, University of Guelph, 50 Stone Rd. E., Guelph, Ontario, N1 G 2W1 Canada.

0043-1354/\$ – see front matter © 2009 Elsevier Ltd. All rights reserved.

doi:10.1016/j.watres.2009.09.042

SWCNT suspensions on the toxicity of the dispersant and point to the potential of non-covalent functionalization with non-toxic dispersants as a method for the preparation of stable aqueous suspensions of biocompatible CNTs.

© 2009 Elsevier Ltd. All rights reserved.

1. Introduction

The discovery (Iijima, 1991) and subsequent extensive characterization of carbon nanotubes (CNTs) have revealed a class of materials with extraordinary electrical, mechanical, and thermal properties (Tasis et al., 2006). The wider application of CNTs in electronic, optical, sensing, and biomedical fields has been impeded by the low solubility of as-produced CNTs in polar liquids and by the strong tendency of CNTs to aggregate due to hydrophobic–hydrophobic interactions (Lin et al., 2004). Dispersing CNTs and ensuring long-term stability of CNTs suspended in a liquid medium have proved especially challenging for aqueous systems.

1.1. Dispersing CNTs in aqueous media

Recent efforts on the development of efficient and facile methods of dispersing CNTs in aqueous media have been focused on the hydrophilization of CNT with molecules that bind to the CNT surface non-covalently (O'Connell et al., 2001; Bandyopadhyaya et al., 2002; Star et al., 2002; Islam et al., 2003; Moore et al., 2003; Didenko et al., 2005; Wang et al., 2005; Bonnet et al., 2007; Grossiord et al., 2007; Hyung et al., 2007; Liu et al., 2007). Such non-covalent functionalization has great promise as the modification-induced changes in the electronic and mechanical properties of CNTs are minimized (Yang et al., 2007). Various surfactants (Islam et al., 2003; Moore et al., 2003; Grossiord et al., 2007), synthetic polymers (e.g., polyvinyl pyrrolidone (O'Connell et al., 2001; Didenko et al., 2005), poly(ethylene glycol) (Vaisman et al., 2006), polyphosphazene (Park et al., 2006)), natural organic matter (NOM) (Hyung et al., 2007; Liu et al., 2007; Saleh et al., 2009), biomolecules (e.g., proteins (Karajanagi et al., 2006; Zong et al., 2007), aminoacids (Georgakilas et al., 2002), DNA (Enyashin et al., 2007)), and carbohydrates (e.g., cyclodextrines (Dodziuk et al., 2003), amylose (Bonnet et al., 2007), starch (Star et al., 2002), and GA (Bandyopadhyaya et al., 2002)) have been evaluated as dispersants for CNTs. Dispersion via non-covalent functionalization is based on the direct contact between a CNT and a dispersant molecule (Liu et al., 1998; Grossiord et al., 2007). Such modification of the CNT surface facilitates the disaggregation (i.e. debundling) of CNT bundles into smaller diameter bundles (Liu et al., 1998) or even individual CNTs (O'Connell et al., 2002; Hyung et al., 2007) and leads to the stabilization of suspended CNTs via steric or electrostatic repulsion mechanisms or both. (See Supporting Documentation (SD), Section S.1.1, for a brief review of mechanisms of non-covalent functionalization of CNTs.)

The dispersion of CNTs in water has been enhanced by mixing (Didenko et al., 2005; Hyung et al., 2007), sonication (Bandyopadhyaya et al., 2002; Liu et al., 2007; Salzmänn et al., 2007), or mixing followed by sonication (O'Connell et al., 2001,

2002; Star et al., 2002; Islam et al., 2003; Moore et al., 2003; McDonald et al., 2006; Grossiord et al., 2007). These treatments were applied both in the absence (Salzmänn et al., 2007) and in the presence of solubilizing agents: NOM (Hyung et al., 2007), Triton X-100 (Islam et al., 2003), Triton X-405 (Chappell et al., 2009), PVP-1300 (Didenko et al., 2005), GA (Bandyopadhyaya et al., 2002), and starch (Star et al., 2002). A three-step approach to solubilizing single-walled carbon nanotubes (SWCNTs) with amylose was suggested by Kim et al. (Kim et al., 2004): dispersion of SWCNT in water by sonication followed by treatment with amylose in dimethylsulfoxide (DMSO)–H₂O mixture, followed by sonication allowing for molecularly controlled encapsulation of CNTs.

1.2. Stability of CNT suspensions in water

Previous studies of the long-term changes in suspensions of dispersed CNTs have focused on monitoring changes in the concentration of suspended CNTs (Jiang and Gao, 2003; Tseng et al., 2006; Lee et al., 2007; Marsh et al., 2007). By measuring UV–vis absorption at certain wavelength: 253 nm (Jiang and Gao, 2003), 300 nm (Sinani et al., 2005), 500 nm (Bahr et al., 2001; Lee et al., 2007), 530 nm (Marsh et al., 2007), and 800 nm (Hyung et al., 2007) the change in the concentration of suspended CNTs with time was determined.

Aqueous suspensions of non-functionalized CNTs are known to be unstable. There are considerable quantitative differences, however, in the reported stability data for non-functionalized CNTs. The concentration of unmodified multi-walled carbon nanotubes (MWCNTs) suspended in deionized water was reported to decline 86 % over 2 h in one study (Marsh et al., 2007) and only 50% over 500 h in another study (Jiang and Gao, 2003). The suspensions of unmodified SWCNTs in deionized water were found to completely precipitate after only 4 h (Tseng et al., 2006).

It was found that non-covalent modification of CNT surface drastically improved the stability of CNT suspensions (Jiang and Gao, 2003; Tseng et al., 2006; Hyung et al., 2007; Lee et al., 2007; Marsh et al., 2007). The stability of the suspension of non-covalently functionalized CNTs was found to be a function of the type (Hyung et al., 2007; Lee et al., 2007) and concentration (Chappell et al., 2009) of the dispersant, CNT length (Marsh et al., 2007) and the presence of inorganic salts in the solution (Saleh et al., 2009). SWCNTs stabilized with oligothiophene-terminated poly(ethylene glycol) produced suspensions that were significantly more stable than CNTs dispersed in water with the aid of sodium dodecyl sulfate (SDS) and Pluronic F127 (Lee et al., 2007). CNT suspensions in model Suwannee River NOM (SRNOM) solutions and in Suwannee River water were found to be considerably more stable than suspensions of CNTs dispersed in 1% aqueous solution of SDS (Hyung et al., 2007). Chappell et al. showed

that the stability of MWCNTs dispersed using two types of humic acids, Triton X-405, Brij 35, and SDS was enhanced in dose-dependent manner (Chappell et al., 2009). In a study of the aggregation kinetics of MWCNTs in aquatic systems, Suwannee River humic acid was shown to significantly enhance stability of MWCNTs suspensions in the presence of monovalent and divalent salts (Saleh et al., 2009). While studying the stability of MWCNTs in water, Marsh and co-workers (Marsh et al., 2007) observed that wrapping of the annealed CNTs with 1% SDS or charge doping increased their stability in the suspension; the authors demonstrated that shorter CNTs form more stable dispersions than longer CNTs of the same diameter. In summary, there is growing evidence that by the appropriate choice of a dispersant that modifies CNT surface non-covalently, highly stable CNT suspensions can be produced. However, to date *there have been no systematic investigations that correlated long-term changes in size and charge of CNTs dispersed via non-covalent functionalization with the dispersion stability.*

1.3. Toxicity of CNTs

1.3.1. Toxicity of CNTs towards eukaryotic cells: cytotoxicity

Most nanomaterial toxicity studies have been performed with mammalian cells, in particular with lung and skin cell cultures reflecting the understanding that the most likely routes of an organism's exposure to nanomaterials are respiratory and dermal contact. With the development of methods of CNT dispersion in aqueous media, the assessment of the toxicity of such dispersed CNTs becomes very important in view of their increased mobility and potential to enter water supplies. While the toxicity of CNTs was studied with respect to the type of the CNT (MWCNT versus SWCNT) (Ding et al., 2005; Jia et al., 2005; Kang et al., 2008a), surface functionalization (Sayes et al., 2006; Yu et al., 2007; Meng et al., 2009; Yun et al., 2009), CNT length (Muller et al., 2005; Kang et al., 2008b; Simon-Deckers et al., 2008), exposure dose (Cherukuri et al., 2006; Flahaut et al., 2006; Sayes et al., 2006; Kang et al., 2007; Pulskamp et al., 2007; Yang et al., 2008, 2009; Ye et al., 2009), degree of purification (Fiorito et al., 2006; Flahaut et al., 2006; Elias et al., 2007; Simon-Deckers et al., 2008), and degree of dispersion (Wick et al., 2007), only very limited information exists on the biocompatibility of CNTs as a function of surface coating.

Several hypotheses have been put forth to explain the likely pathways of CNT toxicity: (i) oxidative stress induced by the formation of reactive oxygen species (ROS) generated at the surface of CNTs (Manna et al., 2005; Yang et al., 2008; Ye et al., 2009); (ii) the presence of residual catalyst, which is used during the CNT manufacturing process (Kang et al., 2008a); (iii) physical contact between a CNT and a cell (Kang et al., 2007); or (iv) a combination of these factors (Kang et al., 2008a). The dispersant used for the stabilization of CNTs in suspension was suggested as another possible cause of the observed nanotube toxicity (Sayes et al., 2006) (See SD, Section S.1.2 for a brief review of possible mechanisms of CNT toxicity).

In most studies of the toxicity of non-covalently functionalized CNTs the dispersants were surfactants. *In vivo* assessment of the toxicity of SWCNTs modified with Pluronic F108 administered intravenously to rabbits showed the

absence of the acute toxicity (Cherukuri et al., 2006). Pluronic F-127-coated MWCNTs did not affect cell viability, apoptosis, and ROS formation in mouse and human neuroblastoma cells (Vittorio et al., 2009), and mouse cerebral cortex (Bardi et al., 2009). In contrast, MWCNTs dispersed using Pluronic F68 caused cell death, changes in cell size and complexity, ROS production, interleukin-8 (IL-8) gene expression and nuclear factor (NF)- κ B activation (Ye et al., 2009). CNTs dispersed using Tween 80 were toxic to mesothelioma cells (Wick et al., 2007), led to an inflammation of murine allergic airway with augmented humoral immunity (Inoue et al., 2009), and induced inflammatory and fibrotic responses when intracheally administered to rats (Muller et al., 2005). More ROS were observed upon exposure of human lung epithelial or primary bronchial epithelial cells to SWCNTs dispersed using dipalmitoylphosphatidylcholine, a major component of lung surfactant (Herzog et al., 2009), as compared to dipalmitoylphosphatidylcholine-free samples. Low toxicity was observed in *in vivo* experiments when SWCNTs were dispersed using Tween 80 and intravenously injected into mice (Yang et al., 2008). In another study, SWCNTs dispersed in 1% SDS aqueous solution showed no cytotoxicity with respect to the human alveolar epithelial cells (Wörle-Knirsch et al., 2006). CNTs dispersed using Pluronic PF-127 solution did not affect viability, apoptosis and ROS generation in the human neuroblastoma cells after 3 days of incubation; however, cell proliferation decreased as incubation time increased to 2 weeks (Vittorio et al., 2009). In the only paper that mentioned the potential toxicity effect of the dispersant, the authors suggested that excess surfactant was responsible for the observed increase in toxicity; in this work, the controlled exposure of cells to 1% Pluronic F108 produced a 10% decrease in the cells viability (Sayes et al., 2006).

Very little is known about the effect of non-covalent wrapping with dispersants other than surfactants on the biocompatibility of CNTs. In vitro cytotoxicity of CNTs wrapped with poly(methyl vinylketone) decorated with α -N-acetylgalactosamine (Chen et al., 2006), nano-1 peptide (Chin et al., 2007) and cholesterol-end-capped poly(2-methacryloyloxyethyl phosphorylcholine) (Xu et al., 2008) were examined after their contact with human lung epithelial-like cells, normal skin fibroblasts and human umbilical vein endothelial cell line. No impact on cell growth and proliferation was demonstrated in all three cases. Cytotoxicity of GA-stabilized MWCNTs upon exposure to A549 cells was observed by LDH, XTT and MTT bioassays in (Simon-Deckers et al., 2008). Two possible reasons were hypothesized to be responsible for this effect: (i) increased availability of GA-stabilized MWCNTs and (ii) different intercellular accumulation pathway of GA-stabilized MWCNTs as compared to when carbon nanotubes were exposed in bundles.

1.3.2. Toxicity of CNTs towards eukaryotic cells: genotoxicity and epigenetic toxicity

Most toxicological studies of CNTs focused on the evaluation of cytotoxicity (Sayes et al., 2006; Elias et al., 2007; Gutierrez et al., 2007; Kang et al., 2007; Wick et al., 2007; Kang et al., 2008a,b; Yang et al., 2008; Bardi et al., 2009; Herzog et al., 2009; Inoue et al., 2009; Kang et al., 2009; Vittorio et al., 2009; Yang et al., 2009). However, genotoxicity (Kang et al., 2008a; Di Sotto et al., 2009; Lindberg et al., 2009; Wirtitzer et al., 2009; Yang et al., 2009) and

epigenetic toxicity (see SD, Section S.1.3) (Upham et al., 1994); (Trosko et al., 1998) are other possible causes of cell damage or other adverse effects. The genotoxicity of SWCNTs dispersed using fetal bovine serum at (5–10) $\mu\text{g}/\text{mL}$ concentration, with respect to primary mouse embryo fibroblasts was demonstrated using Comet assay (Yang et al., 2009). In another recent study, CNTs (dispersed in BEGM cell culture medium and subjected to ultrasonication) induced a dose-dependent increase in DNA damage as indicated by Comet assay and caused a significant increase in micronucleated cells (micronucleus assay) in human bronchial epithelial cells (Lindberg et al., 2009). Kang et al. observed high levels of stress-related gene products in *Escherichia coli* upon its exposure to CNTs, with the quantity and magnitude of expression being much higher in the presence of SWCNTs (Kang et al., 2008a); in this study CNTs were either deposited on a PVDF membrane surface or dispersed in saline solution. No mutagenic effect was observed in *Salmonella* microcosme test with baytubes[®] (high purity MWCNTs agglomerates, sonicated 10 min in deionized water) (Wirnitzer et al., 2009) and in bacterial reverse mutation assay (Ames test) with *Salmonella typhimurium* TA 98 and TA 100 strains and with *E. coli* WP2uvrA strain exposed to MWCNTs dispersed in DMSO (Di Sotto et al., 2009). *There have been no reports to date on the epigenetic toxicity of carbon nanomaterials.*

1.3.3. Toxicity of CNTs in prokaryotic cells

Most toxicity studies have focused on the effect of CNTs on mammalian cell lines. Only limited information exists on the cytotoxic effects of CNTs towards bacterial cells. Recently, antimicrobial activity of SWCNTs (Kang et al., 2007, 2008a, 2009) and MWCNTs (Kang et al., 2008a,b, 2009) either suspended in aqueous solution (Kang et al., 2007, 2008a) or deposited on the surface of a PVDF microfilter (Kang et al., 2007, 2008a,b, 2009) towards gram-negative bacteria (*E. coli* and *Pseudomonas aeruginosa* (Kang et al., 2007, 2008a,b, 2009) and gram-positive (*Staphylococcus epidermidis* and *Bacillus subtilis* (Kang et al., 2009)) bacteria was reported. It was suggested that membrane damage to the cells was caused by the direct physical contact between the CNT and cell (Kang et al., 2007) or by a combination of direct physical contact and oxidative stress (Kang et al., 2008a). No effect on the percentage of *E. coli* inactivation was observed upon exposure of SRNOM-stabilized SWCNTs as compared of SWCNTs dispersed in the absence of SRNOM (Kang et al., 2009). Significant antimicrobial activity of CNTs composite films against *Staphylococcus aureus* and *Staphylococcus warneri* was reported in a separated study (Narayan et al., 2005). In contrast to the findings of above studies, no inhibition of *E. coli* growth and proliferation was reported in a study where microchannel-structured MWCNTs scaffolds were immersed into the culture medium with the cells (Gutierrez et al., 2007).

1.4. Effect of growth media on the toxicity of nanoparticles

The existing literature highlights the importance of the growth media in cytotoxicity testing and links the apparent cytotoxic effect of the nanomaterial to the salt and organic content of the culture and related physicochemical characteristics of the nanomaterial (Lyon et al., 2005; Tong et al.,

2007). Lyon et al. showed that in media with high salt content, the size of nC₆₀ aggregates tends to increase as compared to that observed in low salt media (Lyon et al., 2005). In another study, MWCNTs were found to stimulate growth of unicellular protozoan *Tetrahymena pyriformis* in growth medium, which contained proteose peptone, yeast extract, and glucose; the increase in growth was attributed to the formation of peptone-MWCNTs conjugates, which were taken up by the microorganism (Zhu et al., 2006). While the aforementioned studies indicate that salt and organic composition of the medium, in which exposure studies are performed, may influence the interaction of CNTs with bacteria, *there have been no studies that comparatively evaluated CNT toxicity in growth media with different organic loadings and salt contents.*

1.5. Objectives of this study

This study addressed some of the knowledge gaps identified above. Aqueous suspensions of SWCNTs functionalized by a range of non-covalently bound dispersants of natural (NOM, GA, amylose) and synthetic (PVP, Triton X-100) origin, were prepared and evaluated in terms of their physicochemical and toxicity properties. The study pursued the following objectives:

- (i) *To evaluate the long-term stability and its physicochemical determinants for non-covalently functionalized SWCNTs as a function of dispersant type.* The evolution of the concentration, size, and charge of suspended SWCNTs was studied over the period of 28 days.
- (ii) *To assess time-dependent cytotoxicity of non-covalently functionalized SWCNTs with respect to bacteria and mammalian cells as a function of dispersant type and growth media.* The effect of SWCNTs on *E. coli* was studied by measuring cell viability after 3 h, 24 h, and 48 h of exposure in three types of growth media with different organic loadings and salt contents. The cytotoxicity of dispersed SWCNTs towards mammalian cells was assessed in NDU bioassay with rat liver epithelial cells after 30 min and 24 h of incubation.
- (iii) *To assess time-dependent epigenetic toxicity of non-covalently functionalized SWCNTs as a function of dispersant type.* In this study, we evaluated epigenetic toxicity of the SWCNTs to rat liver epithelial cells as a function of dispersant type in GJIC bioassay after 30 min and 24 h of incubation.

2. Approach

The set of chemically diverse dispersants was chosen based on their demonstrated effectiveness in solubilizing CNTs (Bandyopadhyaya et al., 2002; O'Connell et al., 2002; Star et al., 2002; Islam et al., 2003; Moore et al., 2003; Hyung et al., 2007; Liu et al., 2007) and potential adverse effects (Burnette, 1960; Chourasia and Jain, 2004; Dayeh et al., 2004; Schmitt et al., 2008). NOM, GA and PVP have LD₅₀ doses of (54.8–58.5) mg (intravenous administration in mice) (EMEA, 1999), 2,000 mg (oral administration in rats) (Schmitt et al., 2008), and 100,000 mg (oral administration in rats) (Burnette, 1960) per kg

of body weight, respectively. Amylose has been reported to be used in a colon-specific drug delivery due to its low toxicity and high biodegradability (Chourasia and Jain, 2004). Triton X-100 was reported to be toxic to protozoa, fish, and mammalian cells (Dayeh et al., 2004).

Three batches of dispersed SWCNTs were prepared. The first batch was used to comprehensively evaluate the long-term stability of SWCNT suspensions over a period of 4 weeks in terms of concentration, effective hydrodynamic diameter, and ζ -potential of stabilized SWCNTs.

The second batch was used to evaluate the viability of *E. coli* cells after their contact with dispersed SWCNTs by the quantification of colony forming units. To elucidate the effects of ionic and organic composition of the growth medium, the cytotoxicity of the SWCNTs suspended in three growth media of different organic and salt compositions was evaluated. First, in order to assess the acute cytotoxicity of dispersed SWCNTs, we conducted experiments in 0.1 M NaCl. Then, in order to investigate the effect of SWCNTs on the ability of *E. coli* form colonies over time, we employed three types of growth media: (i) LB medium with higher organic chemical and salt content, (ii) MD medium with low salt content and organic load, and (iii) 0.1 M NaCl solution.

The third batch was used to evaluate cyto- and epigenetic toxicity of the dispersed SWCNTs against rat liver epithelial cells by the (i) NDU and (ii) GJIC bioassays. The NDU assesses cell viability by measuring the accumulation of neutral red dye in lysosomes, which depends on the cell's capacity to maintain pH gradients through the maintaining membrane integrity and production of adenosine triphosphate. The amount of dye incorporated by the cell is quantified spectrophotometrically (Borenfreund and Puerner, 1985). The NDU bioassay has been used to assess cytotoxicity of CNTs (Flahaut et al., 2006). The GJIC bioassay (Borenfreund and Puerner, 1985; Weis et al., 1998; Herner et al., 2001; Satoh et al., 2003) utilizes the ability of epigenetic tumor promoters to alter level of GJIC (Yamasaki, 1990; Trosko et al., 1991). The degree of GJIC was quantified by measuring the distance (area) the fluorescent dye (≤ 1200 Da) travels (occupies) between the cells after a given time. Both NDU and GJIC bioassays were carried out with WB-F344 rat liver epithelial cells exposed to dispersed SWCNTs for different periods of time. The WB-F344 cell line was chosen because these normal diploid rat liver epithelial cells have already used in numerous studies of cytotoxic or epigenetic effects (e.g., Herner et al., 2001) thus allowing us to have a comparative basis.

3. Materials and methods

3.1. CNTs

SWCNTs (purity > 90%), produced by catalytic chemical vapor deposition, were obtained from Cheap Tubes, Inc (Brattleboro, VT) and used as received. The SWCNTs were used as obtained, allowing us to mimic what might occur in the environment. As indicated by the manufacturer, the SWCNTs had an inside diameter in the range of 0.8 nm to 1.6 nm, an outer diameter in the range of 1 nm to 2 nm and were 5 μ m to 30 μ m in length.

3.2. Non-covalent functionalization: dispersants and dispersion procedures

3.2.1. Dispersants

Gum arabic (approx. 250 kDa; a complex mixture of saccharides and glycoproteins obtained from the acacia tree), PVP (approx. 29 kDa), Triton X-100 (approx. 625 Da; polyethylene glycol p-(1,1,3,3-tetramethylbutyl)-phenyl ether) and amylose (molecular weight not specified; a polymeric form of glucose and a constituent of potato starch) were purchased from Sigma-Aldrich (Milwaukee, WI). SRNOM reverse osmosis isolation was obtained from International Humic Substances Society (St Paul, MN). The molecular structure of dispersants used in this study is presented in Fig. 1.

3.2.2. Dispersion procedure

Aqueous solutions of PVP, Triton X-100 were prepared by dissolving PVP (40 mg) and Triton X-100 (0.4 mL) in 40 mL of water and adjusting the pH of both solutions to 7 with 0.1 M HCl. The aqueous solution of GA was prepared by mixing 1 g of GA in 50 mL of water and adjusting the pH of the mixture to 7 with 0.1 M HCl; this mixture was left to settle for 24 h and then 40 mL of supernatant was collected for use in the stability or toxicity studies. To prepare NOM solutions, two flasks of 40 mL of water, each containing 8 mg of NOM, were stirred for 24 h. Each solution was then filtered through a 0.22 μ m filter under vacuum. The pH of one solution was kept at its original value (approx. 3.5) while the pH in another solution was adjusted to 7 with 0.1 M NaOH. SWCNTs were added to the above solutions to result in a 1 mg (SWCNT)/mL loading and were sonicated in Aquasonic 50 T water bath (VWR Scientific Products Corp, West Chester, PA) for 20 min.

SWCNTs were dispersed with amylose based on modified version of the three-step approach reported by Kim et al. (Kim et al., 2004). SWCNTs (40 mg) were sonicated in 25 mL of water (pH 7) at approximately 75 W for 5 min using Sonicator 3000 (Misonix, Inc., Farmingdale, NY) equipped with a microprobe. 100 mg of amylose in 6.28 mL of DMSO were prepared and added to the sonicated suspension of SWCNT in water so that the DMSO/water ratio was 20% by volume. The resulting mixture was sonicated for another 5 min in order to remove the excess amylose and DMSO. The suspension was sonicated, centrifuged and refilled with water four times (See SD, Section S.2.3).

Following the sonication, SWCNTs suspensions were divided into 12 mL aliquots and each aliquot was transferred into 15 mL centrifuge tube. After 24 h standing time, the top 4 mL of each suspension was withdrawn in order to be used in the stability or toxicity studies. Overall, three batches of dispersed SWCNT suspensions were prepared and were used, correspondingly, for 1) the study of the long-term stability of SWCNTs suspensions, 2) the general viability bioassay with *E. coli*, and 3) NDU and GJIC bioassays.

3.3. Physicochemical characterization of SWCNT suspensions

In order to quantitatively assess the long-term stability SWCNT suspensions, a combination of characterization methods was employed.

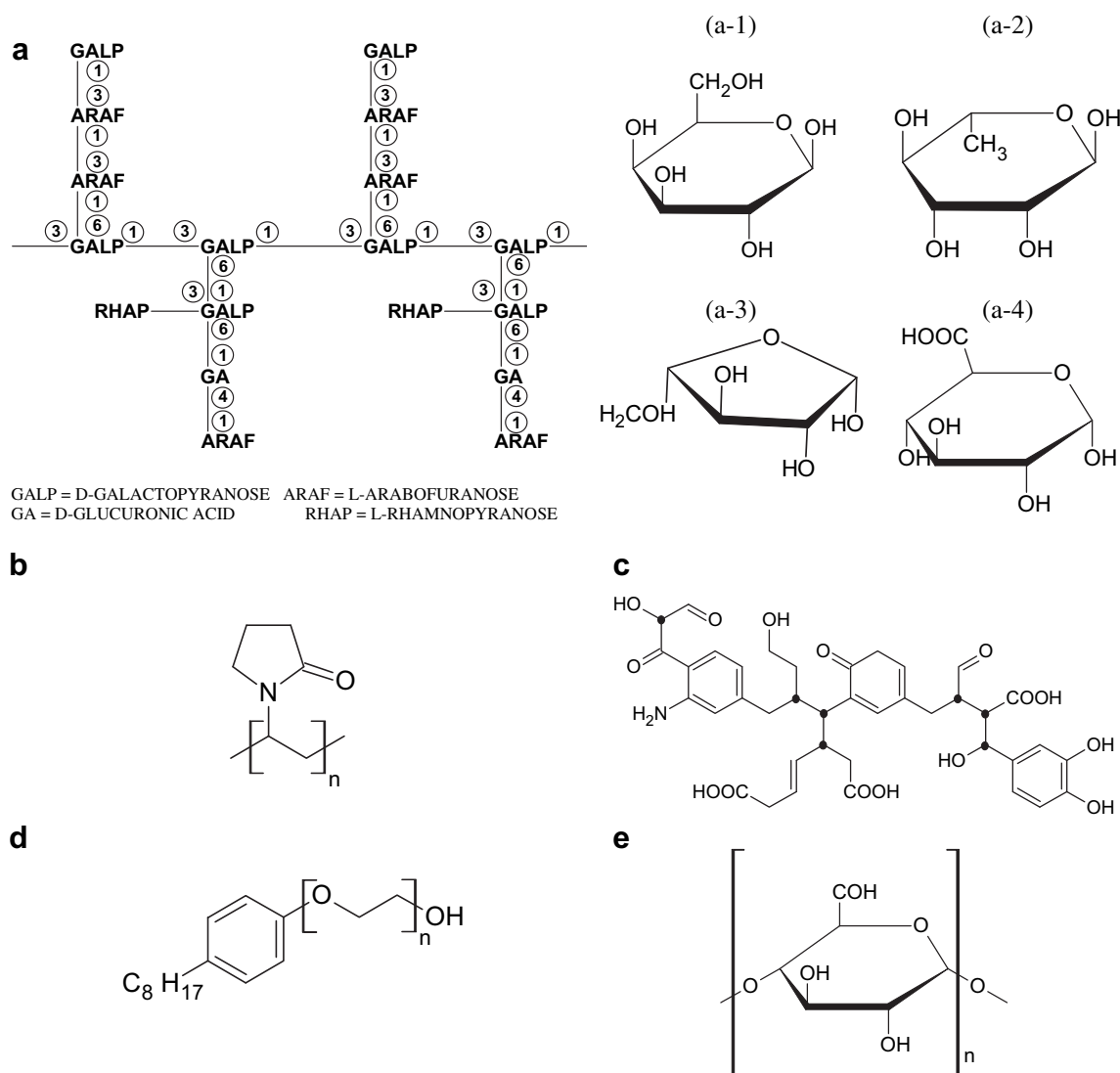


Fig. 1 – Molecular structure of solubilizers: (a) Gum arabic (a-1) galactose, (a-2) rhamnose, (a-3) arabinose, (a-4) gluconic acid; (b) Poly(vinyl pyrrolidone); (c) A building block of humic acids, which has a compositional similarity to SRNOM; Dots represent chiral centers; (d) Triton X-100; (e) Amylose.

3.3.1. UV-vis spectrophotometry. Quantification of SWCNTs concentration in suspension

The absorbance of SWCNT suspensions over the (200–800) nm wavelength range was measured over a period of 4 weeks (Multi-spec 1501, Shimadzu, Kyoto, Japan). For each type of SWCNT suspension prepared, the absorbance of SWCNT-free solution of the corresponding dispersant was used as a baseline.

SWCNT suspensions used in our toxicity studies likely contained both individual and bundled SWCNTs. In fact, DLS measurements indirectly confirmed (see Section 4.2) the presence of dispersed SWCNT bundles and direct TEM imaging (see SD, Section S.3.3, Fig. S5) also showed the presence of SWCNTs bundles (note that TEM results need to be interpreted with caution as evaporation-induced aggregation could have contributed to bundling during TEM sample preparation). Incomplete exfoliation is the most likely and most environmentally relevant scenario; unfortunately, it also

entails difficulties with quantifying the total concentration of suspended nanotubes as larger CNT bundles tend to separate from the suspension.

In this study, we used UV-vis spectrophotometry to estimate the concentration of exfoliated SWCNTs in suspensions. It is known that only fully exfoliated SWCNTs absorb in the (200–1200) nm wavelength range. Bundled NTs do not absorb significantly in this range due to the tunnel coupling between metallic and semiconductive SWNTs (Lauret et al., 2004; Grossiord et al., 2007). Therefore, the UV absorbance by a SWCNT suspension can be used to selectively measure the concentration of individually dispersed (i.e. fully exfoliated or debundled) SWCNTs.

To determine the concentration of suspended exfoliated SWCNTs, we first prepared a separate set of suspensions with ten-fold reduced SWCNT loading with respect to the CNT loading used in long-term stability and toxicity studies. Four suspensions (with PVP, NOM pH 3.5, NOM pH 7, and GA used

as dispersants) with 10-fold reduced SWCNT content (0.1 g/L) were prepared using the same procedures as described in Section 3.2 except that they were subjected to rigorous, prolonged sonication for 1 h at power of (70–80) W using horn sonicator (Sonicator 3000, Misonix, Inc., Farmingdale, NY). No settling of SWCNTs was observed over the short term following the application of this treatment indicating complete dispersion of SWCNTs. UV–vis absorbance spectra were recorded at different dilutions and a calibration curve for absorption at 500 nm (Bahr et al., 2001; Huang et al., 2002; Sinani et al., 2005; Lee et al., 2007; Salzmann et al., 2007) as a function of concentration was constructed, and coefficient of molecular extinction, ϵ , was determined. This coefficient was used to estimate the concentration of exfoliated SWCNTs in suspensions used in long-term stability and toxicity experiments. Note that by subjecting suspended SWCNTs to a very intense sonication treatment we aimed at maximizing the extent of exfoliation; however, it was not possible to ascertain that the exfoliation was complete. Thus coefficients of molecular extinction and exfoliated SWCNT concentrations determined using the recorded calibration curves were estimated values. SWCNT characteristics measured upon the preparation of CNT suspensions are given in Table S1 in SD.

3.3.2. Size and charge of dispersed SWCNTs

The effective hydrodynamic diameter and ζ -potential of suspended SWCNTs were determined after 1, 4, 7, 14, 21, and 28 days of settling. The size and charge were measured by dynamic light scattering (DLS) and phase analysis light scattering techniques, respectively (ZetaPALS, BI-MAS Option, Brookhaven Instrument Corp., Holtsville, NY). The Smoluchowski equation was applied to convert the measured electrophoretic mobility of dispersed SWCNT to ζ -potential. Transmission electron microscopy (TEM) imaging was used as an auxiliary method to aid in the interpretation of dynamic light scattering data (see SD, Sections S.2.5 and S.3.4).

3.4. Toxicity assessment: *E. coli* viability assay

3.4.1. Media preparation

Luria–Bertani (LB) growth medium was prepared according to the standard procedure (Atlas, 1993). Minimal Davis medium with 90% reduced potassium phosphate concentration (MD medium) was prepared (Fortner et al., 2005). 0.1 M NaCl solution was prepared by dissolving 9 g of NaCl in 1 L of water (pH 7) and autoclaving it for 15 min at 1 bar and 121 °C. For the toxicity assessments, each component of LB, MD and NaCl media was prepared in 4-fold higher concentration as compared to original protocol and the aliquot part of the corresponding medium was added to SWCNTs suspension (as further described in “Quantification of cell viability” Section). Luria–Bertani Petri plates were prepared according to the published method (Atlas, 1993).

3.4.2. Preparation of *E. coli* culture

E. coli K12 stock was prepared in glycerol and stored at –80 °C. Prior to use, the stock was defrosted, and 30 mL of LB medium were inoculated with 5 μ L of the stock. After overnight growth at 37 °C, 5 μ L of this suspension was spread onto LB agar plate and cultured at 37 °C. Once distinct colonies were formed, the

agar plate was transferred to the refrigerator and kept at 4 °C for up to one month. *E. coli* suspensions to be used in SWCNT cytotoxicity studies were prepared by scraping one colony from the surface of a Petri plate by aseptic loop and immersing the loop into 10 mL of LB or MD media in a 50 mL centrifuge tube. Tubes were placed on a shaker in an incubator 37 °C for 12 h. When 0.1 M NaCl was used as an exposure medium in colony forming units bioassay, *E. coli* were first grown in the LB medium, centrifuged for 5 min at 2250 rpm and washed with 0.1 M NaCl as follows: the supernatant was decanted and replaced with an equal volume of 0.1 M NaCl, vortexed and resuspended by centrifugation. The washing procedure was repeated twice, presuming that after this treatment most of the remaining organic constituents of LB medium were removed from the *E. coli* suspension.

3.4.3. Quantification of cell viability

The SWCNTs suspension (1.425 mL), growth medium (475 μ L) and 100 μ L of the stock *E. coli* suspension were transferred into a 15 mL centrifuge tube and incubated under gentle shaking at 37 °C. Samples were taken after 3, 24, and 48 h and a series of dilutions (10^4 – 10^6) was prepared for each sample. Five samples of 10 μ L and 20 μ L from each dilution were placed onto an agar plate and incubated at 37 °C until distinct colonies developed. Colony forming units (CFU)/1 mL were calculated for each sample. Each experiment was run in triplicates with negative (bacterial suspension with the corresponding amount of ultrapure water) and vehicle (solution of the corresponding dispersant) controls, herein called vehicle control I and vehicle control II, respectively. The results are reported as a fraction of control (FOC) \pm standard deviation (STD), calculated as the ratio of the average number of colonies grown after *E. coli* exposure to SWCNTs suspensions or vehicle control II to the average number of colonies grown in vehicle control I plates.

3.5. Toxicity assessment: neutral red dye uptake bioassay

For the NDU bioassay we adapted a published procedure (Borenfreund and Puerner, 1985; Weis et al., 1998; Satoh et al., 2003). A solution (0.015 w/v) of neutral red dye (3-amino-7-(dimethylamino)-2-methylphenazine hydrochloride) in D-medium was incubated at 37 °C for 2 h and filtered through a 0.22 μ m syringe filter (Millipore Corp., New Bedford, MA) to remove undissolved dye and ensure sterile conditions. Confluent WB-F344 cells (see SD, Section S.2.6 for details on the preparation of the cells) were exposed to 500 μ L of each of SWCNTs suspension and incubated at 37 °C for 30 min and 24 h under gentle shaking in a humidified atmosphere containing 5% CO₂. After cells were exposed to SWCNTs, the exposure medium was removed by aspiration and the cells were washed with 1 mL of phosphate saline buffer (PBS). Following washing, 2 mL of the neutral red dye solution per plate was added and the cells were incubated for 1 h at 37 °C in the humidified atmosphere containing 5% CO₂. Upon incubation, the cells were rinsed three times with PBS, and 2 mL of aqueous solution containing 1% acetic acid and 50% ethanol was added to each plate to lyse the cells. 1.5 mL of the lysate was transported into 2 mL microcentrifuge tube and the optical density was

recorded at 540 nm using a Beckman DU 7400 diode array detector (Beckman Instruments, Inc., Schaumburg, IL). The background absorbance was measured at 690 nm and then subtracted from the original absorbance. Each experiment was conducted in triplicates. The neutral red dye uptake was reported as the FOC (absorption of neutral red in the chemically treated sample divided by the absorption of neutral red in the nontreated control I sample). FOC values of 1.0 indicates non-cytotoxic response while FOC values <0.8 indicate that less dye was absorbed by cells and that chemical is cytotoxic at that dose (El-Fouly et al., 1987; Satoh et al., 2003).

3.6. Toxicity assessment: gap junction intercellular communication (GJIC) bioassay

The principles of GJIC bioassay were originally described in (Borenfreund and Puerner, 1985) and further developed in (Weis et al., 1998; Herner et al., 2001; Satoh et al., 2003). SWCNTs suspensions (500 μ L) were introduced to the cell culture plates with confluent WB-F344 cells and incubated for 30 min and 24 h at 37 °C in humidified atmosphere containing 5% CO₂ under gentle shaking. Then, cells were washed with PBS solution and 1 mL of 0.05% solution of Lucifer yellow fluorescent dye in PBS buffer was added to each plate. Three different scrapes were made on the bottom of a cell culture plate using a surgical steel scalpel blade. The dye was absorbed through the monolayer of confluent cells. The transfer of dye through gap junctions lasted 3 min, followed by a thorough rinse with PBS solution to remove extracellular dye. Cells were fixed with 0.5 mL of 4% formalin solution in PBS. The migration of the dye in the cells was observed at 200 \times magnification using a Nikon epifluorescence microscope equipped with a Nikon Cool Snap EZ CCD camera and the images were digitally acquired using a Nikon NIS-Elements F2.2 imaging system. The fluorescence area of the dye migration from the scrape line was quantified using Image J 1.40 g (a public domain Java image processing program, <http://rsbweb.nih.gov/ij/index.html>). Each experiment was performed in duplicate with same controls as in the NDU bioassay. Data are reported as the FOC, which is the ratio of the area of dye spread in the chemically treated sample to the area of dye spread in the vehicle control I samples. A FOC value of 1.0 corresponds to full communication between cells, FOC values of (0.5–0.9) represent partial GJIC inhibition, (0.3–0.5) values correspond to significant inhibition of the GJIC and values <0.3 denote complete inhibition of the GJIC (Weis et al., 1998). Student's t-tests at 95% confidence interval were run for all three bioassays to determine whether the difference between the results obtained in the control I plates and the results in the tested plates were significant.

The concentrations of SWCNTs upon addition to suspension of cells in the general *E. coli* viability bioassay, and in NDU and GJIC bioassays are reported in Table 1.

4. Results and discussion

The knowledge of the evolution of physicochemical properties (e.g., charge and size) of dispersed CNTs can provide insights into the basis for both CNT stability and possible toxicity.

4.1. Concentration of dispersed SWCNTs in suspensions

First, SWCNTs were suspended directly in ultrapure water without a dispersant; this suspension was used as a control. After sonication for 20 min, the mixture became a lightly colored suspension that completely separated into a dark subnatant layer and a clear supernatant after only 1 h of settling. In contrast, 20 min of sonication of the SWCNT–water mixture in the presence of a dispersant produced relatively stable colored suspensions (see SD, Fig. S1) that precipitated gradually with the precipitation rate varying as a function of the type of dispersant. The amount of the precipitate that formed at the bottom of a centrifuge tube visibly increased with settling time for all types of SWCNT suspensions. Immediately after sonication, all SWCNT suspensions prepared using the different dispersants appeared black. After 4 weeks of settling, in suspensions of NOM-stabilized and amylose-stabilized SWCNTs the color of the aqueous solution of the dispersant was revealed. After 7 weeks of settling, the color change could be detected in all samples with the suspension of amylose-stabilized SWCNTs (see SD, Fig. S1) undergoing the most dramatic change to an almost transparent supernatant phase (Figure S1 (b)).

The UV–vis absorption measurements were performed to determine the concentration of suspended exfoliated SWCNTs as a function of settling time. The calibration curves for the intensity of the absorbance at 500 nm as a function of SWCNT concentration (see Section 2.3) were recorded for all suspensions (see SD, Fig. S2) except for amylose-stabilized SWCNTs. Because of the observed loss of SWCNTs during centrifugation/washing steps for amylose-dispersed SWCNTs (see SD, Section S.2.3), the concentration of amylose-dispersed SWCNTs could not be measured. The calibration curves were linear ($R^2 \geq 0.99$). The extinction coefficients for suspensions of SWCNTs dispersed using GA-, PVP-, Triton X-100-, NOM (pH 3.5)-, and NOM (pH 7) were determined to be 1.81×10^{-2} , 1.97×10^{-2} , 2.51×10^{-2} , 2.54×10^{-2} , and 2.70×10^{-2} (L mg⁻¹ cm⁻¹), respectively. The concentration of exfoliated SWCNTs in suspension as a function of settling time is given in Fig. 2a.

The dispersion and exfoliation of SWCNTs bundles in the presence of GA and PVP was attributed to the wrapping of a long polymeric chain around the nanotube core (Bandyopadhyaya et al., 2002; Didenko et al., 2005), whereas supra-molecular encapsulation was hypothesized as the mechanism of CNT modification by helical amylose (Kim et al., 2004).

Table 1 – Concentrations of the SWCNTs upon addition to cells in the general viability bioassay with *E. coli*, NRDU bioassay, and GJIC bioassay.

Solubilizer	Concentration of SWCNTs in general <i>E. coli</i> viability bioassay, mg/L	Concentration of SWCNTs in NRDU and GJIC bioassays, mg/L
NOM pH 3.5	68.27	11.22
NOM pH 7.0	40.12	11.93
PVP	77.38	23.42
GA	142.91	34.97
Triton X-100	107.19	26.43

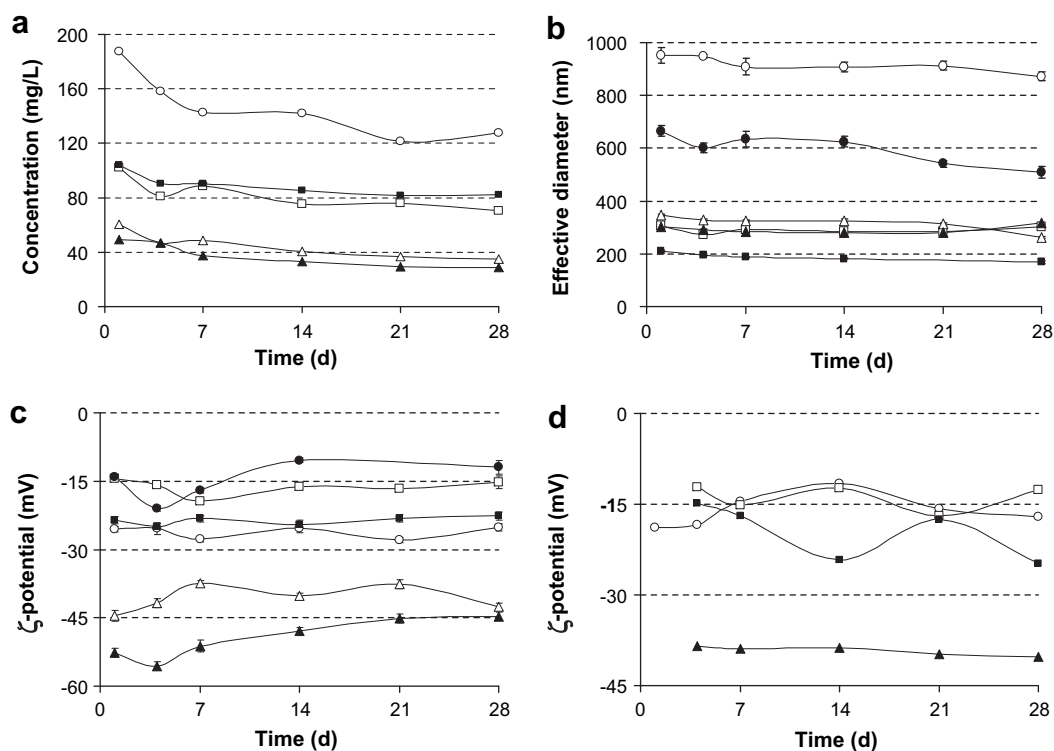


Fig. 2 – The time-dependent characterization of (a) estimated concentration of the exfoliated SWCNTs in the dispersion, (b) effective diameter and (c) ζ -potential of dispersed SWCNTs, and (d) ζ -potential of dispersants alone (—○— for GA/SWCNTs, —□— for PVP/SWCNTs, —△— for NOM3.5/SWCNTs, —▲— for NOM7/SWCNTs, —■— for Triton X-100/SWCNTs, —●— for Amylose/SWCNTs). Notes: (1) The ζ -potential measurement was not conducted for amylose solution, because amylose is not water-soluble under room temperature. (2) Reported are results of only those measurements that were statistically significant, i.e. when sufficiently high photon count rates were recorded in dynamic light scattering measurements. (3) The absorption by suspensions of amylose-stabilized SWCNTs was not measured because the nanotube content in these suspensions could not be precisely determined; this was due to the incomplete separation at the centrifugation step of the suspension preparation process.

Triton X-100 stabilizes nanotubes by the formation of hemimicelles that cover nanotube surface with benzene rings providing π - π stacking between the surfactant molecule and nanotube core (Islam et al., 2003). The exfoliation (debundling) of SWCNTs in the presence of SRNOM was suggested to occur through the interaction of the aromatic moieties of natural organic matter and nanotube surface (Hyung et al., 2007; Liu et al., 2007; Hyung and Kim, 2008). Despite the differences in the physiosorption mechanisms responsible for the stabilization of CNTs in aqueous suspensions, all dispersants were effective, albeit to somewhat different extents.

For all SWCNT suspensions, the calculated values of the concentration of exfoliated SWCNTs correlated well to the visual observations described above. As seen from Fig. 2a, the dispersion efficiency in terms of the concentration of dispersed SWCNTs was a function of the type of the dispersant, with GA producing suspensions having highest concentration of SWCNTs. The data were consistent among the three prepared batches of SWCNTs (see SD, Table S1). Didenko et al. (Didenko et al., 2005) suggested that after covering one single carbon nanotube with a long polymeric molecule, the remaining strands would react with other uncovered or partially covered SWCNTs thus bundling several nanotubes together. We speculate that this mechanism where

one polymer molecule links two or more nanotubes may be responsible for the higher dispersing efficiency of GA (by far the largest molecule among the target dispersants) towards SWCNTs compared to other dispersants. This hypothesis is supported by the measurements of the effective hydrodynamic diameter (Fig. 2b), and the estimation of the length of suspended particles with the size and the length of GA/SWCNTs being higher than those of PVP, Triton X-100 and SRNOM (both pHs). As the measured diameter of GA-stabilized SWCNTs aggregates (which could also be expected to be rather porous) was still relatively small, gravity settling did not lead to a significant removal of GA-stabilized SWCNTs from the dispersion.

When comparing the solubilizing ability of SRNOM at different pH, one could see that SRNOM is a more efficient dispersant at pH 3.5 than at pH 7. This is consistent with the findings by Hyung et al. (Hyung and Kim, 2008) who reported that adsorption of SRNOM to MWCNTs increased when pH decreased due to more compact and coiled conformation of NOM at acidic pHs. When pH increases, carboxylic and phenolic groups of SRNOM deprotonate resulting in higher electrostatic repulsion between a CNT and a SRNOM molecule and, as a consequence, in a lower amount of organic matter adsorbed on the CNT surface. The better dispersion of

SWCNTs at pH 3.5 could also be attributed, in part, to the steric hindrance imposed by SRNOM when a higher surface density of NOM on the surface of CNT bundles results in stronger repulsion between CNTs. This observation is supported by the long-term ζ -potential measurements (Fig. 2c), where the surface charge of stabilized SRNOM/SWCNTs at pH 3.5 became less negative up to day 7, and then stabilized with increasing settling time. At the same time the surface charge of SWCNTs dispersed in SRNOM solution at pH 7 gradually increased after day 5. Indeed, had the electrostatic repulsion been the sole mechanism of SWCNTs stabilization in SRNOM solutions, the surface charge on the SWCNTs would have more rapidly become less negative at pH 3.5 than at pH 7. In summary, in terms of the effectiveness of SWCNT stabilization, the dispersants were ranked as follows: GA > Triton X-100 > PVP > NOM (pH 3.5) > NOM (pH 7).

4.2. Hydrodynamic size of dispersed SWCNTs

The hydrodynamic size of CNTs in a suspension is an important characteristic that affects the stability and, possibly, toxicity of dispersed CNTs. It should be noted that the effective hydrodynamic diameter of suspended SWCNTs measured using DLS can only be used as a very rough estimate. While the DLS data are interpreted with the assumption that the primary scatterers are spherical with an aspect ratio of 1, dispersed SWCNTs are long and tubular, with a very high aspect ratio (see SD, Fig. S3). To obtain a better approximation of the size distribution of dispersed SWCNT, the multimodal size distribution model was used. TEM imaging was employed to obtain auxiliary information on the size and morphology of stabilized SWCNT. Even though the measurement of effective hydrodynamic diameter cannot be relied on to compare the sizes of suspended SWCNTs in different dispersion media, these measurements can be used to compare how the average particle size for a given dispersant changes with settling time. The values of effective diameter as a function of time for different SWCNT suspensions are given in Fig. 2b.

Generally, the effective size of SWCNTs dispersed using Triton X-100, GA and NOM did not change significantly with increasing settling time (Fig. 2b). In the case of amylose-dispersed SWCNTs, a slight decrease in the effective size was observed due to settling of larger and unstable SWCNT aggregates, which left behind more uniformly sized smaller amylose-stabilized CNT clusters. The concentration of SWCNTs in the suspension was negatively correlated with the effective size of SWCNT. The notable apparent exception was the suspension of SWCNTs dispersed using GA. However, it should be noted that the aqueous suspension of GA contained GA colloids of the size that was 1) comparable to the size of dispersed SWCNTs and 2) decreased during the 4 weeks of settling (see SD, Fig. S5). Thus, the effective size measurements for SWCNTs dispersed using GA should be interpreted with caution.

4.3. Charge of dispersed SWCNTs

For all suspensions, the ζ -potential of dispersed SWCNTs was negative and nearly constant over the entire duration of the experiment (Fig. 2c and SD, Table S1). Each ζ -potential

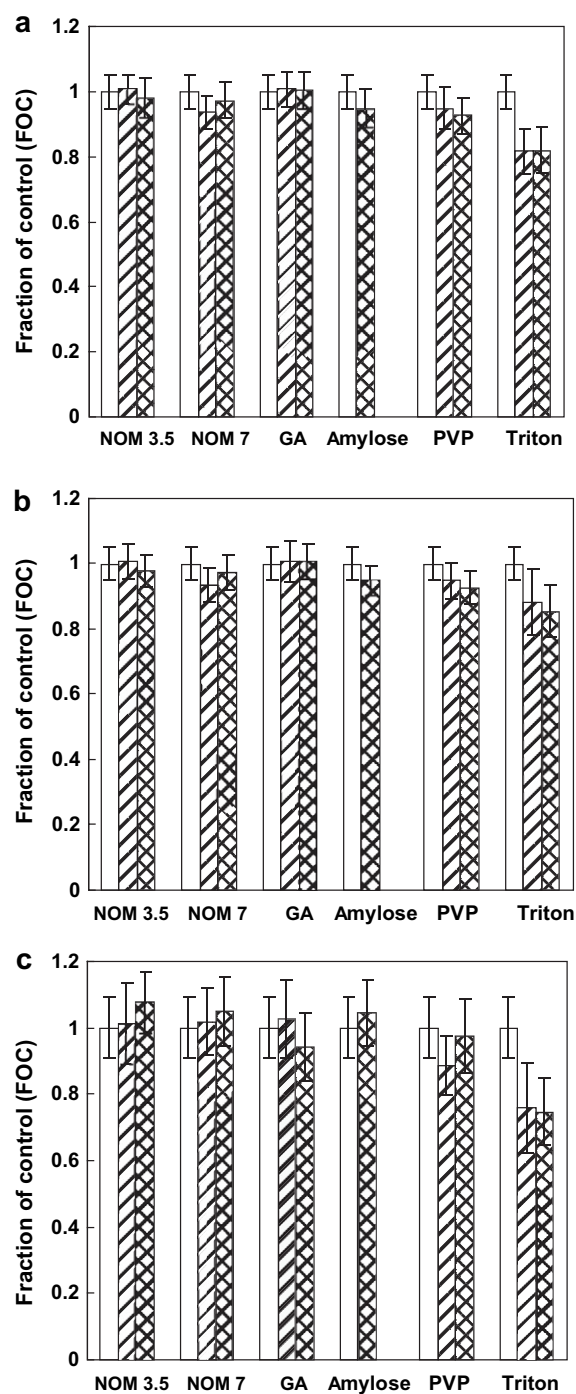


Fig. 3 – Viability of *E. coli* in (a) 0.1 M NaCl, (b) LB medium, and (c) MD medium. Exposure time: (a) 3 h, (b) 48 h, (c) 48 h. Open, hatched and cross-hatched bars correspond to control I, control II and dispersed SWCNTs. In the case of amylose ultrapure water was used as control.

measurement for SWCNT suspensions was accompanied by a measurement of the ζ -potential of the dispersants in a SWCNT-free aqueous solution (Fig. 2d). After 1 d, only the GA solution scattered light sufficiently to enable a statistically meaningful ζ -potential measurement. After 4 d, solutions of NOM (pH 7), PVP, and Triton X-100 also scattered light

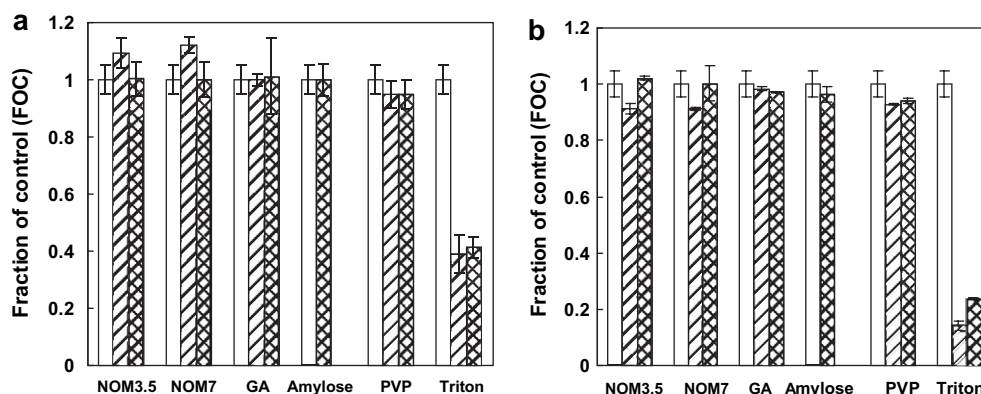


Fig. 4 – Neutral red dye uptake by WB-F344 cells as a function of dispersant type (a – 30 min, b – 24 h of exposure). Open, hatched and cross-hatched bars correspond to control I, control II and dispersed SWCNTs. In the case of amylose control I and control II were ultrapure water.

sufficiently. After 7 d, all the dispersants except for NOM (pH 3.5) achieved acceptable count rates during ζ -potential measurements. The gradual change in the scattering ability of the dispersant solutions may correspond to the aggregation of the dispersant molecules. The dispersants were ranked in order from the most to the least negative ζ -potential of dispersed SWCNTs: NOM (pH 7) > NOM (pH 3.5) > GA \approx Triton X-100 > PVP \approx amylose. The highly negative charge of NOM-stabilized SWCNTs was likely due to the charge of NOM. The low stability of amylose-dispersed SWCNTs could be attributed to the combination of low surface charge and steric repulsion between stabilized SWCNTs in the dispersion.

4.4. Assessment of cell toxicity in prokaryotic and eukaryotic systems

4.4.1. General viability bioassay with *E. coli* (prokaryotic)

Immediately after *E. coli* cells were exposed to SWCNTs suspended in growth medium as well as after 3 h of exposure, no SWCNT aggregation was visually observed (see SD, Table S2) in experiments with all three types of the media – 0.1 M NaCl, MD (medium with lower salt organics content) and LB (medium with higher salt and organics content). After 24 h of incubation, limited precipitation was observed for all SWCNT

suspensions in LB and MD media. After 48 h of incubation more precipitation occurred in each type of media.

No inhibition of *E. coli* colony forming ability was observed after 3 h of incubation with amylose-, NOM-, GA- and PVP-stabilized SWCNTs in 0.1 M NaCl (Fig. 3a). The FOC values did not decline in any of these samples and no significant difference in the influence on CFU counts was found between dispersed SWCNTs and solutions of corresponding dispersants. When the bacteria suspension was brought in contact with Triton X-100-stabilized SWCNTs, approx. 25% loss of the cell viability was measured as compared to vehicle control I samples. However, there was no statistical difference between FOC of Triton-stabilized SWCNTs and the control (solution of Triton X-100 only). It remains unclear if the observed cytotoxicity of these suspensions was due to i) SWCNTs stabilized by Triton X-100 or ii) the residual “free” (i.e. not associated with suspended SWCNTs) Triton X-100 potentially present in the solution or iii) the combined effect of both Triton X-100/SWCNT and dissolved Triton X-100. The complete separation of the Triton X-100/SWCNT and dissolved Triton X-100 could not be accomplished using centrifugation. Even for very long centrifugation times, the supernatant had grayish color indicating that some fraction of SWCNTs was not removed.

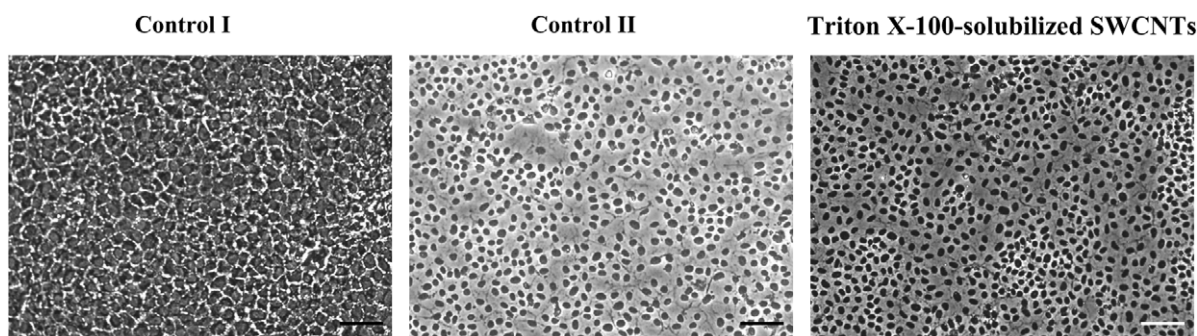


Fig. 5 – Representative phase contrast images of WB-F344 cells incubated with 500 μ L of H₂O (control I), 500 μ L of Triton X-100 (control II) and 500 μ L of Triton X-100-stabilized SWCNTs. Black dots observed in Control II and Triton X-100-solubilized SWCNTs samples correspond to dead WB-F344 cells. All images were taken at 200 \times magnification. Scale bar is 50 μ m.

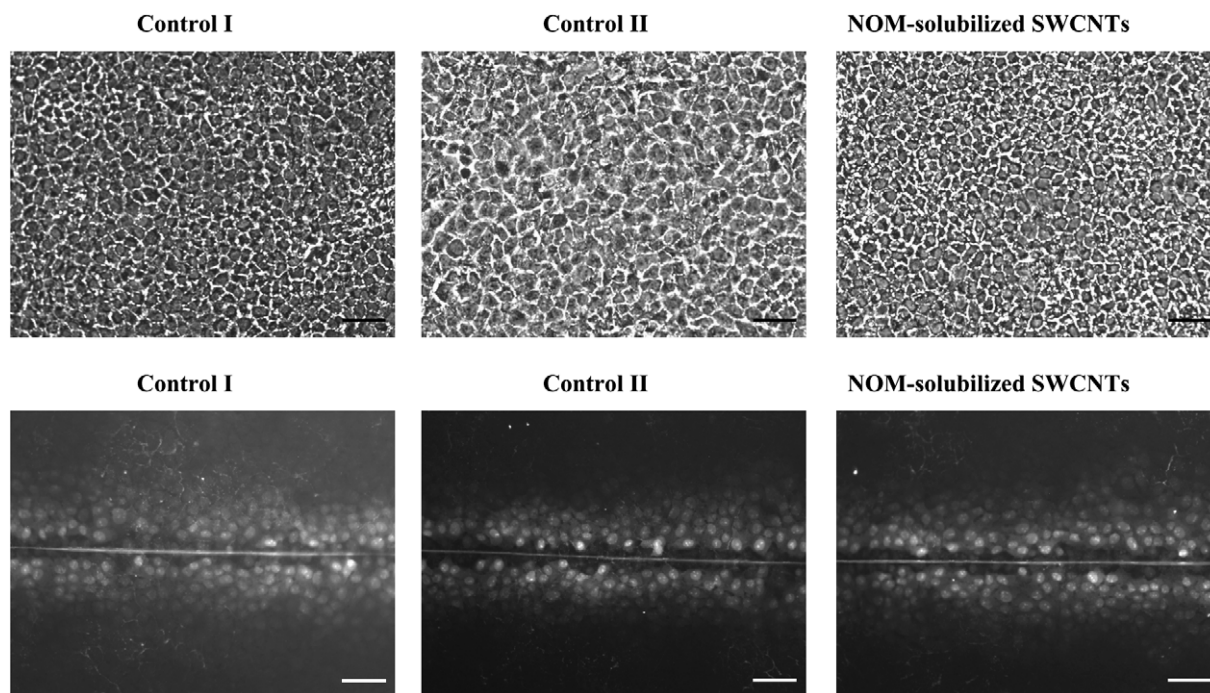


Fig. 6 – Representative phase contrast (upper row) and UV epifluorescent (bottom row) images of WB-F344 cells incubated with 500 μ L of H₂O (control I), 500 μ L of NOM pH 3.5 (control II) and 500 μ L of NOM-stabilized SWCNTs (pH 4). All images were taken at 200 \times magnification. Bright dots correspond to cells that absorb the dye; the absorption is indicative of cellular health. All images were taken at 200 \times magnification. Scale bar is 50 μ m.

The ability of *E. coli* to grow and to form colonies in the presence of amylose-, GA-, PVP-, and NOM-stabilized SWCNTs in LB medium mimicked both control samples regardless of the contact time (see SD, Fig. 3b and Fig. S6). On the contrary, 21 and 18 % mortality rates after 3 h of incubation were observed for *E. coli* in Triton X-100/SWCNTs suspension and Triton X-100 solution, respectively. After 24 h of contact, the number of colonies grown on the Petri plates decreased by 30 % when bacteria were in contact with Triton X-100-stabilized SWCNTs and by 27 % when bacteria were in Triton X-100 only solution (see SD, Fig. S6) as compared to vehicle control I

plates. As the exposure time increased to 48 h, *E. coli* resumed its growth; with FOC of both Triton X-100 suspensions approaching values for vehicle control I sample (Fig. 3b). When dispersed SWCNTs were tested in MD medium, no losses in cell viability for amylose-, GA-, PVP- and NOM-stabilized SWCNTs were measured (Fig. 3c; also see SD, Fig. S7). In the case of Triton X-100 suspensions, the reduction in *E. coli* survival was observed after 3 h of exposure; comparable losses of the *E. coli* viability were also observed for both Triton X-100-stabilized SWCNTs and the Triton X-100 only solution. However, after 24 h of exposure, fewer *E. coli* colonies were

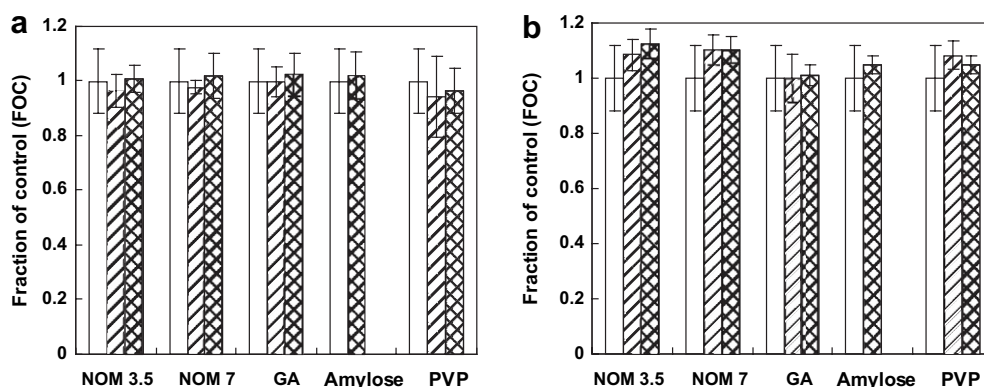


Fig. 7 – GJIC in WB-F344 cells as a function of dispersant type (a – 30 min, b – 24 h of exposure). Open, hatched and cross-hatched bars correspond to control I, control II and dispersed SWCNTs. In the case of amylose control I and control II were ultrapure water.

observed on Petri plates from suspensions of Triton X-100-stabilized SWCNTs and Triton X-100 solution only (vehicle control II) (33 and 44 %, respectively) (see SD, Fig. S7). As the incubation time increased to 48 h, bacterial CFU counts in the presence of both Triton X-100 samples increased and approached that of vehicle control I samples (Fig. 3c).

As was previously mentioned, the exposure of Triton X-100-stabilized SWCNTs to MD medium for 24 h resulted in formation of large flake-like aggregates, which settled out of the suspension. It is possible that this low salt medium induced specific interactions between bacterial cells and Triton X-100-coated SWCNTs, which were suppressed in the medium having a higher ionic strength. This led to a larger decrease in *E. coli* viability in these samples in comparison with the losses in Triton X-100 solution only. Damaged or dead cell attached to the SWCNTs aggregates and formed debris at the bottom of the testing tubes. The simultaneous effect of bacterial and nanoparticles settling out of the solution has been previously described (Tang et al., 2007) where the response of *Shewanella oneidensis* to C_{60} -NH₂ nanoparticles was studied.

The fact that we observed inhibition of *E. coli* viability after 24 h of exposure in MD medium and did not observed this effect in LB medium highlights the importance of growth medium in cytotoxicity testing. Similarly, *E. coli* exposure to SWCNTs, stabilized with amylose, GA, PVP and NOM (both pH) did not affect CFU counts in any of the three media pointing to the importance of the dispersant in the assessments of biocompatibility of CNTs.

4.4.2. NDU cytotoxicity bioassay on eukaryotic cells

The assessment of cytotoxicity was determined by the viable uptake of neutral red into F344-WB rat liver epithelial cells. Nonviable cells lack the ability to absorb this dye. Results (Fig. 4) indicated that SWCNTs dispersed using NOM (pH 3.5), NOM (pH 7), GA, amylose and PVP were not cytotoxic. However, Triton X-100 detergent induced a significant cytotoxic effect independent of SWCNTs. This latter observation can also be seen under phase contrast microscopy of cells treated with Triton X-100 for 30 min (Fig. 5). The morphology of the cells drastically changed from that of the normal control cells, in which the cells became clearer due to loss of most cytosolic contents, except for the cell nuclei. After a 24 h treatment with Triton X-100, the cells completely detached or solubilized from the culture plates (data not shown).

4.5. Assessment of epigenetic toxicity on eukaryotic cells: GJIC bioassay

A representative fluorescent micrograph of the GJIC assay after treatment with (NOM + SWCNTs) is shown in Fig. 6. The migration of the fluorescent dye through several cell layers is an indicator that the gap junction channels are open. After WB-F344 cells were incubated with dispersed SWCNTs suspensions for (1) 30 min and (2) 24 h, there was no significant affect on GJIC for all suspensions tested (Fig. 7). Due to Triton X-100-stabilized SWCNTs being cytotoxic, GJIC was not measured in cells exposed to this mixture. Also, when cells were examined under phase

contrast, no changes in size and shape of the individual cells were detected (Fig. 6). Hence, it can be concluded that under these experimental conditions WB-F344 cells exposed to dispersed SWCNTs retain normal intercellular communication irrespective of the applied treatment.

5. Conclusions

The stability of aqueous suspensions of SWCNTs non-covalently functionalized by a range of natural (gum arabic, amylose, Suwannee River natural organic matter) and synthetic (polyvinyl pyrrolidone, Triton X-100) dispersants that bind to SWCNT surface via different physiosorption mechanisms was evaluated. Despite the differences, all SWCNT suspensions remained relatively stable over a period of 4 weeks as indicated by the evolution of the concentration of suspended exfoliated SWCNT and by the fact that both the average effective hydrodynamic diameter and ζ -potential of suspended SWCNTs were relatively constant. The epigenetic toxicity of dispersed SWCNTs was evaluated for the first time using a gap junctional intercellular communication assay with WB-F344 rat liver epithelial cells resulting in no inhibition by SWCNTs non-covalently functionalized using GA, PVP, amylose, and SRNOM. There were no cytotoxic effects of these SWCNTs suspensions on either the prokaryotic, bacterial (*E. coli*), or eukaryotic (WB-F344 rat liver epithelial) cell types. Only when the dispersant itself was toxic, were losses of cell viability observed. Bacterial CFU counts or neutral red uptake was affected only by SWCNTs dispersed using Triton X-100, which showed cytotoxicity in the SWCNT-free solution (vehicle control II). The results suggest a strong dependence of the toxicity of SWCNT suspensions on the toxicity of the solubilizing agent and point to the potential of non-covalent functionalization with non-toxic dispersants as a method for the preparation of aqueous suspensions of biocompatible CNTs.

Acknowledgements

This work was supported by the National Science Foundation research grants CBET-0608320, CBET-056828 and OISE-0530174, by the National Institute of Environmental Health Sciences grants R01 ES013268-01A2 and Grant-in-Aid for Science Research. We thank Michael Housinger for his assistance with the preparation of SWCNT suspensions. ARR acknowledges the support by Michigan AWWA Fellowship for Water Quality and Treatment Study. The contents of this work are solely the responsibility of the authors and do not necessarily represent the official views of the National Institute of Environmental Health Sciences.

Appendix. Supplementary data

Supplementary data associated with this article can be found in the online version, at doi:10.1016/j.watres.2009.09.042.

REFERENCES

- Atlas, R.M., 1993. Handbook of Microbiological Media. CRC Press, Boca Raton.
- Bahr, J.L., Mickelson, E.D., Bronikowski, M.J., Smalley, R.E., Tour, J.M., 2001. Dissolution of small diameter single-wall carbon nanotubes in organic solvents. *Chemical Communications*, 193–194.
- Bandyopadhyaya, R., Nativ-Roth, E., Regev, O., Yerushalmi-Rozen, R., 2002. Stabilization of individual carbon nanotubes in aqueous solutions. *Nano Letters* 2 (1), 25–28.
- Bardi, G., Tognini, P., Ciofani, G., Raffa, V., Costa, M., Pizzorusso, T., 2009. Pluronic-coated carbon nanotubes do not induce degeneration of cortical neurons in vivo and in vitro. *Nanomedicine: Nanotechnology, Biology, and Medicine* 5, 96–104.
- Bonnet, P., Albertini, D., Bizot, H., Bernard, A., Chauvet, O., 2007. Amylose/SWNT composites: from solution to film – synthesis, characterization and properties. *Composite Science and Technology* 67, 817–821.
- Borenfreund, E., Puerner, J.A., 1985. Toxicology determined in vitro by morphological alterations and neutral red absorption. *Toxicology Letters* 24, 119–124.
- Burnette, L.W., 1960. A review of the physiological properties of PVP. *Proceedings of the Scientific Section of the Toilet Goods Association* 38, 1–4.
- Chappell, M.A., George, A.J., Dontsova, K.M., Porter, B.E., Price, C.L., Zhou, P., Morikawa, E., Kennedy, A.J., Steevens, J.A., 2009. Surfactive stabilization of multi-walled carbon nanotube dispersions with dissolved humic substances. *Environmental Pollution* 157, 1081–1087.
- Chen, X., Tam, U.C., Czapinski, J.L., Lee, G.S., Rabuka, D., Zettl, A., Bertozzi, C.R., 2006. Interfacing carbon nanotubes with living cells. *Journal of American Chemical Society* 128, 6292–6293.
- Cherukuri, P., Gannon, C.J., Leeuw, T.K., Schmidt, H.K., Smalley, R.E., Curley, S.A., Weisman, R.B., 2006. Mammalian pharmacokinetics of carbon nanotubes using intrinsic near-infrared fluorescence. *Proceedings of the National Academy of Sciences* 103, 18882–18886.
- Chin, S.F., Baughman, R.H., Dalton, A.B., Diekmann, G.R., Draper, R.K., Mikoryak, C., Musselman, I.H., Poenitzsch, V.Z., Xie, H., Pantano, P., 2007. Amphiphilic helical peptide enhances the uptake of single-walled carbon nanotubes by living cells. *Experimental Biological Medicine* 232 (9), 1236–1244.
- Chourasia, M.K., Jain, S.K., 2004. Polysaccharides for colon targeted drug delivery. *Drug Delivery* 11 (2), 129–148.
- Dayeh, V.R., Chow, S.L., Schirmer, K., Lynn, D.H., Bols, N.C., 2004. Evaluating the toxicity of Triton X-100 to protozoan, fish, and mammalian cells using fluorescent dyes as indicators of cell viability. *Ecotoxicology and Environmental Safety* 57 (3), 375–382.
- Di Sotto, A., Chiaretti, M., Carru, G.A., Bellucci, S., Mazzantia, G., 2009. Multi-walled carbon nanotubes: lack of mutagenic activity in the bacterial reverse mutation assay. *Toxicology Letters* 184, 192–197.
- Didenko, V.V., Moore, V.C., Baskin, D.S., Smalley, R.E., 2005. Visualization of individual single-walled carbon nanotubes by fluorescent polymer wrapping. *Nano Letters* 5 (8), 1563–1567.
- Ding, L.H., Stilwell, J., Zhang, T.T., Elboudware, J.O., Jiang, H.J., Selegue, J.P., Cooke, P.A., Gray, J.W., Chen, F.F., 2005. Molecular characterization of the cytotoxic mechanism of multiwall carbon nanotubes and nanofibers on human skin fibroblast. *Nano Letters* 5, 2448–2464.
- Dodziuk, H., Ejchart, A., Anczewski, W., Ueda, H., Krinichnaya, E., Dolgonosa, G., Kutner, W., 2003. Water solubilization, determination of the number of different types of single-wall carbon nanotubes and their partial separation with respect to diameters by complexation with h-cyclodextrin. *Chemical Communications*, 986–987.
- El-Fouly, M.H., Trosko, J.E., Chang, C.C., 1987. Scrape-loading and dye transfer: a rapid and simple technique to study gap junctional intercellular communications. *Experimental Cell Research* 168, 422–430.
- Elias, A.L., Carrero-Sanchez, J.C., Terrones, H., Endo, M., Lacleste, H.P., Mauricio, M., 2007. Viability studies of pure carbon- and nitrogen-doped nanotubes with *Entamoeba Histolytica*: from amoebicidal to biocompatible structures. *Small* 3 (10), 1723–1729.
- Enyashin, A.N., Gemming, S., Seifert, G., 2007. DNA-wrapped carbon nanotubes. *Nanotechnology* 18, 245702.
- Fiorito, S., Serafino, A., Andreola, F., Bernier, P., 2006. Effects of fullerenes and single-wall carbon nanotubes on murine and human macrophages. *Carbon* 44, 1100–1105.
- Flahaut, E., Durrieu, M.C., Remy-Zolghadri, M., Bareille, R., Baquey, C., 2006. Investigation of the cytotoxicity of CCVD carbon nanotubes towards human umbilical vein endothelial cells. *Carbon* 44 (6), 1093–1099.
- Fortner, J.D., Lyon, D.Y., Sayes, C.M., Boyd, A.M., Falkner, J.C., Hotze, E.M., Alemany, L.B., Tao, Y.J., Guo, W., Ausman, K.D., Colvin, V.L., Hughes, J.B., 2005. C₆₀ in water: nanocrystal formation and microbial response. *Environmental Science and Technology* 39 (11), 4307–4316.
- Georgakilas, V., Tagmatarchis, N., Pantarotto, D., Bianco, A., Briand, J.-P., Prato, M., 2002. Amino acid functionalisation of water soluble carbon nanotubes. *Chemical Communications*, 3050–3051.
- Grossiord, N., Schhoo, P., Meuldijk, J., Koning, C.E., 2007. Determination of the surface coverage of exfoliated carbon nanotubes by surfactant molecules in aqueous solution. *Langmuir* 23, 3646–3653.
- Gutierrez, M.C., Garcia-Carvajal, Z.Y., Hortiguera, M.J., Yuste, L., Rojo, F., Ferrer, M.L., Monte, F., 2007. Biocompatible MWCNT scaffolds for immobilization and proliferation of *E. coli*. *Journal of Materials Chemistry* 17, 2992–2995.
- Herner, H.A., Trosko, J.E., Masten, S.J., 2001. The epigenetic toxicity of pyrene and related ozonation byproducts containing an aldehyde functional group. *Environmental Science and Technology* 35 (17), 3576–3583.
- Herzog, E., Byrne, H.J., Davoren, M., Casey, A., Duschl, A., Oostingh, G.J., 2009. Dispersion medium modulates oxidative stress response of human lung epithelial cells upon exposure to carbon nanomaterial samples. *Toxicology and Applied Pharmacology* 236, 276–281.
- Huang, W.J., Taylor, S., Fu, K.F., Lin, Y., Zhang, D.H., Hanks, T.W., Rao, A.M., Sun, Y.P., 2002. Attaching proteins to carbon nanotubes via diimide-activated amidation. *Nano Letters* 2 (4), 311–314.
- Humic acids and their sodium salts. EMEA-The European agency for the evaluation of medicinal products. Available via <http://www.emea.europa.eu/pdfs/vet/mrls/055499en.pdf>, 1999.
- Hyung, H., Fortner, J.D., Hughes, J.B., Kim, J.H., 2007. Natural organic matter stabilizes carbon nanotubes in the aqueous phase. *Environmental Science and Technology* 41 (1), 179–184.
- Hyung, H., Kim, J.-H., 2008. Natural organic matter (NOM) adsorption to multi-walled carbon nanotubes: effect of NOM characteristics and water quality parameters. *Environmental Science and Technology* 42 (12), 4416–4421.
- Iijima, S., 1991. Helical microtubules of graphitic carbon. *Nature* 354 (6348), 56–58.
- Inoue, K.-i., Koike, E., Yanagisawa, R., Hirano, S., Nishikawa, M., Takano, H., 2009. Effects of multi-walled carbon nanotubes on a murine allergic airway inflammation model. *Toxicology and Applied Pharmacology* 237 (3), 306–316.

- Islam, M.F., Rojas, E., Bergey, D.M., Johnson, A.T., Yodh, A.G., 2003. High weight fraction surfactant solubilization of single-wall carbon nanotubes in water. *Nano Letters* 3 (2), 269–273.
- Jia, G., Wang, H., Yan, L., Wang, X., Pei, R., Yan, T., Zhao, Y., Guo, X., 2005. Cytotoxicity of carbon nanomaterials: single-wall nanotube, multi-wall nanotube, and fullerene. *Environmental Science and Technology* 39, 1378–1383.
- Jiang, J., Gao, L., 2003. Production of aqueous colloidal dispersions of carbon nanotubes. *Journal of Colloid and Interface Science* 260, 89–94.
- Kang, S., Herzberg, M., Rodrigues, D.F., Elimelech, M., 2008a. Antibacterial effects of carbon nanotubes: size does matter! *Langmuir* 24 (13), 6409–6413.
- Kang, S., Mauter, M.S., Elimelech, M., 2008b. Physicochemical determinants of multiwalled carbon nanotube bacterial cytotoxicity. *Environmental Science and Technology* 42 (19), 7528–7534.
- Kang, S., Mauter, M.S., Elimelech, M., 2009. Microbial cytotoxicity of carbon-based nanomaterials: implications for river water and wastewater effluent. *Environmental Science and Technology* 43 (7), 2648–2653.
- Kang, S., Pinault, M., Pfefferle, L.D., Elimelech, M., 2007. Single-walled carbon nanotubes exhibit strong antimicrobial activity. *Langmuir* 23 (17), 8670–8673.
- Karajanagi, S.S., Yang, H.C., Asuri, P., Sellitto, E., Dordick, J.S., Kane, R.S., 2006. Protein-assisted solubilization of single-walled carbon nanotubes. *Langmuir* 22 (4), 1392–1395.
- Kim, O.-K., Je, J., Baldwin, J.W., Kooi, S., Pehrsson, P.E., Buckley, L.J., 2004. Solubilization of single-wall carbon nanotubes by supramolecular encapsulation of helical amylose. *Journal of American Chemical Society* 125, 4426–4427.
- Lauret, J.-S., Voisin, C., Cassabois, G., Roussignol, P., Delalande, C., Capes, L.E., Valentin, E., Jost, O., 2004. Photocreated carrier dynamics in isolated carbon nanotubes. *Semiconductor Science and Technology* 19, S486–S488.
- Lee, J.U., Huh, J., Kim, K.H., Park, C., Jo, W.H., 2007. Aqueous suspension of carbon nanotubes via non-covalent functionalization with oligothiophene-terminated poly(ethylene glycol). *Carbon* 45, 1051–1057.
- Lin, Y., Taylor, S., Li, H.P., Fernando, K.A.S., Qu, L.W., Wang, W., Gu, L.R., Zhou, B., Sun, Y.P., 2004. Advances toward bioapplications of carbon nanotubes. *Journal of Materials Chemistry* 14 (4), 527–541.
- Lindberg, H.K., Falck, G.C.-M., Suhonen, S., Vippola, M., Vanhalab, E., Catalána, J., Savolainen, K., Norppa, H., 2009. Genotoxicity of nanomaterials: DNA damage and micronuclei induced by carbon nanotubes and graphite nanofibres in human bronchial epithelial cells in vitro. *Toxicology Letters* 186, 166–173.
- Liu, J., Rinzler, A.G., Dai, H.J., Hafner, J.H., Bradley, R.K., Boul, P.J., Lu, A., Iverson, T., Shelimov, K., Huffman, C.B., Rodriguez-Macias, F., Shon, Y.S., Lee, T.R., Colbert, D.T., Smalley, R.E., 1998. Fullerene pipes. *Science* 280 (5367), 1253–1256.
- Liu, Y.Q., Gao, L., Zheng, S., 2007. Debundling of single-walled carbon nanotubes by using natural polyelectrolytes. *Nanotechnology* 18 (36), 365702.
- Lyon, D.Y., Fortner, J.D., Sayes, C.M., Colvin, V.L., Hughes, J.B., 2005. Bacterial cell association and antimicrobial activity of a C60 water suspension. *Environmental Toxicology and Chemistry* 24, 2757–2762.
- Manna, S.K., Sarkar, S., Barr, J., Wise, K., Barrera, E.V., Jejelowo, O., Rice-Ficht, A., Ramesh, G.T., 2005. Single-walled carbon nanotube induces oxidative stress and activates nuclear transcription factor- κ B in human keratinocytes. *Nano Letters* 5, 1676–1684.
- Marsh, D.H., Rance, G.A., Zaka, M.H., Whitby, R.J., Khlobystov, A.N., 2007. Comparison of the stability of multiwalled carbon nanotube dispersions in water. *Physical Chemistry Chemical Physics* 9 (40), 5490–5496.
- McDonald, T.J., Engtrakul, C., Jones, M., Rumbles, G., Heben, M.J., 2006. Kinetics of PL quenching during single-walled carbon nanotube rebundling and diameter-dependent surfactant interactions. *Journal of Physical Chemistry B* 110, 25339–25346.
- Meng, J., Yanga, M., Song, L., Kong, H., Wang, C.Y., Wang, R., Wang, C., Xie, S.S., Xua, H.Y., 2009. Concentration control of carbon nanotubes in aqueous solution and its influence on the growth behavior of fibroblasts. *Colloids and Surfaces B: Biointerfaces* 71, 148–153.
- Moore, V.C., Strano, M.S., Haroz, E.H., Hauge, R.H., Smalley, R.E., Schmidt, J., Talmon, Y., 2003. Individually suspended single-walled carbon nanotubes in various surfactants. *Nano Letters* 3 (10), 1379–1382.
- Muller, J., Huaux, F., Moreau, N., Misson, P., Heilier, J.-F., Delos, M., Arras, M., Fonseca, A., Nagy, J.B., Lison, D., 2005. Respiratory toxicity of multi-wall carbon nanotubes. *Toxicology and Applied Pharmacology* 207 (31), 221–231.
- Narayan, R.J., Berry, C.J., Brigmon, R.L., 2005. Structural and biological properties of carbon nanotube composite films. *Materials Science and Engineering B* 123, 123–129.
- O'Connell, M.J., Bachilo, S.M., Huffman, C.B., Moore, V.C., Strano, M.S., Haroz, E.H., Rialon, K.L., Boul, P.J., Noon, W.H., Kittrell, C., Ma, J., Hauge, R.H., Weisman, R.B., Smalley, R.E., 2002. Band gap fluorescence from individual single-walled carbon nanotubes. *Science* 297, 593–596.
- O'Connell, M.J., Boul, P.J., Ericson, L.M., Huffman, C., Wang, Y., Haroz, E., 2001. Reversible water-solubilization of single-walled carbon nanotubes by polymer wrapping. *Chemical Physics Letters* 342, 265–271.
- Park, H.J., Heo, H.Y., Lee, S.C., Park, M., Lee, S.-S., Kim, J., Chang, J.Y., 2006. Dispersion of single-walled carbon nanotubes in water with polyphosphazene polyelectrolyte. *Journal of Inorganic and Organometallic Polymers and Materials* 16 (4) 359–364.
- Pulskamp, K., Worle-Knirsch, J.M., Hennrich, F., Kern, K., Krug, H.F., 2007. Human lung epithelial cells show biphasic oxidative burst after single-walled carbon nanotube contact. *Carbon* 45, 2241–2249.
- Saleh, N.D., Pfefferle, L.D., Elimelech, M., 2009. Aggregation kinetics of multiwalled carbon nanotubes in aquatic systems: measurements and environmental implications. *Environmental Science and Technology* 42 (21), 7963–7969.
- Salzmann, C.G., Chu, B.T.T., Tobias, G., Llewellyn, S.A., Green, M.L.H., 2007. Quantitative assessment of carbon nanotube dispersions by Raman spectroscopy. *Carbon* 45 (5), 907–912.
- Satoh, A.Y., Trosco, J., Masten, S.J., 2003. Epigenetic toxicity of hydroxylated biphenyls and hydroxylated polychlorinated biphenyls on normal rat liver epithelial cells. *Environmental Science and Technology* 37, 2727–2733.
- Sayes, C.M., Liang, F., Hudson, J.L., Mendoza, J., Guob, W., Beach, J.M., Moore, V.C., Doyle, C.D., West, J.L., Billups, W.E., Ausmanb, K.D., Colvin, V.L., 2006. Functionalization density dependence of single-walled carbon nanotubes cytotoxicity in vitro. *Toxicology Letters* 161, 135–142.
- Schmitt, D., Tran, N., Riefler, S., Jacoby, J., Merkel, D., Marone, P., Naouli, N., 2008. Toxicologic evaluation of modified gum acacia: mutagenicity, acute and subchronic toxicity. *Food and Chemical Toxicology* 46, 1048–1054.
- Simon-Deckers, A., Gouget, B., Mayne-L'Hermiteb, M., Herlin-Boimeb, N., Reynaudb, C., Carrièrea, M., 2008. In vitro investigation of oxide nanoparticle and carbon nanotube toxicity and intracellular accumulation in A549 human pneumocytes. *Toxicology* 253, 137–146.
- Sinani, V.A., Gheith, M.K., Yaroslavov, A.A., Rakhnyanskaya, A.A., Sun, K., Mamedov, A.A., Wicksted, J.P., Kotov, N.A., 2005.

- Aqueous dispersions of single-wall and multiwall carbon nanotubes with designed amphiphilic polycations. *Journal of American Chemical Society* 127 (10), 3463–3472.
- Star, A., Steuerman, D.W., Heath, J.R., Stoddart, J.F., 2002. Starched carbon nanotubes. *Angewandte Chemie International Edition* 41 (14), 2508–2512.
- Tang, Y.J., Ashcroft, J.M., Chen, D., Min, G., Kim, C.-H., Murkhejee, B., Larabell, C., Keasling, J.D., Chen, F.F., 2007. Charge-associated effects of fullerene derivatives on microbial structural integrity and central metabolism. *Nano Letters* 7 (3), 754–760.
- Tasis, D., Tagmatarchis, N., Bianco, A. and Prato, M., 2006. Chemistry of carbon nanotubes. 106 (3), 1105–1136.
- Tong, Z., Bischoff, M., Nies, L., Applegate, B., Turco, R., 2007. Impact of fullerene (C60) on a soil microbial community. *Environmental Science and Technology* 41, 2985–2991.
- Trosko, J.E., Chang, B.V., Madhucar, J.E., Klauning, J.E., 1991. Chemical, oncogene, and growth factor inhibition of gap junctional intercellular communication: an alternative hypothesis to carcinogenesis. *Pathobiology* 58, 265–278.
- Trosko, J.E., Chang, C.-C., Upham, B., Wilson, M., 1998. Epigenetic toxicology as toxicant-induced changes in intracellular signalling leading to altered gap junctional intercellular communication. *Toxicology Letters* 102–103, 71–78.
- Tseng, C.-H., Wang, C.-C., Chen, C.-Y., 2006. Modification of multi-walled carbon nanotubes by plasma treatment and further use as templates for growth of CdS nanocrystals. *Nanotechnology* 17, 5602–5612.
- Upham, B.L., Masten, S.J., Lochwood, B.R., Trosko, J.E., 1994. Nongenotoxic effects of polycyclic aromatic hydrocarbons and their ozonation by-products on the intercellular communication of rat liver epithelial cells. *Fundamental and Applied Toxicology* 23, 470–475.
- Vaisman, L., Marom, G., Wagner, H.D., 2006. Dispersions of surface-modified carbon nanotubes in water-soluble and water-insoluble polymers. *Advanced Functional Materials* 16 (3), 357–363.
- Vittorio, O., Raffa, V. and Cuschieri, A., Influence of purity and surface oxidation on cytotoxicity of multi-wall carbon nanotubes with human neuroblastoma cells. *Nanomedicine: Nanotechnology, Biology, and Medicine*, in press, doi:10.1016/j.nano.2009.02.006.
- Wang, Y., Iqbal, Z., Malhotra, S.V., 2005. Functionalization of carbon nanotubes with amines and enzymes. *Chemical Physics Letters* 402, 96–101.
- Weis, L.M., Rummel, A.M., Masten, S.J., Trosko, J.E., Upham, B.L., 1998. Bay or baylike regions of polycyclic aromatic hydrocarbons were potent inhibitors of gap junctional intercellular communication. *Environmental Health Perspectives* 106 (1), 17–22.
- Wick, P., Manser, P., Limbach, L.K., Dettlaff-Weglikowskab, U., Krumeich, F., Roth, S., Stark, W.J., Bruinink, A., 2007. The degree and kind of agglomeration affect carbon nanotube cytotoxicity. *Toxicology Letters* 168, 121–131.
- Wirnitzer, U., Herbold, B., Voetz, M., Ragot, J., 2009. Studies on the in vitro genotoxicity of baytubes[®], agglomerates of engineered multi-walled carbon-nanotubes (MWCNT). *Toxicology Letters* 186, 160–165.
- Wörle-Knirsch, J.M., Pulskamp, K., Krug, H.F., 2006. Oops they did it again! Carbon nanotubes hoax scientists in viability assays. *Nano Letters* 6 (6), 1261–1268.
- Xu, F.-M., Xu, J.-P., Ji, J., Shen, J.-C., 2008. A novel biomimetic polymer as amphiphilic surfactant for soluble and biocompatible carbon nanotubes (CNTs). *Colloids and Surfaces B: Biointerfaces* 67, 67–72.
- Yamasaki, Y., 1990. Gap junctional intercellular communication and carcinogenesis. *Carcinogenesis* 11, 1051–1058.
- Yang, H., Liu, C., Yang, D., Zhanga, H., Xia, Z., 2009. Comparative study of cytotoxicity, oxidative stress and genotoxicity induced by four typical nanomaterials: the role of particle size, shape and composition. *Journal of Applied Toxicology* 29, 69–78.
- Yang, S.-T., Wang, X., Jia, G., Guc, Y., Wang, T., Nie, H., Ge, C., Wang, H., Liu, Y., 2008. Long-term accumulation and low toxicity of single-walled carbon nanotubes in intravenously exposed mice. *Toxicology Letters* 181, 182–189.
- Yang, Z., Chen, X.H., Chen, C.S., 2007. Noncovalent-wrapped sidewall multi-walled carbon nanotubes functionalization with polyimide. *Polymer Composites* 28 (1), 36–41.
- Ye, S.-F., Wu, Y.-H., Hou, Z.-Q., Zhang, Q.-Q., 2009. ROS and NF- κ B are involved in upregulation of IL-8 in A549 cells exposed to multi-walled carbon nanotubes. *Biochemical and Biophysical Research Communications* 379, 643–648.
- Yu, B.Z., Yang, J.S., Li, W.X., 2007. In vitro capability of multi-walled carbon nanotubes modified with gonadotrophin releasing hormone on killing cancer cells. *Carbon* 45 (10), 1921–1927.
- Yun, Y., Dong, Z., Tan, Z., Schulz, M.J., Shanov, V., 2009. Fibroblast cell behavior on chemically functionalized carbon nanomaterials. *Materials Science and Engineering C* 29, 719–725.
- Zhu, Y., Ran, T., Li, Y., Guo, J., Li, W., 2006. Dependence of the cytotoxicity of multi-walled carbon nanotubes on the culture medium. *Nanotechnology* 16, 4668–4674.
- Zong, S., Cao, Y., Jua, H., 2007. Direct electron transfer of hemoglobin immobilized in multiwalled carbon nanotubes enhanced grafted collagen matrix for electrocatalytic detection of hydrogen peroxide. *Electroanalysis* 19 (7–8), 841–846.

XIV. Steuer, A., Schmidt, A., Labohá, P., **Babica, P.**, Kolb, J.F.* , 2016. Transient suppression of gap junctional intercellular communication after exposure to 100-nanosecond pulsed electric fields. *Bioelectrochemistry* 112, 33–46.



Transient suppression of gap junctional intercellular communication after exposure to 100-nanosecond pulsed electric fields



Anna Steuer^a, Anke Schmidt^a, Petra Labohá^{a,b}, Pavel Babica^b, Juergen F. Kolb^{a,*}

^a Leibniz Institute for Plasma Science and Technology, Greifswald, Germany

^b Research Centre for Toxic Compounds in the Environment (RECETOX), Faculty of Science, Masaryk University, Brno, Czech Republic

ARTICLE INFO

Article history:

Received 27 January 2016

Received in revised form 7 July 2016

Accepted 8 July 2016

Available online 10 July 2016

Keywords:

GJIC

nsPEF

Connexin 43

Cx43

MAP kinase

Actin

ABSTRACT

Gap junctional intercellular communication (GJIC) is an important mechanism that is involved and affected in many diseases and injuries. So far, the effect of nanosecond pulsed electric fields (nsPEFs) on the communication between cells was not investigated. An *in vitro* approach is presented with rat liver epithelial WB-F344 cells grown and exposed in a monolayer. In order to observe sub-lethal effects, cells were exposed to pulsed electric fields with a duration of 100 ns and amplitudes between 10 and 20 kV/cm. GJIC strongly decreased within 15 min after treatment but recovered within 24 h. Gene expression of Cx43 was significantly decreased and associated with a reduced total amount of Cx43 protein. In addition, MAP kinases p38 and Erk1/2, involved in Cx43 phosphorylation, were activated and Cx43 became hyperphosphorylated. Immunofluorescent staining of Cx43 displayed the disassembly of gap junctions. Further, a reorganization of the actin cytoskeleton was observed whereas tight junction protein ZO-1 was not significantly affected. All effects were field- and time-dependent and most pronounced within 30 to 60 min after treatment. A better understanding of a possible manipulation of GJIC by nsPEFs might eventually offer a possibility to develop and improve treatments.

© 2016 Elsevier B.V. All rights reserved.

1. Introduction

Pulsed electric fields applied to living cells can induce different biological effects depending on pulse duration and field strength. Pulses in the range of milli- to microseconds primarily affect the outer membrane, while shorter pulses with duration in the nanosecond range have a more pronounced effect on subcellular structures. Interest in the study of pulsed electric field exposures arises mainly from the potential to induce different biological responses which can be exploited for medical applications. Among those successfully in use in the hospital already are electrochemotherapy by using reversible electroporation [1–5] and tissue ablation by irreversible electroporation [6,7]. Both methods use rather long electrical pulses of microsecond or even millisecond duration. Pulsed electric field exposures with individual pulse durations that are short compared to the charging time of the outer membrane, i.e. nanosecond pulsed electric field (nsPEF) exposures, have been found to induce apoptosis in cancer cells and are currently investigated with respect to cancer treatment [8–13].

The development of medical therapies is associated with the need of a deeper understanding of interactions between pulsed electric fields and cells. Although the fundamental and direct mechanism must be

an effect on charges and dipoles of cellular constituents, subsequent biochemical responses and their complex relationship are deciding on the fate of a cell. A distinction between first or direct physical mechanisms and induced secondary or indirect biochemical processes is sought after to establish a chain of events but often difficult to establish [14, 15]. Investigations on the mechanisms of the interaction of pulsed electric fields with cells were so far mostly done on single cells. Some of the studied effects are for example the formation of pores in the plasma membrane, the release of calcium from intracellular stores or the breakdown of the cytoskeleton [14,16–21]. Conversely, in animal studies in particular the possibility for cancer treatments was intensively investigated [10,12,22]. However, between the study of single cells and the complex responses of tumors in an animal, only little is known about the direct effects of nsPEF on cells that are connected and communicate with each other in a tissue.

Gap junctional intercellular communication (GJIC) is important for the regulation of cell growth control, differentiation and apoptosis. An impaired cell-cell communication is a crucial factor in many diseases such as skin diseases, deafness and cataract [23,24]. Furthermore, it plays an important role in cancer and metastasis formation as well as in wound healing [25–35]. Direct communication between mammalian cells is mediated by gap junctions. These are water-filled pores that directly connect adjacent cells. One connexon (hemichannel) consists of six connexin (Cx) proteins and two connexons form one gap junction (GJ). 21 members of the Cx-gene family are known in humans and 20 in mice, with the

* Corresponding author at: Leibniz Institute for Plasma Science and Technology, Felix-Hausdorff-Strasse 2, 17489 Greifswald, Germany.

E-mail address: juergen.kolb@inp-greifswald.de (J.F. Kolb).

encoded proteins named after their molecular weight, e.g. Cx43. GJs allow the diffusion of ions or signaling molecules with a size up to 1 kDa to adjacent cells. Cell-cell communication is not only regulated by the amount of GJs in the membrane but also by their opening state (gating). The opening state is influenced by different factors such as Cx phosphorylation, membrane polarization and intracellular pH-value and calcium level [36,37]. Cx phosphorylation by mitogen-activated protein (MAP) kinases including extracellular signal regulated kinases (Erk), p38 and C-Jun N-terminal kinases (Jnk) represents probably the most characterized and studied mechanism of GJIC regulation [38–40].

NsPEFs applied to cells can induce the breakdown of the cytoskeleton [20,41,42]. An intact actin and microtubule cytoskeleton is necessary for building and degradation of GJs. After the chemically induced disruption of the cytoskeleton connexin proteins accumulate in the cytoplasm while the amount of membrane-bound connexin decreases. Thus, inhibition of the cytoskeleton is expected to affect GJIC either directly by influencing the mechanisms of the channel transfer or indirectly by disturbing the correct assembly of the GJs [43].

For the study of nsPEF-induced effects on GJIC and the mechanisms involved in its regulation, the rat liver epithelial cells WB-F344 [44] were grown and exposed in monolayers. These non-cancer, stem-like cells have a high expression of Cx43 and, unlike most other cell lines, communicate strongly via GJs *in vitro*. This cell line has been widely used as a model system for the study of gap junctional intercellular communication by Trosko et al. [45–49].

The aim of our experiments was to investigate the effects of sub-lethal exposure conditions. Therefore, we chose a pulse length of 100 ns that has often been used in animal studies [11,13,50,51] and rather mild field strengths of ≤ 35 kV/cm. After the application of trains of 20 pulses to confluent monolayers, GJIC and related parameters and markers were investigated, including gene and protein expression of Cx43 and activation of different MAP kinases. In addition, Cx43 distribution and actin cytoskeleton rearrangements that are directly related to ability of cells to communicate were determined.

2. Materials and methods

2.1. Cell culture

WB-F344 cell line was derived from normal adult male Fischer 344 rat liver by J.W. Grisham and M.S. Tsao of the University of North Carolina at Chapel Hill, Chapel Hill, NC, USA [44], and the culture was obtained from Prof. J. E. Trosko, Michigan State University, East Lansing, MI, USA. WB-F344 cells are diploid, non-tumorigenic, possessing characteristics of normal liver progenitor or bipolar stem cells, whose intrahepatic transplantation into adult syngenic F344 rats results in the morphologic differentiation of these cells into hepatocytes and incorporation into hepatic plates [52]. WB cells express Cx43 and have been extensively characterized for alterations of GJIC in the absence and presence of well-known tumor promoters, growth factors, tumor suppressor genes, and oncogenes [28].

WB-F344 cells were cultured in low-glucose DMEM (#8950614), supplemented with 2 mM L-glutamine, 5% fetal calf serum and 1% penicillin/streptomycin (#4211014) (all purchased from PAN-Biotech GmbH, Aidenbach, Germany) in a humidified CO₂ (5%) incubator. Cells were seeded in 12-well plates. Exposures were done after 48 h of cell growth, when a confluent monolayer was achieved.

2.2. Experimental setup

The experimental setup (Fig. 1) for the application of electric pulses to a monolayer consists of the in-house developed pulse generator, the power supply (FX20R15, Glassman, High Bridge, NJ), a fast oscilloscope (TDS3054, Tektronix, Beaverton, OR) and a high voltage probe (P5100A, Tektronix). The pulse-generator is based on the Blumlein concept and delivers pulses with a duration of 100 ns [53]. The electrode

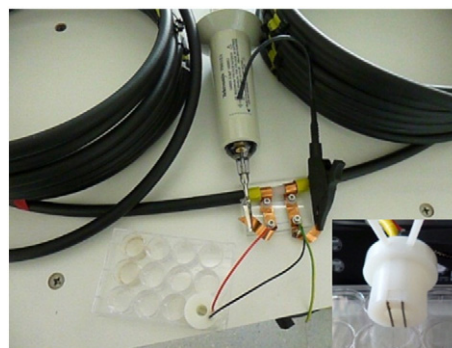


Fig. 1. Overview of the experimental setup with pulse generator, electrode configuration and high voltage probe. Electrodes are embedded in a nylon-cylinder to apply the electric pulses to a monolayer in a 12-well plate.

configuration consists of two parallel stainless steel wires fixed in a plastic cylinder that was tightly fitting in the well of a 12-well plate. The wires have a diameter of 0.8 mm and a gap distance of 5 mm measured from the center of each electrode. The electric field was applied by slightly impressing the electrodes into the monolayer until the electrodes touched the bottom of the well. 20 pulses with amplitudes between 5 and 35 kV/cm were applied.

2.3. MTT assay

3-(4,5-Dimethylthiazol-2-yl)-2,5-diphenyltetrazolium bromide (MTT) was added within 2–10 min after treatment to analyze the respiratory activity of the cells which correlates with cell viability. When a confluent monolayer was achieved cells were exposed to nsPEFs in cell culture medium. Then, cell culture medium was replaced by 500 μ l medium and 50 μ l MTT-solution (5 mg/ml in PBS; AppliChem, Darmstadt, Germany). After 2 h of incubation at 37 °C the MTT-solution was removed and the monolayers were washed once with HBSS. The cells were then lysed with a cell lysing buffer (99.4 ml DMSO, 0.6 ml acetic acid (100%), 10 g SDS). After 5 min incubation time and 5 additional minutes on a shaker the absorbance of the lysate was measured at 550 nm with a reference wavelength of 700 nm (Infinite M200 PRO, Tecan, Männedorf, CH). In each experiment, the weighted absorption values were determined in triplicates for each set of exposure parameters.

2.4. Scrape loading/dye transfer assay

Scrape loading/dye transfer (SLDT) assay was performed to investigate cell-cell communication [54]. After a certain incubation period of the nsPEF treated cell monolayers medium was removed and replaced by 0.05% Lucifer Yellow (L0259, Sigma-Aldrich, Taufkirchen, Germany) and 0.1% dextran conjugated Texas Red (10,000 MW, D-1828, Invitrogen, Darmstadt, Germany) dissolved in PBS. A razor blade was used to make a scrape across the treated cells which were then incubated for 2 min to allow dye uptake by the damaged cells along the scratch. If the cells are connected by functional GJs, the GJ-permeable Lucifer Yellow (LY) diffuses to adjacent cells whereas the GJ-impermeable Texas Red-Dextran (TR-Dx), which serves as loading control and to exclude dye uptake due to electroporation, remains only in the damaged cells. Afterwards, cells were rinsed with PBS and fixed with 4% paraformaldehyde. Finally, monolayers were observed under a fluorescent microscope (Axio Observer D1, Carl Zeiss, Berlin, Germany).

The fluorescent area of the LY migration from the scrape line was quantified by using MATLAB. For this purpose, fluorescence images were converted into black-and-white-images by defining a threshold-value which determined the brightness at which pixels were converted into black and white, respectively. This threshold was kept the same for the evaluation of each experiment. The fluorescent areas of the LY channel of the treated cells were then normalized to the areas of the control

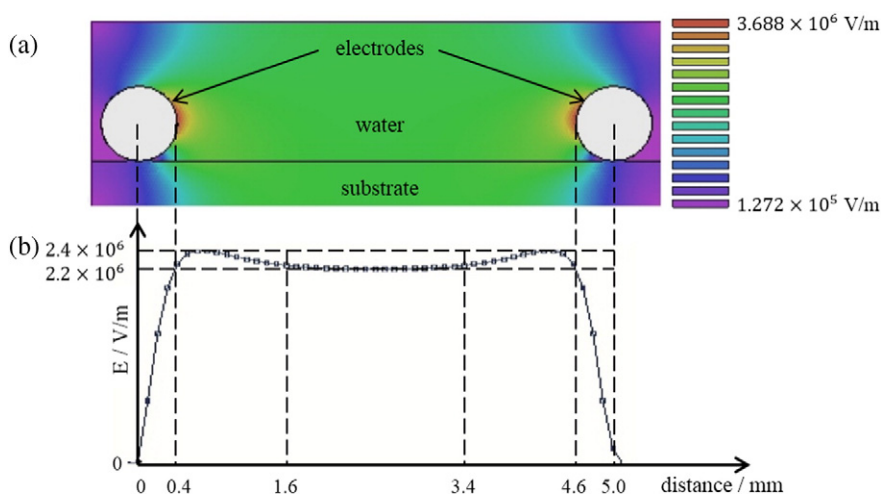


Fig. 2. Color-coded simulation of the electric field distribution of the experimental setup (a) and electric field distribution on the surface of the substrate where the cells are attached (b). For the simulation an applied voltage of 10 kV was set, a gap distance of 5 mm between the electrodes and relative permittivities of 80 for water and of 2 for the substrate.

cells. The fluorescent area of TR had a mean value of 5% which was subtracted from the fluorescent area of LY to quantify only the cells that were involved in GJIC.

2.5. Immunofluorescent staining

Cells were seeded on glass cover slips (# 630-1597, 13 mm diameter, VWR, Darmstadt, Germany) placed in the wells of a 12-well plate to observe the distribution of Cx43, F-actin and ZO-1 in WB-F344 cells by immunofluorescent staining. Cells were treated with nsPEFs when a confluent monolayer was formed. After a desired post-treatment

incubation period cells were fixed with 4% paraformaldehyde and permeabilized with 0.25% Triton X-100 in PBS. Afterwards, cells were incubated at 4 °C overnight with Phalloidin-FITC (Phalloidin, Fluorescein Isothiocyanate Labeled, Sigma-Aldrich, Taufkirchen, Germany) to stain the actin cytoskeleton, together with the primary Cx43-antibody (Cell Signaling #3512, Frankfurt am Main, Germany), diluted in 1% (w/v) BSA/PBS solution to block the unspecific binding sites. The tight junction protein ZO-1 was stained the same way as described above but with the primary antibody rabbit-anti-ZO-1 (QA213066, Life Technologies, Darmstadt, Germany, 1:200 in 1% BSA/PBS) and without concurrently staining of F-actin.

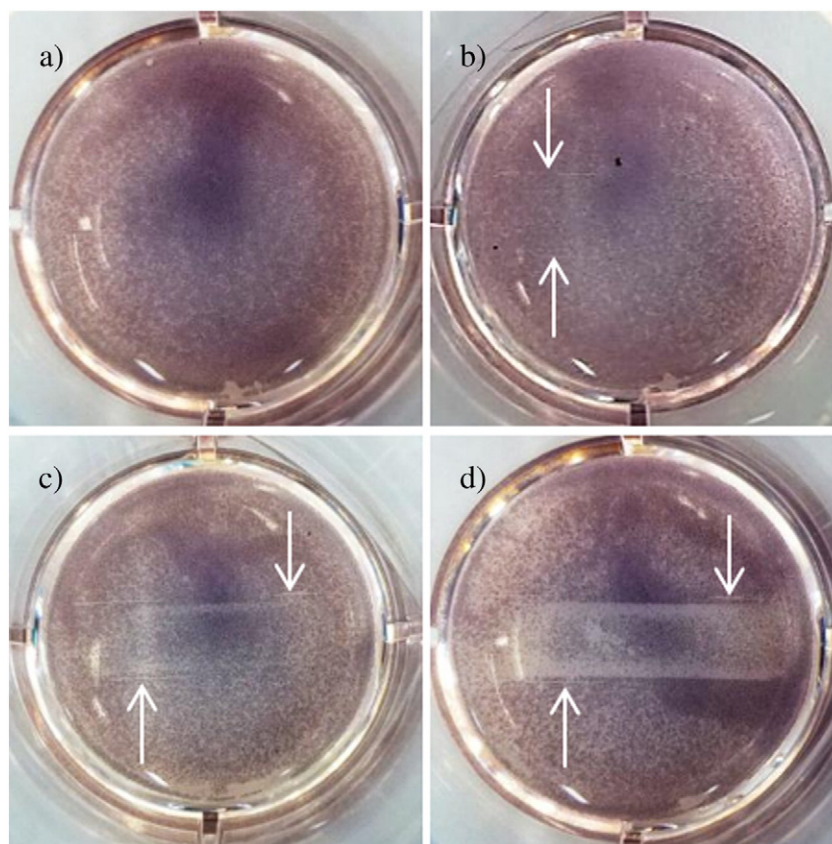


Fig. 3. MTT assay of a control WB-F344 monolayer (a) and after exposure to 20 pulses of 100 ns and 5 kV/cm (b), 15 kV/cm (c) and 25 kV/cm (d) before cell lysis. The white arrows point at the positions of the electrodes. Only the cell survival of the cells between the electrodes was affected.

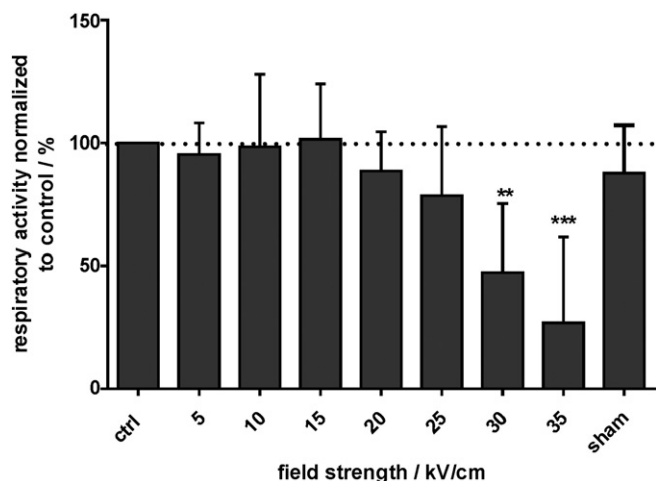


Fig. 4. Viability of WB-F344 cells exposed to 20 pulses of 100 ns and 5–35 kV/cm determined by MTT assay. The diagram shows the mean values \pm SE normalized to control, $n = 4$ (independently repeated experiments).

The following day, cells were incubated with the secondary antibody conjugated with Alexa Fluor 546 (A-11035, Life Technologies) and Hoechst 33342 to stain the nuclei. Finally, samples were observed under a confocal microscope (TCS SP5, Leica, Wetzlar, Germany).

2.6. Quantitative real-time PCR

After nsPEF treatment, cells were washed twice with PBS. For each time point and field strength cells of all wells of one 12-well plate were collected, but only the cells between the electrodes were scraped off for gene analysis. Total RNA was isolated with the RNA MiniKit (Bio&Sell, Feucht, Germany) according to the manufacturer's instructions. 1 μ g RNA was transcribed into cDNA with the Transcriptor First Strand Synthesis Kit (Hofmann-La Roche AG, Basel, CH) according to the manufacturer's instructions. Subsequently, quantitative real-time PCR (qPCR) was done with the RealTime ready Catalog assay GAJ1 for Cx43 and RPL13A for the housekeeping gene, respectively (Hofmann-La Roche AG, Basel, CH), using 100 ng of cDNA. The protocol of the LightCycler 480 (Hofmann-La Roche AG, Basel, CH) included pre-incubation at 95 °C for 10 min, 45 cycles at 95 °C for 10 s, annealing for 30 s at 60 °C, and an amplification step at 72 °C for 1 s.

Final values for gene expression in the treated samples were determined as the ratio of the gene expression in the respective sample related to the control.

2.7. Western blot

Cells were collected the same way as for gene expression analysis. After centrifugation, pellets were suspended in 60 μ l lysis buffer

containing 50 mM Tris, 10 mM EDTA and 1% SDS, and sonicated twice before 15 μ l of 5 \times Laemmli buffer were added. Samples intended for the analysis of p38 and Erk1/2 were heated for 5 min at 95 °C, samples for Cx43 analysis were incubated for 1 h at 37 °C. 30 μ l of each sample (typically about 1 μ g/ μ l) was loaded on Criterion™ TGX Stain-Free™ Precast Gels (Bio-Rad, Hercules, CA). After gel electrophoresis, the TGX Stain-Free™ gels were activated by UV-light to visualize total protein content and then imaged with the Bio-Rad Gel Doc EZ System.

PVDF membranes (Bio-Rad) were equilibrated for 30 s in 96% ethanol, before the separated proteins were blotted on the membranes with the Trans-Blot Turbo Transfer System and imaged with the Gel Doc EZ System. The membranes were blocked for 30 min in a blocking solution of 5% (w/v) non-fat dry milk in Tris-buffered saline with 0.1% of Tween 20 (TBST). After the blocking step the membranes were incubated overnight with the primary antibody diluted 1:1000 in blocking solution at 4 °C, followed by incubation with secondary horseradish peroxidase (HRP)-conjugated goat anti-rabbit antibody (Jackson ImmunoResearch, West Grove, PA) diluted 1:10,000 in blocking solution for 1 h at room temperature. Following, primary antibodies were used, all purchased from New England Biolabs (Ipswich, MA): Cx43 (#3512), p38 (#8690), phosphorylated p38 (#4511), Erk1/2 (#9102), phosphorylated Erk1/2 (#4370). Membranes blotted with p38 and Erk1/2 proteins were used twice, first for the detection of the phosphorylated and then of the non-phosphorylated form. Therefore, membranes were intermittently incubated with harsh stripping solution (62.5 mM Tris, 1% SDS, 100 mM β -mercaptoethanol, pH 6.7) for 20 min at 70 °C. The Cx43-antibody detects total, i.e. phosphorylated as well as non-phosphorylated, Cx43.

Amersham ECL Select (GE Healthcare, Chalfont, UK) was used for the detection of the target proteins, according to the manufacturer's protocol. Chemiluminescent signals were visualized with ImageQuant LAS 4000 (GE Healthcare). Data were evaluated using ImageQuant TL Software (GE Healthcare). Chemiluminescence intensities of specific protein bands were normalized to Stain-Free™ fluorescence intensity of total protein in the corresponding lane. Normalization to total protein has been repeatedly demonstrated to be more reliable and robust method for quantitation of Western blot data than normalization to highly abundant housekeeping proteins loaded in saturating quantities in a typical Western blot experiment [55,56]. In addition, possible changes in many cytoskeletal proteins typically used as a loading control (actin, tubulin) were expected in response to nsPEF treatment, thus standardized method of total protein normalization based on TGX Stain-Free™ technology was used. Data normalized to total protein were then normalized to control.

2.8. Statistics

For the evaluation of the MTT, the SLDT, the qPCR and the Western blot data at least 3 independent experiments for each field strength and time point were performed. Significance was analyzed by one-

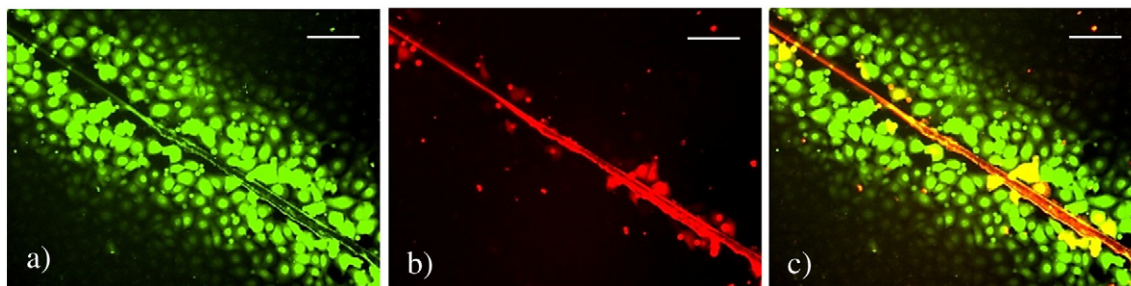


Fig. 5. SLDT assay performed on a control WB-F344 monolayer reveals the propagation of the GJ-permeable dye Lucifer Yellow (a) and the GJ-impermeable dye Texas Red-Dextran (b). While Texas Red-Dextran remains in the damaged cells along the scrape, Lucifer Yellow diffuses to adjacent cells. In (c) the overlay of the two channels is shown (scale bars: 100 μ m). (For interpretation of the references to color in this figure, the reader is referred to the web version of this article.)

way ANOVA with *Dunnett's* post-hoc test with significance levels of p-value < 0.05 (*), p-value < 0.01 (**), and p-value < 0.001 (***).

3. Results

3.1. Electric field distribution

Two parallel wires with a diameter of 0.8 mm each were used as electrodes. The cylindrical electrodes are rather large compared to the size of cells. Furthermore, the electrodes are placed on top of the cells, slightly impressing into the monolayer. Altogether, this results in

some inhomogeneities of the applied electric fields. To estimate the electric field through the monolayer the electric field distribution was simulated with the static electric field simulation software EStat (Field Precision LLC, Albuquerque, NM) with following parameters: gap distance between the electrodes of 5 mm, relative permittivity for water equals 80, a relative permittivity of the substrate of 2 (which is in the range of the material of cell culture dishes), and an applied voltage of 10 kV (Fig. 2).

Fig. 2a shows the color-coded electric field distribution for high voltage pulses applied in water. A cross section of the electric field in the plane of the monolayer, i.e. close to the substrate is shown in Fig. 2b.

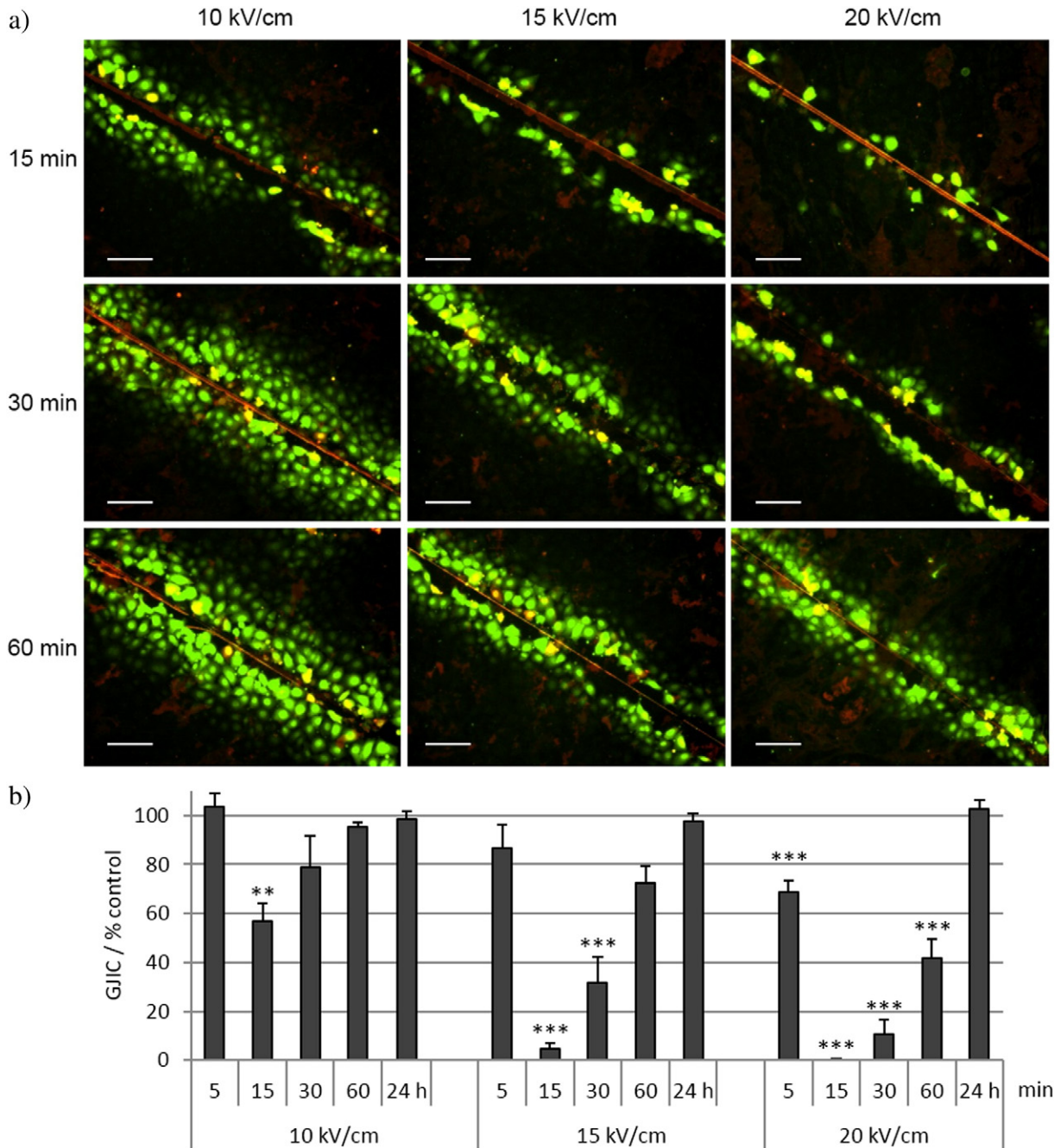


Fig. 6. Impact of nsPEFs on gap junctional intercellular communication intensity. WB-F344 cells were exposed to 20 pulses of 100 ns and 10, 15 or 20 kV/cm. a) Microscopy images of the SLDT assay 15, 30 and 60 min after nsPEF treatment (scale bars: 100 μ m). The figure shows the overlay images of the Lucifer Yellow and the Texas Red channel. b) Evaluated data of the SLDT assay 5, 15, 30, 60 min and 24 h after pulse application. GJIC is affected in a time- and field strength-dependent manner. Data are given as mean values of percentage normalized to control \pm SD.

In a homogenous electric field one would expect a field strength of 20 kV/cm for an applied voltage of 10 kV. For the used wire electrodes that are large in diameter compared to the gap distance, the electric field is slightly higher by about 8% close to the electrodes in comparison to the center of the area of exposure. The simulation shows that overall, the electric field can still be approximated from the applied voltage divided by the nominal electrode distance (center to center) for a width of about 5 mm within reasonable accuracy, especially taking into account fluctuations in pulse amplitude and also with respect to comparison of different parameters. Accordingly, for an applied voltage of 10 kV, in the middle between the electrodes the electric field remains almost constant over a wide distance at a value close to 20 kV/cm.

3.2. Cell viability

Cell survival for different exposure parameters was determined by MTT assay after application of 20 high voltage pulses with field strengths of 5, 10, 15, 20, 25, 30 and 35 kV/cm. Fig. 3 shows typical examples of exposed monolayers after incubation with MTT but before adding cell lysis buffer. The purple color represents the accumulation of insoluble formazan formed by respiratory activity of the cells and thus their viability. The white arrows point out the position of the electrodes during exposures.

For cells that were treated with higher field strengths (15 and 25 kV/cm, Fig. 3c and d) a small gap between the electrode positions and where

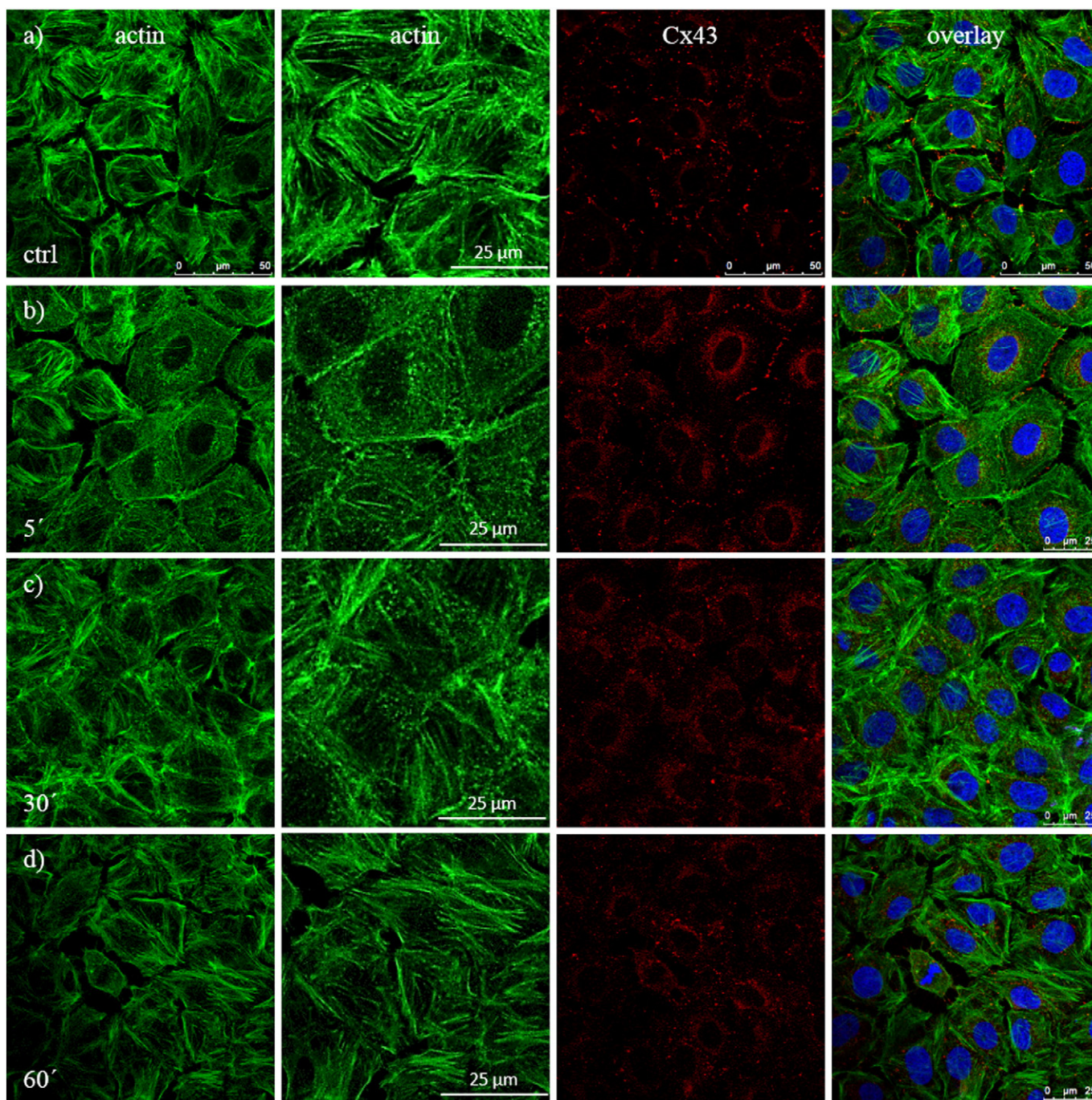


Fig. 7. Staining of Cx43 (red) and actin (green) in a control WB-F344 monolayer (a) and 5, 30 and 60 min after application of 20 pulses of 100 ns and 20 kV/cm (b–d). The images in the second column show an enlarged part of the images of the first column. The actin cytoskeleton is reorganized in a time-dependent manner, also Cx43 distribution changes with time (nuclei are labeled blue). (For interpretation of the references to color in this figure legend, the reader is referred to the web version of this article.)

the electric field starts to have impact on the enzyme activity is visible. Close to the position where the electrodes had contact with the monolayer, the cells did not seem to be affected. This is in agreement with the decreased electric field closer to the contact points as shown by the field simulation (Fig. 2).

After cell lysis, the photometrically measured values of the treated areas were put in relation to the non-treated areas. Therefore, wells containing only non-treated cells were used for control and the mean absorption value of these wells was set to 100% cell survival. The exposed area of the monolayer, i.e. the area between the electrodes, amounts to 23.5% of the whole well area and correspondingly the non-treated part to 76.5%. With these fractions the response and viability in the treated area could be calculated using the following equation with x as absorption of the treated area: absorption (whole well) = $0.765 \cdot \text{ctrl} + 0.235 \cdot x$.

Fig. 4 shows the mean values with standard errors for the corresponding number of surviving cells in the treated areas of 4 independent experiments. The results show that viability of WB-F344 cells remained at control level for an applied field strength up to 15 kV/cm. About 88% of the exposed cells survived exposures with an amplitude of 20 kV/cm. For higher field strengths, viability continuously decreases from 77% for a field strength of 25 kV/cm to a value of about 27% for a field strength of 35 kV/cm.

To ensure that cells fluoresce due to cell-cell communication and not due to pore formation in the membrane, the possibility of electroporation was analyzed by propidium iodide (PI) uptake ($3 \mu\text{M}$ diluted in complete medium) for field strengths up to 20 kV/cm. PI was added to the medium above the cells before and 5, 10 and 15 min after exposure to the high voltage pulses and incubated for 10 min. But even when the cells were treated in presence of PI, no increase of PI-positive cells was detectable indicating that for the chosen exposure parameters no pore formation in the outer cell membrane occurred (data not shown).

3.3. Cell-cell communication

Based on the results on the viability of cells, field strengths of ≤ 20 kV/cm were chosen for exposures to study GJIC since most of the cells (88%) survive the treatment with this amplitude. GJIC was assessed by SLDT assay at 5, 15, 30, 60 min and 24 h after nsPEF treatment. Dye distribution in a control WB-F344 monolayer is illustrated in Fig. 5. The Lucifer Yellow channel represents the dye transfer through GJ-communicating cells (Fig. 5a) and the Texas Red channel depicts the cells where the GJ-impermeable dye was introduced by the razor blade cut (Fig. 5b). Cells that took up both dyes are colored in yellow (Fig. 5c, channels merged).

Different numbers of pulses were applied and the effect on GJIC was tested. The application of 1 pulse (20 kV/cm) had no effect while the application of 100 pulses with a field strengths of 15 kV/cm showed the same effect on cell-cell communication as 20 pulses with 20 kV/cm leading to the inhibition of GJIC (data not shown). For the study of the more pronounced dependency on field strength, a number of 20 pulses but field strengths of 10, 15 or 20 kV/cm were chosen. Fig. 6a shows the overlay microscopy images of the SLDT assay performed on WB-F344 cells 15, 30 and 60 min after nsPEF treatment. The evaluated data for all examined time points were normalized to the control and plotted in a graph (Fig. 6b).

GJIC has changed in a time- and field strength-dependent manner. 5 min after exposure of cells to nsPEFs an amplitude of 10 kV/cm did not affect GJIC whereas field strengths of 15 and 20 kV/cm already lowered intensity of cell-cell communication by about 15 to 30%, respectively, in comparison with the control cells. Decrease in GJIC was most pronounced 15 min after nsPEF treatment. Application of pulses with an amplitude of 20 kV/cm resulted in an almost complete inhibition of GJIC. A field strength of 10 kV/cm decreased cell-cell communication intensity to a value of about 60%, for exposures to 15 kV/cm about 5% of the initial GJIC was retained. 30 min after treatment

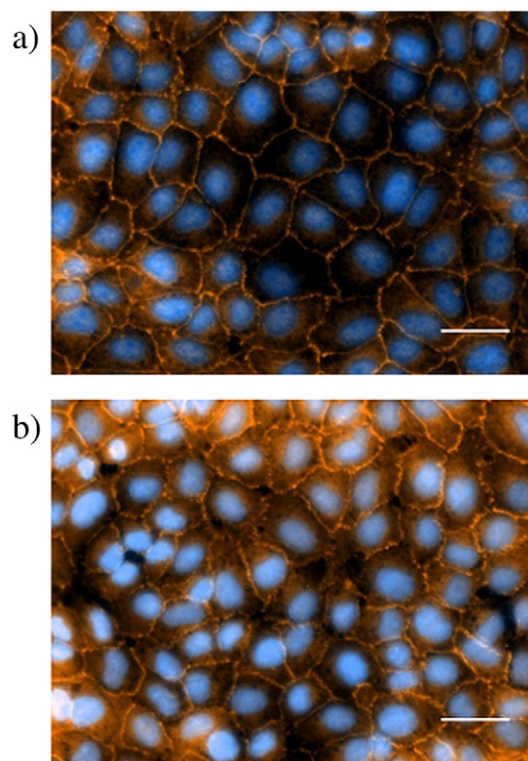


Fig. 8. Staining of ZO-1 (orange) in a control WB-F344 monolayer (a) and 15 min after application of 20 pulses of 100 ns and 20 kV/cm (b). No significant changes of ZO-1 could be detected after exposure to nsPEF compared to control (nuclei are labeled blue; scale bars: 50 μm). (For interpretation of the references to color in this figure legend, the reader is referred to the web version of this article.)

communication intensity rose again to about 80, 30 and 10% for 10, 15 and 20 kV/cm. One hour after treatment, cells that were exposed to 10 kV/cm reached almost control level again, whereas cells that were treated with 15 and 20 kV/cm still had a decreased cell-cell communication intensity of about 70 and 40%, compared to control. 24 h after exposure to nsPEFs no reduced GJIC was detectable anymore for all applied field strengths, showing that the cells survived the investigated field strengths without suffering lasting harm.

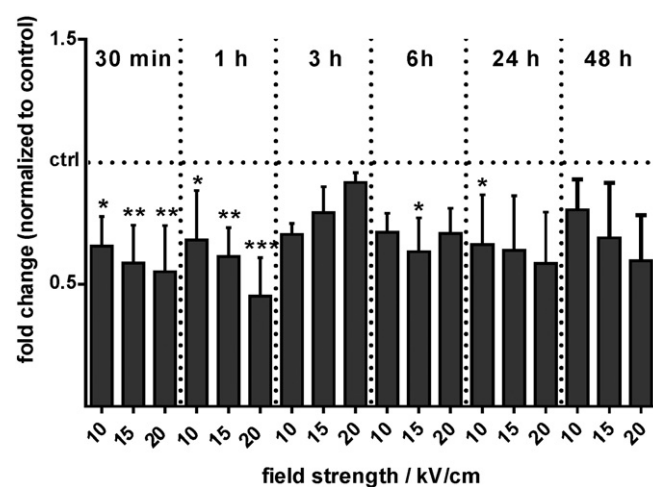


Fig. 9. Quantitative real time PCR for determination of mRNA expression of Cx43. WB-F344 cells were treated with 20 pulses of 100 ns and 10, 15 and 20 kV/cm. Fold changes normalized to control (dashed line) are given as mean values \pm SD.

3.4. Immunofluorescent detection of Cx43, F-actin and ZO-1

In order to elucidate the mechanisms underlying the decreased GJIC after nsPEF treatment, intracellular location of Cx43 and integrity of the actin cytoskeleton were analyzed by immunofluorescent staining. Fig. 7 shows the staining of a control WB-F344 monolayer and monolayers 5, 30 and 60 min after exposure to 20 pulses of 100 ns and 20 kV/cm.

Cells that were not treated showed distinct large and bright spots of Cx43 in the membrane, indicative of GJ plaques, while only little Cx43 could be seen in the cytoplasm (Fig. 7a). Stained actin fibers showed

an evenly distributed intact cytoskeleton with well-defined bundles that are aligned across the entire cell body. For monolayers that were exposed to pulsed electric fields, Cx43 localization was largely unaffected 5 min after nsPEF treatment (Fig. 7b). Cx43 proteins were still integrated in the outer cell membrane but GJ plaques appeared a bit smaller compared with the control and more Cx43 was observed in the cytosol of the treated cells. Only few well-aligned actin fibers could be found anymore. 30 min after exposure almost no Cx43 was visible in the membrane any longer but had apparently translocated to the intracellular volume (Fig. 7c). Cell boundaries that had been outlined by

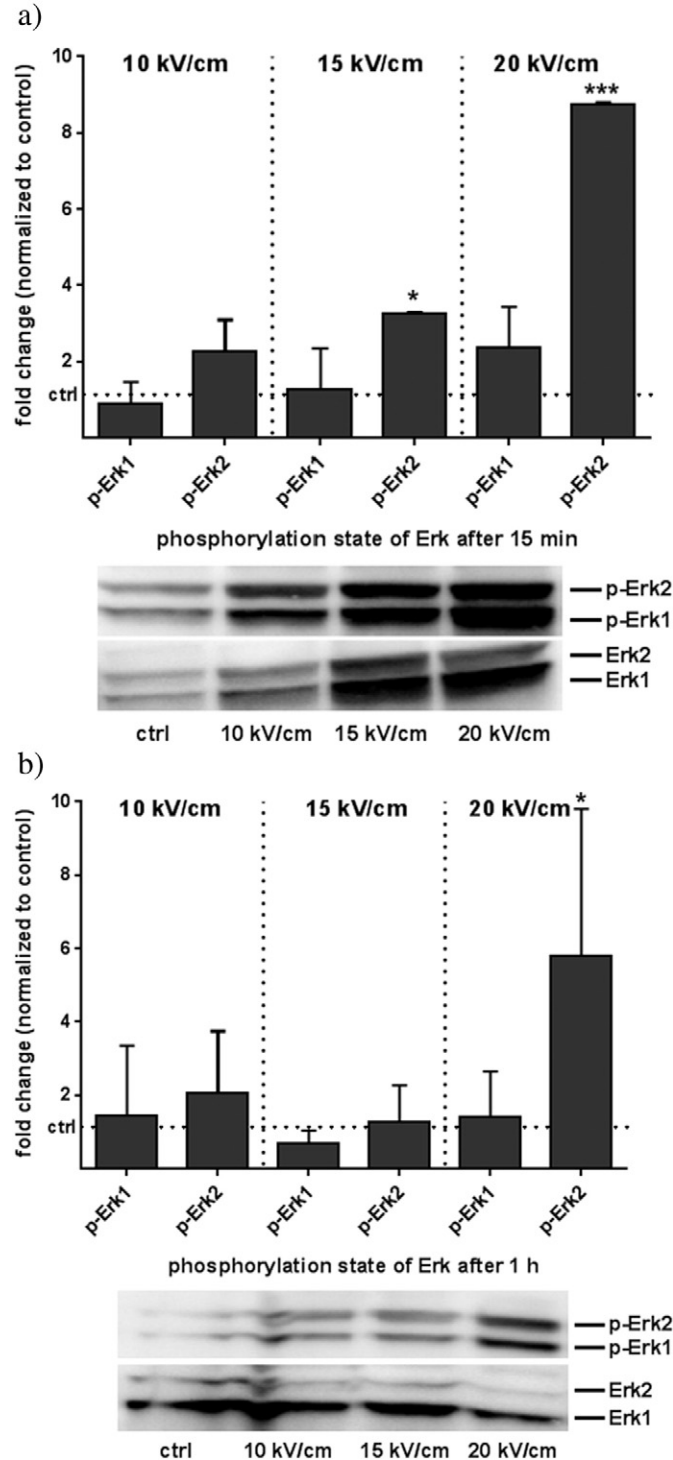


Fig. 10. Western blot analysis for determination of Erk1/2 activation 15 min (a), 1 h (b) and 6 h (c) after application of 20 pulses of 100 ns and 10, 15 and 20 kV/cm. Fold changes normalized to control (dashed line) are given as mean values \pm SD.

Cx43 staining in the controls could no longer be distinguished. Furthermore, the actin cytoskeleton was restructured while cell morphology in general remained unchanged (data not shown). Actin filaments were broken into shorter segments and less organized, i.e. oriented more randomly compared to control cells. 60 min after exposure (Fig. 7d), more Cx43 spots were found again but not yet all were integrated into the plasma membrane. The diffuse fluorescence across the cytosol that hinted at degraded Cx43 decreased in comparison with the results observed 30 min after treatment, indicating a recovery. However, the fluorescence signal was still stronger when compared with the control. Also the cytoskeleton had recovered 60 min after exposure compared to the situation after 30 min although the actin bundles were not yet as organized as in the control cells.

The staining results for cells that were treated with a field of 15 kV/cm were similar to the effects described for the treatment with 20 kV/cm but in general less pronounced (data not shown).

Furthermore, the tight junction protein ZO-1 was stained in order to exclude that cells detached from each other due to nsPEF treatment thus inhibiting communication between cells. In the control monolayer cells were clearly outlined by thin lines of ZO-1 (Fig. 8a). 15 min after exposure to 20 kV/cm boundaries between the cells appear a bit ruffled but cells were not separated from each other (Fig. 8b).

3.5. Quantification of Cx43 gene expression

Gene expression of Cx43 was analyzed by quantitative real-time PCR (qPCR) to determine if degradation of Cx43 that was observed in stained cells after nsPEF treatment is associated with a decreased mRNA level. Cells were treated with 20 pulses of 100 ns and 10, 15 and 20 kV/cm and incubated for 0.5, 1, 3, 6, 24 and 48 h.

Results showed a long lasting and field strength-dependent effect on Cx43 gene expression. Expressions were decreased for almost all investigated time points and for all applied field strengths (Fig. 9). The largest changes were measured for cells treated with 20 kV/cm within 1 h after exposure. Cx43 gene expression decreased to 55% of the initial value within 30 min after treatment and after 1 h to about 45%. 3 h after treatment gene expression had increased almost to control level again, at least for cells treated with a field strength of 20 kV/cm before levels were decreasing again to a value of about 70% after 6 h. Even 24 h after nsPEF treatment, Cx43 transcript levels were still lowered by about 40% compared to control and increased only slightly again within 48 h after exposure. The changes in Cx43 gene expression in the cells treated with field strengths of 10 and 15 kV/cm were similar to monolayers treated with 20 kV/cm but changes between different time points were less pronounced.

3.6. Analysis of MAP kinase activity and Cx43 phosphorylation

GJC is regulated by the number of GJs in the membrane as well as by their opening state which in turn can be affected by the phosphorylation of connexin or the activation of MAP kinases. Therefore, phosphorylation levels of Cx43 and activation of p38 and Erk1/2 were investigated by Western blotting 0.5, 1, 3, 6 h, and in the case of Cx43 also 24 h after application of 20 pulses of 100 ns and 10, 15 and 20 kV/cm.

3.6.1. Activation of Erk1/2

The analysis of Erk1/2 showed a significant field strength-dependent activation of Erk2 within 15 min after treatment in cells exposed to 15 and 20 kV/cm (Fig. 10a). In cells treated with 20 kV/cm, the amount of phosphorylated Erk2 was increased about 9-fold compared to control. In the case of 10 and 15 kV/cm phosphorylation was enhanced about 2-fold and 3-fold, respectively. The amount of phosphorylated Erk1 was only slightly increased for all investigated field strengths. 1 h after nsPEF treatment activation of Erk2 declined compared to 15 min after treatment but was still increased about 6-fold in cells treated with 20 kV/cm (Fig. 10b). In cells exposed to 10 and 15 kV/cm amount of

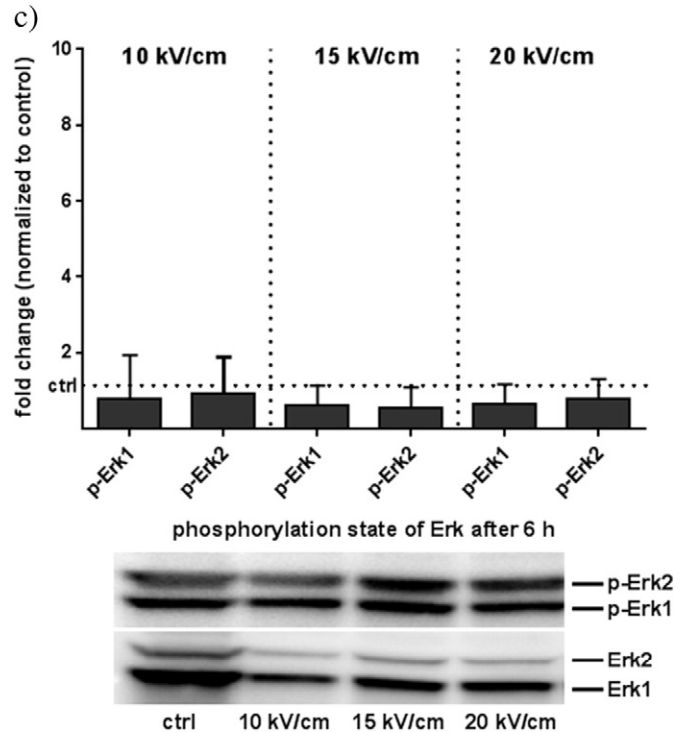


Fig. 10 (continued).

phosphorylated Erk2 was in the range of the control level. Erk1 was not changed at all 1 h after treatment. 6 h after application of nsPEFs no activation of Erk was detectable anymore for all investigated field strengths, neither for Erk1 nor Erk2 (Fig. 10c).

3.6.2. Activation of p38

Analysis of p38 (Fig. 11) showed no activation for up to 3 h after exposure to nsPEFs. The amount of phosphorylated p38 was even slightly below control level. However, p38 was significantly activated in a field strength-dependent manner 6 h after treatment. In cells exposed to 10 kV/cm, the amount of phosphorylated p38 was increased about 3-fold compared to control. In cells treated with 15 kV/cm activation was increased about 4.5-fold and after application of pulses with a field strength of 20 kV/cm 5.5-fold compared to control.

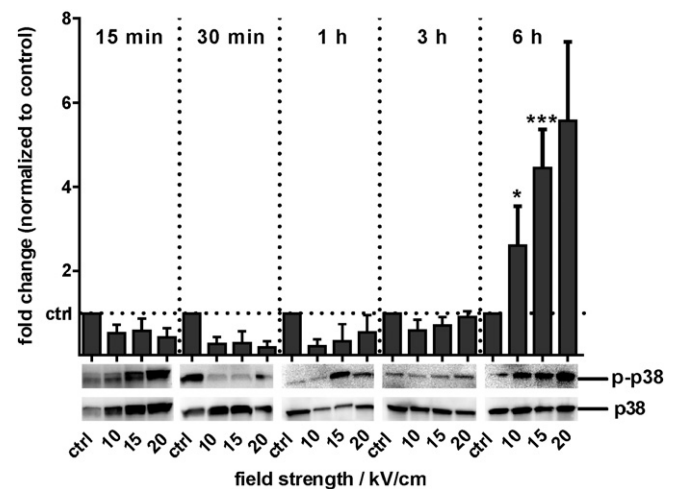


Fig. 11. Western blot analysis for determination of p38 activation 15 and 30 min and 1, 3 and 6 h after application of 20 pulses of 100 ns and 10, 15 and 20 kV/cm. Fold changes normalized to control (dashed line) are given as mean values \pm SD.

3.6.3. Phosphorylation and total amount of Cx43

Protein analysis of Cx43 showed 3 distinct bands reflecting the different phosphorylation states. The P0 band represents the non-phosphorylated, P1 the phosphorylated and P2 the hyperphosphorylated state. Hyperphosphorylation of Cx is associated with inhibition of GJIC.

Analysis of Cx43 after nsPEF treatment revealed a field strength-dependent hyperphosphorylation of Cx43. 30 min after exposure hyperphosphorylation increased about 2.5-fold for cells treated with 10 and 15 kV/cm, and about 3-fold in cells treated with 20 kV/cm (Fig. 12a). The amount of non-phosphorylated (P0) and phosphorylated Cx43 (P1) decreased about by half compared to control for all investigated field strengths. 6 h after exposure, there was almost no change of the phosphorylation pattern compared to control for all applied

field strengths (Fig. 12b). 24 h after application of the high voltage pulses, phosphorylation increased again (Fig. 12c). In cells treated with 10 kV/cm the amount of hyperphosphorylated Cx43 increased about 3-fold compared to control. In cells exposed to 15 kV/cm P2 was about 2-fold enhanced and for 20 kV/cm about 2.5-fold.

Furthermore, changes in the total amount of Cx43 after nsPEF treatment were determined by totaling the values of the P0, P1 and P2 bands (Fig. 13). 30 min after exposure the total amount of Cx43 was significantly reduced by more than half compared to control in cells exposed to 15 and 20 kV/cm. In cells treated with 10 kV/cm Cx43 level was decreased by about 40%. 24 h after application of pulses total amount of Cx43 was in the range of control level for all investigated field strengths.

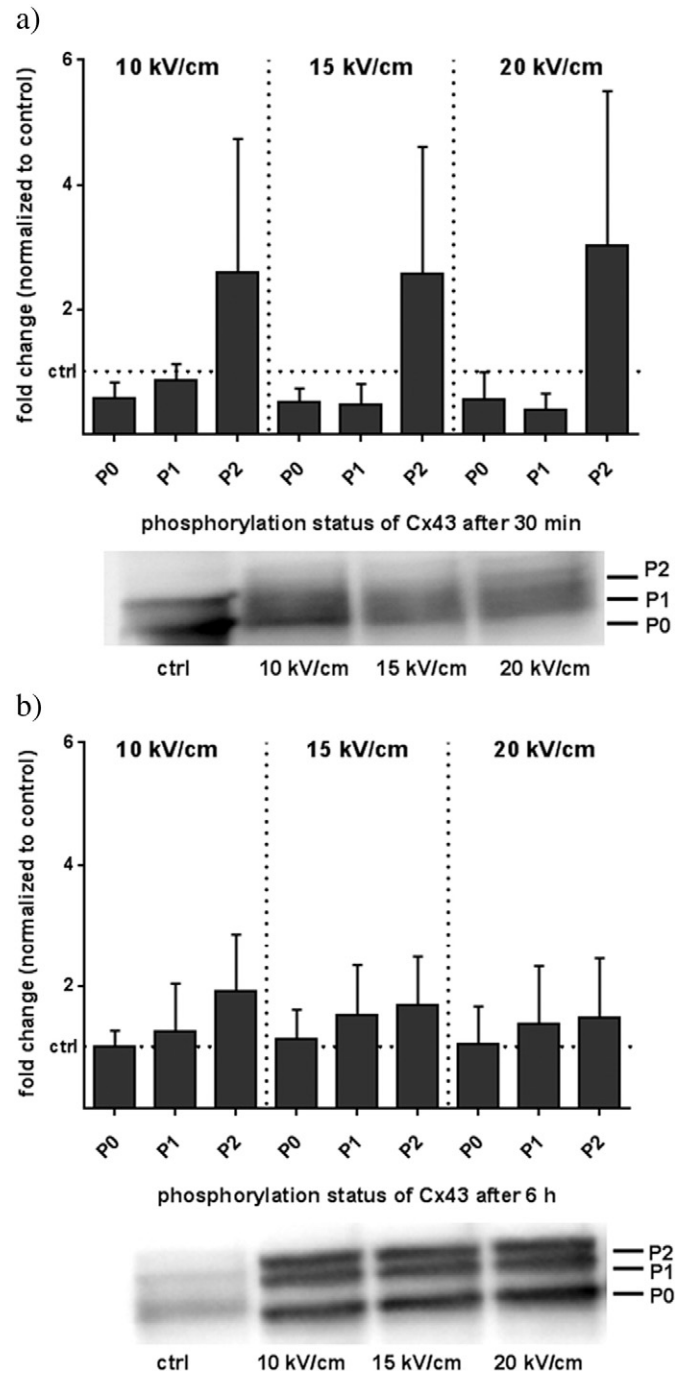


Fig. 12. Western blot analysis of Cx43 protein expression and phosphorylation pattern 30 min (a), 6 h (b) and 24 h (c) after exposure to nsPEFs of 10, 15 and 20 kV/cm. Band P0 represents the lowest phosphorylation state, P2 the hyperphosphorylated state. Fold changes normalized to control (dashed line) are given as mean values \pm SD.

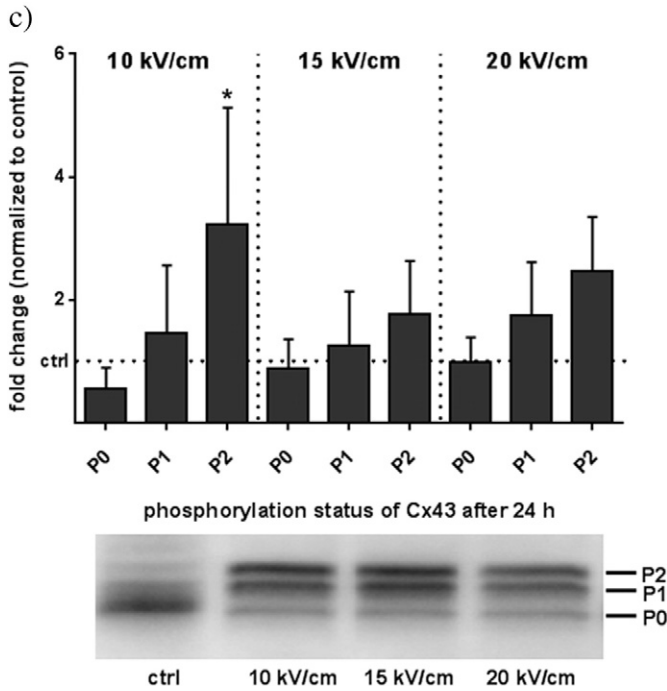


Fig. 12 (continued).

4. Discussion

The results show that exposures to nanosecond pulsed electric fields temporarily change the ability of cells to communicate through gap junctions in a time- and field strength-dependent manner. The fact that cell-cell communication in general can be affected by electric fields has already been demonstrated. The exposure of pre-osteoblastic MC3T3-E1 cells to extremely low-frequency electromagnetic fields of 0–15 G at 60 Hz and 2.3279 mV/m decreased GJIC during their proliferative phase, while the amount and distribution of Cx43 remained unchanged [57]. Western blotting and RT-PCR of breast carcinoma cells after the application of ‘energy controllable steep pulses’ (ECSP) showed a higher expression of Cx43 in the cells compared to control [58]. In contrast, we demonstrated a significantly decreased level of Cx43 mRNA up to 1 h after exposure to nsPEF correlating with the concurrently significantly reduced total amount of Cx43. Changes in Cx43 mRNA and protein level are occurring very quickly in our experiments. Altogether,

changes appear too fast to be explained simply by the downregulation of gene expression which normally takes rather hours than minutes. In comparison to the extended exposure to much lower electric fields this suggests that nsPEFs lead to rapid degradation of Cx43 mRNA and proteins.

Recent research findings and molecular dynamics studies indicate that nsPEFs could have a direct effect on proteins [59,60]. These effects could be mediated by rather fast rise times of the applied electric fields (or high frequency components when describing exposures in the time domain), as reviewed by Beebe [61]. However, detailed interaction mechanisms still need to be investigated. Accordingly, nsPEF might also have a direct effect on the degradation of Cx43 mRNA and proteins that are involved in the synthesis. The cytoskeleton might be affected in a similar manner. However, it is difficult to distinguish this potential effect from other processes that might disturb the cell’s biochemistry and distinguish a single primary effect. Our study in fact confirms that the complex relation of different mechanism has to be considered for an appropriate description of effects.

The downregulation of Cx43 mRNA lasted much longer than the decrease of the corresponding protein level which might be explained as follows. In general, the levels of mRNA and resulting functional protein do not necessarily correlate. As the protein accumulates in the cells, it may act as a repressor of further transcription and signaling because its expression is not needed at a certain stage. Accordingly, it has been suggested that Cx43 can regulate its own production [62]. Moreover, expression of a certain protein might be more or less effective depending on translation of mRNA and post-translational modifications. As Cx43 mRNA is typically expressed at low level under basal conditions, we assume that cells may produce enough Cx43 protein after a certain time despite decreased mRNA levels after nsPEF treatment.

The changes in GJIC could be mediated by several mechanisms that could be directly affected by nsPEFs or instigate a secondary response that is ultimately responsible for the transient decrease. In particular, phosphorylation of Cx43, activation of MAP kinases and the disassembly of the cytoskeleton have been identified as possible key targets.

Phosphorylation of Cx43 is a regulatory event which is involved in GJ assembly, gating, internalization and degradation [63–65]. The induced effects depend on many factors such as connexin and cell type, species, phosphorylation site and the phosphorylation inducing kinases [40]. Activation of MAP kinases represents one of the principal mechanisms responsible for the regulation of GJIC via the phosphorylation of Cx43 which can lead to the closure of GJs and Cx43 internalization. Treatment of cells with 12-*O*-tetradecanoylphorbol-13-acetate (TPA) has been shown to activate protein kinase C (PKC) which in turn activated the MAP kinase Erk. The activation of Erk then led to the induction of Cx43 hyperphosphorylation and GJ internalization and finally resulted in the inhibition of GJIC [66]. In another study it was demonstrated that after exposure of cells to anisomycin, a protein synthesis inhibitor, two other MAP kinases namely p38 and JNK were activated. GJIC was subsequently decreased with an enhanced phosphorylation level of Cx43 and a reduced number of GJs. In this case JNK was unlikely to be involved in the process whereas the activation of p38 had an important role [67]. Like the experiments that are described here, both studies were carried out with WB-F344 cells, establishing this pathway. Furthermore, the activation of MAP kinases by nsPEFs has already been demonstrated, although for a different cell line. Suspended HeLa cells were exposed to electric pulses with similar parameters as chosen for the study presented here. Both, Erk and p38 were strongly activated within 15 min after exposure [68]. In our experiments we also found a significant activation of Erk within 15 min after nsPEF treatment (Fig. 10). But in comparison to the results published for HeLa cells, we obtained an activation of p38 only 6 h after treatment. This might be explained by the fact that the HeLa cells were exposed in suspension and not as a monolayer. Another possibility is that the effects of nsPEFs could be cell-type specific and the same treatment might induce different effects in different cell lines.

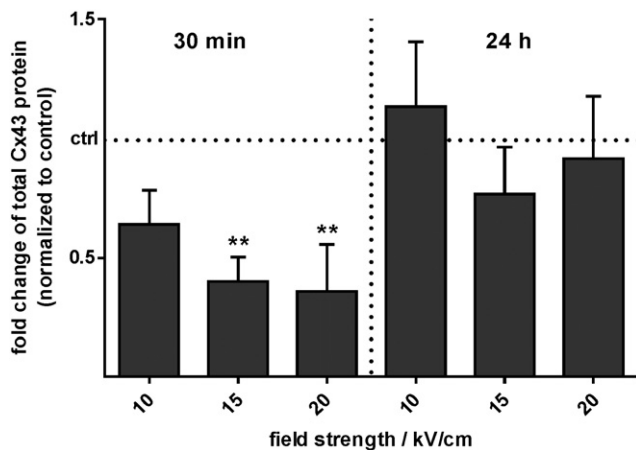


Fig. 13. Quantification of Western blot analysis of Cx43 protein expression 30 min and 24 h after exposure to nsPEFs of 10, 15 and 20 kV/cm. Fold changes normalized to control (dashed line) are given as mean values \pm SD.

Activated Erk as well as p38 can induce a hyperphosphorylation of Cx43. This was observed in our experiments (Fig. 12). Phosphorylation of Cx43 was detected 30 min after exposure to nsPEF and again after 24 h, whereas the phosphorylation pattern was almost unchanged 6 h post-treatment. The activation of MAP kinases as well as the hyperphosphorylation of Cx43 can lead to the disassembly of GJs from the plasma membrane [66,67], which corresponds to the observations after the nsPEF treatment in our experiments. 30 min after exposure almost no GJs could be found in the membrane matching the strongly decreased cell-cell communication. 6 h after nsPEF treatment we obtained activation of p38 and after 24 h a hyperphosphorylation of Cx43 but GJIC was not changed at that point. This might be explained as follows: The early hyperphosphorylation of Cx43 might have been induced by Erk whereas the hyperphosphorylation after 24 h might have been induced by p38. Different modulators can phosphorylate different phosphorylation sites of Cx43 resulting in different effects. Furthermore, a change in connexin phosphorylation does not necessarily result in the inhibition of cell-cell communication. Moreover, it has been reported that some chemicals inhibiting GJIC also activate MAP kinases, but their inhibitory effects are MAPK-independent and mediated via activation of phosphatidylcholine-specific phospholipase C or via not-yet identified mechanisms [69–72]. Thus, more details on mechanisms responsible for the inhibition of GJIC in response to nsPEFs should be further elucidated in future studies.

For the assembly and degradation of GJs an intact cytoskeleton is necessary. Therefore, the inhibition of GJIC could be an indirect effect of nsPEFs on the integrity of the cytoskeleton. Our staining results hinted to a disturbance of the actin fibers (Fig. 7) but not a complete breakdown of the cytoskeleton as described by Stacey et al. [20]. Disturbances of actin filaments might have contributed not only to disassembling of GJs and altered Cx43 degradation but represent structural fluctuations in the cell. These in turn might result in MAP kinase activation. Hence even the effect on the cytoskeleton might again only promote the mechanisms that are associated with MAP kinase activation and phosphorylation of Cx43.

In addition to cytoskeletal interactions, proper formation and function of GJs depends to some degree also on other type of cellular junctions such as tight junctions which maintain the tight connections and cohesions between the cells in the monolayer. Moreover, connexin proteins are known to directly interact with tight junction proteins such as ZO-1 [73,74]. Therefore, we investigated the effect of nsPEFs on the adhesion of cells to each other. We stained the tight junction protein ZO-1 to examine if nsPEF treatment leads to any disturbances of tight junctions which might be responsible for cell detachment and disassembling of GJs. However, we could not detect any significant changes compared to control except that the cell boundaries looked a little bit more ruffled (Fig. 8). Cells did not seem to separate, thus, a mechanical separation of the adjacent cells most likely was not responsible for the observed decrease in cell-cell communication.

Another possible mechanism that is known to be affected by nsPEF and which could have a subsequent effect on the inhibition of GJIC is the depolarization of membranes with an associated possible voltage gating of gap junctions [75,76]. Connexins appear indeed to be sensitive to voltage-dependent conformational changes, which might represent a putative mechanism responsible for the observed effects [77–79]. Voltage gating by pulsed electric fields was also suggested by Kotnik et al. for the application of electroporation pulses of 200 μ s and 1 kV/cm [80]. However, for the exposure conditions that were studied here, i.e. pulsed electric fields of 100 ns and with field strengths \leq 20 kV/cm, no electroporation was actually observed. GJIC inhibition due to depolarization of the membrane is on biological timescales a very fast mechanism and GJ-channel closure should occur within tenths of a second [81]. Despite the likely fast charging of the plasma membrane by nsPEFs, it is doubtful if the transmembrane potential changes that can be induced by nsPEF-exposures can be sustained long enough to be responsible for voltage gating or a direct conformational change of the GJs [82]. Conversely,

triggering an indirect slower effect seems to be more likely and we did indeed observe that GJIC was still only slightly affected by nsPEFs 5 min post-treatment, but a maximum inhibition was observed after 15 min. These results thus indicate that inhibition of GJIC was not mediated by a rapid depolarization-dependent mechanism. The possible increase of intracellular calcium concentration could be a possible trigger for a secondary effect resulting in decreased GJIC by closing the GJs. The release of calcium from intracellular stores has been observed even for nsPEF exposures that were not leading to the poration of the outer membrane [19]. However, further and intricate studies are necessary to elucidate this potential correlation in more detail.

Altogether, the assessment and comparison of different mechanisms that could explain the observed inhibition of GJIC by nsPEFs strongly suggests that for the described exposures, the phosphorylation of Cx43 is the most likely reason. This process is likely to be initiated by the activation of the MAP kinase Erk1/2. With typical timescales for the expression of kinases the communication through GJs is then recovering again. How the effect of nsPEFs on MAP kinases is mediated by nsPEFs needs to be explored in detail.

Decreased GJIC is often associated with the development of cancer. In many tumors, cell-cell communication between the tumor cells themselves as well as between tumor cells and their surrounding healthy cells is inhibited [29,83,84]. As nsPEFs decrease GJIC, it remains to be investigated if exposure of cells to electric fields might induce some malignant transformation of cells. However, for the transient nature of the inhibition of GJIC, a lasting consequence for healthy cells does not seem to be likely unless the reduced communication gives rise to other effects. Conversely, a reduced GJIC could be advantageous in the treatment of other conditions, such as for example wound healing. Cx43 has been found upregulated in certain chronic wounds [31,85–87], and its downregulation has been reported to accelerate wound healing [88,89]. The challenge for the development of respective therapies based on nsPEF will be the transient nature of the inhibited GJIC but should be explored in dedicated studies.

Acknowledgment

The authors gratefully acknowledge the help of Liane Kantz and Theresa Schacht to this study. This work was supported by the German Research Foundation (DFG) under contract no. KO 4644/2-1 and by the Czech Ministry of Education, Youth and Sports (LO1214 and LM2015051).

References

- [1] C.Y. Calvet, L.M. Mir, The promising alliance of anti-cancer electrochemotherapy with immunotherapy, *Cancer Metastasis Rev.* (2016) 1–13.
- [2] M. Cemazar, T. Kotnik, G. Sersa, D. Miklavcic, 24 electroporation for electrochemotherapy and gene therapy, *Electromagnetic Fields in Biology and Medicine* 395 (2015).
- [3] B. Mali, T. Jarm, M. Snoj, G. Sersa, D. Miklavcic, Antitumor effectiveness of electrochemotherapy: a systematic review and meta-analysis, *European Journal of Surgical Oncology (EJSO)* 39 (2013) 4–16.
- [4] P. Queirolo, F. Marincola, F. Spagnolo, Electrochemotherapy for the management of melanoma skin metastasis: a review of the literature and possible combinations with immunotherapy, *Arch. Dermatol. Res.* 306 (2014) 521–526.
- [5] R. Rotunno, F. Marenco, S. Ribero, S. Calvieri, P. Amerio, P. Quaglino, Electrochemotherapy in non-melanoma head and neck skin cancers: a three centers experience and literature review, *Giornale italiano di dermatologia e venerologia: organo ufficiale, Societa italiana di dermatologia e sifilografia* (2015).
- [6] L.G. Campana, A.J.P. Clover, S. Valpione, P. Quaglino, J. Gehl, C. Kunte, M. Snoj, M. Cemazar, C.R. Rossi, D. Miklavcic, Recommendations for improving the quality of reporting clinical electrochemotherapy studies based on qualitative systematic review, *Radiol. Oncol.* 50 (2016) 1–13.
- [7] S. Jahangeer, P. Forde, D. Soden, J. Hinchion, Review of current thermal ablation treatment for lung cancer and the potential of electrochemotherapy as a means for treatment of lung tumours, *Cancer Treat. Rev.* 39 (2013) 862–871.
- [8] S.J. Beebe, X. Chen, J. Liu, K.H. Schoenbach, Nanosecond pulsed electric field ablation of hepatocellular carcinoma, *Engineering in Medicine and Biology Society, EMBC, 2011 Annual International Conference of the IEEE/IEEE 2011*, pp. 6861–6865.
- [9] S.J. Beebe, W.E. Ford, W. Ren, X. Chen, K.H. Schoenbach, Non-ionizing radiation with nanosecond pulsed electric fields as a cancer treatment: in vitro studies,

- Engineering in Medicine and Biology Society, 2009. EMBC 2009. Annual International Conference of the IEEEIEEE 2009, pp. 6509–6512.
- [10] S.J. Beebe, K.H. Schoenbach, R. Heller, Bioelectric applications for treatment of melanoma, *Cancer* 2 (2010) 1731–1770.
- [11] X. Chen, J. Zhuang, J.F. Kolb, K.H. Schoenbach, S.J. Beebe, Long term survival of mice with hepatocellular carcinoma after pulse power ablation with nanosecond pulsed electric fields, *Technology in Cancer Research & Treatment* 11 (2012) 83–93.
- [12] X.H. Chen, J.F. Kolb, R.J. Swanson, K.H. Schoenbach, S.J. Beebe, Apoptosis initiation and angiogenesis inhibition: melanoma targets for nanosecond pulsed electric fields, *Pigment Cell & Melanoma Research* 23 (2010) 554–563.
- [13] R. Nuccitelli, K. Tran, S. Sheikh, B. Athos, M. Kreis, P. Nuccitelli, Optimized nanosecond pulsed electric field therapy can cause murine malignant melanomas to self-destruct with a single treatment, *Int. J. Cancer* 127 (2010) 1727–1736.
- [14] J.C. Weaver, K.C. Smith, A.T. Esser, R.S. Son, T.R. Gowrishankar, A brief overview of electroporation pulse strength-duration space: a region where additional intracellular effects are expected, *Bioelectrochemistry* 87 (2012) 236–243.
- [15] T. Kotnik, D. Miklavčič, Theoretical evaluation of voltage inducement on internal membranes of biological cells exposed to electric fields, *Biophys. J.* 90 (2006) 480–491.
- [16] S.J. Beebe, J. White, P.F. Blackmore, Y. Deng, K. Somers, K.H. Schoenbach, Diverse effects of nanosecond pulsed electric fields on cells and tissues, *DNA Cell Biol.* 22 (2003) 785–796.
- [17] C. Kanthou, S. Kranjc, G. Sersa, G. Tozer, A. Zupanic, M. Cemazar, The endothelial cytoskeleton as a target of electroporation-based therapies, *Mol. Cancer Ther.* 5 (2006) 3145–3152.
- [18] E.S. Buescher, R.R. Smith, K.H. Schoenbach, Submicrosecond intense pulsed electric field effects on intracellular free calcium: mechanisms and effects, *Plasma Science, IEEE Transactions on* 32 (2004) 1563–1572.
- [19] S.S. Scarlett, J.A. White, P.F. Blackmore, K.H. Schoenbach, J.F. Kolb, Regulation of intracellular calcium concentration by nanosecond pulsed electric fields, *Biochimica et Biophysica Acta (BBA)-Biomembranes* 1788 (2009) 1168–1175.
- [20] M. Stacey, P. Fox, S. Buescher, J. Kolb, Nanosecond pulsed electric field induced cytoskeleton, nuclear membrane and telomere damage adversely impact cell survival, *Bioelectrochemistry* 82 (2011) 131–134.
- [21] G.L. Thompson, C. Roth, G. Tolstykh, M. Kuipers, B.L. Ibey, Disruption of the actin cortex contributes to susceptibility of mammalian cells to nanosecond pulsed electric fields, *Bioelectromagnetics* 35 (2014) 262–272.
- [22] M. Breton, L.M. Mir, Microsecond and nanosecond electric pulses in cancer treatments, *Bioelectromagnetics* 33 (2012) 106–123.
- [23] D.P. Kelsell, J. Dunlop, M.B. Hodgins, Human diseases: clues to cracking the connexin code? *Trends Cell Biol.* 11 (2001) 2–6.
- [24] D. Laird, Life cycle of connexins in health and disease, *Biochem. J.* 394 (2006) 527–543.
- [25] G. Carruba, R. Stefano, L. Cocciadiferro, F. Saladino, A. Cristina, E. Tokar, S.T. Quader, M.M. Webber, L. Castagnetta, Intercellular communication and human prostate carcinogenesis, *Ann. N. Y. Acad. Sci.* 963 (2002) 156–168.
- [26] P. Ren, P.P. Mehta, R.J. Ruch, Inhibition of gap junctional intercellular communication by tumor promoters in connexin43 and connexin32-expressing liver cells: cell specificity and role of protein kinase C, *Carcinogenesis* 19 (1998) 169–175.
- [27] J.E. Trosko, The role of stem cells and gap junctional intercellular communication in carcinogenesis, *J. Biochem. Mol. Biol.* 36 (2003) 43–48.
- [28] J.E. Trosko, R.J. Ruch, Cell-cell communication in carcinogenesis, *Front. Biosci.* 3 (1998) d208–d236.
- [29] H. Yamasaki, Aberrant expression and function of gap junctions during carcinogenesis, *Environ. Health Perspect.* 93 (1991) 191.
- [30] D.L. Becker, C. Thrasivoulou, A.R. Phillips, Connexins in wound healing: perspectives in diabetic patients, *Biochimica et Biophysica Acta (BBA)-Biomembranes* 1818 (2012) 2068–2075.
- [31] J.M. Brandner, P. Houdek, B. Husing, C. Kaiser, I. Moll, Connexins 26, 30, and 43: differences among spontaneous, chronic, and accelerated human wound healing, *J. Invest. Dermatol.* 122 (2004) 1310–1320.
- [32] H.P. Ehrlich, T. Diez, Role for gap junctional intercellular communications in wound repair, *Wound Repair Regen.* 11 (2003) 481–489.
- [33] C. Qiu, P. Coutinho, S. Frank, S. Franke, L.-y. Law, P. Martin, C.R. Green, D.L. Becker, Targeting connexin43 expression accelerates the rate of wound repair, *Curr. Biol.* 13 (2003) 1697–1703.
- [34] F. Roberts, M. Al-Husari, U. George, K. Giorgakoudi, J. Caffrey, A. Shabala, C. Bell, E. Chang, S. Webb, J. Ward, Connexins: A Novel Target for Wound Healing, 2010.
- [35] Q. Chang, W. Tang, S. Ahmad, B. Zhou, X. Lin, Gap junction mediated intercellular metabolite transfer in the cochlea is compromised in connexin30 null mice, *PLoS One* 3 (2008) e4088.
- [36] D.C. Spray, R.L. White, A.C. Decarvalho, A.L. Harris, M.V.L. Bennett, Gating of gap junction channels, *Biophys. J.* 45 (1984) 219–230.
- [37] D.F. Hulser, R. Eckert, U. Irmer, A. Krisciukaitis, A. Mindermann, J. Pleiss, B. Rehkopf, J. Sharovskaya, O. Traub, Intercellular communication via gap junction channels, *Bioelectrochem. Bioenerg.* 45 (1998) 55–65.
- [38] B.L. Upham, A.M. Rummel, J.M. Carbone, J.E. Trosko, Y. Ouyang, R.B. Crawford, N.E. Kaminski, Cannabinoids inhibit gap junctional intercellular communication and activate ERK in a rat liver epithelial cell line, *Int. J. Cancer* 104 (2003) 12–18.
- [39] J.-H. Cho, S.-D. Cho, H. Hu, S.-H. Kim, S.K. Lee, Y.-S. Lee, K.-S. Kang, The roles of ERK1/2 and p38 MAP kinases in the preventive mechanisms of mushroom *Phellinus linteus* against the inhibition of gap junctional intercellular communication by hydrogen peroxide, *Carcinogenesis* 23 (2002) 1163–1169.
- [40] L.N. Axelsen, K. Calloe, N.-H. Holstein-Rathlou, M.S. Nielsen, Managing the complexity of communication: regulation of gap junctions by post-translational modification, *Front. Pharmacol.* 4 (2013).
- [41] J.F. Kolb, M. Stacey, Subcellular biological effects of nanosecond pulsed electric fields, *Plasma for Bio-decontamination, Medicine and Food Security*, Springer 2012, pp. 361–379.
- [42] C.J.W. Meulenbergh, V. Todorovic, M. Cemazar, Differential cellular effects of electroporation and electrochemotherapy in monolayers of human microvascular endothelial cells, *PLoS One* 7 (2012).
- [43] D. Giessmann, C. Theiss, W. Breipohl, K. Meller, Microinjection of actin antibodies impaired gap junctional intercellular communication in lens epithelial cells in vitro, *Curr. Eye Res.* 27 (2003) 157–164.
- [44] M.-S. Tsao, J.D. Smith, K.G. Nelson, J.W. Grisham, A diploid epithelial cell line from normal adult rat liver with phenotypic properties of 'oval' cells, *Exp. Cell Res.* 154 (1984) 38–52.
- [45] A.W. de Feijter, D.F. Matesic, R.J. Ruch, X. Guan, C.C. Chang, J.E. Trosko, Localization and function of the connexin 43 gap-junction protein in normal and various oncogene-expressing rat liver epithelial cells, *Mol. Carcinog.* 16 (1996) 203–212.
- [46] A.W. De Feijter, J.S. Ray, C.M. Weghorst, J.E. Klaunig, J.J. Goodman, C.C. Chang, R.J. Ruch, J.E. Trosko, Infection of rat liver epithelial cells with v-Ha-ras: correlation between oncogene expression, gap junctional communication, and tumorigenicity, *Mol. Carcinog.* 3 (1990) 54–67.
- [47] N.D. DeoCampo, M.R. Wilson, J.E. Trosko, Cooperation of bcl-2 and myc in the neoplastic transformation of normal rat liver epithelial cells is related to the down-regulation of gap junction-mediated intercellular communication, *Carcinogenesis* 21 (2000) 1501–1506.
- [48] T. Hayashi, K. Nomata, C.-C. Chang, R.J. Ruch, J.E. Trosko, Cooperative effects of v-myc and c-Ha-ras oncogenes on gap junctional intercellular communication and tumorigenicity in rat liver epithelial cells, *Cancer Lett.* 128 (1998) 145–154.
- [49] Y.-S. Jou, B. Layhe, D.F. Matesic, C.-C. Chang, A.W. de Feijter, L. Lockwood, C.W. Welsch, J.E. Klaunig, J.E. Trosko, Inhibition of gap junctional intercellular communication and malignant transformation of rat liver epithelial cells by neu oncogene, *Carcinogenesis* 16 (1995) 311–317.
- [50] R. Nuccitelli, K. Tran, B. Athos, M. Kreis, P. Nuccitelli, K.S. Chang, E.H. Epstein, J.Y. Tang, Nanoelectroablation therapy for murine basal cell carcinoma, *Biochem. Biophys. Res. Commun.* 424 (2012) 446–450.
- [51] S. Wu, Y. Wang, J. Guo, Q. Chen, J. Zhang, J. Fang, Nanosecond pulsed electric fields as a novel drug free therapy for breast cancer: an in vivo study, *Cancer Lett.* 343 (2014) 268–274.
- [52] W.B. Coleman, A.E. Wennerberg, G.J. Smith, J. Grisham, Regulation of the differentiation of diploid and some aneuploid rat liver epithelial (stemlike) cells by the hepatic microenvironment, *Am. J. Pathol.* 142 (1993) 1373.
- [53] J.F. Kolb, S. Kono, K.H. Schoenbach, Nanosecond pulsed electric field generators for the study of subcellular effects, *Bioelectromagnetics* 27 (2006) 172–187.
- [54] M.H. El-Fouly, J.E. Trosko, C.-C. Chang, Scrape-loading and dye transfer: a rapid and simple technique to study gap junctional intercellular communication, *Exp. Cell Res.* 168 (1987) 422–430.
- [55] A. Gürtler, N. Kunz, M. Gomolka, S. Hornhardt, A.A. Friedl, K. McDonald, J.E. Kohn, A. Posch, Stain-free technology as a normalization tool in Western blot analysis, *Anal. Biochem.* 433 (2013) 105–111.
- [56] S.C. Taylor, T. Berkelman, G. Yadav, M. Hammond, A defined methodology for reliable quantification of Western blot data, *Mol. Biotechnol.* 55 (2013) 217–226.
- [57] D.T. Yamaguchi, J. Huang, D.F. Ma, P.K.C. Wang, Inhibition of gap junction intercellular communication by extremely low-frequency electromagnetic fields in osteoblast-like models is dependent on cell differentiation, *J. Cell. Physiol.* 190 (2002) 180–188.
- [58] D. Xiaojing, H. LiNa, S. CaiXin, Z. YunShan, H. Chuan, L. Cong, L. XiaoDong, M. Yan, Effect of energy controllable steep pulse on gap junction of breast cancer cells, *Tumor* 29 (2009) 310–314.
- [59] P.T. Vernier, Y. Sun, L. Marcu, C.M. Craft, M.A. Gundersen, Nanoelectropulse-induced phosphatidylserine translocation, *Biophys. J.* 86 (2004) 4040–4048.
- [60] Q. Hu, V. Sridhara, R.P. Joshi, J.F. Kolb, K.H. Schoenbach, Molecular dynamics analysis of high electric pulse effects on bilayer membranes containing DPPC and DPPS, *Plasma Science, IEEE Transactions on* 34 (2006) 1405–1411.
- [61] S.J. Beebe, Considering effects of nanosecond pulsed electric fields on proteins, *Bioelectrochemistry* 103 (2015) 52–59.
- [62] M. Vinken, E. Decrock, E. De Vuyst, R. Ponsaerts, C. D'hondt, G. Bultynck, L. Ceelen, T. Vanhaecke, L. Leybaert, V. Rogiers, Connexins: sensors and regulators of cell cycling, *Biochimica et Biophysica Acta (BBA)-Reviews on Cancer* 1815 (2011) 13–25.
- [63] D.W. Laird, Connexin phosphorylation as a regulatory event linked to gap junction internalization and degradation, *Biochimica et Biophysica Acta-Biomembranes* 1711 (2005) 172–182.
- [64] A.P. Moreno, Connexin phosphorylation as a regulatory event linked to channel gating, *Biochimica et Biophysica Acta-Biomembranes* 1711 (2005) 164–171.
- [65] J.L. Solan, P.D. Lampe, Connexin phosphorylation as a regulatory event linked to gap junction channel assembly, *Biochimica et Biophysica Acta-Biomembranes* 1711 (2005) 154–163.
- [66] R.J. Ruch, J.E. Trosko, B.V. Madhukar, Inhibition of connexin43 gap junctional intercellular communication by TPA requires ERK activation, *J. Cell. Biochem.* 83 (2001) 163–169.
- [67] T. Ogawa, T. Hayashi, S. Kyoizumi, Y. Kusunoki, K. Nakachi, D.G. MacPhee, J.E. Trosko, K. Kataoka, N. Yorioka, Anisomycin downregulates gap-junctional intercellular communication via the p38 MAP-kinase pathway, *J. Cell Sci.* 117 (2004) 2087–2096.
- [68] K. Morotomi-Yano, H. Akiyama, K. Yano, Nanosecond pulsed electric fields activate MAPK pathways in human cells, *Arch. Biochem. Biophys.* 515 (2011) 99–106.
- [69] M. Machala, L. Bláha, J. Vondráček, J.E. Trosko, J. Scott, B.L. Upham, Inhibition of gap junctional intercellular communication by noncoplanar polychlorinated biphenyls: inhibitory potencies and screening for potential mode(s) of action, *Toxicol. Sci.* 76 (2003) 102–111.

- [70] I. Sovadinova, P. Babica, H. Böke, E. Kumar, A. Wilke, J.-S. Park, J.E. Trosko, B.L. Upham, Phosphatidylcholine specific PLC-induced dysregulation of gap junctions, a robust cellular response to environmental toxicants, and prevention by resveratrol in a rat liver cell model, *PLoS One* 10 (2015).
- [71] B.L. Upham, L. Bláha, P. Babica, J.S. Park, I. Sovadinova, C. Pudrith, A.M. Rummel, L.M. Weis, K. Sai, P.K. Tithof, Tumor promoting properties of a cigarette smoke prevalent polycyclic aromatic hydrocarbon as indicated by the inhibition of gap junctional intercellular communication via phosphatidylcholine-specific phospholipase C, *Cancer Sci.* 99 (2008) 696–705.
- [72] B.L. Upham, M. Gužvić, J. Scott, J.M. Carbone, L. Blaha, C. Coe, L.L. Li, A.M. Rummel, J.E. Trosko, Inhibition of gap junctional intercellular communication and activation of mitogen-activated protein kinase by tumor-promoting organic peroxides and protection by resveratrol, *Nutr. Cancer* 57 (2007) 38–47.
- [73] B.N. Giepmans, I. Verlaan, W.H. Moolenaar, Connexin-43 interactions with ZO-1 and α - and β -tubulin, *Cell Commun. Adhes.* 8 (2001) 219–223.
- [74] T. Toyofuku, M. Yabuki, K. Otsu, T. Kuzuya, M. Hori, M. Tada, Direct association of the gap junction protein connexin-43 with ZO-1 in cardiac myocytes, *J. Biol. Chem.* 273 (1998) 12725–12731.
- [75] T. Schuster, *Kommunikation Zwischen Zellen: Gap Junctions, Nexus, Elektrische Synapsen*, Akad.-Verlag, 1990.
- [76] F.F. Bukauskas, V.K. Verselis, Gap junction channel gating, *Biochimica et Biophysica Acta (BBA)-Biomembranes* 1662 (2004) 42–60.
- [77] A. Harris, D. Spray, M. Bennett, Kinetic properties of a voltage-dependent junctional conductance, *The Journal of General Physiology* 77 (1981) 95–117.
- [78] V. Valiunas, F.F. Bukauskas, R. Weingart, Conductances and selective permeability of connexin43 gap junction channels examined in neonatal rat heart cells, *Circ. Res.* 80 (1997) 708–719.
- [79] T.A. Bargiello, Q. Tang, S. Oh, T. Kwon, Voltage-dependent conformational changes in connexin channels, *Biochimica et Biophysica Acta (BBA)-Biomembranes* 1818 (2012) 1807–1822.
- [80] T. Kotnik, G. Pucihar, D. Miklavčič, Induced transmembrane voltage and its correlation with electroporation-mediated molecular transport, *The Journal of Membrane Biology* 236 (2010) 3–13.
- [81] P.D. Lampe, A.F. Lau, The effects of connexin phosphorylation on gap junctional communication, *Int. J. Biochem. Cell Biol.* 36 (2004) 1171–1186.
- [82] W. Frey, J.A. White, R.O. Price, P.F. Blackmore, R.P. Joshi, R. Nuccitelli, S.J. Beebe, K.H. Schoenbach, J.F. Kolb, Plasma membrane voltage changes during nanosecond pulsed electric field exposure, *Biophys. J.* 90 (2006) 3608–3615.
- [83] A. Hotz-Wagenblatt, D. Shalloway, Gap junctional communication and neoplastic transformation, *Crit. Rev. Oncog.* 4 (1992) 541–558.
- [84] M.M. Saunders, M.J. Seraj, Z. Li, Z. Zhou, C.R. Winter, D.R. Welch, H.J. Donahue, Breast cancer metastatic potential correlates with a breakdown in homospesific and heterospesific gap junctional intercellular communication, *Cancer Res.* 61 (2001) 1765–1767.
- [85] J. Sutcliffe, K. Chin, C. Thrasivoulou, T. Serena, S. O'Neil, R. Hu, A. White, L. Madden, T. Richards, A. Phillips, Abnormal connexin expression in human chronic wounds, *Br. J. Dermatol.* 173 (2015) 1205–1215.
- [86] C.M. Wang, J. Lincoln, J.E. Cook, D.L. Becker, Abnormal connexin expression underlies delayed wound healing in diabetic skin, *Diabetes* 56 (2007) 2809–2817.
- [87] A. Mendoza-Naranjo, P. Cormie, A.E. Serrano, C.H.M. Wang, C. Thrasivoulou, J.E.S. Sutcliffe, D.J. Gilmartin, J. Tsui, T.E. Serena, A.R.J. Phillips, D.L. Becker, Overexpression of the gap junction protein Cx43 as found in diabetic foot ulcers can retard fibroblast migration, *Cell Biol. Int.* 36 (2012) 661–667.
- [88] B. Cogliati, M. Vincken, T.C. Silva, C.M. Araújo, T.P. Aloia, L.M. Chaible, C.M. Mori, M.L. Dagli, Connexin 43 deficiency accelerates skin wound healing and extracellular matrix remodeling in mice, *J. Dermatol. Sci.* 79 (2015) 50–56.
- [89] M. Hanson, J.P. Derouette, I. Roth, B. Foglia, I. Scerri, T. Dudez, B.R. Kwak, Gap junctional communication in tissue inflammation and repair, *Biochimica Et Biophysica Acta-Biomembranes* 1711 (2005) 197–207.

XV. Steuer, A., Wende, K., **Babica, P.**, Kolb, J.F.*, 2017. Elasticity and tumorigenic characteristics of cells in a monolayer after nanosecond pulsed electric field exposure. *European Biophysics Journal* 46, 567–580.



Elasticity and tumorigenic characteristics of cells in a monolayer after nanosecond pulsed electric field exposure

A. Steuer¹ · K. Wende¹ · P. Babica² · J. F. Kolb¹

Received: 4 January 2017 / Revised: 13 March 2017 / Accepted: 17 March 2017 / Published online: 1 April 2017
© European Biophysical Societies' Association 2017

Abstract Nanosecond pulsed electric fields (nsPEFs) applied to cells can induce different biological effects depending on pulse duration and field strength. One known process is the induction of apoptosis whereby nsPEFs are currently investigated as a novel cancer therapy. Another and probably related change is the breakdown of the cytoskeleton. We investigated the elasticity of rat liver epithelial cells WB-F344 in a monolayer using atomic force microscopy (AFM) with respect to the potential of cells to undergo malignant transformation or to develop a potential to metastasize. We found that the elastic modulus of the cells decreased significantly within the first 8 min after treatment with 20 pulses of 100 ns and with a field strength of 20 kV/cm but was still higher than the elasticity of their tumorigenic counterpart WB-ras. AFM measurements and immunofluorescent staining showed that the cellular actin cytoskeleton became reorganized within 5 min. However, both a colony formation assay and a cell migration assay revealed no significant changes after nsPEF treatment, implying that cells seem not to adopt malignant characteristics associated with metastasis formation despite the induced transient changes to elasticity and cytoskeleton that can be observed for up to 1 h.

Keywords nsPEF · Elasticity · Elastic modulus · AFM · Actin cytoskeleton · Anchorage-independent growth

Introduction

Pulsed electric fields (PEFs) can trigger different biochemical and biophysical pathways in cells. Pulses in the range of milli- to microseconds primarily affect the outer membrane, while shorter pulses with a duration in the nanosecond range can also affect subcellular structures (Beebe et al. 2003). Since nanosecond pulsed electric fields (nsPEFs) can induce apoptosis, they are of interest for the treatment of tumors. Their efficacy was proven in several animal studies for solid tumors (Beebe et al. 2010; Breton and Mir 2012; Chen et al. 2010; Kolb and Stacey 2012). In this context, one of the best-studied pulse lengths is 100 ns (Chen et al. 2012; Nuccitelli et al. 2012, 2010; Wu et al. 2014). Therefore, this pulse duration was also chosen for the study presented here. During treatments, it is likely that not all cells are exposed to fields leading to their death. The exposure might still cause lasting and adverse changes. We investigated how normal cells, in particular their elasticity, are affected after exposure to 100-ns pulses with rather mild field strength so that all cells survive. nsPEFs were applied to cells in monolayers, serving as a simple tissue model in which the cells are stabilized by interactions with their neighbors and with the extracellular matrix. Monolayers thus should recapitulate mechanical properties and responses of adherent cells more relevantly than measurements in single cells.

The elasticity of cells is directly connected to malignancy and invasiveness of cancer cells. Accordingly, invasive cancer cells generally display a lower elastic modulus (Young's modulus, YM) than their non-invasive counterparts (Cross et al. 2008; Jonas et al. 2011; Lekka et al. 1999). Hence, the metastatic potential of cancer cell lines has been predicted from their elasticity (Swaminathan

✉ J. F. Kolb
juergen.kolb@inp-greifswald.de

¹ Leibniz Institute for Plasma Science and Technology, Felix-Hausdorff-Strasse 2, 17489 Greifswald, Germany

² Faculty of Science, Research Centre for Toxic Compounds in the Environment (RECETOX), Masaryk University, Brno, Czech Republic

et al. 2011; Xu et al. 2012). It was demonstrated that the elastic modulus of cancerous human bladder cells was about one magnitude smaller compared to their non-tumorigenic counterpart (Lekka et al. 1999). Metastasizing cells from patient samples from lung, breast and pancreas were more than 70% softer than healthy cells from the same organs (Cross et al. 2007). Another study on patient effusion cells revealed a similar result with tumor cells being about 80% softer than healthy cells (Cross et al. 2008). The investigation of ovarian cell lines with different metastatic potentials showed that cancer cells with the highest metastatic potential were five times softer than cancer cells with the lowest potential (Swaminathan et al. 2011). The cytoskeleton, in particular actin fibers, is the main structure responsible for the stiffness of cells. Furthermore, stiffness inversely correlates with migration and invasion. A change in cell stiffness might be associated with the remodeling of the actin cytoskeleton when the cytoskeletal structure changes from an organized to irregular network (Xu et al. 2012).

That nsPEFs can induce the breakdown of the cytoskeleton in mammalian cells was already shown by Stacey et al. who exposed cervical carcinoma cells HeLa to a single 60-ns pulse with a field strength of 15 kV/cm. They could demonstrate a ruffling of the cell membrane and a rounding of the cell within 4 min after pulsed electric field application but without killing the cells (Stacey et al. 2011). Hence, the cytoskeleton eventually had to have recovered. Chopinet et al. investigated the effect of electroporation pulses on the cytoskeleton and the elasticity of single Chinese hamster ovary (CHO) cells. They found a decrease of about 40% of the elastic modulus that is based on an inner effect related to cytoskeleton destabilization (Chopinet et al. 2014, 2013). In another study, also done with single CHO cells but with nanosecond pulses, Thompson et al. showed likewise a significant decrease of the elastic modulus and an incomplete dissipation of the actin cortex (Thompson et al. 2014). However, it has to be noted that results obtained by AFM measurements display a great variety since they depend on different factors. This needs to be considered with respect to the comparison of the observations. The data in the above-mentioned studies were evaluated for different indentations of the cantilever, which have to be chosen according to tip shape and cell state.

However, so far it is not determined if cells grown and exposed in a monolayer become softer after the application of nsPEFs or if neighboring cells possibly stabilize each other, preventing a general decrease of their elasticity. Furthermore, it is conceivable that cells which were exposed to sublethal PEFs become softer which might suggest a malignant transformation and the potential to form metastases.

In this study, we therefore aimed to determine if the elastic modulus of cells in a monolayer, especially of

normal cells, treated by nsPEFs approaches the elastic modulus of their tumorigenic counterpart and if these cells in consequence show a tumorigenic behavior such as anchorage-independent growth or faster migration.

Materials and methods

Cell line

As our objective was to compare the features of normal cells with those of tumorigenic cells we have chosen two cell lines from the same origin which are thus directly comparable. The first cell line were WB-F344 cells which are diploid liver epithelial cells derived from a normal adult male Fischer 344 rat by J.W. Grisham and M.S. Tsao of the University of North Carolina at Chapel Hill, Chapel Hill, NC, USA (Tsao et al. 1984). WB-F344 cells have characteristics of liver progenitor cells capable of multiple lineage differentiation (Anderson et al. 2007; Fan et al. 2009; Zhou et al. 2010). WB-F344 cells are normal, non-cancerous cells with developed contact inhibition of growth, functional gap junctional intercellular communication (GJIC), inability of anchorage-independent growth and they are non-tumorigenic in vivo (De Feijter et al. 1990; Hayashi et al. 1998). The cell line WB-ras was derived from WB-F344 cells by transformation with H-ras oncogene, which resulted in the neoplastic phenotype of a WB-ras cell characterized by limited contact inhibition of growth, reduced GJIC, increased ability of anchorage-independent growth and tumorigenicity in vivo (De Feijter et al. 1990; Hayashi et al. 1998). Both cultures were obtained from Prof. J. E. Trosko, Michigan State University, East Lansing, MI, USA.

WB-F344 cells were cultured in low-glucose DMEM, supplemented with 2 mM L-glutamine, 5% fetal calf serum and 1% penicillin/streptomycin (medium and supplements purchased from PAN-Biotech GmbH, Aidenbach, Germany). 10^5 cells were seeded in 35-mm Petri dishes and after 24 h, when a confluent monolayer was achieved, used to perform the experiments.

WB-ras cells were cultured in a modified Eagle's minimum essential medium (MEM) but with 1 g/l of sodium bicarbonate and 7.635 g/l of sodium chloride, 1.5× increase in concentrations of all vitamins and all essential amino acids (except L-glutamine, which remains 2 mM), 2× increase of non-essential amino acids (i.e. final concentration 0.2 mM), and 1 mM sodium pyruvate (all supplements purchased from Gibco, Darmstadt, Germany). Furthermore, 1% penicillin/streptomycin was added. Samples were prepared the same way as WB-F344 cells.

Nanosecond pulsed electric field treatment

For the generation of the pulses, an in-house-built Blumlein pulse generator was used which generates pulses with a duration of 100 ns (Fig. 1). The resistance of the monolayer together with the medium was similar to the impedance of the pulse generator of 100 Ω . This pulse length was chosen because it is often used in animal studies (Beebe et al. 2011, 2010; Nuccitelli et al. 2012, 2010). The pulses were delivered by two parallel stainless steel wire electrodes with a diameter of 0.8 mm and a gap distance of 5 mm, which were imbedded in a plastic cylinder. Cells were exposed to 20 pulses with a field strength of 20 kV/cm in full medium by slightly impressing the electrodes into the monolayer. The complete experimental setup including a simulation of the resulting electric field distribution is described in (Steuer et al. 2016).

Atomic force microscopy (AFM) and data analysis

Immediately after nsPEF treatment, cell culture medium was replaced by DMEM supplemented with 25 mM HEPES (Pan-Biotech, Aidenbach, Germany) to stabilize a neutral pH value during the AFM measurement. Subsequently, cells were placed in a Petri dish heater (JPK Instruments, Berlin, Germany) set to 37 °C under the AFM (Nanowizard 3, JPK Instruments, Berlin, Germany). The cantilever (MLCT, Bruker, Camarillo, CA, USA) that was used had a nominal spring constant of 0.03 N/m and a nominal tip radius of 20 nm. Before each experiment, the spring constant was calibrated by thermal noise method. The AFM was operated in QI mode [Quantitative Imaging, JPK, Berlin (JPK Instruments a; JPK Instruments b; Stamoj et al. 2015)] with the following

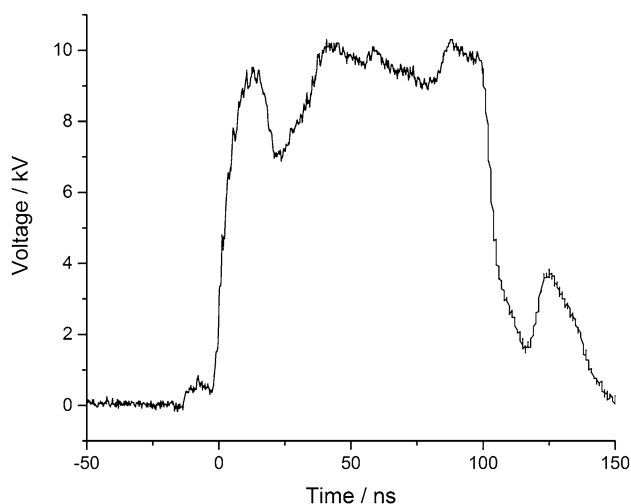


Fig. 1 Image of a typical rectangular 100-ns pulse with an amplitude of 10 kV generated by an in-house-built Blumlein pulse generator

parameters: Z-length 3 μm ; applied force 4 nN; extend/retract speed 15 $\mu\text{m/s}$. 64 \times 64 force curves (in total 4096) were recorded in an area of 30 \times 30 μm^2 . Elasticity of treated cells was measured every 5 min for a period of 28 min at the same position, starting 8 min after the treatment.

Data were analyzed with JPK data processing software (Neumann 2008). In a first step, any offset or tilt from the baseline of the extend curves was removed to find the contact point of the cantilever with the cell surface. Subsequently, the cantilever bending was subtracted from the piezo movement to yield the indentation of the cantilever into the cell. In the last step, the Hertz model was applied to derive the Young's modulus by considering the geometry (shape and angle) of the cantilever tip. For the data evaluation, an indentation depth of 300 nm was chosen, which should reveal the reaction of almost the whole cell without being influenced by the substrate. An indentation in the range of 50 nm mainly reflects the reaction of the cell membrane, while for an indentation deeper than 500 nm, the substrate starts to influence the measurement (Neumann 2008; Roduit et al. 2008). Values were plotted in histograms and fitted with a Gaussian function to exclude "outliers" by using OriginPro 8 software (OriginLab Corporation, Northampton, MA, USA). For further evaluation, the peak values of the Gaussian fits were used. Standard deviations were calculated from the full width of half maximum (FWHM) of the Gaussian fit curves. Significance was analyzed by an unpaired Student's *t* test with significance levels of *p* value < 0.05 (*), *p* value < 0.01 (**) and *p* value < 0.001 (***).

Immunofluorescent staining of the actin cytoskeleton

The actin cytoskeleton was visualized by immunofluorescent staining. Cells were cultured on a glass cover slip until a confluent monolayer had grown. Then, WB-F344 cells were treated with nsPEFs and after an incubation time of 5, 15, 30 and 60 min, cells were fixed with 4% paraformaldehyde and permeabilized with 0.25% Triton X-100 in PBS. Afterwards, cells were incubated at 4 °C over night with fluorescein isothiocyanate-labeled phalloidin (phalloidin-FITC, Sigma-Aldrich, Taufkirchen, Germany). The next day, cover slips were rinsed twice with deionized water and put upside down on microscope slides with the mounting medium Fluoromount™ (Sigma Aldrich, Traunstein, Germany). After 24 h, samples were observed under a confocal microscope (TCS SP5, Leica, Wetzlar, Germany). For comparison, the actin cytoskeleton of untreated WB-F344 and WB-ras cells was also stained.

Cell migration assay

For the investigation of the migration and proliferation of nsPEF-treated cells in comparison to untreated cells, a scratch assay was performed. Therefore, a scratch was made with a pipette tip in a monolayer which resulted in a gap of about 600 μm . In the nsPEF-treated monolayers, the scratch was made orthogonally to the electrode position. Immediately after treatment, medium was exchanged by fresh medium and the cell culture plates were incubated at 37 °C and 5% CO_2 under a microscope (Axiovert 40 CFL, Zeiss, Oberkochen, Germany). Images were taken every 5 min for the next 24 h. Data were evaluated with ZEN software (blue edition, Carl Zeiss MicroImaging GmbH, Jena, Germany). The gap distance of the scratch was measured at three different positions in the image in every thirtieth picture (corresponding to a progression in time of 2.5 h) and gap distance was normalized to the initial gap distance of the scratch.

Colony formation assay

To investigate if nsPEF-treated cells undergo malignant transformation, a soft agar colony formation assay was performed. For this purpose, WB-F344 cells were suspended in a special buffer (2.5 mM KH_2PO_4 , 10 mM K_2HPO_4 , 125 mM saccharose, 2 mM $\text{MgCl}_2 \cdot 6\text{H}_2\text{O}$) and exposed to nsPEFs in 4-mm electroporation cuvettes (VWR International GmbH, Darmstadt, Germany). 5000 cells were suspended in 1 ml 0.33% agarose and layered on top of a solidified base of 1 ml of 1% agarose in a 6-well plate. The cell suspension was covered with a top layer of 1 ml of 0.5% agarose. For all layers, agarose was dissolved in complete medium. Cultures were fed weekly with 0.5 ml of complete medium. Three weeks after plating, colonies were stained with a 1:1 mixture of Giemsa stock solution (Carl Roth, Karlsruhe, Germany) and methanol. For comparison, the assay was also performed with untreated WB-F344 and WB-ras cells.

Results

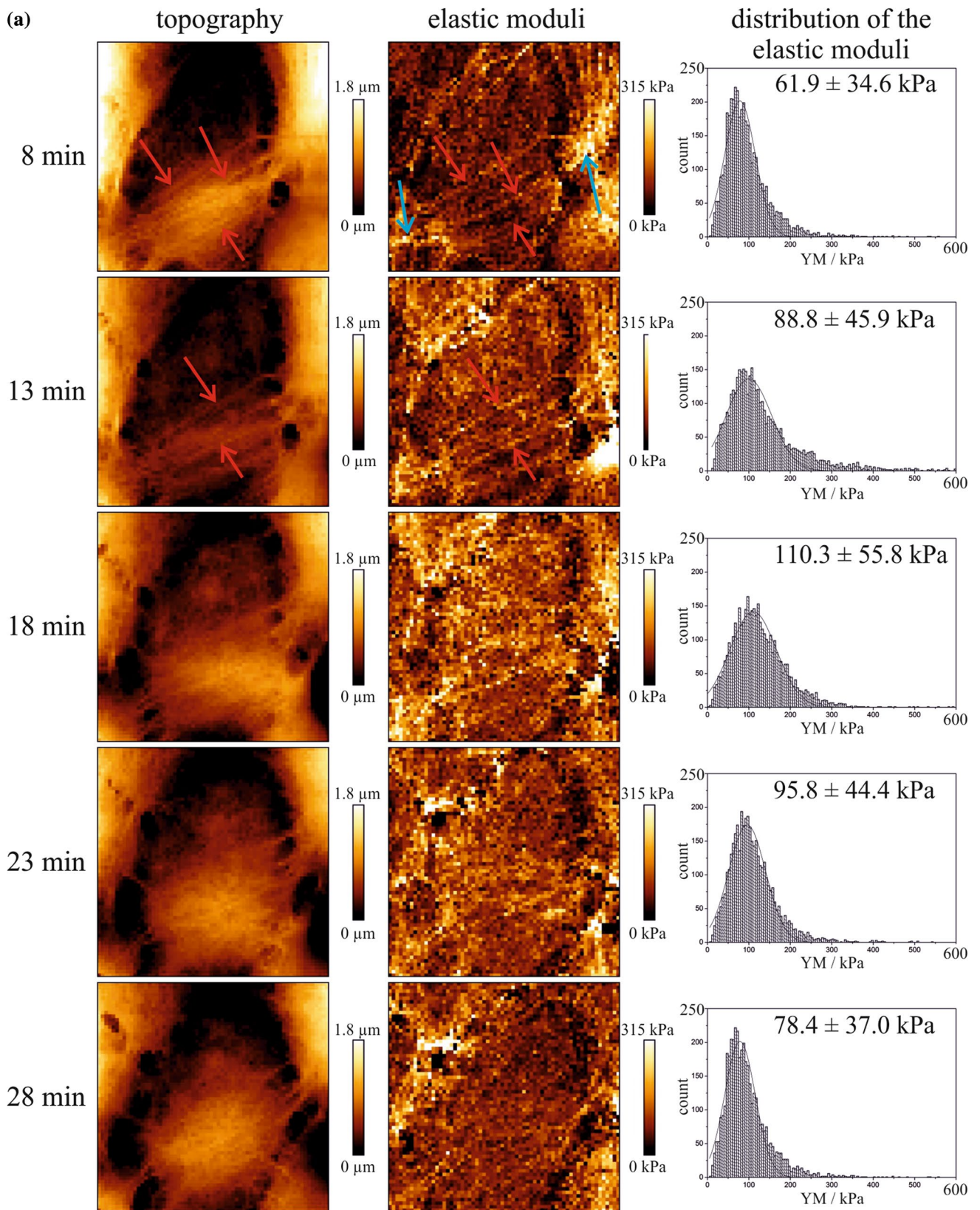
Cell elasticity

The elastic modulus of a randomly chosen patch of the monolayer of WB-F344 cells was measured every 5 min between 8 and 28 min after exposure to nsPEFs. Every patch had an area of $30 \times 30 \mu\text{m}^2$ which was large enough to cover one cell with parts of its neighboring cells. Figure 1a shows a representative example of a cell in a nsPEF-treated monolayer. The left column displays the topography, i.e. the profile. The center column shows

Fig. 2 AFM images of the topography (*left column*) and the elastic moduli (*center column*) of a WB-F344 monolayer (**a**) after the application of 20 pulses of 100 ns and with a field strength of 20 kV/cm, **b** in comparison to an untreated monolayer. Measurements were performed every 5 min between 8 and 28 min after treatment. The right column describes the distribution of the elastic moduli with a Gaussian fit (*x* axis: YM/x_{max} : 600 kPa; *y* axis: $\text{counts}/y_{\text{max}}$: 250). In addition, the peak values \pm standard deviation (SD, derived from the fitted curves) are given. The *red arrows* point at actin fibers and the *blue* ones at the focal adhesions

the color-coded elastic moduli across the same area and the right column shows the correlating distribution (histogram) of the elastic moduli in increments of 5 kPa. The histogram was fitted with a Gaussian curve, which is assuming a normal distribution of elastic moduli. (No arguments are found for the need to use any other model.) This approach is similar to the evaluation conducted by Chopinet et al. (2014, 2013). In addition, the temporal development of the elastic modulus of an untreated monolayer was measured to exclude the possibility that elasticity and actin cytoskeleton changed only due to the measurement procedure (Fig. 1b).

Changes of the actin cytoskeleton are visible in the topographic images as well as in the mapping of the elastic moduli (Fig. 1a, left and center column). Well-defined parallel actin fibers which span across the whole cell were apparent until 13 min after the treatment (red arrows). Between 18 and 28 min after the application of the pulsed electric fields, the shape of the cell changed considerably. The cell became round (but did not lose the contact to its neighboring cells as evidenced by the elastic moduli images) and almost no actin fibers were detectable anymore. The actin fibers appeared to be broken into shorter segments. Also, the focal adhesions (blue arrows) that mechanically link the actin cytoskeleton to the substrate seem disintegrated. The loss of actin fiber structure was confirmed by the distribution of the elastic moduli, depicted in the respective images in the center column, which was becoming more diffuse 13 min after the pulsed electric field treatment. In addition, cell boundaries could no longer be clearly identified. This observation correlates with the measured values of the elastic moduli shown in the histograms (Fig. 2a, right column). In the example presented here, the cells were rather soft with an elastic modulus reaching about 62 kPa (the peak value of the fitted histogram) 8 min after the treatment. Within 18 min after the application of nsPEFs, the cells became stiffer again and the elastic modulus rose to 110 kPa, then decreased again to about 80 kPa. Also, the standard deviations of the elastic moduli values changed considerably after exposures. The value increased from 35 kPa at 8 min after the treatment to 55 kPa after 18 min. 28 min after the application of nsPEFs, the standard deviation was approaching the value of the initial measurement again, although intact actin fibers were not yet visible.



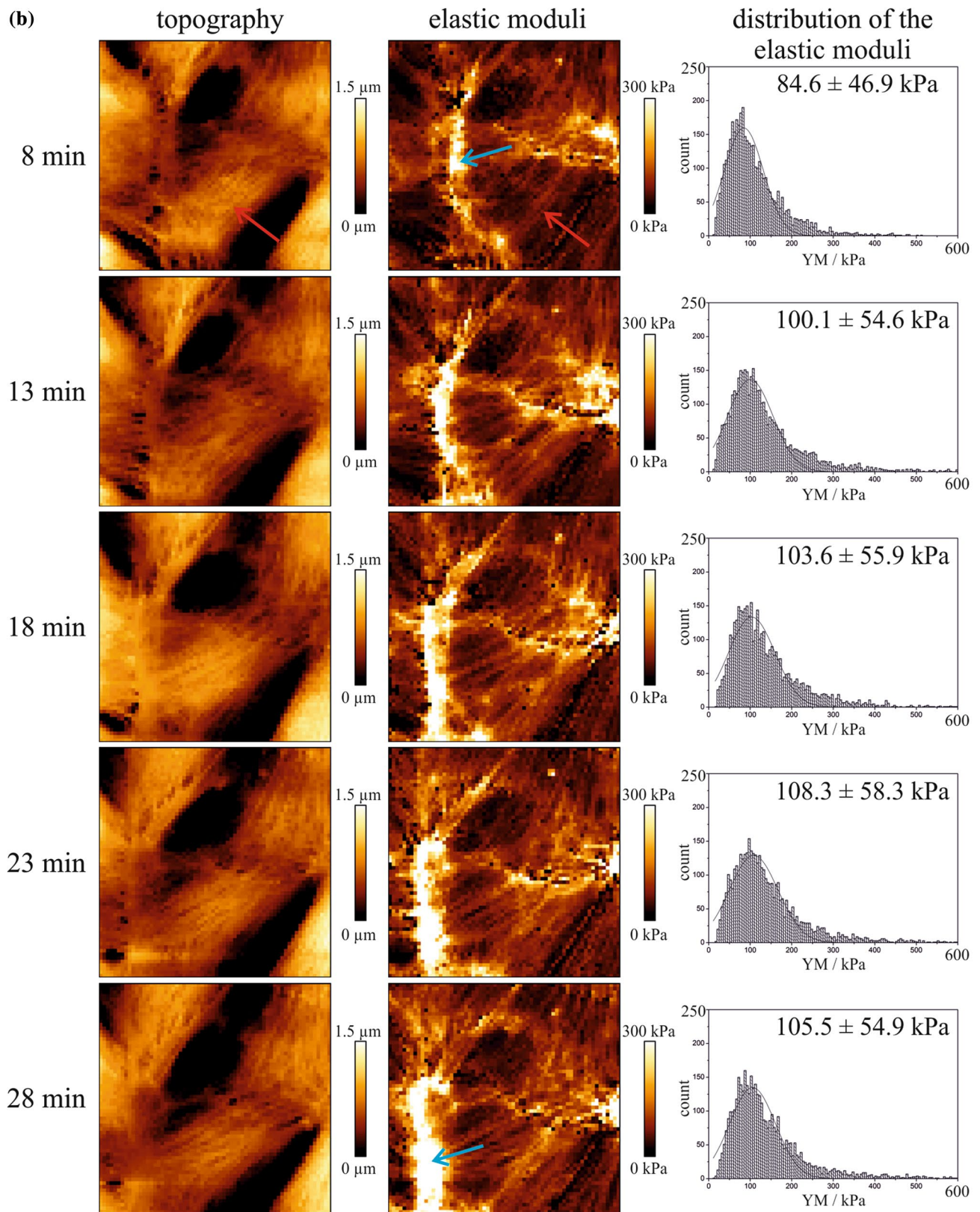


Fig. 2 continued

In comparison, an equivalent time series measured in the untreated cells barely showed any changes with time in topography and in elastic moduli. Cell structure and shape, in particular well-defined actin fibers, were clearly visible in each image (Fig. 2b, left column) and the elastic moduli barely changed (center column). Only the area of the focal adhesions increased (blue arrows), at least at the edges of the cells. Potential changes in focal adhesions existing at the cell's basal lamina were not accessible for the AFM; accordingly, this result does not necessarily reflect the cell's total area of focal adhesions. The structural integrity is also reflected in the distribution of the elastic moduli (right column). The mean value increased from 85 kPa to about 105 kPa. In contrast to treated cells, standard deviations remained largely the same but with generally higher values between 47 and 55 kPa.

Altogether, the temporal development of the elastic modulus was measured on seven different WB-F344 monolayers, exposed in separate and independent experiments. The values for the controls were even determined from 14 samples for WB-F344 and from 5 samples for WB-ras cells. Means of the peak values of the respective Gaussian curves are shown in Fig. 3. Individual peak values were derived by considering every force-distance curve of each overall measurement.

Untreated WB-F344 cells revealed an average elastic modulus of about 61 kPa. After the application of the pulsed electric fields, cells became significantly softer within 8 min, with an elastic modulus barely reaching 43 kPa. Already 13 min after the treatment, the elastic

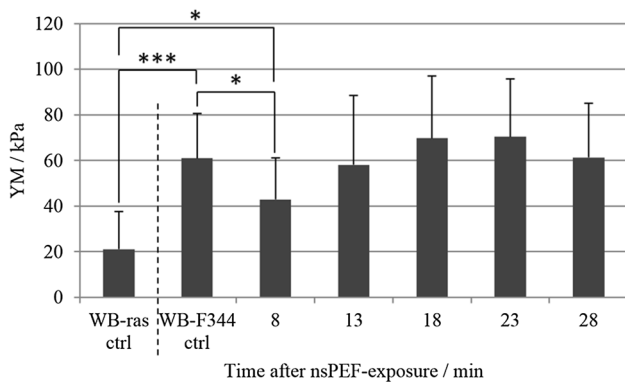


Fig. 3 Temporal development of the elasticity of WB-F344 cells after the application of 20 pulses of 100 ns and with a field strength of 20 kV/cm compared to untreated WB-F344 and untreated WB-ras cells. The graph shows the mean values of the peak values from the Gaussian fits \pm standard deviation (SD). Values for treated WB-F344 cells were derived from 7 independent experiments, values for untreated WB-F344 from 14 and for untreated WB-ras from 5 independent experiments. The error bars correspond to the means of the standard deviations, which were determined for each measurement from the FWHM of the Gaussian fit

modulus approached the control level again with a value of 58 kPa. 18 and 23 min after the treatment, the elastic modulus had increased to 70 kPa and by that slightly, but not significantly, exceeded the elastic modulus of the control. At the last time point of the measurement, 28 min after exposure, cells had regained about the same elasticity as observed for control cells (61 kPa). Hence, for the exposure conditions investigated here, transient changes in the elasticity of cells can be induced for about half an hour. In comparison, tumorigenic WB-ras cells were, in general, considerably softer. With a value of about 20 kPa, the mean elastic modulus of the untreated tumor cells equaled about one-third of the value of untreated WB-F344 cells and about half of the value of treated WB-F344 cells when observed 8 min after the exposure.

Since the elastic moduli were measured in a randomly chosen area of the monolayers, the contribution from cell

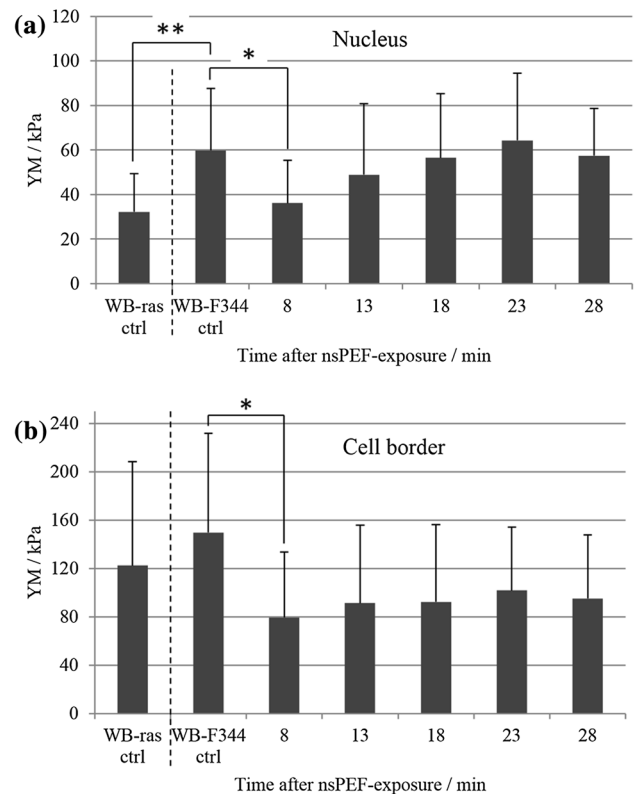


Fig. 4 Temporal development of the elasticity determined **a** across the nucleus and **b** across the border of WB-F344 cells after the application of 20 pulses of 100 ns and with a field strength of 20 kV/cm compared to untreated WB-F344 and WB-ras cells. The graph shows the mean values of the peak values from the Gaussian fits \pm standard deviation (SD). Values for treated WB-F344 cells were derived from 7 independent experiments, values for untreated WB-F344 from 14 and for untreated WB-ras from 5 independent experiments. Attention should be paid to the different ranges of the y axis demonstrating the softer characteristic above the nucleus

areas across the nucleus and the cell border was different for each investigated area. To distinguish differences stemming from the contribution of the nucleus or from changes of structures surrounding it, the effects of nsPEFs on the cell elasticity were evaluated for both regions separately by selecting sections of 25×25 force curves above the nucleus and at the border of the cells, respectively. Figure 4 shows the temporal development of the elastic modulus in the area of the nucleus (a) and the cell's border (b) in comparison to untreated WB-F344 and WB-ras cells.

The average elastic modulus above the nucleus of untreated WB-F344 cells was 60 kPa. 8 min after the application of the nsPEFs, the elastic modulus fell significantly by almost half to 36 kPa, before it increased steadily to 64 kPa within 23 min. 28 min after the exposure, the elastic modulus approached the control level again with a value of 57 kPa. In comparison, the elasticity above the nucleus of the tumorigenic WB-ras cells was 32 kPa, significantly lower than for untreated WB-F344 cells. However, this is only slightly, but not significantly, lower than the elastic modulus of treated WB-F344 cells 8 min after exposure.

The mean elastic modulus in the region at the border of untreated WB-F344 cells was 150 kPa and that for WB-ras cells was 120 kPa. While these values are close, it has to be considered that WB-ras cells were about twice as soft across the nucleus as untreated WB-F344 cells. 8 min after the application of the nsPEFs, the elastic modulus of treated WB-F344 cells decreased to 80 kPa which is only about half of the control level and even lower than values for WB-ras. In the following measurements, the elastic moduli of the cells' borders increased only slightly and ranged between 90 and 100 kPa, but, in contrast to 8 min after exposure, they were not significantly different from the control value anymore.

Actin reorganization

The actin fibers were stained to support the results on the map of elastic moduli concerning the remodeling of the cytoskeleton. Figure 4 shows the fluorescence images of WB-F344 monolayers fixed and stained 5, 15, 30 and 60 min after the treatment with 20 pulses of 100 ns and

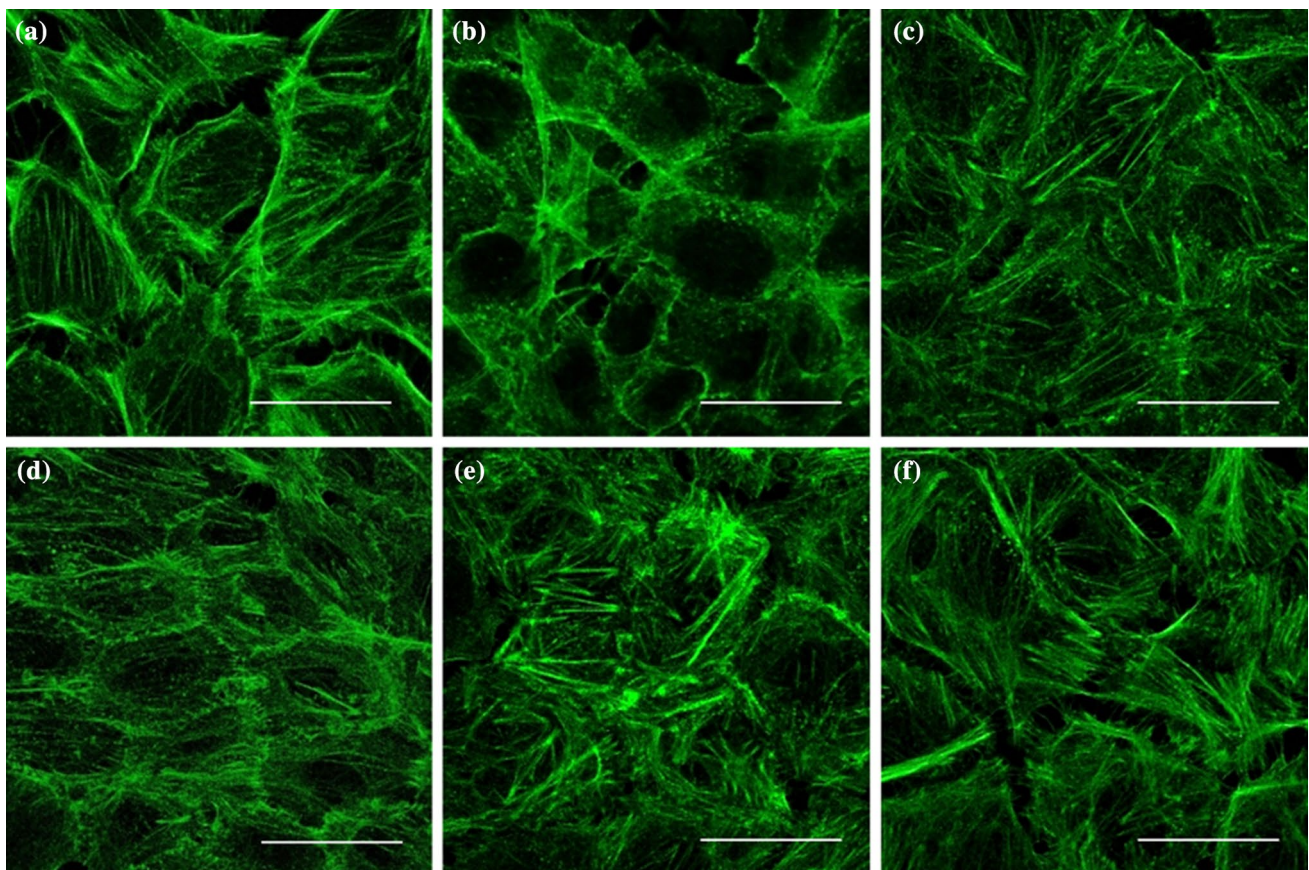


Fig. 5 Immunofluorescent staining of the actin cytoskeleton of **a** untreated WB-F344, **b** untreated WB-ras cells and WB-F344 cells **c** 5 min, **d** 15 min, **e** 30 min and **f** 60 min after the application of 20 pulses of 100 ns and with a field strength of 20 kV/cm. (Scale bars: 25 μ m)

20 kV/cm (c–f), in comparison to images of untreated WB-F344 (a) and WB-ras cells (b).

The actin stress fibers of the untreated WB-F344 cells (Fig. 5a) are well-aligned across the entire cell volume, showing a high degree of organization. In comparison, 5 min after the treatment (Fig. 5c), visible actin filaments were shorter, less organized and randomly oriented. After an additional 10 min (Fig. 5d), only few well-defined stress fibers could still be detected. In addition, a high degree of background fluorescence indicated the presence of oligomeric actin in the cytosol. 30 min after the exposure (Fig. 5e), the appearance was similar to observations after 5 min. Actin fibers were barely aligned and formed a tangled network. Compared with images taken after 15 min, the background fluorescence had declined. 60 min after the treatment, the actin cytoskeleton seemed to recover slowly (Fig. 5f). Actin fibers were more organized and cytosolic actin was reduced. In contrast, the staining of the actin cytoskeleton of tumorigenic WB-ras cells (Fig. 5b) differs considerably from that of WB-F344 cells. In general, no defined actin stress fibers could be detected, corresponding to the small elasticity.

Malignancy and metastatic potential

Cell elasticity is a biomarker not only for invasiveness but also for malignancy in general. After exposure to nsPEFs, the elastic modulus of WB-F344 cells is significantly reduced and approaches values comparable to their tumorigenic counterpart WB-ras (although without quite reaching them). Although the changes are transient, we investigated if the effect is sufficient for normal cells to instigate other tumorigenic characteristics. A scratch assay was performed to determine the potential of nsPEF-treated WB-F344 cells to migrate (Liang et al. 2007). In addition, a soft agar

colony formation assay was conducted to test for malignant transformation.

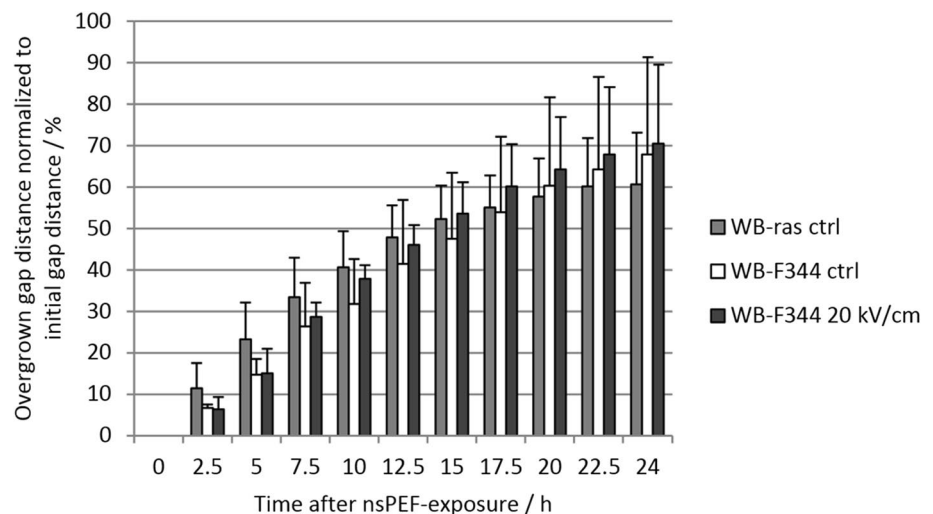
Migration behavior of untreated WB-F344 and WB-ras cells and of WB-F344 cells exposed to nsPEFs was observed for 24 h. The graph in Fig. 6 shows the overgrown distance normalized to the initial gap width with time.

In the first 12.5 h after placing the scratch, the gap in the monolayer of the cancer cell line WB-ras was closing somewhat faster than the gap in the WB-F344 monolayers. This difference in migration velocity was not significant. For the same period, nsPEF-treated and control WB-F344 cells showed a similar migration behavior. During 15 and 24 h after the treatment, proliferation and migration of the WB-ras cells seemed to stagnate. Finally, 60% of the initial gap distance was overgrown while WB-F344 cells kept growing steadily to a value of about 70%. However, altogether, no significant difference in proliferation and migration between nsPEF-treated and untreated WB-F344 and their tumorigenic counterpart WB-ras could be detected.

Besides invasiveness, cell elasticity is also a biomarker for malignancy. Therefore, WB-F344 cells were exposed to nsPEF and tested for anchorage-independent growth (Fig. 7).

Three weeks after plating, cells were stained and images were taken under a microscope (Fig. 7). Untreated WB-F344 cells served as a negative control (Fig. 7a). The arrows point at single cells in the gel which survived the treatment but did not form any colonies. In contrast, the transformed cell line WB-ras did form colonies, visible as large black dots (Fig. 7b). NsPEF-treated WB-F344 cells also did not form any colonies (Fig. 7c), showing no signs of anchorage-independent growth and thus no signs of malignant transformation.

Fig. 6 Bars show mean values \pm standard deviation (SD) of the overgrown gap distance of the scratch in WB-F344 monolayers treated with 20 pulses of 100 ns and with a field strength of 20 kV/cm compared to untreated WB-F344 and untreated WB-ras cells along time. Values were derived from 3 independently repeated experiments



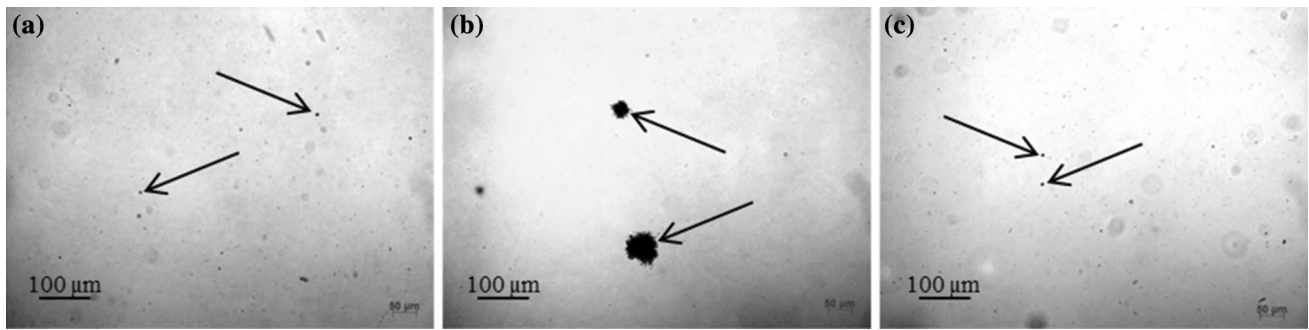


Fig. 7 Colony formation assay of **a** untreated WB-F344 cells, **b** untreated WB-ras cells and **c** WB-F344 cells treated with 20 pulses of 100 ns and with a field strength of 20 kV/cm. Cells were stained with Giemsa 3 weeks after plating

Discussion

The cytoskeleton, in particular actin, is mainly responsible for the elasticity of a cell (Alberts et al. 2012). During carcinogenesis, the elasticity of a cell changes, i.e. cells become softer (Jonas et al. 2011; Lekka et al. 1999; Rother et al. 2014). The main reason for this is the remodeling of the actin cytoskeleton, resulting in a reduced adhesion, a more rounded cell shape and a loss of stress fibers (Ben-Ze'ev 1985; Rao and Cohen 1991). This remodeling is also responsible for an increased motility of the cell, with this promoting the potential formation of metastases (Olson and Sahai 2009; Yamasaki 1991).

Yousafzai et al. found that the highly aggressive breast cancer cells MDA-MB-231 which are relatively soft in isolated conditions, become stiffer (comparable to their normal counterpart) during cell–cell interaction while the less aggressive MCF-7 and the normal HBL-100 cells become softer. Therefore, they hypothesized that cancerous cells might act as normal cells by altering the mechanics of the cell environment (Yousafzai et al. 2016). The other way round, normal cells might act as cancer cells when their mechanical properties are changed. Therefore, the investigation of changes to the cell elasticity for a monolayer is warranted for a better understanding of nsPEF affecting cells in a tissue.

The immunofluorescent staining showed that the application of nsPEFs did induce a reorganization of the actin cytoskeleton in normal WB-F344 cells. This correlates with the topographic images from AFM measurements. Both methods indicate that the actin cytoskeleton was less organized and that actin fibers were broken into shorter segments within a few minutes after exposure to the pulsed electric fields. Regarding the overall elasticity of the measured area, 8 min after the application of the pulses, the stiffness was significantly reduced by about one third compared to untreated WB-F344 cells, but treated cells were still about twice as stiff as their non-treated tumorigenic counterparts.

The results of the immunofluorescent staining did not entirely correspond to the time course of changes to the elasticity. The elastic modulus equaled almost the control level again within 13 min after the treatment while 1 h after the application of the nsPEFs, the actin cytoskeleton had not yet completely recovered. Since microtubules and intermediate filaments contribute minimally to the elasticity of a cell (Buehler 2013; Haga et al. 2000), other yet unknown factors seem to influence the cell elasticity. Structural changes of the plasma membrane might have led to the increase of the elastic modulus, but this possibility has to be investigated further. Pakhomov et al. assumed that the disintegration of the actin cytoskeleton is a result of cell swelling as a consequence of membrane permeabilization (Pakhomov et al. 2014). They exposed single CHO cells to four 600-ns pulses at 19.2 kV/cm and proved an immediate cell membrane poration by the uptake of YO-PRO-1. The downstream effect of cell swelling and the subsequent disassembly of the actin fibers could be prevented by a sucrose buffer. However, in our experiments, no membrane permeabilization was observed for propidium iodide uptake (data not shown). Furthermore, Pakhomov et al. used a pulse length that was six times longer than the one that we used, and in contrast to the 600-ns pulses, 100-ns pulses were probably too short to create pores in the plasma membrane. Besides, we did not observe any change in the cell areas. Although a change in height cannot be excluded, we, in general, conclude that cell swelling due to electroporation is not responsible for the observed disassembly of the cytoskeleton. The exact mechanism which causes the disassembly of the actin cytoskeleton has to be investigated in further studies.

For a deeper insight into the effects of nsPEFs on cell elasticity, elastic moduli for the area above the nucleus and the border of the cells were evaluated separately. The development of the elastic modulus measured above the cell's nuclei was very similar to the elastic modulus of the overall recording. In both cases, the elastic modulus was

significantly decreased 8 min after the application of the nsPEFs and recovered within the following 13 min. The treated cells showed almost the same elasticity above the nucleus as the tumorigenic WB-ras cells. In contrast, the elastic modulus of the cell border of nsPEF-treated cells was by about one third lower compared to those of the border of WB-ras cells and significantly decreased compared to control WB-F344 cells. Within the recorded time frame, the elasticity of the treated cells did not recover in the border area in comparison to the nuclear region. A likely explanation could be that the nucleus itself has a certain elasticity and is able to deform and thus to adapt to changes of the cell shape (Caille et al. 2002). Hence, the effect of the pulsed electric fields could be compensated for by the adaptation of the nucleus. Furthermore, the nucleus fills a large portion of the cell volume for WB-F344 as well as WB-ras cells. Therefore, small values for elastic moduli, as presented in Figs. 1 and 2, are mainly determined by characteristics of the nucleus. That the nucleus might provide the major contribution to the mechanical properties of cells was also suggested by Guilak et al., pointing out the differences between cytoplasmic and nucleic properties (Guilak et al. 2000). Yousafzai et al. confirmed this assumption by comparing two breast cancer cell lines with different aggressiveness with their non-tumorigenic counterparts. They found that all cell lines had significantly different elasticity values above the nuclear region and the leading edge but that the nucleus showed a larger contribution toward the mechanical architecture (Yousafzai et al. 2016).

Not only the elastic moduli of treated but also those of untreated WB-F344 cells had changed by about 20 kPa during the recording of the time series. This might be attributed to small changes in the environment. The use of HEPES might have increased the osmolarity of the medium and thus have led to a shrinking of the cells that was not noticeable under the microscope, and, consequently, to a slight stiffening of the cells. A contribution of temperature changes can also not be completely excluded, although all media were preheated and Petri dishes were put in a Petri dish heater during the measurement. The medium cooled down during the transfer of cells to the AFM, thus eventually leading to potential changes in the fluidity of the plasma membrane and, consequently, to changes of the elastic modulus. Furthermore, the AFM measurements showed that the focal adhesions of the untreated cells became larger with time (Fig. 1b, center column, blue arrows). This might be explained by shear stress caused by hydrodynamic effects due to pipetting for the exchange of the medium, although medium was pipetted very carefully, and removed and added only at the edge of the Petri dish. Additionally, mechanical stress was induced by the cantilever movement during the measurement. Maybe, cells tried to compensate for the stress by enlarging their focal

adhesion areas during the time between individual measurements in the time series. Besides, neither the shape of the cells nor the visible structure of the actin fiber skeleton had changed. However, changes to the elastic modulus by nsPEFs were, in comparison, still much stronger by about 50 kPa. Nevertheless, both treated cells and controls should be affected in the same manner and PEF effects were clearly distinguishable.

The results of our study yielded quite high standard deviations for the elastic moduli. The main reason for this is that the elastic moduli were measured on monolayers, as it was the actual goal. The elasticity strongly depends on the shape of a cell, in particular if it is round or spread on a surface, and, therefore, on the cell density. Round cells require only about one fourth of the force that is required for spread out cells to achieve the same deformation (Caille et al. 2002). Although cells were counted and always the same number of cells was seeded into the Petri dishes, the cell density of the monolayers had a certain statistical variation. The dependency of the standard deviations on the cell density can be confirmed by the fact that they are in the same range for the overall measurement as well as for the separately evaluated data from regions above the nucleus and the cell border. This also shows that the standard deviations essentially did not depend on the chosen area where the elastic moduli have been recorded although depending on the spot, more parts of the cell's border or the nucleus were located in this area.

Effects of PEFs on the elasticity of single cells were previously described by Thompson et al., who performed a study with CHO cells which they exposed to nanosecond pulses (50 or 100 pulses, 10 ns, 150 kV/cm). They executed the measurements on freshly adhered cells which were still round and determined the elastic moduli at an indentation depth of the cantilever of 500 nm (Thompson et al. 2014). The results showed that the elastic modulus decreased by about half and that the actin cytoskeleton partially broke down. This corresponds qualitatively and quantitatively well with our results despite the considerably shorter pulse length and higher field strength. In both Thompson's and our studies, the actin cytoskeleton was restructured after the application of the nsPEFs but not completely broken down.

The exposure to much longer electroporation pulses of 5 ms and a field strength of 400 V/cm was investigated by Chopinet et al. also for CHO cells (Chopinet et al. 2013). Therefore, they determined the elastic modulus at an indentation depth of the cantilever of 50 nm. The elastic moduli of the CHO cells were likewise significantly decreased within 8 min after the application of the electric pulses and started to recover within 17 min. This is similar to our results for shorter nanosecond pulses but in contrast to our study, up to 15 min after the treatment, CHO cells showed an absence of actin fibers under the membrane

which started to recover after 23 min. In comparison, the actin cytoskeleton of the WB-F344 cells changed within 5 min after the application of the nanosecond pulses, but actin fibers could be detected at any time of the measurement and only started to recover 60 min after the treatment. Accordingly, also in the study on the CHO cells, the temporal development of the elastic modulus did not correlate with the changes of the actin cytoskeleton. Chopinet et al. assumed that the softening of the CHO cells is a dynamic process and that besides the direct effects of the electroporation pulses, other effects must have been induced in the cell that affected its elasticity. However, the results of this study are not readily comparable with our study as different cell lines were used which can react differently to PEFs. Moreover, different pulse parameters were investigated with a known primary effect on the cell membrane which might therefore mediate changes to elasticity and cytoskeleton. For electroporation pulses, changes of the osmotic pressure have to be considered and hence a swelling of the cell which can accordingly affect the elasticity of the cell. In addition, elastic moduli were determined at different indentation regimes whereby the cell constituents at the chosen depth (e.g. membrane composition or actin cortex) have an impact on the results.

Cell elasticity is a biomarker for invasiveness as well as for malignancy in general. In addition, rapid induction of cellular events linked to the tumor promotion and malignant transformation after the treatment with nsPEFs has been reported in our previous study, where nsPEFs caused inhibition of GJIC, hyperphosphorylation of gap junctional protein connexin43, and activation of mitogen-activated kinases (MAPKs) Erk1/2 and p38 in WB-F344 cells (Steuer et al. 2016). The observations that nsPEFs can induce several tumor-promoting and carcinogenic events—although some of them transient—in a normal non-tumorigenic cell line could lead to the assumption that nsPEFs might contribute to a malignant transformation associated with permanent changes in the cell phenotype and increase in their tumorigenic features, such as anchorage-independent growth of the cells on soft agar or changes in their motility. The soft agar colony formation assay is a semi-quantitative *in vitro* assay to detect malignant transformation of cells induced by chemicals or other trigger mechanisms. Transformed cells lose their contact inhibition and are therefore able to grow anchorage-independently in a gel. In comparison, normal adherent cells require an attachment to a solid surface to grow and thus cannot form colonies in a gel. Since *in vitro* ability of anchorage-independent growth as well as cell motility correlates well with tumorigenicity *in vivo*, an increase in the frequency of soft agar colony formation or in the cell motility in the scratch assay would indicate a malignant transformation of non-tumorigenic WB-F344

cells after the treatment with nsPEFs. This hypothesis was not confirmed. Treated WB-F344 cells were not able to grow anchorage-independently in the gel and also did not show a significant difference in proliferation and migration in the scratch assay compared to the untreated cells, which indicates that nsPEFs did not induce malignant transformation. Although higher motility of WB-ras than WB-F344 cells in a scratch assay was reported by Lee et al., their experiments were conducted under the arrested growth conditions induced by mitomycin treatment (Lee et al. 2006). The lack of significant difference between motility of WB-ras and WB-F344 cells observed in our scratch assay conducted under the normal cell culture conditions could be a result of comparable and relatively high proliferation rates of both cell lines (Hayashi et al. 1998), when the initially slower wound closure by putatively less motile WB-F344 cells was probably compensated for by their fast proliferation and expansion occurring later on (>15 h post treatment).

Regardless the underlying mechanisms, the results of the soft agar colony formation assay as well as of the scratch assay imply that the application of nsPEFs does not seem to be associated with long-term increase in cell tumorigenic features. Presumably, changes to the mechanical properties that are induced by nsPEFs are too short-lived or not decisive, i.e. an indicator for further events, to result in the tumorigenic characteristics and, for example, also a changed motility. Elasticity already began to recover 13 min after the treatment. In addition, the elastic modulus was still almost twice as high as that of the tumorigenic cells. Besides, actin fibers could still be detected after the application of the pulsed electric fields while WB-ras cells showed almost no actin fibers at all. Similarly, the effects of nsPEFs on GJIC, MAPKs and connexin43 had a transient character (Steuer et al. 2016), which further indicates that these early alterations of tumor-promoting and pro-carcinogenic events caused by sub-cytotoxic treatments with nsPEFs do not lead into the permanent induction of cancer cell behavior or to a malignant transformation of normal cells.

Conclusion

The application of nsPEFs to WB-F344 monolayers significantly decreased the elastic modulus of the cells to a level similar to the elastic modulus of their tumorigenic counterpart WB-ras. However, cells did not develop tumorigenic features such as the ability of anchorage-independent growth or an enhanced migration behavior. From this point of view, nsPEFs seem to be suitable for the treatment of cancer without posing the risk to induce

malignant transformation or enhance the metastatic potential of healthy cells that were incidentally exposed to sub-lethal electric fields. However, it should be noted that the results presented herein were obtained by performing experiments with only one cell line. Accordingly, these results have to be validated for further, in particular human, cell lines and should be extended to *in vivo* studies or at least excised tissues.

Acknowledgements This work was supported by the Czech Ministry of Education, Youth and Sports (LO1214 and LM2015051).

References

- Alberts B, Bray D, Hopkin K, Johnson A, Lewis J, Raff M, Roberts K, Walter P (2012) Lehrbuch der molekularen zellbiologie, vol 4, vollständig überarbeitete auflage. Wiley-VCH, Weinheim
- Anderson PA, Muller-Borer BJ, Esch GL, Coleman WB, Grisham JW, Malouf NN (2007) Calcium signals induce liver stem cells to acquire a cardiac phenotype. *Cell Cycle* 6:1565–1569
- Beebe SJ, White J, Blackmore PF, Deng Y, Somers K, Schoenbach KH (2003) Diverse effects of nanosecond pulsed electric fields on cells and tissues. *DNA Cell Biol* 22:785–796
- Beebe SJ, Schoenbach KH, Heller R (2010) Bioelectric applications for treatment of melanoma. *Cancers* 2:1731–1770
- Beebe SJ, Chen X, Liu J, Schoenbach KH (2011) Nanosecond pulsed electric field ablation of hepatocellular carcinoma Engineering in Medicine and Biology Society, EMBC, 2011 Annual International Conference of the IEEE. IEEE, pp 6861–6865
- Ben-Ze'ev A (1985) The cytoskeleton in cancer cells. *BBA Rev Cancer* 780:197–212
- Breton M, Mir LM (2012) Microsecond and nanosecond electric pulses in cancer treatments. *Bioelectromagnetics* 33:106–123
- Buehler MJ (2013) Mechanical players—the role of intermediate filaments in cell mechanics and organization. *Biophys J* 105:1733–1734
- Caille N, Thoumine O, Tardy Y, Meister J-J (2002) Contribution of the nucleus to the mechanical properties of endothelial cells. *J Biomech* 35:177–187
- Chen X, Kolb JF, Swanson RJ, Schoenbach KH, Beebe SJ (2010) Apoptosis initiation and angiogenesis inhibition: melanoma targets for nanosecond pulsed electric fields. *Pigment cell melanoma Res* 23:554–563
- Chen X, Zhuang J, Kolb JF, Schoenbach KH, Beebe SJ (2012) Long term survival of mice with hepatocellular carcinoma after pulse power ablation with nanosecond pulsed electric fields. *Technol Cancer Res Treat* 11:83–93
- Chopinet L, Roduit C, Rols MP, Dague E (2013) Destabilization induced by electropermeabilization analyzed by atomic force microscopy. *BBA Biomembr* 1828:2223–2229
- Chopinet L, Dague E, Rols MP (2014) AFM sensing cortical actin cytoskeleton destabilization during plasma membrane electropermeabilization. *Cytoskeleton* 71:587–594
- Cross SE, Jin Y-S, Rao J, Gimzewski JK (2007) Nanomechanical analysis of cells from cancer patients. *Nat Nanotechnol* 2:780–783
- Cross SE, Jin YS, Tondre J, Wong R, Rao J, Gimzewski JK (2008) AFM-based analysis of human metastatic cancer cells. *Nanotechnology* 19:384003
- De Feijter AW, Ray JS, Weghorst CM, Klaunig JE, Goodman JI, Chang CC, Ruch RJ, Trosko JE (1990) Infection of rat liver epithelial cells with v-Ha-ras: correlation between oncogene expression, gap junctional communication, and tumorigenicity. *Mol Carcinog* 3:54–67
- Fan J, Shen H, Dai Q, Minuk GY, Burzynski FJ, Gong Y (2009) Bone morphogenetic protein-4 induced Rat hepatic progenitor cell (WB-F344 cell) differentiation toward hepatocyte lineage. *J Cell Physiol* 220:72–81
- Guilak F, Tedrow JR, Burgkart R (2000) Viscoelastic properties of the cell nucleus. *Biochem Biophys Res Commun* 269:781–786
- Haga H, Sasaki S, Kawabata K, Ito E, Ushiki T, Sambongi T (2000) Elasticity mapping of living fibroblasts by AFM and immunofluorescence observation of the cytoskeleton. *Ultramicroscopy* 82:253–258
- Hayashi T, Nomata K, Chang C-C, Ruch RJ, Trosko JE (1998) Cooperative effects of v-myc and c-Ha-ras oncogenes on gap junctional intercellular communication and tumorigenicity in rat liver epithelial cells. *Cancer Lett* 128:145–154
- Jonas O, Mierke CT, Kas JA (2011) Invasive cancer cell lines exhibit biomechanical properties that are distinct from their noninvasive counterparts. *Soft Matter* 7:11488–11495
- JPK Instruments AG a. QI™ mode - Quantitative Imaging with the NanoWizard 3 AFM. Technical Note (jpk-tech-quantitative-imaging.14-1.pdf at www.jpk.com). Accessed 23 Mar 2017
- JPK Instruments AG b. Investigation of living cells using JPK's QI™ mode. Application Note (jpk-app-living-cells-qi.14-1.pdf at www.jpk.com). Accessed 23 Mar 2017
- Kolb JF, Stacey M (2012) Subcellular biological effects of nanosecond pulsed electric fields Plasma for Bio-Decontamination, Medicine and Food Security. Springer, Heidelberg, pp 361–379
- Lee KW, Kim MS, Kang NJ, Kim DH, Surh YJ, Lee HJ, Moon A (2006) H-ras selectively up-regulates MMP-9 and COX-2 through activation of ERK1/2 and NF-κB: an implication for invasive phenotype in rat liver epithelial cells. *Int J Cancer* 119:1767–1775
- Lekka M, Laidler P, Gil D, Lekki J, Stachura Z, Hryniewicz AZ (1999) Elasticity of normal and cancerous human bladder cells studied by scanning force microscopy. *Eur Biophys J Biophys Lett* 28:312–316
- Liang C-C, Park AY, Guan J-L (2007) In vitro scratch assay: a convenient and inexpensive method for analysis of cell migration in vitro. *Nat Protoc* 2:329–333
- Neumann T (2008) Determining the elastic modulus of biological samples using atomic force microscopy. JPK Instruments, Berlin, Germany
- Nuccitelli R, Tran K, Sheikh S, Athos B, Kreis M, Nuccitelli P (2010) Optimized nanosecond pulsed electric field therapy can cause murine malignant melanomas to self-destruct with a single treatment. *Int J Cancer* 127:1727–1736
- Nuccitelli R, Tran K, Athos B, Kreis M, Nuccitelli P, Chang KS, Epstein EH, Tang JY (2012) Nanoelectroablation therapy for murine basal cell carcinoma. *Biochem Biophys Res Commun* 424:446–450
- Olson MF, Sahai E (2009) The actin cytoskeleton in cancer cell motility. *Clin Exp Metas* 26:273–287
- Pakhomov AG, Xiao S, Pakhomova ON, Semenov I, Kuipers MA, Ibey BL (2014) Disassembly of actin structures by nanosecond pulsed electric field is a downstream effect of cell swelling. *Bioelectrochemistry* 100:88–95
- Rao KMK, Cohen HJ (1991) Actin cytoskeletal network in aging and cancer. *Mutat Res DNAGing* 256:139–148
- Roduit C, van der Goot FG, De Los Rios P, Yersin A, Steiner P, Dietler G, Catsicas S, Lafont F, Kasas S (2008) Elastic membrane heterogeneity of living cells revealed by stiff nanoscale membrane domains. *Biophys J* 94:1521–1532
- Rother J, Nöding H, Mey I, Janshoff A (2014) Atomic force microscopy-based microrheology reveals significant differences in

- the viscoelastic response between malign and benign cell lines. *Open Biology* 4:140046
- Stacey M, Fox P, Buescher S, Kolb J (2011) Nanosecond pulsed electric field induced cytoskeleton, nuclear membrane and telomere damage adversely impact cell survival. *Bioelectrochemistry* 82:131–134
- Stamov DR, Kaemmer SB, Hermsdörfer A, Barner J, Jähnke T, Haschke H (2015) BioScience AFM—Capturing dynamics from single molecules to living cells. *Microscopy Today* 23:18–25
- Steuer A, Schmidt A, Labohá P, Babica P, Kolb JF (2016) Transient suppression of gap junctional intercellular communication after exposure to 100-nanosecond pulsed electric fields. *Bioelectrochemistry* 112:33–46
- Swaminathan V, Mythreye K, O'Brien ET, Berchuck A, Blobe GC, Superfine R (2011) Mechanical stiffness grades metastatic potential in patient tumor cells and in cancer cell lines. *Can Res* 71:5075–5080
- Thompson GL, Roth C, Tolstykh G, Kuipers M, Ibey BL (2014) Disruption of the actin cortex contributes to susceptibility of mammalian cells to nanosecond pulsed electric fields. *Bioelectromagnetics* 35:262–272
- Tsao M-S, Smith JD, Nelson KG, Grisham JW (1984) A diploid epithelial cell line from normal adult rat liver with phenotypic properties of 'oval' cells. *Exp Cell Res* 154:38–52
- Wu S, Wang Y, Guo J, Chen Q, Zhang J, Fang J (2014) Nanosecond pulsed electric fields as a novel drug free therapy for breast cancer: an in vivo study. *Cancer Lett* 343:268–274
- Xu WW, Mezencev R, Kim B, Wang LJ, McDonald J, Sulchek T (2012) Cell stiffness is a biomarker of the metastatic potential of ovarian cancer cells. *PLoS One* 7:e46609
- Yamasaki H (1991) Aberrant expression and function of gap junctions during carcinogenesis. *Environ Health Perspect* 93:191
- Yousafzai MS, Coceano G, Mariutti A, Ndoye F, Amin L, Niemela J, Bonin S, Scoles G, Cojoc D (2016) Effect of neighboring cells on cell stiffness measured by optical tweezers indentation. *J Biomed Opt* 21:057004
- Zhou J, Zhao L, Qin L, Wang J, Jia Y, Yao H, Sang C, Hu Q, Shi S, Nan X (2010) Epimorphin regulates bile duct formation via effects on mitosis orientation in rat liver epithelial stem-like cells. *PLoS One* 5:e9732